ANNUAL REPORT

October 1, 1993 to September 30, 1994

Princeton Plasma Physics Laboratory

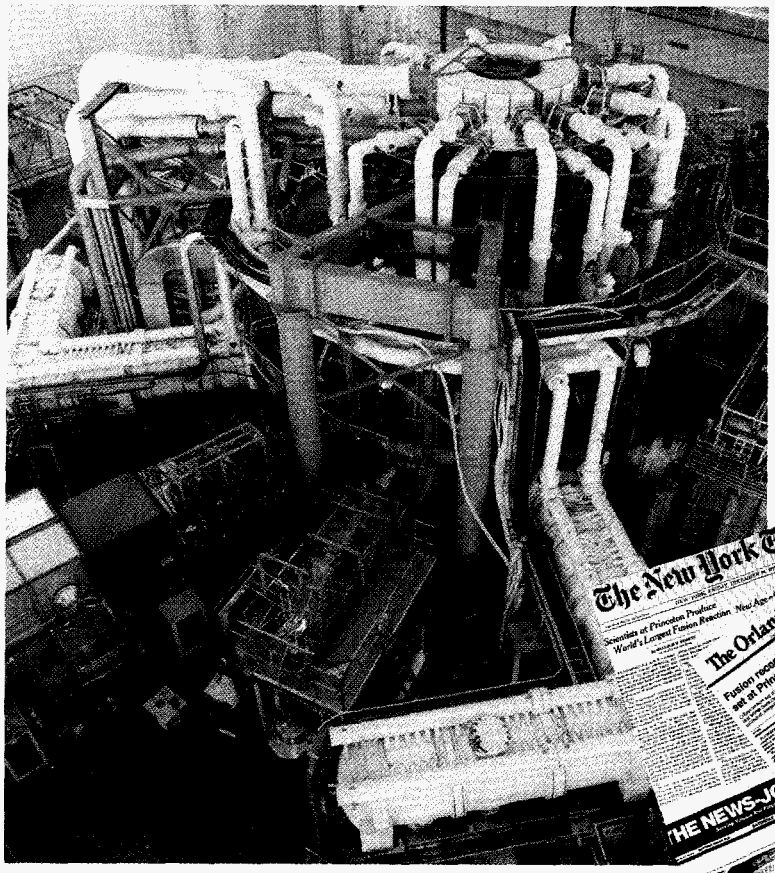

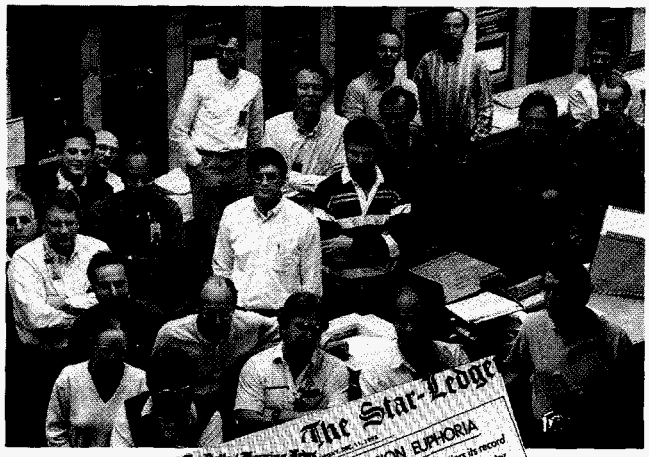

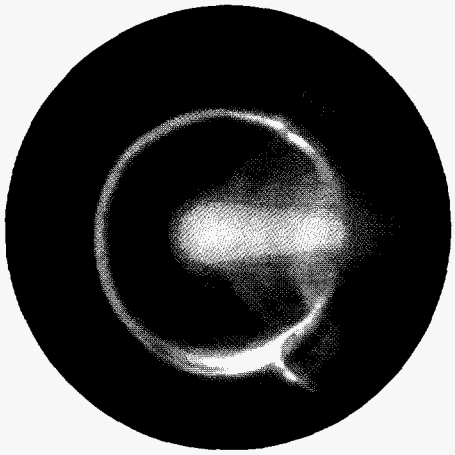

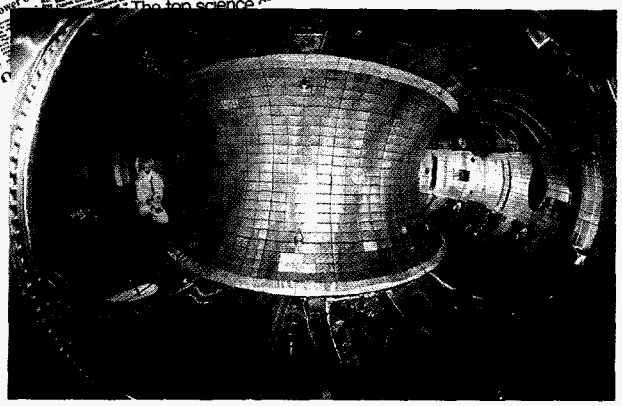

MASTER

PPPL - Q - 52

Cover:

From top left in clockwise direction:

(a) *The Tokamak Fusion Test Reactor—TFTR.*

(b) *Scientists in the TFTR Control Room on December 9, 1993, as they waited for data from the first deuterium-tritium experiments to appear on computer monitors.*

(c) *A collage of newspaper headlines heralding the first U.S. deuterium-tritium experiments in TFTR.*

(d) *Inside the TFTR vacuum vessel.*

(e) *PPPL Principal Research Physicist Russell Hulse receiving the 1993 Nobel Prize for Physics from the King of Sweden.*

(f) *A deuterium-tritium plasma in TFTR.*

Cover Design: Gregory Czechowicz

Funding for the color cover was provided by nonappropriated funds. No Department of Energy funds were used.

Annual Report

Covering the Period October 1, 1993 to September 30, 1994

Princeton University
Plasma Physics Laboratory
Princeton, New Jersey 08543

PPPL-Q-52

DISCLAIMER

Unless otherwise designated, the work in this report is funded by the United States Department of Energy under contract DE-AC02-76-CHO-3073.

Printed in the United States of America

Table of Contents

Preface

The Tokamak Fusion Test Reactor (TFTR) project is well into the experimental phase of its deuterium-tritium (D-T) program, with the objective to derive the maximum amount of experimental data on the behavior of tokamak plasmas containing a significant population of energetic alpha particles. Since the initial D-T experiments in December, 1993, the operational performance of the TFTR, as well as the required tritium-handling and machine maintenance procedures in an activated environment, have improved markedly, so that D-T operation has now become essentially routine, while fully conforming with all of the safety and environmental requirements. During the D-T phase, the machine and auxiliary-systems parameters have also been increased, most notably the toroidal field (to 5.6 T) and the neutral-beam power (to 40 MW). The radio-frequency power in the ion-cyclotron-range of frequencies (ICRF) has been increased to 11 MW.

The results from the initial deuterium-tritium experiments in December, 1993, have been confirmed in subsequent D-T operations. Substantially higher ion temperatures are observed in D-T operation compared with deuterium only, indicating a strongly favorable isotopic mass dependence of ion energy transport in the "supershot" confinement regime. Increments in electron temperature are also observed, which can be accounted for only partially by the direct electron heating by alpha particles, implying that some improvement in electron energy confinement must also be occurring. The number of escaping alpha particles observed on the lost-alpha detectors is consistent with classical predictions of "first orbit" loss. No fluctuations of the type associated with alpha-driven collective instabilities were observed during these experiments.

The further experimental results achieved on TFTR in FY94 have included (i) the production of 10.7 MW of fusion power and 6.5 MJ of fusion energy, with a central fusion power density exceeding that projected for the International Thermonuclear Experimental Reactor (ITER); (ii) the improvement of confinement by further optimization of the lithium-pellet wall-conditioning technique, so that the fusion-triple-product in quasi-steady conditions has more than doubled to 8.3×10^{20} $m^{-3} \cdot sec \cdot keV$; (iii) the identification of the physical mechanisms responsible for the beta-limiting disruptions in TFTR; (iv) the further elucidation of alpha-particle and thermalized helium transport processes in D-T plasmas; and (v) the demonstration of ICRF heating of D-T plasmas in the minority-^{3}He and second-harmonic-tritium modes, and the identification of a promising new radio-frequency method for "mode-conversion current drive (MCCD)."

The overall programmatic mission of the Tokamak Physics Experiment (TPX) is to develop the scientific basis for a compact, continuously operating and economical tokamak fusion reactor. It will do this by demonstrating both the physics and technology needed to extend tokamak operation into the steady-state regime and advances in fundamental tokamak performance parameters on timescales long compared with current-relaxation and plasma-wall equilibration times. Favorable results from the Tokamak Physics Experiment (TPX) are essential to further development of an attractive tokamak fusion reactor and will also benefit the operation of the International Thermonuclear Experimental Reactor. Key contributions will be in the areas of divertor physics and steady-state operation.

Following a successful Conceptual Design Review in March, 1993, the TPX Project began Preliminary (Title 1) Design in October, 1993. Major industrial contracts for the plasma-facing components, the magnet systems, and the vacuum vessel were awarded in FY94, and contracts for systems integration and construction management are now in the final stages of award. Also in FY94, the TPX Project successfully completed a U.S. Department of Energy Management Systems Review to ensure that the management and control systems are in place to proceed with a construction project. The summary conclusions of this

review were that the project management roles and responsibilities are well understood, that a strong industrial systems integration contractor and a construction manager are planned to ensure that all requirements are integrated and controlled, and that, overall, the basic project control functions are in place.

As fiscal year 1994 ends, it becomes clear that the TPX will not receive construction authorization in FY95. Accordingly, the TPX Project is now working on the basis that construction will be authorized in the FY96 budget, and so the FY96 plan calls for the start of Detailed Design and the award of the magnet conductor fabrication contract. The schedule described in the Department of Energy TPX Construction Project Data Sheet, which now reflects the baseline FY96 request, is consistent with a July, 2001, "first plasma" date.

Operation of the Princeton Beta Experiment-Modification (PBX-M) was suspended in November, 1993, due to budget constraints, and most of the staff were transferred at that time to TFTR. Operation of PBX-M is presently planned to resume in January, 1995. Meanwhile, significant machine hardware and auxiliary systems upgrading is taking place.

The theory program continues its strong support for the TFTR D-T experimental program. Theoretical efforts in support of advanced tokamak concepts, including plasma control and disruption avoidance studies and steady-state plasma scenarios for TPX, have been intensified. The Laboratory MHD-theory effort has played the leading role in identifying the reference reversed-shear, second-stability, high-bootstrap regime for TPX. Princeton Plasma Physics Laboratory theorists continue in a leadership role in the development of both gyrokinetic and gyrofluid models in support of the national Numerical Tokamak Project. The theory program continues to develop and support a number of fundamental tokamak physics codes, many of which have become standards worldwide. A new concept for tokamak reactor optimization ("alpha channeling") has been developed. The divertor modeling effort continues to be involved prominently in multi-institutional and international divertor activities, as well as in the design studies for TPX and ITER.

In regard to the ITER Engineering Design Activities, the Laboratory continues to be represented on the Joint Central Team, both in physics at San Diego, California (including the Head of the Physics Integration Unit) and in engineering at Naka, Japan. The Laboratory provides the Home Team Physics Manager, and its involvement in Home Team activities, especially in physics R&D tasks and the physics "expert groups," has increased significantly. The Laboratory continues to provide the Technical Advisory Committee Chair.

A conceptual design study has begun for a National Spherical Tokamak Experiment (NSTX), using hardware from the S-1 device, to explore the physics principles of very-low-aspect-ratio tokamak plasmas. Such "spherical tokamak (ST)" configurations may provide an attractive alternative route to a tokamak reactor with compact size and modest magnet requirements (using normal toroidal-field conductors) or to an attractive volumetric neutron source. The NSTX is designed to test the special physics issues of concern in the very-low-aspect-ratio configuration, including stability at very high beta (approximately 40%), confinement with very high trapped-particle fraction, and high-efficiency noninductive current drive (essential in the reactor application). Although both NSTX and the proposed MAST (Mega-Amp Spherical Tokamak) device at Culham have a plasma current in the 1-MA range, the NSTX complements MAST by having a lower aspect-ratio (1.25), a greater pulse length (5 sec), a nearby conducting wall, and more current-profile control tools (fast-wave current drive and helicity injection, with neutral-beam injection upgrade capability). The NSTX would be located in the Princeton Large Torus (PLT) area.

The small Current Drive Experiment-Upgrade (CDX-U) device continues to pursue innovative current-drive techniques, especially helicity injection, as well as a variety of topics in low-aspect-ratio tokamak physics and a proposed new program in fast-wave heating and current drive in support of National Spherical Tokamak Experiment.

The Laboratory is well advanced in its planning for an expanded program of collaborations on other U.S. and foreign facilities. The goal of the collaborations program will be to provide experienced research personnel, augmented in some cases by engineering support and auxiliary device hardware, to several operating tokamaks for the overall benefit of the U.S. and world fusion effort. The collaborative effort in the near term will include major initiatives on C-Mod (ICRF antenna, divertor diagnostics, divertor modeling), DIII-D (disruption physics, theory of low-to-high confinement mode transitions and energetic-ion MHD effects, ICRF participation, computer support), and increased participation in JT-60U experiments, as well

as continued smaller-scale efforts on JET, ASDEX-U and Tore Supra.

Fiscal year 1994 began with a singularly notable event, namely the award of the 1993 Nobel Prize in Physics to Princeton Plasma Physics Laboratory Principal Research Physicist Russell Hulse and Princeton University Professor Joseph Taylor for their 1974 discovery of the first binary pulsar. Other notable events in the fiscal year were the receipt by Laboratory Director Ronald C. Davidson of the Kaul Foundation Award for Excellence in Science, Education, and Physics, and the award of the 1993 James Clerk Maxwell Prize in Plasma Physics to PPPL Professor Russell Kulsrud.

Awards and Honors

Nobel Prize

In October 1993, Principal Research Physicist Russell Hulse and Princeton University Professor Joseph Taylor received the 1993 Nobel Prize in Physics for their 1974 discovery of the first binary pulsar. It was the first time in the history of the Laboratory that a Nobel Prize was awarded to a Princeton Plasma Physics Laboratory (PPPL) physicist.

At the time of the discovery, Hulse was a University of Massachusetts graduate student who had gone pulsar hunting at the urging of his thesis advisor, Taylor, then a professor at the University of Massachusetts. While using a 300-meter-diameter radio telescope at an observatory in Arecibo, Puerto Rico, Hulse discovered a binary pulsar, which is a twin star system that serves as a rare natural laboratory in which to test Albert Einstein's prediction that moving objects emit gravitational waves, as well as other aspects of Einstein's general theory of relativity.

In preparation for his work, Hulse developed a computer program to sort out the pulsar data collected by the large telescope in Puerto Rico. He expected to detect the characteristic beacons of predictably timed pulses of radio waves that these collapsed stars beam out through the universe.

When Hulse began his search for new pulsars, their existence had been known for just seven years and only about 100 had been discovered. Hulse's search was about 10 times more sensitive than any previous search because it combined the largest available telescope and a dedicated minicomputer devoted to analyzing the signals in great detail. With this increased sensitivity, Hulse was able to detect 40 new pulsars in the small section of the plane of our galaxy (the Milky Way) visible with the Arecibo telescope.

Among the data coming in was one weak pulsed signal that first appeared in July and which was notable at first only for its relatively fast pulses. When Hulse reobserved this particular newly discovered pulsar in August, he noticed that the data was producing inconsistent values for the exact pulsation pe-

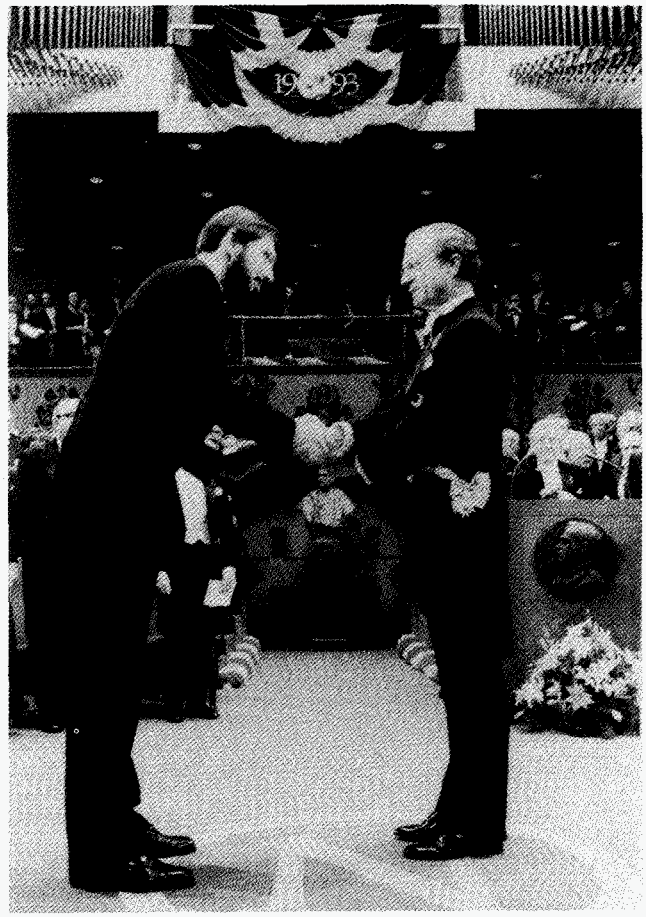

Russell Hulse (left) with the King of Sweden during the Nobel presentation ceremonies.

Joseph Taylor (left) of Princeton University and Russell Hulse of PPPL shared the 1993 Nobel Prize in Physics.

riod. He initially assumed that this was caused by a problem with the observing equipment or his computer programs, since pulsars are very precise and stable stellar "clocks" whose periods can be measured to high accuracy.

Hulse devoted increasing efforts to understanding this puzzling result, and ultimately deduced that the changing pulsation period was indeed real, and not just an instrumental problem. The observed period variations were due to the changing Doppler shifts associated with the orbital motion of the pulsar around another, unseen companion star. Furthermore, he realized that the high orbital velocities and strong gravitational fields associated with this pulsar's orbit would make the system exhibit effects predicted by Einstein's general theory of relativity which would otherwise be very difficult to measure. These effects could now be verified by carefully measuring just the variations in the "ticking" of the pulsar clock which had been so puzzling when the pulsar had been first discovered.

Hulse kept taking the observations, but the data was unlike that for single pulsars. When the periods began repeating, he noticed the pulsar had a predictable pulse rate, but it wasn't alone. It was in orbit around some kind of companion object whose pulses he was also picking up.

This, Hulse discovered, was a binary system — with two stars rotating around a mutual axis. Taylor worked with Hulse in Puerto Rico to affirm and clarify the data and, nearly 20 years later, the two shared the Nobel Prize for Physics.

Hulse, who earned a Ph.D. from the University of Massachusetts in 1975, changed from the field of astrophysics to plasma physics and came to PPPL in 1977. Since entering plasma physics, he has become a leading expert in computational modeling of impurity transport in tokamaks. Taylor continued in the field of pulsar astrophysics, first at the University of Massachusetts and then in the physics department at Princeton University. His continued work on this pulsar has resulted in the best evidence to date for one of the more intriguing predictions of general relativity, that such an orbiting system should emit gravitational waves.

Hulse is presently establishing an advanced computer modeling group at PPPL. Part of the group's efforts will be to develop new approaches to scientific computing that encourage innovative work by enabling the creation of powerful yet easily modifiable computer codes as part of a Cooperative Research and Development Agreement (CRADA). In addition, the group is exploring the educational potential of computer modeling, which can serve as a unique tool for teaching science and the process of scientific investigation.

Jeanne Kuhlman (left), Russell Hulse, and President Bill Clinton.

In addition to his duties at the Laboratory, Hulse has taken on additional speaking and social engagements since winning the Nobel. In December 1993, he attended the Nobel Ceremonies, where he presented an oral lecture on the binary pulsar discovery and dined with Sweden's Queen Sylvia at the Nobel banquet. Prior to the visit to Sweden, where the King of Sweden presented him with the Nobel, Hulse took tea with the Clintons at the White House. Since then, he has been the featured speaker at numerous public and academic lectures at home and abroad.

The Nobel marked the first of three distinguished honors bestowed on Hulse in 1993. He was also recognized for his achievements by being named a Fellow of the American Physical Society (APS) and by being chosen as one of the first three PPPL Distinguished Research Fellows at the Laboratory.

Hulse was honored by the APS "For fundamental contributions in two fields of physics: The discovery by radio astronomy of the first binary pulsar, and the description and computational modeling of processes involving high Z ions in tokamak plasma."

As a recipient of PPPL's newly created Distinguished Research Fellowships, Hulse was cited for his "extraordinary record of creativity and accomplishments in research over an extended period of time."

Awards and Honors in FY94

James L. Anderson
DOE Distinguished Associate Award
U.S. Department of Energy

Dori J. Barnes
Certificate of Accomplishment
Princeton University
Women's Organization

Stefano Bernabei
Fellow
American Physical Society

Ronald C. Davidson
1993 Award for Excellence in Science, Education, and Physics
Kaul Foundation

Russell A. Hulse
1993 Nobel Prize in Physics
The Royal Swedish Academy of Sciences

Fellow
American Physical Society

PPPL Distinguished Research Fellow
Princeton University Plasma Physics Laboratory

1994 Gano Dunn Award
Cooper Union

Charles E. Kessel, Jr.
1994 Excellence in Fusion Engineering
Fusion Power Associates

Russell M. Kulsrud
1993 James Clerk Maxwell Prize in Plasma Physics
American Physical Society

Ernesto Mazzucato
Fellow
American Physical Society

Dale M. Meade
DOE Distinguished Associate Award
U.S. Department of Energy

Susan E. Murphy
Certificate of Accomplishment
Princeton University
Women's Organization

Allan H. Reiman
Fellow
American Physical Society

Timothy J. Riotto
(former co-op student)
Drexel's Outstanding Co-Operative Education Senior for 1994
Drexel University

James M. Scott, III
Certificate of Appreciation
U.S. Department of Energy

James C. Sinnis
DOE Distinguished Associate Award
U.S. Department of Energy

James D. Strachan
PPPL Distinguished Research Fellow
Princeton University Plasma Physics Laboratory

Roscoe B. White
PPPL Distinguished Research Fellow
Princeton University Plasma Physics Laboratory

Michael D. Williams
Fusion Technology Award
Institute of Electrical and Electronics Engineers

King-Lap Wong
Fellow
American Physical Society

Lynne H. Yager
Certificate of Accomplishment
Princeton University
Women's Organization

Stewart J. Zweben
Fellow
American Physical Society

Principal Parameters of Experimental Devices Fiscal Year 1994

Parameters	Experimental Devices		
	TFTR	PBX-M	CDX-U
R (m)	2.6	1.65	0.32
a (m)	0.9	0.3	0.23
I_p (MA)	3.0	0.6	0.02
B_T (T)	5.6[a]	2.0	0.15
τ_{AUX} (sec)	2.0	0.5	0.1
P_{AUX} (MW)			
NB[†]	40 (110 kV)	6 (45 kV)	—
RF	11.4 (40-80 MHz)[b]	2.0 (40-80 MHz)[c]	0.01 (2.45 GHz)[d]
		2.0 (4.6 GHz)[e]	0.2[f]
n(0) (cm^{-3})*	5.0×10^{14}	1.5×10^{14}	5.0×10^{12}
$T_i(0)$ (keV)*	44	5.5	0.04
τ_E (msec)*	550	80	0.1

*These highest values of n, T, and τ were not achieved simultaneously.

[†]Deuterium-Tritium Operations.

[a]At R = 2.48 m, the design basis.

[b]Ion Cyclotron Range of Frequencies (ICRF).

[c]Ion-Bernstein Wave Heating (IBWH) source power.

[d]Electron Cyclotron Heating (ECH) source power.

[e]Lower Hybrid Current Drive (LHCD).

[f]DC-Helicity Injection.

Tokamak Fusion Test Reactor

Excitement filled the air the evening of December 9, 1993, as the first high-power experiments on the Tokamak Fusion Test Reactor (TFTR) with a near-optimum deuterium-tritium (D-T) fuel mixture began. To prevent overcrowding in the control room, red badges conferred entry privileges only to critical operations personnel, while the rest of the Laboratory staff along with media representatives witnessed the action on monitors in the MBG Auditorium and other locations throughout the Lab. As the "shot" clock counted down, those in the control room focused their gaze on a TV monitor which displayed the image of a special scintillator screen located in the TFTR Test Cell. During the high-power phase of a D-T plasma discharge (shot), neutrons from the fusion reactions would excite the scintillator and the otherwise dark screen would light up with the words "Fusion Power" in a circle around the likeness of a lightbulb (see Fig. 1). The brightness of this image provided immediate feedback to researchers on the success or failure of the shot. Cheers from the control room told onlookers that the experiments were successful; stories were broadcast on prime time news, with images such as those shown in Fig. 2 conveying the charged atmosphere of this historic moment in fusion research.

The following *News Alert* was distributed to the staff as they entered the Laboratory the next day:

> TFTR set a world record of about three million watts of controlled fusion power, during the first approximately 50-50 deuterium-tritium (D-T) experiment. The first high-power shot occurred at 11:08 P.M. on Thursday night, December 9," said PPPL Director Ron Davidson. This was the world's first magnetic fusion experiment utilizing a plasma made up of equal parts of deuterium and tritium in a tokamak—the mix required for practical amounts of fusion power.

As a result of this initial experiment and the even better results obtained the next day, there was a burst

Figure 1. *A TV monitor in the TFTR control room viewed this mask placed over a scintillator screen exposed to fusion neutrons near the TFTR machine. The brightness of the image provided scientists with instant feedback about the success or failure of the experiment.*

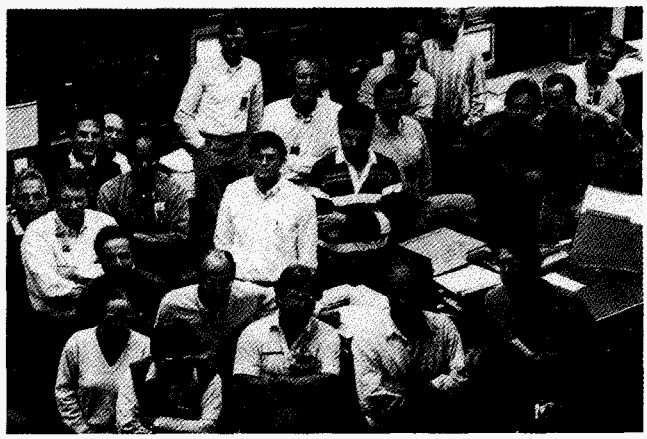

Figure 2. *As the "shot" clock counted down, scientists in the TFTR control room watched the computer monitors with anticipation for data from the first high-powered D-T experiments. (94A0232)*

of media coverage and a multitude of messages of congratulations from coworkers and supporters from around the world. On December 11, Lyman Spitzer, Jr., astronomy professor at Princeton University and the founder in 1951 of the Princeton Plasma Physics Laboratory, wrote in the *New York Times* Op-Ed page:

> Forty years ago Princeton University scientists began experimenting with a promising but challenging idea: if we could replicate the process that powers the sun, we could create a source of virtually unlimited energy. And unlike splitting heavy atoms or burning fossil fuels, this process of fusing light atoms together—fusion—would pose almost no risk and have little adverse environmental impact. On Thursday, America's fusion energy program reached a milestone at Princeton as the Plasma Physics Laboratory began experiments using the fuel that could one day power commercial fusion reactors. This fuel—a mixture of two hydrogen isotopes, deuterium and tritium, in equal portions—should produce the hot gas environment needed for a fusion reaction. ... But to take the next step, scientists need to fully control the mixture of deuterium and tritium, which will produce energetic ions (actually the nuclei of helium atoms) that will hurdle through the hot gas at nearly the speed of light. ... The (TFTR) program will provide for the first time a hot gas in which the effects of the energetic helium ions are observable. This new mixture of gases may exhibit new antics, and scientists will try to find techniques to bring them under control. ... Fusion is a field where patience is necessary. But it is also a field where periodic breakthroughs, like this week's, move us ever closer to the dream of safely harnessing the power of the sun here on earth.

Over the year as more progress was made, the texts of the news articles grew to fill a large book.

The first year of operation with D-T fuel mixtures was highly successful technically, with D-T operation at high power becoming routine sooner than expected, despite the commissioning of several new systems. It was also highly productive scientifically, with plasma performance more favorable with D-T than was anticipated based on previous results with deuterium-only plasmas. Studies were begun to characterize the behavior of the energetic alpha particles, which are a product of the D-T fusion reaction and will ignite the plasmas in future tokamaks.

Through the year, more than 250 experiments using tritium were performed. Here are some of the physics highlights from FY94:

Nov 93	First tritium transport measurements are made with tritium gas puffs.
Dec 93	Obtained record 6.3 MW of fusion power and clear signs of a favorable isotope effect on plasma confinement.
Dec 93	First observations of confined and lost alpha particles in a D-T plasma.
Feb 94	First experiments conducted for ion cyclotron range of frequencies (ICRF) heating of a D-T plasma with second harmonic tritium heating.
Mar 94	High beta poloidal (β_p) D-T plasma obtains high fusion power.
Mar 94	Limiter H-mode (high-confinement mode) achieves an energy confinement enhancement factor H = 4 in a D-T plasma.
May 94	Record 9.2 MW of fusion power obtained.
June 94	First assessment of effects of sawteeth instabilities on plasmas with confined alphas.
July 94	Systematic documentation of the isotope scaling effect.
Sept 94	First assessment of alpha ash transport completed.

The 9.2 MW of fusion power produced in TFTR in May, 1994, is approximately 90 million times that possible in devices in 1974 when TFTR was proposed and about five times that produced in 1991 by the Joint European Tokamak (JET) at Culham, England. At this level of fusion power, the fusion reactivity of a TFTR plasma is comparable to that predicted for the proposed International Thermonuclear Experimental Reactor (ITER), as shown in Fig. 3. Thus, alpha-particle physics studied in TFTR provide initial insight about issues relevant to an ignited reactor plasma.

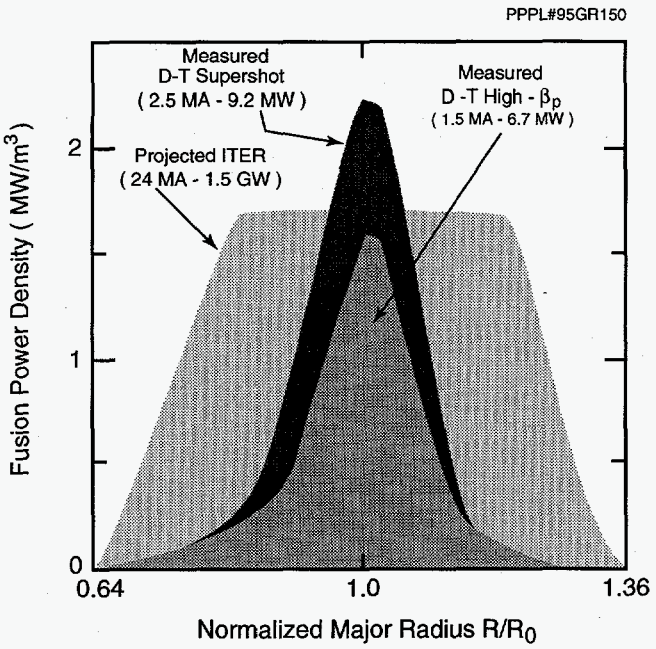

Figure 3. *Deuterium-tritium (D-T) fusion power density profiles projected for the International Thermonuclear Experimental Reactor and measured in TFTR supershot and high-β_p plasma discharges. The D-T fusion power density in TFTR is based on neutron emission profile measurements with an uncertainty of ±15% in the plasma core.*

As shown in Fig. 4, they also continue the steady progress made through the years in magnetic fusion power.

In recognition of the significance of the D-T experiments, TFTR physicists were invited to present lead talks on the results during fiscal year 1994 at national and international meetings, including the American Physical Society's Division of Plasma Physics, the European Physical Society, and the International Atomic Energy Agency (IAEA). These papers, some of which appear in modified form in the TFTR physics section of this report, describe the improvement in plasma performance in D-T plasmas compared to D-only plasmas, the agreement of D-T fusion reactivity with predictions, and the first observations of confined alpha particles. Also included are the first measurements of alpha ash from D-T plasmas, the first results from ICRF heating of D-T plasmas, and the extensive documentation of lost alpha measurements in many interesting scenarios indicating no significant anomalous alpha loss.

In addition to the physics results, the technical achievements during FY94 are also recognized as having important implications for the future of fusion energy development. Through the year, the TFTR staff established a record of safe operation with tritium in a mode which allowed for considerable experimental flexibility. Maintenance and repair activities on the machine and the various subsystems continued to keep the device operating with high reliability. Potentially tritium-contaminated volumes were opened (called "line breaks") more than 100 times for modification and maintenance. The fluorinert toroidal-field coil cooling system commissioned in fiscal year 1993 performed well, removing the burden of having to repair small cooling system leaks in order to continue operation. The neutral-beam systems worked reliably in tritium, and new records for injected power were achieved. The shielding and relocation of diagnostics in preparation for D-T operation was effective and resulted in high reliability for these systems. Calibrations and adjustments were performed as necessary, despite the fact that the machine became progressively more activated. Because of the lack of new installation near the machine during this period, the total level of personnel radiation exposure was actually lower in FY94 than in previous years.

There were two major repair activities on TFTR during fiscal year 1994. The first involved correction of a fabrication flaw in the plumbing of the neutral-beam-source grid masks. Over a two week period, all twelve of the tritium-contaminated neutral-beam sources were safely decontaminated, removed, reworked, and reinstalled. The second repair activity involved vacuum leaks which occurred during high-power radio-frequency heating shots. High-energy ripple-trapped ions caused damage to welds in two

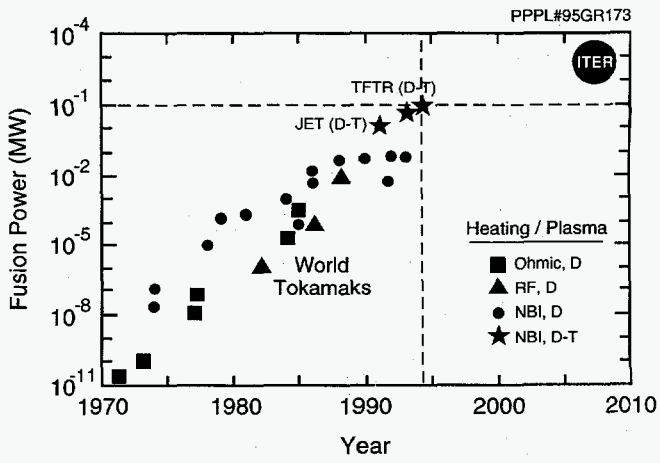

Figure 4. *The performance as measured in fusion power produced by tokamaks around the world by year.*

locations. As described in more detail below, this resulted in a five week suspension of operations. These areas and others, which were vulnerable because of similar machine geometry, were repaired without venting the vacuum vessel.

Many years of preparation were required for operation with deuterium-tritium. Whole new organizations were created, new hardware waited to be commissioned, and a host of new procedures were created to control tritium operations. In FY94, it was satisfying to the staff to be able to test these new systems on real day-to-day problems in dealing with tritium, with a more activated machine, and with new and exciting physics questions. It was even more satisfying when, after many scientific and technical successes, the staff learned in the summer of '94 that TFTR, originally scheduled to stop operations at the end of FY94, would have its program extended one year.

As in previous years, in FY94 the TFTR program benefited greatly from the activities of a host of collaborators from around the world in the critical D-T phase of operations. Table I lists these valuable associations and their contributions.

Details about TFTR achievements in fiscal year 1994 are found in the sections below. Technical experience with the D-T phase of operation is described in the tokamak operations, neutral-beam heating, and tritium systems sections. There is then a section describing alpha diagnostic measurements. Finally, there is a long section on the physics results of the first year of tritium operation, adapted from papers presented by TFTR physicists at the *15th International Conference on Plasma Physics and Controlled Fusion Research* at Seville, Spain, September 26-October 1, 1994.

Tokamak Operations

During 1994, the TFTR operated with high reliability despite the recent commissioning of many of the tritium-related systems. The experimental program was carried out safely and with a minimum of downtime. Installation and operation of a fluorinert-based cooling system for the toroidal-field (TF) coils was successful, ameliorating fears that leaking toroidal-field coil coolant water would cause irreparable damage. The higher radiation levels produced during D-T operation resulted in significantly higher neutron activation of components. Radiological measurements confirm estimates of the radiation levels and indicate that increased neutron production is not a major problem for continued operation of the TFTR. The observed tritium retention in the vacuum vessel is similarly consistent with expectations and does not present a serious obstacle to continued operation of the TFTR. Both routine maintenance and repair of significant vacuum leaks were carried out effectively, despite the higher radiation levels following deuterium-tritium operation. Empirical scaling indicates that the fusion power production in TFTR is limited by high-β instabilities. This implies that operation of TFTR at higher toroidal field would increase fusion power approximately as the fourth power of the toroidal-field current. With the intent of raising the maximum toroidal field in TFTR from 5.2 to 6.0 Tesla, a significant effort was undertaken to examine the coil stresses expected with 6.0 Tesla operation. Upon completion of this analysis, hardware modifications to permit 6.0 Tesla operation were begun. So far, the existing hardware modifications have permitted 5.6 Tesla operation and future modifications are expected to allow 6.0 Tesla operation.

Fluorinert System

To cool the toroidal-field coils for the D-T experiments, an alternate cooling system was installed that utilizes Fluorinert as a coolant. The toroidal-field and poloidal-field coil systems were originally designed for water cooling. In years past, six of the twenty toroidal-field coils developed water leaks which reduced the coils resistance to ground thus posing an electrical hazard. In many cases, repair of these leaks required suspension of TFTR plasma operations for several weeks while the leak was located, the coils were baked to remove water, and, finally, a long curing epoxy seal was applied. A solution was to replace the deionized water with an electrically insulating fluid. Fluorinert was chosen from a host of dielectric fluids because of its compatibility with existing materials in the toroidal-field coil coolant paths, chemical and radiological stability, and its environmental acceptability. Extensive modifications were made to the toroidal-field and poloidal-field cooling systems to integrate the Fluorinert into operation. The Fluorinert system has successfully operated since June, 1993. During the past year, small leaks continued to occur in the toroidal-field coils. Since the leaking Fluorinert did not reduce the resistance to ground, it was possible to continue operation.

Table I. Collaborations on TFTR.

Institution	Country	Research Area
A.F. Ioffe Physical-Technical Institute	Russian Federation	Alpha-Charge-Exchange Diagnostics
Canadian Fusion Fuels Technology Project (CFFTP)	Canada	Edge Plasma Tritium Technology
Columbia University	USA	High Beta Poloidal (β_p)
Ebasco Division of Raytheon Engineers and Constructors, Inc.	USA	Engineering
Ecole Royale Militaire	Belgium	Ion-Cyclotron Radio-Frequency Wave Propagation Modeling
Fusion Physics and Technology, Inc.	USA	Current Profile Measurements
General Atomics (GA)	USA	Alpha-Charge-Exchange Diagnostics
General Physics Corporation	USA	Tritium System Operations Shutdown and Removal Management
Hebrew University of Jerusalem	Israel	Imaging Properties of Doubly Focusing Crystals
I.V. Kurchatov Institute of Atomic Energy	Russian Federation	Lost-Alpha Diagnostics
Japan Atomic Energy Research Institute (JAERI)	Japan	Fusion Product Diagnostics
Joint European Torus (JET)	European Communities United Kingdom	Fusion Product Diagnostics Fiber Optics Evaluation
Lodestar	USA	Ion-Cyclotron Radio-Frequency Modeling Alpha-Particle Modeling
Los Alamos National Laboratory (LANL)	USA	Tritium Handling Pellet and Fusion Products Diagnostics
Massachusetts Institute of Technology (MIT)	USA	Lithium Wall Conditioning Confined Alpha Measurements
National Institute for Fusion Studies (NIFS)	Japan	Neutron Spectroscopy
Northrop Grumman Aerospace and Electronics Corporation	USA	MHD Stability Analysis
Oak Ridge National Laboratory (ORNL)	USA	Ion-Cyclotron Radio-Frequency Modeling Confinement Studies
Sandia National Laboratories (SNL)	USA	Plasma Facing Components
Savannah River Plant	USA	Tritium Gas Waste Reprocessing
Troitsk Institute of Innovative and Thermonuclear Research (TRINITI)	Russian Federation	Alpha Physics NOVA-K Code Analysis Disruptions MHD Stability
University of California at Irvine	USA	Fast Ion Transport
University of California at Los Angeles	USA	Deuterium-Tritium Neutron and Machine Activation Studies
University of Illinois at Urbana	USA	Tritium Retention Studies Modeling
University of Wisconsin at Madison	USA	Fluctuations, MHD, and Confinement Studies

Maintenance Activities

During the course of FY94, maintenance periods were provided to allow individuals and groups time to perform routine maintenance and repairs to their equipment. Some of these activities included inspections of TF coil shim blocks, coil bus connections, and supports; preventive maintenance tasks on a variety of TFTR components such as vacuum, water, neutral beams, and diagnostics; diagnostic shielding upgrades; and Lithium Pellet Injector (LPI) maintenance and wheel changes.

More than 100 line breaks were made ranging from simple breaks in systems that had very low likelihood for tritium to breaks made in the neutral-beam exhaust line that had very severe levels of contamination. In all of these line breaks, there has not been a single exposure of personnel to levels of tritium beyond the allowable limits. In fact, in almost all cases there has been no measurable exposure to personnel. There are presently three portable systems dedicated to performing line breaks. There are two carts that have well-identified components, with operator aids to help identify valves and components, and one cart that is for use by the most experienced technicians in hard-to-reach areas. This cart is a very simple arrangements of valves and fittings.

Vacuum Leak

During a high-power (7-8 MW) ICRF H-minority heating experiment in September, 1994, leaks developed in the TFTR vacuum vessel. The direct cause was the failure of vacuum welds at the joint between the organ pipes and port covers at the bottom of Bays S and K. Associated with the leak was the observation of an influx of manganese into the plasma. Manganese is a minor constituent of stainless steel but it has a fairly high vapor pressure and is readily released when stainless steel is heated. These influxes of manganese had been observed previously in association with radio-frequency (rf) heating under certain conditions. These observations support the idea that high-energy ripple-trapped ions caused the damage. It had been conjectured that ripple-trapped particles were responsible for the damage, since the welds are located far from the plasma and are shielded from direct plasma contact.

High-energy (hundreds of kilo-electron-volts) hydrogen ions in TFTR can drive a toroidicity-induced Alfvén eigenmode (TAE) mode unstable (see the section "TAE Modes and MHD Activity in TFTR D-T Plasmas" below). This mode is easily excited in TFTR during the H-minority ICRF heating used to condition the antennas. The TAE mode causes the ICRF-excited ions to drift radially in and out. If the ions drift into a region of sufficient TF ripple, they become ripple trapped and rapidly drift to the bottom of the vacuum vessel, as shown in Fig. 5.[1] As the ions drift downward, they are focused by the increasing depth of the magnetic well (increasing ripple). About 5% of the high-energy ions are ripple trapped, which can account for the observed melting.

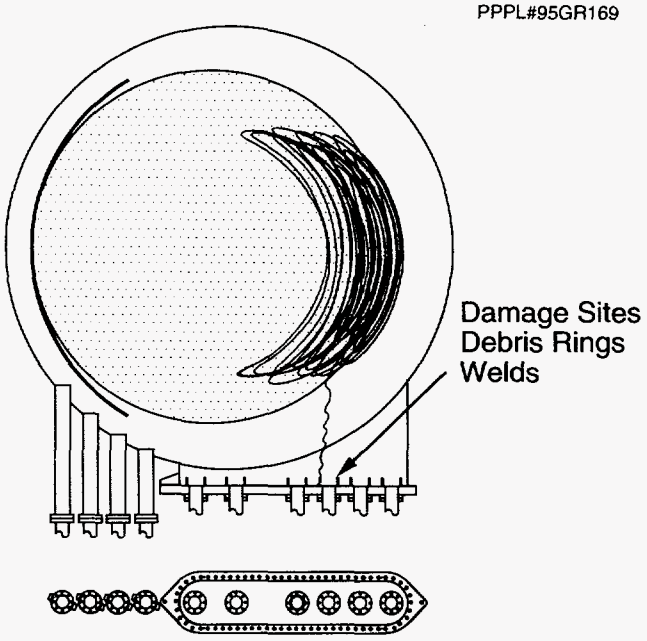

Figure 5. *Shown is the orbit of a single high-energy particle that has been driven by a toroidicity-induced Alfvén eigenmode (TAE) mode instability into the ripple-trapping region and drifted downward out of the plasma. Under certain conditions, a sufficient number of these particles struck the vacuum vessel causing the overheating that resulted in a vacuum weld failure.*

Implications for ITER have been examined. The TF ripple is sufficiently small in ITER, as presently configured, so that essentially no high-energy ions become ripple trapped. Also, the magnitude of the ripple in ITER is below the threshold for stochastic ripple loss, so that ions will not be lost by this mechanism.

During the Fall of 1994, TFTR operations were suspended for five weeks after the vacuum leaks occurred. These leaks were located in a confined-space area with radiation levels of 120 mrem per hour on

contact. An engineering task force was established to review the various repair options and to complete the necessary repairs while the vessel remained under vacuum.

The organ pipe assemblies were initially sealed using a radiation resistant epoxy which could withstand bakeout temperatures of 150 °C. A vacuum can shown in Fig. 6 was then installed around each organ pipe assembly, providing a secondary vacuum barrier between the vessel and the Test Cell atmosphere. Each can was provided with a differential pumping system to maintain this vacuum barrier. These vacuum leak repairs were successfully completed for seven organ pipe assemblies, five of which were modified as a preventive measure due to their high risk locations.

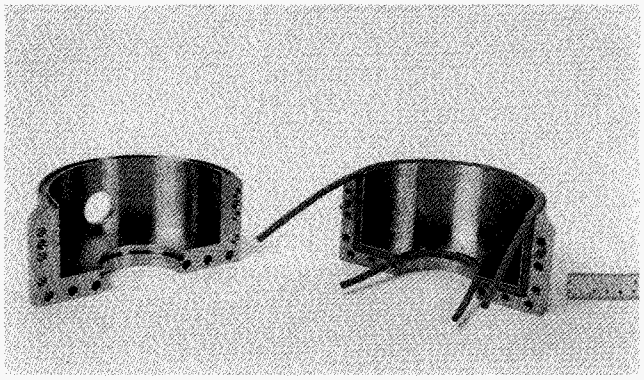

Figure 6. *A photo of the secondary vacuum barrier installed over a leaking weld joint between an organ pipe and a large vessel port cover. (94E0497)*

Conduct of Operations

In FY94, the Conduct of Operations procedure was fully implemented for TFTR to control the way the facility operates. This procedure covers issues ranging from oversight of tritium transfer operations to posting of operator aids. Shown schematically in Fig. 7, a centralized chain of command responsible for the proper implementation of scores of procedures was utilized to coordinate the activities of more that a dozen TFTR subsystems and support organizations. During this period, more than 400 tritium transfer operations, hundreds of line breaks, and approximately 2,000 TFTR and tritium area work permits were safely completed. This mode of operation was instrumental in bringing about the site-wide coordination necessary for the successful introduction of tritium into TFTR in December of 1993 and leading up to the high-power experiments later in the year. These

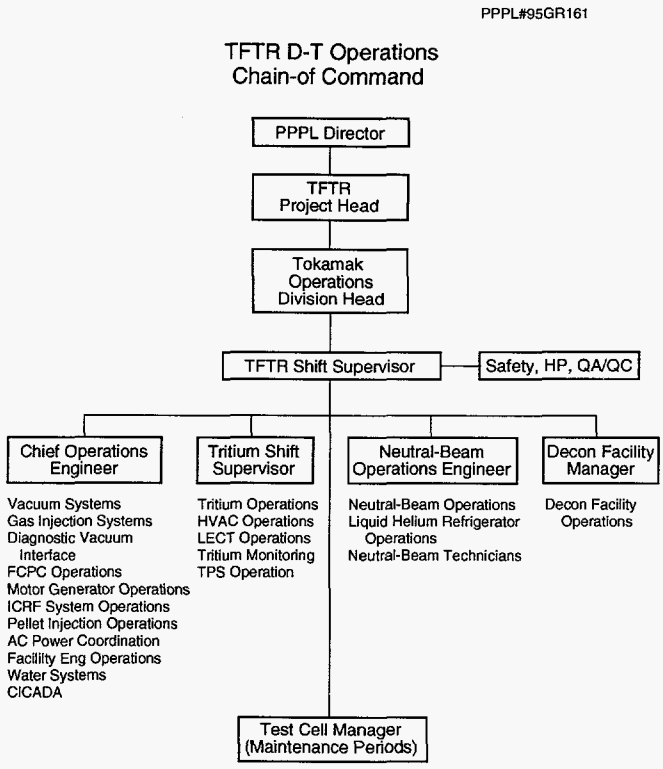

Figure 7. *The deuterium-tritium operations chain of command.*

achievements were accomplished while maintaining complete safety throughout the facility.

Six-Tesla Operation

Before this fiscal year began, the possibility had been recognized of extending operation of TFTR's TF coils to 85 kA (yielding 6 Tesla at R = 2.48 meters), which is beyond their 73-kA designed operating current. Possible benefits for D-T plasma operation had been projected. In preparation for raising the TF operating field level, all loose TF coil case bolts had been retightened during FY93.

Starting in October, 1993, four unused equilibrium-field (EF) power supplies were disconnected from the EF circuit and rewired into the TF circuit. The resulting increase of TF coil loop voltage from 10 kV to 12 kV was commissioned in April, 1994, and immediately allowed extending the TF flattop an additional second at 73 kA without increasing either peak TF coil hot-spot temperature or total energy withdrawn from the motor generator (MG) sets. The MG capability was reviewed and found consistent with raising pulsed operating levels from 950 MVA to 1,200 MVA in support of 6-Tesla operations. Mechanical and ther-

mal capabilities of the TF coils and their structural support systems were reviewed and found to be consistent with 6-Tesla operation without any explicit calculated reduction in the originally designed TFTR fatigue life.

ICRF Operations

The first experiments devoted to ICRF heating of a D-T plasma were conducted in February and March of 1994. These experiments measured the efficiency of heating a D-T supershot plasma via the second harmonic cyclotron resonance of the tritium ions. This heating scheme had been the one that was envisioned eight years before when the operation frequency of the ICRF system was specified. The tritium ion concentration was varied, as well as the magnetic-field strength, while 10-Hz amplitude modulated rf power was applied. The amplitude modulation allowed a detailed experimental determination of the heating profiles to be obtained. Next, ICRF power was used to investigate the TAE mode threshold in D-T plasmas. The threshold was observed to drop from approximately 5.2 MW to about 4 MW when the plasma was changed from D-D to D-T. Some of this effect has been ascribed to the additional alpha drive in D-T plasmas and some to a change in the stability threshold due to the change in ion composition. Finally, a series of experiments on electron heating and current drive was carried out. These included both direct electron heating and heating via the mode-converted ion-Bernstein wave. Direct centralized fast-wave current drive was performed at a frequency of 63.6 MHz with the plasma preheated with 43-MHz H-minority heating. A driven current of 70 kA was inferred from the change in loop voltage observed. A new, highly efficient, mode-conversion regime was demonstrated. This regime is highlighted by its strong single-pass damping which allows strong localized electron heating both on and off axis. Modulation experiments show strongly localized electron heating which can be positioned from r/a = 0 to r/a = 0.6. Ion cyclotron range of frequencies operation into D-T plasmas was achieved with a reliability of 88%.

To support the above experiments, several changes were made to the ICRF system. These changes were confined to the control systems and did not apply to the antennas or matching systems. A radial plasma position feedback system was completed and tested for supershot plasmas. This system adds a signal to the plasma radial position feedback circuitry that adjusts the plasma position to hold the antenna loading resistance constant. Antenna phase control circuitry was added that locked the phase between individual elements within an antenna and from antenna to antenna. This phase control is necessary to obtain the traveling wave spectrum required for the current-drive experiments. Multiple arc detection circuitry in conjunction with the phase control was perfected and played a role in the high reliability factor achieved for D-T operations. Finally, a novel circuit for arc detection based on sensing the second harmonic content of the antenna power was developed. When fully implemented, this should allow discrimination between high reflected power levels due to plasma effects and those due to arcing in the antenna or feed lines. This will prove extremely useful in future multi-element antennas.

Radiation and Activation

Neutronics and shielding efficiency measurements for TFTR were performed in collaboration with the University of California at Los Angeles (UCLA), the U.S. Department of Energy's (DOE) Environmental Measurement's Laboratory (EML), and the Los Alamos National Laboratory (LANL) during high-power D-T operations with record neutron yields.

Direct measurements were made of D-T neutron-induced radioactivity in many materials of interest to ITER in a realistic tokamak fusion reactor environment.[2] Neutron activation foil measurements were performed to characterize neutron spectra close to the plasma, near the outside vessel walls, and at the Test Cell inner walls. Measurements were made of streaming through diagnostic penetrations in the Test Cell shield walls to guide the development of fast ITER radiation shielding codes.[3]

Extensive measurements were made to characterize machine activation. Figure 8 shows machine activation peaking during D-T operations and decaying significantly during D-D operations and maintenance.

Deuterium-tritium shielding efficiency measurements of neutron and gamma dose-equivalents were performed at the inside and outside Test Cell walls, in nearby work areas, at the R = 125 m site boundary, and out to the nearest property lines at R = 180 m. At some locations, special neutron gamma spectral measurements were made. Figure 9 shows the radial dependence of the neutron and gamma dose-equivalents

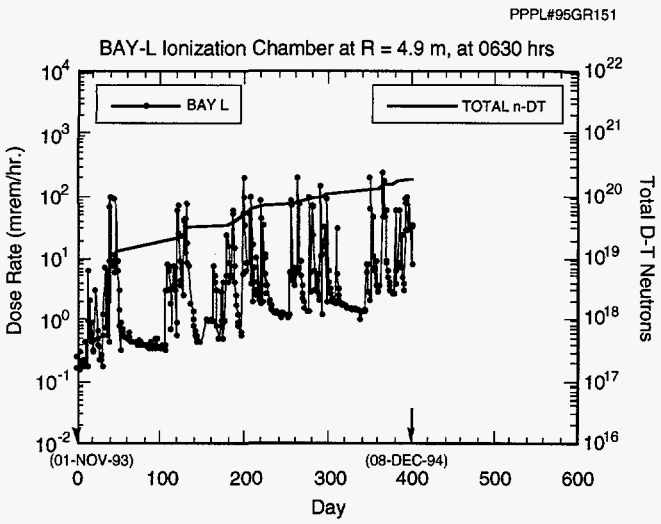

Figure 8. *The TFTR activation dose rate near base of vessel about one meter outboard of the outer vessel hardware. Midplane vessel contact dose rates inboard of the ionization chambers are of order ten greater.*

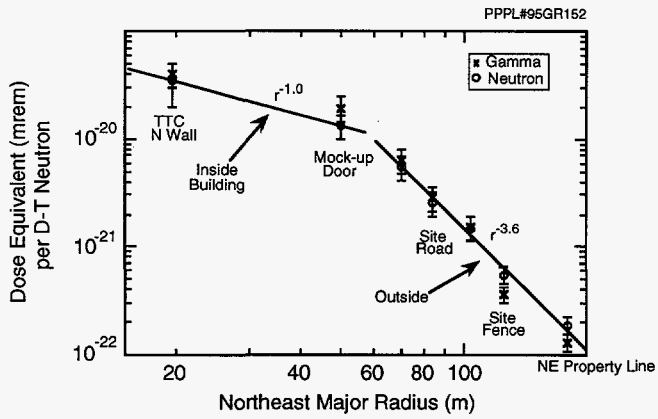

Figure 9. *Log-log plot of neutron and gamma dose-equivalent per TFTR deuterium-tritium neutron measured versus major radius (m) in the northeastward direction toward the nearest property line.*

per TFTR D-T neutron from the outer North Test Cell wall in the Mock-up Building out to the nearest northeastward property line at 180 m. Figure 10 shows the direct proportionality of the neutron radiation field to source neutron strength at the northeastward 125-m site fence and at the 180-m property line. The measured dose-equivalents per TFTR neutron were used to confirm that the expected neutron production in calendar year 1994 was consistent with the design objective of limiting the total dose-equivalent at the property line, from all sources and pathways, to less than 10 mrem per year.[4,5]

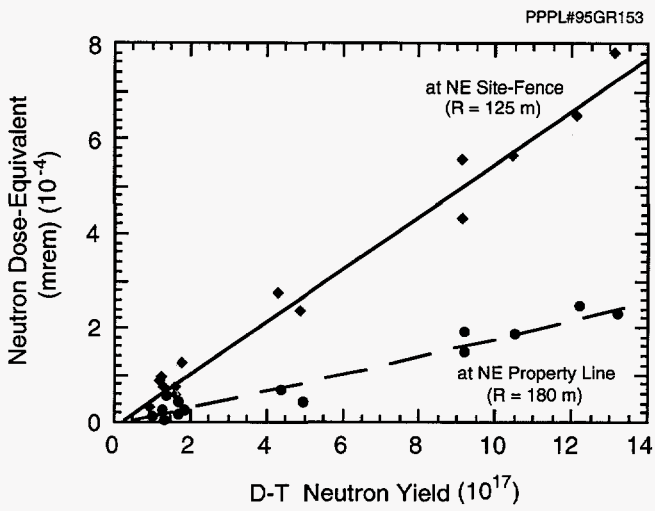

Figure 10. *Measured neutron dose-equivalent per TFTR deuterium-tritium neutron at the northeastward site fence (R = 125 m) and at the property line (R = 180 m). The measured dose-equivalents are directly proportional to neutron source strength.*

Table II summarizes the contributions to the annual dose-equivalent at the northeastward property line from all sources and pathways. It is seen that the dominant contribution is due to activated air and natural tritium losses. The activated air and tritium transport to the property line were conservatively estimated using a regulatory-mandated semi-gaussian plume model. The relatively low measured northeastward property line annual dose-equivalent accrued from the effectiveness of the Test Cell north supplementary shielding, the empirically discovered decrease in D-T to D-D dose-equivalent ratio with distance,[5] and the reduced TFTR experimental schedule. These results demonstrate that the TFTR radiation shielding efficiency is qualified for extended D-T operations, with yields exceeding 3×10^{21} D-T neutrons per year.

Tritium Retention

Tritium used in the D-T experiments in TFTR is supplied to the plasma primarily by neutral-beam injection (NBI). A much smaller amount (less than 1%) was supplied by gas puffing in separate experiments. Therefore, the issue of tritium retention in TFTR deals primarily with tritium consumed by the neutral beams. Most of this tritium (approximately 95%) is trapped on the neutral-beam cryopanels and subsequently sent to the gas-holding tanks for processing. Of the remaining 5%, about half is injected into the plasma and half is deposited on the beam dumps. The

Table II. Summary of Contributions to the Maximum Annual Dose-Equivalent during Deuterium-Tritium (D-T) Operations at Nearest Northeast Property Line from All Sources and Pathways.

Radiation Path	mrem/Neutron	Total CY93	Total CY94
D-D Neutron Yield		$7.0 \pm 0.7 \times 10^{18}$	
D-T Neutron Yield		$1.65 \pm 0.1 \times 10^{19}$	$\sim 1.9 \times 10^{20}$
Direct Neutrons from D-D Neutrons	$<1.5 \times 10^{-22}$	$<1.1 \pm 0.1 \times 10^{-3}$	
Direct Gammas from D-D Neutrons	$<4.1 \pm 2.7 \times 10^{-22}$	$3.0 \pm 1.9 \times 10^{-3}$	
Direct Neutrons from D-T Neutrons	$1.9 \pm 0.4 \times 10^{-22}$	$3.1 \pm 0.7 \times 10^{-3}$	3.6×10^{-2}
Direct Gammas from D-T Neutrons	$1.3 \pm 0.2 \times 10^{-22}$	$2.1 \pm 0.3 \times 10^{-3}$	2.5×10^{-2}
Estimated Air Activated by D-D Neutrons	3.4×10^{-22}	2.4×10^{-3}	
Estimated Air Activated by D-T Neutrons	7.3×10^{-22}	1.2×10^{-2}	1.4×10^{-1}
Liquid Nitrogen Activated by D-T Neutrons	2.0×10^{-23}	3.3×10^{-4}	3.8×10^{-3}
Normal Tritium Loss	2.6×10^{-3} mrem/Ci		
Calendar Year 1993	<50 Ci	<0.13	
Calendar Year 1994	<140 Ci		<0.36
Annual Property Line Dose-Equivalent		<0.15	<0.56

internal beamline surface (total area about 1,000 m^2) including beam dumps is expected to retain about 200 Ci per beamline. A fraction of the tritium injected into the plasma as energetic tritons is co-deposited with graphite in regions of net deposition on the graphite limiters. The total amount of tritium injected into TFTR by NBI up to December 30, 1994, is 2.4×10^{23} tritons or 11,500 Ci. Past measurements of deuterium retention on TFTR indicate that the amount of deuterium retained in the graphite limiters and the walls of TFTR is 20-60% of the total amount of deuterium injected by neutral beams. If tritium is retained in the same fraction as deuterium (approximately 50%), it is expected that 5,750 Ci will be retained in the limiter and walls of TFTR and 800 Ci in the neutral-beam lines. The expected total of 6,550 Ci is to be compared with the approximate 11,000 Ci retained tritium found by subtracting the total amount of tritium processed through the gas-holding tanks from the tritium delivered and consumed by TFTR (approximately 300,000 Ci). This is to be compared to the regulatory limit of 20,000 Ci retained tritium.

Operations with Tritium Neutral Beams

The major portion of the power to heat the TFTR plasma is supplied by the neutral-beam-injection system.[6] After commencing injection in 1984, the neutral-beam system has primarily produced deuterium beams for injection into deuterium tokamak plasmas, although some hydrogen (protium) operation was also carried out during the early life of the system. Over the ensuing years, the beam system matured,[7] regularly injecting at neutral-particle power levels in excess of 25 MW and reaching a peak of more than 33 MW by 1993.

At the same time, progress on the tokamak was changing the role envisioned for the neutral beams during the final deuterium-tritium (D-T) phase of TFTR operations. The TFTR neutral-beam systems were originally planned with the intent that they would not be used to produce tritium beams and, in fact, the initial design included large focal plane shutter valves to sharply limit the flow of tritium from the tokamak into the beamlines. The final phase of TFTR operation was originally intended to consist of operation with a plasma mixture of roughly 50:50 deuterium and tritium to produce a high fusion power yield (10 MW). However, it was believed that this optimum mix of deuterium and tritium could be maintained by controlling the ratio of isotopes fed into the tokamak vacuum vessel through gas puff valves. This was a reasonable assumption at the time in light of the short beam-pulse capability (0.5 sec) specified for the initial ion sources and, more importantly, the high edge-recycling plasma regime (now known as Low-confinement mode[8] or L-mode) that was ubiquitous in the 1970s. This regime is characterized by broad density profiles and high rates of gas reflux at the plasma periphery.

More recently, operation in the supershot mode[9] has shown energy confinement improvements over the L-mode of factors of two and more and has yielded substantially higher fusion reactivities than could be achieved with L-mode discharges. Supershots can be achieved when neutral beams are used to heat and fuel low-density target plasmas in which the edge recycling is strongly reduced by conditioning the tokamak limiters to reduce the accessible gas in the surface region. Supershots typically have high electron temperatures (10-12 keV), very high ion temperatures (20-40 keV), and strongly peaked density profiles (peak electron density/average electron density of roughly 2.5-3). The fusion reactivity is even more strongly peaked in the supershot core, where the beam-supplied particles maintain the peaked density.

Since many of the thermal particles in the strongly reacting core of a supershot (as well as, of course, all of the slowing-down beam particles) come from the injected beams, the composition of the neutral beams became crucial once it was apparent that the supershot regime offered the route of highest fusion power yields in TFTR. In order to maintain the optimum isotope mix in the core, it would be necessary to have at least half of the twelve ion sources operating with tritium feedstock. This became even more important with the decision to replace the original half-second ion sources with long-pulse ion sources (capable of 30 sec operation, but limited by the power-handling capability of beamline components to pulses of a few seconds). Although global particle confinement times are typically significantly shorter than 0.5 sec, the core density usually grows during a supershot, so for pulses of extended length it is potentially even more important to be able to use tritium in the beams.

An extensive set of experiments was carried out to study possible operating scenarios with tritium[10] and the effects of tritium upon ion source insulators and breakdown effects in gas feed lines,[11] as well as a study of the gas flow at the source-neutralizer interface.[12] In addition, a new feedback-controlled tritium-hardened beamline gas feed system[13] was built to efficiently utilize the relatively small quantities of tritium (about 18-22 kilocuries) that would be available for use in a given batch.

Tritium Neutral-Beam Operations

Tritium operations began in November of 1993 with a set of experiments using trace quantities of tritium in the neutral beams. The ion sources were run on a premixed feedstock of roughly 2% tritium and 98% deuterium. This permitted the full TFTR tritium system and the beamline tritium valves to be exercised while using relatively small amounts of tritium, and it permitted the tokamak's diagnostics to be checked in the presence of a moderate flux of the 14-MeV neutrons resulting from deuterium-tritium fusion reactions.

After successfully completing the trace tritium experiments, which entailed firing some dozens of trace-tritium shots into the plasma, full deuterium-tritium operation commenced in December of 1994. In this phase, each source is fired into the plasma with a feedstock of either pure deuterium or nominally pure tritium. Thus, the total injected beam isotopic composition in the plasma core is determined by how many of the twelve ion sources are run on tritium and how many on deuterium. The isotopic balance is controlled in this manner because the neutral beamlines potentially could be damaged by running the ion sources on arbitrary mixtures of deuterium and tritium. This is because a significant portion of the accelerated positive ion beam remains unneutralized after emerging from the gas neutralizer cell. These residual ions are magnetically deflected out of the neutral beam onto water-cooled ion dumps. These dumps are designed to accommodate the three momentum components normally present in single isotope beams resulting from the accelerated atomic ions and breakup products arising in the neutralizer from accelerated diatomic and triatomic ions. When two isotopes are used at the same time, additional components occur. In the case of trace tritium, some of the unneutralized residual tritium ions are under deflected, missing the dumps and hitting other beamline components. At low concentrations, the power density in the misdirected ions is insufficient to cause damage, but with higher admixtures melting could result. In practice, the stepwise quantization in the core plasma isotope mix that results from running with only one isotope at a time in any given source has not proved to be a significant limitation in conducting experiments.

A more severe constraint results from the low on-site inventory of tritium allowed for TFTR [50 kilocuries (kCi) for the site and a maximum of 25 kCi in any system]. Of this, the amount that is actually usable by the neutral beams for multisource tritium shots during a one-to-five day experimental run period is typically 18 kCi or a little more. Each of the twelve ion sources uses roughly 100 Ci in establishing a stable tritium plasma suitable for ion extraction. Additionally, each source then uses approximately 100 Ci per second of beam extraction Thus, for an experiment using one-second-beam pulses, each source shot uses about 200 Ci. Accordingly, a usable allotment of 18 kCi means that around 90 tritium source shots are available in a few-day period. For high fusion-power shots with six of the twelve ion sources operating with tritium, this translates into about 15 tokamak plasma discharges.

During deuterium operation, the ion sources and the beam extraction and acceleration grids are conditioned and then maintained at their chosen operating voltage by firing a beam pulse every 2.5 minutes. This is usually either a full-length pulse into a retractable beamline calorimeter or, in the case of well-conditioned ion sources, a 50-msec beam pulse into the tokamak wall armor (extracted from a full-length arc pulse). With only of order 90 source shots available from a tritium batch, it is clear that conditioning sources with tritium-beam pulses prior to injecting with them into tokamak plasmas would result in virtually all the tritium being consumed by the conditioning pulses and, thus, almost no useful shots into the tokamak. Accordingly, all source conditioning pulses are fired with deuterium feedstock, as are preparation shots for tritium-beam injection. Just prior to a tritium shot, the acceleration voltage is increased by a few percent to partially compensate for the fact that the optimum perveance for minimum beam divergence in these Pierce-focused grids is lower for tritium than for deuterium. The tritium is pulsed through a system which is completely separate from the one for deuterium to avoid cross-contamination. After the tritium-injection shot, the acceleration voltage is reduced to its earlier value, and the source is returned to deuterium conditioning (50-msec beam pulses into the tokamak armor) and deuterium-beam injection until the next tritium shot is required.

This tritium operating scenario has proven to work well. The reliability of the ion sources on tritium-injection shots has tended to be somewhat better than for the corresponding deuterium shots, except for some cases in which the gas valves in the tritium supply manifold malfunctioned. The improved source reliability is probability due to the fact that the current density at near-optimum perveance in tritium is lower than for deuterium. Analysis of the Doppler-shifted spectrum of the beams indicates that the isotopic changeover in the source is quite efficient, with a residual deuterium impurity of roughly 2% in the tritium beams, and less than 0.5% tritium (the estimated measurement limit) in the deuterium beams.[14] The contamination of the deuterium is lower because the source undergoes several (and often many) deuterium conditioning pulses before a deuterium tokamak injection pulse is fired, whereas a tritium-injection pulse is always preceded by deuterium conditioning pulses.

Figure 11 shows a spectrum of a tritium shot with the accompanying minority components due to deuterium. In addition, the tritium shots tend to have minor amounts of other contaminants (protium and He^3 at the fractional percent level) that come in the tritium as supplied.

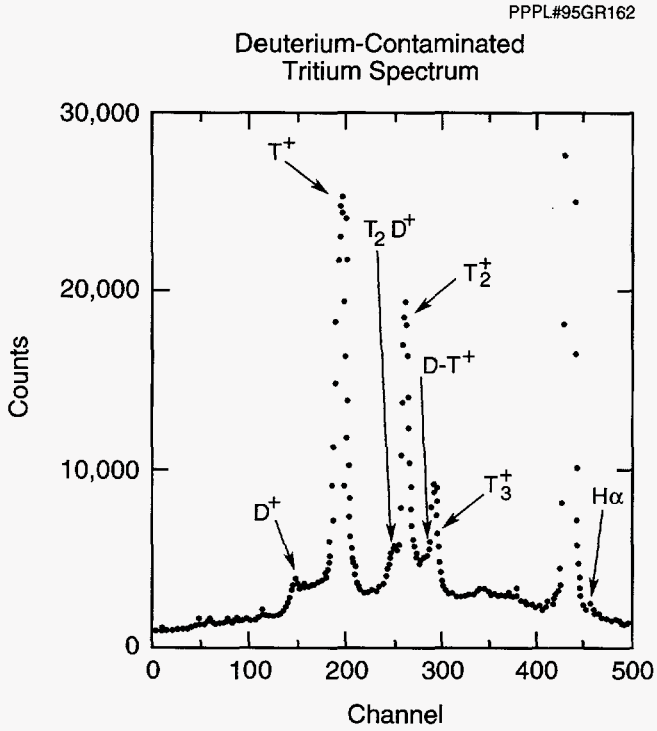

Figure 11. *Doppler-shifted spectrum of the atomic and molecular components in the beam extracted from a TFTR ion source. This is a tritium shot with minority deuterium contamination arising from preceeding deuterim conditioning shots. The extracted beam is 73% T^+, 22% T_2^+, 4% T_3^+, 1.3% D^+, 0.4% D-T^+, and less than 0.1% T_2D^+.*

Doppler-shift spectroscopy measurements indicate that tritium and deuterium yield similar mixtures of the extracted atomic and molecular ions. For deuterium the extracted ion fractions are approximately 0.72±0.04 D^+, 0.22±0.02 D_2^+, and 0.06±0.01 D_3^+, essentially the same as the 0.72±0.04 T^+, 0.23±0.02 T_2^+, and 0.05±0.01 T_3^+ for tritium.[14] The molecular components in either case dissociate in the neutralizer gas cell into particles with one-half and one-third of the acceleration energy. Since, at a given acceleration voltage, the tritium velocity is lower, and thus the equilibrium neutralization efficiency is higher, than is the case for deuterium, a larger fraction of the tritium beam is neutralized for injection into the tokamak than with deuterium. With an acceleration voltage in the 95-120 keV range, this difference is much more pronounced for the faster atomic component than for the slower molecular breakup fragments. Thus, the neutral-tritium beam delivered to the tokamak carries a somewhat larger fraction of its power in the full-energy component than does a deuterium beam at the same acceleration voltage. For instance, at an acceleration energy of 100 kV, the neutral-beam-power fractions for the full, one-half, and one-third energy components are 0.68/0.26/0.06, respectively, for tritium as compared to 0.64/0.28/0.08, respectively, for deuterium. During most of the TFTR neutral-beam-injection experiments, the tritium neutral-beam power per source has been about 10% higher than for deuterium due to the higher neutralization efficiency, the somewhat overdense operation at higher than optimum perveance in tritium, and the higher acceleration voltage used to obtain partial perveance match.

In the initial years of TFTR neutral-beam operation, the beam feedstock gas was all introduced into the ion source, where a portion of it was ionized, while the rest flowed through the acceleration grids into a conductance-limiting duct that forms the neutralizer. After several years, an additional gas feed point was added midway down the neutralizer so that deuterium could be added to ensure that the beam was never under neutralized. The gas feed to the source consisted of a length of insulating plastic tubing which crossed a sulfur hexafluoride (SF_6)-filled source enclosure (the ion source is run at the acceleration potential of up to 120 kV so that the neutralizer can be run at ground potential with the rest of the beamline). Any leak of the tubing or its couplings would result in a mixture of SF_6 and tritium, which was thought to be a particularly onerous mixture to process in the tritium cleanup system. In order to produce a more robust tritium feed path, the primary gas feed point was moved from the ion source to a point in the neutralizer just downstream of the ion source ground (exit) grid, and the mid-neutralizer gas feed was eliminated altogether. In addition to avoiding the SF_6, feeding the tritium at ground potential had the advantage that the entire feed path could be composed of rigid double-jacketed stainless steel tubing with very little chance of leakage to air. The ground feed just downstream of the grids requires about 15% more tritium throughput to maintain source operability than if all the gas were supplied directly to the source arc chamber, but it requires less than if the mid-neutralizer feed were still in use as well.

A relatively small portion of the tritium fed into the neutral beamlines is actually injected into the tokamak plasma. During the injection pulse, about 10% of the tritium enters the plasma as beam, and a much smaller fraction (of order 0.5-1%) enters as cold gas during the beam and one-second prebeam phase. Thus, the great majority (>95%) of the tritium accumulates immediately on the neutral-beam cryocondensation pumps along with whatever tritium subsequently comes back from the tokamak. Every few days these liquid-helium-cooled panels are warmed up to drive off the frozen tritium, along with a much greater quantity of deuterium, so that the gas can be pumped away by turbopumps to the tritium processing system.[15]

Tritium Neutral-Beam Operation Experience

Over the course of the months since tritium-beam operations commenced, these operations have come to be routine in essentially every regard, notable perhaps both for what has happened as well as what has not happened. Hundreds of tritium source shots have been fired into tokamak plasma discharges and every one of the 12 source positions has been used. A maximum of eight sources have fired tritium beams at the same time. A maximum of 24.3 MW of neutral tritium was injected with seven sources, while the maximum injected power with combined deuterium and tritium beams was 39.6 MW. On the other hand, there have been no significant leaks of tritium from the neutral beams or their gas system to air and only small (one to a few curies) controlled stack releases when sources were removed. Swab tests on the epoxy insulators of the ion source accelerators indicate that there has been no detectable permeation through them. There have been a number of ion source problems unrelated to tritium operation which required sources to be removed and replaced or removed and modified. More than a dozen source removal operations have been performed without incident after repeated pump and purge cycles reduced the level of tritium remaining adsorbed on source surfaces. Experience has shown that very little tritium is removed if dry nitrogen is employed as the purge gas, but that ordinary (moist) air rapidly removes it. Typically, about a curie is removed from a source in this manner before it is disconnected from a beamline. There have also been a number of repairs made to the tritium feed valves which entailed opening the gas system to air, and these have also become routine. Thus, a large neutral-beam system is not only operating over an extended period with tritium, but doing so in a routine day-in, day-out manner as part of a nuclear facility.

Post-Tritium Neutral-Beam Operations

After the completion of tritium operations on TFTR, the tokamak is to be shutdown to make way for the Tokamak Physics Experiment (TPX), a tokamak with superconducting coils to study advanced modes of operation for reactors. The beamlines will be decontaminated. This will be carried out largely through pump and purge cycles with moist air to remove absorbed tritium and by operations with deuterium beams to drive out most of the implanted tritium. Afterwards, at least one beamline and its power supplies will be modified to allow 1000-second pulses on the TPX.

Tritium Processing and Management during D-T Experiments

Stable operations of tritium systems provide for safe, routine D-T operation of TFTR. In the preparation for D-T operation, in the commissioning of the tritium systems, and in the operation of the "Nuclear Facility" several key lessons have been learned. They include: the facility must take the lead in interpreting the applicable regulations and orders and then seek regulator approval; the use of ultrahigh vacuum technology in tritium system design and construction simplifies and enhances operations and maintenance; and central facility control under a single supervisory position is crucial to safely orchestrate operational and maintenance activities.

The TFTR tritium systems have had a challenging history.[16] Designed in the 70s and installed in the early 80s, the systems do not have the benefit of ultrahigh vacuum or tritium equipment that has been developed and marketed in the intervening years. The tritium system was initially commissioned with deuterium in 1993 and final commissioning with tritium in late 1993 and early 1994. In this section, the systems are described briefly and the problems and les-

sons learned associated with preparation for achieving Nuclear Facility status and for commissioning and maintenance of the systems are discussed.

Tritium Systems Configuration

Figure 12 schematically shows the fueling path for the TFTR tritium systems. In a typical shipment, 10 to 20 kCi of tritium is delivered to TFTR in an a container, called an LP-50, specifically approved for its use by the U.S. Department of Transportation. With a nominal volume of 50 liters, the product container, with approximately 100 Torr of tritium gas, is loaded into the Tritium Receiving and Analytical Glove Box (TRAGB), which is a part of the Tritium Storage and Delivery System (TSDS). The tritium is transferred to one of three uranium gutter beds (U-bed) for storage. Once tritium is requested, the U-bed to be used is heated, driving off the tritium. The tritium is sent to a calibrated volume where the temperature and pressure of the gas is measured and inventoried (PVT measurement for pressure, volume, and temperature, which is related to the number of tritium molecules by the Ideal Gas Law). The gas may be analyzed for purity at this point by a quadrupole mass spectrometer (QMS).

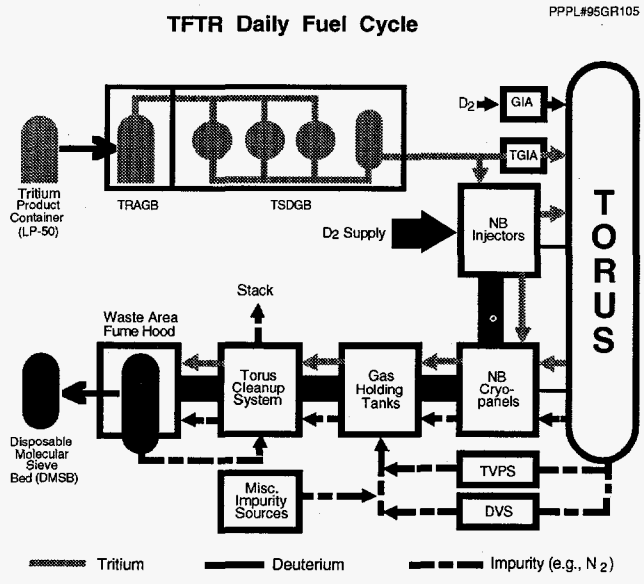

Figure 12. *The TFTR daily fuel cycle. The flow of hydrogenic species through TFTR. The line widths are related to the relative amount of hydrogenic gas moved between systems. As can be seen, much more deuterium is supplied to the neutral beams than tritium. Of all of the gas delivered to the neutral-beam injectors, less than 5% is injected. See text for explanation and key to acronyms.*

The tritium gas is then delivered to the Tritium Gas Delivery Manifold (TGDM). This supply line is coaxial in construction with the inner conductor comprised of a capillary line with a 1.6-mm inner diameter. The outer, secondary containment is 13-mm tubing and is under vacuum. An ion gauge and a QMS monitors this vacuum and delivery of tritium is inhibited if vacuum is lost or if mass 6 (T_2) components are observed. The small inner diameter is employed to minimize the tritium inventory in this 120-m line. The tritium is supplied by the TGDM to the Tritium Gas Injection Assemblies (TGIAs) and the Neutral-Beam Tritium Gas Injectors (NBTGIs), Fig. 13.

The two TGIAs provide direct injection of tritium gas into the torus. These have been used for transport studies but are rarely used for fueling plasma discharges (shots).

The primary method for fueling TFTR plasma discharges is by the neutral-beam injectors (NBI). For a typical D-T plasma discharge, six of the twelve ion sources are fueled with tritium and the other six are fueled with deuterium. The tritium inventory in the sources prior to the shot is approximately 5-6 kCi. The gas is injected into the ion source, where a fraction is accelerated and a larger fraction enters the neutral-beam line and acts to neutralize about one-half of the accelerated beam. The neutral-beam line enclosures contain boiling liquid-helium-cooled cryopanels that pump more than 95% of the gas injected into the ion source. This means that less than 5% of the gas delivered to the source for a shot is actually injected into a plasma discharge. Subsequent to the shot, the cryopanels pump the gas particles from the discharge along with any impurities that were generated. During the time between shots, the ion sources are conditioned every 2.5 minutes using pulses of deuterium gas, which is also collected on the cryopanels. Because of this extensive conditioning, the fraction of the total gas that is injected into the beamline is only about 1% tritium.

Once operation of the machine is complete for the day, the neutral-beam cryopanels are regenerated by warming them up to a temperature where the hydrogenic species are evaporated and pumped into the Gas Holding Tanks (GHTs) in the tritium area.

Gas from the torus is directly pumped to the GHTs through the Torus Vacuum Pumping System (TVPS). This system is only used during nonoperational periods, being valved off during plasma discharge operations and, hence, a very small fraction (approximately

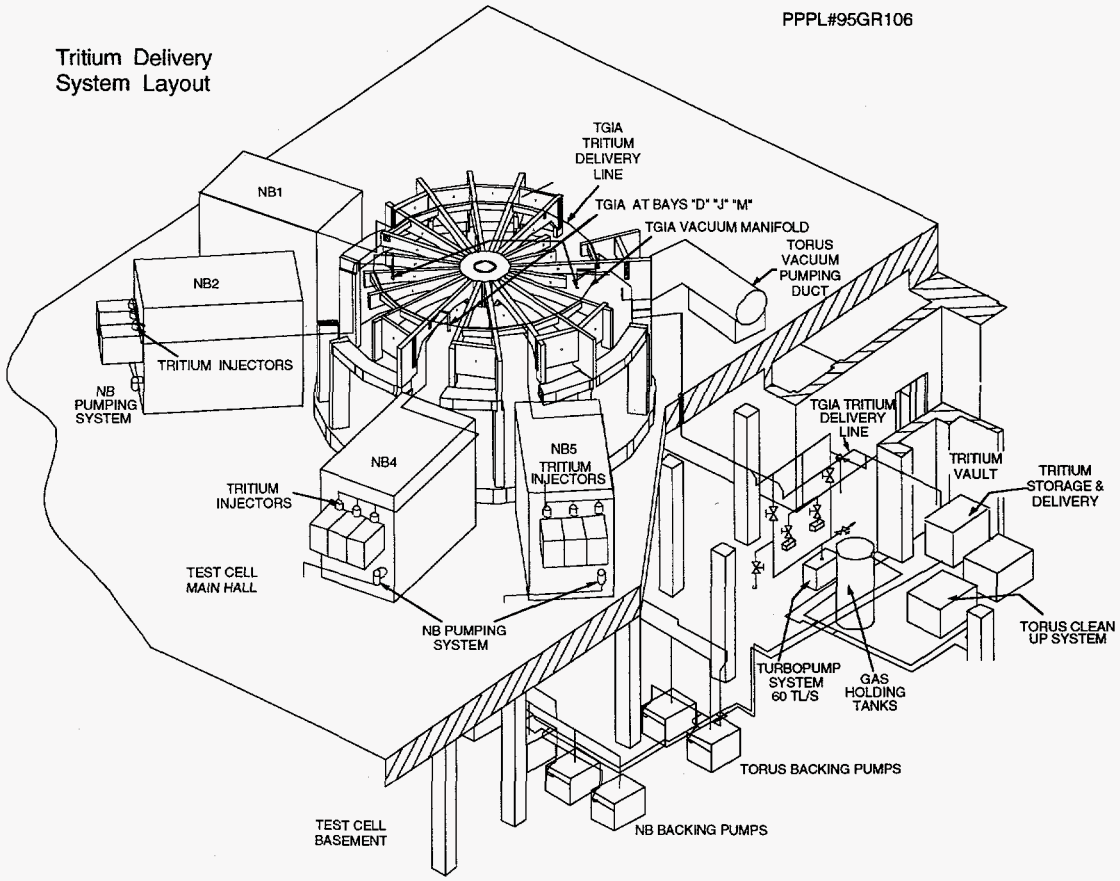

Figure 13. *Projection view of the TFTR tritium systems. The Tritium Storage and Delivery System (TSDS) is located in the basement in the Tritium Vault. A coaxial line carries the tritium to the two Tritium Gas Injector Assemblies (TGIAs) for direct injection into the torus and to the 12 ion sources, three on each neutral beam. For a typical D-T plasma discharge approximately 5 kCi of tritium is loaded into six of the neutral-beam injectors and the remaining six are charged with deuterium.*

1%) of the gas from the torus, primarily outgassing, is transported to the holding tanks via the TVPS. Another channel to the GHTs is through the several diagnostic devices that are open to the torus during plasma discharge operation. The aggregate gas load from these Diagnostic Vacuum Systems (DVS) is small (less than 1%) due to the limited conductance of these systems to the torus.

The gas in the GHTs is composed of the regenerated fueling gas (99% deuterium, 1% tritium) and assorted other impurity gas such as nitrogen (from purging) and hydrocarbons generated in the tokamak. The gases are pumped into the process stream, 4% gas from the GHTs into the working gas (nitrogen), of the Torus Cleanup System (TCS). The process gas is pumped over a catalyst, which oxidizes the active components, forming moisture. The process stream is then passed through Disposable Molecular Sieve Beds (DMSBs). The moisture, containing the tritium oxide is deposited on the DMSB. The gas is passed over a second DMSB and through a large fixed molecular sieve bed. This ensures that only a small fraction of the original tritium remains in the process stream (less than 0.1%.) A small amount of the detritiated process gas is then vented to the stack. The process gas is then returned to the start of the TCS loop.

There are two types of DMSBs: Type A, which is used to bury the tritium waste, has a limit of 1 kCi of tritium and 3.6 kg of water. Type B, which is used to store the tritium until it is removed and reprocessed at the Savannah River Site, has a limit of 25 kCi of tritium and 3.2 kg of water.

To date, approximately 200 kCi of tritium has been received, of which approximately 134 kCi has been shipped off-site (32 kCi as elemental and 102 kCi as oxide). The total amount of tritium delivered into the machine has been about 107 kCi, and approximately 120 kCi has been processed into oxide.

Maintenance of Tritium Systems

During commissioning, a number of tritium leaks were detected. The leaks tended to be difficult to locate (especially oxide leaks) due to contamination of nearby surfaces, giving false positive indication by hand-held ion chambers. This was abated somewhat by starving the cleanup systems of oxygen, thereby minimizing oxide formation and exposure of personnel to oxide. Most external leaks were found to be in gaskets: elastomeric gaskets permeating tritium and metal gaskets leaking due to improper installation or thermal cycling. Some valve throughput leaks were observed. Such leaks do not present a direct threat to exposure of personnel, but they are considered serious because areas of the system cannot be isolated, giving false indications of leaks or preventing isolation of parts of the system required for maintenance.

During the commissioning phase, the design of the tritium systems led to extreme difficulty in performing corrective and periodic maintenance because of insufficient purge paths and lack of properly implemented joining techniques (ultrahigh vacuum flanges). Parts of the system that were found to be defective were repaired and upgraded to facilitate pumping and purging of the systems and components were replaced with more tritium-compatible equipment. Similar results were experienced during subsequent periodic and corrective maintenance of the systems.

Whenever the tritium envelope is opened (a line break), reduction of the tritium concentration is achieved by purging with dry inert gas and followed, typically, with a room air (moist) purge to reduce the surface contamination of tritium oxide. It has been found that systems that are easily and quickly maintained greatly reduce complications (exposure, releases) during line breaks. Ready accessibility (in a glove box or in the open) of components and providing numerous purge paths are key to rapid and efficient maintenance. It is important to realize that speed and efficiency is central to reducing exposure to tritium.

Segregation of low-tritium-concentration streams from high-concentration streams greatly reduces the requirements for purging and high-tech components in the low-concentration streams. Again this efficiency manifests itself in reduced exposure time and therefore in reduced dose.

Another finding was that the rooms exposed to systems leaking tritium (HTO) developed surface contamination (approximately 1,000-10,000 disintegrations per minute/100 cm^2) that cleaned-up (about a day) with good room air exchange. This result enhances operation since it reduces exposure and eliminates the need for protective clothing after a brief time period.

Tritium Inventory

Tritium inventory was recognized early on as a critical task in the overall management of the tritium process. Tritium inventory and accountability methods are mandated by Department of Energy Order 5633.3 therefore a series of procedures and a Material Control and Accountability (MC&A) Plan were developed. This Plan called for the daily resolution of all transactions (movements) of tritium from one location to another. This self-imposed requirement far exceeded the frequency requirements of the Order. It was recognized, however, that given the small quantities of tritium in use and the large throughput (10% of the site inventory is installed in the injection planums prior to a shot), as well as the 25-kCi limit in any one location, a careful accounting would be required to keep track of events as they happened.

In addition to the accountability issues and the design basis limit, an important research issue required careful tritium accounting. The amount of tritium retained by the tokamak and its ancillary systems has been studied and estimated for several years, both as a general research issue for fusion reactors but also in particular for TFTR given its very low-inventory limits. Measurement of the amount of tritium trapped in the tokamak system was recognized as difficult, given that is it determined by inventory. By carefully measuring the tritium injected into the neutral beams and the torus (a PVT measurement) and subtracting similarly careful measurements of tritium returned to the GHTs (by sampling the activity and measuring it with one of two parallel plate ionization chambers), a small difference is expected and is a measure of what is retained by the tokamak (primarily in the torus in a co-deposited layer.) Any error in these measurements would lead to large errors in the vessel inventory account.

After several weeks of D-T operation (with a hiatus for completion of the shakedown repairs), a discrepancy was detected by a divergence in account balance sheets and delivery versus shipment balance. It was recognized that on-site inventory was growing relative to the amount calculated by merely subtract-

ing shipments off-site from deliveries on-site. This coupled with the fact that the in-vessel inventory was growing negative (more tritium was measured leaving the vessel than was injected) implicated the parallel plate ionization chamber as systematically reading too high. This systematic error would explain the negative balance growing in the torus account and also explain the growing on-site inventory. By over reporting the amount of tritium in the Disposable Molecular Sieve Beds, more tritium was being kept on-site than was expected. A physical inventory of the tritium was performed and an *in-situ* calibration of the flat plate ion chambers were performed.

The major finding of the calibration of the parallel plate ion chambers was that, although they were linear over the tritium concentration range covered at TFTR, the factory calibration was incorrect and they were systematically reading 30% too high (see Fig. 14). Using the new calibration numbers, the discrepancy disappeared and, together with the physical inventory, the accounts were balanced. However, there is still sufficient measurement uncertainty so that definitive conclusions cannot be drawn about tritium retention in the vessel.

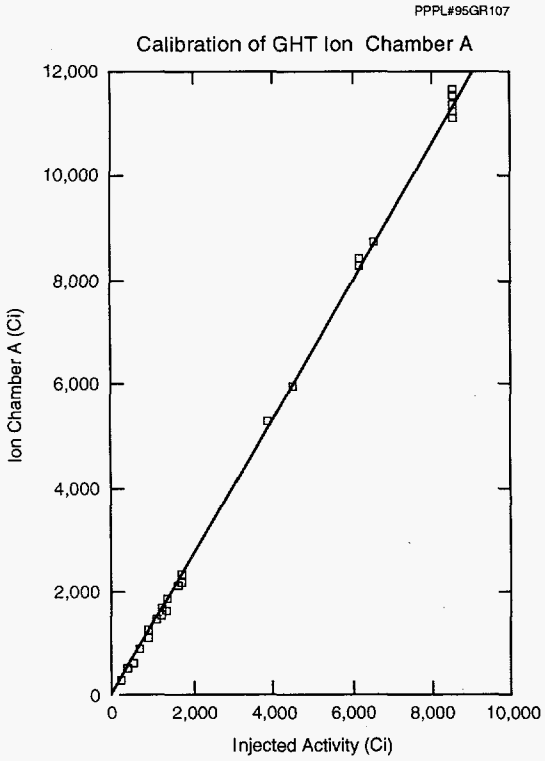

Figure 14. *Gas holding tank (GHT) ionization chamber in-process calibration. Data indicate a large systmatic error (30%), but it is highly linear with low random error.*

Several improvements to the process of inventory control and accounting were subsequently made: the role of Nuclear Material Custodian (NMC), the person who tracks and is responsible for tritium movement, was shifted to the TFTR Shift Supervisor; strict adherence to daily tritium accounting is enforced; and a comparison of the ion chamber measurements are made on a daily basis to ensure that a large systematic error will not reoccur.

It was learned that low-inventory limits and high-tritium throughput require a high level of (quasi-real-time) tracking. It was also learned that the Nuclear Material Custodian must have sufficient authority to halt operation when required, especially in support of the daily record keeping. Another important lesson was the realization that in-process calibration of primary inventory instrumentation is required to assure accurate measurement.

Alpha-Particle Measurements

In preparation for the TFTR D-T phase, diagnostics were added and modified to detect alpha particles—both those which are confined within the core of plasma, as well as those which escape at the plasma edge. This section summarizes the first alpha-particle measurements.

Lost Alpha Probe Measurements of Lost Alphas

The lost alpha probes, which previously were extensively used to study fusion product losses in deuterium-only plasmas,[17] played an important role in many of the D-T experiments. These scintillator probes, located at 90°, 60°, 45°, and 20° below the outer midplane, were extensively modified for D-T operation.[18] Light produced when fusion products escaping the plasma strike the scintillators is imaged onto fiber optics which carry it to detectors located in the Test Cell Basement. A schematic of the detector system is shown in Fig. 15. One of the more satisfying features of the previous probe studies of D-D fusion product loss was the agreement with models of first-orbit loss, which predict large loss fractions at low plasma current for the 90° detector. Recent results in Fig. 16 show the lost-alpha fraction collected by the 90° probe as a function of plasma current for D-T plas-

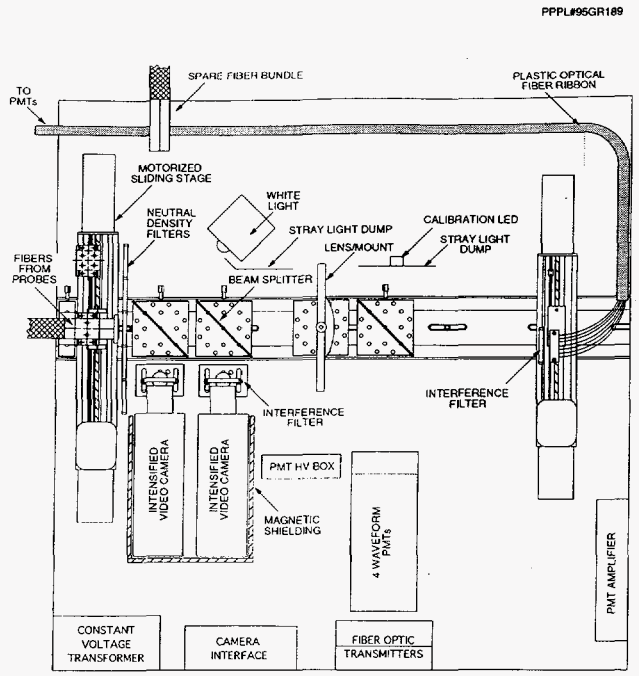

Figure. 15. *Layout of the Lost Alpha Probe Detector System. (95GR189)*

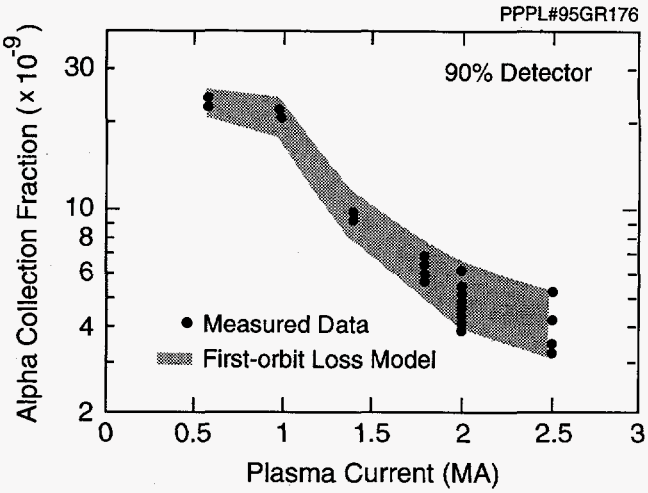

Figure 16. *The alpha-particle loss fraction captured by the lost alpha detector at the bottom of the vacuum vessel in the ion ∇B direction.*

mas. Also shown are predictions from a first-orbit loss model which matches the data in absolute magnitude, plasma current dependence, and pitch-angle distribution. For 2.5-MA discharges, the first-orbit loss is about 3%. For detectors closer to the midplane, the first-orbit loss model does not adequately fit the losses from D or D-T plasmas. Collisional and stochastic toroidal-field ripple losses are being investigated to explain the pitch-angle distribution and magnitude of the losses observed there.

In both D and T plasmas, MHD activity with low toroidal and poloidal mode numbers is observed to increase the loss of fusion products. Both minor and major disruptions produce substantial losses of alpha particles. In a major disruption, about 20% of the alpha stored energy is observed to be lost in approximately 2 msec during the thermal quench phase, while the plasma current is unchanged. The loss is preferentially to the bottom of the vessel which is on the ion drift direction. The design of in-vessel components in a reactor will have to accommodate the localized heat flux from alpha particles during a plasma disruption.

Good alpha-particle confinement is needed for ignition of future fusion devices. There is a concern that alpha confinement may be affected by instabilities driven by the presence of the energetic alphas. The lost alpha probes have shown (see Fig. 66 of the section entitled Deuterium-Tritium Plasmas in the High Poloidal Beta Regime) that there is no significant increase in lost alphas as the alpha source rate increases.

Alpha-CHERS Measurements of Confined Alphas

The alpha-particle charge-exchange recombination spectroscopy (α-CHERS) diagnostic is a spectroscopic diagnostic for measurement of confined, non-thermal alpha particles produced by D-T fusion reactions in TFTR.[19-21] This project is a collaboration between the University of Wisconsin and the Princeton Plasma Physics Laboratory (PPPL). During the 1993-94 D-T campaign on TFTR, alphas with energies up to 0.7 MeV were observed by the α-CHERS in the core of a sawtooth-free plasma discharge.[22] The observed spectra are in good agreement with predicted spectra based on TRANSP code calculations of the alpha-energy distribution, and the decay of the alpha distribution following the turnoff of the tritium beams (alpha source) is clearly seen. These observations confirm that the confinement and slowing down of the alphas in this energy range is close to neoclassical.

The visible He^+ line at 468.6 nm is excited by charge-exchange recombination of alphas with neutral-beam atoms, and the Doppler shift of the emission due to alphas with energies up to 0.7 MeV is observed. The alpha signal is less than 1% of the background bremsstrahlung intensity and is near the

wings of the much brighter thermal He^+ line; as a result, extraction of the alpha signal from this background requires excellent photon statistics.[23] As shown schematically in Fig. 17, the instrumentation consists of high-throughput light collection optics on TFTR which are fiber optically coupled to three high-throughput visible spectrometers, each equipped with a low-noise, high-quantum efficiency, high-dynamic range CCD camera detector. Each spectrometer views a single spatial channel at a time, allowing three spatial points to be observed during a single plasma discharge. A total of five spatial channels are available and may be remotely selected. Measurements are typically averaged over a 0.1-0.4 sec interval to achieve a signal-to-noise ratio of 5-10. Detection of nonthermal helium ions by α-CHERS was experimentally demonstrated previously by observation of ^3He ions with energies up to 400 keV produced by ion cyclotron range of frequencies heating.

A D-T experiment designed to optimize the α-CHERS signal was performed this year. Supershot plasma discharges similar to those described by Strachan, *et al.*[24] were used and had the following parameters: toroidal magnetic field $B_t = 5.1$ T, plasma current $I_p = 2.0$ MA, major radius R = 2.52 m, and minor radius a = 0.87 m. Both deuterium and tritium beams were injected for 1.3 sec to maximize the alpha density in the lower-energy range observed by α-CHERS; the deuterium beams were kept on for an additional 0.7 sec to allow the thermalization of the alphas to be observed following turnoff of the alpha source.

Figure 18 shows α-CHERS data from a plasma discharge in which no sawteeth occurred prior to the observation period. The thermal He^+ 468.6-nm line, background bremsstrahlung, and a number of weaker background impurity lines emitted primarily by low-ionization states of carbon at the plasma edge are clearly seen. The background impurity lines were removed from the spectrum by fitting them with a Gaussian-line profile convolved with the measured instrumental line shape, and subtracting the fit from the data, leaving a signal consisting of the thermal He^+ line and the bremsstrahlung background. This line removal process does not increase the noise level of the data above that of photon statistics. Each D-T plasma discharge performed in this experiment had a companion D-D discharge with similar plasma parameters, and thus bremsstrahlung of similar intensity and identical wavelength dependence. Line removal was performed on both the D-T and deuterium shots, and the D-D and D-T spectra were normalized to each other in the wavelength region corresponding to alpha energies of 0.75-1.05 MeV, where the spectrum is predicted to be pure bremsstrahlung. The data are then binned in the spectral direction to improve the signal-to-noise ratio.

Figure 19 shows the resulting alpha signal at r/a = 0.3 averaged over a 0.4 sec period centered at 4.5 sec, which is during the deuterium-beam-only diag-

PPPL#95GR174

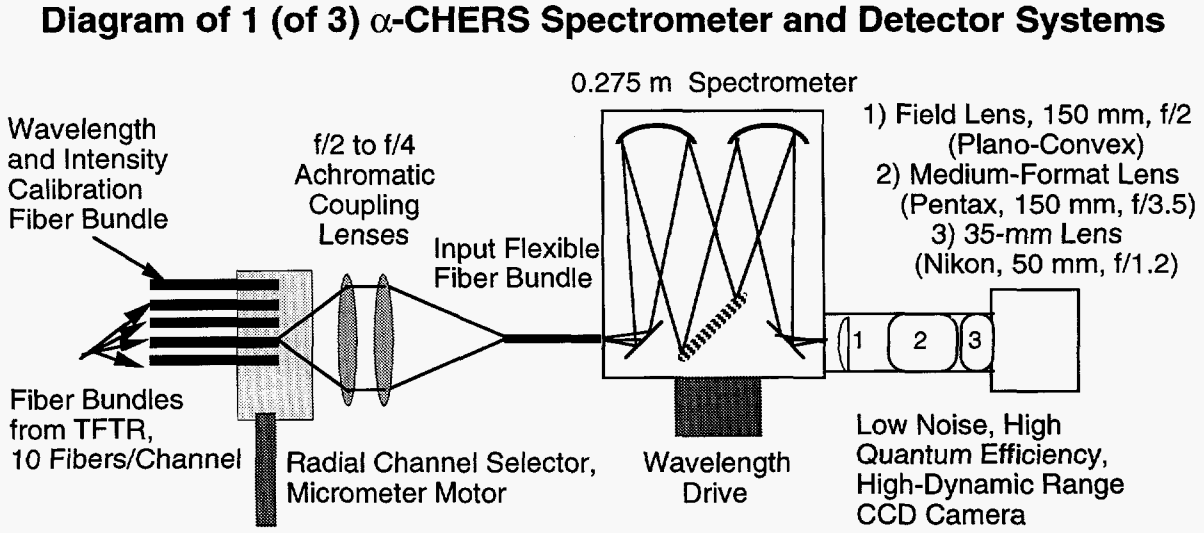

Figure 17. *Schematic of the α-CHERS spectrometer and detector system.*

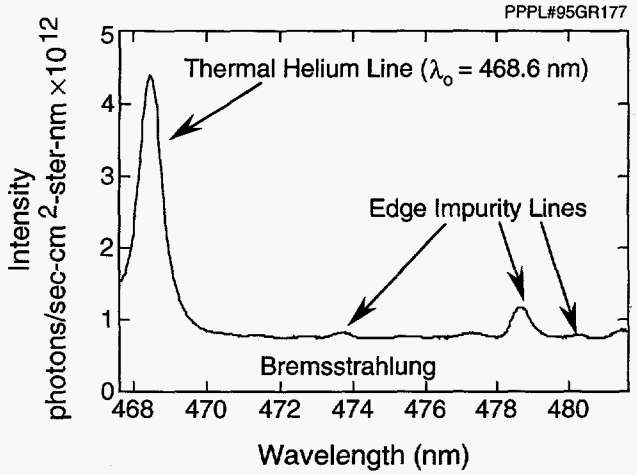

Figure 18. *The α-CHERS spectrum showing thermal He+ line, bremsstrahlung continuum, and edge impurity lines.*

nostic phase of the plasma discharge. The α-CHERS has an absolute radiometric calibration, and the signal shown is an absolute intensity measurement. Also shown is a predicted signal based on the alpha-distribution function calculated by the TRANSP kinetic analysis code; the measured and calculated signals are not normalized to each other. The good agreement between the measured and calculated signals indicates that the slowing-down alpha-energy distribution is close to neoclassical and that no significant anomalous losses of the fast alphas occurs in these plasma discharges.

The signal-to-noise ratio of this data set is sufficient for signal averaging over smaller time intervals of 100 msec to permit observation of the alpha slowing down. The time evolution of the measured and predicted signals at four times extending over 0.4 sec during the deuterium-beam-only phase is shown in Fig. 20. Both the measured and calculated spectra exhibit a decay of the alpha distribution to lower energies that is consistent with classical slowing down.

The results shown here are from a plasma discharge in which no sawteeth occurred. Other plasma discharges with sawteeth prior to the observation period show a reduced intensity of the alpha signal, indicating that sawteeth may be depleting the alpha density at the observation radius. Future D-T experiments will be performed on TFTR to study the effects of sawteeth on confined alphas in detail.

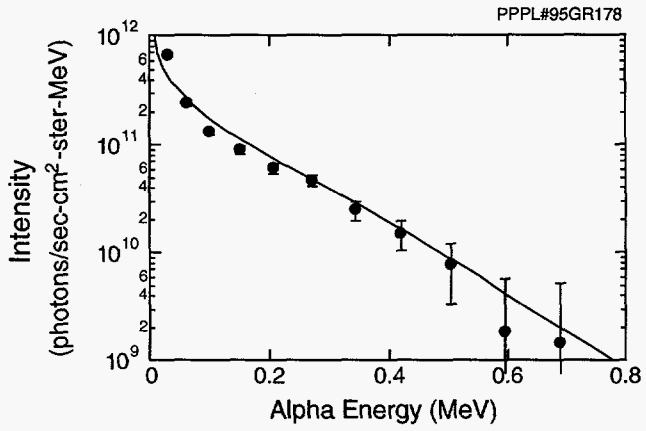

Figure 19. *Fast-alpha signal (ŧ) measured at r/a = 0.3 averaged over the time interval 4.3-4.7 sec and spectrum calculated from the TRANSP code alpha distribution (—) at 4.5 sec.*

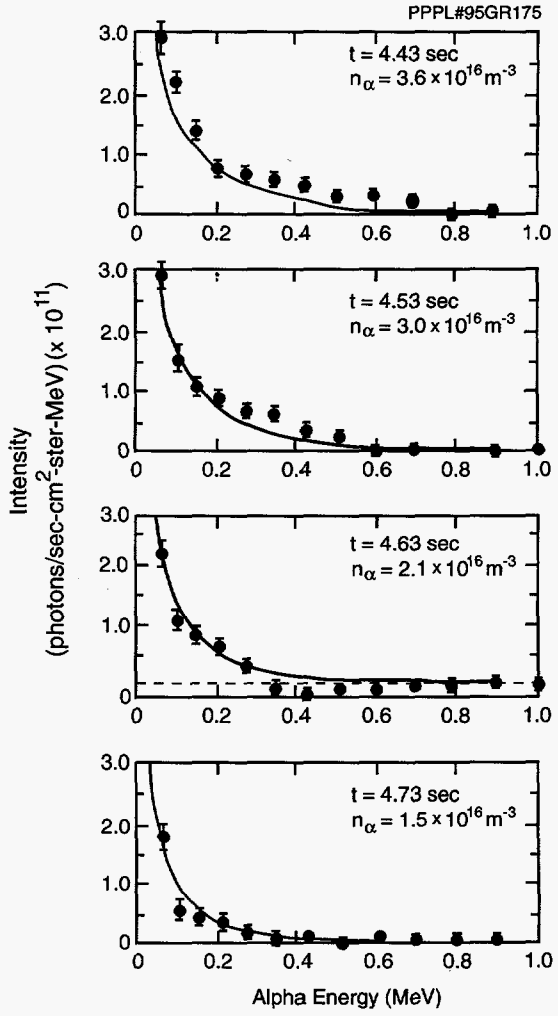

Figure 20. *Time evolution of alpha distribution at four time points during the thermalization process, showing decay of the distribution to lower energies following beam turnoff at 4.1 sec; r/a = 0.3 and integration time of 0.1 sec. The filled circles (ŧ) denote the α-CHERS measurement and the line (—) indicates spectrum calculated from the TRANSP code alpha distribution.*

Pellet Charge-Exchange Measurements of Confined Alphas

Radially resolved energetic confined-alpha energy spectra were obtained using the Pellet Charge-Exchange (PCX) diagnostic during the TFTR 1993-1994 D-T experimental campaign. The PCX project is a collaboration between General Atomics, the A.F. Ioffe Physical-Technical Institute, and PPPL. The diagnostic utilizes the ablation cloud from an impurity pellet as a target for alpha charge-exchange.[25] In the case of lithium (Li) pellets, the incident confined alpha will undergo both the double charge-exchange ($He^{2+} + Li^{+} \rightarrow He^{0} + Li^{3+}$) and sequential single charge-exchange ($He^{2+} + Li^{+} \rightarrow He^{+} + Li^{2+}$ followed by $He^{+} + Li^{+} \rightarrow He^{0} + Li^{2+}$) reactions without losing much of their energy. Hence, the technique provides an excellent method for measuring the "confined" alpha-energy distribution. A mass and energy resolving Neutral Particle Analyzer (NPA) detects the escaping neutral alphas. The NPA is a E||B mass and energy analyzer with eight ZnS(Ag) scintillation detectors. The analyzer has an energy range of 0.2-3.5 MeV, with a dynamic range of $E_{max}/E_{min} = 3.8$ and energy resolution $6.2 \leq \Delta E/E(\%) \leq 9.8$. The Lithium Pellet Injector (LPI) injects cylindrical lithium pellets with approximately 7×10^{19} atoms and velocities in the range of 400-600 m/sec. For diagnostic purposes, two pellets can be injected into a plasma discharge with a minimum temporal spacing of 2 msec. The LPI injects the pellets radially on the midplane. The NPA sightline can be configured to view the ablation cloud at different toroidal distances from the pellet. Presently, the NPA axis is positioned at an oblique angle of 2.75° with the LPI axis (about 12 cm from the pellet at R = 3.0 m). In preparation for D-T operation, a neutron and gamma radiation shield was installed for the analyzer. The shield consists of four inches of lead inside six inches of borated polyethylene, encasing the NPA almost completely. The measured shield attenuation is 150× for 14-MeV neutrons and 500× for 2.45-MeV neutrons.

While the primary purpose of the PCX diagnostic is to study confined alphas, the instrument is often operated to measure radio-frequency-driven tail ions and tritium ions.[26] These secondary measurements serve a dual purpose of providing instrumental calibration and enabling the study of other fast ions. During H-minority heating experiments, active and passive (without the use of lithium pellet) measurements of the energetic hydrogen tail (Fig. 21) was simultaneously obtained. In the passive mode, energetic H^{+} charge-exchanged with hydrogen-like carbon impurity ions (C^{5+}) in the plasma center. The neutralization rate ($\sigma v_{H^{+}}$) is approximately constant in the energy range of interest. The agreement between the active and passive measurement gives us good confidence in our model for the neutralization probability used to analyze fast-ion spectra.

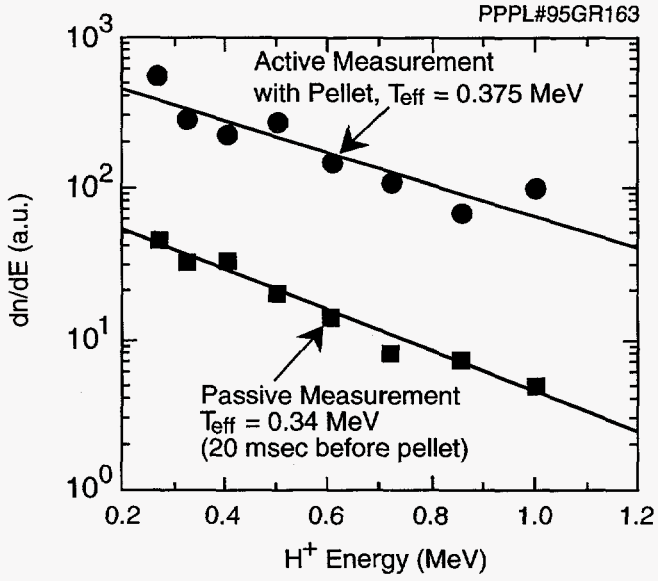

Figure 21. *Active and passive measurements of radio-frequency-driven H^{+} tail ions yield similar effective tail temperature.*

During D-T operations in the 1993-94 campaign on TFTR, the PCX diagnostic obtained the first measurements of confined-alpha particles in a tokamak.[27-28] The first example is from a current ramp experiment (I_p = 1.7-0.9 MA) where the lithium pellet penetrated to the plasma center. Comparison with the TRANSP code simulation yields very good agreement indicating alphas with large perpendicular velocity in the plasma core are well confined with a classical slowing-down energy spectrum (Fig. 22). In a similar deuterium-only plasma discharge, tritium ions from D-D fusion reactions were measured. The ratio of the measured triton-to-alpha signal agrees with the TRANSP code prediction as shown in Fig. 22.

The measured alpha-energy spectra agree well with TRANSP code predictions near the plasma cen-

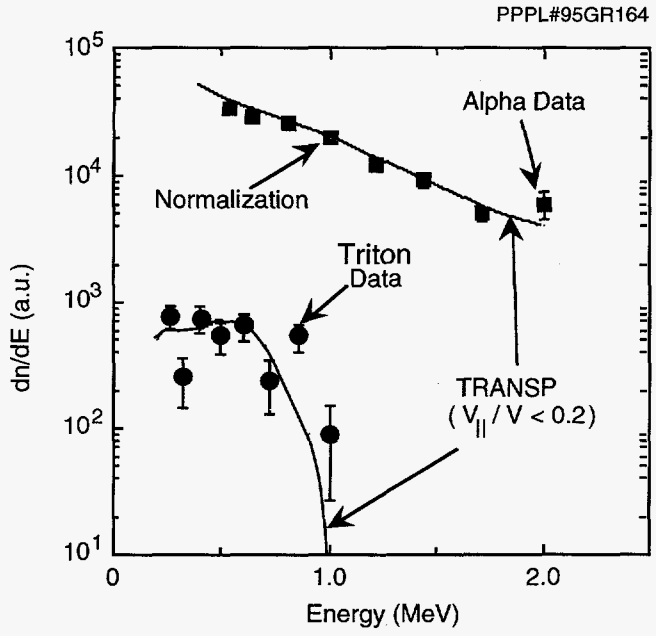

Figure 22. *Alpha and triton energy spectra at the plasma core. The ratio of the measured signal agrees well with TRANSP code simulations.*

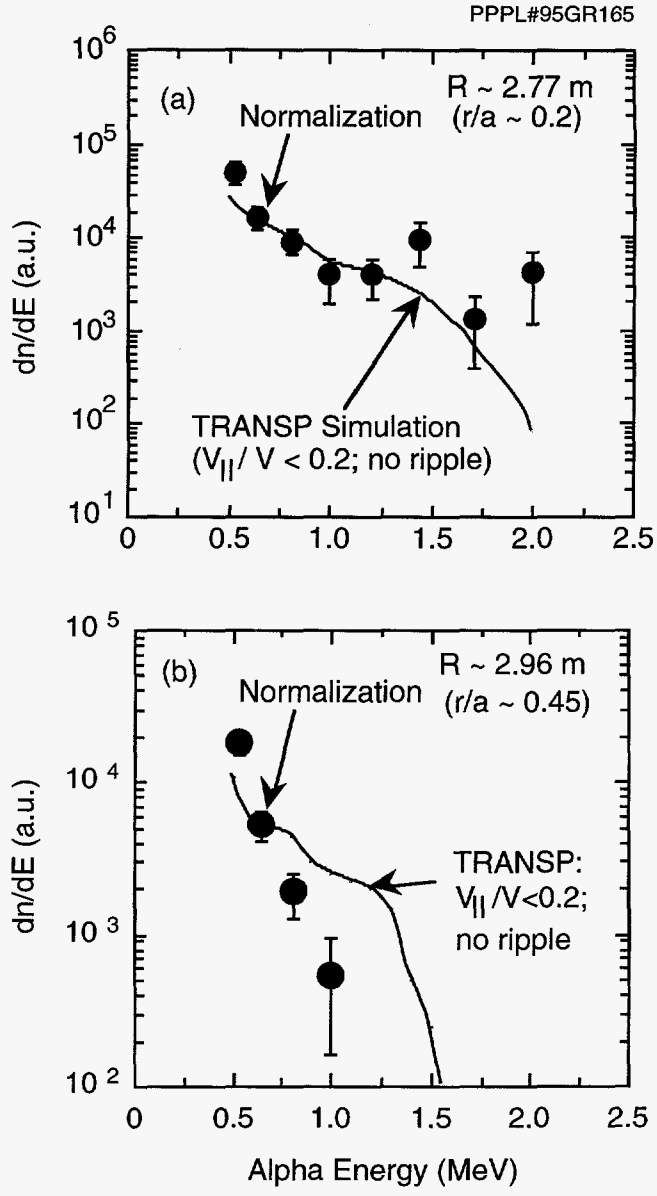

Figure 23. *Alpha-energy spectra at different radial location in a high current (I_p = 2.5 MA) discharge. The pellet charge-exchange data agrees with TRANSP modeling near the plasma center (a), but the agreement is poorer at r/a > 0.3 (b).*

ter, but differences arise outside r/a = 0.3. This observation is shown in Fig. 23. The main plasma parameters of the discharges are: I_p = 2.5 MA, B_t = 5.1 T, R = 2.52 m, a = 0.87 m, neutral-beam injection power P_{NBI} = 30 MW. There were several large sawteeth after neutral-beam injection turnoff but before pellet injection. The lithium pellet was injected 500 msec after beam injection and the pellet penetrated to 2.75 m (r/a ~ 0.2). The trapped alpha-energy spectrum near the core (r/a ~ 0.2) agrees relatively well with TRANSP simulations, while the PCX data differ from TRANSP simulations at the outer edge (r/a > 0.3). Possible explanations for the disagreement at larger radii are: (1) the TRANSP simulation did not include toroidal-field ripple effects; alphas in the sightline are very sensitive to ripple-induced losses, particularly at large radii, (2) uncertainty in the TRANSP modeling of Z_{eff} at the plasma edge, (3) uncertainty in the TRANSP modeling of the edge recycling and neutral density, (4) poor Monte Carlo statistics in the modeling, (5) the TRANSP code averages more than 100 msec to gain better statistics which is the same order as the alpha slowing-down time at the edge, and (6) the TRANSP simulation does not include fast-ion mixing due to sawteeth oscillation, which may be altering the alpha distribution.

Fusion Power Production in TFTR

Since December 1993, the TFTR has been operated with mixed deuterium-tritium plasmas at plasma densities and temperatures near those expected in a reactor such as the International Thermonuclear Experimental Reactor (ITER). A major thrust of the ex-

periments being conducted with high concentrations of tritium is the study of the energetic D-T fusion alpha particles in the plasma, including their confinement and transport, their role in the energy balance, and their potential for exciting instabilities. Since the possibilities for observing both self-heating of the plasma by the D-T fusion products and the collective instabilities excited by them generally increase with the D-T fusion rate, the second area of interest has spurred efforts to maximize the fusion power production in TFTR.

This section presents the techniques that have been used to produce high D-T reactivity in TFTR plasmas. The optimization of the D-T power within the constraints imposed by the available heating power, the energy confinement, and the plasma stability are discussed. The modeling of the fusion reactivity based on measured plasma parameters is then addressed. Finally, the possibilities for further improvements in the D-T fusion performance of TFTR are discussed.

Regime of D-T Operation

For producing high D-T fusion yields in TFTR, injection of high-power tritium and deuterium neutral beams has proved most successful.[24,29] In the "preliminary tritium experiment" in the Joint European Torus (JET),[30] the tritium was also introduced through neutral-beam injection (NBI). In TFTR, the twelve neutral-beam sources inject almost tangentially; six of the sources inject co-parallel and six inject counter-parallel to the plasma current. For most of these experiments, each source was operated with either pure deuterium or pure tritium gas, although in an initial series of experiments, sources were also operated with a mixture of 2% tritium in deuterium.

For deuterium NBI, the highest D-D fusion rates in TFTR have been obtained in the supershot regime,[31] characterized by very high central ion temperatures, $T_i(0) = 20\text{-}35$ keV $>> T_e(0) = 10\text{-}12$ keV, highly peaked profiles of the density and ion temperature, a broad electron temperature profile, and enhanced confinement relative to the predictions of low-confinement mode (L-mode) scaling. This regime was also used for most of the high D-T fusion yield experiments. In the D-T experiment in JET, a similar mode of operation with $T_i(0) > T_e(0)$ was used, although in that case, the divertor plasma also showed characteristics of high-confinement mode (H-mode) confinement.[30] Supershots in TFTR are produced with NBI heating when the edge recycling of hydrogenic species and carbon are reduced so that the plasma core is fueled predominantly by the injected neutrals. In addition to the enhanced confinement, this provides the advantage for D-T experiments that the central ion-species mix can be varied by changing the fraction of sources injecting tritium. In TFTR, the reduction in edge recycling that can be achieved by running repeated low-density ohmically heated plasmas has been extended through the injection of solid lithium pellets (1-4 pellets) into the Ohmic phase of the plasma discharge.[32] The plasma density perturbation from the pellets, which are injected 1.5-0.5 sec prior to NBI, has largely decayed by the start of the NBI; even in plasmas with multiple conditioning pellets, lithium is not a significant source of plasma dilution during NBI. Each pellet contains typically 4×10^{20} atoms, which corresponds to coverage of roughly one monolayer of lithium on the limiter surface. The use of lithium-pellet conditioning has increased the plasma current at which the supershot characteristics are obtained to 2.5 MA and increased the highest energy confinement time achieved to 0.27 sec in a plasma with 21 MW neutral-beam injection. In deuterium supershots, there is a strong dependence of the peak fusion reaction rate on the total plasma energy, W_{tot}, during NBI[33] and similar dependence was expected with D-T.[34] For maximum D-T fusion yield, therefore, operation at high plasma current and toroidal magnetic field was necessary to maximize the β limit, which has been found to scale in supershots similarly to the Troyon limit,[35] so that $W_{tot,max} \propto I_p B_t$ for fixed plasma size.

The experiments described in this section were conducted in plasmas with major radii of 2.45-2.52 m (minor radius 0.80-0.87 m, nominally circular cross section, with a toroidal carbon limiter on the inboard side) at a toroidal magnetic field 4.6-5.1 T. The plasma current was in the range $I_p = 1.0\text{-}2.5$ MA, held constant during NBI, and the total NBI power was in the range 5-34 MW.

The D-T fusion yield from TFTR is measured with a number of detectors for the 14-MeV neutrons.[36] The total rate is measured by ^{4}He-recoil detectors, silicon surface barrier detectors, ZnS scintillators, and a set of fission detectors (^{235}U and ^{238}U) with overlapping operating ranges to provide wide dynamic range. Most of these detectors have been absolutely calibrated using a standard D-T neutron source *in situ*.[37] The total yield for each pulse is measured by an elemental sample activation analyzer which provides neutron

energy discrimination and which, coupled with a neutron transport code, is also absolutely calibrated.[38] The scintillators and ^{4}He-recoil detectors are collimated along ten lines of sight across a poloidal cross section to provide data on the neutron source profile. The various detectors have different sensitivities to the 2.5-MeV neutrons from the d(d,n)^{3}He reaction and the 14.1-MeV neutrons from the d(t,n)^{4}He reaction, allowing the rates of the two reactions to be separated for plasmas with a small tritium content. The D-T neutron rates used in this section are generally derived from one of the fission detectors operating in its current-measurement mode. The calibration of this mode, which is expected to be linear for D-T neutron rates up to 10^{19} sec^{-1}, was derived from an uncertainty-weighted mean of four absolutely calibrated measurements for the first high-power tritium shots in December, 1993.[36] From time to time since then, variations of up to 10% have been observed between this and other measurements of the total D-T fusion rate. The overall accuracy of the D-T neutron rates is believed to be ±7%.

Figure 24 shows the time evolution of the D-T fusion power (using the total reaction energy of 17.6 MeV per D-T neutron) and plasma stored energy for four plasmas from a sequence leading up to the discharge

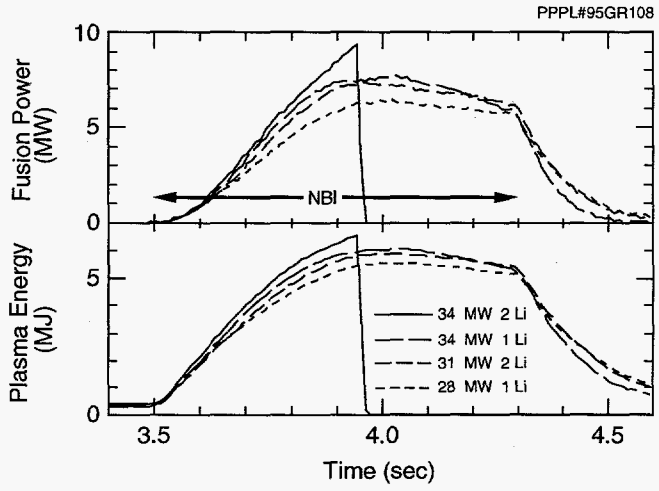

Figure 24. *Evolution of the D-T fusion power and the plasma stored energy for a series of plasmas with mixed deuterium and tritium neutral-beam injection leading up to the plasma discharge which produced the highest instantaneous fusion power. Plasma discharges with deuterium-NBI only were interspersed in this sequence. One or two lithium pellets were injected into the plasma prior to neutral-beam injection. Plasma parameters: major radius R = 2.52 m, minor radius a = 0.87 m, toroidal magnetic field B_t = 5.1 T, and plasma current I_p = 2.5 MA.*

producing the highest instantaneous power of 9.3±0.7 MW. The plasma energy is determined from magnetic data and includes the energy in the nonthermalized injected deuterons and tritons. In this sequence, the neutral-beam power and the amount of lithium conditioning were progressively increased. Only discharges with tritium NBI are shown in Fig. 24; shots with deuterium NBI only were interspersed between the tritium shots. The final shot in the sequence disrupted after 0.44 sec of neutral-beam injection, when the plasma reached the β limit at a total plasma stored energy of 6.5 MJ, corresponding to a Troyon-normalized-β, β_N ($=10^8\beta_t aB_t/I_p$ where β_t is the total toroidal β and a is the plasma minor radius) of 1.9. A similar β limit has been found to apply to deuterium "High-β_p" plasmas in the Japanese tokamak JT-60U, which exhibit many similarities to TFTR supershots, including high ion temperatures and peaked pressure profiles.

Figure 25 shows the peak fusion power, averaged over a 40 msec interval, as a function of total heating power (NBI plus Ohmic power; the latter is, however, negligible for $P_{tot} > 10$ MW) for the data set of supershots with NBI auxiliary heating only and with more than 20% of the NBI power in tritium. The plasmas with extensive lithium pellet conditioning are distinguished. A nonlinear dependence of the D-T fusion power on the heating power is apparent in these data. The highest ratio Q of the fusion power to the total heating power, $Q \approx 0.27$, was obtained on two discharges, one being the highest power discharge. In this discharge, immediately before the disruption, the rate of increase of plasma energy was still 7.5 MW out of a total heating power of 34 MW, demonstrating that stability rather than energy confinement now imposes the limit on the D-T performance in TFTR. The central toroidal β is calculated to have reached 5% in this plasma. A rapidly growing, toroidally localized mode with ballooning character was detected in the electron temperature profile immediately before this disruption. This is described in more detail below in section on "TAE Modes and MHD activity in TFTR D-T Plasmas." The shot producing 5.6 MW with only 21 MW neutral-beam injection was conditioned with four lithium pellets in the ohmically heated phase prior to the NBI and achieved a transient confinement time of 0.27 sec (averaged over an energy confinement time) which is approximately 2.4 times the prediction of ITER-89P scaling,[39] based on an average ion mass of 2.5.

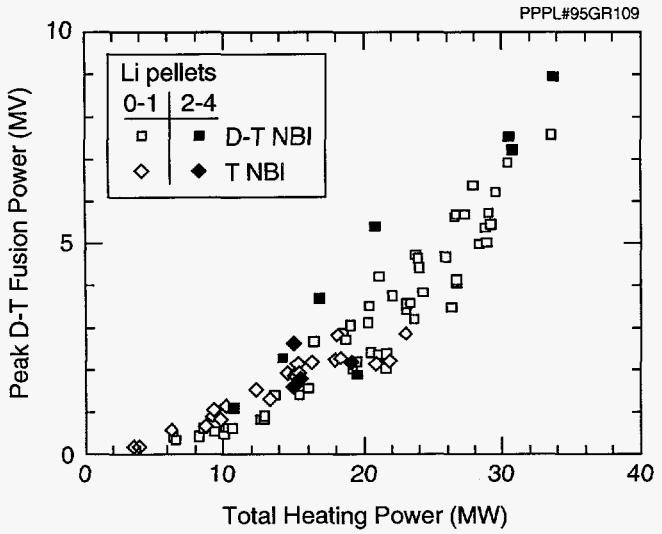

Figure 25. *Peak D-T fusion power as a function of total input power (neutral-beam injection plus Ohmic power). The data are for supershots with at least one neutral-beam injector source injecting pure tritium. Plasma discharges with tritium neutral-beam injection only are distinguished. Improved performance is made possible by lithium-pellet injection.*

The peak fusion powers from D-T and nominally D-only supershots at the same NBI power under similar conditions have been compared. Since there is a small amount of tritium present in any nominally D-only plasma taken soon after a D-T shot, as a result of tritium influx from the limiter, the D-T reaction component is subtracted from the nominally D-only data in calculating this power ratio. In the experiment to maximize fusion power, the D-T component of the reaction rate in the D-only plasmas tended to increase secularly through the NBI pulse, whereas, the D-D component generally peaked after about 0.5 sec. Comparison of the plasmas shown in Fig. 24 with D-only shots from the same experiment having the same plasma current (2.5 MA) and number of lithium pellets, yields a ratio P_{DT}/P_{DD} of 135±7 "at constant neutral-beam power." A similar ratio is obtained for the subset of discharges with the same major radius (2.52 m) but at a plasma current of 2.0 MA.

In discussing the relative fusion reactivity, it is also necessary to consider the confinement differences between D-T and D-only plasmas, since the fusion rate varies strongly with plasma energy.[33] As discussed in detail in the following section, "Heating and Transport in TFTR D-T Plasmas," the global energy confinement of plasmas with significant tritium NBI is substantially higher than in equivalent plasmas with deuterium NBI only. Figure 26 shows the fusion power production from comparable D-T and D-only plasmas plotted against the scaling $W_{tot}^{1.91} q_a^{0.32} V_p^{-1}$, where V_p is the plasma volume and q_a the edge safety factor q, and the exponents on W_{tot} and q_a were determined by regression analysis. The exponent of W_{tot} is close to that expected for thermalized D-T plasmas with ion temperatures in the range 10-20 keV (where the local D-T fusion power density varies approximately as $n_i^2 T_i^2$) having similar pressure profile shapes and in which the electron stored energy is a constant fraction of the total. The factor $q_a^{0.32}$ represents a tendency for the pressure profile to broaden and the fraction of the total energy in the ions to decrease with plasma current. The data include supershots both with and without lithium pellets. The D-T plasmas are restricted to those with a tritium NBI power fraction between 0.35 and 0.75. The root-mean-square deviation of the data about the fit is about 7% for the whole data set. From this data, the ratio of the fusion power between the D-T and D-only supershots "at constant plasma energy" is 115±15. This ratio is less than the maximum of about 210 expected for thermalized D-T and D-only plasmas at a temperature of 10 keV, because in supershots, the ion temperatures are higher and the nonthermal ion component increases the reactivity in D-only plasmas, and because there are small systematic differences in the profiles between D-T and D-only supershots.

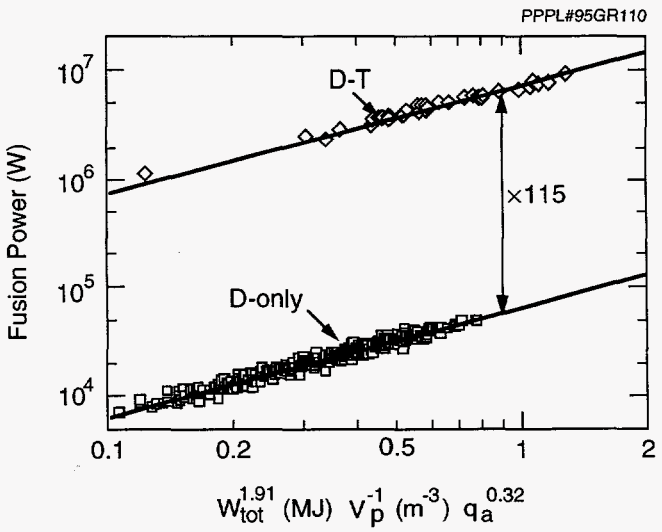

Figure 26. *Peak fusion power from both D-T and D-only supershots with neutral-beam-injection heating plotted against the common scaling expression determined by a regression fit. The D-T plasmas are restricted to those with close to the optimum fraction of tritium neutral-beam injection.*

Modeling of the D-T Reactivity

The time evolution of the fusion reactivity in TFTR has been analyzed with the TRANSP code.[40] The deposition, orbit loss, and slowing down of the injected tritium and deuterium neutrals are calculated using the measured profiles of the electron density and the electron and ion temperatures. The beam-injected ions are transferred to the thermal ion population when their energy reaches $1.5kT_i$, where T_i is the local ion temperature. The profile of the total ion density is calculated using the visible bremsstrahlung for the total Z_{eff} and X-ray measurements of the metallic contribution to Z_{eff}. Spectroscopy shows that carbon is the dominant low-Z impurity. A source of uncertainty in the analysis is the role of the edge fueling in determining the overall mix of deuterium and tritium in the center. High-resolution spectroscopy of the hydrogen isotope line radiation from the plasma edge[41] has confirmed that, as expected from the history of the limiter exposure to plasmas, the edge fueling is dominated by deuterium, with a smaller component of hydrogen, typically 10-20%, and relatively little tritium influx, less than 10%. Comparisons between plasmas with varying fractions of deuterium and tritium injection have demonstrated that the fueling of the core of supershots by this edge recycling is quite significant. The D-T neutron rate normalized to the scaling $W_{tot}^{1.91}q_a^{0.32}V_p^{-1}$ is shown in Fig. 27 as a function of the tritium NBI fraction, $F_T = P_T/(P_T + P_D)$, where P_T, P_D are the tritium and deuterium NBI powers, respectively, for plasmas with $P_{NBI} > 10$ MW and at least one source injecting tritium. The fitted parabola, which is constrained at $F_T = 0$ to the level typical for D-only plasmas in D-T experiments, peaks at $F_T \approx 0.6$ and is broader than would be expected in the absence of edge fueling. In plasmas with tritium injection only, the normalized D-T neutron rate averages about 65% that for the optimal mix of deuterium and tritium sources and shows more variability since it depends on the edge influx. In plasmas with deuterium NBI only, the tritium content is small and depends on the tritium exposure of the limiter during the preceding discharges. However, because of its much larger fusion probability, the tritium in D-only plasmas can produce a D-T reactivity comparable to or larger than the D-D reactivity. A model for the tritium and deuterium transport which describes reasonably well the dependence of the D-T and D-D neutron rates on the tritium fueling fraction has been developed.[42]

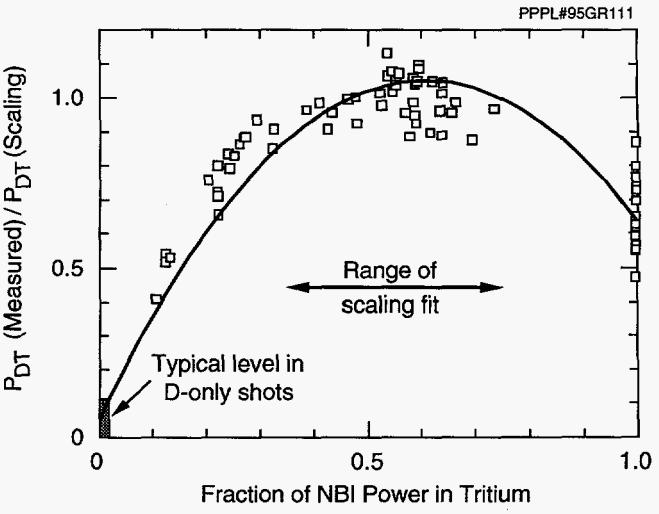

Figure 27. *Dependence of the normalized D-T fusion power on the fraction of tritium-NBI in the total neutral-beam injection power. The D-T fusion rate is normalized to the scaling expression (Fig. 26) to remove the effect of the energy confinement on the D-T power. The range over which the scaling expression was fitted and the range of D-T power for D-only plasmas are indicated.*

The measured and calculated time evolutions of the total D-T fusion power and plasma energy are compared in Fig. 28 for the discharge (76771) producing 7.2 MW (Fig. 24). The slight decay of the D-T power after 0.45 sec of heating is reproduced by the calculation, indicating that this decay arises from the classical effects which are included in the model (in particular, changes in temperature and density profiles) and is not caused by an anomalous loss of injected-beam ions. The data from the collimated neutron detector array is also used to constrain the fueling and particle transport models. At the time of peak fusion power, the central electron and ion temperatures in this plasma were 11 and 30 keV, respectively, and the central electron and fuel (deuteron plus triton) densities were 7.3×10^{19} and 5.0×10^{19} m^{-3}, respectively. The peakedness of the fuel ion pressure profile, which is appropriately characterized by the parameter $\langle U_{DT}^2 \rangle / \langle U_{DT} \rangle^2$, where U_{DT} is the energy density of the deuterons and tritons and $\langle\ \rangle$ represents the volume average, reached 2.1.

For the subset of D-T plasmas in Fig. 25 that have been analyzed in detail by the TRANSP code (46 shots), the model generally matches the total plasma energy within 10% and the total D-T neutron rate within 25%. The discrepancies in the D-T rate and the plasma energy are correlated so that the modeled

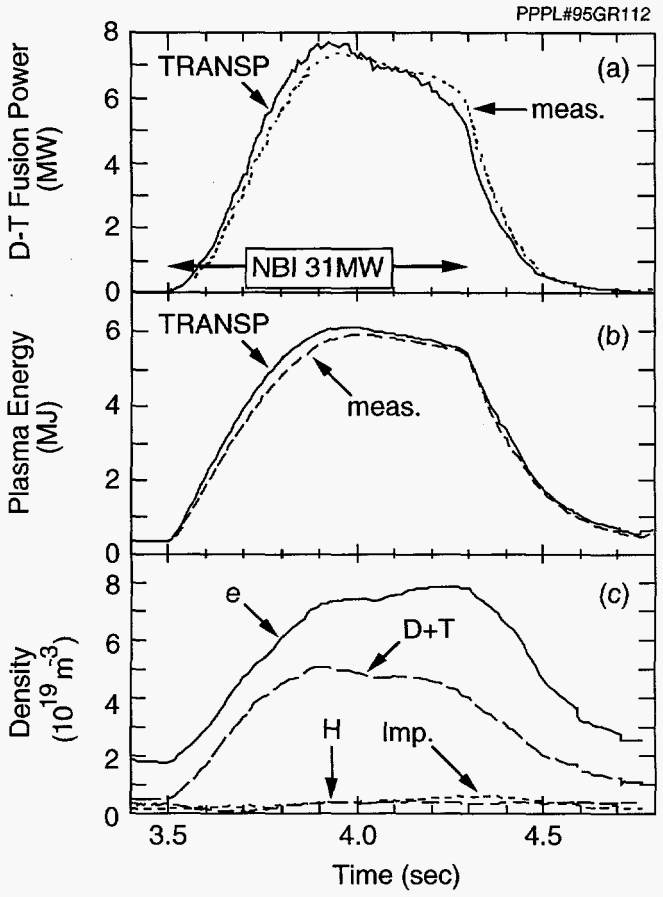

Figure 28. *Comparisons of (a) the D-T fusion power and (b) the plasma energy calculated by the TRANSP code with measurements for shot 76771. Panel (c) shows the inferred densities of the various plasma species.*

and measured ratios P_{fus}/W^2_{tot} agree within a 10% standard deviation for the D-T plasmas. For similar D-only plasmas experiments during the D-T campaign, the TRANSP calculations of the plasma energy are generally in agreement with the measurements, but the fusion rates do not agree quite as well. As a result, the TRANSP code predicts that there should be a ratio of about 135 between the fusion powers from D-T and D-only supershots at constant plasma energy, which is about 20% higher than the measured ratio.

Summary

For discharge 76771, the local Q, defined as the ratio of the fusion power density to the total heating power density (neutral-beam and Ohmic power) was about 0.4 at the plasma center. The plasma with exceptional confinement produced by lithium conditioning which achieved a global Q of 0.27 (discharge 77309, Fig. 25), is calculated to have reached a central Q of 0.5. The central fusion power densities achieved in the high-performance TFTR supershots, typically about 1.5 MW m^{-3}, are essentially the same as those for pure, isothermal D-T plasmas at the optimum temperature for reactivity ($T_e = T_i \approx 15$ keV) having the same total energy density. For discharge 76771, this "equivalent thermonuclear" plasma would have $n_e = n_T + n_D \approx 1 \times 10^{20}$ m^{-3}. Although the NBI provides the dominant heating and fueling in supershots, at the plasma center, the nonthermal ion distribution does not increase the D-T reactivity compared to that of a plasma having a locally Maxwellian ion distribution with the same total fuel energy and particle densities. The hot-ion ($T_i > T_e$) nature of these plasmas essentially compensates for the dilution of the fuel density relative to the electron density.

Assuming that the central plasma energy density is limited, either by confinement or the local β limit for the present magnetic-field strength, the reactivity is currently being reduced below that which could be achieved both by the presence of impurities [$Z_{eff}(0) \approx 2.0$ typically at the time of peak fusion power] and by the hydrogen component fueled by the limiter. In the discharge that achieved exceptional confinement and Q (77309), the fraction of hydrogen in the edge recycling was particularly high. Modeling with the TRANSP code suggests that increases of 20% in the central fusion power density might be possible in similar plasma conditions to this discharge with the normal recycling composition. Experiments to modify the contact of the plasma with the limiter to control the recycling during the NBI pulse are also planned.

Since the β limit is now providing a fundamental limitation on the achievable D-T performance in TFTR, plans are also being made to increase the toroidal magnetic field by up to 16% for a limited number of pulses. Such an increase could raise the central plasma energy density at the β limit by up to 30% and, if the present scaling is maintained, the achievable D-T fusion power by up to 70%.

Heating and Transport in TFTR D-T Plasmas

One of the most striking features of initial operation at high power with significant tritium concentration was improved energy confinement. In this section, the variation of tokamak energy confinement and

transport with isotopic mass is analyzed for TFTR deuterium and deuterium-tritium plasmas in the supershot regime. The isotopic mass dependence is of fundamental interest for developing an understanding of tokamak transport and to accurately project confinement for future ignited reactors, such as ITER. Previous experiments on a variety of devices compared confinement and transport in hydrogen (H) and deuterium plasmas, with a wide range of results that were summarized in the ITER-confinement scalings[39] as $\tau_E \propto A^{\sim 0.5}$, where τ_E is the global energy confinement time and A is the ion mass

The plasmas studied here are in the enhanced-confinement supershot regime,[31,33] characterized by high ion temperature (approximately 30 keV), high fusion reactivity, confinement enhancement of up to three times L-mode scalings, and peaked density profiles. These plasmas are fueled by either pure deuterium or pure tritium neutral-beam injection to maximize the isotopic effects and to minimize contributions from fusion-produced alpha particles to the plasma stored energy or heating. The plasmas studied have $I_p = 1.6$ MA, $R = 2.52$ m, $B_t = 4.8$ T, and include power scans up to injected power $P_{NBI} \sim 23$ MW of either nearly balanced co- and counter-tangential NBI or co-tangential only NBI. All plasmas discussed achieve transport equilibrium within the 1.4 sec heating pulse, with no significant confinement degradation or MHD instabilities.

This section will discuss the isotopic mass scaling of the energy confinement time of D-T plasmas, followed by analysis of the plasma profiles and heating and the inferred scaling of the local transport.

Plasma Conditions and Global Scaling

Figure 29 shows the variation of the total plasma stored energy W_{tot} (from magnetic measurements) with injected power for either deuterium-NBI or tritium-NBI, for both near-balanced injection and co-only (unbalanced) injection. The total plasma stored energy is consistently enhanced by about 25% for tritium-NBI plasmas relative to comparable deuterium-NBI plasmas, except at low values of injected power. Similar enhancements are observed with higher power tritium-NBI (20-30 MW) and higher plasmas currents (1.8-2.0 MA).[29,43] Plasmas with mixed deuterium and tritium-NBI show intermediate levels of improvement. As previously observed in the supershot regime,[44]

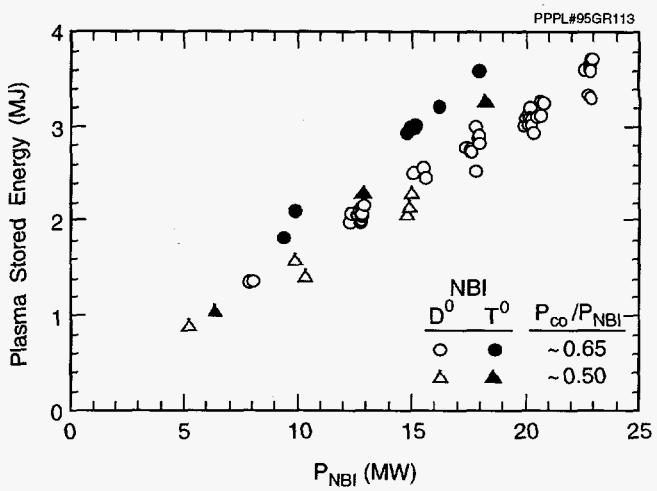

Figure 29. *Variation of stored energy with injected power for deuterium (D) and tritium (T) fueled supershots, with $I_p = 1.6$ MA and either balanced injection ($P_{co}/P_{NBI} = 0.5$) or slightly co-injection ($P_{co}/P_{NBI} = 0.65$).*

energy confinement is optimized in both tritium-NBI and deuterium-NBI plasmas, with slightly more co- than counter-injected power, $P_{co}/P_{NBI} \sim 0.65$. By comparison, the confinement time for plasmas with balanced injection ($P_{co}/P_{NBI} = 0.5$), is about 10% lower. For the highest power tritium-NBI discharges, the classically expected alpha-particle stored energy is approximately 90 kJ, or 2.5% of the total plasma stored energy, and the resulting heating power is less than 47 kW relative to $P_{NBI} = 18$ MW.

For the tritium-NBI plasmas shown in Fig. 29, the limiter hydrogenic recycling influx, as measured by $H_\alpha/D_\alpha/T_\alpha$ spectroscopy,[45] is dominated by deuterium with only about 2% due to tritium and about 18% due to hydrogen. From measurements of the deuterium-tritium neutron emission profile, the tritium fraction of the thermal hydrogenic ions within $r/a = 0.5$ is calculated to be about 60% for the highest power tritium-NBI plasma. Thus a significant portion of the central thermal hydrogenic ion density is due to particles originating from the limiter. For the low-power tritium-NBI plasmas, the thermal tritium fraction is calculated to be about 28%, explaining its smaller confinement enhancement above similar deuterium-NBI plasmas.

The fraction of injected power radiated in these plasmas is about 25% at high power, and about 30% for $P_{NBI} \sim 5$ MW. The radiated power fraction in tritium-NBI plasmas is lower by 3%, on average, than for similar power deuterium-NBI plasmas, resulting in slightly higher limiter power loading with tritium-

NBI. The radiation is emitted near the plasma edge, as measured by bolometer arrays, and is negligible in the plasma core. When comparing matched deuterium-NBI and tritium-NBI plasmas at a given injected power, the edge hydrogenic recycling remains constant to within 5-10%. The edge CII emission is often up to 20% higher in tritium-NBI plasmas. In deuterium-NBI plasmas, higher edge CII emission correlates with "lower" confinement. Thus, neither radiated power nor edge recycling appears to play a significant role in the observed confinement improvement with tritium-NBI, in contrast to hydrogen/deuterium (H/D) isotopic comparisons on ASDEX (Axially Symmetric Divertor Experiment) at Garching, Germany.[46]

Profile Analysis

In order to understand the origin of the improved confinement with tritium-NBI, these plasmas are analyzed using the one-dimensional steady-state transport analysis code SNAP and the 1-1/2 dimensional time-dependent code TRANSP[47] using the experimentally measured temperature and density profiles. Electron temperature [$T_e(r,t)$] is measured by ECE (electron cyclotron emission) spectroscopy and Thomson scattering, ion temperature [$T_i(r,t)$] and toroidal rotation velocity [$v_\phi(r,t)$] are measured by carbon charge-exchange recombination spectroscopy (CHERS), and electron density [$n_e(r,t)$] is measured by a ten-channel infrared interferometer array. The ion depletion is calculated using tangential visible-bremsstrahlung measurements for Z_{eff} and X-ray spectroscopic measurements of metallic concentrations.

Due to the change in the beam-neutral velocities between deuterium-NBI and tritium-NBI, at fixed acceleration voltage, the CHERS measurements suffer a systematic offset in the apparent ion temperature and toroidal rotation velocity due to the variation of the carbon charge-exchange emission cross section with the relative velocity between the hydrogenic neutral and the C^{6+} ion.[48,49] This effect has been verified by comparing CHERS measurements of the same D-T plasma made using either deuterium or tritium doping beams, and by comparing measurements of spinning plasmas using co- and counter-directed neutral beams, as a function of plasma rotation velocity. The offsets are found to be in good agreement with simulations of the charge-exchange spectral line shape and position. The modeling is based on emission cross sections for the n = 8-7 transition of C^{5+} (6292 Å) from a published fit to experimental and theoretical capture cross sections.[50] This effect is largest for the toroidal rotation velocity measurement in high ion temperature plasmas with low velocity neutral beams, such as tritium-NBI or with co-only injection into a high velocity plasma. The ion temperature and toroidal rotation velocity measurements used for this analysis (for both tritium-NBI and deuterium-NBI) are corrected for this effect using the beam deposition calculations in the SNAP and TRANSP codes to calculate the fast neutral energy spectrum in the plasma frame. As shown in Fig. 30, this correction results in a substantial increase in the toroidal rotation velocity, but only a modest increase (≤10%) in the central ion temperature. The correction to the toroidal rotation velocity reaches approximately 2.3×10^5 m/sec for $T_i \sim$ 30 keV. The correction to the ion temperature decreases rapidly at lower temperatures and is ≤5% for $T_i \leq 20$ keV. The difference between the measured carbon-ion temperature and the deuterium temperature due to finite equipartition times is calculated to be less than 1.5 keV for the high injected power plasmas.

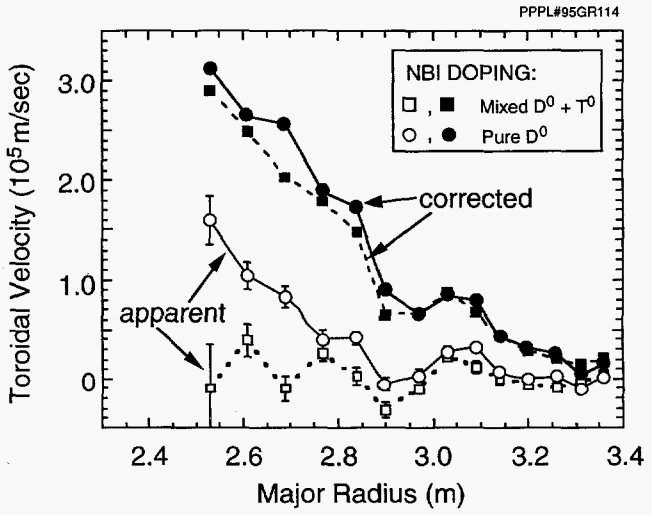

Figure 30. *Comparison of toroidal rotational velocity v_ϕ profiles measured by carbon charge-exchange recombination spectroscopy using deuterium or mixed deuterium-tritium doping beams, with and without correction for the energy dependence of the charge-exchange cross section.*

Comparing carefully matched sets of deuterium-NBI and tritium-NBI plasmas, for which all the externally controlled discharge parameters and the target plasma are nominally identical, a consistent and clear improvement in plasma performance is observed with tritium-NBI. As shown in Fig. 31, tritium-NBI

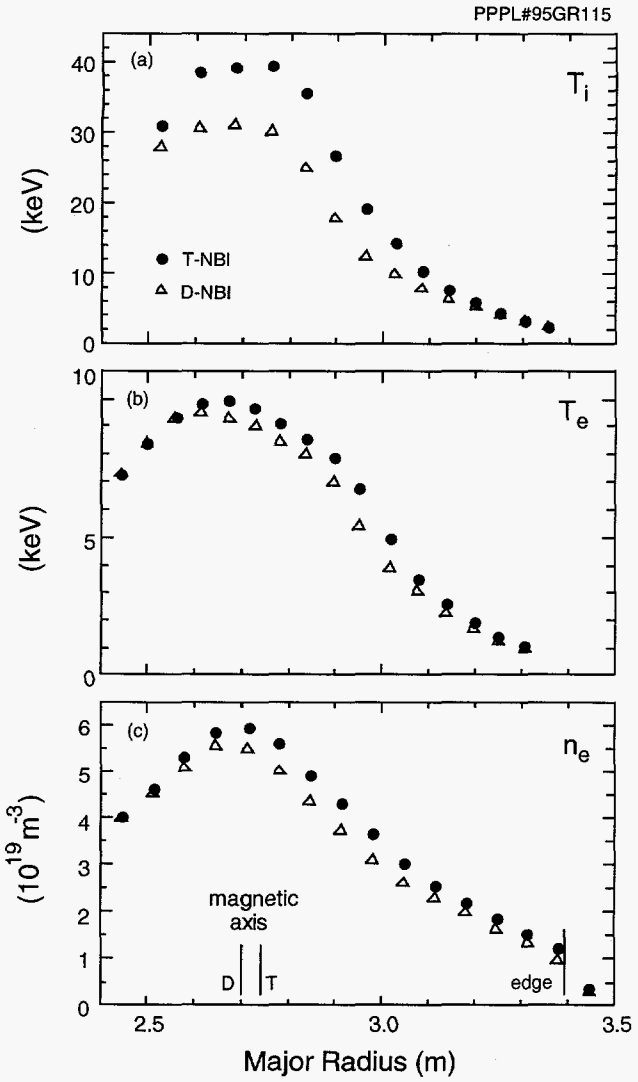

Figure 31. *Comparison of measured profiles of ion and electron temperatures (T_i and T_e, respectively) and electron density (n_e) in deuterium and tritium plasmas, for I_p = 1.6 MA and P_{NBI} = 18 MW. Note that the Shafranov shift of the profiles has changed due to the change in stored energy between deuterium-NBI and tritium-NBI.*

plasmas typically have an about 25% higher central ion temperature and a 5-10% higher central electron temperature. (The increase in the electron temperature is most apparent in measurements by electron cyclotron emission spectroscopy and is consistently smaller in the Thomson scattering measurements.) The central Z_{eff} for the tritium-NBI plasma is 2.3, while the deuterium-NBI plasma has Z_{eff} = 2.5. The measured plasma density profiles have the same shape, but the deuterium-NBI plasma density is about 10% lower. Within the cluster of other deuterium-NBI plasmas with P_{NBI} = 18 MW in Fig. 29 are plasmas with the same Z_{eff} or electron density profile as the tritium-NBI plasma. Due to their larger total plasma stored energy, the tritium-NBI profiles show a larger Shafranov shift than the deuterium-NBI profiles. For high injected power, 65-80% of the increase in the total plasma stored energy is accounted for by the increase in the thermal ion and electron energy content, with the rest due to the expected classical increase in the circulating beam particles and the small contribution from alpha particles.

Transport Analysis

The SNAP and TRANSP codes model the deposition of the injected beam neutral atoms, and the subsequent slowing down and losses of the fast ions. To assess the consistency of the diagnostics and kinetic modeling, the magnetically measured energy content W_{mag} is compared with the kinetic stored energy W_{kin} calculated from the measured thermal temperature and density profiles and the modeled beam-ion distribution function. Using the ECE electron temperature measurements, the kinetic stored energy is within 10% of the magnetically measured energy content, which is within their combined uncertainties. The Thomson scattering electron temperature measurement has a lower central electron temperature and a broader profile than the ECE measurement, resulting in an increased calculated kinetic stored energy. The resulting kinetic stored energy is consistently higher than the magnetically measured energy content by about 10% at high injected power and 20% higher at P_{NBI} = 5 MW. Because of this higher level of disagreement, only results based on ECE electron temperature measurements will be discussed here.

There are a number of classically expected differences between tritium- and deuterium-neutral-beam heating which are included in the analysis. For tritium-NBI, the lower beam particle velocity results in a broadened deposition profile, increased beam heating of thermal ions, and decreased beam heating of electrons. The effects on the ion heating roughly cancel, but the core ion energy flux is reduced in tritium-NBI plasmas due to the increased ion-electron equilibration power, see Fig. 32. The beam electron heating is substantially reduced with tritium-NBI, but this is more than compensated for by the increase in ion-electron equilibration power.

The accuracy of the beam-deposition modeling has also been tested for both the deuterium-NBI and tri-

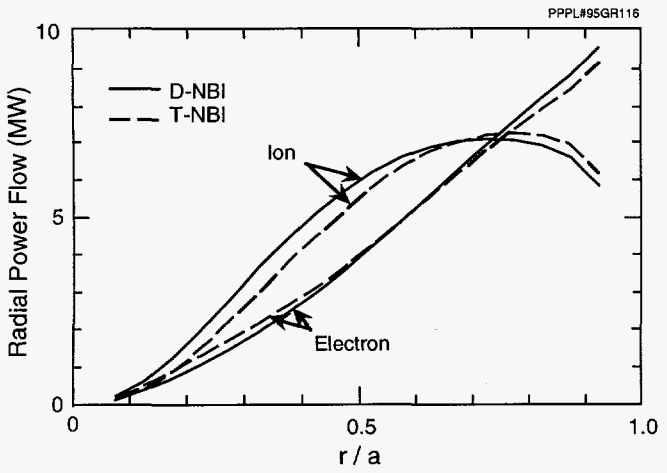

Figure 32. The calculated profiles of the ion and electron power flows in the deuterium and tritium neutral-beam-injected plasmas of Fig. 31.

tium-NBI plasmas by comparing the rate of rise of the central plasma density at the initiation of beam injection with the calculated electron source rate. The calculated and measured central particle source rate due to beam injection agree to better than 10%.

As previously observed in supershots,[9] energy transport near the magnetic axis is dominated by 1.5Γ T convective losses, particularly for the higher-temperature tritium-NBI plasmas. At r ~ a/2, the convective losses are small, and the transport is dominated by conduction. In order to treat the transport in both regions and to avoid prescribing a particular convective multiplier, the local transport is characterized and compared between plasmas in terms of "total" effective diffusivities $\chi_{i,e}^{tot}$

$$Q_{i,e} \equiv - \chi_{i,e}^{tot} n_{i,e} \nabla T_{i,e} ,$$

$$\Gamma_e \equiv - D_e \nabla n_e ,$$

where Q_i and Q_e are the total ion and electron radial energy fluxes, respectively, Γ_e is the electron radial particle flux, and $n_i = \Sigma_j n_j$ is the total thermal ion density.

Isotopic Content

The isotopic content of the plasma must be measured in order to understand any transport variations observed. In the deuterium-NBI plasmas, the absence of a significant tritium density is confirmed by the measured low level of D-T fusion neutron emission. In the tritium-NBI plasmas, the wall recycling deuterium influx is a significant source of particles, and leads to a significant deuterium density n_D throughout the plasma. The thermal deuterium density profile is determined from the measured D-T neutron emission profile and the calculated plasma D-T reactivity profiles for beam-thermal and thermal-thermal reactions using the TRANSP code, constrained by the total hydrogenic-ion thermal density determined by depletion of the electron density. The D-T neutron emission profile is measured by a ten-channel collimated neutron-detector array. It is assumed that hydrogen density $[n_H(r)]$ and deuterium density $[n_D(r)]$ have the same profile and are in the same ratio as the measured edge hydrogen-alpha H_α and deuterium-alpha D_α intensities, since the only source of hydrogen and deuterium is edge recycling in tritium-NBI plasmas. The central deuterium density is found to rise slowly during the equilibrium phase of the neutral-beam injection pulse in approximately fixed ratio to the edge deuterium-alpha D_α emission. Typical inferred equilibrium deuterium density and tritium density n_T profiles are shown in Fig. 33. Note that the deuterium density profile is relatively flat, indicating the absence of any significant deuterium particle pinch

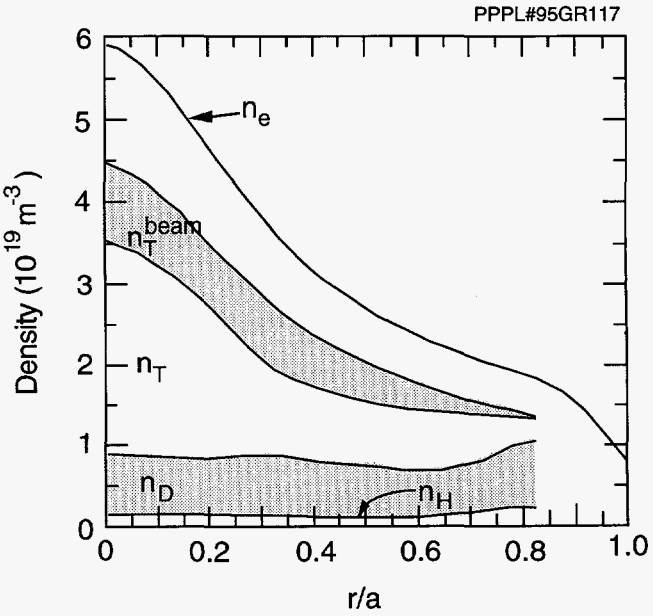

Figure 33. The hydrogen n_H, deuterium n_D, tritium n_T, tritium beam n_T^{beam}, and electron densities in the tritium-NBI plasma of Fig. 31. Each region represents the density of the indicated species. The deuterium and tritium densities are determined from the measured D-T neutron emission profile and the plasma reactivity profiles calculated by the TRANSP code.

in these cases. The implied absence of a significant ion-particle pinch in these plasmas is similar to the results of the tritium gas puffing experiments described below in the section "Tritium Transport, Influx, and Helium Ash Measurements on TFTR during D-T Operation."

Energy and Particle Transport

Figure 34 compares the inferred local diffusivities for the matched tritium-NBI and deuterium-NBI plasmas of Fig. 31. The power balance analysis consistently indicates that the higher ion temperature gradient observed during tritium-NBI, in the presence of reduced net ion heating, is due to a reduction of the ion thermal diffusivity χ_i^{tot} by a factor of approximately two for r/a ≤ 0.5. The lack of substantial change in the density gradient, despite the broader beam deposition profile with tritium-NBI, is interpreted as a drop in the core electron particle diffusivity D_e by about 20%. The electron thermal diffusivity χ_e^{tot} is often observed to be higher in the core with tritium-NBI, but can be lower near r/a ~ 0.5 by about 10%. As shown in Fig. 35, this strong reduction in ion thermal diffusivity and weak reduction in electron thermal diffusivity is clearly present throughout the dataset, except at low power where the fractional tritium density is small.

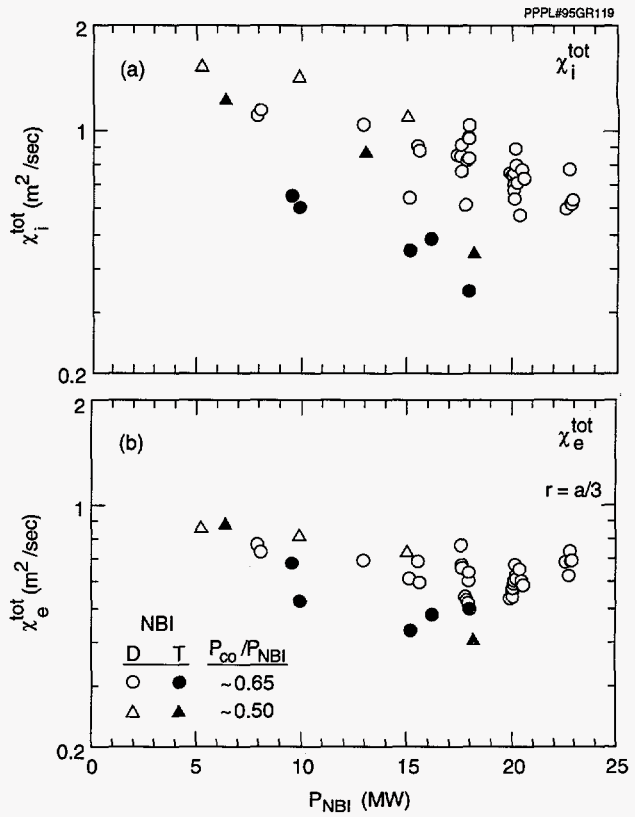

Figure 35. *Variation of (a) ion thermal diffusivity χ_i^{tot} and (b) electron thermal diffusivity χ_e^{tot}, with injected power P_{NBI} at r/a =1/3.*

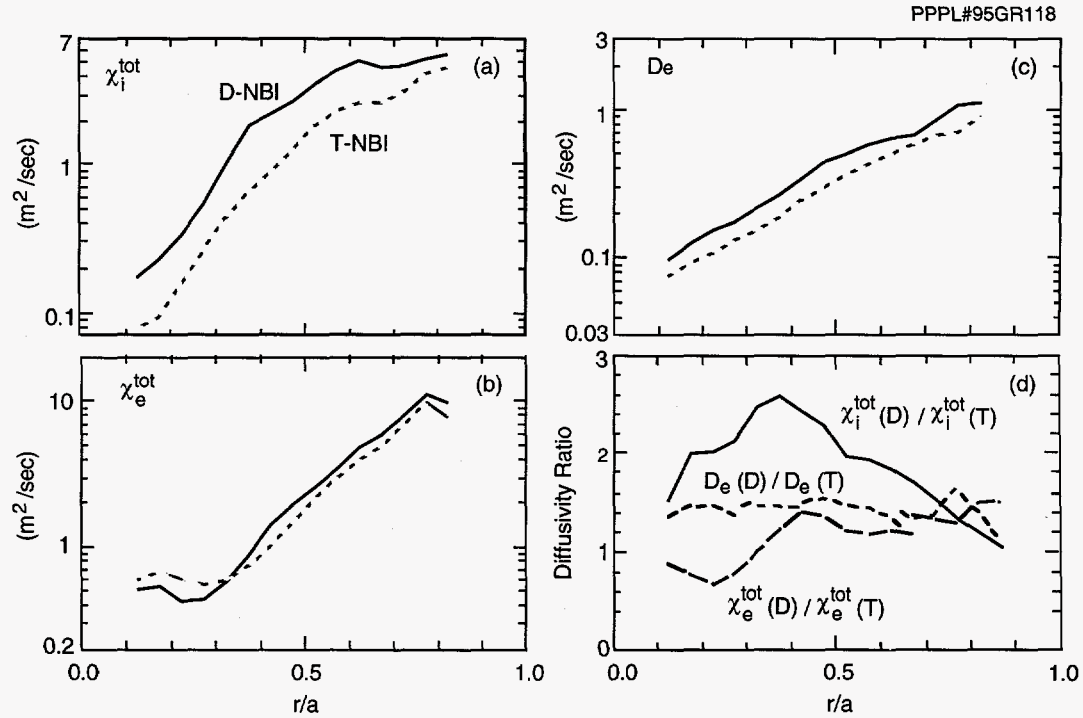

Figure 34. *Comparison of transport coefficients inferred between the deuterium- and tritium-NBI plasmas of Fig. 31, (a) ion thermal diffusivity χ_i^{tot}, (b) electron thermal diffusivity χ_e^{tot}, (c) electron particle diffusivity D_e, (d) ratio of the deuterium- and tritium-NBI.*

The isotopic mix of these plasma has been characterized by the average mass of the central thermal hydrogenic ions <A> within r/a = 0.5, since this radius contains more than three fourths of the thermal stored energy. This volume-averaged mass is approximately equal to the local average hydrogenic mass at r = a/3. The plasmas studied range from <A> = 1.9 (deuterium-NBI) to <A> = 2.1 (with 6.4 MW tritium-NBI) to <A> = 2.5 (with 18 MW tritium-NBI). Thus, the core of the 18-MW tritium-NBI plasmas has the same average isotopic mix as expected for ITER and future reactors. The observed variations of the plasma parameters and transport coefficients for the tritium-NBI plasmas relative to the matched deuterium-NBI plasmas can be expressed as a power law dependence on <A>. Strong dependencies on <A> are inferred, due to the strong variations observed and the moderate range of <A> studied. The total stored energy analyzed in this fashion scales as $W_{tot} \propto \langle A \rangle^{0.82\pm0.05}$ and the thermal stored energy scales as $W_{thermal} \propto \langle A \rangle^{0.89\pm0.10}$. In the plasma core, r/a ~ 1/3, $\chi_i^{tot} \propto \langle A \rangle^{-2.6\pm0.3}$ and $D_e \propto \langle A \rangle^{-1.4\pm0.2}$ for fixed injected power. The uncertainties indicated for these scalings represent the standard deviations on the fits to the nominal data points. The variation in electron thermal diffusivity is much smaller than for ion thermal diffusivity or electron particle diffusivity and may not be significant.

Momentum Transport

The isotopic scaling of the momentum transport is measured in a companion scan of the applied neutral-beam torque using unidirectional co-only injection. As shown in Fig. 36, the central angular momentum density is about 50% higher for tritium-NBI than for deuterium-NBI at fixed injected torque. Much of the increase in momentum density is due to the higher tritium mass. The momentum transport is analyzed in terms of an angular momentum diffusivity

$$\Gamma_\phi \equiv - \chi_\phi^{tot} R\, n_i\, m_i\, \nabla v_\phi ,$$

where Γ_ϕ is the radial flux of angular momentum. Figure 37 compares the inferred momentum diffusivity χ_ϕ^{tot} for tritium-NBI and deuterium-NBI plasmas in the torque scan at r/a ~ 1/3. For the highest torque tritium-NBI plasma, achieved with P_{NBI} = 12 MW, the inferred momentum diffusivity was reduced by about 30% relative to similar deuterium-NBI plasmas.

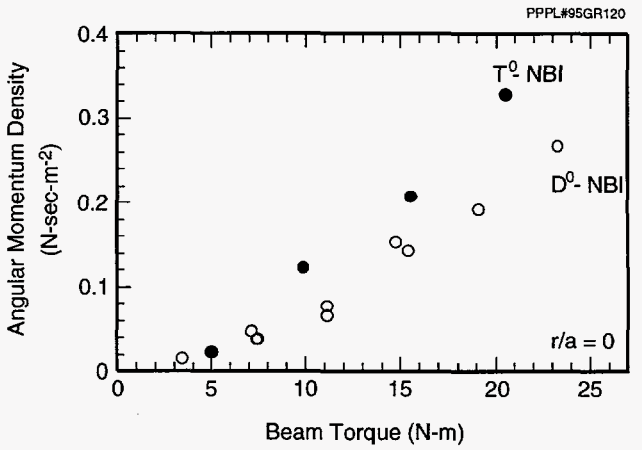

Figure 36. Increase in central angular momentum density with increasing applied beam torque with unidirectional co-only injection for both tritium-NBI and deuterium-NBI.

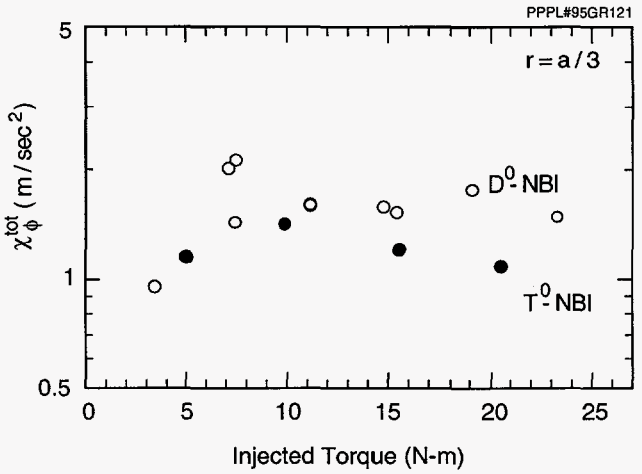

Figure 37. Comparison of the inferred momentum diffusivity χ_ϕ^{tot} for deuterium- and tritium-NBI versus the injected-beam torque.

This reduction is similar to the reduction of the inferred momentum diffusivity found for near-balanced plasmas at this power level, and it supports previous observations that the momentum and the ion-thermal transport are correlated and may be due to the same mechanism.

Discussion

The observed strong decrease in the inferred momentum diffusivity with isotopic mass is opposite to what is expected for simple gyro-Bohm theoretical transport models. However, these models are showing increasing sophistication in their nonlinear treatment of experimental conditions, such as the presence

of multiple-ion species and nonthermal ions.[51,52] Adequate comparison with these models will await numerical simulation of the experimental conditions. These results are also to be contrasted with studies[53] of isotopic scaling between hydrogen and deuterium L-mode plasmas in TFTR, where only a weak improvement in the thermal confinement was observed, and no significant change in ion-energy transport was found.

Previous studies of transport in deuterium supershots have noted a favorable correlation of the inferred momentum diffusivity with the ion temperature and other related parameters,[54] with ion thermal diffusivity varying roughly as the inverse of the ion temperature ($1/T_i$) in the plasma core. In addition, a number of the microturbulence theories predict a strong dependence of the plasma transport on the ratio of ion temperature to electron temperature (T_i/T_e). Such dependencies could amplify an intrinsic isotopic dependence and make it appear to be stronger. However, as shown in Fig. 38, by comparing tritium-NBI plasmas with deuterium-NBI plasmas of slightly higher injected power, the isotopic variation in the ion thermal diffusivity at r = a/3 is clearly apparent at fixed local ion temperature. Despite the differences in injected power, the cluster of tritium-NBI and deuterium-NBI points near $T_i \sim 15$ keV on Fig. 38 have the same local values of electron density and electron density scale length (L_{n_e}) to better than 10%. There is no significant difference observed in either the toroidal rotation velocity (v_ϕ) or in the gradient toroidal rotation velocity (∇v_ϕ) for these plasmas. The tritium-NBI plasmas have about 10% lower values of L_{T_i} and L_{T_e}, indicating slightly stronger gradients, which would be expected by ion-temperature gradient-turbulence models to correlate with "increased" transport. Both the tritium-NBI and deuterium-NBI plasmas have $T_i/T_e = 2.9 \pm 0.1$. Thus, the strong change in the ion thermal diffusivity is not due to a dependence on other local thermal plasma parameters, and it appears to depend only on the change in isotopic content.

If the dependence on the average mass of the central thermal hydrogenic ions <A> is expressed at approximately constant local plasma parameters, particularly constant ion temperature, the relation $\chi_i^{tot} \propto \langle A \rangle^{-1.8 \pm 0.2}$ is inferred. It is interesting that, when combined with the correlation of the ion thermal diffusivity and the inverse of the ion temperature, this implies that roughly $\chi_i \propto A^{-1} \rho_i^2$ (for fixed B) opposite

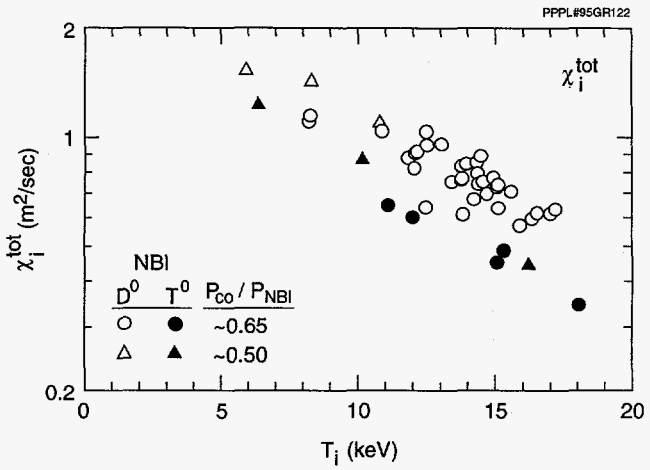

Figure 38. Variation of ion thermal diffusivity χ_i^{tot} with ion temperature T_i at r/a = 1/3.

to the gyro-Bohm dependence. This disagreement with the theoretical scalings is much stronger than that implied by the global scalings.

Summary

The confinement and local transport have been analyzed in high-confinement supershot plasmas heated by either deuterium or tritium neutral beams. For strongly heated plasmas, tritium-fueled plasmas have 25% higher stored energy and energy confinement than comparable deuterium-fueled plasmas, implying that $W_{tot} \propto \langle A \rangle^{0.82 \pm 0.05}$ for these plasmas. Of this increase in stored energy, 65-80% is due to the thermal plasma, resulting in a thermal confinement scaling of $W_{thermal} \propto \langle A \rangle^{0.89 \pm 0.10}$. Analysis of the thermal transport indicates that most of the improvement is due to a large drop in ion thermal diffusivity and a small decrease in electron thermal diffusivity. The implied isotopic mass scalings are $\chi_i^{tot} \propto \langle A \rangle^{-2.6 \pm 0.3}$ and $D_e \propto \langle A \rangle^{-1.4 \pm 0.2}$ for fixed injected power. A similar decrease is observed for the inferred momentum diffusivity in plasmas with unidirectional injection. For fixed "local" plasma parameters, in particular fixed ion temperature, an approximate scaling of $\chi_i^{tot} \propto \langle A \rangle^{-1.8 \pm 0.2}$ is obtained. The observed isotopic variation of ion thermal diffusivity cannot be explained by a simple dependence on T_i/T_e or by its previously observed correlation with the inverse of the ion temperature in the supershot regime. These strong scalings of ion thermal diffusivity and energy confinement in D-T plasmas have very favorable implications for D-T operation in ITER and future reactors.

TAE Modes and MHD Activity in D-T Plasmas

A topic of concern for ITER and other D-T burning devices is the potential for destabilization of the plasma due to the presence of a high-energy fusion alpha population. The high-power deuterium and tritium experiments on TFTR have produced fusion alpha parameters similar to those expected on ITER. The achieved values for alpha parameters affecting stability, β_α/β and the $R\nabla\beta_\alpha$, in TFTR deuterium-tritium shots are one-half to one-third those predicted in the ITER Engineering Design Activity. Studies of the initial TFTR deuterium-tritium plasmas find no evidence that the presence of the fast fusion alpha population has affected the stability of MHD, with the possible exception of toroidal Alfvén eigenmodes (TAEs). The initial TFTR deuterium-tritium plasmas had MHD activity similar to that commonly seen in deuterium plasmas. Operation of TFTR at plasma currents of 2.0-2.5 MA has greatly reduced the deleterious effects of MHD commonly observed at lower currents. Even at these higher currents, the performance of TFTR is limited by β-limit disruptions. The effects of MHD on D-T fusion alphas was similar to effects observed on other fusion products in D-only plasmas.

MHD Activity in the Initial Deuterium-Tritium Plasmas

Low m and n (m/n = 2/1, 3/2, 1/1, etc.) coherent MHD modes have been observed in the initial D-T plasmas on TFTR. The amplitude, frequency of occurrence, and effect on plasma performance are similar to those observed in comparison D-only plasmas. The saturated level of the MHD activity agrees well with the predictions of the neoclassical model of MHD modes.[55] However, the theoretical models of the MHD behavior do not, as yet, explain why the higher m's (3, 4 or 5) are more commonly observed than the m,n = 2,1. Modeling of the effect of MHD on confinement suggests that the MHD can be responsible for up to a 30% decrease in the energy confinement time in the worst cases,[56] consistent with the degradations observed. In cases of weak MHD, typical of most of the higher current plasmas ($I_p > 2.0$ MA, $q_{sh} < 4$), the effect is usually less than 5%. The decrease in neutron rate is consistent with the changes in the equilibrium plasma. It does not appear necessary to assume anomalous losses of fast beam ions to explain this decrease. Enhanced losses of fusion alphas, correlated with the presence of MHD, are observed in D-T plasmas. The losses are similar to those previously reported for D-D plasmas.[17]

Fishbone and sawtooth activity have also been observed in D-T plasmas. At present, there is no evidence that fusion alphas have affected sawtooth or fishbone stability. There is a tendency for the fishbone activity to be stronger in D-T plasmas; however, that may be more correlated with the somewhat broader pressure profiles often found in D-T plasmas, as compared to D-only plasmas under similar conditions.

The β Limit and Disruptions in Deuterium-Tritium Plasmas

The D-T fusion power which TFTR can produce is limited by pressure-driven instabilities which can cause major or minor disruptions. The disruptive β limit in D-only NBI-heated plasmas and D-T NBI-heated plasmas appears to be similar. The β limit follows approximately the dependence predicted in the Troyon formula. The time history of the normalized toroidal β [$\beta_N = a_p(m)\ B_t(T)\ \beta_t/I_p(MA)$] for three D-T plasma discharges which include a major and minor disruption are shown in Fig. 39. In this set of data, as well as the broader data set including D-only operation, there is some variation in the normalized toroidal β (β_N) which can be reached before major or minor disruptions occur. The variations may be correlated

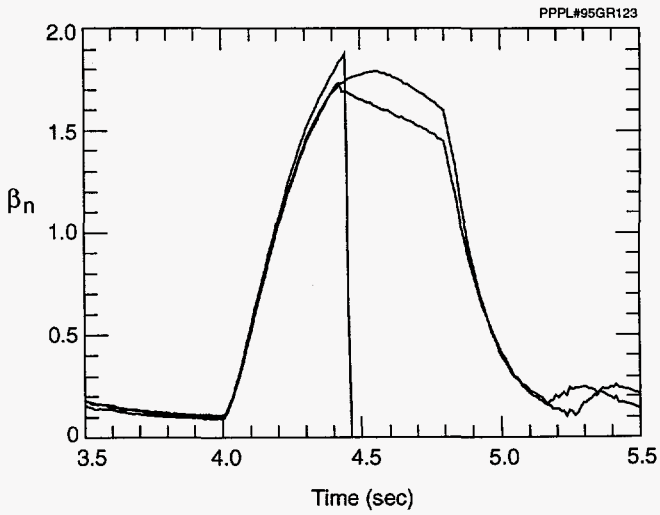

Figure 39. *Time evolution of normalized toroidal beta (β_N) for three of the highest fusion power D-T plasma discharges.*

with changes in the peakedness of the plasma pressure profile. Some of the variation might also be attributed to a slightly stronger dependence on minor radius than is predicted in the Troyon formalism.

The high-β disruption in D-only or D-T plasmas appears to be the result of a combination of an n=1 internal kink coupled to an external kink mode and a toroidally and poloidally localized ballooning mode.[57] In Fig. 40 is shown contour plots of the electron temperature as measured at a 500-kHz digitizing rate by the two electron cyclotron emission grating polychromators separated by 126° in the toroidal direction. The simultaneous absence of the ballooning mode on one grating polychromator, and its presence on the second, clearly demonstrates the toroidal localization of the mode. The ratio of the frequency of the ballooning mode and the n=1 kink indicate that the ballooning mode has a toroidal wave number of about 10-15 (assuming only toroidal rotation). The kink mode can have a growth rate in excess of 10^4/sec. This growth rate is much faster than the Sweet-Parker or tearing-mode growth rates, and slower than the ideal growth rate. The experimentally observed growth rates are in reasonable agreement with the growth rate for collisionless plasmas. Here, the inertia of the plasma plays a more important role than the resistivity[58] and the growth rate is given approximately by $\gamma\tau_{Alfvén} = q'\rho_s/q$ or $\gamma \approx 3 \times 10^4$/sec.

The radial structure of the kink mode suggests coupling of a predominantly internal kink to a weaker external kink. The profile of the radial displacement of the flux surface due to the kink (and the ballooning

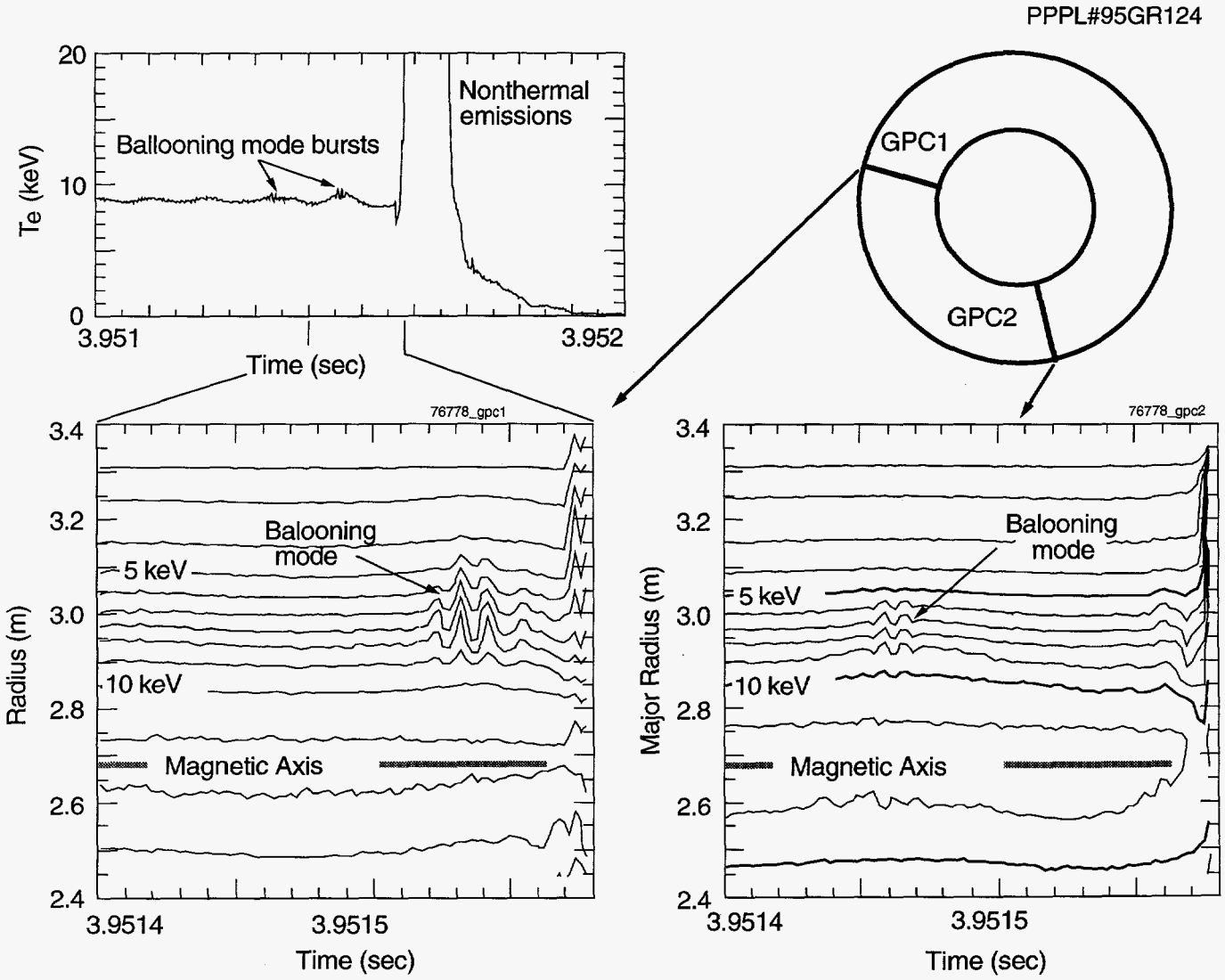

Figure 40. *Contours of electron temperature prior to a high-β disruption showing the n=1 kink and ballooning precursors.*

mode) for a D-T plasma discharge generating a peak fusion power greater than 9 MW is shown in Fig. 41. For comparison is the radial displacement as predicted by the PEST stability code. While the PEST code predicts that the n=1 kink is unstable for this disrupting plasma, it also in general predicts that most supershot plasmas are similarly unstable, as the safety factor on axis q(0) is typically less than unity[59] and the plasma pressure is sufficient to drive an ideal mode.

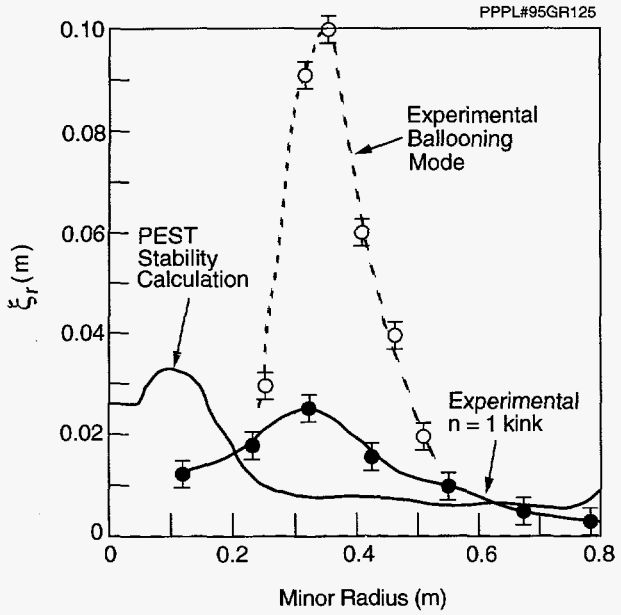

Figure 41. *Radial profile of the radial displacement of the flux surface experimentally measured and compared to the linear PEST code calculation.*

The kink mode can locally decrease the magnetic shear and increase the local pressure gradient so that the ballooning mode is locally destabilized. The thermal quench phase may result from destruction of flux surfaces by the nonlinear growth of the n=1 kink, possibly aided by the presence of the ballooning modes. There is no evidence for a global magnetic reconnection as is seen in high-density disruptions. The electron temperature collapses on a time scale of several hundred μsec with no local flatspots, indicating that the magnetic geometry is destroyed uniformly over the plasma cross section. The thermal quench phase is typically preceded by a large nonthermal ECE burst. The burst is at least 10 to 20 times larger than is predicted by the fast compression of electrons by a rapidly growing internal kink displacement.[60]

Minor disruptions are more commonly observed than major disruptions. The type of precursor activity and the parameter regime in which they appear are very similar to those for the major disruptions. While the minor disruptions do not result in termination of the plasma discharge, they do result in strongly degraded performance, compromising the usefulness of such plasma discharges for D-T physics studies. While the minor disruptions result in a central electron temperature drop and a burst of H_α emission from the plasma edge, they are not related to either sawteeth (which have a resistive precursor and a reconnection in the core) or edge localized modes (the H_α burst results from a transient deposition of plasma energy from the core, rather than the plasma edge, on the limiter). The minor disruptions can cause a transient burst of fusion product losses. Figure 42 shows the lost alpha detector signal from which it is estimated that 0.1% of the confined fast alphas were lost in several hundred μsecs. The loss is smaller than in major disruptions, where up to 20% of the stored energy in the fast alpha population may be lost in several bursts spanning a few msec. This level and rate of alpha loss could cause severe damage to internal hardware in ITER.

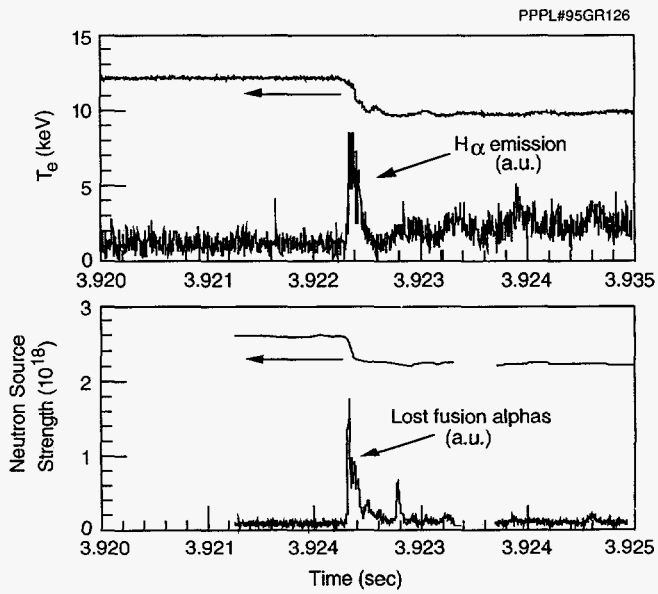

Figure 42. *Central electron temperature, edge H_α, global neutron rate, and lost-alpha rate through a minor disruption.*

Toroidal Alfvén Eigenmodes Studies

In ITER and future fusion reactors, the toroidal Alfvén eigenmode (TAE) activity may result in en-

hanced fusion alpha losses, causing decreased performance and endangering internal components. An important goal of the TFTR D-T experiments is to improve the theoretical understanding of toroidal Alfvén eigenmodes, resulting in a higher level of confidence in code simulations of TAE activity in ITER. Fluctuations in the TAE range of frequencies have been observed under many conditions in TFTR, including shots with NBI at low magnetic field, ICRF H-minority heated plasmas, supershots, L-mode plasmas and in Ohmic shots with pellet injection. Figure 43 compares the observed frequency of magnetic fluctuations to a semi-empirical scaling relation for the expected TAE frequencies.

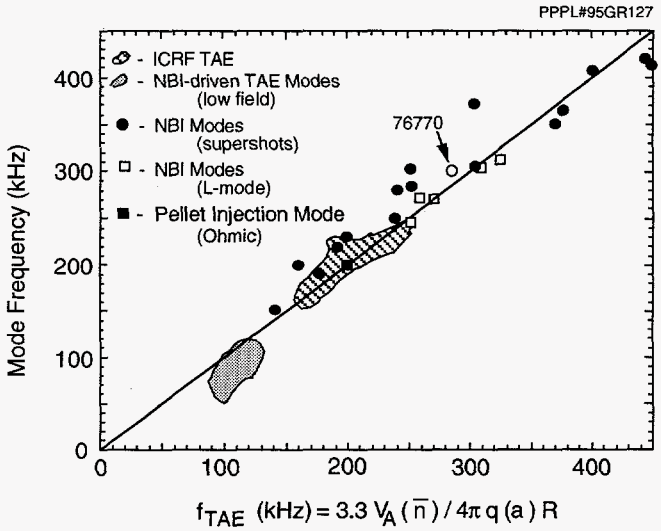

Figure 43. *Scaling of the TAE activity frequency versus a semi-empirical scaling relation.*

The toroidal Alfvén eigenmode is a natural resonance of the plasma for which the frequency is determined by the ratio of the plasma mass to the restoring force due to sheared displacement of the magnetic field. The modes are usually damped by several mechanisms including Landau damping on the electrons, beam ions, and thermal ions. The modes are destabilized by a super-Alfvénic fast-ion population.

An extensive series of experiments on TAE modes driven by fast ions from neutral-beam injection[61] at B_t = 1-1.2 T and ICRF heating of an H-minority species[62] at B_t = 3 T has been carried out on TFTR for the purposes of experimentally verifying the instability thresholds predicted by the theoretical models. The range of parameters covered by these experiments is indicated by the shaded regions shown in Figure 43. These experiments have been very useful in the benchmarking and improvement of the codes which are used to predict alpha-driven TAE behavior in TFTR and ITER.

The TAE activity is primarily studied using the Mirnov coil system to measure the magnetic fluctuations at the plasma edge and the reflectometer for measurements of density fluctuations in the plasma interior. The TAE modes have also been observed with the beam emission spectroscopy (BES) system and the electron cyclotron emission (ECE) grating polychromator. The Mirnov system is used to measure the toroidal wave number of TAE modes and the reflectometer provides an internal measure of the TAE mode amplitude.

In experiments using ICRF H-minority heating to create a super-Alfvénic fast-ion tail, a cluster of very narrow peaks in the frequency spectrum are typically observed. The separate peaks, corresponding to different toroidal mode numbers n, are separated by 2 to 4 kHz. The measured toroidal mode numbers range from as low as three in the low-current ICRF plasmas to higher than eight at higher plasma currents. Calculations of the mode frequency and stability with the NOVA-K code find reasonable agreement with the measured frequency. Figure 44 shows the magnetic fluctuation spectrum from an ICRF-heated plasma with the experimentally determined toroidal mode numbers from the Mirnov coil array[63] and the theoretically calculated TAE frequencies marked. The TAE modes have also been observed with 64-MHz ICRF

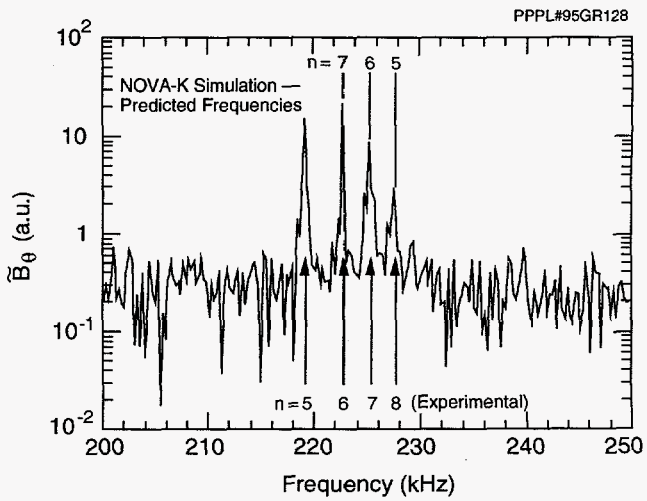

Figure 44. *Comparison of the measured magnetic fluctuation spectrum and toroidal mode numbers to NOVA-K code predictions.*

H-minority heating at a toroidal field of 4.6 T. In these experiments, the Mirnov and reflectometer spectra tend to have just one or two strong peaks (Fig. 45). The toroidal mode number is found to increase with increasing plasma current, dropping from n=6 at 1.8 MA to n=3 at 1.4 MA.

The fast-ion loss was measured and the level of loss was correlated with the measured amplitude of TAE activity over roughly two orders of magnitude.[17] These experiments used both ICRF-tail and NBI fast-ion-driven TAE modes. The TAE-induced diffusion of a trapped fast-ion population is suspected of being the source of ripple-trapped ions responsible for the recently detected damage to the TFTR vacuum vessel.

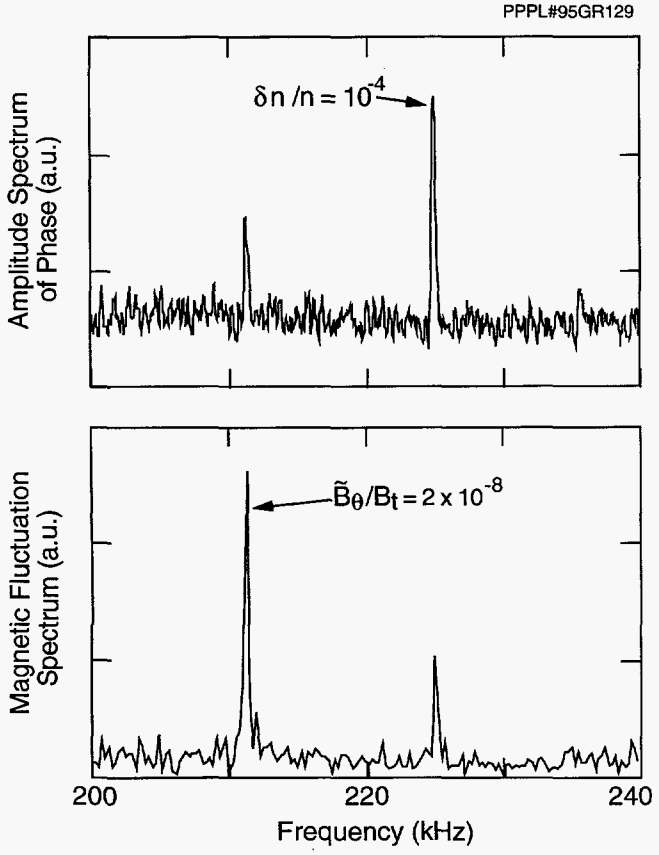

Figure 45. *Reflectometer and Mirnov coil spectra for ion cyclotron range of frequencies plasma discharge.*

Toroidal Alfvén Eigenmodes in Deuterium-Tritium Plasmas

The highest fusion power shots on TFTR have produced fast-alpha populations comparable with some dimensionless alpha parameters comparable to the projected fast-alpha populations for ITER, e.g., $R\nabla\beta_\alpha$. In Fig. 46 is shown the typical structure of a TAE mode, superimposed on the alpha-pressure profile as calculated in the TRANSP code. The amplitudes of the TAE modes peak at large minor radius and are typically only weakly coupled to the fusion alphas. In typical TFTR deuterium-tritium supershots, the thermal and beam ion Landau damping are stronger than the fusion-alpha drive. Experiments were successfully done to reduce the thermal ion Landau damping; however, the alpha-drive was still not sufficient to overcome the beam ion Landau damping.[64,65]

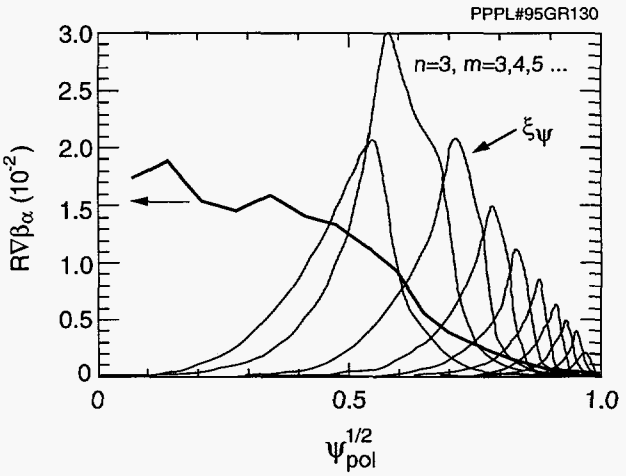

Figure 46. *Typical toroidal Alfvén eigenmode (TAE) mode structure as calculated with the NOVA-K code.*

Experimentally the search for alpha-driven TAE activity in D-T plasmas is complicated by the presence of a mode near the expected TAE frequency in both D-D and D-T neutral-beam-injection heated plasmas. The mode has a relatively broad peak in frequency, with a spectral width of about 50 kHz at 300 kHz. The frequency of the NBI-driven activity is found to approximately fit the semi-empirical scaling relation developed from the H-minority ICRF and low-toroidal-field (B_t = 1 T) NBI-driven TAE mode data (Fig. 43). A mode at similar frequency has also been observed near the plasma center with the reflectometer; it is not known at this time whether the modes are the same. The toroidal mode number found for this peak is n=0. Nonlinear numerical simulations of TAE modes by Spong[66] have predicted that the interactions of multiple TAE modes would result in an n=0 mode. The modes may represent a "thermal" level of excitation or be driven by fast-beam ions. For these plasmas, the beam-ion velocity is one-third to one-fifth the Alfvén velocity.

In Fig. 47 is shown the spectrum of the edge magnetic fluctuations for a D-T plasma discharge with 7.5 MW of fusion power and for a similar plasma discharge at 6.5 MW and a D-only shot. The mode amplitude has increased by a factor of 2-3 in the 7.5 MW discharge. The NOVA-K code[64] finds n=5 and n=6 core-localized modes in the region where q < 1 in this plasma (Fig. 48). The localization of the mode near the plasma core increases the coupling of the fusion alphas, which makes the mode unstable. The calculated TAE mode frequency from the NOVA code was about 250 kHz, lower than the experimental frequency of 300 kHz. In this experiment the toroidal mode number was not measured.

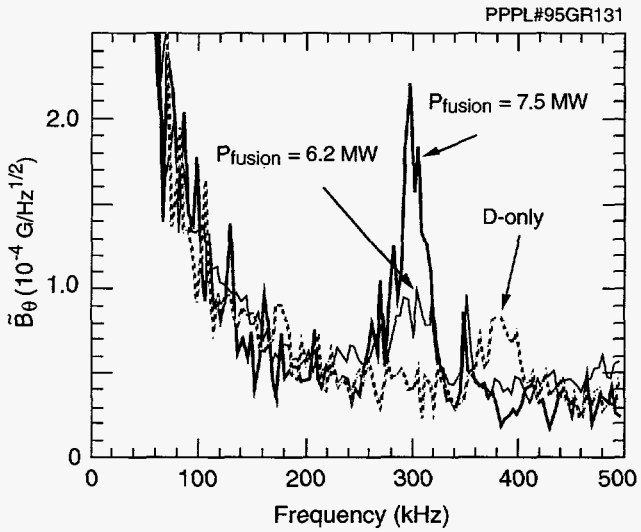

Figure 47. Spectrum of magnetic fluctuations for D-T plasmas generating 7.5 MW and 6.5 MW, and for a D-only plasma.

Discussion

The high-power D-T experiments in TFTR have provided the first look at the effect on MHD activity of a fusion alpha population similar to that expected in ITER. In the TFTR D-T experiments to date, there is no evidence for alpha loss due to alpha-driven instabilities; however, one of the highest fusion power plasma discharges may have evidence of alpha-driven TAE activity. Theoretical calculations suggest that presently achieved alpha parameters in TFTR are close to the stability threshold for alpha-driven TAE modes. Low-m MHD, fishbones, and disruptions appear very much the same in D-only and D-T plasmas. At the higher currents used in the D-T experiments, the performance of TFTR is still limited by β-limit disruptions. Studies of the β-limiting disruptions with

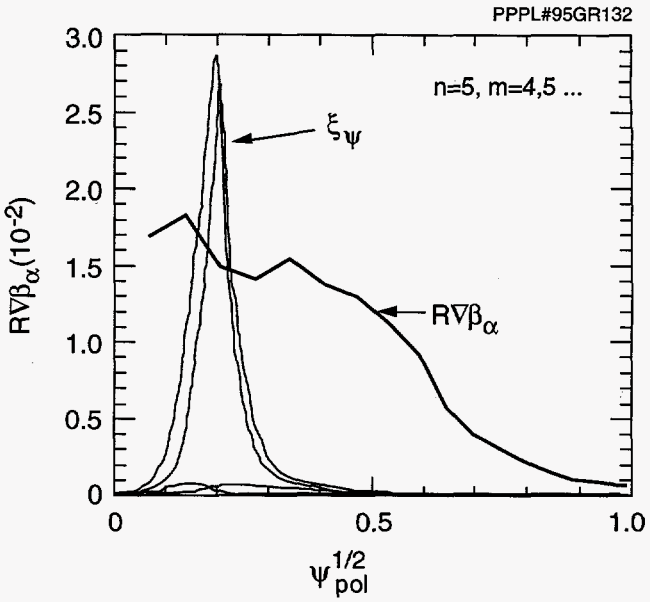

Figure 48. The NOVA-K code calculation of the mode structure for the 7.5 MW fusion power plasma discharge.

the extensive MHD diagnostics set has provided valuable information on the structure of the disruption precursors. In particular, TFTR has provided the first clear evidence of strong ballooning activity in high normalized toroidal beta plasmas. The enhanced loss of D-T fusion alphas during MHD activity, e.g., (2,1) modes, is similar to that observed in D-only plasmas for other fusion products.

ICRF Heating of D-T Plasmas in TFTR

Future D-T fusion devices, such as the ITER, emphasize ion cyclotron range of frequencies (ICRF) heating, but until now no experimental database has been available to provide a benchmark for the radio-frequency (rf) computer codes which predict performance in plasmas containing tritium. The TFTR has performed the first experiments which combine ICRF heating with tritium plasmas.

The deuterium-tritium ICRF program on TFTR has two major objectives: first to study D-T radio-frequency physics and second to enhance the performance of D-T supershot plasmas,[31] and eventually L-mode plasmas. Plasma reactivity can be increased by directly heating tritium ions via second harmonic ICRF. Significant increases in the central electron temperature of supershot plasmas via heating by collisions

with minority tail ions[67] or direct electron heating may result in lengthened alpha-particle slowing times and increased alpha-particle pressure in D-T plasmas.

Initial experiments on TFTR were directed primarily towards investigating the rf physics of ICRF-heated plasmas containing tritium. These experiments were conducted at 43 MHz with out-of-phase current strap excitation into D-T plasmas fueled by 18-24 MW of approximately 100 keV neutral-beam-injection. Results from twenty-one ICRF-heated D-T plasmas which have explored n_T/n_e concentrations from approximately 6% to 40% are discussed. In addition, the toroidal field was scanned to vary the location of the second harmonic tritium resonance from R = 2.6 m to 3.0 m in full bore (R = 2.62 m, a = 0.96 m) plasmas with the Shafranov-shifted magnetic axis at R ~ 2.8 m. Of these D-T plasmas, 16 plasma discharges utilized 90% power modulation (f_{mod} = 5-10 Hz) to investigate the relative strength of the possible heating mechanisms.

Plasma Performance

The maximum ICRF power coupled thus far into a D-T plasma has been 5.8 MW with a 2% ^{3}He minority species and 4.9 MW without a ^{3}He minority. Some plasmas had ^{3}He added to avoid eigenmode effects on the ICRF coupling. The rf power was launched by up to four antennas[68] at the midplane, on the low-field side of the plasma. Figure 49 shows the evolution of two D-T plasmas heated by 23.5 MW of neutral-beam injection. The plasma discharge shown by the solid line had an additional 5.5 MW of ICRF heating [Fig. 49(a)]. Both plasmas had a 2% ^{3}He minority, and 60% of the beam-injected power was in tritium. Based on comparisons of the measured D-T neutron production rate with the rate calculated by the SNAP time-independent equilibrium code,[69] the tritium fraction at the center of the plasma, $n_T/(n_T + n_D + n_H)$, appears to be only 25-30% due to significant deuterium (and minimal tritium) recycling from the carbon limiters on the

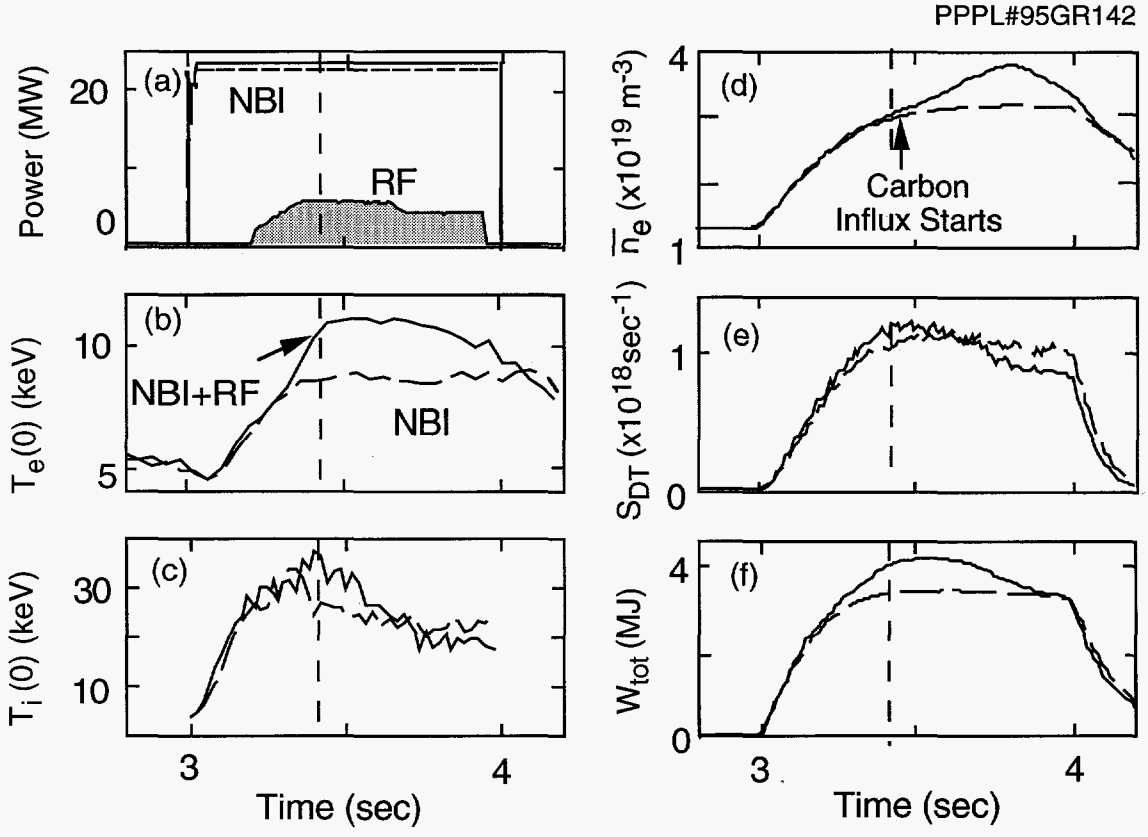

Figure 49. Time evolution of (a) the neutral-beam-injection and ICRF power, (b) central electron temperature, (c) central ion temperature, (d) line-averaged density, (e) D-T neutron production rate, and (f) magnetically measured stored energy for two plasmas with 23.5 MW of neutral-beam-injection (60% in tritium). The plasma indicated by the solid line had 5.5 MW of 43 MHz ion cyclotron range of frequencies heating. Both plasmas had a 2% ^{3}He minority, the ^{3}He fundamental resonance is degenerate with the $2\Omega_T$ resonance.

inner and outer walls. In the core, $n_H/(n_T + n_D + n_H)$ is assumed to be about 5%, half the edge value measured by spectroscopy. For the two plasmas in Fig. 49, the magnetic field at the Shafranov-shifted magnetic axis was 4.2 T, placing the second harmonic tritium (and fundamental ^{3}He minority) resonance at the axis. With the addition of ICRF, the central electron temperature, measured by electron cyclotron emission, increased from 8 to 10.5 keV at 3.4 sec [Fig. 49(b)], due to fast wave direct electron heating (via Landau damping and transit time magnetic pumping) and heating by collisions with minority tail ions. The central ion temperature, measured by charge-exchange recombination spectroscopy, initially increased from 26 to 36 keV at 3.4 sec [Fig. 49(c)]. However, it later decreased as an enhanced carbon influx[70] developed. This carbon influx also resulted in increased line-averaged density [Fig. 49(d)] approximately 400 msec after the start of ICRF heating. Prior to this influx, the stored energy (W_{tot}) increased from 3.4 to 4.1 MJ [Fig. 49(f)] with the addition of radio-frequency, and the excess perpendicular component of the stored energy ($W_{ex\perp} = 3W_\perp - 2W_{tot}$) increased by 200-250 kJ due to the presence of an rf tail. There was also a 10% enhancement in the D-T neutron production rate to approximately 1.2×10^{18} sec^{-1}. Figure 50 shows the ion and electron temperature profiles at 3.4 sec (the time of peak performance). A significant increase in temperature is seen out to r/a ~ 0.3. The core ion heating observed is consistent with $2\Omega_T$ heating, since an analogous increase in core heating was noticeably absent in D-^{3}He minority experiments.[67] A deuterium-tritium plasma, which was essentially identical to the ICRF-heated plasma discharge shown in Fig. 50, but with no ^{3}He minority and only 4.4 MW of ICRF, reached a core ion temperature of 32 keV.

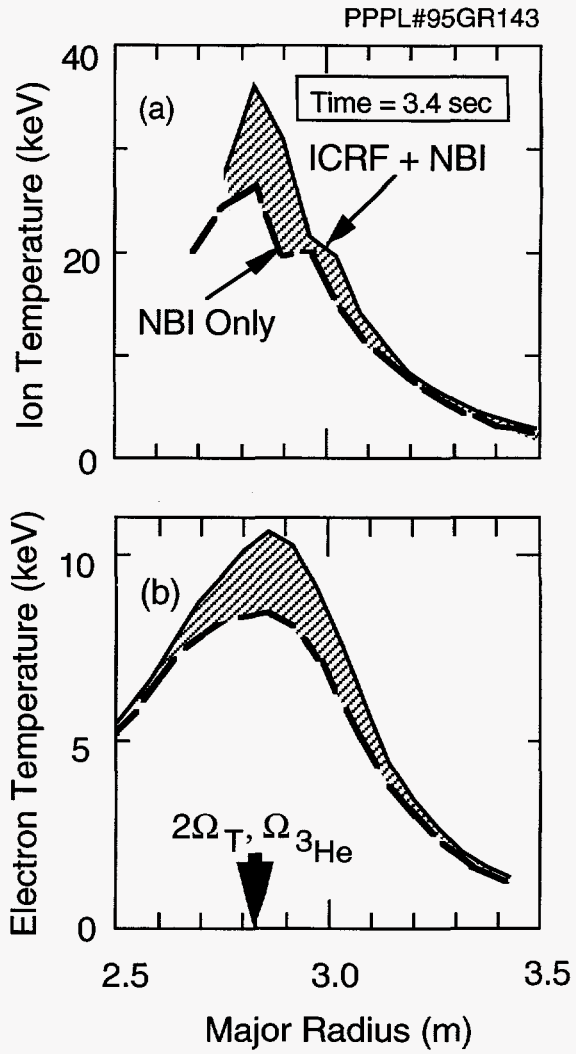

Figure 50. *Comparison of (a) ion and (b) electron temperature profiles for the two D-T plasmas in Fig. 49 at the time shown by the vertical dashed line in Fig. 49. The plasma discharge indicated by the bold solid line had 5.5 MW of ICRF heating.*

Radio-Frequency Physics

Radio-frequency power modulation[71] provides a technique for studying the power deposition directly. Sixteen of the ICRF-heated D-T discharges utilized 90% power modulation (f_{mod} = 5-10 Hz). The changes in the electron temperature and density profiles were measured by electron cyclotron emission and multichord, far-infrared interferometry, respectively. The electron temperature response showed no delay, consistent with direct electron heating. Density modulation contributed up to 10% to the calculated power absorbed directly by electrons.

Figure 51 shows the fraction of power absorbed by ions and electrons during rf modulation as a function of the fraction of neutral-beam power in tritium for three plasmas with the $2\Omega_T$ resonance at the magnetic axis. Although no ^{3}He minority was added to these plasmas, there may have been about 0.2% ^{3}He concentration remaining from prior D-^{3}He discharges. The neutral-beam-injection and rf powers for this scan were 17-20 MW and 3.6-3.8 MW, respectively. The absorbed power fraction is calculated noting that about 10% of the rf power is lost in the antennas. The total power absorbed by the plasma, determined from the modulation in the magnetic measurement, was typi-

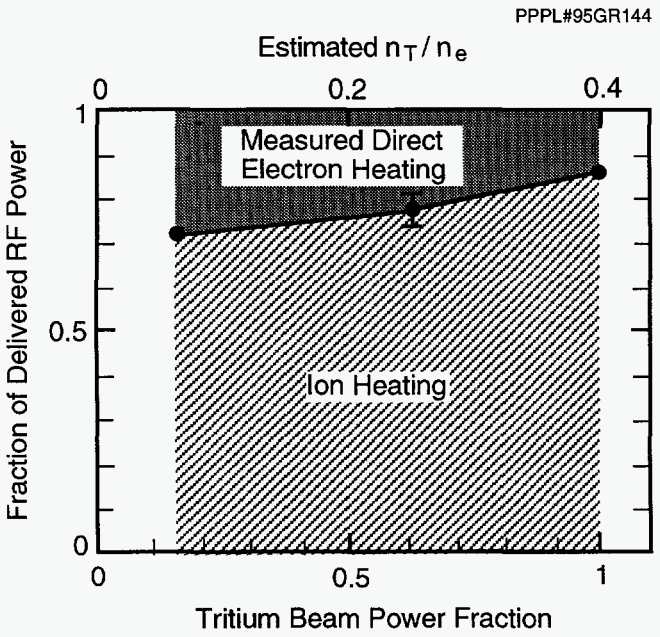

Figure 51. *Fraction of radio-frequency power delivered directly to electrons and ions as a function of tritium-beam power fraction during radio-frequency modulation. Data are for plasmas with no ^3He minority, 3.6-3.8 MW of radio-frequency power input to the antenna, 17-20 MW of neutral-beam injection and with the $2\Omega_T$ resonance at the magnetic axis.*

cally 80%±15% of the power leaving the antenna. The electron absorbed power fraction decreased from 25% to 15% when the tritium-beam fraction increased from 15% to 100% (the corresponding estimated increase in the ratio of the tritium density to electron density n_T/n_e was from about 6% to about 40%). This behavior is expected as a result of the competition between direct electron heating and $2\Omega_T$ heating of the tritium-beam ions. There is also possibly some mode conversion, although because of the limited tritium fraction and magnetic field, the mode conversion around the two-ion hybrid resonance did not move far enough into the core to enable detection in the present experiments.

The rf modulation results for the plasma with a 60% tritium-beam fraction in Fig. 51 were compared in detail with two independent computer codes. In the first, a single-time-point analysis was done with the PICES code,[72] a two-dimensional (2-D), reduced-order, full-wave code, using multiple toroidal mode numbers weighted by the antenna spectrum. The predicted power deposition profiles were calculated using the experimental temperature and density profiles (including beam ions with an effective temperature of approximately 60 keV on axis). Of the rf power leaving the antenna (about 10% antenna loss), 36% was absorbed at the $2\Omega_T$ resonance near the core (26% going to tritium beams and 10% to thermal tritium) and 7% was absorbed at the deuterium (and carbon) fundamental resonance located at r/a ~ 0.8. Twenty-six percent of the rf power was absorbed directly by electron Landau damping and transit time magnetic pumping near the core, in good agreement with the rf modulation data. This code also calculates that approximately 30% of the rf power is absorbed at the intersection of deuterium ion fundamental resonance (R ~ 2.1 m) and the mode conversion layer near the last closed flux surface. There is so far no experimental evidence supporting or refuting this effect. A time-dependent analysis of the power deposition profiles was also obtained for the same plasma with the TRANSP transport analysis code.[47] The rf package in TRANSP consists of the 2-D reduced-order wave solver, SPRUCE,[73] combined with the bounce-averaged Fokker-Planck solver, the FPP code.[74] Power deposition was computed for a single toroidal mode number representative of the peak of the launched antenna spectrum. Experimental density and temperature profiles were used for the thermal ions and electrons, while the beam density and effective temperature profiles were obtained using the Monte Carlo beam deposition subroutines. From this analysis, the ratio of the ion-to-electron power absorption is about 3.3, with 80% of the ion heating occurring within r/a = 0.6. These results are in relatively close agreement with the data.

Figure 52 shows the result of varying the toroidal magnetic field to scan the location of the $2\Omega_T$ resonance from R = 2.5 m to R = 3.0 m (the Shafranov-shifted axis was at approximately R = 2.8 m). Data are shown for four deuterium-tritium plasmas with 60% of the neutral-beam power in tritium. The neutral-beam injection and rf powers for this scan were 18.5-21 MW and 3.7-4.9 MW, respectively. The plasma current was adjusted to maintain a relatively constant edge safety factor. The rf power fraction absorbed directly by electrons increased from 15% to 25% as the $2\Omega_T$ resonance was moved from the low- to the high-field side of the plasma column. Since the direct electron heating peaks on axis, placing the $2\Omega_T$ resonance between the antenna and the core would be expected to reduce the direct electron heating fraction as observed.

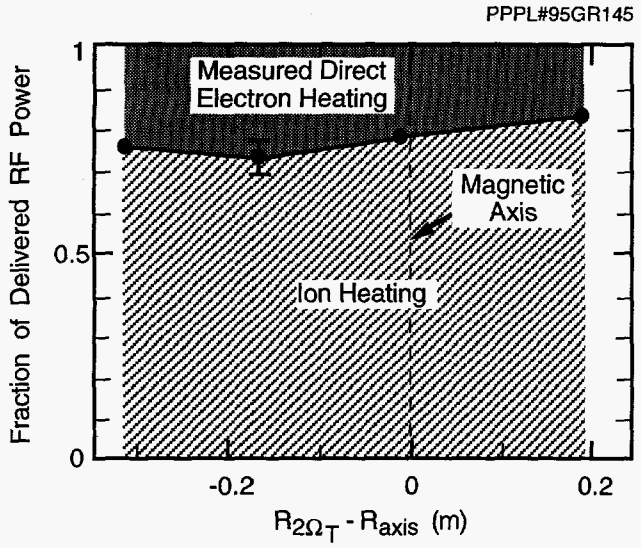

Figure 52. *Fraction of radio-frequency power delivered directly to electrons and ions as a function of the distance of the $2\Omega_T$ resonance from the magnetic axis. Data are for plasmas with no ^{3}He minority, 3.7-4.9 MW of radio-frequency power input to the antenna, 18.5-21 MW of neutral-beam injection and approximately 60% of the injected power in tritium.*

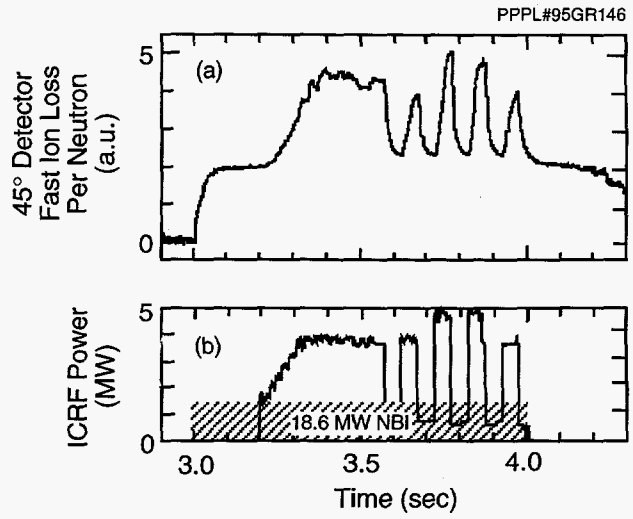

Figure 53. *(a) Neutron-normalized fast-ion loss rate to a detector 45° below the midplane as a function of time and (b) the corresponding radio-frequency power evolution. During the time indicated by the shaded region, 7.1 MW of deuterium and 11.5 MW of tritium neutral-beam power were injected. The portion of the loss which is synchronous with the ICRF power waveform is due to the loss of tritium tail ions.*

RF-Induced Fast-Ion Losses

During ICRF heating of deuterium-tritium plasmas with no ^{3}He, the detectors which measure escaping fast ions[75] indicated two sorts of fast-ion losses, in addition to first-orbit loss of alpha particles. The first of these, illustrated in Fig. 53, was the loss, at the detectors 45° and 60° below the outer midplane, of approximately 600 keV tritium ions accelerated by the ICRF waves. The magnitude of the loss was modulated synchronously with the applied ICRF power. The characteristic interval for these losses to reach a steady level was approximately 50 msec, significantly shorter than the 100 msec required to produce a proton tail in hydrogen-minority heating. This is consistent with 100-keV beam-injected tritons being heated at their second harmonic, since a tail can be created more rapidly from hot ions than from bulk ions and, furthermore, $2\Omega_T$ heating preferentially heats hotter ions. This unambiguous observation of tritium tail ions confirms that $2\Omega_T$ heating occurred in these plasma discharges.

The second type of fast-ion loss was the ICRF-induced loss of alpha particles to the detector at 90° below the midplane. As depicted in Fig. 54, the ICRF-induced loss is modulated with the rf power and can be as much as 50% of the first-orbit loss rate, with only 4 MW of applied power. The rf-induced loss appears in the detector at the pitch angle of the fattest banana orbit. It is concluded that the loss is caused

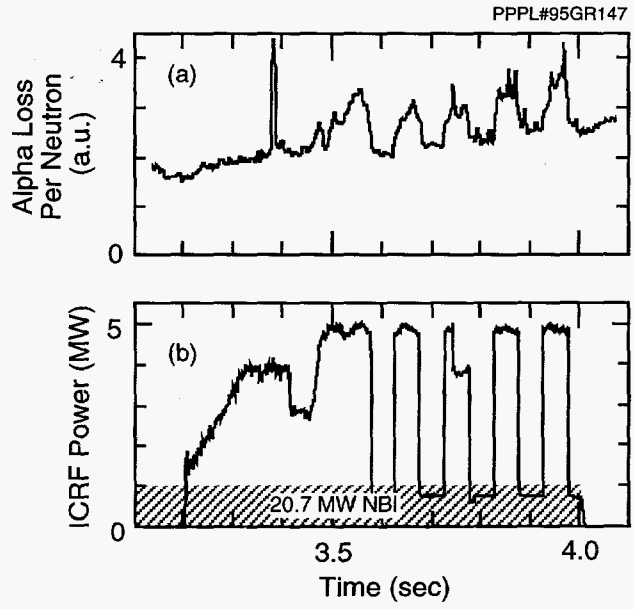

Figure 54. *(a) Neutron-normalized alpha loss rate to a detector 90° below the midplane as a function of time and (b) the corresponding radio-frequency power evolution. During the time indicated by the shaded region, 9.1 MW of deuterium and 11.6 MW of tritium neutral-beam power were injected.*

by marginally passing alphas being heated by the waves and converted into marginally trapped particles which then strike the vessel wall.[76] To date, only birth energy alphas have been expelled by this process, and so it is unlikely to be useful as an ash removal technique.

Mode-Conversion Studies in TFTR

An increasing emphasis is being placed on control of the q-profile in order to access advanced tokamak operating regimes. Enhanced plasma performance in the TFTR,[77] in the JET,[78] and in the DIII-D device[79] has been attributed to reversed shear operation. Reversed shear operating scenarios are planned for the Tokamak Physics Experiment (TPX)[80] and the ITER. The ability to drive off-axis currents noninductively is a key requirement for such scenarios.

The initial experimental demonstration of a technique which can provide either on- or off-axis electron heating and current drive is described below. A fast magnetosonic wave is launched using low-field-side ICRF antennas in a multiple ion species plasma with parameters chosen to yield efficient mode conversion to a low-parallel phase velocity, strongly damped ion-Bernstein wave (IBW).[81] Ion species mixes which maximize mode conversion include D-^{3}He, ^{4}He-^{3}He, D-T-^{3}He, and D-T, where the fractional ion densities of the species are comparable. In TFTR, the present range of toroidal field and ICRF-generator frequencies do not permit mode conversion studies in D-T plasmas. Heating has been demonstrated in TFTR with D-^{4}He-^{3}He and D-T-^{3}He plasmas. Experiments in mode conversion current drive have also begun. Previous theoretical studies of the ray trajectory of the mode-converted IBW in the case of high-parallel phase velocities have indicated that no net directivity would be obtained.[82] Here, where the mode-converted IBW has a low-parallel phase velocity, the electron response is experimentally found to be sensitive to the direction of the launched wave.

The use of a high poloidal mode number IBW to "channel" power directly from the alpha particles to ion heating has also been recently discussed.[83] In TFTR, the effect of the mode-converted IBW on the small population of alpha particles in a L-mode plasma with neutral-beam-fueled D-T and puffed ^{3}He is under investigation. Simulations predict that the IBW will diffuse the alpha-particle population in both space and energy. This quasilinear diffusion is expected to depend on the toroidal direction of IBW propagation. The alpha-particle current to the lost alpha detectors[84] should therefore be dependent on the toroidal direction of the IBW and hence the launched fast wave.

Efficient Mode-Conversion Heating and Current Drive

Efficient single-pass mode conversion in a multiple ion species plasma, such as D-T, has been discussed in detail elsewhere.[81,85] Briefly, the fast wave is cut off at surfaces defined by the conditions $n_\parallel^2 = L, R$; where $n_\parallel = ck_\parallel/\omega$, and $k_\parallel$ is the parallel wavenumber. Mode conversion occurs at the ion-ion hybrid resonance defined by $n_\parallel^2 = S$. The functions R, L, and S are defined by Stix.[86] Previous treatments have neglected the $n_\parallel^2 = R$ cutoff, considering mode conversion at a cutoff-resonance pair. However, if the ion species mix, central density, and toroidal magnetic field are correctly chosen, these surfaces form a closely spaced cutoff-resonance-cutoff triplet for some value of $k_\parallel$. An increase in the "single-pass" mode-conversion efficiency of up to a factor of four over the cutoff-resonance pair case results. Numerical modeling of the D-^{3}He or ^{4}He-^{3}He and D-T-^{3}He ion systems indicates that single-pass mode-conversion efficiencies in excess of 90% can be achieved. Efficient mode conversion is obtained at the mode-conversion triplet for high $n_\parallel$, so that the resultant ion-Bernstein wave is excited with $v_\phi/v_{T_e} < 1$ and is rapidly damped on electrons. If the mode-converted ion-Bernstein wave is directional then current drive will result. Unlike direct fast-wave current drive which is always localized to the plasma axis, the radial location of the mode-conversion surface and hence the driven current can be varied by the species mix or magnetic-field strength. Current-drive efficiency is expected to be comparable to fast-wave current drive.

Mode-Conversion Heating Experiments

Experiments using ^{3}He, ^{4}He, and D Ohmic target plasmas in TFTR have demonstrated mode-conversion electron heating. The electron temperature (T_e) rise with near-axis mode conversion is shown in Fig. 55(a). A Thomson scattering electron temperature profile taken at 2.8 sec during this plasma discharge is shown in Fig. 55(b). Heating occurs at the mode-conversion layer, remote from the ion cyclotron reso-

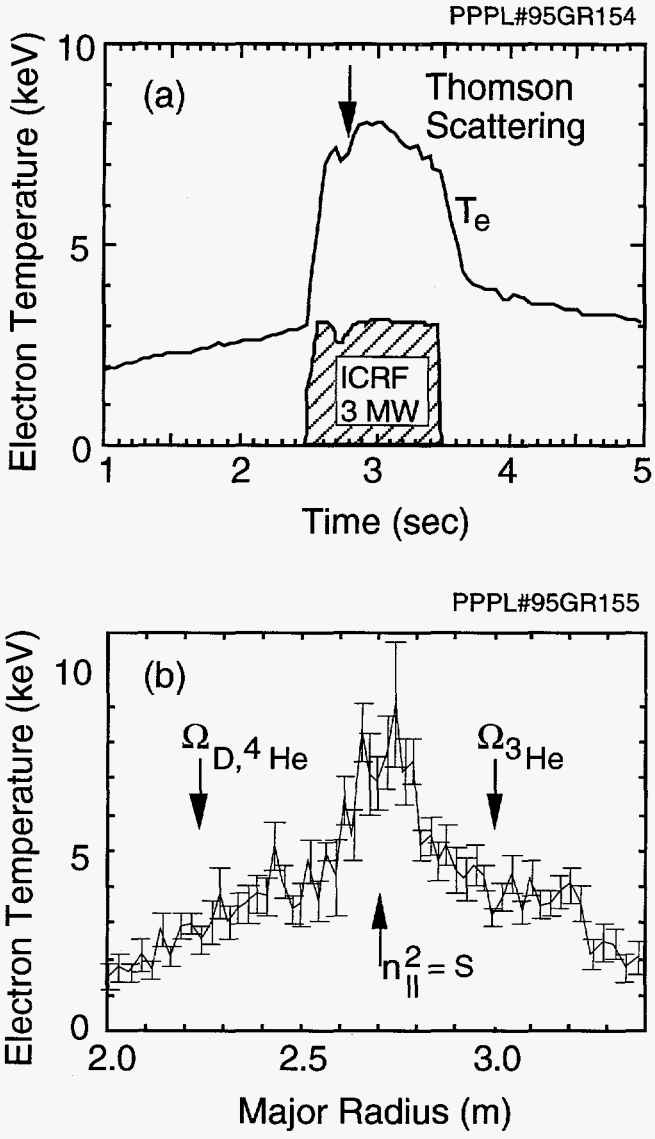

Figure 55. (a) Time evolution of the central electron temperature for on-axis mode conversion heating, derived from electron cyclotron emission measurements and (b) radial profile of the electron temperature from Thomson scattering at 2.8 seconds.

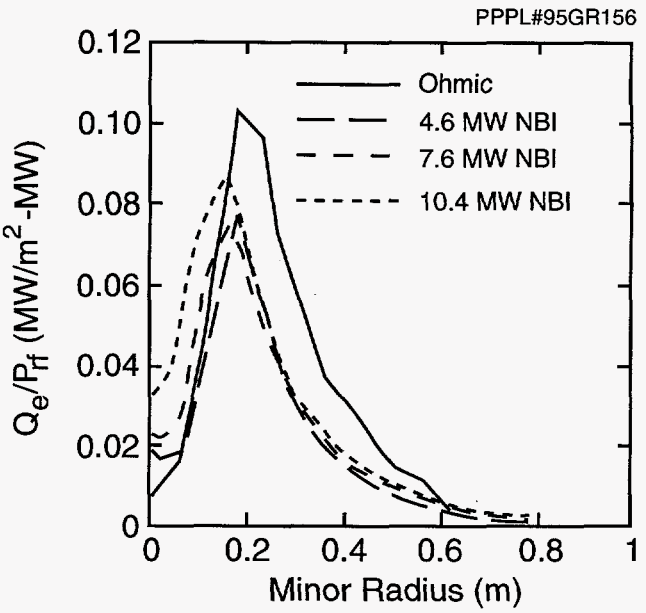

Figure 56. Electron power deposition profile, derived from power modulation techniques, for off-axis mode conversion, for Ohmic- and NBI-heated target plasmas with electron density $n_e(0) = 4\text{-}5 \times 10^{19}$ m^{-3} and helium fraction $n_{3He}/n_e = 0.12$.

nances. In Fig. 56, the measured electron power deposition profile is shown for off-axis mode conversion, for an Ohmic target plasma, and for plasmas with 4.6, 7.6, and 10.6 MW of neutral-beam injection (NBI). The power deposition profile was measured using Fourier transform techniques with 10-Hz radio-frequency power modulation.[87] Power deposition is localized to the mode-conversion layer on the high-field side of the axis for both the Ohmic- and NBI-heated plasma discharges. Peak ion temperature in the neutral-beam-fueled L-mode target plasma discharges was measured to be 5-7 keV by charge-exchange recombination spectroscopy (CHERS). Modeling of the radio-frequency-heated Ohmic discharge with the FELICE code[88] predicts that the fraction of ICRF power coupled to electrons should be 0.86, while the experimentally observed fraction is 0.7. The predicted and observed power deposition radii are in agreement to less than five centimeters. The modeling used parabolic density and temperature profiles with central density $n_e(0) = 4 \times 10^{19}$ m^{-3}, helium concentration $n_{3He}/n_e = 0.2$, central electron temperature $T_e(0) = 5$ keV, where the electron temperature is obtained from electron cyclotron emission measurements, and central ion temperature $T_i(0) = 4$ keV, based on X-ray crystal spectrometry and CHERS results for similar plasma discharges. The experimentally measured central electron power deposition is small for the Ohmic target case, indicating that the single-pass mode-conversion efficiency is larger by an order of magnitude than the single-pass absorption for direct fast-wave electron heating. Single-pass direct fast-wave electron absorption is calculated to be about 5%, from which it is inferred that the single-pass mode-conversion efficiency is approximately 50%. The fraction of power absorbed near the axis for the neutral-beam-injection-heated plasma discharges is difficult to estimate due to strong sawtooth mixing.

The location of the mode-conversion layer can be controlled by adjusting either the toroidal magnetic field (B_t) or the ion species ratio. In Fig. 57 the measured radius of electron power deposition as a function of the toroidal field is shown for constant density [$n_e(0) = 4 \times 10^{19}$ m^{-3}] and ^{3}He fraction (0.14). The power deposition radius occurs within a few centimeters of the $n_{\|}^2 = S$ layer. In Fig. 58 the measured fraction of the radio-frequency power coupled to electrons at the mode-conversion surface is shown for plasma discharges in which the mode-conversion radius is varied through either the species fraction or the toroidal field. Plasma discharges with 4.0 T < B_t < 4.8 T and 0.1 < n_{3He}/n_e < 0.3 are included. The central density was $n_e(0)$ = 4-5 × 10^{19} m^{-3} and the central ion temperature was $T_i(0)$ = 4-7 keV. Up to 80% of the ICRF power is mode converted, with greater than 50% typical for a wide range of deposition radii. The fraction of power mode converted and coupled to electrons rises with ^{3}He concentration, as shown in Fig. 59. Here B_t = 4.5 T while other plasma conditions were as noted for Fig. 58. Relatively little mode-conversion electron heating is found for NBI-heated plasma discharges with low ^{3}He fractions (less than 0.1), where minority ion heating of the ^{3}He population becomes significant.

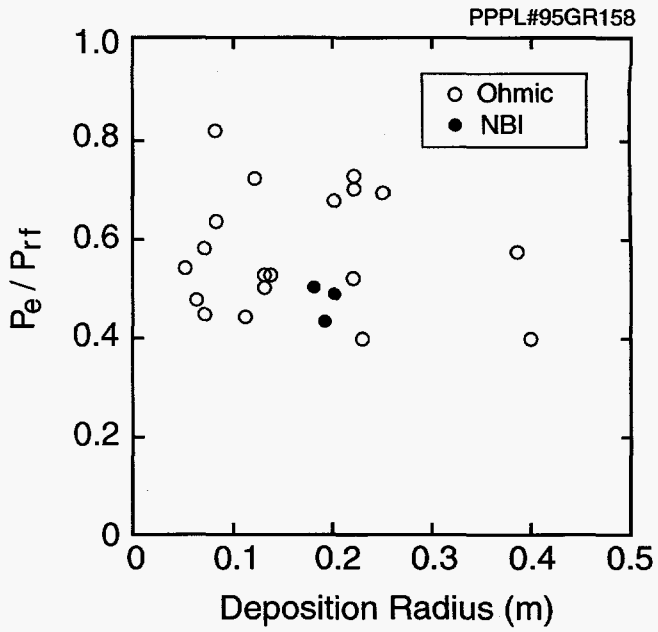

Figure 58. *Fraction of power coupled to electrons at the mode-conversion surface as a function of the radius of the mode-conversion surface. For these plasma discharges 4.0 T < B_t < 4.8 T, 0.1 < n_{3He}/n_e < 0.3, and $n_e(0)$ = 4-5 × 10^{19} m^{-3}. The solid circles indicate neutral-beam-injection-heated plasma discharges.*

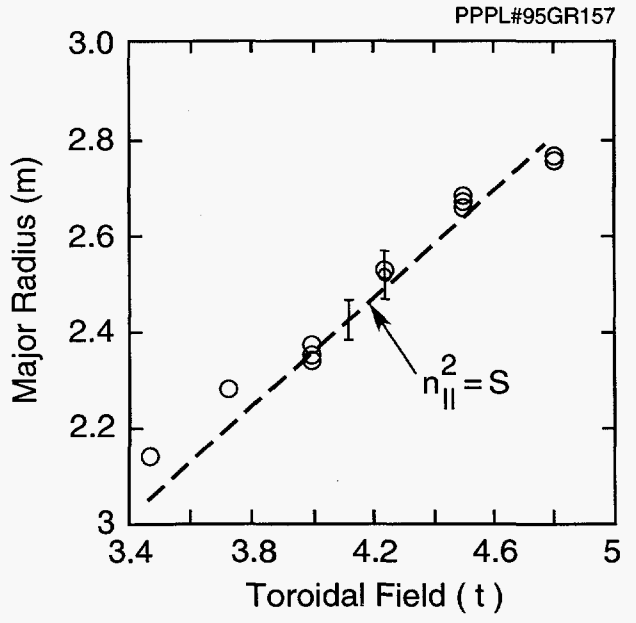

Figure 57. *Observed radius of electron power deposition as a function of the toroidal field for constant ^{3}He fraction (n_{3He}/n_e = 0.14) and constant density [$n_e(0) = 4 \times 10^{19}$ m^{-3}]. The open circles indicate the experimentally observed radii of deposition; the dashed line denotes the calculated position of the mode-conversion surface.*

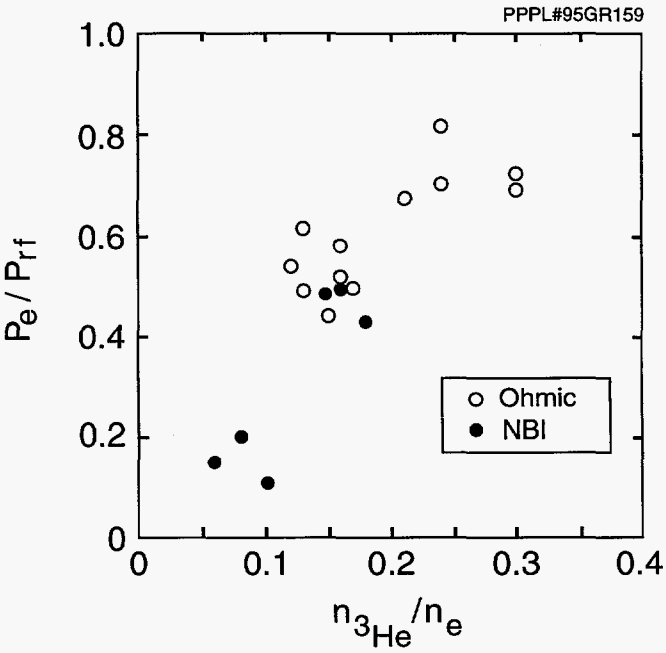

Figure 59. *Fraction of power coupled to electrons at the mode-conversion surface as a function of the ^{3}He fraction for constant toroidal field (4.5 T) and density [$n_e(0) = 4 \times 10^{19}$ m^{-3}]. The solid circles indicate neutral-beam-injection-heated plasma discharges.*

Mode-Conversion Current Drive

Initial mode-conversion current-drive experiments used Ohmic D-^{4}He-^{3}He target plasmas, with two of the two-strap TFTR antennas each phased at 90° to provide a directional fast-wave launch at $k_{\|}$ (antenna) = 7 m^{-1}. The mode-conversion layer was located near the plasma axis, with $n_{^3He}/n_e = 0.12$, $B_t = 4.5$ T, and $n_e(0) = 4 \times 10^{19}$ m^{-3}. The electron temperature response depended on the antenna phasing, and hence the direction of the fast-wave launch, as shown in Fig. 60. This result indicates that the IBW directivity depends on the directivity of the fast wave. However, the surface loop voltage was substantially the same during the 0.8-sec radio-frequency pulse with co (i.e., parallel to the electron current) and counter fast-wave launches. Subsequent TRANSP code modeling of these 1.2-MA plasma discharges indicates that centrally driven currents in the expected 100-200 kA range would not be reflected in the surface voltage on these time scales. Future current-drive experiments will be performed in lower-current plasma discharges with on- and off-axis electron coupling, 2-sec radio-frequency pulses, and measurement of the current profile by motional Stark effect to permit a more direct observation of noninductive currents.

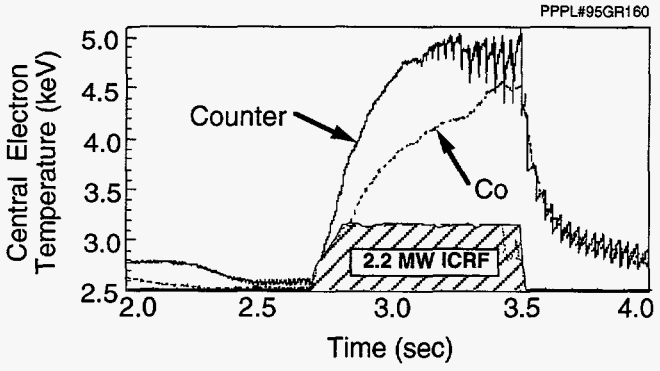

Figure 60. *Electron temperature evolution during directional (90°) fast-wave launch parallel to the Ohmic current (co) and antiparallel to the Ohmic current (counter). Here $n_e(0) = 4 \times 10^{19}$ m^{-3}, $B_t = 4.5$ T, and $I_p = 1.2$ MA.*

Results in D-T-^{3}He Plasmas

Ion-Bernstein wave/alpha-particle interactions were investigated in a L-mode D-T-^{3}He plasma with D-T supplied via neutral-beam injection while ^{3}He was supplied by gas puffing. Five plasma discharges with 2.3 MW of deuterium neutral-beam injection and 2.9 MW of tritium neutral-beam injection into a 1.6-MA plasma were produced as mode-conversion targets. The mode-conversion layer was located near the plasma axis, and the radio-frequency power was modulated at 10 Hz. No corresponding modulation in the lost alpha signal, normalized to the neutron rate, was seen. Hence, at the power levels employed for these initial experiments (2 MW), IBW heating of the alpha particles is not discernible relative to collisional pitch-angle scattering into the alpha-particle loss cone. It should be noted that the mode-converted power fraction in these experiments was low (about 0.2), probably due to low on-axis ^{3}He concentration (less than 0.1), with a resultant onset of minority ion heating (see Fig. 59). During these experiments, significant levels of $<|\delta n_e(k_r, \omega = \omega_{rf})|>$ were observed with microwave scattering[89] at k ~ 5-11 cm^{-1} in the horizontal midplane near the location of the mode-conversion layer. A precise determination of the peak mode wavenumber and correlation with the expected IBW dispersion will be attempted in future experiments at higher toroidal field and ^{3}He concentrations.

Channeling of Alpha-Particle Power

Poloidally propagating waves with small phase velocities[90] are required for effective alpha channeling. Such waves extract power from energetic alpha particles, while diffusing them radially. The mode-converted IBW has the necessary wave properties.[83] If alpha-particle power can be channeled effectively to ions, the power density can be doubled in a fusion reactor.[91] Ray-tracing studies for TFTR parameters, with $T_e = 10$ keV, $T_i = 20$ keV, predict that with suitable toroidal phasing and a frequency of 35 MHz, high-poloidal wavenumber ion-Bernstein waves could be excited off the horizontal midplane of the plasma by mode conversion.[92]

The present TFTR range of operating frequencies and toroidal fields do not permit near-axis excitation of an IBW in a D-T plasma. However, microwave scattering and reflectometry in D and D-T-^{3}He plasmas will be used to investigate the propagation of the IBW. Preliminary evidence of high wavenumber modes in the midplane has already been obtained. With toroidal phasing of the ICRF antennas, such as is already utilized in the current-drive experiments, the prediction of up-down asymmetries in the poloidal wavenumber will be investigated with microwave scattering. Mode conversion in a D-T-^{3}He low-confinement

mode plasma provides a small population of alpha particles to test the interaction. Because of the up-down asymmetry in IBW propagation, reversal of the toroidal launch direction should produce observable differences in the energy of the outwardly diffused alpha particles detected with the lost-alpha probes.

Deuterium-Tritium Plasmas in the High Poloidal Beta Regime

The economics of a fusion power plant based on the tokamak concept can be significantly improved if the plasma stability and energy confinement, usually parameterized by the Troyon normalized beta,[93] $\beta_N \equiv 10^8 <\beta_t> aB_0/I_p$, and energy confinement enhancement factor,[39] $H \equiv \tau_E/\tau_{E\ ITER\text{-}89P}$, could be enhanced. Present reactor design studies[94] show that 50% reductions in the cost of electricity and the capital cost of the plant can be obtained with "advanced tokamak" operation at high $H \leq 4$ and $\beta_N \leq 6$ compared to more conventional tokamak operating parameters. Advanced tokamak plasmas in steady-state operation have been considered in both the ARIES (Advanced Reactor Innovation Evaluation Study)[95] and SSTR (Steady-State Tokamak Reactor)[96] designs.

Operation at high poloidal beta (β_p) has the additional benefit of reduced plasma current (I_p) which reduces the requirements for noninductive current drive, increases the fraction of transport-induced bootstrap current, and reduces the adverse consequences of disruptions. The advantages of this operating regime have been understood for some time and large experimental tokamak programs including TFTR,[97] JT-60U,[98] and DIII-D[99] have produced and studied high-β_p plasmas. Operation at high H and β_N has been achieved by modifying the plasma current and pressure profiles,[97,100,101] and the shape of the outer boundary.[102,103]

Prior to the use of deuterium and tritium in TFTR, high diamagnetic poloidal beta $\beta_p^{dia} = 5.9$ [up to the equilibrium limit,[104] $\beta_N^{dia} = 4.9$ and $H \equiv \tau_E/\tau_{E\ ITER\text{-}89P} = 3.6$ (with $\beta_N^{dia} = 4.5$ and $H = 3.5$ reached simultaneously)] conditions had been obtained in deuterium plasmas at $I_p < 0.5$ MA by actively peaking the current profile and creating a plasma with increased internal inductance, ℓ_i.[97] Here, $\beta_p^{dia} \equiv 2\mu_0 <p_\perp>/<<B_p>>^2$ where $<p_\perp>$ is the volume-averaged transverse plasma pressure and $<<B_p>>$ is the line average of the poloidal magnetic field over the outer flux surface. In addition, high-β_p plasmas with an on-axis safety factor $q(0) > 2$ and low magnetic-field shear in the core had been created with access to the second stability region.[105] Recently, a separate set of experiments has produced plasmas with a high on-axis safety factor exhibiting a reversal in the magnetic-field shear and enhanced-confinement properties.[106,94] Similar "high ℓ_i" and "high q(0)" operating scenarios are planned to be produced and studied under steady-state plasma conditions in the proposed Tokamak Physics Experiment (TPX).[107]

The experiments described here are the first to utilize nominally equal concentrations of D and T in high poloidal beta plasmas in TFTR with current and density profiles optimized for high normalized beta and high energy confinement enhancement factor. The purpose of these experiments is to demonstrate the ability to produce significant levels of fusion power with these plasmas and to examine the characteristics of these plasma discharges in the presence of D-T fusion alpha particles. Both "high ℓ_i" and "moderate q(0)" ($1 \leq q(0) \leq 1.5$) operating scenarios are considered in the present study.

The ability of high-β_p plasmas to generate significant levels of fusion power at reduced plasma current is illustrated in Fig. 61. Here, the peak D-T fusion power (P_F) is plotted as a function of plasma current for TFTR supershot plasmas with plasma current I_p

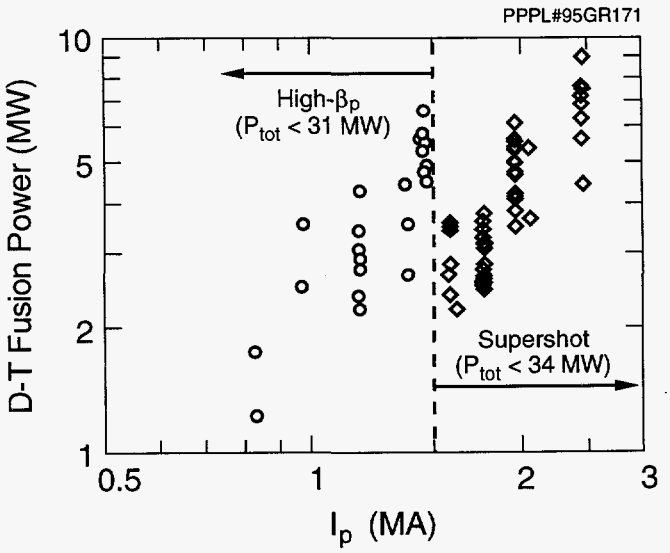

Figure 61. *Deuterium-tritium fusion power versus plasma current for TFTR high-β_p and supershot plasmas*

$\geq$ 1.5 MA and high-β_p plasmas at lower plasma current. Up to 6.7 MW of fusion power was produced in a nondisruptive high-β_p plasma with auxiliary heating power P_{tot} = 31 MW, I_p = 1.46 MA, and $q^* \equiv 5[a^2B_0/R_pI_p(MA)](1+\kappa^2)/2 = 4.7$. This value of q^* is in the range presently being considered in advanced tokamak reactor design studies. The fraction of fusion reactions by thermal-ion collisions, beam-ion collisions with other beam ions, and beam-ion collisions with thermal ions, as computed by the TRANSP code[108] were 34%, 10%, and 56%, respectively. This level of fusion power is 90% of the maximum power produced in a nondisruptive supershot plasma, but at 2/3 of the plasma current.

Experimental Parameters of High-β_N Plasmas

The increase in internal inductance required to produce high-β_N plasmas in TFTR was produced by rapidly decreasing the plasma current from I_p = 1.65-2.5 MA to 0.85-1.46 MA in a deuterium plasma with toroidal magnetic field B_t = 4.6-5.1 T and major radius R = 2.45-2.6 m during a period of neutral-beam injection in the co-direction [Fig. 62(a)]. Addition of counter-injected beams later in the discharge produced the desired power level P_{tot} = 16-31 MW with a nominally equal number of D and T sources. The fraction of auxiliary heating power due to injected tritium neutral-beam power was in the range 0.45-0.72. Electron and ion temperatures reached 11 keV and 35 keV, respectively, with peak electron densities of up to 8×10^{19} m^{-3}. Noninductive current of up to 55% has been computed by the TRANSP code at I_p = 1.46 MA with a 35% contribution from the bootstrap current. The thermal plasma comprised 65% of the total stored energy in the highest density plasmas. Determination of the safety factor profile using motional Stark effect (MSE) measurements of the magnetic-field pitch-angle indicate that $q(0) \leq 1$ for plasmas with $I_p \geq 1$ MA.

High-β_p D-T plasmas with moderate q(0), I_p = 0.85 MA, R = 2.6 m, and $P_{tot} \leq 17$ MW were produced in a manner similar to that described above to test the recent theoretical result[65] indicating that the alpha-particle-driven toroidal Alfvén eigenmode (TAE)[109] can be destabilized if q(0) could be raised to a value between 1.2 and 1.5. In this case, $\beta_p^{dia} = 2.9$, $\beta_N^{dia} = 2.8$, H = 4.2, and P_F = 1.8 MW were attained and preliminary equilibrium modeling using MSE data shows q(0) = 1.4.

Advanced tokamak operation in deuterium-tritium produced a relatively large alpha-particle beta (β_α) for a given plasma current. The on-axis value [$\beta_\alpha(0)$] of 1.6×10^{-3} was computed by the TRANSP code for the I_p = 1.2 MA deuterium-tritium plasma shown in Fig. 62. This value is the same as has been obtained in a deuterium-tritium supershot plasma with I_p = 1.8 MA. At I_p = 1.2 MA, the alpha-particle beta profile is slightly broader. An on-axis alpha particle beta of 2.5×10^{-3} was generated in the plasma with P_F = 6.7 MW. The plasma at moderate on-axis safety factor had a peak $\beta_\alpha(0) = 0.9 \times 10^{-3}$.

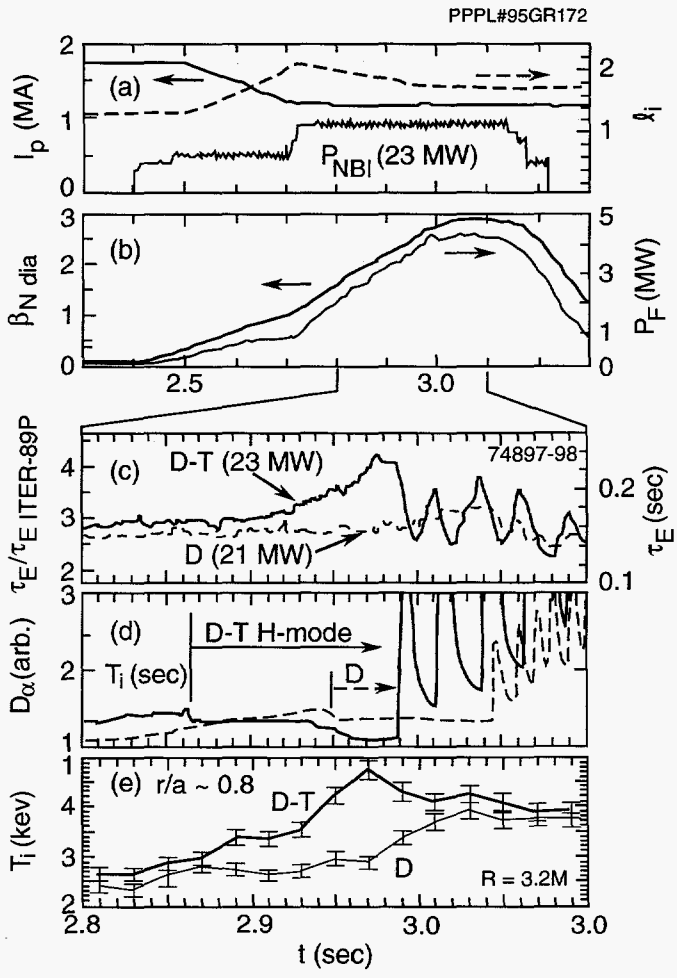

Figure 62. *Time history waveforms for a high-β_p deuterium-tritium H-mode plasma and comparison to an equivalent deuterium plasma discharge. Shown in this figure are (a) the plasma current, plasma internal inductance, and neutral-beam heating, (b) diamagnetic normalized beta and deuterium-tritium fusion power, (c) energy confinement enhancement factor and confinement time, (d) D_α emission, and (e) edge ion temperature.*

Enhanced Confinement and the D-T Limiter H-Mode

Producing enhanced energy confinement involved a reduction in particle recycling. This was obtained in both D and D-T plasmas when the plasma discharge made a transition to a limiter H-mode,[110] or by lithium-pellet conditioning[32] of the limiter. Limiter conditioning has allowed energy confinement (τ_E) at $I_p > 1$ MA to reach a value of 0.2 sec at 1.5 MA. This is a significant improvement compared to the maximum value of $\tau_E = 0.14$ sec reached before the use of lithium pellets in high-β_p plasmas.[111] Similar increases in energy confinement have been observed in sequences of deuterium plasmas which utilize lithium conditioning before and/or after neutral-beam injection. The greatest improvements were obtained when pellets were injected before NBI. The combination of limiter conditioning, operation using D-T, and transition to a limiter H-mode has produced a maximum value of $\tau_E = 0.26$ sec.

The general characteristics of edge localized modes (ELMs), precursor MHD activity to β-collapse, and disruptions are similar in D and D-T plasmas. High-frequency "grassy" ELMs occur in low-power H-mode plasma discharges, while large-amplitude, low-frequency (about 40 Hz in Fig. 62) "giant" ELMs are more likely to occur in D-T plasmas with relatively broad pressure profiles and high normalized beta. Deuterium-tritium H-mode plasmas exhibit an earlier transition time, a longer ELM-free phase, and a greater drop in D_α light when compared to equivalent deuterium plasmas.

Transitions to the high-β_p H-mode in equivalent D and D-T plasmas are shown in Fig. 62(c-e). While a significant increase in energy confinement was observed in the deuterium plasma during the MHD-quiescent "ELM-free" phase of the H-mode, a greater increase (of approximately 40%) was observed in the D-T plasma[112] and an energy confinement enhancement factor of 4.3 (using an average isotopic mass of 2.3) was attained. This improvement was transient, since the onset of the first ELM caused a decrease in energy confinement. However, a recovery of enhanced energy confinement was observed during the relaxation period of the ELMs.

Since transition to the H-mode occurred during the initial rise of the plasma stored energy during NBI, the plasma density and temperature increased up to the onset time of the first ELM. However, while the edge electron temperature and density steadily increased, the edge ion temperature displayed a more rapid increase in both D-T and D plasmas at the time of the H-mode transition [Fig. 62(e)]. At this time, the effective total ion thermal diffusivity, $\chi_i^{tot} \equiv -q_i/n_i^{th}\nabla T_i$ as computed by the TRANSP code decreased in both D-T and D comparison plasmas (Fig. 63). Here, q_i is the ion heat flux and n_i^{th} is the thermal-ion density. A larger change in ion temperature and total ion thermal diffusivity occurred in D-T plasmas as compared to equivalent deuterium discharges.

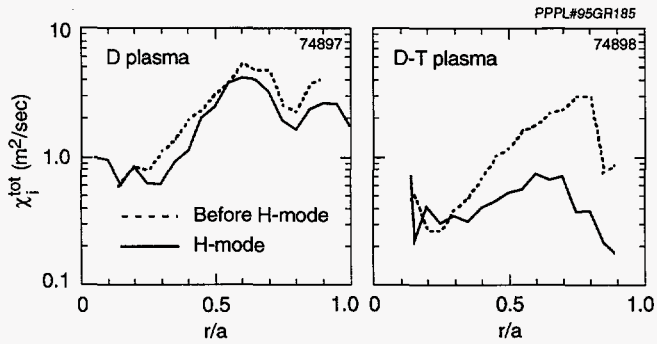

Figure 63. *Reduction in χ_i^{tot} for the D-T and deuterium plasmas shown in Fig. 62 before the H-mode transition and during the ELM-free H-mode phase. The largest change was observed during the ELM-free phase of deuterium-tritium H-mode plasmas at a normalized minor radius r/a ≥ 0.5.*

After the onset of ELMs, the increase in both the edge temperature and density ceased. The edge electron temperature decreased during an ELM burst but recovered its original value before the next ELM burst. In addition, the edge ion temperature in D-T plasmas decreased to the value reached in the equivalent deuterium plasma. This matching of the ion temperature profile, which appeared to be caused by the ELMs, generally extended from the plasma edge to a normalized minor radius r/a = 0.65.

The range of the energy confinement enhancement factor and the normalized beta achieved during the D-T phase of TFTR operation is shown in Fig. 64. The highest values of the energy confinement enhancement factor (up to 4.5) were reached transiently during the ELM-free H-mode phase, during which time the rate of change of the total store energy divided by the heating power $[(dW_{tot}/dt)/P_{NBI}]$ was maximized (exceeding 40% in some plasma discharges). While the largest value of the energy confinement enhancement factor occurred in a deuterium plasma at $I_p = 1$ MA, D-T plasmas produced the larger energy confinement

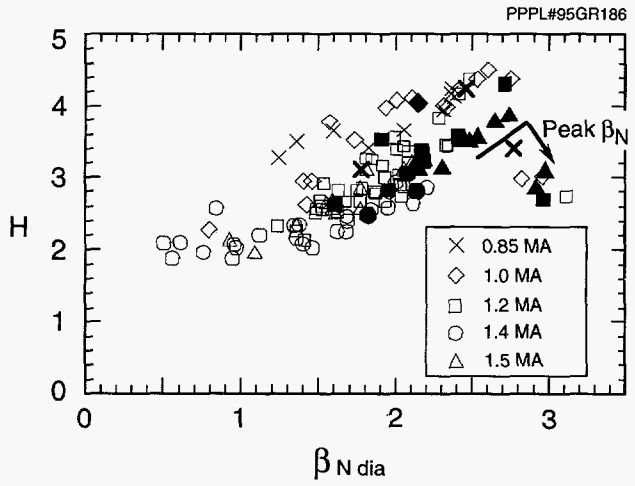

Figure 64. *Range of normalized beta β_N and energy confinement enhancement factor H reached by high-β_p plasmas during the D-T phase. The different symbols indicate varying plasma current. The majority of the data shown was taken at the time of peak H. The data shown by the arrow was taken at the time of peak β_N. Solid or bold symbols indicate a plasma in which D-T was used. None of the plasmas represented terminated in disruption.*

enhancement factor at equal auxiliary heating power and plasma current. Also indicated in Fig. 64 are the values of normalized beta and energy confinement enhancement factor for some plasmas at the time of maximum normalized beta (where $dW_{tot}/dt = 0$). The high-β_p plasma with the highest fusion power output, $P_F = 6.7$ MW, reached during the ELMing phase of the discharge had H = 3.1 and $\beta_N^{dia} = 3$.

Stability of High-β_N Plasmas

Plasma stability limited the improvement in energy confinement for plasmas with high energy confinement enhancement factor. The first high-β_p D-T experiments were concentrated on reaching enhanced performance while simultaneously minimizing the probability of major disruptions. Based on results from prior deuterium plasma operation, the diamagnetic normalized beta stability limit was determined for a given plasma current time history, and a value of diamagnetic normalized beta 15% below this limit was chosen as a target value for D-T operation. This technique was almost entirely successful. Out of 134 plasma discharges in which neutral beams were injected, only three major disruptions were produced, each one occurring "below" the reduced target value of diamagnetic normalized beta. Two of these disruptions occurred in deuterium plasmas for which the electron density profile peakedness, $F_{Ne} \equiv n_e(0)/\langle n_e \rangle_{volume}$ became excessively large. This observation of a reduced normalized beta limit at increased density peakedness is consistent with ideal-MHD stability analyses of n=1 kink/ballooning modes performed for TFTR deuterium plasmas.[111] The result of these calculations showed that the increase in the diamagnetic normalized beta observed in plasmas with increased internal inductance can be eliminated by increased peaking of the plasma pressure profile. The excessive density peaking was created by excessive limiter conditioning using lithium. This conditioning typically caused a reduction of particle recycling that allowed increased neutral-beam penetration and caused the electron density profile peakedness to rise (with a corresponding increase in energy confinement). The plasma disruptions that occurred below the target value of the diamagnetic normalized beta had $F_{Ne} = 3.4$, while a more common value for high-β_p plasmas is 2.5.

The peakedness of the deuterium-tritium neutron source strength as measured with a neutron collimator (an indicator of the pressure profile peakedness) was found to be a useful diagnostic in examining the MHD stability. Deuterium-tritium plasmas either disrupted or suffered a β-collapse when the neutron profile peakedness rapidly increased to a value of $P_{SN} \equiv S_N(0)/\langle S_N \rangle_{volume} \sim 10$ (Fig. 65). Such large values of the neutron peaking factor were obtained only with D-T operation or lithium-pellet injection. These β-limiting events occurred at a normalized beta less than the observed disruptive limit of deuterium plasmas with less peaked pressure profiles.

A "secondary ballooning instability"[113] was clearly observed as a precursor to the D-T plasma disruption and the toroidally localized nature of this mode was established by observing electron temperature fluctuations at two distinct toroidal locations. Details of this instability can be found in the section above "TAE Modes and MHD Activity in D-T Plasmas."

Alpha-driven TAE instabilities have not yet been observed in high-β_p D-T plasmas. The TAE mode stability analysis of plasmas with high internal inductance and $q(0) \leq 1$ is consistent with this observation. The on-axis alpha-particle beta $[\beta_\alpha(0)]$ required to drive the least stable toroidal mode number (n) was computed to be 9.0×10^{-3} for the n=4 mode in the D-T plasma shown in Fig. 62. This level is 5.6 times greater than the peak on-axis alpha-particle beta reached in this discharge. High-β_p plasmas at moderate on-axis

safety factor that were also observed to be stable are computed to be stable, but have on-axis alpha-particle beta significantly closer to the unstable boundary. Preliminary analysis of the D-T plasma with q(0) = 1.4 yields an instability threshold of $\beta_\alpha(0) = 2.1 \times 10^{-3}$ for the n=1 mode, which is a factor of 2.2 larger than the peak on-axis alpha-particle beta generated in this plasma discharge.

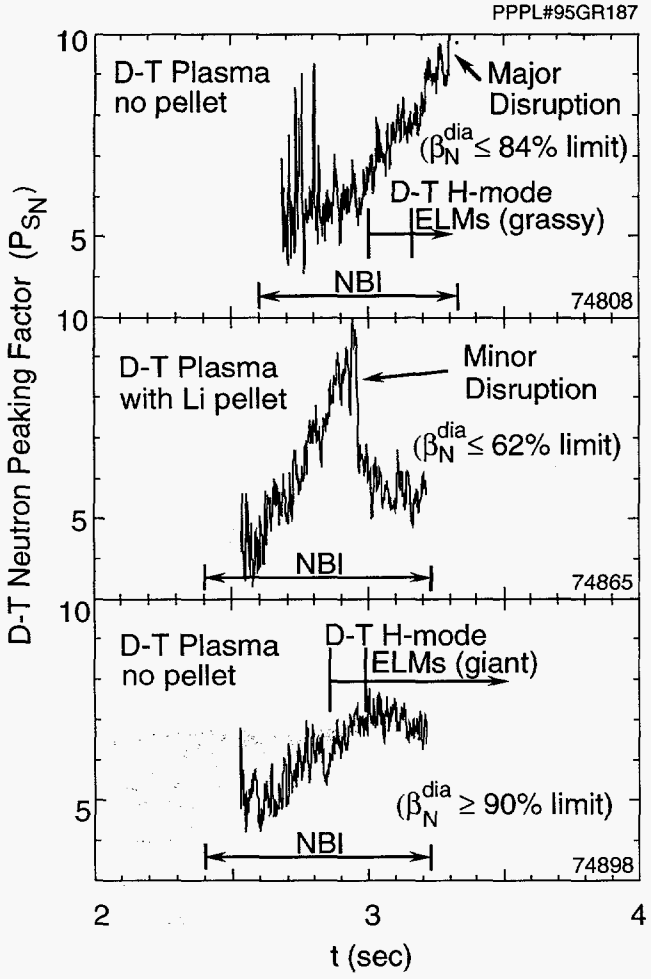

Figure 65. *Time evolution of D-T neutron peakedness in plasmas of varying MHD stability. Plasma with $P_{SN} \sim 10$ encountered major and minor disruptions at reduced diamagnetic normalized beta β_N^{dia}. Plasmas with lower peakedness were stable at greater than 90% of the anticipated β_N^{dia} limit.*

Alpha-Particle Confinement in High-β_N Plasmas

Confinement of alpha particles in high poloidal beta plasmas appears to be classical and large losses due to collective effects have not been observed. The alpha-particle loss fraction does not increase as the fusion reactivity increases (Fig. 66). High poloidal beta plasmas with I_p = 1.5 MA and higher plasma internal inductance experience alpha loss similar to 2.0-MA supershot plasmas with a lower plasma internal inductance. Due to the peaked current profile produced in the high-β_p plasmas, first-orbit losses are less than in a plasma with lower internal inductance and equal plasma current. Modeling of experimental D-T plasmas using the TRANSP code shows that at I_p = 1 MA, 17% of the alpha particles are lost with ℓ_i = 2.2 as opposed to 34% with ℓ_i = 1.2.

The ELMs also have a small but measurable effect on the D-T fusion alpha-particle loss. The alpha-particle detector mounted at a poloidal position 90° below the outboard midplane of the torus measured a fluctuation in amplitude of less than 10%, approximately in phase with the ELM bursts. The detector mounted at 45° below the outboard midplane showed a 15% fluctuation that was out of phase with the ELM bursts. This modest poloidal redistribution of particle loss may be important for ITER, in which even a few percent loss of the alpha-particle population could damage first-wall components.

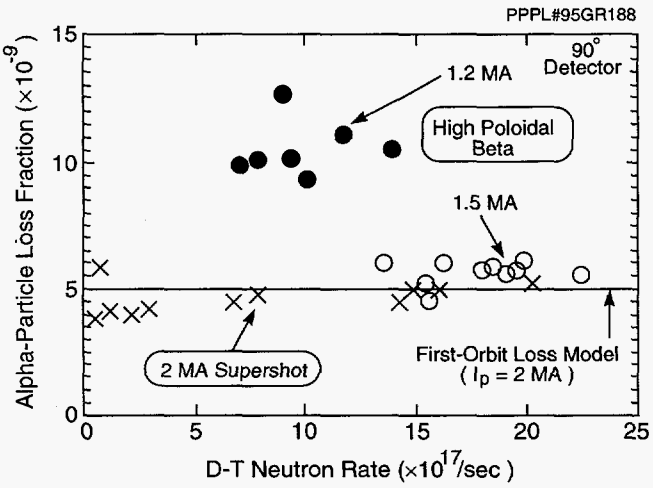

Figure 66. *Alpha-particle loss as a function of D-T neutron reactivity in high-performance TFTR plasma regimes.*

Conclusion

The initial TFTR D-T experiments performed in the high-β_p "advanced tokamak" regime have begun to address issues important to future tokamak reactors designed to operate in this regime. Significant fusion power production (6.7 MW) has been demonstrated at β_N^{dia} = 3, H = 3.1, and q* = 4.7 with a central

fusion power density (1.6 MW/m^3) at the level of the present ITER design (1.7 MW/m^3). In these plasmas, peaking the current profile allowed fusion power production similar to supershot plasmas, but at two thirds of the plasma current. Operation with D-T produced an increase in energy confinement of approximately 40% in an enhanced limiter H-mode. Confinement of alpha particles was classical, with no large loss due to collective effects. Alpha-particle losses due to ELMs are small, but are at a level that may be significant to the operation of ITER. The alpha-particle-driven TAE has not been observed to date in these plasmas. Deuterium-tritium plasmas with high internal inductance and $q(0) \leq 1$ are computed to have an adequate margin against TAE instability. However, plasmas with a moderate on-axis safety factor might encounter TAE instability at higher auxiliary heating power since TFTR D-T plasmas are presently about a factor of two below the computed instability boundary. Future experiments are planned to test the TAE thresholds at $q(0) \sim 1.4$ by increasing the on-axis alpha-particle beta in these plasmas.

Tritium Transport, Influx, and Helium Ash Measurements on TFTR during D-T Operation

Tritium operation in TFTR[24,29] has provided a unique opportunity to study hydrogenic and helium-ash particle dynamics in reactor-relevant plasmas. Here, separate measurements of tritium transport, tritium flux from the limiter, and helium ash are reported.

The enhancement factor of approximately 100 in the deuterium-tritium neutron cross section, compared to that for deuterium-deuterium reactions, makes tritium an attractive particle source for studying transport, influx from the limiter, and fueling efficiency. This has motivated the development of neutron techniques[114,115] to measure hydrogenic-ion transport with similar accuracy to spectroscopic measurement of impurity transport and interferometric measurement of electron transport. Measurement of hydrogenic-ion transport is fundamental to understanding the physics of plasma transport. In addition, characterization of local tritium ion transport is important to future reactors, such as ITER, because plasma transport directly impacts reactor density profile control.[116,117] Density profile control may provide operational flexibility to meet the requirements of stable core fusion power production and edge density control. Edge density control directly affects impurity influx, particle flux to the divertor, and helium-exhaust removal. Furthermore, edge density control may require gas puffing, making particle fueling efficiency also an important issue. A pulsed-gas valve on TFTR has been used to inject small amounts of tritium gas into deuterium neutral-beam-heated plasmas during tritium transport experiments ($n_T/n_D \leq 2\%$). These experiments have resulted in the first measurement of tritium transport coefficients in the form of a diffusivity (D_T) and convective velocity (V_T).

In a plasma optimized for helium-ash production ($n_T/n_D \approx 1$), helium transport has been observed with charge-exchange recombination spectroscopy. In terms of future reactors, the viability of removing helium ash depends upon the local relationship between the core energy transport and the thermal helium transport, as well as the edge helium transport and the pumping speed.[118-121] Before this work, helium had been introduced by gas valves to study transport and ash removal.[122,123]

The first spectroscopic observations of the tritium Balmer-alpha line have shown excellent sensitivity, and revealed tritium influx from the limiter at levels of up to 9% of the total hydrogenic influx. These measurements provide a unique opportunity to study tritium edge physics and are being used to benchmark current models of neutral velocities and limiter erosion and redeposition important for ITER and other D-T tokamaks.

Tritium Transport

Measurement of hydrogenic-ion transport has remained elusive, because no spectroscopic technique has been identified with sufficient accuracy to measure the local ion density. Fusion product techniques have been used to study ^{3}He transport with limited spatial resolution, and a similar approach has been proposed to infer the trace tritium density in a deuterium plasma from the 14.1-MeV t(d,n)α and 2.5-MeV d(d,n)^{3}He neutron emissivities.[114,115] In the tritium-beam experiments on the Joint European Torus, the local 14.1-MeV t(d,n)α and 2.5-MeV d(d,n)^{3}He neutron emissivity profiles have been measured, and the transport was studied using various mixing models

to predict the local evolution of tritium and deuterium, with global introduction of tritium by neutral-beam injection.[124,125]

On TFTR, tritium transport has been studied by puffing small amounts of tritium gas into deuterium neutral-beam-fueled plasmas. The local 14.1-MeV t(d,n)α and 2.5-MeV d(d,n)^{3}He neutron emissivity profiles were measured, and the ion-density profile was inferred.[126] The introduction of the tritium in the form of a small gas puff permits the application of perturbative transport analysis techniques to ascertain the local transport coefficients.[127,128] Because the amount of tritium before the gas puff is very small ($n_T/n_D \leq 0.001$), the transport coefficients represent the tritium transport coefficients for the background plasma. These results represent the first measurement of hydrogenic-ion transport coefficients, in the form of a diffusivity and convective velocity in a tokamak plasma.

The experiment examined tritium transport in high-performance, low-recycling, neutral-beam-fueled plasmas, referred to as supershots. The specific plasma condition investigated was previously studied for electron, helium, and impurity transport.[123] The neutral beams were injected counter tangential and cotangential to the plasma current, to minimize plasma rotation, and were fueled with deuterium neutrals at a maximum energy of approximately 100 keV and at 14 MW of power. The tokamak operating parameters included a toroidal magnetic field of $B_t = 4.8$ T, a major radius of R = 2.45 m, a minor radius of a = 0.8 m, and a plasma current of $I_p = 1.15$ MA. The central electron and ion temperatures were $T_e(0) \approx 7.5$ keV and $T_i(0) \approx 25$ keV, respectively, and the central electron density was $n_e(0) \approx 5 \times 10^{19}$ m^{-3}. The global energy confinement time for this plasma was 0.16 sec, which is approximately three times the ITER-89P L-mode confinement scaling. The deuterium neutral beams were injected from 3 to 4 sec. A tritium puff of gas (40 Pa-m^3/sec for 0.016 sec) was applied at 3.5 sec and resulted in approximately a factor of two increase in the total neutron source strength. It was estimated that the ratio of central tritium to deuterium density is $n_T(0)/n_D(0) \approx 0.01$.

The main diagnostics on TFTR for tritium studies are three different collimated neutron detector systems: a five channel ^{4}He proportional counter array that is sensitive only to the 14.1-MeV t(d,n)α neutrons, a ten channel NE-451 ZnS detector array that is sensitive to both the 14.1-MeV t(d,n)α and 2.5-MeV d(d,n)^{3}He neutrons, and a second ten channel array with less sensitive ZnS wafer scintillators.[129-133] The proportional counters and the NE-451 scintillators were absolutely calibrated *in situ* using a D-T neutron generator.[133-135] Figure 67 shows the time evolution of the local 14.1-MeV t(d,n)α neutron emissivity profile after the injection of the tritium gas puff near 3.5 sec, as measured by the ZnS detector array. The 14.1-MeV t(d,n)α neutron emissivity is determined from the total chordal neutron measurement by subtracting the 2.5-MeV d(d,n)^{3}He neutron contribution measured in similar deuterium plasma discharges and Abel inverting the resulting chordal neutron profile.[126] In Fig. 67 the local neutron emissivity due to the tritium gas puff begins hollow and quickly peaks up within 0.05 sec. The early hollow character of the neutron emissivity is indicative of a hollow tritium density profile during the early time of its evolution.

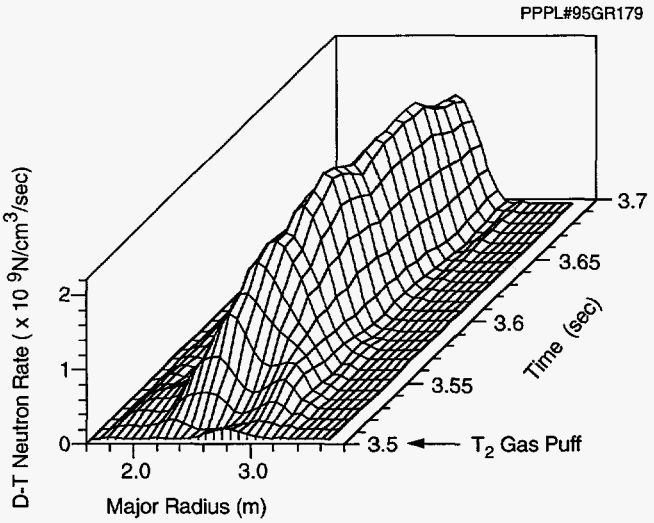

Figure 67. *Local 14.1-MeV t(d,n)α neutron emissivity profile resulting from a pure tritium gas puff. The 14-MeV neutron profile starts out hollow and rapidly becomes peaked.*

Nuclear techniques for measuring plasma ion density have been described by Strachan, *et al.*[114,115] The techniques rely upon the majority of the neutrons originating from beam-target reactions. By taking the ratios of the deuterium-deuterium and deuterium-tritium reaction rates, I_{DT}/I_{DD}, the beam species mix, neutral-beam deposition, beam ion-orbit losses on the first orbit, beam power, and beam slowing down time do not enter the measurement:

$$I_{DT}/I_{DD} \approx n_T/n_D \; 67.3 \exp(0.72/T_i^{0.33}) ,$$

where T_i is the ion temperature in keV. In the supershot studied here, approximately 65% of the 2.5-MeV d(d,n)^{3}He neutrons are from beam-target reactions and the remainder are thermonuclear and beam-beam reactions. Furthermore, only 50% of the central 2.5-MeV d(d,n)^{3}He neutrons are from beam-target reactions. To take the thermonuclear neutron contribution into account, a new scale factor for the above equation can be calculated. Here an alternate algorithm was designed to infer the ion density profile. A response function, similar to a Green's function, is calculated relating the tritium ion density, $n_T(r,t)$, from the measured 14.1-MeV t(d,n)α neutron emissivity measurement, $S_{DT}(r,t)$, for this plasma discharge. The analysis code TRANSP,[47] using the measured plasma density, temperatures, Z_{eff}, magnetics, and the NBI parameters, computes the local 14.1-MeV t(d,n)α neutron emissivity, $S^*_{DT}(r,t)$, for a constant amount of tritium density, $n^*_T = 5 \times 10^{17}$ m^{-3}, at each plasma radius and for all time. This represents the 14.1-MeV t(d,n)α neutron response for a fixed amount of tritium in the plasma including both beam-target and thermonuclear reactions. Then, the plasma tritium density, $n_T(r,t)$, can be estimated from the measured 14.1-MeV t(d,n)α neutron emissivity measurement, $S_{DT}(r,t)$, according to the simple relation

$$n_T(r,t) \approx n^*_T S_{DT}(r,t)/S^*_{DT}(r,t) .$$

The Green's function here is $n^*_T/S^*_{DT}(r,t)$. The tritium density evolution obtained by this technique for the small gas puff is shown in Fig. 68. The profile starts out hollow, fills in as tritium diffuses into the core, and reaches a slightly peaked shape in about 0.1 sec. This behavior is similar to that of the electrons, previously measured on TFTR.[136] Note that the peak of the profile is near R = 2.67 m, which is within one centimeter of the position of the magnetic axis. The profile shape is somewhat less peaked than the deuterium density profile inferred from the electron density profile and the Z_{eff} profile, and the helium and carbon profiles measured with charge-exchange recombination spectroscopy.[122,137] The differences in the profile shapes can be partly attributed to the limited spatial resolution of the neutron measurements in the core of the plasma and a 15% uncertainty in the neutron calibration.

The time-dependent density profile and the gas puff source are used in the TRANSP analysis code to calculate the tritium particle flux, $\Gamma(r,t)$, from the one-dimensional particle balance equation: $\partial n/\partial t = -\nabla\cdot\Gamma + S$, where S is the tritium source. Then at each radius, r, a regression analysis of the particle flux is used to determine the transport coefficients according to the relationship

$$\Gamma(r,t) = -D_T(r)\, \nabla n(r,t) + V_T(r)\, n(r,t) ,$$

where $D_T(r)$ and $V_T(r)$ are the local tritium transport coefficients. The same techniques have been used in the study of electron particle transport.[127,128]

Figure 69 shows the tritium transport coefficients, $D_T(r)$ and $V_T(r)$, as determined from multiple regression analysis. In addition, the transport coefficients of ^{4}He measured by charge-exchange recombination spectroscopy on similar plasma discharges are shown for comparison.[123] Also included in the plot is the deuterium thermal conductivity determined from equilibrium power balance analysis. The diffusivities are all similar in magnitude and profile shape: $D_T \sim D_{He} \sim \chi_D$. The similarity of the diffusivities has been observed in previous perturbative transport experiments on TFTR and is a prominent characteristic of transport due to drift-like microinstabilities.[122,123,127] In addition, the similarity in the diffusivities has been

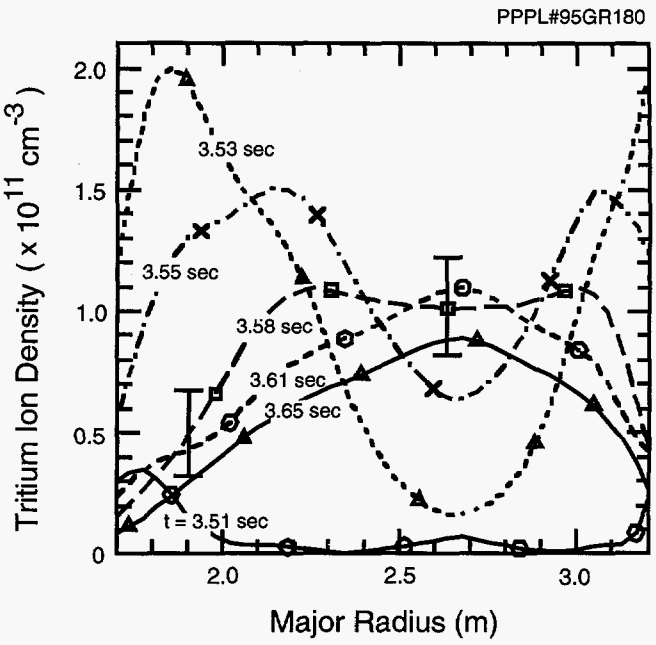

Figure 68. *Evolution of tritium density profile inferred from the neutron emissivity profiles for a pure tritium gas puff. The tritium profile starts out hollow and fills in about 0.1 sec, showing diffusive transport. The same characteristics were observed in previous electron transport studies.*

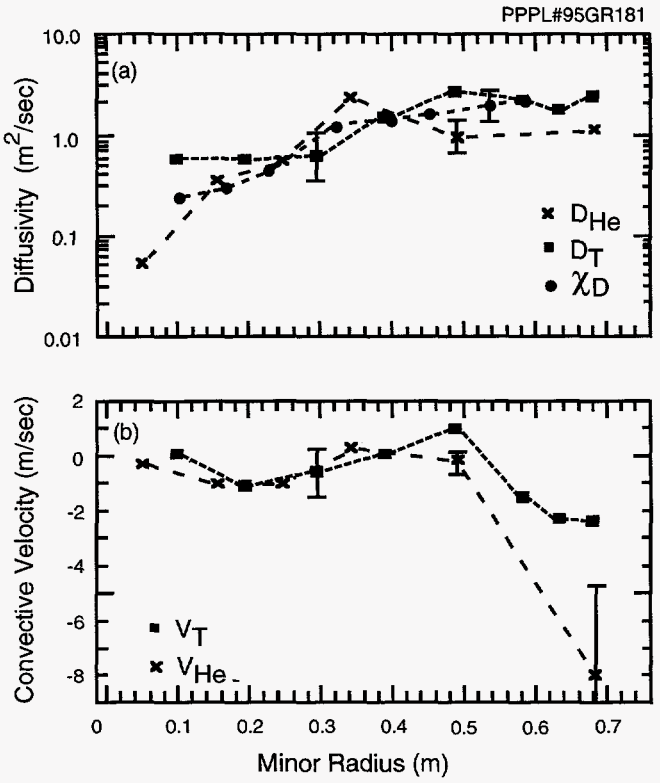

Figure 69. *Comparison of tritium and helium particle diffusivities (a) and convective velocities (b). The diffusivities of tritium, helium, and heat are of similar magnitudes. These are attractive characteristics for future reactors like the International Thermonuclear Experimental Reactor.*

shown to be attractive with regard to helium-ash removal for future reactors, such as ITER.[123] There is an inward pinch in the tritium transport coefficients, and it is also similar to the helium values, except for a large value at the plasma edge for helium. Within the error bars, the tritium pinch is also consistent with neoclassical values for $r < 0.5$ m. Furthermore, the chordal D-T neutron data can be simulated with the measured diffusivities, the measured pinch values for $r > 0.5$ m, and neoclassical values for $r < 0.5$ m.

A quasilinear transport model, predominantly due to E×B drift, is applied to the present experimental data.[138] Here, the eigenmodes and eigenfrequencies of electrostatic and electromagnetic modes are calculated in toroidal geometry. The electron and ion temperature profiles, electron density profile, carbon density profile, and Z_{eff} profile are used in the quasilinear calculation. The beam-ion energy distribution and the ion density are calculated by TRANSP and are also used. The ratio of V/D is calculated at r/a = 0.2 and 0.5 for the ion species D, T, and ^{4}He. These ratios are compared to the present tritium and the previous ^{4}He results.[123] At r/a = 0.2, there is good agreement between the model and measurements: the model estimates V/D ≈ -2.4 m^{-1} for helium, V/D ≈ -3.2 m^{-1} for tritium, and D/χ ≈ 1.2 while the experimental values are V/D ≈ -2.6 m^{-1} for helium, V/D ≈ -1.6 m^{-1} for tritium, and D/χ ≈ 1.5. The comparison at r/a = 0.5 is not as favorable and may be influenced by the measured carbon density profile having a local maximum there, and the transport model being sensitive to the impurity density profile. These transport properties of fusion fuel and helium ash will be further pursued.

With the measurements of the ion density profile evolution, the fueling efficiency, defined as the ratio of tritium delivered to the plasma to the amount of tritium gas injected by the gas valve, can be determined. From the pure gas puffs and from previous trace tritium puffs (2% tritium and 98% deuterium), the fueling efficiency was estimated to be approximately 15%, although the tritium-recycling coefficient was estimated to be about 2-5% from modeling the neutron data with the TRANSP code and spectroscopic measurements indicate smaller values. The total number of tritium ions as a function of time, N_T, for the gas puff was calculated. The decay time constant for N_T is the effective tritium particle confinement time, $\tau_p^*(T)$, and for this plasma discharge is 0.16 sec. During the same time period, the energy confinement time was 0.14 sec. The tritium effective particle confinement time can be compared to that for deuterium, $\tau_p^*(D)$, just after the termination of neutral-beam injection, NBI. When NBI ceases, the major central fueling source in the plasma core stops and the subsequent density decay can be used to determine the global effective particle confinement time. For the same plasma discharge, the global τ_p^* is found to be 0.21 sec and the energy confinement time is 0.15 sec. To the extent that these two decay constants can be compared, the tritium pump-out is faster than the deuterium pump-out, indicating that the tritium pumping by the limiter is faster than deuterium pumping.

Helium-Ash Measurements

Deuterium-tritium operation provides a unique opportunity to measure alpha-ash production. Initial measurements of radial ash profiles have been made using charge-exchange recombination spectroscopy (CHERS). The n = 4-3 line of He^+ (4686 Å), emitted

after charge-exchange of He^{2+} with beam neutrals, was observed with a fiber optic viewing array coupled to a 0.6-m Czerny-Turner spectrometer. Two similar plasmas were investigated, one with deuterium- and tritium-beam injection (21 MW), and the other with deuterium injection only (22 MW). The plasma had a current of 2.0 MA, a toroidal magnetic field of 4.8 T, a major radius of 2.52 m, and a minor radius of 0.87 cm. Five co-injecting and four counter-injecting neutral beams were used. In the D-T plasma, four of the sources injected tritium. After 1.3 sec of the 2 sec neutral-beam pulse, four of the nine neutral-beam sources terminated injection, reducing the heating power to 12 MW in both cases. This caused the plasma temperature to decrease, increasing the alpha-particle slowing-down rate and increasing the population of moderate energy alpha particles, as well as the thermalized ash. Thermal helium profiles were evaluated for the two plasmas using the measured thermal-helium-line brightnesses. During the lower-power phase of the plasmas, a clear increase in the thermal-helium-spectral brightness is observed in the D-T plasma, but not in the D-D case. In addition, differences in the thermal-helium-line brightnesses in similar D-D plasmas are an order of magnitude smaller than in this D-T/D-D plasma pair. The thermal helium profiles, consisting entirely of background helium in the D-D plasma and of background helium and ash in the D-T case, indicate that the local helium density increased by at least 30% in the D-T case as compared to the D-D plasma by the end of neutral-beam injection.

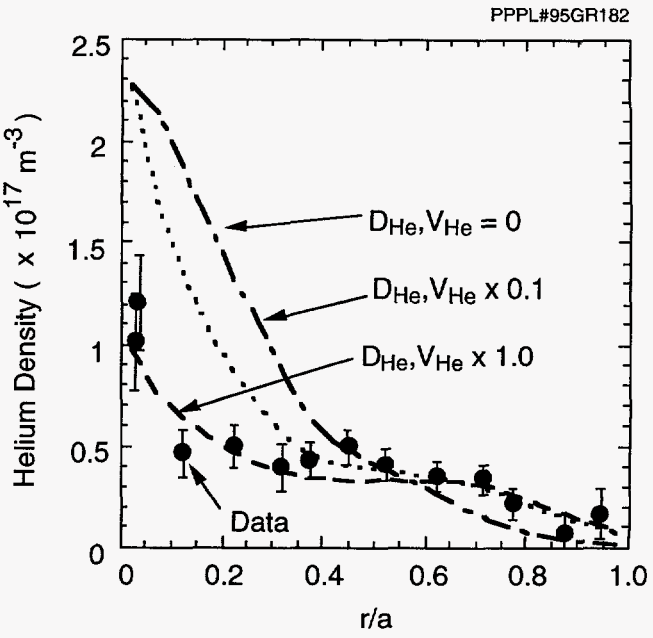

Figure 70. *Measured and modeled alpha-ash density profiles. The data are the difference of the profiles measured from a D-D (#76529) and a D-T (#76528) plasma discharge, and was measured at the end of the neutral-beam-injection phase. The residual represents an approximately 30% increase in the helium density in the D-T case as compared to the D-D case. The data are normalized to the modeled profiles by choosing the integrated total particle number to be equal to that of the three simulated profiles. Shown are the results assuming that the transport coefficients D_{He} and V_{He} are the same as those from Ref. 123. Also shown are results assuming no thermal-ash transport, as well as results assuming D_{He} and V_{He} are one-tenth the measured values.*

The difference in the amplitude of the profiles measured at the end of beam injection is used as a measure of the ash buildup. The residual helium-ash profile, obtained by integrating over the last 100 msec of neutral-beam injection, is shown in Fig. 70. Error bar estimates include the effects of uncertainties in background subtraction, beam attenuation, and correction for ion plume emission.[139] The profile is characterized by a broad pedestal and a central peak. These characteristics are similar to those of the background helium profiles observed in other deuterium plasmas following gas puffing, as well as the background helium profiles in these two plasmas. As discussed in Ref. 123, the values of D_{He} and V_{He} shown in Fig. 69 yield profiles with similar characteristics, without the presence of a central source.

Using the transport rates shown in Fig. 69, the helium profile shape was predicted with the TRANSP code. In addition to the transport, the calculation includes the effect of creation and thermalization of the alpha particles. The measured profile shape is in good agreement with predictions and indicates that the shape determination is dominated by transport, not the presence of the central source. Also shown are the ash profiles obtained under the assumption of no thermal-helium transport, along with the case for which the diffusion and convection were reduced by a factor of ten from the nominal values. The measured profile was normalized by choosing the integrated total particle number to be near that of the three cases shown (the integral varies by no more than 20% between the three cases). Agreement is clearly better in the case using the measured transport coefficients. These measurements, taken together with the transport coefficients measurements and the modeling, provide evidence that the ash transports readily from the ash

source region out to the plasma boundary. This supports earlier inferences from the gas puff data that a reactor with helium and energy transport properties similar to these supershots is compatible with sustained ignition: the ratio of the energy transport rates to the thermal-helium-particle transport rates is favorable. Further dedicated experiments will be performed to determine the alpha-ash-particle transport coefficients in D-T plasmas themselves, as will experiments in long-pulse, constant-power neutral-beam plasmas of both low and high recycling.

Measurements of Tritium Influx from the Limiter

The first spectroscopic measurements of tritium Balmer-alpha (T_α) emission from a fusion plasma were made on TFTR using a Fabry-Perot interferometer.[45] The data are a measure of the fueling of the plasma by tritium accumulated in the TFTR limiter, with additional contributions from neutral tritium generated by charge-exchange of plasma ions. Recycling is an important factor in plasma performance and core plasma composition, but it is more difficult to control than the beam fueling. Some of the tritium injected by neutral beams is retained on the plasma facing surface of the limiter and is available to be recycled on the next plasma discharge; the remainder may be retained on the vacuum vessel wall, buried by co-deposition in the limiter or pumped out. Tritium co-deposition is potentially very important for ITER, and it is therefore important to understand this process in existing experiments. Even for surface materials like beryllium (Be), which involve a much lower tritium co-deposition fraction than carbon (e.g., about 1% hydrogen in beryllium versus up to 40% hydrogen in carbon), the beryllium erosion rate in ITER may be so high that significant amounts of tritium may be trapped by co-deposition. Such tritium trapping raises safety and operational concerns. The use of carbon (under current consideration as a candidate surface material) in ITER is crucially dependent on obtaining acceptably low tritium trapping.

Neutral tritium has a Balmer-alpha transition, T_α, that is analogous to the H_α and D_α transitions long used in edge plasma diagnostics. This line has not previously been observed in fusion plasmas. In TFTR, H_α, D_α, and T_α emission occurs in the inner plasma edge region where the plasma typically contacts a toroidal belt limiter that is constructed from graphite tiles. The emission is collected by a telescope and transferred via a fiber optic cable to a remote Fabry-Perot interferometer, which analyzes the spectrum (for more details see Ref. 45). The T_α intensity is expected to be low, even with 100% tritium NBI, because the principle source of T_α is tritium desorption from the limiter and this is highly diluted with deuterium from previous plasma discharges. In addition, the line is partially blended with the short wavelength wing of the D_α profile. However, the excellent reproducibility of the D_α line shape in the plasma discharges and the high optical efficiency (high signal level) available from the Fabry-Perot interferometer enabled T_α to be measured at levels down to 2% of the total hydrogenic influx. Figure 71 shows an overlay of the line profiles from a tritium-beam-fueled plasma discharge and an earlier deuterium comparison discharge. A clear displacement can be seen in the line profile of the tritium discharge at the T_α wavelength, as expected from earlier simulations of the composite line profile. The T_α line may be seen most clearly in a plot of the difference between the profiles amplified by a factor four shown in the lower part of Fig. 71. By integrating under the difference profile and comparing to the integral of the total, the ratio $T_\alpha/(H_\alpha+D_\alpha+T_\alpha)$ was estimated to be 5%±2%. The highest level of T_α observed to date is 9%.

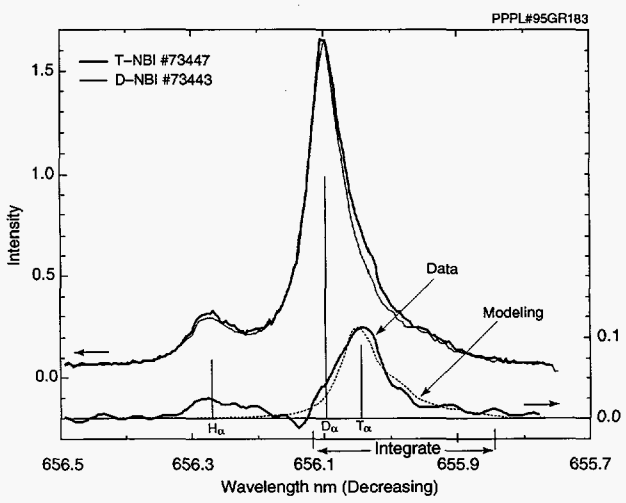

Figure 71. *Comparison of the normalized line profiles from plasma discharge #73447 (100% tritium neutral-beam injection) in bold and an earlier deuterium comparison plasma discharge before tritium injection (#73443; thin trace). A small displacement can be seen on the plasma discharge wavelength side of the profile. The lower traces show the difference between these profiles magnified by a factor four (scale on the right-hand side) and an initial prediction of the T_α profile by the neutrals code DEGAS (dotted line).*

The spectral line profile maps the (nonthermal) velocity distribution of neutral hydrogen isotopes at the plasma edge. Also shown in Fig. 71 is an overlay of a T_α-line profile calculated by the Monte-Carlo neutral transport code DEGAS.[140] Such comparisons have highlighted ways to improve the treatment of sputtering and dissociation in DEGAS that are currently in progress. In deuterium-only NBI plasma discharges following tritium NBI, T_α emission persists for several discharges. This can be seen in the Fig. 72 insert which shows the T_α history after a sequence of major tritium NBI discharges. Also shown is the tritium/deuterium density ratio, n_T/n_D, in the core of the plasma derived from the measured D-T/D-D neutron ratio.[141] The TRANSP modeling of the neutron emission per tritium ion in the inner 20% of the plasma radius predicts, in deuterium-beam-heated discharges, that the ratio of n_D/n_T is $(187\pm5)^{-1}$ of the D-T to D-D neutron ratio. These data fit an exponential relation with a 7.5 discharge decay constant. The long-term decay of tritium was considerably slower (Fig. 72). After the above experimental period, there was a period without tritium NBI (#73461-74430), the latter part of which included deuterium-NBI discharges, permitting neutron measurements of the core tritium/deuterium density ratio (T_α emission was too weak to be identified in these plasma discharges). In the 500 plasma discharges following #73955, the D-T/D-D neutron ratio declined from 0.4 to 0.1 and hence the core n_T/n_D declined from 0.002 to 0.0005. These data fit an exponential decay with a decay constant of 404 discharges. This pattern of rapid and then slow decay was also observed in earlier deuterium-hydrogen exchange experiments performed previously on TFTR[142] and in the preliminary tritium experiment at JET.[143] This behavior was interpreted in terms of an initial rapid dilution of adsorbed and near surface atoms by NBI fueling followed by a slow diffusion of atoms from the bulk to the limiter surface. A quantitative analysis using the REDEP three-dimensional erosion/redeposition code[144] is in progress, and is expected to provide key information for model validation and future predictive capability for both erosion/redeposition and tritium co-deposition codes for ITER and other D-T tokamaks.

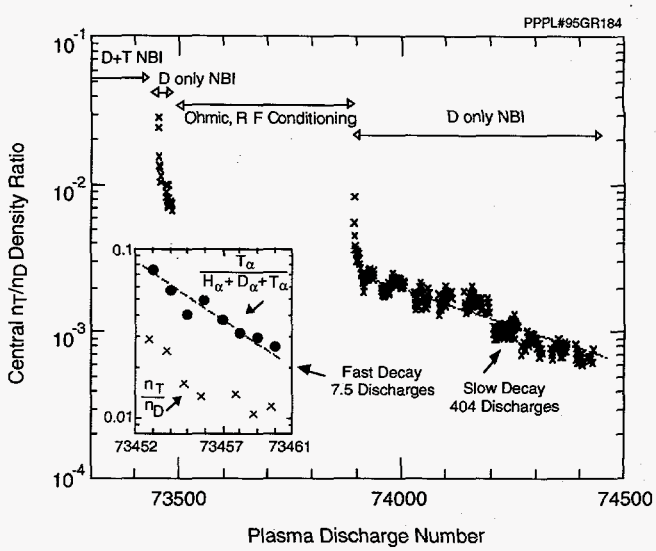

Figure 72. *The decay, in between periods of tritium injection, of the central (r/a < 0.2) tritium/deuterium density ratio as derived from the D-T/D-D neutron ratio. The long-term decay (starting at plasma discharge #73950) followed a 404 plasma discharge decay constant. The short-term decay is shown in the inset: (•) is the $T_\alpha/(H_\alpha + D_\alpha + T_\alpha)$ ratio showing the tritium influx from the limiter and (x) the central tritium/deuterium density over nine deuterium plasma discharges following a sequence of tritium-NBI plasma discharges. (Plasma discharges #73453-#73462 were 100% deuterium NBI with the exception of #73457 which had one tritium and seven deuterium NBI sources.)*

Summary

Extended tritium operation on TFTR has provided a unique opportunity to study tritium and helium-ash transport. For the first time the transport coefficients of a hydrogenic-ion specie in the form of a diffusivity and convective velocity (D_T, V_T) are measured. When compared to previous helium transport results,[123] it is observed that the tritium, helium, and thermal diffusivities are of similar magnitude. The tritium inward pinch velocity, within its error bars, is consistent with neoclassical values for $r < 0.5$ m and is substantially greater than neoclassical values for radii $r > 0.5$ m. Furthermore, the helium ash in a D-T plasma has been measured for the first time. Its transport appears to be consistent with previous measurements of transport coefficients for helium introduced to the plasma by gas puffing.[123] As observed in previous transport studies where helium was introduced by gas puffing,[123] the helium-ash diffusivity is on the order of the thermal diffusivity. All of the experimental results outlined above have been shown to be consistent with theoretically calculated E×B drift transport. This is important to the understanding of light ion transport and helps validate the theoretical model for future design of reactors.

The above mentioned experimental results have an impact on the design and operation of future reactors, like ITER. As discussed in Ref. 123, supershot-like transport coefficients would lead to some buildup of helium ash on axis in a reactor, but because the plasma volume is small in this region, fusion reactivity will be degraded by only 10%, and ignition will still be sustained. Furthermore, the tritium transport is an integral component, along with the density fueling and divertor pumping, in determining the density profile. Achieving density control in a reactor is important in balancing the requirements of stable core fusion energy production and edge density control. The tritium results offer a strong inward pinch for radii $r > 0.5$ m in a supershot plasma. Within the error bars, the pinch at $r < 0.5$ m is consistent with neoclassical values. Additional measurements are planned to characterize tritium and helium transport in L-mode and H-mode plasmas in TFTR.

The first spectroscopic observations of the tritium Balmer-alpha line have shown excellent sensitivity and revealed tritium influx from the limiter at levels of up to 9% of the total hydrogenic influx. These measurements provide a unique opportunity to study tritium edge physics. The line profiles reflect the H, D, T edge velocities and are being used to benchmark and improve the Monte-Carlo neutral transport code DEGAS. The decay of tritium influx in plasma discharges after tritium-beam injection was directly observed in T_α measurements and in the resulting decline in the central n_D/n_T density obtained from neutron data. These data fit a pattern of initial rapid decay (7.5 discharge decay constant) followed by a much longer decay (404 discharge decay constant). This pattern is being analyzed using the REDEP erosion/redeposition code and will provide key information for ITER and other D-T machines.

References

1 R. White, E. Fredrickson, D. Darrow, *et al.*, "Toroidal Alfvén Eigenmode-Induced Ripple Trapping," Plasma Phys. **2** (1995) 2871.

2 Anil Kumar, Mohamed A. Abdou, Cris W. Barnes, H.W. Kugel, and M.J. Loughlin, "Radioactivity Measurements of ITER Materials using the TFTR D-T Neutron Field," Fus. Eng. and Design **28** (1995) 415-428.

3 Anil Kumar, Mohamed A. Abdou, and H.W. Kugel "Characterization of TFTR Shielding Penetrations of ITER Relevance in D-T Neutron Field," Fus. Eng. and Design **28** (1995) 492-503.

4 H.W. Kugel, G. Ascione, S. Elwood, *et al.*, "TFTR Radiation Contour and Shielding Efficiency Measurements during D-D Operations," Fusion Technol. **26** (1994) 963.

5 H.W. Kugel, G. Ascione, S. Elwood, *et al.*, "Measurements of Tokamak Fusion Test Reactor D-T Radiation Shielding Efficiency," Fus. Eng. and Design **28** (1995) 534-544.

6 L.R. Grisham, H.P. Eubank, J.H. Kamperschroer, *et al.*, "The Neutral Beam Heating System for the Tokamak Fusion Test Reactor," Nucl. Intrum. and Methods **B10/11** (1985) 478-482.

7 L.R. Grisham for the TFTR Group, "TFTR Neutral Beam Operations and Results," Plasma Devices and Operations **3** (1994) 187-197.

8 Robert J. Goldston, "Energy Confinement Scaling in Tokamaks: Some Implications of Recent Experiments with Ohmic and Strong Auxiliary Heating," Plasma Phys. and Contr. Fus. **26** (1984) 87-103.

9 M.C. Zarnstorff, V. Arunasalam, C.W. Barnes, *et al.*, "Transport in TFTR Supershots," in *Plasma Physics and Controlled Nuclear Fusion Research 1988* (Proc. 12th Int. Conf., Nice, France, 1988), Vol. **1** (International Atomic Energy Agency, Vienna, 1989) 183.

10 L.R. Grisham, H.F. Dylla, M.D. Williams, K. Wright, and R. Causey, "Tritium Neutral Beams for the Tokamak Fusion Test Reactor," J. Vac. Sci. Technol. A **7** (1989) 944.

11 L.R. Grisham, H. Falter, R. Causey, W. Chrisman, *et al.*, "Experiments with High-Voltage Insulators in the Presence of Tritium," Rev. Sci. Instrum. **62** (1991) 376.

12 L.R. Grisham, H.D. Falter, R. Hemsworth, and G. Deschamps, "Extracted Beam Composition with a Mixed Isotope Feed to a Neutral-Beam System," Rev. Sci. Instrum. **60** (1989) 3730.

13 M.E. Oldaker, J.E. Lawson, and K.E. Wright, "Installation, Preoperational Testing, and Initial Operation of the TFTR Neutral Beam Deuterium-Tritium Gas Delivery System," in *Fusion Engineering* (Proc. 15th IEEE/NPSS Symp., Hyannis, MA, 1993), Vol. **1** (Institute of Electrical and Electronic Engineers, Piscataway, New Jersey, 1994) 487.

14 J.H. Kamperschroer, L.R. Grisham, L.J. Lagin, *et al.*, "Observation of Doppler-Shifted Tα Emission from TFTR Tritium Neutral Beams," Princeton University Plasma Physics Laboratory Report PPPL-2996 (June 1994) 14 pp.

15 R.A.P. Sissingh and R.L. Rossmassler, "Tritium Facility at TFTR," Fus. Eng. and Design **12** (1990) 383.

[16] J.L. Anderson, R.A.P. Sissingh, C.A. Gentile, and R.L. Rossmassler, "Initial Testing of the Tritium Systems at the Tokamak Fusion Test Reactor," in *Fusion Engineering* (Proc. 15th IEEE/NPSS Symp., Hyannis, MA, 1993), Vol. **1** (Institute of Electrical and Electronic Engineers, Piscataway, New Jersey, 1994) 208-211.

[17] S.J. Zweben, C.E. Bush, C.S. Chang, *et al.*, "Anomalous Losses of Deuterium-Deuterium Fusion Products in the Tokamak Fusion Test Reactor," Phys. Plasmas **1** (1994) 1469.

[18] D.S. Darrow, H.W. Herrmann, D.W. Johnson, *et al.*, "Measurement of Loss of DT Fusion Products using Scintillator Detectors in TFTR (Invited)," Rev. Sci. Instrum. **66** (1995) 476.

[19] G.R. McKee, R.J. Fonck, T.A. Thorson, and B.C. Stratton *et al.*, "Implementation of the α-CHERS Diagnostic for D-T Operation of TFTR," Rev. Sci. Instrum. **66** (1995) 643-645.

[20] B.C. Stratton, R.J. Fonck, Y.J. Kim, *et al.*, "Alpha-CHERS: A Spectroscopic Experiment to Detect Nonthermal Alpha Particles on TFTR," Rev. Sci. Instrum. **63** (1992) 5179.

[21] T. Thorson, G. McKee, R.J. Fonck, and B. Stratton, "Spectrometer System and Detector Tests for the TFTR Alpha-CHERS Experiment," Rev. Sci. Instrum. **63** (1992) 5182.

[22] G. McKee, R. Fonck, B. Stratton, *et al.*, "Confined Alpha Distribution Measurements in a Deuterium-Tritium Tokamak Plasma," Phys. Rev. Letts. **75** (1995) 649-652.

[23] B.C. Stratton, R.J. Fonck, G. McKee, *et al.*, "Spectroscopic Observation of 0-300 keV ^{3}He Ions Produced by ICRF Heating in TFTR," Nucl. Fus. **34** (1994) 734.

[24] J.D. Strachan, H. Adler, P. Alling, *et al.*, "Fusion Power Production from TFTR Plasmas Fueled with Deuterium and Tritium," Phys. Rev. Lett. **72** (1994) 3526.

[25] R.K. Fisher, J.M McChesney, A.W. Howald, *et al.*, "Alpha Particle Diagnostics using Impurity Pellet Injection (Invited)," Rev. Sci. Instrum. **63** (1992) 4499-4504.

[26] S.S. Medley, R.K. Fisher, A.V. Khudoleev, *et al.*, "Initial Operation of the Alpha Charge Exchange Diagnostic using Impurity Pellet Injection into Deuterium Plasmas on TFTR," in *Controlled Fusion and Plasma Physics* (Proc. 20th EPS Conf., Lisboa, Portugal, 1993), edited by J.A. Costa Cabral, M.E. Manso, F.M. Serra, and F.C. Schüller, Contributed Papers Vol. **17C** (Part III) (European Physical Society, 1993) 1183-1186.

[27] H.H. Duong, R.K. Fisher, D.K. Mansfield, *et al.*, "Measurements of the Fast Confined Alphas in TFTR using Pellet Charge Exchange (Abstract)," Bull. Am. Phys. Soc. **39** (1994) 1679.

[28] R.K. Fisher, H.H. Duong, J.M. McChesney, *et al.*, Bull. Am. Phys. Soc. (November 1994).

[29] R.J. Hawryluk, H. Adler, P. Alling, *et al.*, "Confinement and Heating of a Deuterium-Tritium Plasma," Phys. Rev. Lett. **72** (1994) 3530.

[30] JET Team, "Fusion Energy Production from a Deuterium-Tritium Plasma in the JET Tokamak," Nucl. Fus. **32** (1992) 187.

[31] J.D. Strachan, M. Bitter, A.T. Ramsey, *et al.*, "High-Temperature Plasmas in the Tokamak Fusion Test Reactor, Phys. Rev. Lett. **58** (1987) 1004.

[32] J.A. Snipes, E.S. Marmar, J.L. Terry, M.G. Bell, R.V. Budny, *et al.*, "Wall Conditioning with Impurity Pellet Injection on TFTR," J. Nucl. Mater. **196-198** (1992) 686; D.L. Jassby, D.K. Mansfield, M.G. Bell, *et al.*, "High-Performance Supershots in TFTR with Lithium Pellet Injection," Princeton University Plasma Physics Laboratory Report PPPL-2940 (September 1993) 17 pp.

[33] M.G. Bell, V. Arunasalam, C.W. Barnes, *et al.*, "An Overview of TFTR Confinement with Intense Neutral Beam Heating," in *Plasma Physics and Controlled Nuclear Fusion Research 1988* (Proc. 12th Int. Conf., Nice, France, 1988), Vol. **1** (International Atomic Energy Agency, Vienna, 1989) 27.

[34] R.V. Budny, M.G. Bell, H. Biglari, *et al.*, "Simulations of Deuterium-Tritium Experiments in TFTR," Nucl. Fus. **32** (1992) 429.

[35] F. Troyon, R. Gruber, H. Saurenmann, S. Semenzato, and S. Succi, "MHD-Limits to Plasma Confinement," Plasma Phys. Contr. Fus. **26** (1984) 209.

[36] L.C Johnson, Cris W. Barnes, H.H. Duong, *et al.*, "Cross Calibration of Neutron Detectors for Deuterium-Tritium Operation in TFTR, Rev. Sci. Instrum. **66** (1995) 894.

[37] D.L. Jassby, Cris W. Barnes, L.D. Johnson, *et al.*, "Absolute Calibration of Tokamak Fusion Test Reactor Neutron Detectors for D-T Plasma Operation," Rev. Sci. Instrum. **66** (1995) 891.

[38] Cris W. Barnes, Alvin R. Larson, G. LeMunyan, and M.J. Loughlin, "Measurements of DT and DD Neutron Yields by Neutron Activation on the Tokamak Fusion Test Reactor," Rev. Sci. Instrum. **66** (1995) 898.

[39] P.N. Yushmanov, T. Takizuka, K.S. Riedel, *et al.*, "Scalings for Tokamak Energy Confinement," Nucl. Fus. **30** (1990) 1999.

[40] R.V. Budny, "A Standard DT Supershot Simulation," Nucl. Fus. **34** (1994) 1247.

[41] C.H. Skinner, H. Adler, R.V. Budny, *et al.*, "First Measurements of Tritium Recycling in TFTR," Nucl. Fus. **35** (1995) 143.

[42] R.V. Budny, H. Adler, M.B. Bell, *et al.*, "Analysis of a High Fusion Power TFTR Supershot," to be published

as Princeton University Plasma Physics Laboratory Report PPPL-3039, 55 pp.

43 S.D. Scott, D.R. Ernst, M. Murakami, *et al.*, "Isotopic Scaling of Transport in Deuterium-Tritium Plasmas," Physica Scripta **51** (1995) 394-401.

44 R.J. Hawryluk, V. Arunasalam, M.G. Bell, *et al.*, "TFTR Plasma Regimes," in *Plasma Physics and Controlled Nuclear Fusion Research 1986* (Proc. 11th Int. Conf., Kyoto, Japan, 1986), Vol. **1** (International Atomic Energy Agency, Vienna, 1987) 51.

45 C.H. Skinner, D.P. Stotler, H. Adler, and A.T. Ramsey, "Spectroscopic Diagnostics of Tritium Recycling in TFTR," Rev. Sci. Instrum. **66** (1995) 646.

46 M. Bessenrodt-Weberpals, F. Wagner, ASDEX Team, *et al.*, "The Isotope Effect in ASDEX," Nucl. Fus. **33** (1993) 1205.

47 R.J. Hawryluk, "An Empirical Approach to Tokamak Transport," in *Physics of Plasmas Close to Thermonuclear Conditions* (Proc. of Course, Varenna, Italy, 1979), edited by B. Coppi, G.G. Leotta, D. Pfirsch, R. Pozzoli, and E. Sindoni, Vol. **1** (Commission of the European Communities, Brussels, Belgium, 1980) 19.

48 R.B. Howell, R.J. Fonck, R.J. Knize, and K.P. Jaehnig, "Corrections to Charge Exchange Spectroscopic Measurements in TFTR Due to Energy-Dependent Excitation Rates," Rev. Sci. Instrum. **59** (1988) 1521.

49 M.G. von Hellermann, W. Mandl, H.P. Summers, *et al.*, "Visible Charge Exchange Spectroscopy at JET," Rev. Sci. Instrum. **61** (1990) 3479.

50 R.K. Janev, R.A. Phaneuf, H. Tawara, and T. Shirai, "Recommended Cross Sections for State-Selective Electron Capture in Collisions of C^{6+} and O^{8+} Ions with Atomic Hydrogen," Atomic Data and Nuclear Data Tables **55** (1993) 201-232.

51 W. Dorland, M. Kotschenreuther, M.A. Beer, *et al.*, "Comparisons of Nonlinear Toroidal Turbulence Simulations with Experiment," in *Plasma Physics and Controlled Nuclear Fusion Research 1994* (Proc. 15th Int. Conf., Seville, Spain, 1994), paper IAEA-CN-60/D-P-I-6, to be published in 1995 by the International Atomic Energy Agency, Vienna.

52 G. Hammett, *et al.*, "Advances in Simulating Tokamak Turbulent Transport," in *Plasma Physics and Controlled Nuclear Fusion Research 1994* (Proc. 15th Int. Conf., Seville, Spain, 1994), paper IAEA-CN-60/D-2-II-1, to be published in 1995 by the International Atomic Energy Agency, Vienna.

53 C.W. Barnes, *et al.*, private communication.

54 D.M. Meade, V. Arunasalam, C.W. Barnes, *et al.*, "Recent TFTR Results," in *Plasma Physics and Controlled Nuclear Fusion Research 1990* (Proc. 13th Int. Conf., Washington, D.C., USA, 1990), Vol. **1** (International Atomic Energy Agency, Vienna, 1991) 9.

55 Z. Chang, J.D. Callen, C.C. Hegna, *et al.*, "Observation of Nonlinear Neoclassical ∇_p-Driven Tearing Modes in TFTR," Princeton University Plasma Physics Laboratory Report PPPL-2988 (September 1994) 13 pp.

56 Z. Chang, E.D. Fredrickson, J.D. Callen, *et al.*, "Transport Effects of Low (m,n) MHD Modes on TFTR Supershots," Nucl. Fus. **34** (1994) 1309-1336.

57 E.D. Fredrickson, K. McGuire, A. Janos, *et al.*, "β Limit Disruptions in the TFTR Tokamak," Princeton University Plasma Physics Laboratory Report PPPL-3023 (1994) 46 pp; to be published in Physics of Plasmas in November 1995.

58 J.F. Drake, "Kinetic Theory of m=1 Internal Instabilities," Phys. Fluids **21** (1978) 1777.

59 F.M. Levinton, L. Zakharov, S.H. Batha, J. Manickam, and M.C. Zarnstorff, "Stabilization and Onset of Sawteeth in TFTR," Phys. Rev. Lett. **72** (1994) 2895.

60 R.J. Hastie, "Change in Electron Cyclotron Emission during a Sawtooth Collapse," JET Laboratory Report JET-R(94)03 (May 1994).

61 K.L.Wong, R. Durst, R.J. Fonck, *et al.*, "Investigation of Global Alfvén Instabilities in the Tokamak Fusion Test Reactor," Phys. Fluids B **4** (1992) 2122.

62 J.R. Wilson, M.G. Bell, H. Biglari, *et al.*, "ICRF Heating on TFTR—Effect on Stability and Performance," in *Plasma Physics and Controlled Nuclear Fusion Research 1992* (Proc. 14th Int. Conf., Würzburg, Germany, 1992), Vol. **1** (International Atomic Energy Agency, Vienna, 1993) 661-673.

63 E. Fredrickson, K.M. McGuire, and Z.Y. Chang, "Results from the TFTR High-Frequency Toroidal Mirnov Array for Detection of Modes in the Alfvén Range of Frequencies," Rev. Sci. Instrum. **66** (1995) 813.

64 C.Z. Cheng, R. Budny, L. Chen, *et al.*, "Energetic Particle Effects on MHD Modes and Transport," in *Plasma Physics and Controlled Nuclear Fusion Research 1994* (Proc. 15th Int. Conf., Seville, Spain, 1994), paper IAEA-CN-60/D-3-III-2, to be published in 1995 by the International Atomic Energy Agency, Vienna.

65 D. Spong, *et al.*, "Energetic Particle Destabilization of Shear Alfvén Waves in Stellarators and Tokamaks," in *Plasma Physics and Controlled Nuclear Fusion Research 1994* (Proc. 15th Int. Conf., Seville, Spain, 1994), paper D-P-II-3, to be published in 1995 by the International Atomic Energy Agency, Vienna.

66 D.A. Spong, B.A. Carreras, and C.L. Hedrick, "Nonlinear Evolution of the Toroidal Alfvén Instability using a Gyrofluid Model," Phys. Plasmas **1** (1994) 1503.

67 G. Taylor, J.R. Wilson, R.C. Goldfinger, *et al.*, "ICRF Heating of TFTR Deuterium Supershot Plasmas in the ^{3}He Minority Regime," Plasma Phys. Contr. Fus. **36** (1994) 523-542.

[68] G. Schilling, "Overview of TFTR ICRF Results (Invited)," in *Radio-Frequency Power in Plasmas* (Proc. 10th Topical Conf., Boston, 1993), edited by Miklos Porkolab and Joel Hosea, AIP Conference Proceedings **289** (American Institute of Physics, New York, 1993) 3; J.R. Wilson, *et al.*, in *Fusion Technology* (Proc. 18th Symp., Karlsruhe, Germany, 1994) to be published.

[69] H.H. Towner, R.J. Goldston, G.W. Hammett, *et al.*, "Data Analysis on TFTR using the SNAP Transport Code," Rev. Sci. Instrum. **63** (1992) 4753.

[70] A.T. Ramsey, C.E. Bush, H.F. Dylla, *et al.*, "Enhanced Carbon Influx into TFTR Supershots," Nucl. Fus. **31** (1991) 1811.

[71] D.J. Gambier, M.P. Evrard, J. Adam, *et al.*, "ICRF Power Deposition Profile and Determination of the Electron Thermal Diffusivity by Modulation Experiments in JET," Nucl. Fus. **30** (1990) 23; M. Murkami, E. Fredrickson, E.F. Jaeger, *et al.*, "ICRF Direct Electron Heating Experiments in TFTR," in *Controlled Fusion and Plasma Physics* (Proc. 20th EPS Conf., Lisboa, Portugal, 1993), edited by J.A. Costa Cabral, M.E. Manso, F.M. Serra, and F.C. Schüller, Contributed Papers Vol. **17C** (Part III) (European Physical Society, 1993) 981.

[72] E.F. Jaeger, D.B. Batchelor, and D.C. Stallings, "Influence of Various Physics Phenomena on Fast Wave Current Drive in Tokamaks," Nucl. Fus. **33** (1993) 179.

[73] D.N. Smithe, P.L. Colestock, R.J. Kashuba, and T. Kammash, "An Algorithm for the Calculation of Three-Dimensional ICRF Fields in Tokamak Geometry," Nucl. Fus. **27** (1987) 1319.

[74] G.W. Hammett, "Fast Ion Studies of Ion Cyclotron Heating in the PLT Tokamak," Ph.D. Thesis, Princeton University (1986).

[75] S.J. Zweben, R.L. Boivin, M. Diesso, S. Hayes, *et al.*, "Loss of Alpha-Like MeV Fusion Products from TFTR," Nucl. Fus. **30** (1990) 1551; D.S. Darrow, H.W. Herrmann, D.W. Johnson, *et al.*, "Measurement of Loss of DT Fusion Products using Scintillator Detectors in TFTR (Invited)," Rev. Sci. Instrum. **66** (1995) 476.

[76] D.S. Darrow, S.J. Zweben, R.V. Budny, *et al.*, "ICRF-Induced DD Fusion Product Losses in TFTR," Princeton University Plasma Physics Laboratory Report PPPL-2975 (1994) 16 pp.

[77] F.M. Levinton, M.C. Zarnstorff, S.H. Batha, *et al.*, "Improved Confinement with Reversed Magnetic Shear," Princeton University Plasma Physics Laboratory Report PPPL-3117 (1995) 15 pp.

[78] P. Kupschus, B. Balet, D. Bartlett, *et al.*, "High Thermonuclear Yield on JET by Combining Enhanced Plasma Performance of ICRH-Heated, Pellet-Peaked Density Profiles with H-Mode Confinement," in *Controlled Fusion and Plasma Physics* (Proc. 18th EPS Conf., Berlin, Germany, 1991), edited by P. Bachmann and D.C. Robinson, Contributed Papers Vol. **15C** (Part I) (European Physical Society, 1991) I-1.

[79] D-III-D Team, "Recent D-III-D Results," in *Plasma Physics and Controlled Nuclear Fusion Research 1992* (Proc. 14th Int. Conf., Würzburg, Germany, 1992), Vol. **1** (International Atomic Energy Agency, Vienna, 1993) 41-55.

[80] W.M Nevins, R.J. Goldston, D.N. Hill, *et al.*, "Mission and Design of the Tokamak Physics Experiment/ Steady State Advanced Tokamak (TPX/SSAT)," in *Plasma Physics and Controlled Nuclear Fusion Research 1992* (Proc. 14th Int. Conf., Würzburg, Germany, 1992), Vol. **3** (International Atomic Energy Agency, Vienna, 1993) 279.

[81] R. Majeski, C.K. Phillips, and J.R. Wilson, "Electron Heating and Current Drive by Mode Converted Slow Waves," Phys. Rev. Lett. **73**, (1994) 2204.

[82] A.K. Ram and A. Bers, "Propagation and Damping of Mode Converted Ion-Bernstein Waves in Toroidal Plasmas," Phys. Fluids B **3** (1991) 1059.

[83] N.J. Fisch, E.J. Valeo, C.F.F. Karney, and R. Majeski, "Possibility of Using Ion-Bernstein Waves for Alpha Power Extraction in Tokamaks," in *Controlled Fusion and Plasma Physics* (Proc. 21th EPS Conf., Montpellier, France, 1994), edited by E. Joffrin, P. Platz, and P.E. Stott, Contributed Papers Vol. **18B** (Part II) (European Physical Society, 1994) 640.

[84] S.J. Zweben, R. Boivin, S.L. Liew, *et al.*, "Constrains on Escaping Alpha Particle Detectors for Ignited Tokamaks," Rev. Sci. Instrum. **61** (1990) 3505.

[85] V. Fuchs, *et al.*, in *Controlled Fusion and Plasma Physics* (Proc. 21th EPS Conf., Montpellier, France (1994), edited by E. Joffrin, P. Platz, and P.E. Stott, Contributed Papers Vol. (Part) (European Physical Society, 1994)

[86] T.H. Stix, *Waves in Plasmas*, American Institute of Physics, New York (1992).

[87] M. Murkami, E. Fredrickson, E.F. Jaeger, *et al.*, "ICRF Direct Electron Heating Experiments in TFTR," in *Controlled Fusion and Plasma Physics* (Proc. 20th EPS Conf., Lisboa, Portugal, 1993), edited by J.A. Costa Cabral, M.E. Manso, F.M. Serra, and F.C. Schüller, Contributed Papers Vol. **17C** (Part III) (European Physical Society, 1993) 981.

[88] M. Brambilla, "Theory of Bernstein Wave Coupling with Loop Antennas," Nucl. Fus. **28** (1988) 549.

[89] N. Bretz, P. Efthimion, J. Doane, and A. Kritz, "X-Mode Scattering for the Measurement of Density Fluctuations on TFTR (Invited)," Rev. Sci. Instrum. **59** (1988) 1538.

[90] Nathaniel J. Fisch and Jean-Marcel Rax, "Interaction of Energetic Alpha Particles with Intense Lower Hybrid Waves," Phys. Rev. Lett. **69** (1992) 612.

91 N.J. Fisch and M.C. Herrman, "Utility of Extracting α-Particle Energy by Waves," Princeton University Plasma Physics Laboratory Report PPPL-2989 (1994) 60 pp.

92 E.J. Valeo and N.J. Fisch, "Excitation of Large Θ Ion-Bernstein Waves in Tokamaks," Princeton University Plasma Physics Laboratory Report PPPL-3000 (September 1994) 13 pp.

93 F. Troyon and R. Gruber, "A Semi-Empirical Scaling Law for the β-Limit in Tokamaks," Phys. Lett. **110A** (1985) 29.

94 R.J. Goldston, S.H. Batha, R.H. Bulmer, *et al.*, "Advanced Tokamak Physics — Status and Prospects," Plasma Phys. Contr. Fus. **36** (1994) B213-B227 and references therein; L.J. Perkins, *et al.*, submitted to Nucl. Fus.

95 F. Najmabadi, R.W. Conn, J.R. Bartlit, *et al.*, "The ARIES Tokamak Fusion Reactor Study," in *Fusion Engineering* (Proc. 13th IEEE Symp., Knoxville, TN, 1989), edited by M.S. Lubell, M.B. Nestor, and S.F. Vaughan, IEEE Catalog No. 89CH2820-9, Vol. **2** (Institute of Electrical and Electronics Engineers, Piscataway, New Jersey, 1990) 1021.

96 M. Kikuchi, "Steady State Tokamak Reactor Based on the Bootstrap Current," Nucl. Fus. **30** (1991) 265.

97 S.A. Sabbagh, R.A. Gross, M.E. Mauel, *et al.*, "High Poloidal Beta Equilibrium in the Tokamak Fusion Test Reactor Limited by a Natural Inboard Poloidal Field Null," Phys. Fluids B **3** (1991) 2277.

98 S. Ishida, M. Matsuoka, M. Kikuchi, *et al.*, "Enhanced Confinement of High Bootstrap Current Discharges in JT-60U," in *Plasma Physics and Controlled Nuclear Fusion Research 1992* (Proc. 14th Int. Conf., Würzburg, Germany, 1992), Vol. **1** (International Atomic Energy Agency, Vienna, 1993) 219-233.

99 P.A. Politzer, T. Casper, C.B. Forest, *et al.*, "Evolution of High β_p Plasmas with Improved Stability and Confinement," Phys. Plasmas **1** (1994) 1545.

100 J.R. Ferron, L.L. Lao, T.S. Taylor, *et al.*, "Improved Confinement and Stability in the DIII-D Tokamak Obtained through Modification of the Current Profile," Phys. Fluids B **5** (1993) 2532.

101 Y. Kamada, K. Ushigusa, O. Naito, *et al.*, "Non-Inductively Current Driven H-Mode with High β_N and High β_p Values in JT-60U," Nucl. Fus. **34** (1994) 1605.

102 G.A. Navratil, R.A. Gross, M.E. Mauel, *et al.*, "Study of High Poloidal Beta Plasmas in TFTR and DIII-D," in *Plasma Physics and Controlled Nuclear Fusion Research 1992* (Proc. 13th Int. Conf., Washington, D.C., USA, 1990), Vol. **1** (International Atomic Energy Agency, Vienna, 1991) 209-218.

103 L.L. Lao, J.R. Ferron, T.S. Taylor, *et al.*, "High Internal Inductance Improved Confinement H-Mode Discharges Obtained with an Elongation Ramp Technique in the DIII-D Tokamak," Phys. Rev. Lett. **70** (1993) 3435.

104 M.E. Mauel, G.A. Navratil, S.A. Sabbagh, *et al.*, "Operation at the Tokamak Equilibrium Poloidal Beta Limit in TFTR," Nucl. Fus. **32** (1992) 1468.

105 S.A. Sabbagh, High-n Ballooning Instabilities and Access to the Second Stability Region in TFTR (Invited)," Bull. Am. Phys. Soc. **38** (1993) 1984.

106 F.M. Levinton, S.H. Batha, R. Budny, *et al.*, "Experimental Observation of Negative Magnetic Shear in TFTR and its Effect on Transport," (Abstract Only), Bull. Am. Phys. Soc. **39** (1994) 1679.

107 G.H. Neilson, D.B. Batchelor, P.K. Moduszewski, *et al.*, "Mission and Physics Design of the Tokamak Physics Experiment," Fusion Techno. **26** (1994) 343.

108 R.J. Goldston, D.C. McCune, H.H. Towner, S.L. Davis, *et al.*, "New Techniques for Calculating Heat and Particle Source Rates due to Neutral Beam Injection in Axisymmetric Tokamaks," J. Comput. Phys. **43** (1981) 61-78.

109 C.Z. Cheng, Liu Chen, and M.S. Chance, "High-n Ideal and Resistive Shear Alfvén Waves in Tokamaks," Ann. Phys. **161** (1985) 21-47.

110 C.E. Bush, R.J. Goldston, S.D. Scott, *et al.*, "Peaked Density Profiles in Circular-Limiter H Modes on the TFTR Tokamak," Phys. Rev. Lett. **65** (1990) 424.

111 M.E. Mauel, G.A. Navratil, S.A. Sabbagh, *et al.*, "Achieving High Fusion Reactivity in High Poloidal Beta Discharges in TFTR," in *Plasma Physics and Controlled Nuclear Fusion Research 1992* (Proc. 14th Int. Conf., Würzburg, Germany, 1992), Vol. **1** (International Atomic Energy Agency, Vienna, 1993) 205-217.

112 C.E. Bush, S.A. Sabbagh, R.E. Bell, *et al.*, "Initial H-Mode Experiments in DT Plasmas on TFTR," in *Controlled Fusion and Plasma Physics* (Proc. 21th EPS Conf., Montpellier, France, 1994), edited by E. Joffrin, P. Platz, and P.E. Stott, Contributed Papers Vol. **18B** (Part I) (European Physical Society, 1994) 354.

113 Y. Nagayama, S.A. Sabbagh, J. Manickam, *et al.*, "Observation of Ballooning Modes in High-Temperature Tokamak Plasmas," Phys. Rev. Lett. **69** (1992) 2376; M.N. Bussac and R. Pellat, "Nonlinear Evolution of the Internal Kink in Tokamaks," Phys. Rev. Lett. **59** (1987) 2650.

114 J.D. Strachan, R.E. Chrien, and W.W. Heidbrink, "Measurement of Plasma Density using Nuclear Techniques," J. Vac. Sci. Technol. A **1** (1983) 811.

115 J.D. Strachan and A. Chan, "Helium Transport in TFTR, "Nucl. Fus. **27** (1987) 1025.

116 W.A. Houlberg, S.E. Attenberger, and M.J. Grapperhaus, "Density Profile Control in a Fusion Reactor using Pellet Injection," Nucl. Fus. **34** (1994) 93.

117 K. Borrass, S.A. Cohen, R.B. Campbell, *et al.*, "Plasma Operation Control in ITER," in *Plasma Physics and Controlled Nuclear Fusion Research 1992* (Proc. 13th Int. Conf., Washington, D.C., USA, 1990), Vol. **3** (International Atomic Energy Agency, Vienna, 1991) 343.

118 F. Engelmann and A. Nocentini, "Helium Exhaust in Tokamak Fusion Reactors," Comments Plasma Phys. Contr. Fus. **5** (1980) 253-260.

119 R.J. Taylor, B.D. Fried, and G.J. Morales, "Burn Threshold for Fusion Plasmas with Helium Accumulation," Comments Plasma Phys. Cont. Fus. **13** (1990) 227-237.

120 M.H. Redi, S.A. Cohen, and E.J. Synakowski, "Transport Simulations of Helium Exhaust in ITER using Recent Data from TFTR, TEXTOR, and JT-60," Nucl. Fus. **31** (1991) 1689.

121 D.L. Hillis, K.H. Finken, J.T. Hogan, *et al.*, "Helium Exhaust and Transport Studies with ALT-II Pump Limiter in the TEXTOR Tokamak," Phys. Rev. Lett. **65** (1990) 2382.

122 E.J. Synakowski, B.C. Stratton, P.C. Efthimion, *et al.* "Measurements of Radial Profiles of He^{2+} Transport Coefficients on the TFTR Tokamak," Phys. Rev. Lett. **65** (1990) 2255.

123 E.J. Synakowski, P.C. Efthimion, G. Rewoldt, *et al.*, "Helium, Iron, and Electron Particle Transport and Energy Transport Studies on the Tokamak Fusion Test Reactor," Phys. Fluids B **5** (1993) 2215.

124 F.B. Marcus, J.M. Adams, B. Balet, *et al.*, "Neutron Emission Profile Measurements during the First Tritium Experiments at JET," Nucl. Fus. **33** (1993) 1325.

125 B. Balet, P.M. Stubberfield, D. Dorba, *et al.*, "Particle and Energy Transport during the First Tritium Experiments on JET," Nucl. Fus. **33** (1993) 1345.

126 L.C. Johnson, P.C. Efthimion, J.D. Strachan, *et al.*, "Tritium Transport Studies on TFTR," in *Controlled Fusion and Plasma Physics* (Proc. 21th EPS Conf., Montpellier, France, 1994), edited by E. Joffrin, P. Platz, and P.E. Stott, Contributed Papers Vol. **18B** (Part I) (European Physical Society, 1994) 182.

127 P.C. Efthimion, D.K. Mansfield, B.C. Stratton, *et al.*, "Observation of Temperature-Dependent Transport in the TFTR Tokamak," Phys. Rev. Lett. **66** (1991) 421.

128 P.C. Efthimion, M. Bitter, E.D. Fredrickson, *et al.*, "Transport Studies on TFTR Utilizing Perturbation Techniques," in *Plasma Physics and Controlled Nuclear Fusion Research 1988* (Proc. 12th Int. Conf., Nice, France, 1988), Vol. **1** (International Atomic Energy Agency, Vienna, 1989) 307-321.

129 A.L. Roquemore, R.C. Chouinard, M. Diesso, *et al.*, "TFTR Multichannel Neutron Collimator," Rev. Sci. Instrum. **61** (1990) 3163.

130 L.C. Johnson, "Validation of Spatial Profile Measurements of Neutron Emission in TFTR Plasmas (Invited)," Rev. Sci. Instrum. **63** (1992) 4517.

131 A.L. Roquemore, L.C. Johnson, and S. von Goeler, "Performance of the Upgraded Multichannel Neutron Collimator," Rev. Sci. Instrum. **66** (1995) 916-918.

132 J. Scott McCauley and J.D. Strachan, "Measurement of DT Neutron Emission from TFTR with Helium-4 Proportional Recoil Counters," Rev. Sci. Instrum. **63** (1992) 4536.

133 J.D. Strachan, Cris W. Barnes, M. Diesso, *et al.*, "Absolute Calibration of TFTR Helium Proportional Counters (Abstract)," Rev. Sci. Instrum. **66** (1995) 897.

134 D.L. Jassby, Cris W. Barnes, L.C. Johnson, *et al.*, "Absolute Calibration of Tokamak Fusion Test Reactor Neutron Detectors for D-T Plasma Operation," Rev. Sci. Instrum. **66** (1995) 891.

135 A.L. Roquemore, D.L. Jassby, L.C. Johnson, and J.D. Strachan, "Performance of a 14-MeV Neutron Generator as in *In Situ* Calibration Source for TFTR," in *Fusion Engineering* (Proc. 15th IEEE/NPSS Symp., Hyannis, MA, 1993), Vol. **1** (Institute of Electrical and Electronic Engineers, Piscataway, New Jersey, 1994) 114.

136 D.K. Mansfield, P.C. Efthimion, R.A. Hulse, *et al.*, "Particle Confinement Studies on Ohmically-Heated Plasmas in TFTR using Gas Modulation Techniques," in *Controlled Fusion and Plasma Physics* (Proc. 14th EPS Conf., Madrid, Spain, 1987), edited by F. Engelmann and J.L. Alvarez Rivas, Contributed Papers Vol. **11D** (Part I) (European Physical Society, 1987) 314-317.

137 R.J. Fonck and R.A. Hulse, "He^{++} Transport in the PDX Tokamak," Phys. Rev. Lett. **52** (1984) 530.

138 G. Rewoldt and W.M. Tang, "Toroidal Microinstability Studies of High-Temperature Tokamaks," Phys. Fluids B **2** (1990) 318

139 R.J. Fonck, D.S. Darrow, and K.P. Jaehnig, "Determination of Plasma-Ion Velocity Distribution via Charge-Exhange Recombination Spectroscopy," Phys. Rev. A **29** (1984) 3288.

140 D. Heifitz, D. Post, M. Petravic, J. Weisheit, and G. Bateman, "A Monte-Carlo Model of Netural-Particle Transport in Diverted Plasmas," J. Comput. Phys. **46** (1982) 309-327.

141 C.H. Skinner, H. Adler, R.V. Budny, *et al.*, "First Measurements of Tritium Recycling in TFTR," Princeton University Plasma Physics Laboratory Report PPPL- 2993 (June 1994) 21 pp.

142 P.H. LaMarche, H.F. Dylla, P.J. McCarthy, and M. Ulrickson, "Hydrogen Isotope Exchange and Conditioning in Graphic Limiters used in the Tokamak Fusion Test Reactor," J. Vac. Sci. Technol. A **4** (1986) 1198.

143 P. Andrew, J.P. Coad, J. Ehrenbert, D.H.J. Goodall, L.D. Horton, *et al.*, "Experiments on the Release of Tritium from the First Wall of JET," Nucl. Fus. **33** (1993) 1389.

144 T.Q. Hua and J.N. Brooks, "Analysis of Erosion and Transport of Carbon Impurity in the TFTR Inner Bumper Limiter Region," J. Nucl. Mater. **196-198** (1992) 514-519.

Princeton Beta Experiment-Modification

The goal of the Princeton Beta Experiment-Modification (PBX-M) Project is to improve the attractiveness of the tokamak as a fusion reactor concept. The PBX-M approach is to show the practicality of controlling the plasma current and pressure distributions to achieve stable advanced operating regimes and avoid plasma disruptions. The PBX-M is particularly well-suited for this task because it can explore concepts which are direct prototypes for the Tokamak Physics Experiment (TPX) and other future devices.

The PBX-M was operated in October and November of 1993 to complete experiments demonstrating the modification of the plasma current profile with lower-hybrid current drive (LHCD).[1] During this brief period, further work was also done with Ion-Bernstein wave (IBW) heating and neutral-beam injection (NBI) to investigate plasma discharges with a high central density. These plasmas were confirmed to be in a new tokamak operating regime that was first discovered on PBX-M. The new regime has been labeled the CH-mode (for "core H-mode"). This improved confinement mode, achieved with modest IBW power, is characterized by the formation of a core transport barrier, and it has stimulated widespread experimental and theoretical interest.[2,3]

Due to budgetary restrictions, the remainder of FY94 was devoted to facility upgrades and data analysis. The defective klystron for LHCD System 2 (high-$n_{\|}$) was repaired, so all eight tubes are now available for full-power operations. A new configuration for the LHCD couplers was also designed. The original arrangement consisted of two couplers located above and below the horizontal midplane of PBX-M, each capable of launching lower-hybrid waves with different parallel wavelengths. Arcing was observed in the gap between them, and the new geometry is intended to eliminate this by bringing the ends of the couplers together. Fabrication and installation are planned for the next fiscal year.

Among the most significant accomplishments in FY94 were:

- Analysis of NBI-heated plasma discharges with and without LHCD indicated that beam-driven currents themselves are not causing q(0) to rise above unity. This conclusion was based on equilibria reconstructed with the three-dimensional (3-D) Variational Moments Equilibrium Code, which uses magnetic-field pitch-angle profiles from the multichannel motional Stark effect (MSE) diagnostic and thermal pressure profiles from the multipoint Thomson scattering (TVTS) diagnostic. The VMEC results have also shown that in PBX-M, lower-hybrid current drive is more effective in raising the central safety factor q(0) in hydrogen plasmas than in deuterium discharges.
- The formation of an inner transport barrier, coincident with the radio-frequency (rf) power deposition profile, was documented in cases where IBW heating was applied to NBI-heated high-confinement mode (H-mode) plasmas. Analysis of soft X-ray emissivity profiles showed that during the initial phase of IBW heating, edge-localize-mode-driven thermal losses were reduced at the location of the barrier.[4] As the rf heating progressed, the inner transport barrier dominated the confinement zone as strong kinetic gradients appeared in the plasma core, and the discharge entered the CH-mode.
- Measurements with both the soft X-ray diode array and the multichannel third harmonic electron cyclotron emission (ECE) diagnostic

during the CH-mode indicated the presence of high-frequency modes with ballooning-like characteristics.[4] Examination of the impurity behavior during IBW heating indicated that the global impurity confinement time followed the improved confinement of the bulk plasma.[5] The deuterium behavior dominated the properties of these discharges.

- Further studies of edge plasma conditions were performed. An analysis of measurements obtained with amplitude modulation (AM) reflectometry showed that the plasma is moved away from the IBW antenna by the ponderomotive force during the application of rf power.[6] Bicoherence analysis of fast reciprocating probe data before and after the H-mode transition supported the relationship between plasma turbulence and magnetic shear.[7,8]

Equilibrium Modification with LHCD

The 3-D Variational Moments Equilibrium Code (VMEC)[9] is used to reconstruct PBX-M equilibria from external flux loop measurements and internal MSE magnetic-field data. The code first interpolates between MSE magnetic-field pitch-angle points and other discrete measurements with cubic spline fits and uses the resulting continuous functions to solve the Grad-Shafranov equation. A typical PBX-M equilibrium takes 25 to 35 sec on an IBM RISC-6000 workstation, which makes reconstructions possible between shots. The MSE pitch-angle data and VMEC fit for the Ohmic target plasma typically used in LHCD experiments is shown in Fig. 1.

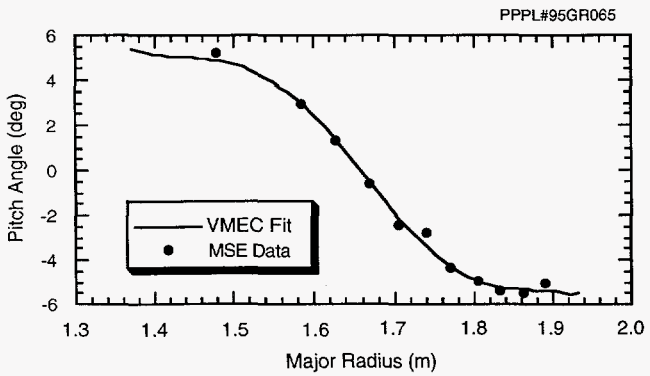

Figure 1. *Motional stark effect data and VMEC code fit for an Ohmic plasma.*

A stable operational path to high β_p can be found by first increasing the central "safety factor," or q(0), with off-axis LHCD in an Ohmic discharge and then heating the plasma with NBI.[10] This was attempted experimentally, and MSE measurements were obtained for the initial Ohmic plasma, the phase with LHCD alone, and combined LHCD and NBI. The VMEC equilibria constrained with MSE measurements were taken in each of these cases. For a 180-kA Ohmic discharge, q(0) = 0.93. Evaluation of systematic and random errors suggest an uncertainty of about 10%.[11] This value of q(0) is consistent with the presence of sawtooth oscillations.

The addition of 0.3 MW of LHCD raised q(0) to 1.15 and the suppression of sawtooth oscillations and m/n=1/1 modes was observed. After 175 msec of NBI at the 0.5-MW level, β_p doubled from 0.5 to 1.0. This was primarily due to the increase in density caused by the neutral-beam heating without sawtooth activity, and the central profile peaking is evident in Fig. 2. The discharge remained quiescent to magnetohydrodynamic (MHD) activity, however, and the central q stayed above 1 [q(0) = 1.1].

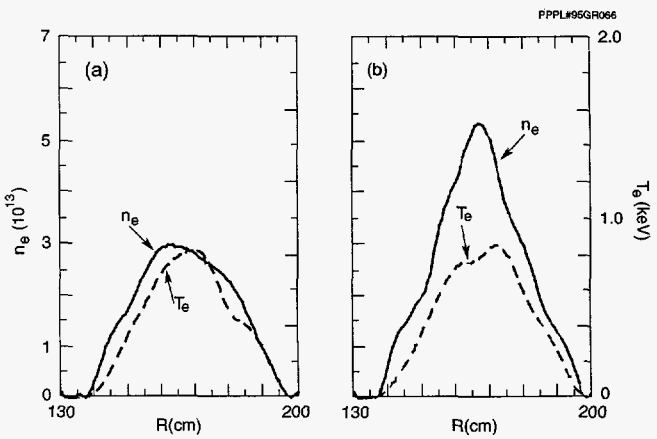

Figure 2. *Electron temperature (T_e) and density (n_e) profiles before (a) and after (b) addition of neutral-beam injection (NBI) to a plasma with lower-hybrid current drive. The β_p increased from 0.5 to 1.0 with the application of 0.5 MW of NBI power.*

To determine if beam-driven currents themselves could maintain q(0) above 1, discharges having NBI alone were compared with plasmas where LHCD and NBI were combined. The corresponding current density profiles are shown in Fig. 3. A measure of the shape of the current distribution is the ratio of the central current density to its value near the mid-minor radius point, j(0)/j(r = 15 cm). This was 2.2 for the

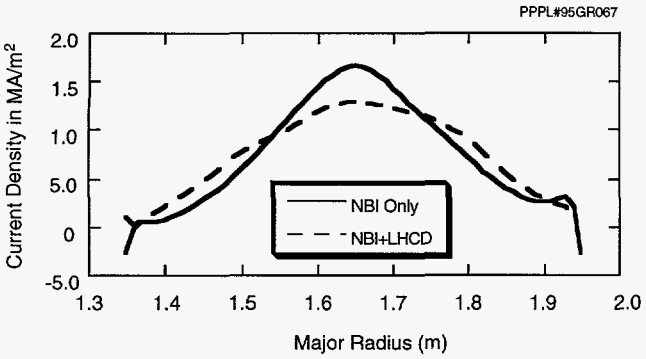

Figure 3. *Comparison of current density profiles with NBI only and combined NBI and LHCD.*

Ohmic plasma and 2.4 for discharges with NBI only. With both NBI and LHCD, however, the ratio falls to 1.4, which corresponds to a profile that is clearly broader and shows more off-axis current than in the NBI only case. The central q was 0.87 for the plasma with NBI only, and sawtooth oscillations were present as in the Ohmic discharge. In all of these cases (Ohmic, NBI only, and NBI combined with LHCD), the plasma current was 180 kA and the toroidal field was 13.5 kG.

The q(0) was increased above one in both hydrogen and deuterium plasmas (Fig. 4). The absence of hydrogen data at higher rf power was due to limitations in run time, but it was still possible to observe that the sawtooth crash behaved differently in the two cases. In hydrogen discharges, the sawtooth crash radius and the radial location of the precursor of the m/n=1/1 mode shrinks monotonically during the LHCD, until q(0) exceeds one. For deuterium plasmas, however, the sawtooth oscillations are suppressed promptly when LHCD power is applied, even though q(0) remains below one. A very weak residual 1/1-mode

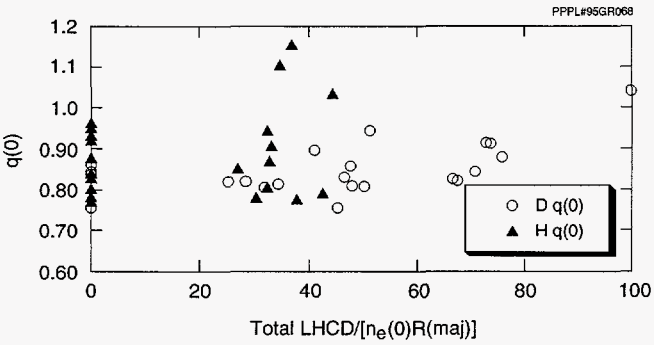

Figure 4. *Central safety factor q(0) as a function of radio-frequency power normalized to density (n_e) and major radius for hydrogen (H) and deuterium (D) plasmas.*

remains near the magnetic axis until q(0) eventually rises above one. The longer time it takes for q(0) to increase in these discharges under a given LHCD condition may explain the data in Fig. 4, where the change in q(0) is more modest in deuterium than in hydrogen at the same ratio of rf power to electron density. The cause of the prompt sawtooth suppression in deuterium discharges and the details of the consequences of the 1/1-mode on the increase in q(0) are currently under investigation.

Ion-Bernstein Wave Physics

Profile Loss during ELM's

In IBW experiments, approximately 0.3 MW of IBW power were injected into an H-mode discharge (2 MW of NBI) to modify the pressure and the current profile (Fig. 5). The IBW power deposition was located at the fifth harmonic deuterium ion-cyclotron ($5\Omega_D$) resonance layer, which was at $r \approx a/3$.[12] The plasma current in these discharges was 250 kA, toroidal magnetic field 1.5 T, major radius 165 cm, midplane halfwidth 30 cm, and elongation and triangularity 1.55 and 0.55, respectively. An increase in the central particle and energy confinement time in the core after 580 msec was associated with the injection of IBW.[13] The increase in central confinement was exhibited by an increase in the plasma diamagnetism and deuterium-deuterium neutron production rate.[13] The induced peaking, due to the application of IBW power to the H-mode phase, radically changed the character of the MHD behavior.

Three distinctive periods in the discharge were observed during the IBW-induced density peaking (Fig. 5). A weak transport barrier first formed in the core of the plasma, where the discharge was still in the H-mode (denoted in figure as "core transport barrier formation"). At that time, thermal losses by IBW-modified ELMs were greatly reduced at the location of the barrier between the q = 1 and q = 2 surfaces. The second phase (denoted in figure as "CH-mode formation") was characterized by the cessation of ELMs. This marked the onset of the formation of high core confinement (CH-mode). In the last period (denoted in figure as "CH-mode saturation"), the increase in the core confinement was limited by MHD activity.

Very shortly after the start of the IBW injection, the ELM-free H-mode period was terminated by the

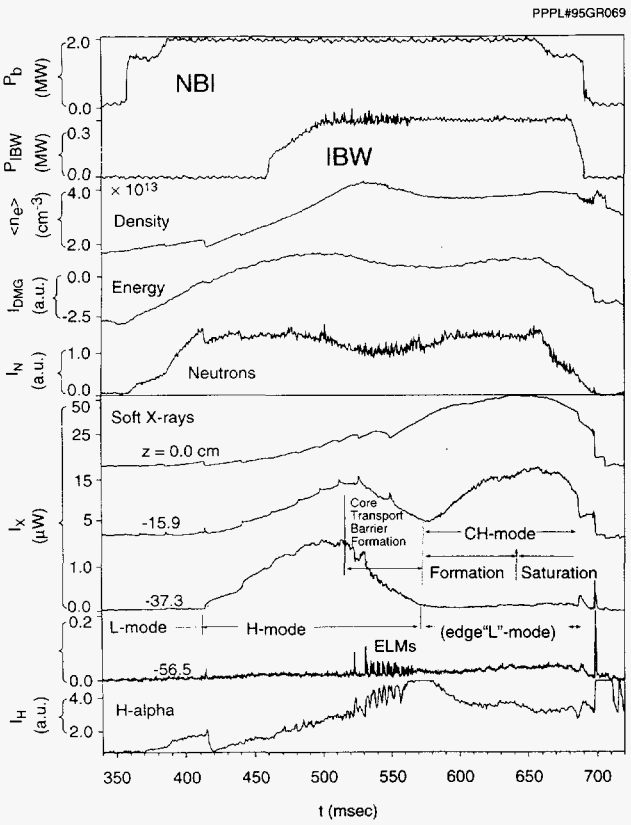

Figure 5. Typical neutral-beam-assisted IBW plasma discharge. Discharge parameters: P_b = neutral-beam-injection power, P_{IBW} = Ion-Bernstein wave power, $<n_e>$ = line-averaged density, I_{DMG} = noncompensated diamagnetic loop signal showing the plasma energy evolution, I_N = neutron rate signal, I_X = soft X-ray diode signals at four positions (z=0, -15.9, -37.3, and -56.5 cm) in the plasma, and I_H = H-alpha signal.

appearance of a series of a closely spaced ELMs, lasting from 520 to 570 msec (lowermost two traces in Fig. 5). During the ELM activity, the sawteeth were suppressed and the core transport barrier began to form. Sawteeth suppression was also observed 50 msec after the full IBW power was applied. This did not occur in the absence of IBW heating during discharges with comparable levels of NBI power. The stored energy (W_{tot}) for NBI-heated plasmas with and without IBW was calculated from the measured discharge parameters using the transport code TRANSP.[14] The results showed that W_{tot} for the CH-mode exceeds the NBI-only H-mode value.

The formation of the core transport barrier modified the ELMs, such that the thermal losses observed in soft X-rays were reduced at the barrier location. Figure 6 shows a comparison between IBW-modified ELMs [Fig. 6(a)] and the usual ELMs [Fig. 6(b)]. Here, z is the vertical distance of the diode line-of-sight to the midplane at the major radius R_0 = 165 cm. The ELM losses in an H-mode discharge without IBW heating normally penetrated deep into the confinement region. These losses start from a well-defined inversion radius of z = 40 cm, reach a maximum at z = 18 cm, and then decrease toward the center.

In the H-mode with IBW heating, the loss profiles were modified by the core transport barrier. The IBW-modified ELMs were triggered roughly at the same inversion radius near the edge. At z = 15 cm, however, they were responsible for a substantially smaller loss minimum between two loss maxima, indicating a "plugging" of the energy loss channel at this location. This minimum loss position coincides closely with the maximum in the density and pressure gradients and the maximum velocity shear, i.e., the location of a weak transport barrier created by the IBW.[12] The ELMs eventually stop, and at that time, the strong core barrier formation (the CH-mode) starts.

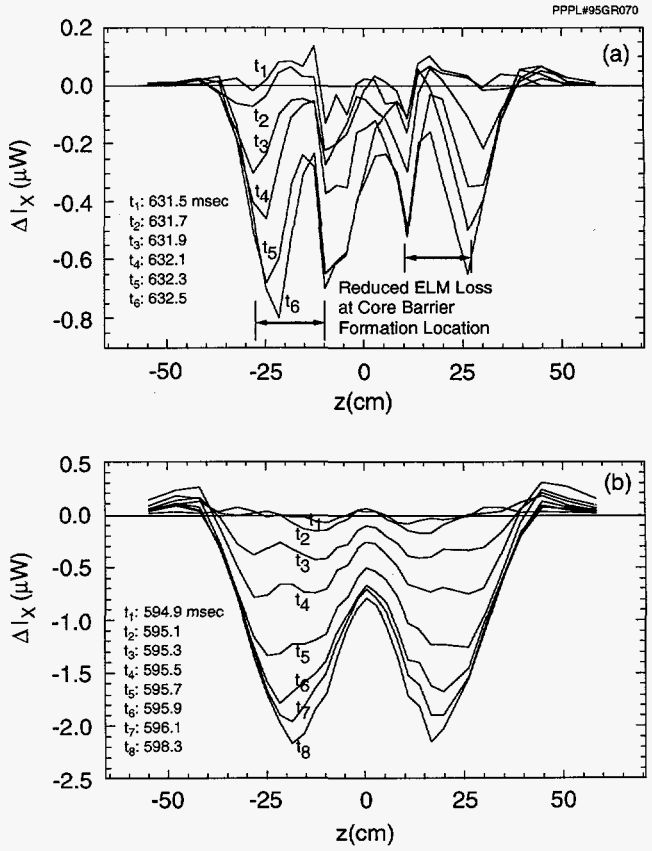

Figure 6. Time evolution of soft X-ray edge localized mode (ELM) loss profiles for (a) modified ELM during H-mode with IBW injection and (b) during H-mode with NBI only.

High-Frequency MHD with IBW and NBI

Immediately after the cessation of the ELMs (at 570 msec in Fig. 5), several plasma parameters began to peak in the core: density, electron and ion temperature, and toroidal velocity.[12] This profile peaking usually lasted for about 50 msec, and it was usually an MHD-quiescent period with an occasional single burst of a medium amplitude m=1/n=1 mode, which died out in 10 to 20 msec in most cases. Only in peaked pressure profile IBW+NBI discharges has high-frequency bursting in the core region been observed.

The bursting high-frequency modes were responsible for limiting the CH-mode in the majority of discharges. These modes occur over a frequency range between 70 and 350 kHz, and many of these modes—sometimes as many as ten—were excited simultaneously in different radial locations between the q = 1 and q = 2 surfaces. An example is shown in Fig. 7.

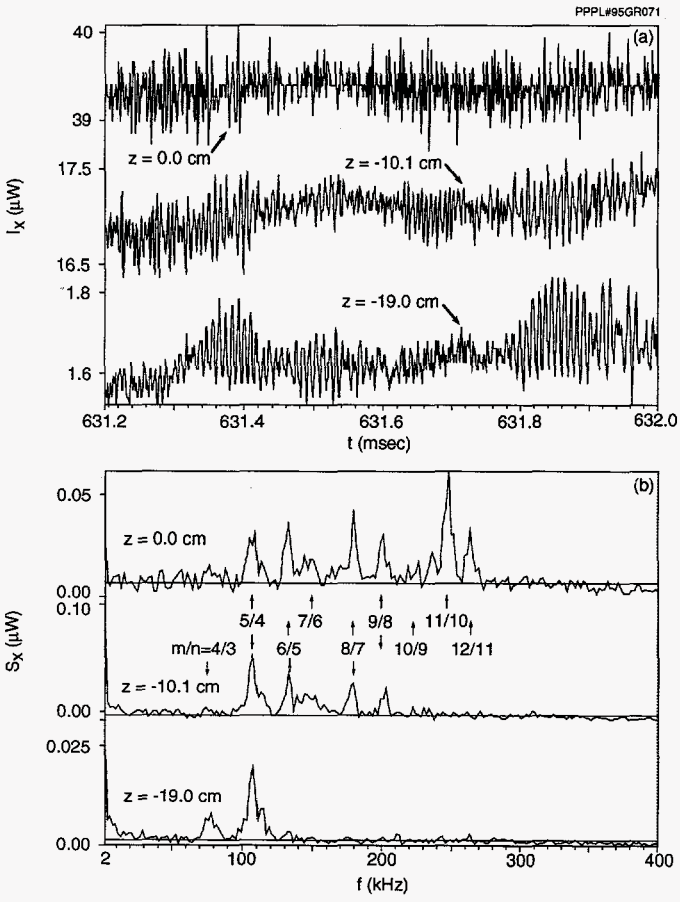

Figure 7. *Bursting mode during the saturation in density peaking. (a) Soft X-ray fluctuations at different plasma positions (z). (b) Power spectra for the X-ray signals in (a).*

The burst duration of individual modes was as short as 100 μsec. The main bursts were irregularly spaced, with repetition rates between 1 and 2 kHz. The spectra of these bursts, depicted in the lower half of Fig. 7, show many modes.

The m-numbers of these modes have been established either from the soft X-ray fluctuation profile or from the slope of the phase change across the soft X-ray diodes. The n-number has been either measured by the Mirnov coils, or inferred from the m-number and mode location. The mode numbers, increasing linearly with the mode frequency, are related by n=m-1, with the m-numbers for the highest frequencies as high as m=14 or higher. The modes were well-localized on shells in the region between q = 1.25 (m=5/n=4) and q = 1.08 (m=14/n=13), with q = m/(m-1) and possibly q = m/(m-2) in some cases. This region coincided with the location of the core transport barrier.

The frequency of these modes appeared to be simply the toroidal plasma rotation frequency at the location of the mode ($f = nv_t/2\pi R$). The amplitude of these modes was just strong enough to provide a self-regulation of the pressure and density gradients in the core transport barrier region. With increasing frequency, the spectral peaks of Fig. 7 moved more and more toward the center diodes. Detailed analysis of the amplitude and phase dependence of the mode on minor radius is consistent with a ballooning-like character for the high-m modes. The ECE heterodyne radiometry measurements (utilizing the third harmonic electron cyclotron emission) of the same high-frequency modes also showed a strong localization of these modes and ballooning-like behavior.

The soft saturation of the CH-mode that is coincident with the bursting high-frequency modes poses two questions: are these modes responsible for the confinement limit, and what is the driving mechanism for these modes? The close association between the appearance of the modes and the limiting of the core confinement increase is a strong indication that these modes are the cause. Concerning the driving mechanism, MHD stability calculations with the PEST code, which included wall effects, have shown that the external kink is stabilized in these discharges. Infinite-n CAMINO code calculations have shown that ballooning modes are marginally unstable in approximately the same region of the plasma where the bursting high-frequency modes were observed.

The fact that the higher-m modes showed ballooning-like effects supports the picture that these modes

might be ballooning modes. In addition, these modes also appeared at the location of the highest pressure gradient, and they seemed to limit the growth of the gradient. This further suggests that they are ballooning modes, since they might be driven by the pressure gradient. The bursting high-frequency modes are nonpropagating, with frequencies given by the harmonics of the Doppler frequency, so they are not likely to be kinetic ballooning modes or toroidicity-induced Aflvén eigenmodes.

In a few discharges, the m=1/n=1 burst developed into a continuous and strong mode without 2/1 and 3/1 components, and it usually began to grow during the CH-mode formation stage. The strong m=1/n=1 mode appeared to be more effective in stopping the growth in the temperature and density gradients than the high-frequency bursting modes, thus preventing the core transport barrier from developing fully and reducing the confinement. Appearing with this mode was a 1 kHz, m=2/n=2 mode and a 150 kHz, m=6/n=6 (or 5) mode. These three modes interact nonlinearly.[15] Further study of the strong m=1/n=1 mode awaits more careful measurements of q(0) and the safety factor shear dq/dr at q = 1 when experimental operations resume.

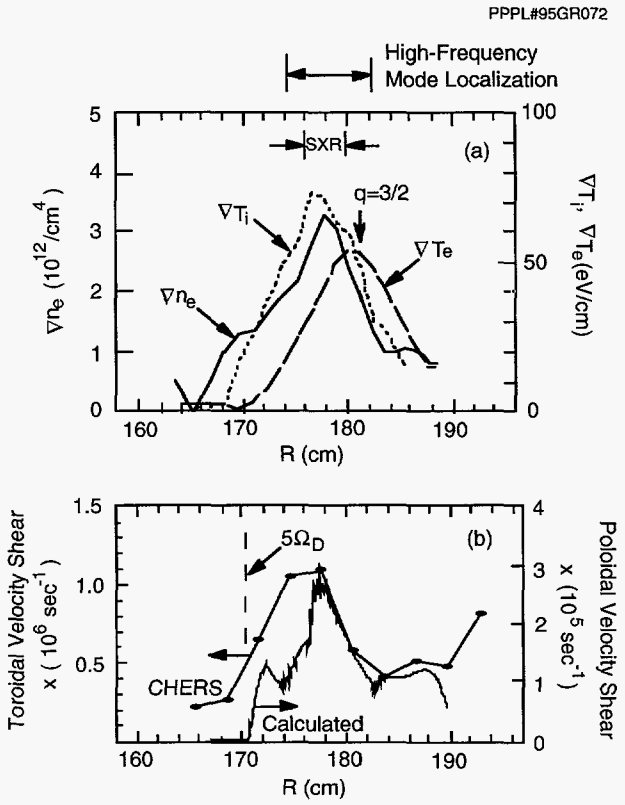

Figure 8. *(a) Composite of radial profiles of gradients [density (n_e) and ion and electron temperatures (T_i, T_e)]. The location of the electron energy barrier from the soft X-ray (SXR) measurements and the region where the high-frequency mode occurs is also indicated. (b) Profiles of CHERS measured toroidal shear and calculated poloidal shear.*

Comparison of Transport Barrier Formation and Sheared Flow Model

The radial profiles of the absolute values of the electron temperature T_e, ion temperature T_i, and density n_e gradients are shown in Fig. 8(a). The H-mode has a strong density gradient in the edge region. For the CH-mode, the strong density gradient region is moved well into the plasma core. The CH-mode also has a strong electron temperature gradient in the core region (R ≈ 178 cm), well above the experimental error bars. These large gradients suggest the existence of an H-mode-like transport barrier near the mid-radius region.

Similar gradients can be also seen in the ion temperature profile. The observed location of the soft X-ray ELM barrier (R ≈ 176-178 cm) is indicated in Fig. 8(a). In the strong pressure gradient region, ballooning-like high-frequency (75-350 kHz) MHD fluctuations are observed. In Fig. 8(b), the V_ϕ gradient and the calculated IBW-induced poloidal sheared flow are shown, with their locations coinciding relatively well with the observed barrier location. The electron temperature gradient appears to occur at a slightly larger radius than the rest of the barrier locations. It might be conjectured that the electron temperature gradient may be influenced by the presence of the nearby q = 3/2 surface. Transport analyses have also shown that the toroidal momentum and ion thermal diffusivities are lower during the CH-mode than for the preceding H-mode phase.

In the PBX-M ion-Bernstein wave experiments, the peaking of density was observed not only in the CH-mode (with NBI heating) but also in the Ohmic discharges. In a typical Ohmic discharge, the application of modest IBW power (100 kW) for $5\Omega_D$ resonance heating is usually sufficient to cause the density peaking. Also, in previous IBW experiments on JIPPTII-U at the National Institute of Fusion Studies at Nagoya, Japan, third harmonic hydrogen resonance heating caused peaking of the density and pressure profiles in Ohmic-heated and NBI-heated L-mode (low-confinement mode) circular plasmas.[16] Therefore, profile

peaking by IBW heating appears to be associated with the presence of a resonant absorption layer in the plasma. The occurrence of peaking for the case with strong wave absorption is consistent with the sheared flow model.[3,12] In addition, the observed required power in PBX-M for density peaking is on the order of 100 kW (for circular Ohmic parameters) and 300 kW (for bean-shaped CH-mode parameters), which is consistent with the IBW power required by the sheared flow model.[3,12]

In one experiment with a circular Ohmic plasma on PBX-M, the IBW ion cyclotron heating layer was moved to the high-field side of the plasma by going down to the lower cyclotron harmonic frequency ($\omega < 4\Omega_D$) with the reduced transmitter frequency of 42 MHz. This configuration makes the heating layer inaccessible to the externally launched IBW, since the IBW rays are radially reflected near the plasma axis without any damping. The inward and outward going waves tend to cancel the poloidal drive and, therefore, little sheared flow is expected.[12] No density profile peaking was observed in more than 100 shots under these conditions, even at higher IBW power (≈200 kW), thus lending further support to the sheared flow model.

Impurity Behavior during IBW Heating

In PBX-M, it is usually observed that influxes of both low-Z and high-Z impurities increase during IBW injection in all types of operation,[5] although rates can be minimized by boronization of the vacuum vessel.[17] For example, 340 kW of IBW heating power can raise the central iron and nickel concentrations by more than an order of magnitude. The central confinement of the bulk plasma also increases, as shown by the peaking of the electron density profiles. The radiated power profile, as determined from a 15-channel bolometer array, tends to be hollow prior to the introduction of the IBW, but becomes more peaked until a "soft" disruption occurs about 300 msec after the application of the rf power.

The peripheral carbon and oxygen emissions grow by factors of five, while the metallic impurities increase to the point where their lines are the dominant features in the vacuum ultraviolet spectrum. The data indicate that the strong rise in the radiation from ions such as Fe XVI and Ni XVIII occur not only because of the increased influx, but also as a result of the impurities becoming more centrally concentrated. This conclusion is based on comparing the strength of the unresolved lines from low-ionization stages in the region around 200 Å to the strengths of the sodium-like and magnesium-like ions. The former increase by about a factor of five during IBW heating, while the latter rise by factors of at least twenty.

When IBW heating is used in conjunction with NBI, impurity transport depends on whether the discharges are in the L-mode or H-mode. In a typical L-mode discharge, 2.5 MW of NBI raises the radiation from the metallic ions by about a factor of two over levels during Ohmic heating alone. The addition of 340 kW of IBW heating further increases the metallic emissions by about another factor of five. The transport coefficients are not significantly changed, in that there is no build-up of impurities, and the plasma remains in the L-mode. If a discharge makes a transition to the H-mode during NBI, the impurity confinement time appears to increase at the onset, but no strong central peaking of the metallic profiles occurs. However, the addition of IBW power raises the losses by a factor of four, and the profiles become very narrow. In addition, the electron temperature profile frequently evolves to a flat or slightly hollow shape in these cases.

When the plasma makes a transition to the H-mode shortly after the start of NBI (Fig. 9), the emissions from the peripheral regions, such as O V and C III radiation, drop as the electron temperature gradient steepens. These signals then rise to pre-H-mode levels when IBW heating is applied, and a greater in-

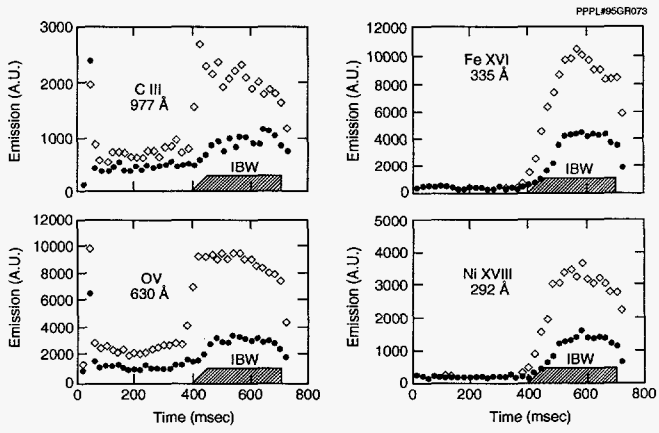

Figure 9. Evolution of spectral line radiation during IBW heating in an H-mode plasma. The closed circles are for neutral-beam injection only and the open diamonds are for neutral-beam injection plus ion-Bernstein waves.

flux of impurities occurs. In contrast, the metallic emissions show minor changes when there is NBI alone, and the intensities of Fe XVI and Ni XVIII only grow rapidly with the addition of IBW power. After about 150 msec of rf heating, there is a sharp drop in signal strength. This is apparently due to a strong pinch that compresses the iron and nickel towards the center, rather than a decrease in impurity influx. This interpretation is evident from the Fe XXIII and Ni XXV resonance lines, which increase during this interval. The tendency toward central peaking of the impurities is also observed in the profiles of the fully stripped oxygen, as deduced from charge-exchange excitation measurements. These data show that impurity pinching during IBW heating is also evident for low-Z ions.

Edge Physics

Edge Density Profile Measurements during IBW Heating

In IBW heating experiments, the ponderomotive force is particularly strong because the antenna electric field is mainly parallel to the magnetic field of the tokamak. The ponderomotive potential is given by the following expression.[18]

$$\Psi_{rf} = 10^2 F^{-2} | E_{\|} |^2.$$

Here, F is the applied rf frequency in units of 100 MHz and $E_{\|}$ is the parallel electric field in statvolts/cm. The ponderomotive potential can be important for low-frequency experiments in the 10 to 100 MHz range. At F = 30 and $E_{\|} = 1$, for example, Ψ_{rf} is about 1 keV, which is higher than the plasma temperature. Therefore, a substantial density modification can be expected.

The ponderomotive potential, if very large, can cause a density "hole" to develop in front of the antenna, and this can lead to nonlinear coupling effects. Therefore, the edge physics must be known when IBW power is applied to insure good heating efficiency. Thus, the measurement of the edge density profile close to the antenna becomes a very important means of understanding the wave coupling physics in IBW heating experiments.

The amplitude modulation (AM) reflectometer horns on PBX-M were installed adjacent to the Faraday shield of one of the IBW antennas. Profiles from the AM reflectometer were matched to the Thomson scattering data to determine their absolute spatial location. Edge density profiles for discharges with two different levels of IBW heating power are shown in Fig. 10. These data demonstrate the power dependence of the "hole," or density depletion, in front of the IBW antenna.[6]

These measurements are consistent with observations from other experiments. The modification of the rf antenna coupling due to the ponderomotive potential has been previously investigated for the case of lower-hybrid waves,[19,20] and similar effects have been reported for IBW on ACT-I[21] and Doublet-III-D (DIII-D).[22] In DIII-D, increasing the rf power was also observed to move the plasma away from the antenna, and this could be interpreted as evidence for a ponderomotive density depletion effect. However, no direct measurements of the edge density profile modification due to IBW heating as a function of time during a single discharge have been reported until the experiments on PBX-M.

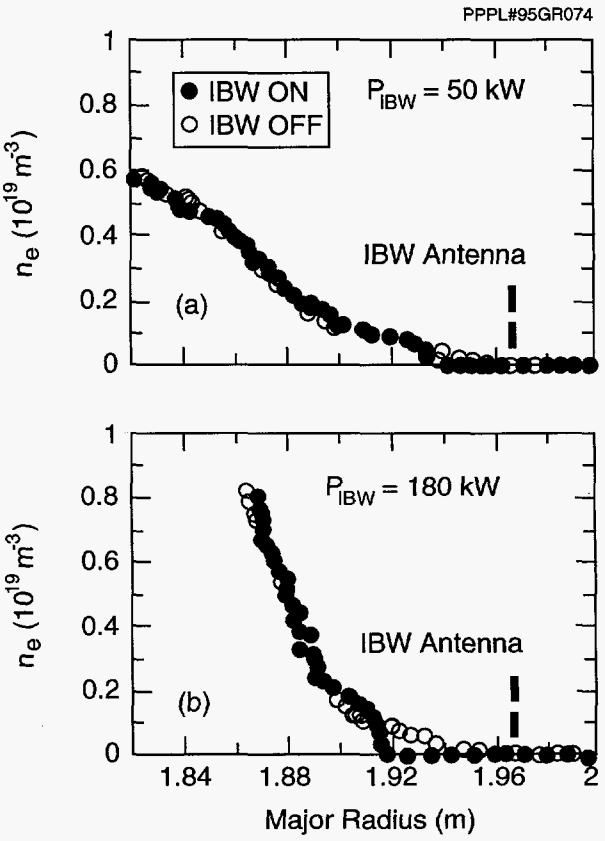

Figure 10. *Density profiles measured in the vicinity of the IBW antenna at two different rf powers: (a) P_{IBW} = 50 kW and (b) P_{IBW} = 180 kW.*

Fluctuation Analysis of Langmuir Probe Data

The fast reciprocating probe on PBX-M was inserted up to 0.7 cm inside the separatrix during H-mode plasmas with NBI.[7,8] In these discharges, a strong negative electric field is observed [Fig. 11(a)]. At the time of the H-mode transition, a suppression of the ion saturation current and the floating potential occurs. The effective turbulent diffusion coefficient is diminished by an order of magnitude [Fig. 11(b)], which is consistent with reduced edge transport. Steep edge density gradients form in the region $0.8 < r/a < 1$ within a few msec of the L-to-H transition, which is faster than the edge transport time.

The probe data indicate that the fluctuation propagation direction reverses over a narrow (≈0.3 cm) layer just inside the last closed flux surface during the H-mode. This is shown in Fig. 11(c), and it is consistent with the development of a negative radial electric field. There is a similar flow reversal during the L-mode, but the shear is a factor of two to three smaller, and it reaches a maximum at several centimeters inside the last closed flux surface. In addition, the probe measurements show that a highly localized, radially narrow coherent mode is present just inside the last closed flux surface during the H-mode.

Similar observations have been made on DIII-D, where far infrared collective scattering results, for example, have indicated that coincident with the L-to-H transition, there is a large reduction in the electron density fluctuation level at the plasma edge. This is the region where the radial electric field, as determined from the toroidal and poloidal rotation profiles of an impurity species, is negative. After the L-to-H transition in DIII-D, the fluctuation spectra broaden, which is indicative of increased electric field shear where the electron density fluctuation level is reduced.[23]

The standard linear spectral analysis (power spectrum) provides experimental information on the amplitude and phase behavior of the individual Fourier components. However, it does not give any information about the coupling between different spectral components. The use of bispectral analysis, on the other hand, allows discrimination between waves spontaneously excited by the plasma and those generated by nonlinear coupling mechanisms.[24]

The bicoherency measures the fraction of the fluctuation power at a frequency f which is phase correlated with the spectral components at the frequencies f_1 and f_2 obeying the summation rule $f = f_1 \pm f_2$. The bicoherency is bounded between 0 and 1. When it is equal to one, the fluctuations at frequency f are completely coupled with the frequency components at frequency f_1 and f_2, and they are completely uncoupled for a value of zero. The bicoherence has been computed for Langmuir probe measurements taken in the plasma bulk side of the velocity shear location ($r\text{-}a_{shear} \approx -2$ cm) in PBX-M. Significant values for the bico-

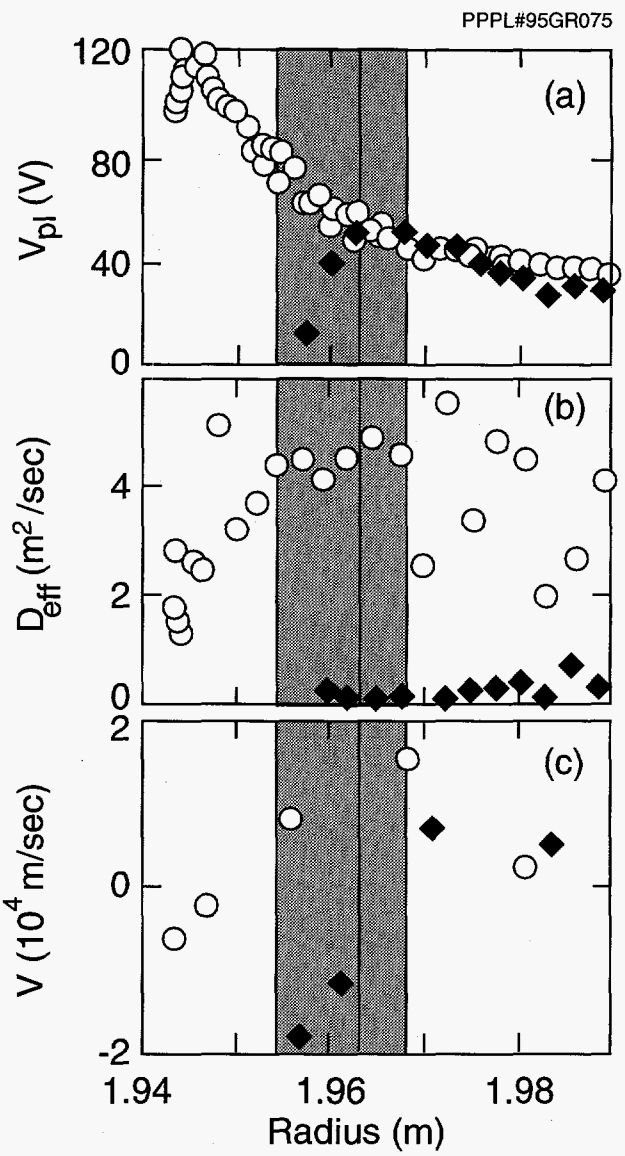

Figure 11. *Radial profiles in L-mode (open circles) and H-mode (closed diamonds) plasma discharges: (a) plasma potential, (b) effective diffusion coefficient, and (c) poloidal fluctuation propagation velocities. The shaded region indicates the separatrix position estimated from an equilibrium reconstruction.*

herence have been obtained in the plasma edge region, which may indicate long-wavelength drift-wave turbulence.[25]

Graduate Studies and General Education Programs

High school and undergraduate college students (Summer Science Awards Program) and a high school teacher (Teacher Research Associates Program) participated in data analysis and assisted in the development of an advanced plasma control system for PBX-M in the summer of 1994. The teacher made a presentation on his analysis of hard X-ray imaging data at the American Physical Society's Division of Plasma Physics meeting in November, 1994. The Massachusetts Institute of Technology (MIT) student in residence at PPPL successfully defended his thesis on fluctuation measurements with the third harmonic electron cyclotron emission diagnostic in July, 1994. Graduate student projects nearing completion include AM reflectometry for density profile measurements (Centro de Investigaciones Energetics Medioambientales y Technologicas or CIEMAT) in Madrid, Spain, the oblique ECE diagnostic for fast electron transport measurements (Princeton), and the vertically viewing ECE diagnostic using the signal from a transient LHCD pulse to determine plasma parameters (Princeton).

A postdoctoral research scientist from MIT continued to work on equilibrium reconstruction and analysis of LHCD data. The International Atomic Energy Agency postdoctoral fellow from the Hungarian Academy of Sciences, who was in residence at PPPL in FY93, continued his analysis of hard X-ray distributions during LHCD at his home institution.

Collaborations with Other Institutions

Researchers from several fusion laboratories and university groups participated in the analysis of data from PBX-M operations in FY93 and early FY94. The Oak Ridge National Laboratory (ORNL) had primary responsibility for impurity analysis, and it had a leading role in the study of plasma fluctuations. ORNL also completed development of VMEC, which incorporates data from the multichannel motional Stark effect diagnostic of Fusion Physics and Technology for equilibrium reconstruction. The MIT group continued their participation in LHCD physics and the analysis of fluctuation data from their third harmonic electron cyclotron emission diagnostic. Scientists from the University of California at Los Angeles continued their edge profile and turbulence studies, which also involved physicists and graduate students from CIEMAT. The quasilinear analysis of IBW absorption by electrons was a collaborative effort with Associazione-ENEA, Frascati, Italy. There was also a visiting scientist from Association-CEA, Cadarache, France, who participated in the analysis of MHD phenomena during LHCD.

References

[1] Princeton University Plasma Physics Laboratory Annual Report PPPL-Q-51 (October 1, 1992 to September 30, 1993) 39.

[2] S.-I. Itoh, K. Itoh, and A. Fukuyama, "Physics of Edge Plasmas in Enhanced Confinement Modes," J. Nucl. Mater. **220-222** (1995) 117-131.

[3] P.H. Diamond, *et al.*, "Dynamics of the L to H Transition, ELM's VH-Mode Evolution and RF Driven Confinement Control in Tokamaks," in *Plasma Physics and Controlled Nuclear Fusion Research 1994* (Proc. 15th Int. Conf., Seville, Spain, 1994) Paper IAEA-CN-60/D-2-II-6, to be published by the International Atomic Energy Agency in 1995.

[4] S. Sesnic, S. Batha, R. Bell, *et al.*, "MHD Behavior During RF Current Profile Control Experiments in PBX-M," in *Plasma Physics and Controlled Nuclear Fusion 1994* (Proc. 15th Int. Conf., Seville, Spain, 1994), Paper IAEA-CN-60/A3/5-P-12, to be published by the International Atomic Energy Agency in 1995.

[5] R.C. Isler, A.P. Post-Zwicker, S.F. Paul, *et al.*, "Impurity Behavior During Ion-Bernstein Wave Heating in PBX-M," in *Controlled Fusion and Plasma Physics* (Proc. 21st EPS Conf., Montpellier, France, 1994), edited by E. Joffrin, P. Platz, and P.E. Stott, Contributed Papers Vol. **18B** (Part I), (European Physical Society, 1994) 42.

[6] E. de la Luna, J. Sanchez, V. Zhuravlev, *et al.*, "Edge Density Profile Measurements on PBX-M Using an Amplitude Modulation Reflectometer," in *Controlled Fusion and Plasma Physics* (Proc. 21st EPS Conf., Montpellier, France, 1994) edited by E. Joffrin, P.

Platz, and P.E. Stott, Contributed Papers Vol. **18B** (Part **III**), (European Physical Society, 1994) 1180.

[7] R.D. Bengtson, R. Bell, L. Blush, *et al.*, "Control of Edge Turbulence in PBX-M and TEXT-U," in *Plasma Physics and Controlled Nuclear Fusion Research 1994* (Proc. 15th Int. Conf., Seville, Spain, 1994), Paper IAEA-CN-60/A-4-II-2, to be published by the International Atomic Energy Agency in 1995.

[8] C. Hidalgo, T. Estrada, E. Sanchez, *et al.*, "Nonlinear Phenomena, Turbulence and Anomalous Transport in Fusion Plasmas," in *Plasma Physics and Controlled Nuclear Fusion 1994* (Proc. 15th Int. Conf., Seville, Spain, 1994) Paper IAEA-CN-60/A2-4-P-15, to be published by the International Atomic Energy Agency in 1995.

[9] S.P. Hirshman, D.K. Lee, F.M. Levinton, *et al.*, "Equilibrium Reconstruction of the Safety Factor Profile in Tokamaks from Motional Stark Effect Data," Phys. Plasmas **1** (1994) 2277.

[10] S. Bernabei, R. Bell, M. Change, *et al.*, "Experimental Exploration of Profile Control in the Princeton Beta Experiment-Modified (PBX-M) Tokamak," Phys. Fluids B **5** (1993) 2562.

[11] F. Levinton, S.H. Batha, M. Yamada, and M.C. Zarnstorff, "q-profile Measurements in the Tokamak Fusion Test Reactor," Phys. Fluids B **5** (1993) 2554.

[12] M. Ono, B. LeBlanc, H. Kugel, *et al.*, "Formation of Core Transport Barrier and CH-Mode by Ion-Bernstein Wave Heating in PBX-M," *Plasma Physics and Controlled Nuclear Fusion 1994* (Proc. 15th Int. Conf., Seville, Spain, 1994) Paper IAEA-CN-60/A-3-I-7, to be published by the International Atomic Energy Agency in 1995.

[13] B. LeBlanc, R. Bell, J. Dunlap, *et al.*, "Core Profile and Transport Improvement During IBWH in PBX-M," *Controlled Fusion and Plasma Physics* (Proc. 21st EPS Conf., Montpellier, France, 1994) edited by E. Joffrin, P. Platz, and P.E. Stott, Contributed Papers Vol. **18B** (Part **I**), (European Physical Society, 1994) 186.

[14] R. J. Hawryluk, "An Empirical Approach to Tokamak Transport," in *Physics of Plasmas Close to Thermonuclear Conditions* (Proc. of Course, Varenna, Italy, 1979) Vol. **1** (Commission of the European Communities, Brussels, Belgium, 1980) 19.

[15] S. Sesnic, R. Kaita, S. Kaye, *et al.*, "Non-Linear Coupling of Low-n Modes in PBX-M," Nucl. Fusion **34** (1994) 1365.

[16] T. Seki, R. Kumazawa, T. Watari, *et al.*, "High Frequency Ion Bernstein Wave Heating Experiment in the JIPP T-IIU Tokamak," Nucl. Fusion **32** (1992) 2189.

[17] H.W. Kugel, J. Timberlake, R. Bell, *et al.*, "Real-Time Boronization in PBX-M using Erosion of Solid Boronized Targets," J. Nucl. Mater. **220-222** (1995) 636-640.

[18] M. Ono, "Ion Bernstein Wave Heating Research," Phys. Fluids B **5** (1993) 241.

[19] G.J. Morales, "Coupling of Lower-Hybrid Radiation at the Plasma Edge," Phys. Fluids **20** (1977) 1164.

[20] J. R. Wilson and K. L. Wong, "Ponderomotive Force Effects on Slow-Wave Coupling," Phys. Fluids **25** (1982) 675.

[21] F. Skiff, "Linear and Non-Linear Excitation of Slow Waves in the Ion Cyclotron Frequency Range," Ph. D. Thesis, Princeton University (1985).

[22] M.J. Mayberry, R.I. Pinsker, C.C. Petty, *et al.*, "Ion Bernstein Wave Antenna Loading Measurements on the DIII-D Tokamak," Nucl. Fusion **33** (1993) 627.

[23] C. L. Rettig, W.A. Peebles, K.H. Burrell, *et al.*, "Edge Turbulence Reduction at the L-H Transition in DIII-D," Nucl. Fusion **33** (1993) 643.

[24] Ch. Ritz, E.J. Powers, and R.D. Bengtson, "Experimental Measurement of Three-Wave Coupling and Energy Cascading," Phys. Fluids B **1** (1989) 153.

[25] B.A. Carreras, K. Sidikman, P.H. Diamond, *et al.*, "Theory of Shear Flow Effects on Long-Wavelength Drift Wave Turbulence," Phys. Fluids B **4** (1992) 3115.

Current Drive Experiment-Upgrade

The research program of the Current Drive Experiment-Upgrade (CDX-U) is presently focusing on the physics of spherical tokamak (ST) plasmas. In particular, the emphasis is placed on the critical physics issues related to performance projections and design of future mega-amp-level spherical tokamak experiments such as the National Spherical Tokamak Experiment (NSTX). If the plasma confinement and stability in the ST regime proves to be favorable, then such a configuration could evolve into a relatively compact neutron source facility, as well as an attractive advanced high-β tokamak reactor. The ST configuration also lends itself naturally to the investigation of trapped particles and related physical processes such as trapped-particle-driven microturbulence and associated plasma transport and neoclassical bootstrap current generation.

With the installation of a high-performance Ohmic solenoid in FY94, the CDX-U has been used to investigate many important physics issues such as the Ohmic start-up of ST plasmas in the presence of a toroidally continuous vacuum vessel and the plasma current or q(a) limits of the plasmas. At present, four major areas of ST-relevant research are being pursued on CDX-U:

(1) Operational limits of the inductively and noninductively driven ST plasma;

(2) MHD instabilities in ST plasmas;

(3) Electron-ripple injection for improving ST plasma confinement; and

(4) Physics of high harmonic fast waves for heating and current drive of ST plasmas.

To support the above physics investigations, the CDX-U device was designed to afford maximum plasma access for diagnostics. To provide plasma profile information, a Fabry-Perot Doppler interferometer, a microwave current and density imaging system, and an improved magnetic diagnostic system were developed. As an advanced diagnostic to measure microturbulence, a CO_2 phase-contrast-imaging system was developed under separate U.S. Department of Energy Applied Physics and Technology funding. To measure the electron temperature profile in CDX-U, an addition of a multipass Thomson scattering system and soft X-ray diagnostics will be developed.

Spherical Tokamak Research Results

Efficient Tokamak Start-up Technique

In designing low-aspect-ratio tokamaks like the CDX-U, a toroidally continuous vacuum vessel wall design is necessary because of the tight "inner leg" space. This design will be beneficial for advanced tokamaks where a toroidal insulating break will be difficult to implement and for larger CDX-U-like "spherical tokamaks." A potential problem of this design is that plasma initiation can be hampered because poloidal magnetic fields created by wall eddy currents induced during Ohmic heating start-up can make the plasma current MHD unstable. Studies of CDX-U Ohmic start-up in the presence of significant wall eddy currents can provide benchmarks for future spherical tokamak experiments.

The initial three-month period of Ohmic operation was devoted to measuring and properly modeling the induced-wall-eddy current. This time varying eddy current must be compensated for by properly programming the poloidal-field coils. With the aid of the Tokamak Simulation Code and other computer models developed by CDX-U scientists, proper poloi-

dal-field waveforms were determined and applied, resulting in a stable tokamak plasma discharge. Combining Ohmic heating with electron cyclotron resonance heating (ECRH), it was possible to start-up the tokamak plasma efficiently with almost arbitrarily low loop voltages ($V_{loop} \leq 1$ V).

Plasma current generating efficiency of 1.7 kA per mV-sec was obtained up to a plasma current I_p = 53 kA. Figure 1 shows the maximum plasma current obtained thus far in CDX-U Ohmic discharges as a function of volt-second expenditure for various discharges. This measure of Ohmic heating efficiency can be seen to improve slightly with increasing plasma current, suggesting an increasing average temperature with plasma current. The maximum current ramp-up rate attained is 10 kA per msec. An Ejima coefficient of 0.4 was routinely obtained. The observed efficiency and the ramp-up rate dropped only by 10% when toroidal-field current I_{tf} was reduced by a factor of 2.3 (from I_{tf} = 160 kA to 70 kA).

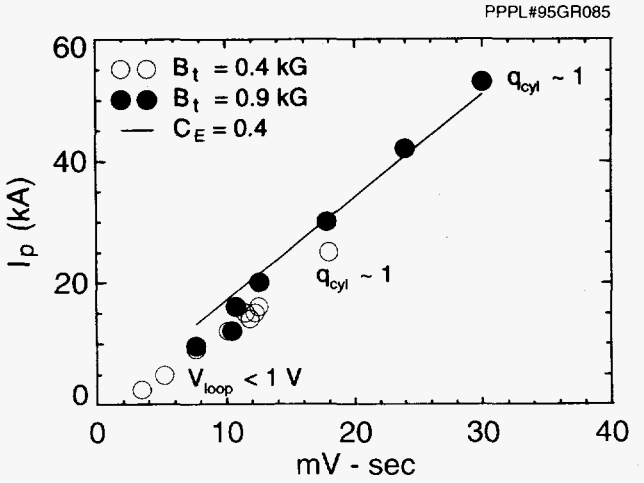

Figure 1. Ohmic plasma current (I_p) as a function of millivolt-second (mV-sec) expenditure for various plasma discharges. The toroidal magnetic-field is B_t and C_E is the Ejima Coefficient.

Exploring the Plasma Current Limit

The plasma current limit in a low-aspect-ratio tokamak (LART) is of interest, since predicted performance improvements in parameters such as plasma beta limit, plasma confinement, reactivity, etc., depend on how much current a given LART can support [limit in q(a)] without undesirable effects such as MHD instabilities and plasma disruptions. Figure 1 shows the progress in plasma current during FY94. The maximum current increased to more than 50 kA. A q(a) (q refers here to MHD q unless otherwise noted) value below 4 was obtained with the cylindrical-q near one, which is a record in a LART plasma. The plasma discharge time increased from less than 1 msec to 20-30 msec. The long discharge time shows that the plasma has very low resistivity, indicative of a hot core electron temperature. Typical plasma parameters for these low q(a), low-aspect-ratio plasmas were: major radius R = 0.34 m, minor radius a = 0.22 m, line-integrated density $n_eL \approx (4.5\text{-}10) \times 10^{17}$ m^{-2}, and an estimated electron temperature in the range of 100-200 eV from charge-state analysis of carbon lines. These parameters indicate that the plasma is already in the low-collisionality regime $\nu_e^* \approx$ 0.1-0.3, where trapped-particle effects become important.

Taking advantage of the relative insensitivity of the plasma current to the toroidal magnetic field, it was possible to attain q(a) ≤ 5 plasma discharges with various toroidal magnetic fields. Maximum plasma current obtained thus far in CDX-U Ohmic plasmas, as a function of toroidal field, is shown in Fig. 2. Maximum plasma currents at given toroidal magnetic fields appear to be limited to q(a) ≥ 3-4 ($q_{cyl} \geq 1$) and q(0) ≈ 1.

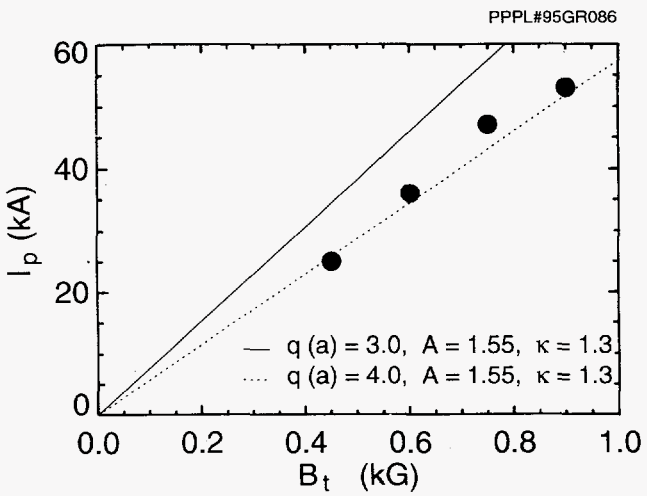

Figure 2. Maximum plasma current (I_p) obtained as a function of toroidal magnetic-field (B_t) strength. The safety factor at the edge is q(a), A is aspect ratio, and K is elongation.

Investigating MHD Activity

As the plasma current limit is approached, the MHD instability activity is observed to increase as

shown in Fig. 3. The MHD activity often leads to an abrupt termination of the plasma discharge. The mode number of the dominant MHD instability has been measured to be n=1 and m=1 and 2. The MHD instability appeared to be prominent in the outer region

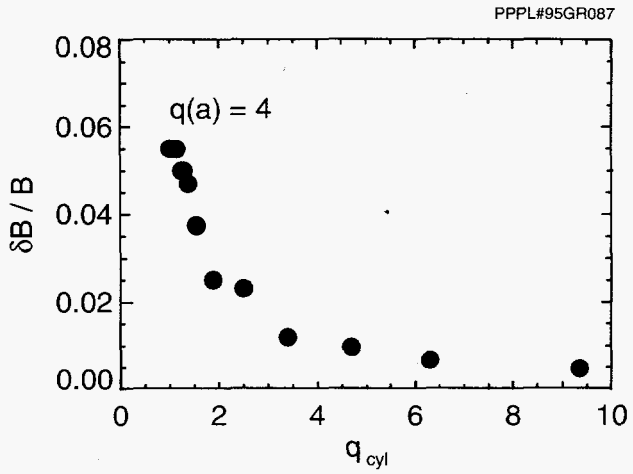

Figure 3. *Measured MHD fluctuation levels as a function of safety factor q_{cyl} and normalized measured fluctuation level $\delta B/B$.*

(lower field) of the plasma. The radial structure of these modes shows a dip in the vertical magnetic-field fluctuation $\delta B_Z/B_Z$ signal but not in the radial magnetic-field fluctuation $\delta B_R/B_Z$ signal, as shown in Fig. 4, which suggests the possible existence of large magnetic islands at the low-field side. As the central safety factor q(0) drops below one, these islands can couple with m=1/n=1 sawteeth and terminate the plasma

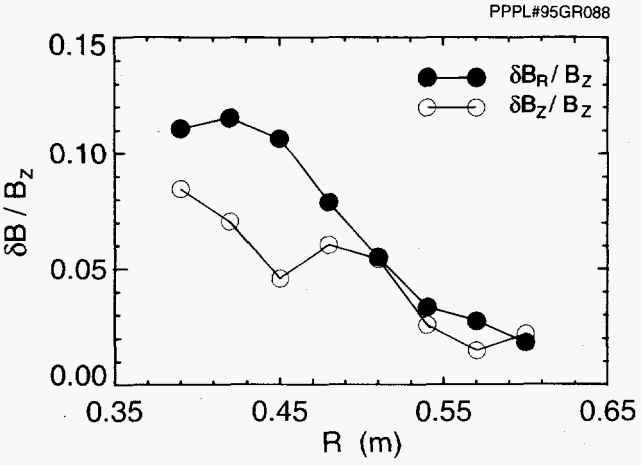

Figure 4. *Radial structure of measured magnetic fluctuations.*

abruptly. The q(0) of maximum plasma current discharges for various toroidal magnetic fields were estimated from equilibrium reconstruction to be near one, supporting the above conjecture. More detailed studies on these modes continue. Possible stabilization schemes such as dc-helicity injection (current profile flattening) are being studied.

Electron-Ripple Injection to Improve Confinement

In order to develop a nonintrusive technique to induce a high-confinement mode (H-mode) of tokamak plasmas, a scheme based on electron-ripple injection (ERI) is being studied in CDX-U. This technique utilizes externally generated, spatially localized magnetic ripple fields in conjunction with electron cyclotron resonance heating to generate a radial electric field which is believed to play a critical role for H-mode transition. A series of preliminary experiments were done in previous years and the combined effects of ripple trapping and electron heating by cyclotron resonance heating were observed. In order to quantify the effects of cyclotron resonance heating on electrons, the kinetic calculation of temperature anisotropy of resonant electrons in a tokamak plasma has been attempted. Results show the ratio of perpendicular to parallel temperature can be as large as 15 with moderate input wave power. In addition, a Monte-Carlo guiding-center electron-orbit code was written to understand the behavior of the energetic electrons' influenced in the presence of ripple fields.

Figure 5 shows a cross-sectional view of the time trace of guiding-center trajectories of a 1.5-keV electron launched from the point where the ripple strength is 0.88%. As shown in the figure, the energetic electron is locally trapped toroidally for about 3 msec while experiencing downward drifts. Due to the increase of Coulomb collisions and decrease in mirror ratio as it moves toward the plasma center, the ripple-trapped electron then becomes detrapped and has more freedom to move in the toroidal direction. The electron follows a banana orbit and, at the same time, loses its energy to background particles by Coulomb drag. As time advances, it eventually becomes a passing particle and is thermalized. The accumulation of these electrons results in charging up the flux surface negatively and produces radially inward electric field. Based on these results, efforts will be made to complete the development of the electron-ripple injection

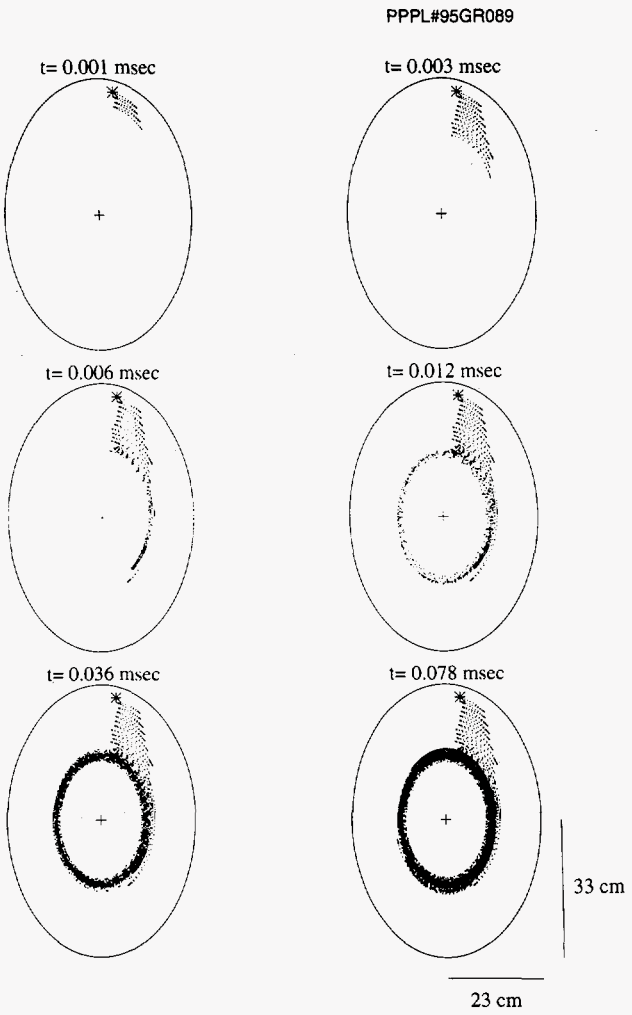

Figure 5. A cross-sectional view of the time trace for guiding-center trajectories of ripple-injected electrons.

technique in the near future. If this prototype injector is successful on CDX-U, it can be applied to larger-size future devices.

NSTX Design and ST Stability Study

To explore the ST physics at more reactor-relevant plasma parameters than those in present small devices such as CDX-U, a design study of a new, medium-sized ST facility (R = 80 cm, a = 64 cm, and I_p = 1 MA), the National Spherical Tokamak Experiment (NSTX), is being done. This device aims to test the ST concept as a basis for a volumetric neutron source and/or advanced fuel fusion reactor. Design and operational experience with the CDX-U tokamak (which is similar but smaller in size by a factor of 2.5) significantly benefits the NSTX design effort. The NSTX center stack with toroidal-field and Ohmic-heating coils has been designed similarly to that in the CDX-U device, including demountable outer toroidal-field sections. The vacuum vessel has been designed without any toroidal electrical break.

Important issues with regard to the ST are its strong advantage in achievable beta in the first stability regime and its limitations for plasma current drive mechanisms. Numerical study of the ballooning and m=1, 2, 3 kink stability limits has found that the stable normalized beta limit increases as the aspect ratio is reduced, indicating enhanced ideal-MHD stability. Further, by raising q(0) well above unity, MHD stable equilibria with beta in excess of 40% and high bootstrap fractions (greater than 80%) in NSTX parameters have been found. These results, if demonstrated, can profoundly impact future advanced reactor designs.

Other Activities

A CO_2-Laser-Based Tangential Imaging Diagnostic

This is a novel diagnostic technique that is presently being developed on CDX-U. Its purpose is to measure two-dimensional images of plasma density fluctuations in toroidal plasma devices. The system employs a CO_2 laser operating at 10.6 μm. The laser beam is expanded to an 8-cm diameter and is directed horizontally through two sodium chloride (NaCl) windows and through the core of the CDX-U plasma. A geometrical projection of the plasma density fluctuations is formed on the beam cross section; the fluctuation profile is then measured using a novel variation of the phase contrast imaging technique. An array of 16 liquid-nitrogen-cooled, MCT photoconductors is used to sense the image. A spatial resolution of 0.5 cm is obtained, which may be further improved with the use of a magnifying lens. The maximum measurable wavelength is limited by the beam size to 8 cm. The time evolution of the density fluctuations is measured at sampling rates of up to 5 MHz.

It has been demonstrated theoretically that an accurate reconstruction of the fluctuation profile localized to the plane of tangency between the beam and the magnetic-field lines is possible. The imaging technique is based on this work, which states that the

projection of the density fluctuations through the plasma is approximately a convolution of the density fluctuations at the tangency plane with a shift-invariant point spread function.

Recent calibration results obtained using sound waves indicate that density fluctuations down to approximately 1×10^9 cm^{-3} root-mean-square (corresponding to phase fluctuations of 1.4×10^{-6} rad), can be measured. Preliminary plasma measurements indicate that fluctuations in the CDX-U plasma are of measurable amplitude. A more thorough set of plasma measurements, including the characterization of the plasma density fluctuation k-spectrum, coherence length, and mode structure, are presently underway.

Graduate Student Education

The CDX-U continues in its role as an excellent experimental plasma physics facility for graduate student training. In FY94, three thesis graduate students and one first-year graduate student worked on the experiment. Cary Forest received the 1994 American Physical Society's Simon Ramo award for his experimental thesis work performed on the CDX-U.

Collaborations

In FY94, the CDX-U group hosted visiting scientists from the Instituto Nacional de Pesquisas Espaciais (INPE), Brazil, and the University of Tromso, Norway, and continued a collaboration on a multipass Thomson scattering system with the GLOBUS-M group at the Ioffe Institute at St. Petersburg, Russian Federation. The engineering design of the ruby laser and the detection system for the multipass Thomson scattering system was completed, and fabrication started on most of the system components. The system is expected to be installed during FY95.

References

[1] C.B. Forest, Y.S. Hwang, M. Ono, G. Greene, *et al.*, "Investigation of the Formation of a Fully Pressure-Driven Tokamak," Phys. Plasmas **1** (May 1994) 1568-1575.

[2] Y.S. Hwang, M. Yamada, T.G. Jones, M. Ono, *et al.*, "Exploration of Low-Aspect-Ratio Tokamak Regimes in CDX-U and TS-3 Devices," in *Plasma Physics and Controlled Nuclear Fusion Research 1994* (Proc. 15th Int. Conf., Seville, Spain, 1994), paper IAEA-CN-60/A5-II-6-2, to be published by the International Atomic Energy Agency, Vienna, 1995.

[3] Y.S. Hwang, T.G. Jones, M.Ono, W. Choe, *et al.*, "Exploration of Low-Aspect-Ratio Tokamak Regimes in CDX-U," in *IAEA Technical Committee Meeting on Research Using Small Tokamaks* (Madrid, Spain, September 1994).

[4] M. Ono and the CDX-U and CCT Groups, "Improvement of Tokamak Performance by Injection of Electrons," in *New Ideas in Tokamak Confinement Research, Trends in Physics*, M.N. Rosenbluth, editor-in-chief (American Institute of Physics Press, 1994) 410.

Tokamak Physics Experiment

The Conceptual Design for the Tokamak Physics Experiment (TPX) was completed during fiscal year 1993. The Preliminary Design formally began at the beginning of fiscal year 1994. Funding for FY94 was approximately 19 M$. This funding was directed towards design activities and support for R&D tasks, industrial contract development, and safety documentation development.

A large fraction of the design and R&D effort during FY94 was focused on the tokamak and, in turn, on the tokamak magnets. The reason for this emphasis is because the magnets require a large design and R&D effort and are critical to the project schedule.

Although contract development did not represent a majority of the project activity, it did receive a high priority because of the need to award the design contracts to proceed with the design activities. The quality of the contracts and associated contractors demonstrates the strong interest and support of industry for the TPX Project.

The development and review of the Tokamak Fusion Test Reactor Shutdown and Removal/TPX Environmental Assessment was completed during FY94. A "Finding of No Significant Impact" was published by the U.S. Department of Energy (DOE) in the Federal Register in December 1994 completing this lengthy National Environmental Policy Act process.

The Preliminary Safety Analysis Report for TPX is being developed by the Idaho National Engineering Laboratory and will be reviewed by the Laboratory. The report will be submitted to the Department of Energy's Princeton Area Office for review and comment. Following completion of the review by the Princeton Area Office, the report will be forwarded to the Chicago Operations Office.

The TPX is a national project involving a large number of U.S. fusion laboratories, universities, and industries. This report summarizes the work of these institutions. The institutional assignments are given in Table I.

Configuration

The TPX not only incorporates new physics, but also pioneers new technologies to be used in the International Thermonuclear Experimental Reactor (ITER) and other future fusion devices. The TPX will be the first tokamak with fully superconducting magnetic field coils using advanced conductors. It will have internal nuclear shielding, will use robotics for machine maintenance, and will remove the continuous, concentrated heat flow from the plasma with new dispersal techniques and with special materials that are actively cooled.

Superconducting Magnets

Superconducting coils, will be needed for a tokamak fusion device to generate net electrical power. Both ITER and TPX will use advanced niobium-tin (Nb_3Sn) wires in cable-in-conduit conductors. Niobium-tin, a brittle material, requires a fabrication technology that is different from that used for more conventional niobium-titanium coils.

Internal Shielding

The TPX will require shielding to prevent fusion neutrons from heating the superconducting magnets and to allow hands-on maintenance outside the vacuum vessel. The shielding system is illustrated in Fig. 1. The double-walled titanium vessel will be filled with borated water between its inner and outer walls to absorb the neutrons. Layers of insulation will separate the vacuum vessel wall at 150 °C and the superconducting magnets at -269 °C, each of which must withstand very significant structural forces.

High-Heat-Flux Continuous Cooling

In tokamaks, heat flows along a thin layer at the edge of the plasma exposing the surfaces of the plasma

Table I. The TPX Work Breakdown Structure Showing Institutional Responsibilities

No.	Work Breakdown Structure	Contractual Responsibility	Design Organization
11	Plasma Facing Components	PPPL	Industry
12	Vacuum Vessel	PPPL	Industry
13/14	Magnets	LLNL/MIT	Industry
15	Cryostat	LLNL	Industry
16	Tokamak Support Structure	PPPL	PPPL
17	Tokamak Assembly and Integration Test	PPPL	Industry
18	Tokamak Shielding	ORNL	ORNL
19	Field Error Correction and Fast Vertical Position Control Coils	PPPL	Industry
21	Neutral-Beam Injection	PPPL	PPPL
22	Electron Cyclotron Heating/ECCD	—	—
23	Ion Cyclotron Heating/FWCD	ORNL	ORNL/Industry
24	Lower-Hybrid Heating/LHCD	ORNL	ORNL/Industry
31	Fuel Storage and Delivery	PPPL	PPPL
32	Pellet Injection		
33	Radiation Monitoring and Tritium Cleanup	PPPL	PPPL
34	Vacuum Pumping	ORNL	ORNL/Industry
4X	Power Systems	PPPL	PPPL/Industry
5X	Maintenance Systems	ORNL	Industry
61	Central Instrumentation and Control	PPPL/LLNL	PPPL/LLNL
62	Diagnostics	PPPL	Fusion Institutions
71	Building Modifications and Site Improvements	PPPL	Industry
72	Cryogenic Equipment	LLNL	Industry
73	Heating and Cooling	PPPL	Industry
74	Test Cell Penetrations	PPPL	Industry
81	Preparations for Operations	PPPL	PPPL
91	Management and Administration	PPPL	PPPL
92	Safety Documentation	INEL	INEL/PPPL
93	Project Physics	Fusion Institutions	Fusion Institutions
94	Systems Integration	PPPL	Industry
95	Construction Management	PPPL	Industry

All hardware fabricated by Industry.

PPPL = Princeton Plasma Physics Laboratory
LLNL = Lawrence Livermore National Laboratory
MIT = Massachusetts Institute of Technology
ORNL = Oak Ridge National Laboratory
INEL = Idaho National Engineering Laboratory

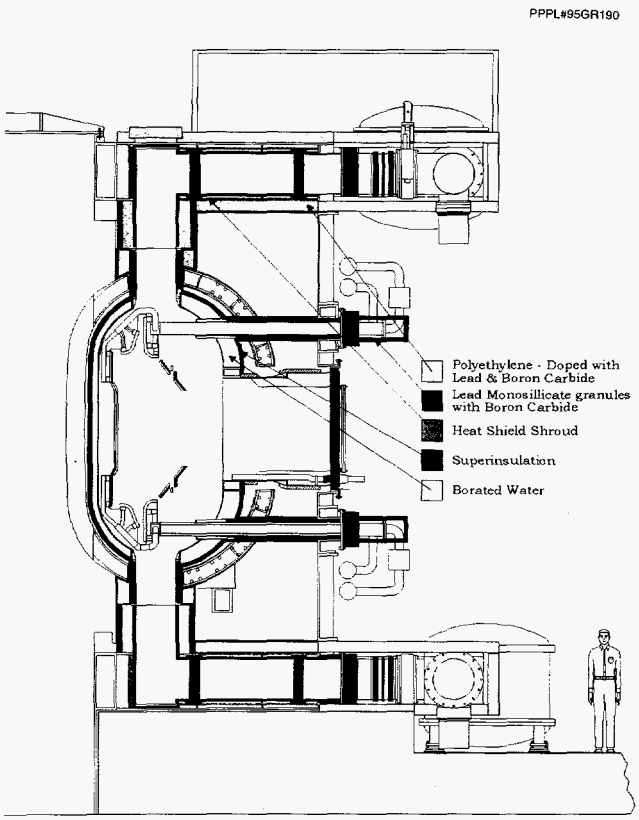

Figure 1. *The TPX Shielding Concept. Various layers of insulation separate the vacuum vessel wall at 150 °C and the superconducting magnets at -269 °C.*

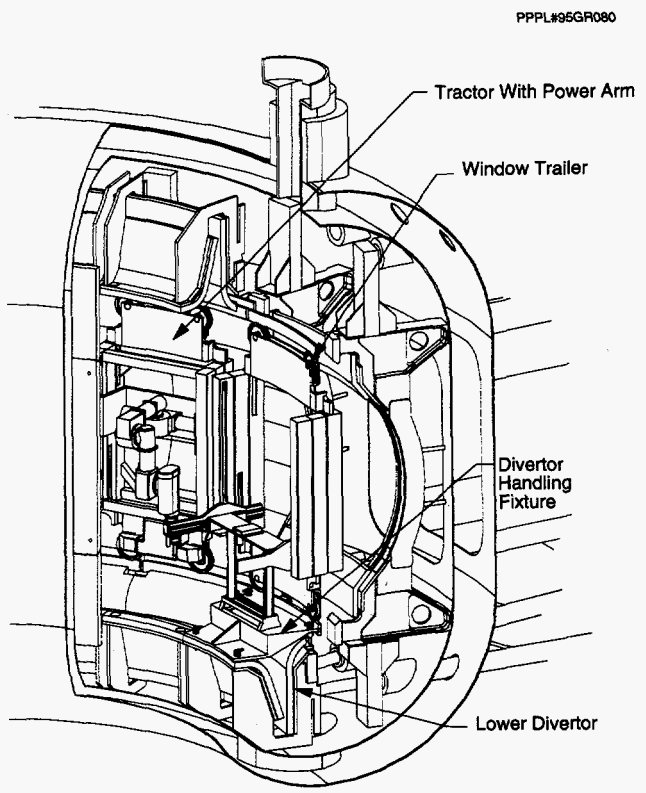

Figure 2. *The TPX Maintenance System (by the Oak Ridge National Laboratory).*

chamber to high thermal loads. These surfaces require special materials, durably bonded to cooled substrates. In addition, innovative physics techniques are needed to disperse the heat over a wide area of the chamber surfaces because the unprecedented thermal loads of TPX and ITER—continuing for 1,000 seconds or more—will exceed the heat-absorption capacity of all known materials. The heat dispersal techniques developed in TPX will be critical for the success of ITER and of the later Demonstration Power Reactor (DEMO).

Robotics for Maintenance

Fusion neutrons will activate structures inside the shield, but the use of titanium for the vacuum vessel will markedly reduce the amount of radioactivity. Nevertheless, robotics will be required for maintenance of hardware inside the vacuum vessel. Among TPX's features will be a unique system of permanently installed rails inside the vacuum vessel, dexterous manipulators, and parts that are designed for easy maintenance by the robotic system. The TPX Maintenance system is shown in Fig. 2.

Configurational Improvements

Since the Conceptual Design was completed and reviewed in a formal Conceptual Design Review in March 1993, several modifications and changes have been made in the configurational design of TPX.

In the Conceptual Design there was 8.8 inches for structure and cooling manifolds between the back of the inboard limiter and the vacuum vessel. The possibility was created to reduced this space to 2.85 inches, allowing an "additional" 5.8 inches to be added to the magnet and vacuum vessel envelopes for magnet design and optimization. This reduction was achieved by reshaping the inboard passive plates and repositioning the inboard divertor, by moving all of the coolant connections for the inboard limiter and passive stabilizer to the plasma facing side, and by routing

the plumbing to between the two walls of the vacuum vessel.

The Conceptual Design featured a double-walled vacuum vessel with leaded glass shield tiles (doped with boron carbide) mechanically attached to its outside surface. The space between the two walls of the vessel was filled with 150 °C water for cooling during normal tokamak operations and for shielding. Analyses performed after the Conceptual Design Review indicate that the leaded glass tiles can be eliminated without compromising shielding performance. This is accomplished by increasing (by one inch on the inboard midplane) the vacuum vessel envelope to fill the space occupied by the tiles and by borating the shielding water. This new configuration has the added advantages of eliminating a worrisome failure mode [i.e., a cracked tile creating a thermal short between the 5 K cold mass and the 423 K (or 150 °C) vacuum vessel and/or degrading of the shielding effectiveness] and reducing the cost of the shielding.

The pipes to feed and return coolant to and from the inboard limiter and passive stabilizers are routed between the two walls of the vacuum vessel. Connections to these pipes must be made from the plasma facing surface on the inboard limiters and passive stabilizers, as in the Conceptual Design for the inboard limiter. A design concept has been developed for a remotely maintainable coolant connection.

The inboard limiter and passive stabilizer module has carbon-carbon composite tiles attached to a copper substrate. As in the Conceptual Design, the tiles will be either bolted or brazed to the substrate depending on the heat flux. The tiles on the toroidal limiters (and most of the armor between the inboard limiters) will be bolted, since the heat flux is less than 1 MW/m^2. The tiles will be brazed to the substrate in armor regions subject to neutral-beam shine-through, where the heat flux is greater than 1 MW/m^2.

The inner leg of the toroidal-field (TF) coil has been moved 5.7 inches further outboard resulting in a peak toroidal field which is lower by 0.5 T, i.e., 8.4 T in the proposed new design versus 8.9 T in the Conceptual Design. In addition to lowering the peak field, the number of strands in the superconductor has been increased from 405 to 486, thus improving its performance.

The outer leg of the TF coil has been moved back 2.0 inches to provide space for the expanded TF coil case. The inside width of the standard vacuum vessel port has been reduced to 37.0 inches (from 38.0 inches) and the neutral-beam port has been reconfigured. The neutral-beam plasma tangency radii have been reduced by 3 cm to 1.97 m (it was 2.0 m) and the beam has been moved six inches closer to the plasma. The local geometry of the vertical vacuum vessel duct (that passes between the TF coil) has been elongated radially and narrowed toroidally to accommodate the increased size of the TF coil case, as well as the additional space for shielding and assembly gaps.

In the poloidal-field (PF) system, the outer diameter of the central solenoid coils increased by 1.7 inches. The larger cross-sectional area allows the flux swing requirement to be met at lower field which tends to decrease the cost of the system. A series of poloidal-field optimization studies were performed. These studies led to a final set of cost-optimized PF coils that meets the MHD (magnetohydrodynamic) equilibrium flexibility requirements, satisfies physics and engineering constraints on plasma initiation, and is capable of an inductively driven HC scenario.

TPX Physics

The TPX physics team sets the performance requirements for the TPX facility and its various subsystems in order to provide the hardware capabilities needed for the TPX mission. Physics analyses are carried out in support of the engineering design, and the physics management coordinates voluntary physics research and development activities for TPX within the U.S. fusion program. The TPX diagnostics team is responsible for the design and construction of the TPX baseline diagnostics and for ensuring that machine interfaces for all diagnostics (including anticipated upgrades) are properly designed.

The physics and diagnostics teams are national in makeup, consisting of about 30 participants from fusion laboratories, universities, and industries in the United States. Physics issues are discussed with the TPX Program Advisory Committee, which meets quarterly and serves as a standing physics review board for the Project.

Physics Management and Integration

An experimental plan was developed for the first ten years of TPX operation, in collaboration with the Program Advisory Committee. The experimental program is divided into four research areas: plasma con-

trol, advanced tokamak operating regimes, steady-state divertors, and steady-state integration. For each of these areas, detailed research tasks, milestones, and hardware upgrade requirements were identified. The major goal proposed for the first five years is to demonstrate a high-performance advanced-tokamak scenario for 1,000 seconds pulses under active plasma control. The major goal for the later phase (also about five years) is to develop a tokamak scenario that will be prototypical for ITER upgrades and DEMO design. Envisioned in the plan are hardware upgrades for heating power increases, divertor modifications, diagnostic additions, and pulse-length extension.

Magnetics

The physics team played a major role in optimizing the design of the poloidal-field coils to meet physics requirements at minimum cost.

An important requirement is to be able to support full-current steady-state equilibria over a wide range of plasma pressures and current-profile shapes. In fact, the required operating space was expanded slightly to accommodate the reversed-shear scenario. However, it was possible to relax the constraints on plasma shape, allowing wider tolerances in the shape control points, and still have the plasma fit within the internal hardware geometry. The plasma initiation scenario was reoptimized to provide a larger field null, while reducing the voltage, a trade-off that was clearly indicated by recent tokamak operating experience. The poloidal-field coil configuration was developed by systematic optimization of the coil positions and cross-section shapes, while satisfying tokamak configuration constraints, superconductor engineering allowables, and physics requirements. The cost of the system was minimized within these constraints.

Magnetohydrodynamic physics analysis tasks addressed the stabilization of external modes with the nonaxisymmetric conducting structure in TPX, and the role of plasma rotation. An interface between the PEST stability code and the SPARK three-dimensional electromagnetic code was developed so that the mode eigenfunction consistent with the structure geometry could be determined. This is currently being done in the single-toroidal-mode approximation, while toroidal mode coupling will be added in the future. For testing the overall method, a simple code based on cylindrical geometry was written and used to successfully test the interface. In parallel, the MH3D code was used to study the effects of plasma rotation and finite wall resistivity on mode stabilization. The existence of a cold mantle region between the plasma and resistive wall appears to be crucial in the ability to stabilize with reasonable velocities. Vertical flows connect the wall and core plasma edge through the mantle, allowing eddy currents to flow at the edge and provide stabilization. The amount of current depends on the viscosity, which is an important component of the plasma model.

Heating and Current Drive

The ACCOME current-drive simulation code was used to develop steady-state tokamak operating scenarios consistent with the baseline TPX heating systems and MHD equilibrium. Models for the bootstrap current and for neutral-beam, fast-wave, and lower-hybrid current drive are included. The density and temperature profiles are specified with the help of a zero-dimensional model to ensure consistency with global power balance requirements.

Two model operating modes of the baseline TPX, an ARIES-I, and a reversed-shear mode were developed. While the full heating system is needed in both cases, more than ninety per cent of the fast-wave power is unused for current profile control. In the ARIES-I case, a small fast-wave current is driven in the forward direction to obtain $q = 1.3$ on axis. In the reversed-shear case, the fast-wave current is driven in the reverse direction and the lower-hybrid current drive is critical in maintaining a negative-shear region out to $r/a \approx 0.8$. These modeling studies show that the ability to vary the direction of the on-axis fast-wave current drive is important for control, even though only a small fraction of the available ion cyclotron range of frequencies (ICRF) heating power may be needed for this purpose. Lower-hybrid current drive is needed to control the profile in the outer half of the plasma, and is particularly important for reversed-shear configurations.

Based on these studies, a recommendation was made to increase the lower-hybrid power from 1.5 MW to 3.0 MW and to reduce the ICRF power from 8 MW to 6 MW. This is aimed at improving (at approximately constant heating power) the off-axis profile control capability to make the system more robust to uncertainties in the profiles, at the expense of on-axis current drive which is more than adequate.

Power and Particle Handling

The divertor physics group developed design guidelines for the plasma-facing component engineers and worked to optimize to the divertor configuration.

Following a review of the operating experience on tokamaks and of laboratory data on the outgassing properties of graphite, the physics group decided to relax the requirement for the plasma-facing components (PFC) inter-shot temperature. The minimum temperature will be reduced from 150 °C to 50 °C, subject to the constraint that the plasma facing components and vacuum vessel be at the same temperature. This change will allow engineering to simplify the design of the cooling system and provide more design of options without compromising the ability to achieve the physics objectives of TPX. It is likely that a temperature slightly above the new minimum will be used because of the operational requirements of the boron-water shield.

The issue of erosion lifetime was examined. It was concluded that one-centimeter-thick carbon armor would allow for, nominally, three years of full deuterium-deuterium operation before 70% of the tile thickness eroded. This was based on peak erosion rates evaluated using the REDEP code. No allowance was made for moving the strike point to broaden the erosion pattern. This will be sufficient to allow the first divertor to survive the first four years of TPX operation, since the first two years have limited full-performance operating time.

The role of the central divertor baffle is being studied in an effort to optimize the configuration. It was concluded that the gap between the baffle and the inner target plate should be sealed to prevent gas leakage from the plenum back to the plasma. The benefits of this gap as a pumping slot proved to be minimal. The contour of the baffle is being studied to see if it can be flattened to allow greater plasma shape flexibility. The baffle helps to isolate the two divertor legs and to direct gas toward the pump ducts to improve particle throughput. Using the DEGAS code, it was found that a five centimeters lowering of the baffle near the inner strike point provided the same neutral retention as the reference configuration. The particle throughput to the pumps and the fraction of gas reaching the core plasma were examined. Both remained the same within error bars for the two baffle shapes considered. Encouraged by this, a study was begun to determine whether the contour could be flattened even further into a straight surface, making it considerably cheaper.

Diagnostics

A plan was developed for procuring the 28 diagnostics included in the TPX Project baseline. These diagnostics will be designed and fabricated by national laboratories, universities, and industry. Contractor responsibilities will be broad, extending from conceptual design through fabrication and participation in the installation and testing. Since it is inappropriate for national laboratories to compete with universities and industry, it was necessary to decide in advance which type of organization (either "national laboratory" or "industry and university") would be solicited as the prime contractor for a given diagnostic. The diagnostics were then grouped into eighteen procurement packages, and an "acquisition path" was chosen for each package. Seven of the packages will be procured from "industry and universities" through normal competitive procurement processes; the remaining eleven will be acquired from "national laboratories." In order to make use of the diagnostic capabilities of small businesses and university groups, an outreach program will be implemented to make such organizations aware of TPX diagnostic plans and to solicit their interests. The larger organizations with lead responsibilities will be expected to involve these smaller, more specialized groups as partners through teaming arrangements.

Contracts

During FY94, four major design contracts were awarded and work is nearing completion on management support contracts. The design contracts point toward and include options for fabrication. They are for the design of the vacuum vessel, plasma facing components, toroidal-field magnets, and poloidal-field magnets. Two contracts were signed at the Princeton Plasma Physics Laboratory (PPPL) on June 9, 1994, for the preliminary and final designs and associated R&D for the vacuum vessel and plasma facing components. The $26 million Plasma Facing Component contract was awarded to General Atomics teamed with McDonnell Douglas Corporation, the Rocketdyne Division of Rockwell International Corporation, and

Raytheon Engineers and Constructors, Inc. (Ebasco Division). The $8.3 million vacuum vessel contract was awarded to the Ebasco Division of Raytheon Engineers and Constructors teamed with McDonnell Douglas Corporation and General Atomics. Both contracts can be renegotiated at their conclusion to include the actual hardware manufacture and installation and test support.

The magnet design is a Lawrence Livermore National Laboratory (LLNL) responsibility. Lawrence Livermore National Laboratory has selected contractors for the preliminary design of the two superconducting magnet systems. Babcock and Wilcox (B&W), a McDermott Company with facilities in Lynchburg, Virginia was awarded a $3.26 million contract for preliminary design and R&D of the 16 coil, toroidal-field system. Babcock and Wilcox will be working with its subcontractor, General Atomics, on these magnets. Westinghouse Electric Corporation's Marine Division in Sunnyvale, California, was awarded a $3.99 million contract for preliminary design and R&D of the 14 ring-shaped coils that make up the poloidal-field system. Westinghouse will have as subcontractors Northrop Grumman Aerospace & Electronics of Bethpage, New York, and Everson Electric Company of Bethlehem, Pennsylvania. When the Phase I preliminary design is complete in nine months, Westinghouse and B&W will compete to conduct the remaining design and fabrication work on both magnet systems, with one or both expected to continue to work on the project.

The management support contracts include the Tokamak Construction Management contract and the Systems Integration Support contract. It is expected that these contracts will be awarded early in calendar year 1995.

The scope of work for the Tokamak Construction Management contract is dominated by the assembly of the primary TPX Project hardware. However, the contractor will be involved in the early stages of the design to assure compatibility of the design with manufacture and assembly requirements.

The scope of work for the Systems Integration Support contract includes a broad range of systems engineering activities to bring industrial expertise to the technical management of the TPX Project. Examples of these activities include configuration management, design integration, and interface control.

Superconducting Magnet System

Fiscal year 1994 was a busy and productive year for TPX Magnet System development. The design of both the toroidal-field and poloidal-field magnets (shown in Fig. 3) evolved, and substantial progress was made in the development of the TPX superconductors and quench detection sensors. The TPX magnet team grew considerably—industrial personnel were brought on board in magnet design and R&D, as well as in strand and conductor fabrication. Additional DOE laboratory personnel were added to help manage and direct the expanded team efforts.

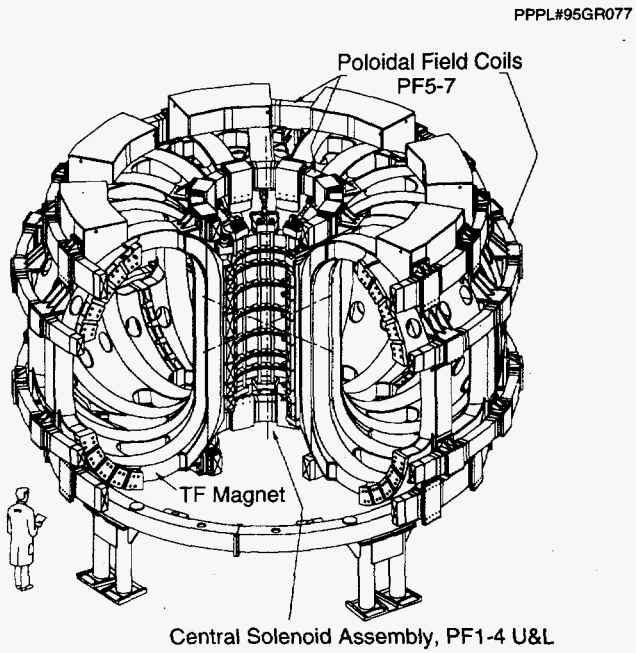

Figure 3. *The TPX Superconducting Magnet System.*

In the design of the magnet system, there were some marginal areas of performance in the 1993 Conceptual Design. The toroidal-field coils needed to have more superconductor in order to meet the overall performance specifications with the nuclear heat load, while staying within the design criteria. As part of the critical configuration review held in January 1994, changes to the plasma facing components plumbing and to the vacuum vessel on the inboard side of the plasma allowed the toroidal-field magnet inner leg to

move outward and the central solenoid to grow in diameter. The TF conductor was increased from 405 superconducting strands to 486 strands, the strand copper to superconductor ratio was reduced from 3.5:1 to 2.5:1 and the conductor shape was changed from square to rectangular. With these changes the TF coils now meet all operating requirements, while staying within the design criteria. The two-coil TF assembly is shown in Fig. 4.

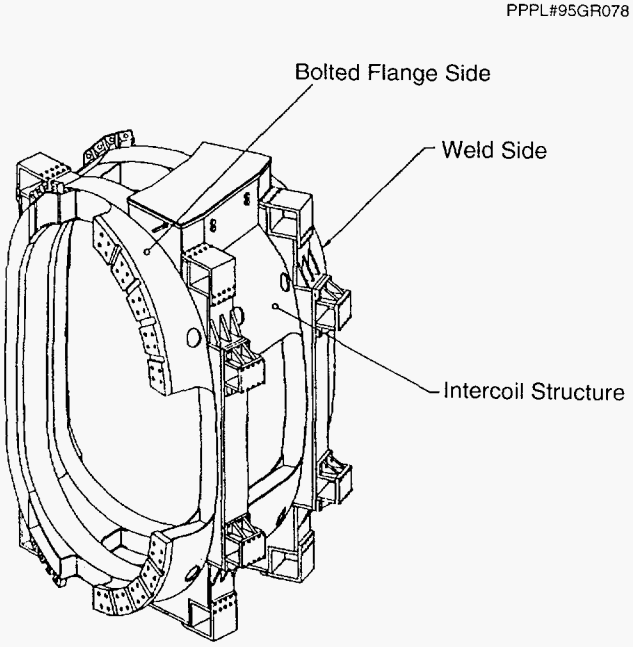

Figure 4. *Two-coil toroidal-field assembly with outer poloidal-field supports. This two-coil assembly is the primary building block of the toroidal-field system.*

In the Conceptual Design, the poloidal-field could operate at the nominal high current scenario and the lower current scenario, but could not operate at all of the flexibility points. In a collaborative effort with the TPX physics team, the PF coils have been optimized for all modes of operation, while minimizing cost. The primary changes were in the central solenoid, where the overall diameter increased, and the total number of turns decreased. All of the PF coil cross sections were changed from an approximately square configuration to a taller and radially thinner rectangular cross section. The number of turns per coil was revised, the number of superconducting strands per conductor adjusted, and pure copper strands added for protection purposes. The new PF coil configuration is shown in Fig. 5. The revised PF coil design can now operate at all flexibility points while meeting the design criteria.

The preliminary design of the TPX superconducting magnet system by industry is underway, with the toroidal-field system design being done by the industrial team lead by Babcock and Wilcox, and the poloidal-field system design being done by the Westinghouse team. Since the contracts were awarded in July of 1994, the primary design activity has been transferred from LLNL, the Massachusetts Institute of Technology and PPPL to the magnet contractors. Funding limitations have caused some delays in the overall schedule, but the preliminary design is now expected to be completed in September 1995.

Both magnet contractor teams have made good progress, having submitted all of the plans covering the work required during this preliminary design phase. Three technical interchange and management meetings lead by LLNL, have been held with the Babcock and Wilcox and Westinghouse teams and the TPX Project.

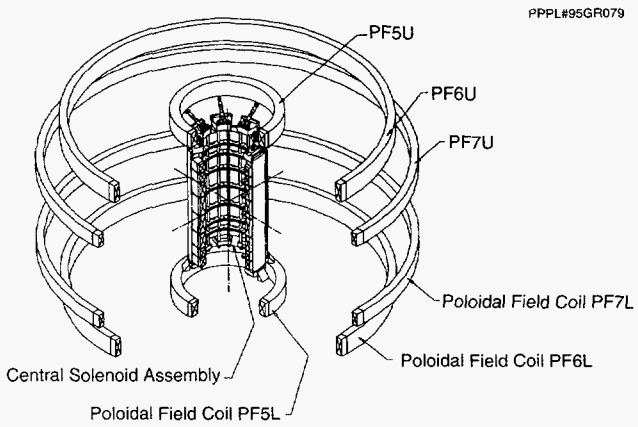

Figure 5. *Isometric view of TPX poloidal-field system.*

Preliminary Design for the TF System

The three-dimensional electromagnetic model of the toroidal-field system was completed by the B&W team responsible for the Preliminary Design of the TF system, and the resulting loads linked into the structural models. A structural model of a TF quadrant (four toroidal-field magnets and structure), was created and analysis is underway, with detailed mod-

els of specific areas being analyzed. The B&W manufacturing R&D responsibilities include: the development of conductor-forming processes used in making the magnets and superconductor reaction process development. A one-eighth scale model of the TF coil was produced using copper conductor to understand the transitions that must be made between turns when forming the magnet. An initial thermal analytical model for the reaction process was created and initial results obtained.

Preliminary Design for the PF System

The Westinghouse team designing the PF magnet system has completed the electromagnetic model, verifying the peak magnetic fields in the poloidal-field conductors. These loads are being analyzed as part of the two-dimensional structural analysis of the central solenoid, as well as the three-dimensional analysis of the PF magnets. The Westinghouse R&D activities include magnet insulation system development and helium hydraulic connection process development. Trade studies of the insulation system are underway. Initial shear test results have been obtained on small samples of candidate insulation systems. Initial processes for penetrating the conduit and welding on the helium connections have been proposed.

Conductor Testing

One of the major areas of development in the TPX superconducting magnet program is the development of the conductors for those magnets. These conductors use a cable-in-conduit-conductor approach, where superconducting wires (called strands) are placed inside a heavy-walled tube or conduit. The strands are the most important part of the conductor, since they carry the electric current. The structural support for the cable is provided by the conduit. Supercritical helium flows through the conduit, cooling the strands to a superconducting temperature. The TPX superconducting strands are similar to previously developed superconductors, but have slightly different characteristics. The toroidal-field strands are different from the poloidal-field strands due to the differences in the operating conditions.

In order to demonstrate the capability for producing the strands required for TPX, a total of six samples for strand of about 25 kilograms each were obtained; four for PF strand and two for TF strand. An additional TF-strand sample was obtained for a third TF strand developed by a vendor at his own expense. Final tests of all of the strands are in progress, but initial results show that vendors were able to meet specifications for residual resistivity, hysteresis loss, and piece length, but had mixed success in meeting critical current requirements. Two of the four PF-strand types were close to meeting the critical current, and two of the three TF-strand types exceeded the critical current requirements. The successful strands will be made into 27 strand subcables. They will then be tested to demonstrate ramping capability. The full-size demonstration conductors will be tested to demonstrate operational capabilities at full current, full magnet field, and temperature with the time varying conditions expected during operation.

Production size quantities will then be ordered, subject to construction approved by Congress; and the successful vendors are expected to be able to continue to produce superconducting strand that meets TPX needs.

Titanium Corrosion Testing

Titanium corrosion testing is nearing completion at the Oak Ridge National Laboratory (ORNL) and results to date support the use of a titanium vacuum vessel in TPX. The corrosion testing was required to demonstrate the compatibility of the titanium vacuum vessel with borated water. Borated water is proposed to fill the annulus of the double-walled vacuum vessel to provide effective radiation shielding. Borating the water with 110 grams per liter of boric acid is sufficient to reduce the nuclear heating in the TF coil set and limit the activation of components external to the vacuum vessel.

Two types of corrosion-related tests have been undertaken. The tests include a Constant Elongation Rate Tensile or CERT test to determine the susceptibility of the titanium to stress corrosion cracking, and the development of polarization curves to investigate whether corrosion rates will be enhanced by MHD-generated voltages. The MHD effects must be considered since the borated water is an electrolyte, and flow of electrolyte in the magnetic field of TPX will generate voltages that may enhance the corrosion rate. The titanium alloys that were tested include Ti-6Al-4V

(vacuum vessel structure) and Ti-3Al-2.5V (piping). The CERT test involves pulling a tensile specimen immersed in borated water at a constant strain rate of about 1×10^{-6} per sec (one "microstrain" per second). The continuous straining is intended to disrupt the protective passivation layer on the specimen to expose reactive metal to the solution in localized areas. If stress corrosion cracking is a potential problem, the specimen will fail faster than if tested in air, and the fracture surfaces will indicate nonductile failure.

Results of the CERT tests confirm that stress corrosion should not be a problem for Ti-6Al-4V or Ti-3Al-2.5V. Welded and unwelded specimens were tested in air and in borated water at 150 °C. The specimens behaved the same in air as in the borated water, with strength, elongation, and time to failure nearly identical. All the samples exhibited ductile failure, and none of the samples showed any evidence of stress corrosion. There were some strength differences between the initial set of welded samples and the unwelded samples. However, subsequent samples taken from plate welded by McDonnell Douglass (prototypical of the actual vessel manufacturing processes), showed no degradation in strength.

The Remote Maintenance Mock-Up

Remote maintenance tooling and operations have evolved substantially over the fifty years of the nuclear age; however, it continues to be an expensive, time consuming, and technically complex business. While remote maintenance is unavoidable in TPX, three essential measures are being taken to insure that the difficulties and expense are minimized. First, a combination of shielding and low-activation titanium structure are being used to permit hands-on dexterous maintenance. Second, the responsibility for maintenance procedures and special purpose tooling have been assigned to the component designers to insure effective interface and planning. And, third, mock-up demonstration of remote maintenance operations is required throughout the design, fabrication, and testing of the relevant TPX systems.

These measures were fully implemented in 1994. The first two, low-activation material and tooling design responsibility, were key elements of vendor procurements issued during the year. The third element, mock-up design verification, began with the construction and installation of the TPX preliminary maintenance mock-up at ORNL. It is the first in a series of progressively more elaborate mock-up facilities planned throughout the life of the TPX design and operation.

Figure 6 shows the basic TPX preliminary maintenance mock-up with a prototype maintenance vehicle installed. This assembly reproduces the critically limited working space inside the TPX vessel, enabling early full-scale modeling of maintenance tooling concepts. A remote maintenance test plan, jointly prepared with General Atomics, identifies specific issues to be addressed in the preliminary mock-up. The proposed tests will enable the plasma facing components design team to specify important in-vessel features, such as fastener access, weld joint configurations, and tile attachments. Evaluations of lighting, viewing, and umbilical concepts will also be undertaken to confirm key elements of the TPX maintenance system concept.

The preliminary TPX maintenance mock-up serves several supplementary purposes, particularly as a tool to educate potential vendors responding to the Remote Systems Request for Proposal to be issued in 1995 and for use by the diagnostics groups in the conceptual design of probes and sensors.

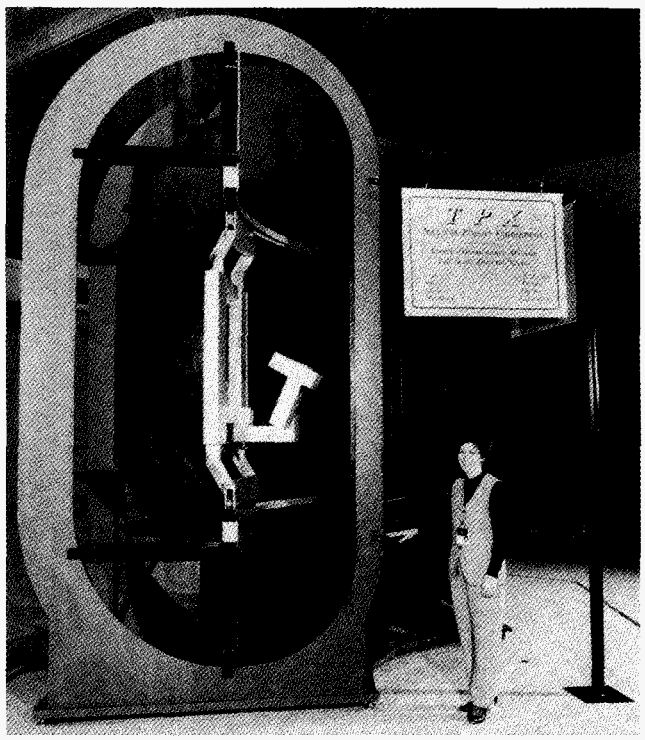

Figure 6. *The basic TPX preliminary maintenance mock-up with a prototype maintenance vehicle installed. (95E0491)*

Ion Cyclotron System

Antenna Design

The TPX ion cyclotron heating antenna design was updated with changes that respond to configuration changes of the vacuum vessel, as well as changes that improve the design. In particular, the antenna was shortened to fit in a new "standard" horizontal port. Antenna assembly procedure, which was not well-defined in the Conceptual Design Review, has been studied, and a realistic procedure has been determined.

Results from recent neutronics calculations performed at PPPL provide encouraging possibilities to simplify the antenna. Based on the calculations, it may be possible to use straight rigid coax in the antenna instead of the present design, in which the coax has two right-angle bends. The bends were put in during the Conceptual Design to decrease neutron streaming through the coax, since at the time no good neutronics calculations were available.

Antenna R&D

The issues for the ion cyclotron antenna revolve around the questions: Can an antenna be fabricated from titanium? Will it then survive in the TPX environment? During the year, a test-piece titanium Faraday shield specimen was fabricated by industry. Welds and tube bends appear completely satisfactory and give increased confidence that an antenna constructed of titanium can be built. In addition, a successful nickel plating technique was developed at ORNL, and an industrial vendor was found that can nickel plate titanium.

The main remaining issue for titanium fabrication concerns protecting the titanium from hydrogen embrittlement in the TPX environment. It is hoped that nickel plating will protect the titanium from this peril, but a R&D program must be carried out to demonstrate that this will work. This will be done in the coming year.

Tuning and Matching Design

A series of meetings were held with the TPX physics team to determine what changes in requirements for the tuning and matching system are needed. To summarize, the results are:

1. Improved feedback control of mismatches induced by changes in plasma loading by controlling the plasma position.
2. Improved feedback control of mismatches due to plasma-induced changes in the strap inductance by controlling the radio-frequency (approximately ±100 kHz).
3. Increased capability to vary the current-drive efficiency between discharges and to change it (within limits "To Be Determined") during a plasma discharge. Changing current drive during a discharge will be done by changing the phase between transmitters driving the antennas; how this can best be implemented will be studied in the next year.

A study was begun of fast phase-shifting components, available now or under development, that could be used in the TPX ion cyclotron heating system to control antenna spectrum. These components might also be used in the antenna tuning and matching system. Fast phase-shifters that can operate over a range of 60 degrees, while operating at 2 MW under high voltage standing wave ratio, are needed. Both electromechanical and electromagnetic units were studied, with tentative time response requirements spanning 2 secs down to 20 msec. From what has been learned thus far, it doesn't look like an electromechanical device to do fast phase shifting at high power will work, even when considering a 2-sec response time. The speed and accuracy would be impossible to attain in a reliable mechanical unit. The AFT company is already at work developing fusion-related components for General Atomics. In the next year, it is expected that a clearer picture of whether or not the active components in AFT's fast ferrite tuners can be used in TPX as fast phase shifters.

Based on financial constraints, it was determined not to install any electromagnetic matching units during the construction or initial operation of TPX. However, the system will be designed so that these units can easily be installed to increase the matching capability if needed in the future.

Lower-Hybrid System

Launcher Design

Initial studies indicate it will be possible to redesign the lower-hybrid launcher so that it can fit in a standard port. Neutronics analysis indicates that the neutron attenuation in such a launcher should be adequate to allow hands-on maintenance of the back of the launcher.

A significant problem still exists with the launcher design. The design of the vacuum windows uses a titanium frame holding ceramic windows that have been brazed into the frame. The frame is sealed to the waveguides with metal O-rings. The problem is that when the assembly is subjected to 350 °C bakeout temperatures, the difference in the thermal expansion coefficient of the copper waveguides and the titanium flange causes unacceptable differential thermal expansion, which may cause a leak in the O-ring seal. Work is continuing on this problem. If the windows are moved outside the port, external pumping will be needed for the long evacuated waveguides.

Launcher R&D

High temperature brazes of a copper and a Glidcop test stack were completed using non-noble alloys. The copper test was completely successful. The Glidcop stack test was generally successful, but it suffered some small edge delamination and warping. There was also evidence of diffusion of silver through the protective copper layer. The results of the program are being evaluated before further testing continues.

Phase Control and RF Sources

The baseline design is for a system that supplies 1.5 MW of lower-hybrid power to the plasma, with a 3-MW lower-hybrid launcher. It appears that the TPX Project may modify the requirements to deliver 3 MW of lower-hybrid power to the plasma. This will entail the procurement and installation of an additional 1.5 MW of lower-hybrid sources, power supplies, and splitter and phase control systems. At present, the 1.5-MW system klystrons are planned to be located in the basement of the test cell, near the launcher to reduce radio-frequency losses. However, it is not clear that there will be room for a 3-MW system in the test cell area. A 6-MW system was designed this past year; for a system of this size, it is clear that space external to the test cell area will be needed, possibly requiring the construction of an additional building to house the radio-frequency sources. A study of the space requirements for a 3-MW system will be made in the next year.

Diagnostic Acquisition

A diagnostic acquisition plan was developed in FY94 and approved by DOE. The TPX Project baseline includes 28 plasma diagnostics, which have been grouped into eighteen procurement packages. These will be designed and fabricated by national laboratories, universities, and industry. Contractor responsibilities will be broad, including physics requirements definition, design, fabrication, and participation in the installation and testing. The TPX Project's diagnostic team will work closely with the contractors in setting the requirements and making cost-performance tradeoffs in order to stay within the available budget. The contractors will be chosen through competitive selection processes. However, since it is inappropriate for national laboratories to compete with universities and industry, it is necessary to decide in advance which type of organization (either "national laboratory" or "industry and university") will be solicited as the prime contractor for a given diagnostic. The DOE therefore asked the TPX Project for recommendations on these "acquisition path" decisions for each of the eighteen baseline packages.

The Project's recommendations are given in Table II. In each case, the project management team chose the acquisition path that it believes offers the better chance of providing equipment that will meet the TPX performance requirements within budget and schedule constraints. The successful contractor team must be capable in all aspects of diagnostic construction, including project management and integration, physics definition, engineering, and manufacture. Experience in the construction and operation of diagnostics for fusion confinement experiments was used as the primary indicator in assessing where the best relevant capabilities exist. In many cases, it is expected that the best overall capability is likely to be provided by a multi-institutional team rather than a single organization. In those cases, the acquisition path is determined by whether laboratory or industry and university leadership is more appropriate. Historically, the involvement of industry and universities in laboratory-led diagnostic projects has been quite successful. Small university groups and businesses have critical capabilities in physics and technology that should be utilized. A program will be developed to actively promote the participation of such groups through teaming arrangements with the larger organizations.

The acquisition plan was presented first to the DOE Office of Fusion Energy and then to the TPX National Council at its May 1994 meeting. The Council endorsed the approach adopted for the selection process, including the requirement for DOE approval,

Table II. Acquisition Paths Recommended for TPX Diagnostics.

Procurement Package	Recommended Path
Magnetic Diagnostics	Industry or University
Motional Stark Effect and Charge Exchange Recombination	National Laboratory
Thomson Scattering	Industry or University
ECH Heterodyne Radiometer	National Laboratory
Millimeter Interferometer	Industry or University
Visible Spectrometers	National Laboratory
Visible Monitor Arrays	National Laboratory
Bolometer Arrays	National Laboratory
Visible and Infrared TV's	National Laboratory
UV Survey Spectrometer	Industry or University
Hard X-ray Detectors	National Laboratory
Soft X-ray Arrays	National Laboratory
Epithermal Neutron Detectors	National Laboratory
Fast Neutron Pressure Gauges	National Laboratory
Thermocouples	National Laboratory
Fixed Edge Probes	Industry or University
Vacuum Monitors	Industry or University
Glow Discharge Probes	Industry or University

while remaining neutral with respect to the actual recommendations made. The proposed acquisition path was approved by DOE in a letter to the Project dated September 23, 1994.

Environmental Assessment

The National Environmental Policy Act (NEPA) activity for TPX focuses on the preparation, review, and approval of the Environmental Assessment (EA). Work on the Environmental Assessment has been complicated by the need to address the TFTR Shutdown and Removal (S&R), since this activity must precede the planned TPX construction in the TFTR Test Cell. The construction of TPX and the shutdown and removal of TFTR are "connected actions," and must be addressed in the same NEPA document, according to federal regulations. In addition, the NEPA requirement to consider alternatives to the proposed action created a number of "combinations" of possible actions—S&R with no TPX, S&R with TPX at another location, or delayed S&R with TPX at PPPL—that have had to be evaluated in the Environmental Assessment. Also included in the Environmental Assessment are two additional planned construction activities "connected" to S&R and/or TPX—the construction of the radioactive waste storage building and a new storm-water detention cell.

The Environmental Assessment is being prepared by the Idaho National Engineering Laboratory Fusion Safety Group, with close coordination by the TPX Environmental, Safety and Health Manager, who is also PPPL's NEPA Compliance Manager. The Environmental Assessment will be reviewed and commented on by PPPL, by the U.S. Department of Energy's Princeton Area Office, Chicago Headquarters, Energy Research, General Counsel, the Environmental and Health Office, and by the State of New Jersey Department of Environmental Protection. The assessment will include evaluations of potential air, water, visual, noise, land use, socioeconomic, chemical, and radiological impacts.

The Department of Energy's NEPA regulations indicate that major systems acquisitions such as TPX normally require the preparation of an Environmental Impact Statement. However, based on the analyses in the Environmental Assessment, the DOE determined that the more costly and time-consuming Environmental Impact Statement was not required for TPX, and published a Proposed Finding of No Significant Impact (PFONSI) in the Federal Register for public review on October 5, 1994. The PFONSI will be distributed to federal, state, and local government officials. Copies of the Environmental Assessment and PFONSI will be placed in area libraries for public inspection. Additionally, a public meeting will be held to present the Environmental Assessment findings to the public.

Preliminary Safety Analysis Report

The draft Preliminary Safety Analysis Report (PSAR) for the TPX is being prepared by the Fusion Safety Program Group at the Idaho National Engineering Laboratory. It will be submitted to the Department of Energy's Princeton Area Office for review and comment. Following completion of the review by the Princeton Area Office, the PSAR will be forwarded to the Chicago Operations Office.

Based on guidance from the Princeton Area Office, the Chicago Operations Office, and the Office of Fusion Energy, the PSAR will incorporate the "Graded Approach" philosophy as outlined in the *Preparation Guide for U.S. Department of Energy Nonreactor Nuclear Facility Safety Analysis Reports*, and will also follow the 20-chapter format recommended in the *Nuclear Safety Analysis Reports*.

The TPX design is based on deuterium-deuterium operation, but does not preclude future deuterium-tritium operation. The PSAR will address the deuterium-deuterium operation phase; it will be revised if the Tokamak Physics Experiment is upgraded for deuterium-tritium operations. For TPX to maintain a classification as a "nonnuclear facility," the tritium inventory will be kept below 1,000 curies during the deuterium-deuterium operation phase.

A preliminary hazards analysis for TPX was conducted and is being documented in the PSAR. For the analysis, a generic list of hazards was first screened to eliminate "incredible" and "standard industrial hazards." ("Incredible" is defined as having a frequency of occurrence less than 1×10^{-6} per year. "Standard industrial hazards" are those that are routinely encountered in general industry and construction, and for which national codes exist to guide safe design and operation.) The hazards remaining after the screening were chemical exposure, explosion, fire, and ionizing radiation exposure. Risks levels for these hazards were assessed. Table III summarizes the results.

Table III. Results of TPX Risk Assessment

	Risk Level (Probability × Consequence)		
Hazard	**Normal Condition**	**Abnormal Condition**	**Accident Condition**
Chemical	Negligible	Negligible	Negligible
Fire	Negligible	Low	Low
Explosion	Negligible	Negligible	Negligible
Ionizing Radiation	Low	Negligible	Negligible

International Thermonuclear Experimental Reactor

In FY94, the Princeton Plasma Physics Laboratory (PPPL) continued to increase its involvement in the physics and engineering activities of the International Thermonuclear Experimental Reactor (ITER). The ITER is a collaboration of the governments of Japan, the European Community, the Russian Federation, and the United States targeted at designing and building a magnetic fusion engineering test reactor. The conceptual design for ITER was carried out by an international design team located at the Max Planck Institut für Plasmaphysik in Garching, Germany, from 1988 to 1990. The present phase of the ITER is a six-year Engineering Design Activity (EDA) which began in mid-July of 1992 and is led by a Joint Central Team (JCT) at three design centers, located in San Diego, California; Naka, Japan; and Garching, Germany.

The Joint Central Team is supported by institutions of each of the ITER partners through "Home Teams." The ITER Council is advised on technical issues by the Technical Advisory Committee. In 1994, the physics research program in support of ITER was formalized by the establishment of seven ITER Physics Expert Groups and the ITER Physics Committee. The PPPL participates in the ITER Joint Central Team U.S. Home Team, on the Technical Advisory Committee, in the ITER Physics Expert Groups, and on the ITER Physics Committee. By the end of FY94, two PPPL physicists and two PPPL engineers were working on the Joint Central Team.

Princeton Plasma Physics Laboratory personnel serve in leadership roles as Head of the JCT Physics Integration Unit, as chair of the ITER Technical Advisory Committee, as the Physics Manager for the U.S. Home Team (which coordinates the U.S. physics participation in the ITER design), and as Task Area Leaders for Plasma Diagnostics and Divertor and Disruptions. Other PPPL staff and projects provide scientific and engineering support on design and research and development tasks.

In physics research, PPPL contributes strongly both by participation of PPPL research staff in the ITER physics research structure and by performance of ITER-relevant physics research. A PPPL researcher serves as one of two U.S. "Senior Scientists" on the ITER Physics Committee and another PPPL researcher serves as chairperson of the international ITER Physics Expert Group on Diagnostics. Five other PPPL researchers serve as members of ITER Physics Expert Groups on Confinement Modeling and Databases; Divertor Physics; Divertor Modeling and Databases; Disruptions, Plasma Control, and MHD; and Energetic Particles, Heating and Current Drive.

Physics Design Studies at PPPL

The PPPL continued its ITER design work with the U.S. Home Team, which is responsible for all U.S. design and technology research and development in support of the ITER Engineering Design Activity. The team is responsible for coordinating, with guidance from the U.S. Department of Energy (DOE), all of the design work performed by institutions in the U.S. in support of the design work of the Joint Central Team and the technology research and development required to validate the design.

The United States ITER Home Team is led by Dr. Charles Baker of the University of California-San Diego. The U.S. ITER Home Team Management consists of a Home Team Leader and Managers for Physics, In-Vessel Systems, Ex-Vessel Systems, and Engineering (Fig. 1). The Physics Manager, from PPPL, is

PPPL#95GR076

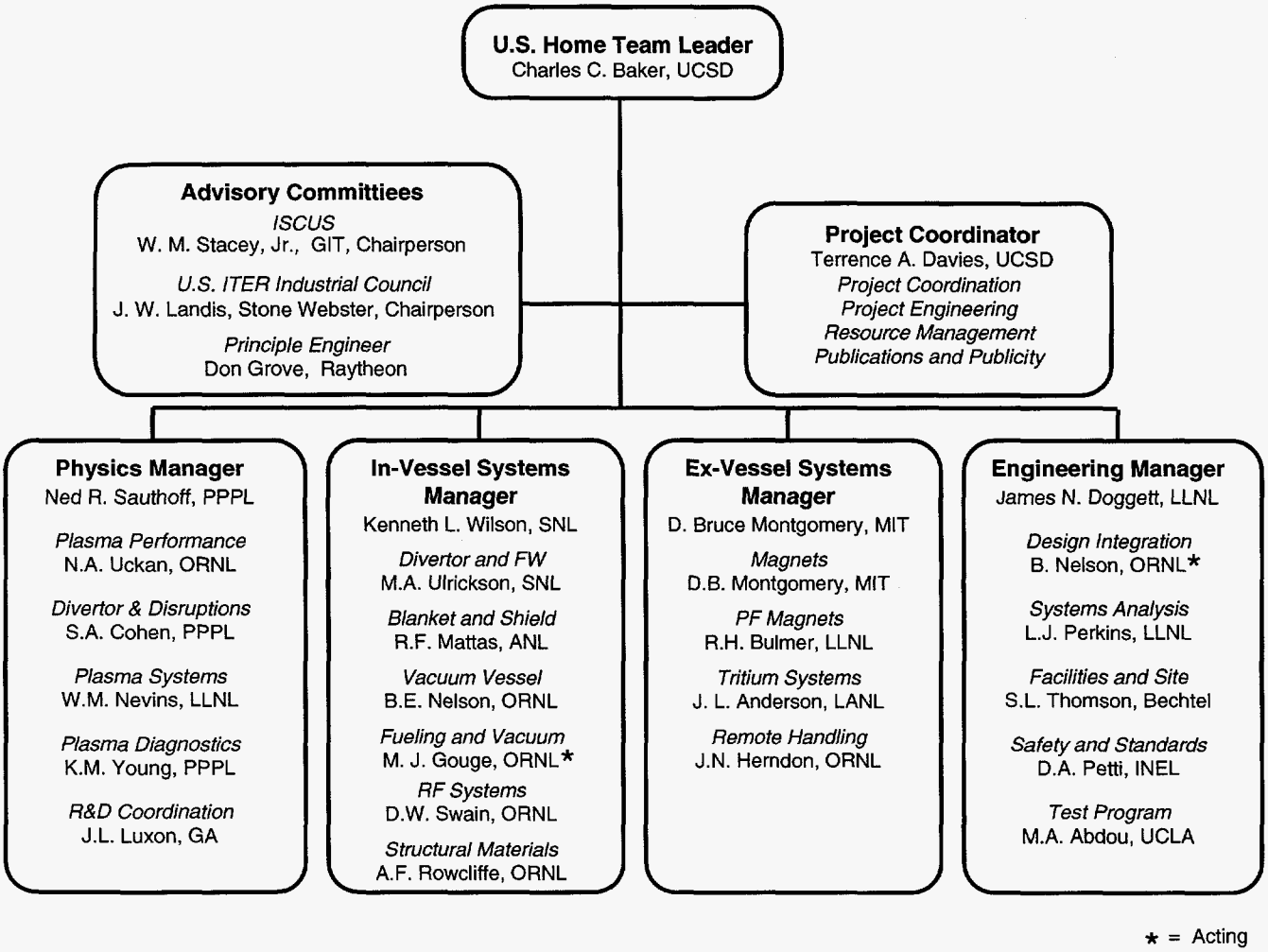

Figure 1. *U.S. National Organization for the International Thermonuclear Experimental Reactor.*

responsible for coordinating the ITER design activities of physicists from institutions in the U.S. with the work coordinated by Task Area Leaders. The Task Area Leader for plasma diagnostics, from PPPL, is responsible for coordinating the U.S. support of the design of the plasma diagnostics systems for ITER and for the diagnostics research and development (R&D) in the U.S. The Task Area Leader for Divertor and Disruptions, also from PPPL, coordinates the U.S. support of the design of the ITER divertor design and the system requirements for plasma disruptions. Each of these activities involves researchers from institutions spread across the United States.

During 1994, the PPPL ITER physics design group contributed to ITER in the areas of (1) axisymmetric plasma simulation and magnetics design, (2) MHD (magnetohydrodynamic) stability analyses, (3) alpha-particle physics, (4) divertor analysis, and (5) diagnostic design.

Axisymmetric Plasma Simulation & Magnetics Design

The PPPL-developed Tokamak Simulation Code (TSC) played an increasingly central role in the design of the ITER Poloidal Field System and in disruption simulations. The PPPL team developed both reference plasma discharge scenarios and requirements for flexibility requirements on the current and voltage capabilities of the ITER magnets. This work included the development of optimal plasma start-up trajectories based on stability and transport consid-

erations and the development of stable paths for shutting down the reference plasma while avoiding disruptions. Working with groups at the Oak Ridge National Laboratory (ORNL) and the Idaho National Engineering Laboratory (INEL), PPPL scientists developed tools for predicting the loads imposed on in-vessel components by off-normal plasma disruptions. These simulated events include the intense thermal and current quenches and the generation of halo currents and runaway electrons during the disruption.

MHD Stability Analyses

A team of MHD stability experts from the PPPL Theory Division worked with the ITER Joint Central Team, groups at ORNL, Lawrence Livermore National Laboratory (LLNL), the Massachusetts Institute of Technology (MIT), and General Atomics, and other international groups in investigating the MHD stability properties of several proposed ITER operating points. The L-mode (low-confinement mode) profiles were found to be stable with a wide stability margin even without a close-fitting conducting wall. As the plasma beta increases, fine-scale ballooning instabilities are predicted to set in before the global kink mode, implying that the beta limit would be soft, rather than disruptive. The standard H-mode (high-confinement mode) profiles were found to be stable, but with a smaller stability margin. Resistive stability studies performed with the PEST-III code also indicate stability when the central safety factor is above one. The PPPL team also played a lead role in the multi-institutional studies of the possibility of ITER operating in an advanced tokamak physics regime. A high-beta, high-bootstrap fraction, low-current, fully noninductive plasma discharge was developed that is stable to all MHD modes in the presence of a nearby conducting wall. This mode demonstrates that advanced tokamak concepts could be explored in a later phase of ITER operation.

Alpha-Particle Physics

Alpha effects on Toroidicity-Induced Alfvén Eigenmode (TAE) modes in ITER have been studied by employing the NOVA-K code.[1-3] Based on very flat PRETOR code plasma profiles, NOVA-K calculation finds that TAE modes are stable. However, the PRETOR profiles may be unrealistic. For a more realistic ITER equilibrium, the TAE growth rate increases with density, and thus the critical alpha-particle beta decreases with density. Ion-Landau damping is the dominant damping mechanism and increases rapidly with ion beta. However, the alpha drive also increases with ion beta. The stability boundary in the density-temperature space POPCON code diagram shows that TAE modes may be unstable for normal ITER operations. In actual ITER experiments, there may be other high-energy particle species, such as ion cyclotron resonance heating minority tail ions and high-energy beam ions, which can contribute additional TAE instability drive and lower the TAE threshold. On the other hand, safety factor and density profiles can be controlled to provide continuum damping and stabilize the TAE modes. Therefore, TAE stability in ITER needs to be investigated further with more realistic plasma profiles and additional particle species. From these investigations it is also realized that higher-density ($n > 20$) TAE modes may be important. To properly study these modes, additional physics of ion finite Larmor radius (FLR) effects will be added to the NOVA-K code and a high-density TAE stability code will be developed.

PPPL researchers assessed the effects of the trapped-particle precessional drift frequency on the energetic particle effects on sawteeth stabilization and on fishbone excitation. The precessional drift frequency is a function of plasma geometry, plasma beta, particle energy, and pitch angle. Finite inverse aspect ratio, plasma beta, and plasma shaping effects can significantly enhance the trapped-particle drift reversal domain in the pitch-angle space and reduce the precessional drift frequency. Due to uniform pitch-angle distribution of alphas, the magnetic drift reversal can significantly modify the stability thresholds for sawteeth stabilization and excitation of fishbone modes.[4] The reduction of precessional drift magnitude and drift reversal effects on the sawtooth stabilization is small, but the critical alpha-particle beta for exciting fishbone modes can be much lower than previous result.[5] The thermal ion diamagnetic drift effect (ion FLR effect) has a strong destabilizing effect on the fishbone mode when the ion diamagnetic drift frequency is comparable with the trapped-alpha precessional drift frequency, but has a stabilizing effect on the ideal-MHD kink mode.

Divertor Analysis

The PPPL researcher who serves as task area leader for divertors coordinated the modeling of ITER

divertor plasmas using a spectrum of plasma and neutral gas models.

Diagnostic Design

Design and Technology R&D work in ITER diagnostics focused on studies of access requirements and of the effects of irradiation on the essential characteristics of materials in ITER diagnostic systems. Generic access studies analyzed the views of the ITER plasma needed to perform measurements for plasma control, performance assessment, and understanding; these views were translated into requirements for space in the in-vessel structure. Irradiation studies investigated degradation of electrical insulation, window and optical fiber transparency, and mirror reflectivity under neutron irradiation.

ITER Physics Research at PPPL

In 1994, the physics research program was formalized with the establishment of an ITER Physics Committee and seven ITER Physics Expert Groups, charged with compiling the Physics R&D needs for the ITER design, with assessing the adequacy of coverage by the physics research programs planned by the four parties, and with working to coordinate the parties' physics research programs.

The Laboratory has made significant contributions in the topical areas of each of the seven expert groups.

Confinement Physics

The PPPL Theory Division continued to play a leading role in the development of state-of-the-art analytic and computational techniques to provide the understanding of plasma transport needed for realistic confinement projections. These theoretical models have been successfully applied to the interpretation of experimental trends observed in TFTR, DIII-D (Doublet-III-D at General Atomics), etc. and have encompassed key issues such as measured fluctuation spectra, shear flow effects, trace-element and impurity transport trends, etc. With regard to ITER-specific initiatives, state-of-the-art models for sawteeth behavior and core transport trends have been developed and tested against the relevant TFTR-database, and they are now being incorporated into time-dependent transport modeling codes such as BALDUR.

Confinement Modeling and Databases

Work in this area over the past year has involved collection and analysis of global confinement data for L-modes and H-modes. The PPPL involvement has focused on coordinating the update and analysis of the L-mode data, while contributing to the analysis of the H-mode and threshold data. A PPPL researcher first-authored the ITER Database Group paper at this year's International Atomic Energy Agency's (IAEA) meeting in Seville, Spain. The L-mode database update effort has involved the collection of more than 2,000 time slices of data from more than twelve tokamaks. The scope of this present effort transcends that of previous L-mode efforts in the attention being paid to the contribution of fast particles to the global stored energy. Knowing this will allow the development of thermal energy confinement time scalings, something that up to now has been limited to H-mode data. This has gained increasing importance recently with realization that the H-mode scalings are inherently highly uncertain because of the number of as yet unquantified parameters that control the confinement quality of the plasma discharge. These include details of the edge localized modes or ELMs and the ratio of main chamber to divertor pressure. The robustness of the L-mode provides a much better defined and quantified baseline from which to deduce confinement behavior and its enhancement. The initial version of the L-mode database has been assembled and is undergoing validation.

Divertor Physics

The PPPL member of the Divertor Physics Expert Group participated in the identification of physics R&D needs in the divertor area and in compiling a report on worldwide divertor configurations and planned upgrades.

Divertor Modeling and Databases

The PPPL member of the Divertor Modeling and Database Expert Group participated in the compilation of physics R&D needs in the preparation of databases and development of models.

Disruptions, Plasma Control, and MHD

PPPL researchers have been active both in participating in the expert group meetings in this area and in responding to requests from the working group. The m=1 mode has been identified as a potential problem in an inductively driven high-current burning plasma such as ITER. The PPPL team is studying the onset of this mode in the high-powered D-T regimes in TFTR and has developed a theory and modeling capability to predict its consequences in ITER. Another area stimulated by working groups request is the integrated disruption model. PPPL researchers participate in a joint research activity involving ORNL, INEL, Argonne National Laboratory (ANL), and several universities in extending the TSC disruption model to include additional effects such as wall vaporization, including vapor shielding and impurity influx phenomena.

Energetic Particles, Heating, and Current Drive

The main activities of PPPL researchers in Energetic Particle, Heating, and Current Drive Physics were to help formulate a list of ITER Research Needs in this area and to contribute to the IAEA paper on ITER Alpha Physics. The identified ITER research needs include analysis of the high-density TAE mode stability of ITER and of MHD and toroidal-field ripple-induced alpha-particle loss. These topics are being actively studied by the PPPL theory group and through experiments on TFTR. An e-mail bulletin board for this group was set up through PPPL.

Diagnostics

The creation of the Expert Group in Diagnostics in the summer led to some clear direction on the requirements of the plasma parameters to be measured. The measurement resolution requirements for the diagnostic instrumentation were also provided toward the end of the year. Until that time, the diagnostic effort had been mostly based on the study of some problem areas identified within the U.S. Home Team and on specific support requests from the Joint Central Team. Considerable help was given to the new leadership of Diagnostics within the JCT in preparing the measurement lists for consideration by the Expert Group.

A study of the feasibility of diagnostics making use of the emitted X-rays, culminating in the preparation of two reports, was completed. The capability for doing fluctuation studies in the ITER plasma environment was also examined at PPPL. Support of the JCT magnetic diagnostic design activity by General Atomics was supervised and a start was made to looking at access routes for diagnostics through the vacuum vessel, the blankets, necessary shielding, and the cryostat. Ideas were developed and the U.S. undertook to work on neutron and microwave diagnostic access.

The study of radiation effects on fiber optics in the real fusion-neutron environment of TFTR, including the advantages of running the fiber hot to reduce the transient absorption effect, has affected thinking about the use of fibers close to ITER. This "voluntary physics" activity was a component of a significant R&D program within the U.S. on radiation effects on ceramics, fiber optics, and diagnostic components (e.g., mirrors) managed from PPPL.

Computer Communications

Rapid communication with electronic mail, including the exchange of computer files, is crucial to the coordination of the national and international ITER activities. The PPPL Computer Division continued its development and support of electronic communication throughout the U.S. ITER organization and the maintenance of the electronic document management system. Electronic mail is handled using the EUDORA program developed by the National Center for Supercomputing Applications at the University of Illinois. All of the U.S. ITER staff and many of the foreign ITER staff have been connected to this software. The software allows any ITER person connected to INTERNET to use the ITER UNIX fileserver from a Macintosh, IBM PC, SUN workstation, etc. In this way, important ITER documents, design drawings, etc., are almost instantly available to anyone working on ITER regardless of their location.

References

[1] C.Z. Cheng, R. Budny, L. Chen, *et al.*, "Energetic Particle Effects on MHD Modes and Transport," in *Plasma Physics and Controlled Nuclear Fusion Re-*

search 1994 (Proc. 15th Int. Conf., Seville, Spain, 1994), paper CN-60/D-3-III-2 (IAEA, Vienna, 1995), to be published.

[2] C.Z. Cheng, "Kinetic Extensions of Magnetohydrodynamics for Axisymmetric Toroidal Plasmas," Physics Reports **211** (1992) 31-51.

[3] G.Y. Fu, C.Z. Cheng, and K.L. Wong, "Stability of the Toroidicity-Induced Alfvén Eigenmode in Axisymmetric Toroidal Equilibria," Phys. Fluids B **5** (1993) 4040.

[4] Y. Wu, C.Z. Cheng, and R.B. White, "Alpha Particle Effects on the Internal Kink and Fishbone Modes," Phys. Plasmas **1** (1994) 3369.

[5] B. Coppi, S. Migliuolo, F. Pegoraro, and F. Porcelli, "Global Modes and High-Energy Particles in Ignited Plasmas," Phys. Fluids B **2** (1990) 927.

Collaborations

With the pending conclusion of the Tokamak Fusion Test Reactor (TFTR) experimental program in September 1994 (now deferred to September 1995), it was clearly necessary that the Laboratory set up collaborations with other fusion-related organizations to enable scientific and technical expertise gained on TFTR to be extended to other operating tokamaks in the near-future years. A program involving detailed negotiations with fusion facilities worldwide was set up and, building on those negotiations, some initial experimental and theoretical collaborations were begun.

In particular, negotiations with the staffs of Alcator C-Mod (Massachusetts Institute of Technology), DIII-D (General Atomics), JET (European Community), and JT-60U (Japan Atomic Energy Research Institute) were held and programs developed for collaborations, with the U.S. Department of Energy's Office of Fusion Energy fully informed at all times. Less detailed discussions were held with the staffs of ASDEX-U (Germany), Tore-Supra (France), FTU (Frascati, Tokamak Upgrade, Italy), TEXTOR (Germany), and LHD (Large Helical Device, Japan) about future work, but these activities will necessarily be of much smaller scale. In addition to management-level discussions, some specific visits were made by physicists to discuss their own particular participation in the collaborative activities.

The contributions made directly to these non-PPPL fusion programs in fiscal year 1994 are described below.

Alcator C-Mod

RF Antenna Design and Source Move

The aim of the Massachusetts Institute of Technology (MIT) Alcator C-Mod program is to test divertor physics in a high magnetic field, high density tokamak. In order to fully test divertor schemes, a high-power flow into the divertor region is required. The C-Mod device has an auxiliary heating system composed of two ion cyclotron range of frequencies (ICRF) antennas and two fixed-frequency 80-MHz transmitters. The goal of the Princeton Plasma Physics Laboratory-MIT collaboration is to double the auxiliary heating power from four to eight megawatts by providing two variable (40-80 MHz) frequency transmitters and an additional ICRF antenna. The additional power is to be made available in FY96.

During FY94, preliminary discussions took place between MIT and Princeton Plasma Physics Laboratory (PPPL) engineers and physicists to lay the groundwork for the transfer of two ICRF transmitters from TFTR and the design and construction of a new ICRF antenna. Source engineers prepared a preliminary layout of the source location at MIT and the needed utilities. In addition, MIT sent a description of their control interfaces so that PPPL engineers could prepare duplicates for the additional transmitters. Since the transmitters will remain in operation on TFTR until the end of FY95, coordinated planning will be required to prepare for the quick transfer of transmitters in FY96.

PPPL has prepared a conceptual design for a four-strap ICRF antenna. This antenna proposal features a novel insulated Faraday shield and completely inductively decoupled radiating elements. The antenna would be suitable for both heating and current drive. The concept was presented at MIT, and PPPL was encouraged to go ahead with detailed design and analysis. Fabrication of a full-scale electrical mock-up of the design was begun.

Divertor Thomson Scattering System

This is a collaboration between PPPL, MIT, and Princeton Scientific Instruments which seeks to make use of Small Business Innovative Research funding along with commitments by PPPL and MIT to build, install, and operate a Thomson scattering diagnostic system to make measurements of the electron temperature and density in the C-Mod divertor along a line through the lower x-point of the C-Mod divertor. PPPL's responsibilities now include procurement, testing, and installation of the laser; design and installa-

tion of beam optics; testing and calibration of the collection optics, polychromator, and detectors; and development of the data acquisition system, as well as operation of the system once installed. In FY94, this collaboration used PPPL Laboratory Program Development Activity (LPDA) funds for travel to MIT to establish the initial intentions of the collaborators and later again to attend design reviews. This support has lead to significant commitments from all concerned to achieve installation of the complete system in the summer of FY95.

Divertor Modeling

The divertor modeling collaboration with MIT is concerned primarily with using the DEGAS Monte-Carlo neutral transport code to simulate the H-alpha emissions from the divertor and first wall of Alcator C-Mod. Because of the extensive scrape-off layer diagnostics installed on C-Mod, a minimum number of assumptions are required to provide DEGAS with the plasma density and temperature information it requires. An example computational mesh is shown together with the C-Mod vacuum vessel, divertor targets, and H-alpha viewing chords in Fig. 1.

The DEGAS code also needs data about ion fluxes to the divertor targets and other first-wall surfaces. Reference 1 describes two different models used to compute the flux to the targets from the parallel ion flux measured by probes. Recent work on a high-recycling plasma discharge indicates that the model in which the surface flux is just the parallel flux times the sine of the angle of field line incidence is consistent with the overall power balance in Alcator C-Mod. However, the present DEGAS simulations suggest that this model is unable to reproduce the observed pattern of hydrogen Balmer-alpha emissions from the divertor region. The second model in which the surface flux is equal to the measured parallel flux times a constant does a better job in this regard, but predicts an electron cooling rate due to neutral gas which exceeds the power flowing into the scrape-off layer.

Detached Alcator C-Mod plasmas will also be modeled with the DEGAS code. In this case, the simple conduction-based model used to interpolate between diagnostics[1] is no longer valid. Although eventually it should be possible to use detailed two-dimensional plasma simulations to fill this need, present work is focused on simple analytic or even empirical prescriptions.

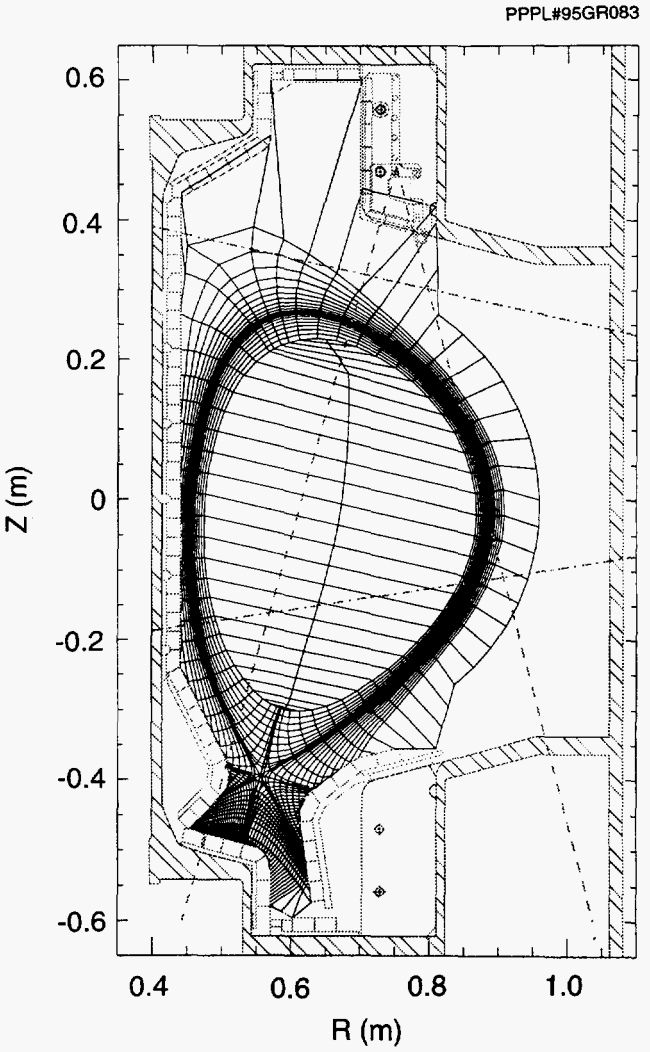

Figure 1. *Plasma mesh used in DEGAS code simulations of Alcator C-Mod divertor modeling. The ranges of the divertor and inner wall H-alpha arrays are indicated by dashed and dash-dot lines, respectively.*

DIII-D

Analysis

The state-of-the-art NOVA-K code for analyzing energetic-particle behavior in tokamak plasmas was eagerly sought by General Atomics' DIII-D group. This capability was very effectively transferred to GA within this collaboration, and subsequently led to a prominent paper[2] at the International Atomic Energy Agency's (IAEA) 15th International Conference on *Plasma Physics and Controlled Nuclear Fusion Research* held at Seville, Spain, in September 1994,

which included results from the analysis of toroidicity-induced Alfvén Eigenmode (TAE) experiments on DIII-D.

Another resource from PPPL highly desirable by the GA group was the FULL comprehensive kinetic stability code.[3] This code has been interfaced with DIII-D equilibria of interest and has produced results which will be presented at the American Physical Society's Division of Plasma Physics meeting in November 1994. In particular, representative high-ℓ_i high-confinement mode (H-mode) and very high-confinement mode (VH-mode) discharges have been analyzed for the radial variation of the linear growth rates and real frequencies of the toroidal drift mode destabilized by the combined effects of ion temperature gradients and trapped particles. In the absence of toroidal plasma rotation, the toroidal drift mode is unstable only in a fairly narrow radial region for both shots. In addition, an approximate toroidal rotation model has been implemented, to account for radially local and nonlocal stabilizing effects. In future work, analysis of high beta-poloidal and negative magnetic shear DIII-D plasma discharges is planned.

With regard to edge physics analysis of particular interest to GA, a newly developed theoretical model has been applied to the interpretation of the low-confinement mode (L-mode) to H-mode and H-mode to VH-mode transition phenomena observed on DIII-D. The previous two-point nonlinear theory of flow-shear-induced fluctuation suppression in near circular, high-aspect-ratio toroidal plasma[4] was extended to arbitrary shape, finite-aspect-ratio toroidal plasma. These results were then applied to a more realistic quantitative comparison of experimental data from H-mode and VH-mode divertor plasmas in DIII-D. The in-out asymmetry of fluctuation reduction behavior can be explained in the context of flux expansion and poloidal variation of the local magnetic-field pitch on a given flux surface. The charge-exchange-induced parallel momentum damping is predicted to reduce the flow shearing rate. This could offer a partial understanding of the experimental observation that the presence of neutral particles has adverse effects on L-mode to H-mode and H-mode to VH-mode transitions.

Computer Software

As part of the goal to assist the DIII-D group to improve their operational capability, a start has been made to provide improvements in the computer software. A PPPL software engineer spent several months at DIII-D. His initial goals were to learn the overall computer system at DIII-D, to learn the data flow from DIII-D experimental observations through data analysis and archiving, to design and implement a shot logger program (SLP) to be written in Interactive Data Language (IDL) to allow monitoring of SLP at PPPL, and to facilitate the sharing of computer analysis codes between the two institutions.

The primary function of the SLP program (now 90% complete) is to allow an on-site person to log shot information during the experimental runs at DIII-D. The SLP will read in DIII-D plasma discharge data automatically, perform analysis, plot data sets, and produce a shot log and a good shot list. Collaborating sites will be able to follow results during the experimental runs by entering the program in monitor mode.

The installation of PPPL's TRANSP analysis code on the HP workstation platforms is now possible at General Atomics.

JT-60U

Analysis

PPPL's expertise in the energetic particle area was actively sought by the JT-60U (Japan Tokamak-60 Upgrade) project. The Laboratory collaborated with the JT-60U group to study TAE activity on JT-60U ICRF experiments as well as JT-60SU (Japan Tokamak-Super Upgrade) design. Three papers on this work were written and presented at the 1994 International Conference on *Plasma Physics and Controlled Nuclear Fusion Research* at Seville, Spain in September, 1994.[5,6,7]

With regard to the collaborative studies in the area of magnetohydrodynamics (MHD) analysis, a prominent topic involved the severe problem posed by edge localized modes (ELMs) in JT-60U. The possibility that the ELM in JT-60U might be due to low-n kink modes was investigated, with special emphasis on the significance of the current pedestal and edge pressure gradient. An interface between the JT-60U equilibrium codes and the PEST codes was implemented. The plasma discharges of interest are single-null divertor cases, and have up-down asymmetry. This interface will be useful for future collaborations involving Princeton codes, including BALLOON, CAMINO, ORBIT, NOVA, PEST-I, PEST-II, and PEST-III, as well as the comprehensive kinetic stability code of Rewoldt and Tang.[3]

With regard to specific results, an equilibrium representing a JT-60U plasma discharge including a single-null geometry was analyzed. This equilibrium was characterized by two significant features near the plasma edge — a large pressure gradient and a current pedestal. Stability analysis of the resulting equilibrium showed it was strongly unstable to low-n external kinks. To determine the underlying forces of the instability, two equilibrium sequences were then generated: the first with reduced pressure gradient near the edge and the second with reduced parallel current near the edge. This would help to clarify the role of the pressure gradient and the current pedestal.

Stability analysis showed that only the current reduction is effective in stabilizing the mode. Even with the pressure gradient reduced to zero, the instability could not be stabilized. This suggests that the observed MHD is due to current-driven kinks rather than pressure-driven ballooning modes. This result was considered to be quite important by the JT-60U group and was subsequently incorporated into two of their IAEA papers. They also proposed continuing such studies to address other topics, e.g., triangularity and role of bootstrap current.

LHCD Collaboration

Lower-hybrid current profile control is a central component of the Princeton Beta Experiment-Modification's (PBX-M) and JT-60U's programs. In FY94, there were several contacts between the lower-hybrid groups, and PPPL physicists spent a total of six man-weeks at Japan Atomic Energy Research Institute.

The main issue is to be able to generate the radio-frequency current in a predetermined off-axis location, while avoiding the destabilization of MHD modes. This requires certain characteristics for the lower-hybrid system, like flexibility of the spectrum generated, more power and longer pulse length; in addition, specific diagnostics are needed to assess the efficacy of the current modification. The PBX-M and JT-60U systems have a mixture of these requirements: the flexibility and diagnostics of PBX-M are better, while JT-60U has more power and longer pulse length at its disposal. In addition, the target plasmas are somewhat different, which contributes to make the exchanges particularly interesting and complete.

Exchange of information on more mundane topics, such as wave coupling, have helped us to understand some unusual results in our experiments.

Radial Thomson Scattering System Consultation

Consultations started in FY93 to investigate the feasibility of installing a new Thomson scattering system on JT-60U continued. This system would use a radial midplane laser beam viewed from the lower outside port of the vessel. This geometry would provide more complete radial profiles, including the core regions of nearly all popular JT-60U configurations. Over the last year, the JT-60U group has accomplished much toward the goal of installing this system during the installation of the Negative Ion Beam in early 1996. It has been determined that an inner wall viewing dump is feasible and assembly of a polychromator and the detector hardware has begun.

ASDEX-Upgrade

The Axially Symmetric Divertor Experiment-Upgrade or AUG device was built to study the use of divertors for reducing impurity production, lessening energy load on the walls, and improving energy confinement time — issues important to the International Thermonuclear Experimental Reactor (ITER). Participation by PPPL personnel in experiments on the AUG tokamak is performed under the framework of the International Energy Agency (IEA) Implementing Agreement on a Cooperative Program for the Investigation of Toroidal Physics in, and Plasma Technologies of, Tokamaks with Poloidal Field Divertors: International Energy Agency ASDEX/ASDEX-Upgrade Agreement. These activities are part of a U.S.-wide Department of Energy-coordinated program at ASDEX-Upgrade.

In each year since its inception in 1991, the DOE/AUG implementing agreement has supported nearly a man-year of effort by PPPL scientists on ASDEX and ASDEX-U. Typically, five PPPL scientists participate yearly. The collaboration has benefited from the strong involvement of colleagues from the Canadian Fusion Fuels Technology Project and the Courant Institute of Mathematical Physics at New York University.

In FY94, four PPPL-funded scientists spent a total of eight months at the Institut für Plasmaphysik (IPP) in Garching, Germany and about three months at PPPL. They developed models of divertor plasmas and acquired and analyzed data on divertor plasmas. A total of 18 papers were co-authored by the PPPL

participants, with most published in the Proceeding of the 21st European Physical Society Conference on *Controlled Fusion and Plasma Physics* held in Montpellier, France, in 1994.

Results

Using two fast-scanning Langmuir probes, three-millimeter resolution measurements of radial plasma profiles were performed approximately five centimeters above both the inner and outer divertor plates during Ohmic- and neutral-beam-heated operation. At low and moderate plasma density, the outer divertor is found to be hotter and less dense than the inner divertor, although there appears to be plasma pressure balance between the two divertors. At high density, a strong x-point Marfe develops and both divertor fans enter a state termed "partial detachment" in which the particle flux to the plate in the region of the separatrix strike points drops significantly. The particle fluxes and plasma temperature further out in the scrape-off layer for both inner and outer fans increase during partial detachment. Stable "full detachment" has not been observed.

During the last year, the neutral-beam power available has increased to more than 10 MW, allowing studies of detachment under high-power conditions. The results are qualitatively similar to those attained under Ohmic conditions, i.e., partial detachment, starting first at the separatrix, is the rule. Figure 2 shows the plasma density profile across the outer plate under 7 MW of heating (grad-B drift towards the x-point) at a moderate density of 7.5×10^{19} m^{-3} and a high density of 1.0×10^{20} m^{-3}. Figure 3 similarly shows the electron temperature profiles. The high-density discharge shows a region of "detachment" of radial extent approximately five centimeters immediately adjacent to the separatrix where the density is low. The same region shows a decrease in the plasma temperature in comparison to the moderate density shot.

Numerical stabilization of the linearized form of the source terms for the B2 fluid code, as they are computed by the EIRENE Monte-Carlo code, was explored. The target case was a particular problematical ASDEX-Upgrade calculation in which carbon line radiation dominates the energy balance in the divertor and for which the B2/EIRENE coupling did not converge. The numerical stabilization succeeded to turn this into a smoothly converging calculation.

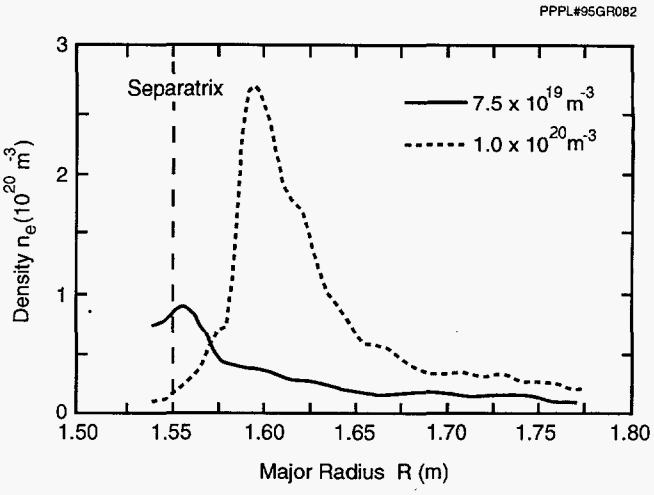

Figure 2. *Plasma density, measured 0.05 meter above the outer divertor plate for two core plasma densities.*

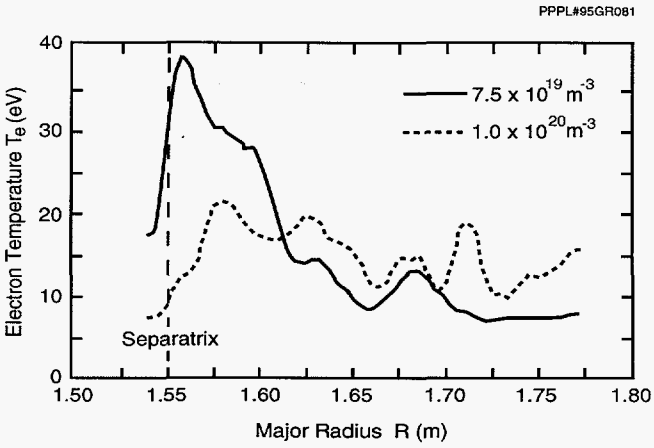

Figure 3. *Electron temperature measured 0.05 meter above the outer plate for the same two core plasma densities as in Fig. 2. Partial detachment, a drop in electron temperature and density at the strike point (separatrix intersection with the divertor plate) is observed for the higher density case.*

FORTRAN code implementation of a fluid neutral gas description in the Garching version of the B2.5 code was started and issues of coupling EIRENE to the latest (B3) version of the fluid code explored. The implementation of the full multispecies parallel transport in the formulation of Boley, Hirshman, Zhdanov, and Igitkhanov was started. It was found important to incorporate the process of charge-exchange impurity recombination in the Garching calculations.

The B2/EIRENE code was upgraded to allow large concentrations of impurities. Excitation and radiation rates were modified to include collisional radiative effects expected to be of dominant importance at high density. In this way, cold divertor plasma studies can be made for ITER. Such studies are also important to

Marfes and detached plasmas presently found on operating tokamaks. Impurity radiation has been shown to be much more efficient at removing plasma energy than charge-exchange. The stability of the Marfe solutions found is open to question because of their slow migration to and above the x-point.

A DOE/IPP-sponsored workshop on disruptions was held at MIT in March 1994, in coordination with the AUG/DOE Executive Committee Meeting to discuss these results with other U.S. partners in the AUG/DOE activities.

Tore Supra and TEXTOR

The Princeton Plasma Physics Laboratory participates in the U.S. Department of Energy-sponsored collaborations with Tore Supra (Superconducting Torus tokamak at Cadarache, France) and with TEXTOR (Tokamak Experiment for Technologically Oriented Research, Jülich, Germany). Other participants in the collaboration with Tore Supra include the Oak Ridge National Laboratory, the Sandia National Laboratory (Albuquerque), and General Atomics. Other participants in the collaboration with TEXTOR include the University of California at Los Angeles and the Oak Ridge National Laboratory.

The emphasis of the PPPL contributions is in modeling core plasma phenomena to better understand the plasma physics. Various codes, such as the TRANSP plasma analysis code, the PEST MHD equilibrium code, and the ORBIT fast-ion code are being used to analyze plasma discharges.

The PPPL efforts at Tore Supra have been concentrated on studying the effects of lower-hybrid heating and current drive and of ion-cyclotron resonance heating. Various plasma discharges, selected by Tore Supra physicists as especially interesting, are being studied in detail. These include plasma discharges with ion cyclotron resonance heating that exhibited "monster sawteeth" with long periods. Others with long durations of lower-hybrid current drive and a ramp down of the plasma current have exceptionally efficient heating of the electrons. The electron temperature became very peaked, obtaining peak values near 10 keV. Other plasma discharges with constant plasma current and lower-hybrid heating current drive also have enhanced-energy confinement, typically 1.4 times the L-mode values.

The q_{MHD} profiles in Tore Supra plasmas are measured with a five-channel Faraday rotation system, and the results indicate that the discharges with lower-hybrid current drive have negative shear near the center and evolve in time to values above one at the center. These results stimulated speculations that the negative shear led to the improved electron confinement, and that the inner regions of the discharge were near second stability. The TRANSP code modeling of these discharges uses a lower-hybrid ray tracing and damping code, LSC, developed at PPPL for analyzing experimental results from PBX-M. Analysis of the Tore Supra discharges using TRANSP/LSC are based on kinetic measurements from far infrared interferometer, electron-cyclotron-emission, and Thomson-scattering diagnostics. Assuming neoclassical resistivity, and using the measured visible bremsstrahlung emission to derive Z_{eff}, the analysis results for the temporal and spatial variation of the q-profile showed good agreement with the measured variations. The analysis indicated a negative shear region near the center, brought about by a slightly off-axis lower-hybrid current drive, coupled with a contribution from the bootstrap current.

Ballooning stability analysis indicates that the computed current and pressure profiles, while not directly in the second stability region, provided free access to that regime near the center of the discharge. Results have been reported in References 8-11.

The ORBIT code is being developed to study the interaction of high-energy ions with magnetohydrodynamic modes. It will be applied to the suppression of sawteeth by the high-energy ions excited by ion-cyclotron range of frequencies heating. This code uses orbit averaging of motion in either analytic or numerically generated equilibria through Hamiltonian guiding-center equations. A dispersion relation is used to evaluate the effect of the particles on the linear mode. Generic behavior of the solutions of the dispersion relation have been analyzed and the dominant contributions of the different components of the particle distribution function have been identified. Numerical convergence of Monte-Carlo simulations have been analyzed. The code gives an accurate means of comparing experimental results with predictions of kinetic magnetohydrodynamics. The method can be extended to include self-consistent modifications of the particle orbits by the mode, and hence the nonlinear dynamics of the coupled system. Results have been reported in Reference 12.

PPPL has several collaborations with TEXTOR. One area of collaboration is with the team from the

École Royal Militaire from Brussels, Belgium, developing and using the TRANSP code to analyze TEXTOR plasma discharges such as the I-mode discharges that exhibit enhanced-energy confinement. Modeling results are discussed in Reference 13. The scaling characteristics of I-mode discharges are similar to those of supershots in TFTR and high-beta discharges in JT-60U. These similarities are being investigated further.

PPPL scientists are collaborating with a TEXTOR group working to improve the TRANSP modeling of ICRF heating. The ICRF modeling has been improved by computing the electromagnetic field in the plasma on a fine grid consisting of 200 by 200 radial points. This feature is being incorporated into the TRANSP code, and will improve the accuracy of ICRF mode-conversion calculations. This improvement will be very useful for TFTR, since recent experiments with mode conversion in TFTR have achieved very interesting results. The present unmodified TRANSP code calculation is inaccurate for modeling these experiments. The coding of the improvement is progressing well.

A second improvement being worked on will add the capability for calculating ICRF heating of neutral-beam-injected ions using Monte-Carlo techniques. The improved version uses a Monte-Carlo operator that accelerates the beam ions when they traverse the ICRF resonance region. The TRANSP code runs of TFTR discharges have been given to the TEXTOR team to use to test and debug the improved code.

Another collaboration between the PPPL and TEXTOR teams investigates sawteeth in TEXTOR plasma discharges using the Faraday rotation diagnostic. These measurements have been very successful for time scales longer than the sawtooth crash time. Faster data is needed to resolve the magnetic structure during the crash itself. A new channel with ten microsecond time resolution has been installed during the TEXTOR maintenance period. The data measured by the new channel will be used to study the poloidal angle dependence of the magnetic structure of the m=n=1 MHD mode during the crash. This has not been measured previously in hot plasmas.

References

1 D.P. Stotler, J.A. Snipes, G.M. McCracken, *et al.*, "Modeling of Alcator C-Mod Divertor Plasmas in High Recycling and Detached Regimes," in *Plasma Physics and Controlled Nuclear Fusion Research 1994* (Proc. 15th Int. Conf., Seville, Spain, 1994), paper IAEA-CN-60/D-III-1-2 (IAEA, Vienna, 1995), to be published.

2 C.Z. Cheng, R. Budny, L. Chen, *et al.*, "Energetic Particle Effects on MHD Modes and Transport," in *Plasma Physics and Controlled Nuclear Fusion Research 1994* (Proc. 15th Int. Conf., Seville, Spain, 1994), paper IAEA-CN-60/D-3-III-2 (IAEA, Vienna, 1995), to be published.

3 G. Rewoldt, W.M. Tang, and R.J. Hastie, "Collisional Effects on Kinetic Electromagnetic Modes and Associated Quasilinear Transport," Phys. Fluids **30** (1987) 807.

4 T. S. Hahm, "Rotation Shear Induced Fluctuation Decorrelation in a Toroidal Plasma," Phys. Plasmas **1** (1994) 2940.

5 M. Saigusa, H. Kimura, T. Fujii, *et al.*, "Comprehensive Studies on Second Harmonic ICRF Heating in JT-60U," *in Plasma Physics and Controlled Nuclear Fusion Research 1994* (Proc. 15th Int. Conf., Seville, Spain, 1994), paper IAEA-CN-60/A-3-I-5 (IAEA, Vienna, 1995), to be published.

6 Ninomiya, *et al.*, "Conceptual Design of JT-60 Super Upgrade," in *Plasma Physics and Controlled Nuclear Fusion Research 1994* (Proc. 15th Int. Conf., Seville, Spain, 1994), paper IAEA-CN-60/F-1-I-1 (IAEA, Vienna, 1995), to be published.

7 M. Kikuchi, *et al.*, "Recent JT-60U Results Towards Steady State Operation of Tokamak," in *Plasma Physics and Controlled Nuclear Fusion Research 1994* (Proc. 15th Int. Conf., Seville, Spain, 1994), paper IAEA-CN-60/A-1-I-3 (IAEA, Vienna, 1995), to be published.

8 D. Moreau, B. Saoutic, G. Agarici, *et al.*, "RF Heating and Current Drive in Tore Supra," in *Plasma Physics and Controlled Nuclear Fusion Research 1992* (Proc. 14th Int. Conf., Würzburg, Germany, 1992), Vol. **1** (IAEA, Vienna, 1993) 649-660.

9 G. Agarici, J.P. Allibert, J.M. Ane, *et al.*, "'Recent Results of the TORE SUPRA Tokamak," in *Plasma Physics and Controlled Nuclear Fusion Research 1992* (Proc. 14th Int. Conf., Würzburg, Germany, 1992), Vol. **1** (IAEA, Vienna, 1993) 79-96.

10 G.T. Hoang, D. Moreau, E. Joffrin, *et al.*, "Lower Hybrid Enhance Performance in Tore Supra," in Radio-Frequency Power in Plasmas (Proc. 10th Topical Conf., Boston, MA, 1993), edited by Miklos Porkolab and Joel Hosea, AIP Conference Proceedings **289** (American Institute of Physics, New York, 1993) page 107.

11 G.T. Hoang, C. Gil, E. Joffrin, *et al.*, "Improved Confinement in High ℓ_i Lower Hybrid Driven Steady State Plasmas in Tore Supra," Nucl. Fusion **34** (1994) 75-85.

12 M. Zabiego, R.B. White, Y. Wu, *et al.*, "Analytical and Numerical Analyses of Sawteeth Stabilization with On-Axis ICRH Tore Supra," in *Plasma Physics*

and Controlled Nuclear Fusion Research 1994 (Proc. 15th Int. Conf., Seville, Spain, 1994) paper D-3-III-4-1 (R (IAEA, Vienna, 1995) to be published.

[13] Ongena, H. Conrads, M. Gaigneaux, *et al*, "Improved Confinement in TEXTOR," Nuclear Fusion **33** (1993) 283-300.

Low-Temperature Plasma Research

Low-temperature plasmas, well-known for their importance in technological and scientific endeavors such as illumination, lasers, spacecraft thrusters, microwave amplifiers, magnetic fusion reactor heat exhaust components, plasma torches, and high-temperature chemistry, have grown immensely in commercial value to a number of materials fabrication processes. These include the etching of complex patterns for microelectronic and microoptical components and the deposition of tribological, magnetic, optical, decorative, insulating, conducting, polymeric, and catalytic thin films.

Research in the low-temperature plasma branch at the Laboratory has activities in several of these areas, with strong concentration on two: fusion reactor divertors and surface erosion by hyperthermal neutral particles. Such erosion processes have applications in low-earth orbit phenomena and electronic materials fabrication. The low-temperature research efforts at PPPL are aimed at obtaining a deeper understanding of the plasma and plasma-surface-interaction processes that are operative in the weakly ionized regime. From this basis, practical applications for the associated generic techniques are developed. These research activities provide Princeton University students with opportunities for education and training in the diverse disciplines embodied in plasma science and technology.

Divertor Research for ITER

Two topics important to the International Thermonuclear Experimental Reactor (ITER) have been studied in a linear plasma device called the Princeton Divertor Simulator (PDS). One topic is plasma transport at high gas pressure. The second topic is tritium reduction in the exhaust stream by the use of permeable materials.

The PDS device produces quasi-steady-state, dense, warm plasmas with typical parameters of electron density $n_e = 6 \times 10^{19}$ m^{-3} and electron temperature $T_e = 5$ eV. The plasma is a magnetized (B ~ 0.4 T) column, about 0.01 m in radius and up to 0.3 m in length, terminating on a typically metal end plate. About 1 kW of microwave power at 2.45 GHz is supplied to the plasma through a waveguide in cutoff. This geometry, in conjunction with the plasma properties, promotes the generation and absorption of lower-hybrid waves. Nearly any working gas can be used. Our divertor studies have concentrated on helium and hydrogen.

Plasma Transport at High Gas Pressure

The high gas pressure approach to reducing the peak heat load, named gas-target divertor (GTD), was first proposed by Tenney in 1973. It has been the subject of several experimental studies. Nevertheless, a new phenomenon has been uncovered — a steady-state, highly localized, thermal collapse of the electron temperature from around 5 to 0.5 eV — whose detailed behavior is reminiscent of a stationary ion-acoustic double layer. The first detailed comparisons between the measured plasma parameters and those predicted by truly two-dimensional fluid plasma models have also been achieved. Moreover, the first (and in detailed) measurements of the effects on plasma parameters of a deeply inclined (87°) end plate have been made. Below, the thermal collapse is discussed.

The observations of thermal collapse were made with scanning Langmuir probes and an optical multichannel analyzer. Figures 1 and 2 show the measured axial electron temperature, ion density, space potential, and floating potential. For helium plasmas flowing into a chamber filled with helium gas to a pressure of 130 mTorr, a thermal collapse from about 4 to below 0.5 eV is seen to occur between 10 and 12 cm

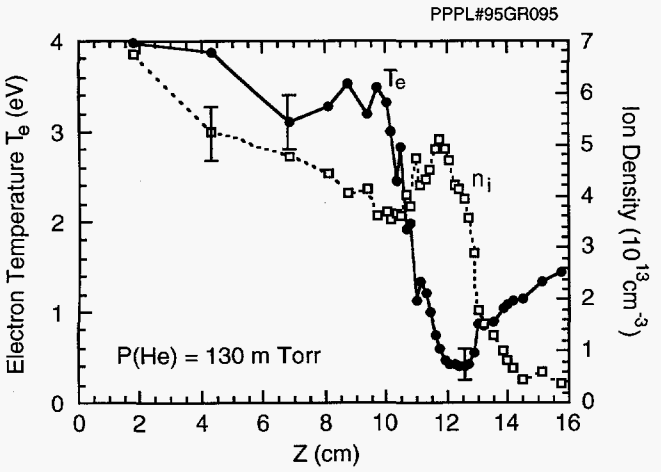

Figure 1. *Axial electron temperature and ion density measured for a magnetized helium plasma flowing into a helium-gas-filled chamber. A collapse of temperature to below 0.5 eV is seen.*

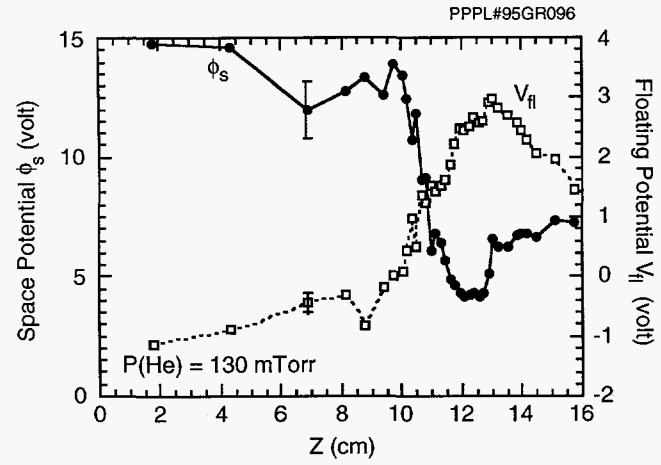

Figure 2. *Axial space and floating potentials for the plasma discharges whose parameters are shown in Fig. 1. Note the steep gradient in space potential in the region of thermal collapse.*

from the exit of the plasma source. A similarly shaped step in space potential is observed. The power flow to the end plate was reduced a factor of 40, perhaps as a result of the profound effect of plasma potential gradient on electron heat transport. No appreciable radial transport was seen. In the region beyond the thermal collapse, intense recombination radiation from n = 3-9 levels to the n = 2 level were observed. Resonance radiation, n = 2 to 1, was not observed, consistent with the calculated opacity of the surrounding ground-state neutral gas. Equally intriguing is the ability to control the occurrence of the thermal collapse by small variations in the electrical bias, of order $4T_e$, applied to the metal end plate. Virtually none of these phenomena have been predicted by the models used to design ITER. Hence, major insights into the important divertor-region physics may be gained on the PDS that will ensure that the ITER divertor functions as needed.

Tritium Reduction by Permeable Materials

It has been proposed to reduce the tritium content in ITER's exhaust stream by employing the phenomenon named superpermeation by A. Livshits. In this process, the rate of hydrogen transport through select materials, such as palladium, is enhanced by factors exceeding 10^9 compared with that of molecular hydrogen by the conversion of the gas phase molecular hydrogen to atomic, allowing the hydrogen transport process to avoid the molecular dissociation activation barrier at the material's surface. The conversion is done in the PDS by directing a hydrogen plasma onto the metal end plate. The ions reflect as neutrals, predominantly atomic, and free flow onto a nearby palladium membrane. A schematic of the measured hydrogen flux transmitted through the far side of the membrane is shown in Fig. 3. Note that exposure to gaseous molecular hydrogen fluxes produce no appreciable permeation. The decrease in flux, upon

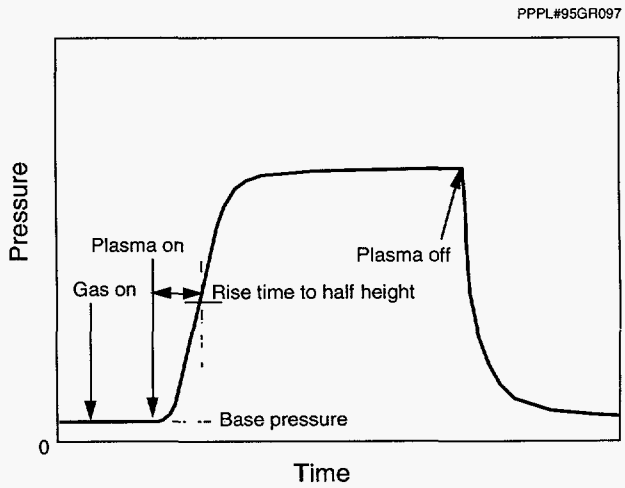

Figure 3. *Schematic of the measured hydrogen flux transmitted through the far side of a superpermeable membrane. Exposure to gaseous molecular hydrogen fluxes produce no appreciable permeation, while exposure to atomic hydrogen produces a rapid increase in permeation.*

termination of the plasma, is modeled by a diffusion equation, with recombination boundary conditions. The solution of this equation predicts a linear behavior of the function G[ϕ(t)], where ϕ(t) is the time-dependent permeating flux.

The constant of proportionality depends on the surface recombination rates (k_r) of the front [superscript (1)] and rear [superscript (2)] surfaces, and the thickness of the membrane (x_0). This behavior is clearly seen in Fig. 4, validating the understanding of the process and allowing an engineering design for a prototype to proceed.

$$G(t) \equiv \ln\left[\frac{\sqrt{\phi_p(t)}+\sqrt{\phi_p(t=\infty)}}{\sqrt{\phi_p(t)}-\sqrt{\phi_p(t=\infty)}}\right]_0^t = 4\frac{c'\,(k_r^{(1)}+k_r^{(2)})}{x_0}t$$

PPPL#95GR098

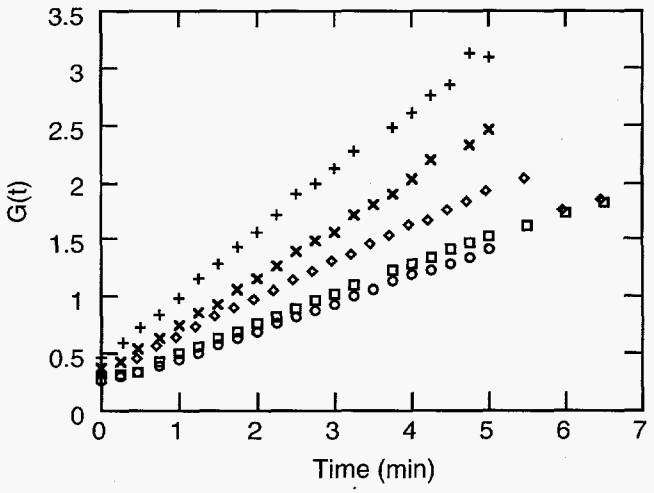

Figure 4. *Time dependence of G(t) after cessation of the hyperthermal atomic hydrogen beam. The linear behavior matches the theory described by the equation and gives a measure of the recombination rates at the front and rear palladium surfaces.*

Materials Processing with Hyperthermal Neutrals

Individual atoms, ions or radicals impacting surfaces can cause the removal of surface atoms by chemical or sputtering processes. Chemical processes may occur at relatively low impact energies, around approximately 1 eV, particularly if the impacting species are highly reactive. Sputtering, in contrast, requires more than 100 eV for rapid erosion rates to be attained.

The selective and highly anisotropic removal of material in semiconductor fabrication is generally called etching and is of great commercial value. At the higher energies typical of sputtering, damage detrimental to the crystalline structure may occur, hence chemical etching is preferred. Plasmas have long provided the desired erosion rates, selectivity, and anisotropy. However, as surface features have shrunk to below 0.5 μ, problems with direct plasma etching appear. The two main ones are: (1) damage to the semiconductor due to exposure to ultraviolet light generated in plasmas by electron impact excitation, and (2) damage due to charge build-up on thin insulating surfaces, and subsequent arcing. To avoid these, intense hyperthermal neutral particle beams of reactive gases such as atomic oxygen, chlorine, and fluorine are being developed. These sources will also have use in qualifying materials for use in low-earth orbit.

The method is surface neutralization of plasma ions. The plasma is responsible for the fragmentation and ionization of the less reactive oxygen, fluoride, and chloride molecules into their constituent atoms and ions. These are directed onto a biased target and reflected as neutrals, retaining, after reflection, about half of their incident energy. The PDS was the second source of hyperthermal neutrals at PPPL, the first being a pulsed toroidal device named ACT-I. As a research tool, the PDS is exceedingly valuable. However, it has several drawbacks for production-oriented etching. The first, which will eventually be overcome, is that it runs at a low-duty factor, typically less than 10%. Secondly, plasma light still reaches the target because of the extended plasma region. Thirdly, the magnetic field requires nearly 150 kW of electrical power. And lastly, the magnetic field extends rather far from the apparatus, declining to less than 100 G only at distances greater than 2 m. This can adversely affect other nearby equipment.

To overcome these problems, a new source has been conceived which unites a magnetron (sputtering) configuration with a microwave-heated cavity, see Fig. 5. The plasma formed in this manner is located

out of line-of-sight to the target, in a small region where a moderate, about 2 kG, magnetic field is provided by a relatively low-power, about 2 kW, electromagnet. In such a configuration, the plasma may be overdense, in part because $\omega < \omega_{ce}$ near the magnetron cathode. In the first set of experiments, a steady-state oxygen plasma with 300 W of absorbed μ-wave power at 2.45 GHz was formed. The current to the cathode was 0.5 A when the oxygen pressure in the cavity was 2×10^{-3} T. The use of μ-wave power has allowed the bias on the magnetron cathode to be reduced to below 10 volts, hence sputtering of the cathode is minimized. Within the sample chamber, the pressure was 2×10^{-4} T because of the low conductance of the collimator. Plasma parameters of $n_e = 2 \times 10^{11}$ cm^{-3} and $T_e \approx 4.6$ eV were measured with a single Langmuir probe. Removal of a photoresist film by the stream of particles coming from this source has been observed. The research program for next year will focus on optimization of the source and its operational modes, quantification of the species, flux, and energy of the atomic and molecular beam, and analysis of the parametric dependencies of the etching process.

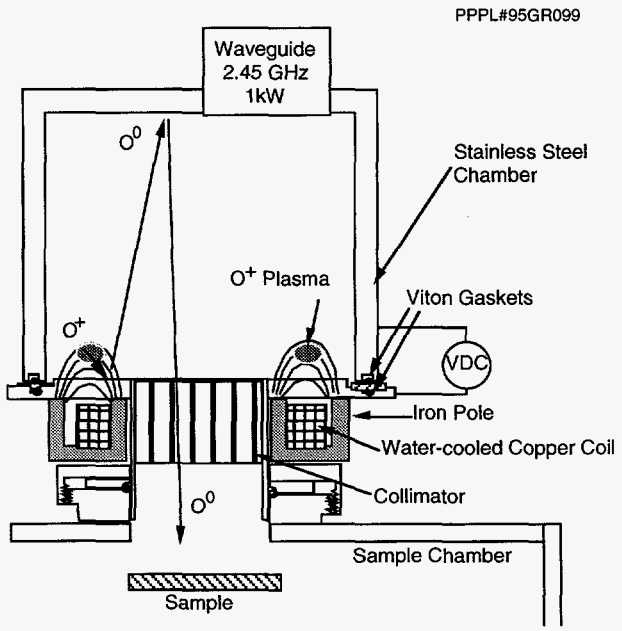

Figure 5. *Schematic of the hyperthermal atomic beam (HAB) apparatus. An oxygen plasma, formed by electron cyclotron resonance and cavity mode operation in a sputtering magnetron configuration, is neutralized on the biased cathode. Reflected neutrals may exit through the collimator and impact the sample.*

Electron Diffusion Gauge Experiments

The purpose of the Electron Diffusion Gauge (EDG) experiment is to establish a primary pressure standard in the ultrahigh vacuum regime (less than 10^{-7} Torr) using the properties of pure electron plasmas. Because the confined plasma relaxes to a well-known equilibrium, small deviations can be accurately characterized. For this experiment, there is a measurable plasma expansion resulting from collisions with background neutral helium gas. The confinement of the EDG plasma was demonstrated in previous experiments. In FY93, the EDG operating regime was explored and pressure-dependent operation was demonstrated. In FY94, density scaling laws for plasma confinement were investigated and subsequently used to estimate the range of parameters where the pressure can be accurately determined. Research on the EDG was designed to establish two conditions about plasma behavior: (1) The presence of gas in the system is a small perturbation to the rigid-rotor equilibrium so that the plasma is in a state of successive equilibria. This is shown from the fact that the relaxation to equilibrium is faster than the transport processes. (2) The diffusion due to field asymmetries is smaller than the diffusion due to the background gas so the field asymmetries can be neglected.

Methodology

This experimental configuration consists of a Malmberg trap that uses a combination of magnetic and electrostatic trapping to confine the electrons for several tens of seconds. A Malmberg trap achieves a radial force balance between the space-charge expansion and the inward $\mathbf{j} \times \mathbf{B}$ force from the plasma rotation and the uniform axial magnetic field. In this equilibrium, the rotation frequency is independent of radius, i.e., the plasma is a rigid rotor. Longitudinal confinement is provided by electric fields produced by biased collinear cylinders. Unlike a neutral plasma, these single-species plasmas conserve angular momentum so particle collisions do not lead to plasma transport. In the absence of nonuniformities or misalignments of the confining fields, the equilibrium is perfectly confined and most of the electrons never reach the wall. In practical, imperfect systems with imperfections as low as 0.1%, the angular momentum changes slowly, leading to radial expansion of the plasma and a finite confinement time even at the base pressure.

If neutral gas is present, collisions between electrons and neutrals result in an additional loss of angular momentum and an increased in the rate of plasma expansion. If the contribution from field asymmetries can be accurately subtracted, the expansion due to neutral gas collisions can be found, providing the basis for the pressure measurement. Using a calculated value for the elastic momentum transfer cross section of the neutrals (the velocity distribution as calculated from the equilibrium), the rate of expansion provides a more accurate determination of neutral gas density (or pressure, given the ambient temperature) than other types of pressure gauges.

The electron source is thermionic emission from a resistively heated filament. The electrons stream down the magnetic field into the trapping region. The farthest cylinder is held at a negative electric potential and reflects the electrons. After the trapping region is populated with electrons, the cylinder nearest the filament is brought to the same negative potential and a trapped-electron cloud is formed.

The evolution of the plasma is measured by abruptly removing the potential from the far cylinder, allowing the plasma to escape along the field lines. The charge distribution is measured with a collector consisting of an axially movable plate for collecting the bulk of the electrons and a Faraday cup behind an aperture for measuring the charge density at a particular radial position. The position of the aper-

ture is moved radially to establish a profile. Because the measurement requires the termination of the plasma, the profile must be determined from a sequence of plasma discharges. The radial velocity distribution is found by releasing the plasma with a variety of sector potentials. A time-of-flight measurement is made to determine the parallel temperature for high-energy electrons. Experiments elsewhere have demonstrated that the high-energy parallel temperature is equal to the perpendicular temperature unless perturbed. If the plasma temperature is spatially uniform, then the plasma total energy and angular momentum can be determined.

Experimental Results

Measurements of the total charge, angular momentum, and energy of the plasma as a function of time and control parameters were made. The angular momentum is calculated from the radial profile of the plasma and the energy from measurements of the axial temperature.

The principal results are that there are properties of internal transport that are inconsistent with existing theory. A new result establishes that pressure transport can lead to the formation of rigid-rotor equilibria identical to those generated by internal transport, but with lower temperatures.

Interpretation is complicated by the fact that the characteristic electron temperature for pressure-driven equilibrium is lower than that for internal transport. The ramifications are that absolute velocity distribution cannot be determined from the equilibrium alone and therefore absolute pressure cannot be established unambiguously without an additional electron temperature measurement. However, this system is suitable for relative pressure measurements.

Pressure-induced transport was found over a large range of pressure (10^{-10} to 10^{-4} Torr) with residual gas in the chamber (primarily hydrogen as determined with a quadrupole residual gas analyzer). The increase of relaxation rate with pressure was measured. The scatter in the data was only about 8% over five orders of magnitude.

Acknowledgments

Research in FY94 was supported in part by the Office of Naval Research under Grant No. N00014-92-F-0058. Previous work supported by grants from the National Institute of Standards and Technology. The SMC Corporation loaned certain equipment.

Theoretical Studies

The Theory Division Group has several roles in the Princeton Plasma Physics Laboratory's (PPPL) research program: It works with experimental groups to interpret results of experiments and suggests new experimental approaches. It works to propose new theories for existing phenomena and undiscovered phenomena. It develops theoretical and computational tools which will have impact in future research. And, it works to aid in machine design for future experiments. In addition, the Theory Division staff play a major role in the Graduate Studies Program and have involvement in non-fusion areas of plasma physics. The group also has an extensive ongoing collaborative effort with groups in the U.S. and abroad. Some of the major research efforts for FY94 include:

- Improvements of the tokamak concept as a fusion reactor. These include advanced tokamak operating regimes, having high beta, high confinement, and high-bootstrap fraction, as well as innovative techniques for more efficiently utilizing fusion products and the power they provide, including "alpha channeling," and "frequency sweeping" or "chirping" for ash-removal and plasma profile control.
- Studies to improve the understanding of plasma transport. Using both analytic and numerical tools, progress has been made in a range of transport issues of current interest including: transport due to drift-type and toroidicity-induced Alfvén eigenmodes (TAE); the effect of toroidal flow and flow-shear on turbulent and neoclassical transport; the effects on drift-wave transport of the reversed-shear and low-aspect-ratio configurations contemplated in the advanced tokamak studies; and transport scalings with ion mass, system size, plasma current, and other important physical parameters. In studying these and other problems, the Theory Division Group has developed an array of major codes, including toroidal gyrokinetic and gyrofluid codes, a hybrid-MHD/kinetic code, an upgrade of the ORBIT guiding-center code incorporating self-consistent effects, the DIA code for solving statistical closures, and comprehensive stability codes.
- Comparison of experimental results with theory for sawtooth stabilization studies, for analysis of TAE modes, and for the comparison of experimental profiles and predictions obtained purely from gyrofluid and gyrokinetic simulations.

This report includes four major theoretical physics sections covering magnetohydrodynamics, microinstabilities and transport, energetic-particle phenomena, and non-fusion studies. There is substantial overlap among these categories. For example, some magnetohydrodynamic (MHD) studies must account for kinetic effects from energetic particles and, conversely, MHD effects can play an important role in energetic-particle transport and in microinstabilities.

Magnetohydrodynamics

Advanced Tokamak Studies

Advanced tokamak studies concentrate on high-confinement, high-beta, and high-bootstrap fraction steady-state tokamak operating modes. If these modes of operation are fully developed, they could lead to much less expensive tokamak demonstration power plants and to a significantly reduced cost of electricity from fusion compared to that implied by a pulsed, low-β_N International Thermonuclear Experimental Reactor-like device. Advanced tokamak studies have been performed in the areas of resistive-wall stabilization, ponderomotive stabilization, and the kinetic basis for improved confinement. The last of these is discussed in the Microinstabilities and Transport section below.

Resistive-Wall Mode Studies

Many of the new, attractive, tokamak configurations rely on ideal-wall stabilization of the low-n free-

boundary modes. Real walls, however, are not ideal and are subject to the resistive-wall instability. A new mechanism for stabilizing this resistive wall is being studied.[1] This mechanism relies on plasma rotation, viscosity, and inertia. A stable window in the position of the resistive wall, similar to that of Bondeson and Ward,[2] is shown to exist for reasonable values of the rotation frequency.

Bondeson and Ward[2] recently demonstrated the existence of a narrow window for placement of a resistive wall, which results in complete stabilization of beta-driven external kinks. The stabilization, which requires sonic rotation, is ascribed to toroidal coupling of the plasma perturbation to sound waves and Landau damping. The possibility of complete stabilization has encouraged consideration of additional damping mechanisms, which can increase the size of the stable window.

The MH3D code is an initial value, nonlinear, three-dimensional (3-D) toroidal, resistive, compressible MHD code, which here is used to study the stabilization of external kink modes. (Further applications are discussed below.) In the present application, a high-conductivity plasma core region is surrounded by a low-temperature resistive mantle, too resistive to carry any significant perturbed current. Plasma flows are allowed in the mantle as well as the core. Anomalous viscosity μ is included in the momentum equation as a prescribed function of radius. Using a cylindrical plasma model and a rotating resistive wall, typical results are shown in Fig. 1, which is a plot of linear growth rate γ versus wall-rotation frequency Ω for a single helicity m/n=2/1 external kink resistive-wall mode at zero beta.

The q = 2 rational surface lies at $r_s = 1.05$ and the critical radius at which a perfectly conducting wall stabilizes the kink is $r_c = 1.20$. Results are shown for three values of the anomalous viscosity. Length and time are given in units of minor radius and Alfvén time, respectively. All variables are nondimensionalized by scaling length and time with respect to minor radius and Alfvén time, respectively.

Consider first curve (1) corresponding to $\mu = 10^{-5}$, a value consistent with typical plasma edge parameters. Rotation is initially destabilizing; however, increased slippage between the mode and wall frequencies (see dashed curve for mode frequency) causes a roll-over in growth rate versus wall-rotation frequency, and complete stabilization is obtained at $\Omega_{crit} \approx 0.06$. Curves (2) and (3) show that decreasing the viscosity

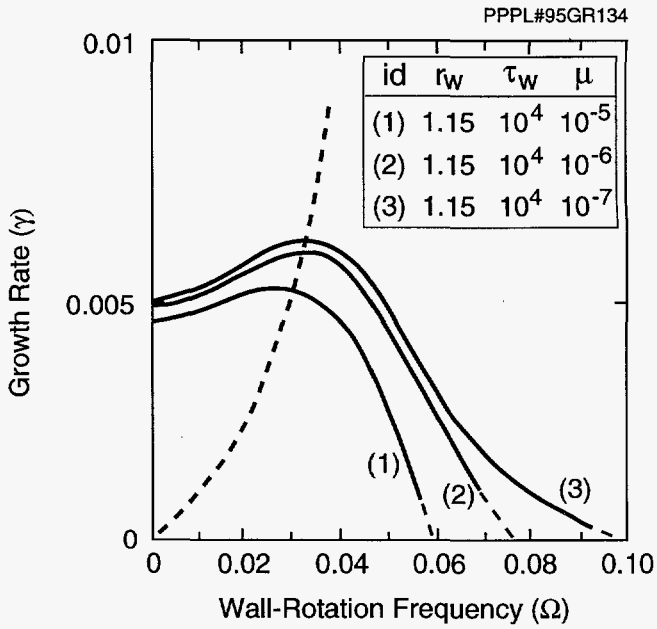

Figure 1. *Linear growth rate γ versus wall-rotation frequency Ω illustrating the rotational stabilization of an external kink.*

makes stabilization by rotation more difficult. By varying the viscosity profile, it is found that it is the anomalous viscosity at the edge of the plasma core, rather than the anomalous viscosity in the mantle, that dominates the stabilization of the resistive-wall mode. The resistive-wall eigenfunctions show the importance of the restriction on plasma motion caused by the mantle inertia: the mantle allows flows which restrict the edge core plasma displacement, leading to stabilizing edge eddy currents.

Using the linearized incompressible equations of reduced MHD and treating the resistive wall in the thin wall limit, a dispersion relation may be derived which exhibits good qualitative, and fair quantitative, agreement with the MH3D results and provides additional understanding of the role of viscosity in stabilizing wall modes in the presence of rotation.

Feedback Stabilization using Ponderomotive Forces

Another feedback mechanism which is being studied is that realized through radio-frequency-ponderomotive force. While this technique has been tried with some success in mirror machines, it has not yet been demonstrated that these forces can be effective on global modes like the kink in large-scale devices. An experiment of this kind has been proposed by the Princeton Beta Experiment-Modification researchers

using the present ion-Bernstein wave (IBW) system as the feedback agent. As a prelude to the experiment and theoretical simulation on the helical modes, a proof-of-principle experiment has been proposed to see how effective the ponderomotive force can be for controlling the axisymmetric position of a plasma discharge. The formulation for such a n = 0 equilibrium modification has been worked out by Myra[3] and incorporated into the TSC code for a theoretical simulation.

Nonlinear MHD with the MH3D Code

As noted earlier, the MH3D code is an initial value, nonlinear, 3-D toroidal, resistive, compressible MHD code. The code has been extended for more realistic simulation of tokamak plasma discharges. A vacuum region and resistive wall were added for the study of external mode stabilization by plasma rotation, described above.

The MHD model treats the plasma as a single fluid. A more realistic two-fluid model, representing ion and electron fluids, has been added to the code and is presently being benchmarked with analytic results.

The MH3D-K code is another extension of MH3D code, which includes hot-particle effects.[4] The code treats thermal species as fluids and hot-particle species as gyrokinetic particles. The MH3D-K code has been used to study linear and nonlinear evolution of TAE modes driven by hot particles.[5] It was found that wave-particle trapping is the nonlinear saturation mechanism for the cases studied. The corresponding density profile flattening of hot particles is observed. The saturation amplitude is proportional to the square of the linear growth rate, as expected from an analytic theory.

Unstructured mesh capability is presently being added to the MH3D code for a more efficient representation of plasma geometries.

Sawtooth Stabilization in D-D and D-T Regimes

The sawtooth stabilization criterion in the Tokamak Fusion Test Reactor (TFTR) deuterium-deuterium (D-D) plasmas has been intensively compared with new TFTR regimes during deuterium-tritium (D-T) plasma experiments of the past year. Earlier,[6] the criterion was checked in 13 plasma discharges with the motional Stark effect (MSE) diagnostic measurements of the q-profile (in D-D regimes with neutral-beam injection and plasma current of 1.4 to 1.8 MA).

At present, more than 200 discharges have been scanned using the plasma profiles obtained from TRANSP code plasma analysis. Although without MSE data this comparison is subject to some uncertainty, it allows the test of the theory in new regimes with higher plasma current (up to 2.7 MA), with both D-D and D-T plasmas with a combination of neutral-beam-injection and ion-cyclotron range-of-frequencies heating. With a few exceptions, the criterion of sawtooth stabilization works in all TFTR regimes, as well as in the presence of other MHD activities like fishbones and minor disruptions (in a beta range up to the disruption level).

Based on these results, it can be concluded that a much improved understanding of sawtooth suppression in tokamak plasmas has been obtained. Although many issues of sawtooth oscillations remain still unresolved, this theory determines the sawtooth-free operational space and, in particular, the achievable values of the central safety factor.

PEST and SPARK Code Coupling for δW Analysis with 3-D Ideal Walls

Real tokamak walls are intrinsically three-dimensional. To analyze ideal time-scale stabilization due to 3-D ideal conducting walls, the PEST-VACUUM codes have been coupled to the 3-D SPARK electromagnetics code, suitably modified to calculate the perturbed magnetic field from the induced wall currents using the PEST perturbations as its driver.[7] For each surface poloidal harmonic of the PEST displacement, the SPARK code is used to find the 3-D magnetic perturbation $\delta\mathbf{B}_s$ which, when driven by the fields obtained from PEST code, combine with them to satisfy the appropriate boundary conditions at the 3-D shell. The traditional PEST treatment for two-dimensional (2-D) vacuum-wall systems solves Laplace's equation for the magnetic scalar potential using collocation techniques for the integral equations generated by Green's second identity. The effects of the wall are incorporated directly into the resolving matrix for the potential. Now, for 3-D wall systems, the vacuum treatment is reformulated into several

steps to linearly superpose distinct contributions coming from (a) the plasma "in the absence of the shell" and from (b) the shell "in the absence of the plasma" but driven by the plasma perturbations, while ensuring that the boundary conditions are appropriately taken on the "total" magnetic field. A modified vacuum energy matrix is finally calculated which is spectrally filtered in toroidal angle for input to PEST.

The SPARK code is used for step (b) for eventual 3-D applications. Meanwhile, it has been verified in a cylindrical limit (where vacuum fields are easily analyzed in terms of Bessel functions), and in a toroidal case with poloidal cuts in an axisymmetric shell, that the new vacuum PEST algorithm gives identical results compared with the traditional PEST treatment. The coupled PEST/SPARK code significantly extends the capability of PEST to allow an assessment of the stabilizing influence of a perfectly conducting wall with arbitrary poloidal and toroidal variation.

Advances in the PIES Code

In collaboration with P. Merkel (Garching) and A. Salas (Madrid), work on the PIES code has continued.[8] Merkel has implemented an interface with the NESTOR code[9] so that the PIES code can operate with the plasma-vacuum interface treated as a free boundary. Successful application has been made to a simple Wendelstein 7-A configuration and work is progressing to make it useful for more complicated systems. Some of the computational techniques used in the code have been changed and improved to make the code more robust and accurate. In particular, more careful determination of the position of island edges, together with an improved algorithm for flattening the pressure and current in the islands, has dramatically improved the convergence properties of the code.

Applications of the code have been made to the W7-X Helias, the TJ-II Heliac, the LHD stellarator, and the MHH configuration which is being used for a stellarator power plant study.[10] A typical result is given in Fig. 2, for a $<\beta> = 2.35\%$ MHH equilibrium.

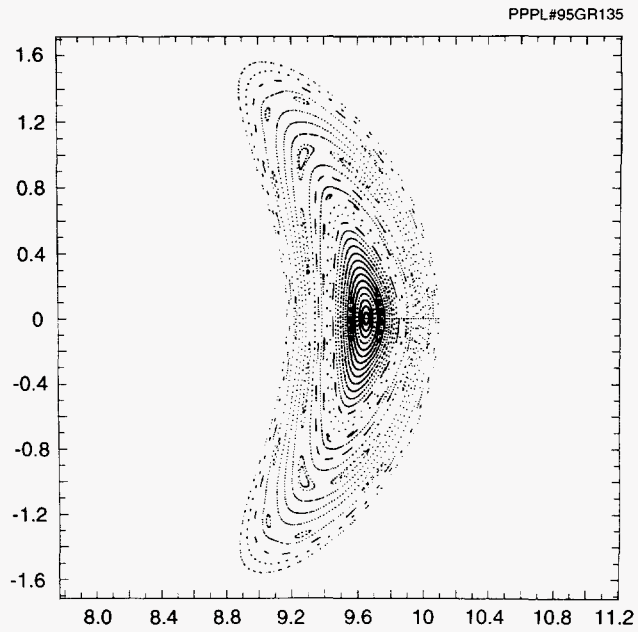

Figure 2. *Magnetic surfaces for the MHH configuration with* $<\beta> = 2.35\%$ at the $\phi = 0$ *cross section.*

Stability of External Modes in a Diverted Tokamak

In the presence of a nonaxisymmetric perturbation, it has been found[11] that a poloidally diverted tokamak plasma develops open field line regions of differing topology separated by singular surfaces. The singular surfaces play a role analogous to that of rational toroidal flux surfaces, in terms of constraining ideal-MHD motion and thus constraining the free energy that can be tapped by ideal-MHD instabilities. The effect on external modes, such as external kink modes and certain types of ELMs (edge localized modes), is stabilizing. Nonaxisymmetric fields which can give rise to the singular open surfaces are produced self-consistently by the nonlinear evolution of a free-boundary MHD mode, are produced by field errors, and could be imposed expressly for the purpose of influencing the MHD modes through the constraints introduced by the singular surfaces. In the absence of the effect, external kink modes which resonate with rational surfaces near the divertor separatrix would enter a nonlinear phase of rapid growth when they break the rational surface. A simple model has been used to numerically explore the structure of the open field lines and the structure of the singular surfaces, in particular.

Sweeping Equilibrium and Stability Code

Understanding disruption phenomena in tokamak plasmas requires a comprehensive comparison of nonideal theoretical models with experimental databases. For these purposes, a special "sweeping" method

to solve equilibrium and stability problems has been developed.[12] The method provides automatic control of its accuracy without time-consuming convergence studies.

At present, the method has been successfully applied to solve the Grad-Shafranov equation. A new fast equilibrium code, SESC, also uses the new "sweeping" technique and has many advanced features:

- It provides an appropriate polynomial description of the equilibrium, containing all necessary derivatives for the theory.
- It has both interactive and conveyor modes, allowing scanning of experimental databases on tokamaks.
- It does not require benchmarking and can check the accuracy of existing codes.
- It contains an optimal combination of the spectral representation of the plasma core and a boundary layer representation near the separatrix.
- Its solution contains complete information about axisymmetric instabilities and, thus, does not require separate studies of n=0 stability.
- It is excellent as an equilibrium solver for TRANSP, TSC, ASTRA, and DINA plasma evolution codes with a simplest form of the Newton iterations.

The full version of SESC will contain calculations of ideal and nonideal linear stability and will be used for extensive comparison of the theory with experiments on TFTR and other machines.

Extended Energy Principle

An analysis[13] by B. Lehnert,[14] who challenged the validity of the Extended Energy Principle,[15] has been carried through. It has been found that Lehnert lost a term in his calculation.

The Energy Principle Paper reduced the stability problem to one of minimizing a functional $\delta W_B(\xi,\xi)$ subject only to the constraint that the normal component of **B** be continuous across the perturbed plasma-vacuum surface. In the Extended Energy Principle, the system is MHD unstable if, and only if, this functional is negative. Bernstein *et al.*[15] showed that, if a perturbation ξ which does not satisfy pressure balance can be found which makes δW_B negative, then a modified one, $\tilde{\xi} = \xi + \varepsilon\eta\nabla\psi$, exists which does satisfy pressure balance and has the same negative potential energy. Here η is nearly independent of ψ everywhere except in a narrow region between $\psi_S(1 - \varepsilon)$ and ψ_S at the plasma edge with ε arbitrarily small. In this region it changes rapidly, such that $\varepsilon B^2 |\nabla\psi|^2 \partial\eta/\partial\psi = O(\varepsilon^0)$. This small modification of the perturbation makes ξ satisfy the pressure balance at the plasma-vacuum interface and introduces only an infinitesimal change in δW_B. It creates a large current just inside the plasma surface which interacts with the local field to produce a stabilizing force. However, in the Extended Energy Principle this force was transformed to the torsional Alfvén wave contribution $\tilde{Q}_{||}^2$ in δW_B by an integration by parts.

Lehnert incorrectly criticized the extension of the energy principle to unrestricted test functions ξ. He ignored a surface integral that came from an integration by parts and then argued that a surface current **K**, which must be imposed to provide pressure balance, will add an additional contribution to the force $\mathbf{F}(\xi)$ in the functional δW_L, which should be stabilizing. The analysis showed that this additional term just cancels the term that he lost.

Microinstabilities and Transport

Microinstability Analysis of Advanced Tokamaks

Kinetic theory analysis relevant to advanced tokamak configurations has been carried out in support of the negative magnetic shear scenarios of special interest to the Tokamak Physics Experiment (TPX) and the International Thermonuclear Experimental Reactor (ITER) and the low-aspect-ratio scenarios appropriate for the proposed National Spherical Tokamak Experiment (NSTX) experiment. In particular, the implications of drift-type microinstabilities are addressed. These high-n modes are destabilized by the combined effects of ion-temperature gradients and trapped particles. The present studies have focused on applications of comprehensive kinetic microinstability calculations[16,17] (using the FULL code) to general tokamak equilibria.

In examining the influence of negative magnetic shear on microinstabilities, previous work[18] has been

extended to investigate the sensitivity of the results to changes in local values of the magnetic shear and the ion-temperature gradient. Results indicate that the linear growth rates have a large safety margin for stability with respect to the ion-temperature gradient, but only a small one for the magnetic shear, i.e., the magnetic shear has to be kept sufficiently negative in order to achieve complete stabilization for these modes.

With regard to the low-aspect-ratio investigations, a sequence of MHD equilibria[19] of varying aspect ratio have been calculated numerically using parameters of the newly proposed NSTX experiment.

The linear growth rate for the dominant mode is found to be fairly constant for (horizontal) aspect ratio $A = R/a > 1.75$, but there is rapid stabilization as A decreases from 1.75 down to 1.5, where this particular mode becomes completely stable. Other modes that are less affected by magnetic drifts could be less stabilized. This stabilization is mainly due to the decrease in the bad curvature with decreasing aspect ratio, with a corresponding decrease in the orbit-average magnetic drift for the trapped particles. The encouraging results from these studies thus indicate that the dominant branch of the toroidal drift mode should be strongly stabilized by low (horizontal) aspect ratio, typically for $A < 1.75$. This has been demonstrated for a variety of plasma boundary shapes and profile parameters. These findings suggest significant reduction in the transport, but do not imply absolute stability to microturbulence.

Microinstability Analysis of TFTR Deuterium-Tritium Plasmas

Recent deuterium-tritium plasmas in the TFTR experiments have given evidence of a surprisingly strong favorable isotopic dependence in confinement. This has motivated analysis of the linear stability and associated quasilinear transport of prominent microinstabilities such as the toroidal-drift mode (trapped-electron-η_i mode) and the kinetic MHD ballooning mode. In particular, the scaling with ion mass of the linear growth rates was analyzed using the FULL code.[17] In general, it was found that the growth rates do decrease strongly with ion mass (after maximizing the growth rate over n or $k_\theta\rho_i$), though the scaling exponent depends on the particular mode studied and

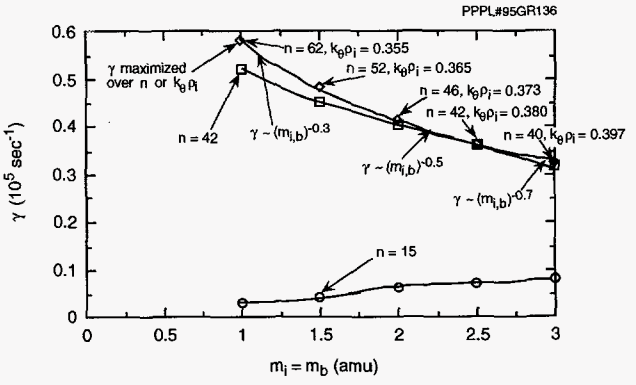

Figure 3. *Linear growth rates for TFTR D-T shot 73268 at r/a = 0.475 for the electrostatic toroidal-drift mode including electrons, background ions, beam ions, hot alpha particles, and impurity ions.*

the magnetic surface chosen. This trend is illustrated in Fig. 3 for parameters corresponding to a representative TFTR deuterium-tritium plasma discharge. Also, the relationship of the transport coefficients for H, D, T, He^3, and He^4 has been investigated. It is found that, as is true for all multispecies microinstability studies, the equilibrium profile details strongly influence the results.

Microinstability Analysis of DIII-D High-Performance Plasma Discharges

As part of a collaboration between General Atomics and the PPPL Theory Division, the kinetic stability properties in a number of high-performance discharges from the DIII-D (Doublet III-D) experiment have been analyzed utilizing the FULL stability code.[16] This code has been interfaced with equilibria specific to DIII-D plasmas. Experimentally measured equilibrium profile data, along with internal and external magnetic data, were used, and the corresponding MHD equilibria were computed numerically. In particular, a high-ℓ_i high-confinement mode (H-mode) case and a very high-confinement mode (VH-mode) case were considered, and a high-β_p case and a low-to-negative magnetic shear case are planned. An assessment of the influence of velocity-shear flow on these instabilities has also been initiated. Representative results from these studies are illustrated in Fig. 4 where the radial variation of the linear growth rate and real frequency for the high-ℓ_i H-mode case are shown.

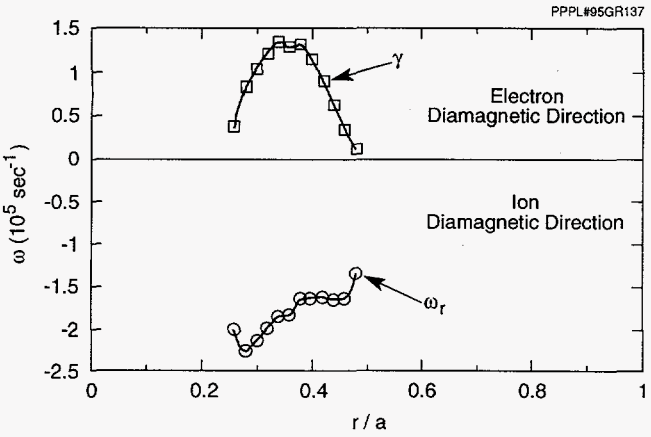

Figure 4. *Linear growth rates and real frequencies for DIII-D high-ℓ_i H-mode shot 73715 at t = 2.5 sec for the toroidal-drift mode at $k_\theta\rho_i = 0.42$, including impurity and beam species. Here, $V_{tor} = 0$.*

Trapped-Ion Mode in Toroidally Rotating Plasmas

The influence of radially sheared toroidal flows on trapped-ion modes has been investigated using a two-dimensional eigenmode code. These radially extended instabilities may play a significant role in accounting for the Bohm-like confinement trends observed in recent tokamak experiments. The electrostatic drift kinetic equation was obtained from the general nonlinear gyrokinetic equation in rotating plasmas.[20] In the long perpendicular wavelength limit $k_r\rho_{bi} << 1$, where ρ_{bi} is the average trapped-ion banana width, the resulting eigenmode equation becomes a coupled system of second-order differential equations for the poloidal harmonics. These equations were solved using finite element methods. Numerical results from the analysis of low and medium toroidal mode number instabilities have been obtained using representative TFTR low-confinement mode (L-mode) input parameters. Contour plots in the X-Z plane of the perturbed electrostatic potential for such an instability with toroidal mode number n=4 are shown in Fig. 5 for several values of the Mach number M_0 on the magnetic axis.

Gyrokinetic Simulations

The gyrokinetic particle simulation group at PPPL continues to be an important contributor to the Numerical Tokamak Project (NTP), a national consortium sponsored by the Department of Energy for the

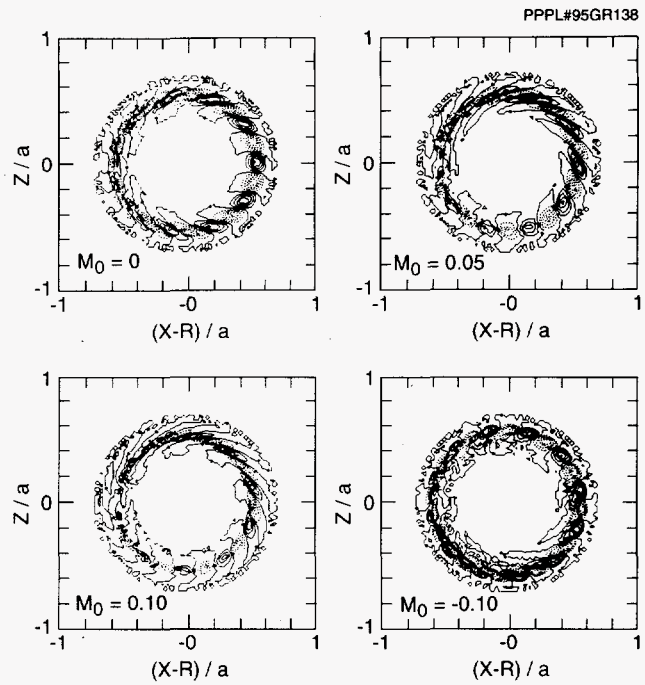

Figure 5. *Poloidal cross-sections of the eigenfunctions for selected values of the Mach number M_0 on the magnetic axis.*

High Performance Computing and Communication Initiative (HPCCI). Presently, the 3-D global toroidal gyrokinetic particle code, GET3D,[21] runs in dedicated mode on the C90s at the National Energy Research Supercomputing Center (NERSC), the CM-5 at the Advanced Computing Laboratory at the Los Alamos National Laboratory, and the Pittsburgh Supercomputing Center (PSC). This code is presently being ported to the new massively parallel platform, the Cray T3D, at these sites.

The code has been used to pursue several research areas of major current interest, synopsized below.

Mass Scaling of Turbulent Transport

Studies of the scaling with ion mass of the ion thermal diffusivity, χ_i, due to the ion temperature gradient (ITG) driven instability have been carried out. The observed favorable mass scaling is believed to be the result of mode-coupling to the long wavelength modes, for which the radial mode widths are related more to the equilibrium scale lengths than to the ion gyroradii.

Turbulent Transport and Flow Shear

The effects of ambipolar (or purely radial) electric field, nonlinearly generated by the unstable ITG modes, have been investigated.[22] It is found that the

global nature of the ion-temperature-gradient mode and its long radial correlation length makes it less effective in influencing the nonlinear evolution of the unstable modes. As a result, transport is typically only reduced by 30-40% from its value in the absence of the ambipolar field.

Turbulent Transport and Gyrokinetic Interpretation

A detailed analysis of the transport in full-volume gyrokinetic simulations of tokamak plasmas is being carried out,[23,24] toward developing a reliable first-principles transport theory for these systems. Two complementary lines of investigation have been followed:

(1) Studying the scalings of transport with important plasma parameters. Two asymptotic regimes of global scaling have been found, a small-system scaling (for a/ρ_i less than about 64) and a large-system scaling (for a/ρ_i greater than 64), of which the latter is more relevant to existing experiments, and of obvious importance in extrapolation to future devices such as ITER. The larger systems have transport close to that predicted by the standard simple estimates for transport by drift-wave turbulence (viz., Bohm or gyro-Bohm) in scaling with a/ρ_i, temperature, magnetic field, ion mass, safety factor, and minor radius, but lying much closer to Bohm, which appears to be the result better supported theoretically.

(2) The development of the first-principles theory, using the gyrokinetic data to guide the validity of assumptions and approximations. It is found that the essential transport physics is held in a greatly reduced set (a few tens) of the thousands of harmonics kept by the full simulation, and the coefficients determining the dynamics of this reduced system have been inferred from the gyrokinetic data. The nonlinear power transfer predicted by the inferred nonlinear coupling coefficients M_{kpq} are consistent with the characteristic downshift in the $<k_\theta>$-spectrum observed previously in going from the linear to the turbulent phase. An explanation of the downshift is given from the resemblance of the reduced system to the Hasegawa-Mima or Terry-Horton systems. These manifest an analogous downshift in slab geometry, and have M_{kpq} resembling those inferred from the gyrokinetic data.

Collisional Toroidal Gyrokinetic Simulations

A neoclassical version of the code has been applied to the investigation of sheared flow effects in toroidal plasmas.[25] An accurate collision operator conserving momentum and energy has been developed and implemented. Simulation results using the operator are found to agree very well with neoclassical theory. For example, it is dynamically demonstrated in these multispecies simulations that like-particle collisions produce no particle flux and that the neoclassical fluxes are ambipolar for an ion-electron plasma.

In the presence of toroidal mass flow, simulation results are in agreement with the analytical neoclassical theory of Hinton and Wong. The poloidal electric field associated with toroidal mass flow is found to enhance density-gradient-driven electron-particle flux and the bootstrap current, while reducing temperature-gradient-driven flux and current. Finally, neoclassical theory in a steep gradient profile is examined by taking into account finite-banana-width effects. In general, the present work demonstrates a valuable new capability for studying important aspects of neoclassical transport inaccessible by conventional analytical calculation processes.

Electromagnetic Effects and Nonadiabatic Electrons

Development is underway to include electromagnetic effects in a 3-D flux tube code. A zero-electron-inertia fluid model has been derived from moments of the drift kinetic equation by taking $m_e \rightarrow 0$ but with $T_{\|e}$ finite, avoiding all accuracy or stability constraints on $k_\| v_{te} \Delta t$, as well as particle noise associated with electron free streaming. This approach is a natural extension of present 3-D toroidal gyrokinetic simulations to include effects of electron $\mathbf{E} \times \mathbf{B}$ flow, electron pressure gradient (e.g., ω_{*e}), and, most importantly, the electron parallel current, which in turn is used to include electromagnetic perturbations $\Delta B_\perp$ perpendicular to the equilibrium B-field.

This GK-ZEM-Hybrid model will first be used to study the β dependence of χ_i from ITG driven microturbulence modified by $\Delta B_\perp$. In the future, such a

model may be useful for studying both bulk and energetic ion-kinetic effects on MHD modes. All ion components would be fully kinetic and nonlinear. The $\Delta B_{\|}$ can be calculated by perpendicular pressure balance.

Gyrofluid Simulations

Significant advances have also been made in comprehensive gyrofluid simulations of tokamak plasma turbulence, leading to encouraging comparisons with experimental measurements. These simulations now include a number of effects important for realistic comparisons with experiments, including toroidal geometry and the associated toroidal curvature destabilization mechanisms,[26,27] turbulence-generated fine-scale poloidal flows,[26,28] kinetic effects such as Landau-damping and gyro-averaging,[28] impurities and beams,[28] all in a high-resolution field-line coordinate system.[29]

Researchers at the Institute for Fusion Studies (IFS) at the University of Texas,[30,31] in collaboration with PPPL, have developed a model for the ion thermal conductivity χ_i based on these nonlinear gyrofluid simulations[26] and a linear gyrokinetic code for a more accurate determination of critical temperature gradients and quasilinear estimates of χ_e/χ_i. Careful comparisons have been carried out with a wide range of TFTR experiments. This IFS-PPPL transport model contains several scaling trends that might be expected from various previous theories, but it is unique in being directly based on first-principles, detailed, toroidal simulations. The simulations indicate that the ITG mode is the dominant instability for most TFTR L-mode plasmas. However, even the ITG mode is found to be only marginally unstable in the inner half of many plasmas, leading naturally to a $\chi_i(r)$ that increases with minor radius over most of the plasma. The predicted $\chi_i(r)$ eventually gets too small very near the plasma edge, where some other transport mechanism presumably dominates, so the comparisons with experiments have focused on the core region ($r/a < 0.85$) using the temperature at $r/a = 0.85$ as a boundary condition. The present IFS-PPPL transport model focuses on regimes where the ITG instability is dominant, and uses a quasilinear estimate of χ_e. The nonlinear gyrofluid simulations have recently been extended to include a sophisticated model of trapped electrons,[26, 32] so we can now begin to study regimes dominated by the trapped-electron mode, and we can study particle transport in addition to heat transport.

This first-principles thermal transport model (with no experimentally adjustable parameters) has been compared with the core region ($r/a < 0.85$) of more than 50 TFTR L-mode discharges, typically predicting the ion and electron temperature profiles $T_i(r)$ and $T_e(r)$, respectively, within the experimental error bars throughout the confinement zone. An example of this is found in the power scan in (Fig. 6). The dramatic increase of the central ion temperature observed in supershots (from 5 keV to 30 keV) is also reproduced (Fig. 7), though in order to get the detailed temperature profile shapes correct it appears necessary to upgrade the transport model to include the collisionless trapped-electron mode. A number of effects are responsible for the improved supershot performance, but the key mechanism appears to be via high T_i/T_e (the ratio of ion to electron temperature), which raises the threshold for the ITG instability and lowers the conductive part of the ion heat flux so that the (experimentally measured) convection part dominates near the core. The low edge recycling of a supershot

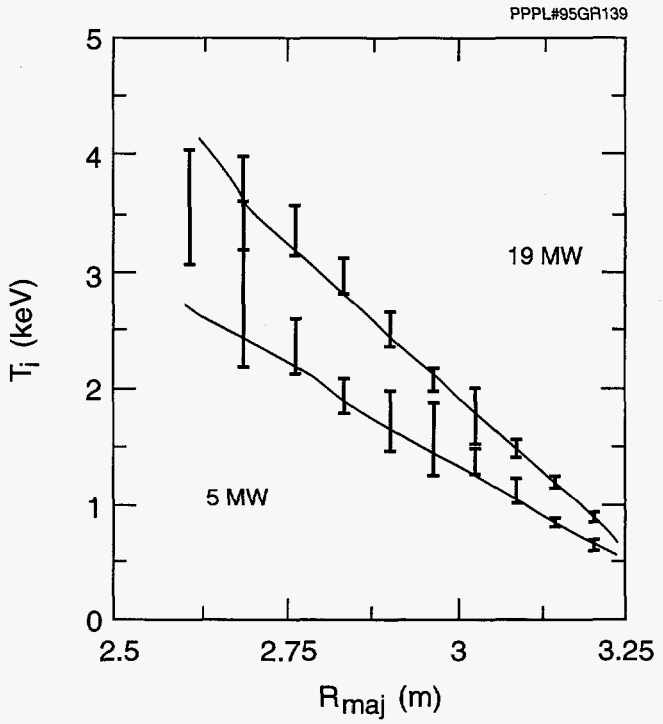

Figure 6. *The IFS-PPPL transport model compared with a TFTR power scan. The predicted $T_i(r)$ profiles (line) agree reasonably well with the measured profiles (error bars) as the power is varied a factor of 4. (From Ref. 30.) Here, and in Fig. 7, the model is used to predict the temperature in the main plasma region ($r/a < 0.85$) using $r/a = 0.85$ as a boundary condition.*

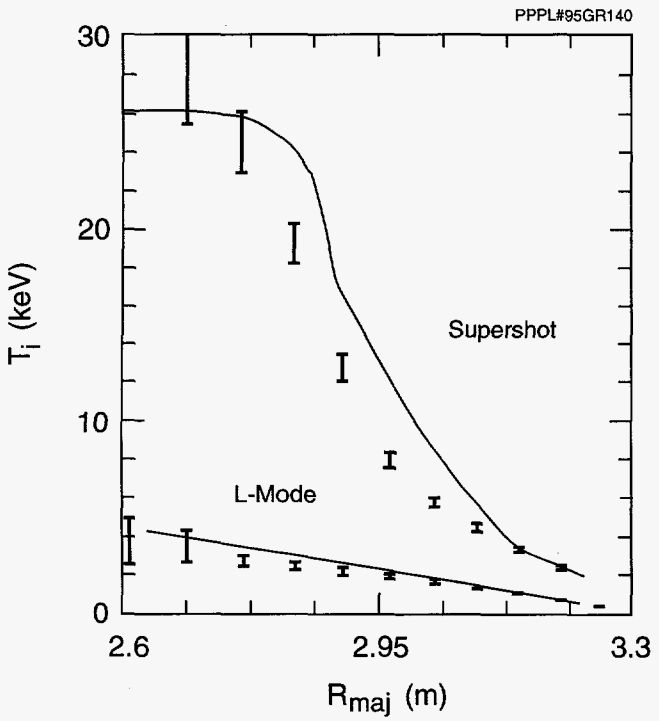

Figure 7. *The IFS-PPPL transport model (line) compared with a TFTR L-mode/supershot pair (error bars). The simulations capture much of the enormous variation in the ion temperature between supershots and L-modes. Nonlinear simulations that include trapped-electron dynamics will probably fit the data better. (From Ref. 30.)*

gives a high edge ion temperature, which eventually leads to enhanced confinement all the way in to the core.

This level of quantitative agreement with experiments is very encouraging, but there are a number of transport issues which remain under study, such as the edge region, favorable isotope scaling in supershots, Bohm scaling in L-mode, density transport, various perturbative and time-dependent phenomena, effects of elongation and triangularity, high beta, etc. Possible explanations for some of these effects are being pursued, one of them being the issue of Bohm versus gyro-Bohm scaling. The marginal stability effects in the IFS-PPPL transport model (and using the measurements at r/a = 0.85 as a boundary condition) can partially mask the raw gyro-Bohm scaling of the model so it is closer to the Bohm scaling results on TFTR than a purely gyro-Bohm scaling. Results from flux-tube versus full-torus simulations suggest the existence of a transition from Bohm to gyro-Bohm scaling,[32] but a detailed theory of this transition has not yet been worked out. The D-IIID has recently found experimental evidence of such transitions in various regimes.[33]

Analytic Theory of Turbulent Transport in Sheared Flows

The enhanced decorrelation of fluctuations by the combined effects of the $\mathbf{E} \times \mathbf{B}$ flow (V_E) shear, the parallel flow ($V_\parallel$) shear, and the magnetic shear has been studied in toroidal geometry. A two-point nonlinear analysis previously utilized in a cylindrical model[34] shows that the reduction of the radial correlation length below its ambient turbulence value Δr_0 is characterized by the ratio between the shearing rate ω_s and the ambient turbulence scattering rate $\Delta\omega_r$. The derived shearing rate is given by

$$\omega_s^2 = (\Delta r_0)^2\{(1/\Delta\phi^2)[(\partial/\partial r)(qV_E/r)]^2 + (1/\Delta\eta^2)[(\partial/\partial r)(V_\parallel/qR)]^2\},$$

where $\Delta\phi$ and $\Delta\eta$ are the correlation angles of the ambient turbulence along the toroidal and parallel directions. This result deviates significantly from the cylindrical result for high magnetic shear or for ballooning-like fluctuations. For suppression of flutelike fluctuations, only the radial shear of qV_E/r contributes, and the radial shear of $V_\parallel/qR$ is irrelevant regardless of the plasma rotation direction. Recent magnetic braking experiments on the Doublet III-D very-high confinement modes show a clear reduction in thermal diffusivity in the region where the shear of $Er/RB_\theta (\propto qV_E/r)$ is significant.

Analytic Nonlinear Theory of High-n TAE Modes

The nonlinear interactions of high-mode-number TAE modes, mediated via Compton scattering off the bulk ions, have been investigated. It has been shown that the nonlinear $\mathbf{J}_\perp \times \mathbf{B}_\perp$ ponderomotive force produced by the TAEs' interaction drives sound-wave-like density fluctuations with low phase velocity which can resonantly interact with the bulk ion parallel motion. Consequently, fluctuation energy of the TAEs is transferred to lower frequency and eventually absorbed by linearly stable TAEs near the lower shear-Alfvén continuum, leading to nonlinear saturation. An explicit expression for the saturated magnetic fluctuation amplitude has been derived.

Foundations: Analytic Theory of Turbulent Transport

One of the foremost issues in the theory of fusion plasmas is to understand and systematically calculate transport—e.g., of particles and heat—driven by turbulent fluctuations. Historically, a variety of theories have been advanced,[35] but these have mostly proven to be too asystematic and ad-hoc to provide more than dimensionally correct formulas in which numerical coefficients and dependence on dimensionless parameters such as the ratio of linear growth rate γ to real frequency ω remain undetermined. Recently, the importance of realizability (statistics compatible with a positive-definite probability density function) has been stressed,[36] and the Realizable Markovian Closure (RMC) has been developed[36,37] as an efficiently computable cousin of the direct-interaction approximation.[38] The RMC has been applied to the Hasegawa-Wakatani (H-W) model[39] of resistive drift-wave turbulence.

The H-W model consists of coupled nonlinear equations for fluctuations of potential ϕ and density n. It furnishes an important paradigm for plasma turbulence dominated by the $\mathbf{E} \times \mathbf{B}$ nonlinearity in the presence of background gradients, it is self-excited, and it determines a self-consistent, nonlinear phase shift to which the particle transport is proportional. It is controlled by the adiabaticity parameter α, inversely proportional to resistivity: $\alpha \to \infty$ defines the adiabatic limit, in which $n \to \phi$ and a forced/dissipative Hasegawa-Mima equation[40,41] is recovered; $\alpha \to 0$ defines the hydrodynamic limit, in which n is essentially passively advected by ϕ.

The predictions of the RMC for the particle transport coefficient[42] are shown in Fig. 8. The line of short dashes is the result of a direct pseudospectral simulation; the solid line is the result of the analytic theory. Clearly, excellent agreement is found, both qualitatively and, in particular, quantitatively. For comparison, the prediction of a quasilinear theory is also shown (line of longer dashes) that obviously grossly overestimates the transport in the hydrodynamic limit. Although not shown, similar excellent agreement is found for the salient features of the wave number spectrum, such as the overall level, shape, and position of the peak wave number.

The dramatic depression of the hydrodynamic flux from its quasilinear value has been previously observed in the literature and attributed[43] to the formation of intermittent "coherent structures" (CS). The present calculations show that this interpretation is in error: The RMC is a second-order closure that does not capture the detailed higher-order statistics of CS, yet predicts the transport very accurately. (The presence of CS is observed in higher-order statistics like the kurtosis.) Indeed, the existence of the depression can be explained qualitatively on the basis of the rigorous spectral balance equation, which dictates that the nonlinear damping η is balanced by the sum of the linear growth rate and (positive-definite) nonlinear noise. (Simple resonance-broadening theory[35] omits the latter contribution.) A random-walk argument combined with an estimate of the nonlinear correlation time $\propto \eta^{-1}$ then leads to the depression.[42]

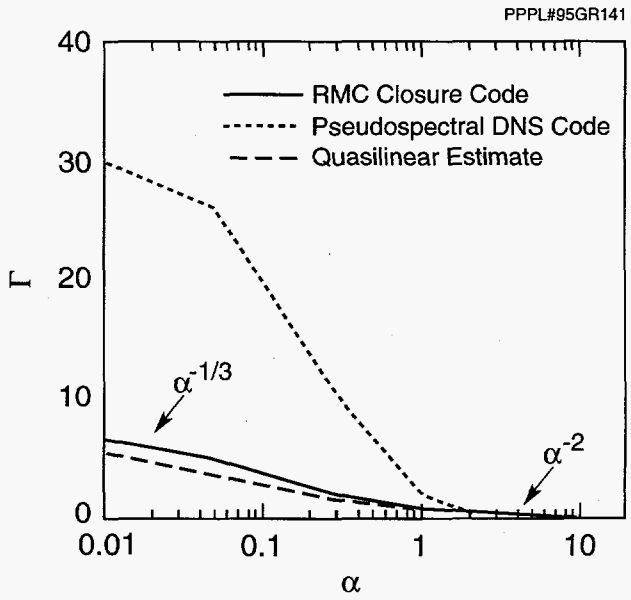

Figure 8. *Particle flux for Hasegawa-Wakatani model as a function of adiabaticity parameter. (a) Line of short dashes: direct numerical simulation. (b) Solid line: Realizable Markovian Closure. (c) Line of longer dashes: quasilinear theory.*

Energetic-Particle Phenomena

In a fusion reactor, unanticipated loss of energetic/alpha particles can result in heating efficiency degradation, serious wall damage, impurity influx, major operational control problems, and even a failure to sustain ignition. Neutral-beam injection and ion-cyclotron range of frequencies experiments in tokamaks have indicated that collective MHD modes, such as fishbones, and TAE modes can be strongly destabi-

lized by energetic ions and can cause significant fast-ion loss. On the other hand, proper excitation of plasma modes might perform beneficial functions, such as a direct coupling of alpha power to the fuel ions, and removal of helium ash. The following summarizes the research the Theory Division has pursued during FY94 on both aspects of energetic particle effects.

Tokamak Optimization by Channeling Alpha-Particle Power

An economically superior development path to a tokamak reactor may be possible, if alpha-particle power can be extracted by plasma waves, and if the wave power is then channeled to fast fuel ions. If 75% of the alpha-particle power is so channeled in a D-T reactor, then the fusion power density grows by about a factor of two at constant plasma beta.[44] In previous work, it has been shown that the channeling is best accomplished by waves with small poloidal phase velocity.[45] Such waves extract power from energetic alpha particles while diffusing them to the plasma periphery, incidentally exhausting the helium ash. These waves may also be phased toroidally, thus accomplishing simultaneously the current-drive function.

The lower-hybrid wave has the necessary wave features,[45] but the off-midplane, mode-converted ion-Bernstein wave (IBW) is easier to excite.[46] In a deuterium-rich D-T mixture, with proper toroidal phasing, this wave appears to be eminently suitable for channeling, because it damps on the tritium tail, while it attains poloidal phase velocities small enough to divert alpha power.[47]

The idea here is that the mode conversion surface is vertical, so the IBW emerges with a high horizontal wavenumber, which, if the mode conversion takes place sufficiently off the horizontal midplane is essentially with a high poloidal wavenumber, something required by the theory. The interaction of alpha particles with the IBW then occurs in a narrow vertical slab. On any magnetic surface, essentially all the alpha particles sample the wave region. Those alpha particles satisfying the resonance condition as they pass through the vertical slab are kicked to a larger minor radius if they lose energy to the wave and are kicked to a smaller minor radius if they gain energy from the wave. Particles are extracted as they near the periphery, so that a diffusion gradient is maintained along the path stretching from the center at high energy to the edge at low energy.

The reactor envisioned here will depart from present designs in several important ways, such as: it is dominated by the presence of radio-frequency power; fuel ions are necessarily drawn to the center while being heated; the electron heat confinement is purposely made poor; the ion temperature is much greater than the electron temperature; and the alpha energy is unavailable to drive "unwanted" instabilities. Because of the large benefit in channeling, other tokamak plasma parameters, such as elongation or triangularity, might also be designed with a view to optimizing the wave physics.

Frequency Sweeping for Energy-Selective Transport

The new technique of "frequency-sweeping"[48] or "chirping"[49] permits one to induce nondiffusive, energy-selective transport in energetic ions, which can be applied to perform a number of important functions in a fusion device. The technique has been shown[48] to have the necessary energy-selective properties to provide an energetically inexpensive means of ash removal. More preliminary work also shows it to be promising as a means of profile control, providing a bootstrap seed-current, as well as tailoring the energetic transport characteristics induced by alpha-channeling schemes.

Self-Consistent Energetic-Particle Interactions with Kinetically Modified MHD

The guiding-center code ORBIT has been extended[50,51] to allow detailed quasilinear analysis of fishbone excitation and sawtooth stability, and the effect of these modes on the high-energy particle distributions. A similar modification has been performed to study the saturation of the toroidal Alfvén eigenmode (TAE) due to the resonant trapping of particles. These codes provide important tools for the study of alpha-particle effects in ignition experiments.

Energetic-Particle Effects on TAE Modes

The TAE mode[52] has received increasing attention recently. It has been shown theoretically and ex-

perimentally that the mode can be destabilized by energetic/alpha particles in tokamak plasmas. The TAE mode is important because it may degrade the confinement of fusion alpha-particles in an ignited tokamak plasma.

In the past year, the NOVA-K code[53] has been used to study TAE stability in TFTR D-T experiments and in ITER.[54] The NOVA-K code is a global kinetic/MHD stability code. The code evaluates TAE stability for general tokamak plasma equilibria. It includes energetic-particle drive with finite-orbit-width effects, Landau damping of thermal species, Landau damping of beam ions, and collisional damping of trapped electrons. For instability, the energetic-particle drive must overcome the sum of all damping.

In typical TFTR D-T experiments, there is no alpha-driven TAE instability. The NOVA-K code also predicts the TAE to be stable. However, in D-T shot #76770, the magnetic fluctuation near the TAE frequency is enhanced over that in the equivalent D-D shot. On the other hand, the NOVA-K calculation shows that a core-localized TAE exists due to slightly broader pressure profile and this mode is unstable. The core-localized TAE can exist due to the effects of finite aspect ratio.[55] In summary, the NOVA-K results of TAE stability are consistent with the TFTR D-T experiments.

The stability of TAE modes in ITER has also been studied based on the ITER Engineering Design Activity design parameters. For PRETOR plasma profiles (very flat pressure and q profiles for $r/a < 0.7$), the NOVA-K calculation finds that TAE modes are stable (up to $n = 7$). However, the PRETOR profiles are probably unrealistic and more realistic plasma profiles have been employed for the NOVA-K TAE stability calculation. In these cases, it is found that the core-localized TAE modes exist and become unstable for $n > 12$.

Energetic-Particle Effects on Sawteeth and Fishbones

An important parameter in determining the energetic/alpha-particle effects on sawteeth stabilization and excitation of fishbone modes is the trapped-particle precessional drift frequency. The precessional drift frequency is a function of plasma geometry, plasma beta, particle energy, and pitch angle. In particular, it has been found that the magnetic drift reversal can significantly modify the stability thresholds for sawteeth stabilization and excitation of fishbone modes.[56] Finite inverse aspect ratio, plasma beta, and plasma shaping effects can significantly enhance the trapped-particle drift reversal domain in pitch-angle space and reduce the bounced-averaged precessional drift frequency.

The reduction of the precessional drift and drift-reversal effects on sawtooth stabilization is small. However, the critical alpha-particle beta for exciting fishbone modes can be much lower than an earlier result.[57] Moreover, the fishbone mode can be destabilized for total plasma beta below the ideal-MHD n=1 kink threshold. The thermal ion diamagnetic drift (ion FLR effect) effect has also been studied and found to have a strong destabilizing effect on the fishbone mode when the ion diamagnetic drift frequency is comparable with the trapped alpha precessional drift frequency, but has a stabilizing effect on the ideal-MHD kink mode.

Alfvén Cyclotron Instability for Understanding Ion Cyclotron Emissions

Experiments in the PDX (Poloidal Divertor Experiment, predecessor to PBX-M), the TFR (French tokamak), the JET (Joint European Torus, in England), and the TFTR have revealed intense (up to 10,000 times the background signal) high-frequency ion cyclotron emission (ICE) with frequency spectrum peaks at multiple deuterium cyclotron frequency evaluated near the outer plasma edge at midplane. To understand the ICE, a theory of Alfvén cyclotron instability (ACI) has been developed which explains all major features of the observed ICE.[58]

Non-Fusion Studies

Space Physics

Ionosphere and Neutral Gas Simulations

A particle simulation model has been developed[59] to study a neutral gas/ionosphere interaction experiment conducted on board the space shuttle. The model includes self-consistent plasma dynamics and plasma-neutral gas interaction to model the xenon gas release into the ionosphere. It has been shown that an anomalously rapid neutral ionization caused by the plasma instabilities can explain the space observations con-

firming Alfvén's original idea of Critical Ionization Velocity.

Two- and Three-Dimensional Magnetospheric Equilibria

Self-consistent two-dimensional (2-D) and three-dimensional (3-D) magnetospheric equilibria with anisotropic pressure and rotation have been studied numerically by solving the inverse equilibrium equations in an optimal flux coordinate system.[60,61] The effect of rotation is to expand the plasma outward by the centrifugal force. At high rotation rate a magnetodisc structure can be formed with thin current sheet and cusp-like magnetic-field configuration near the equatorial plane.

Kinetic-MHD Theory of Ballooning-Mirror Instability

A kinetic-MHD eigenmode stability analysis of low-frequency ballooning-mirror instabilities has been performed to understand the excitation mechanism of Pc 4-5 waves observed in the magnetospheric anisotropic pressure plasmas.[62]

For wave frequency smaller than the energetic trapped-particle magnetic drift frequency, which is much smaller than the bounce frequency, the energetic trapped particles experience a bounce-averaged wave structure. For modes with north-south symmetric structure of the compressional magnetic field, the energetic trapped particles experience a finite bounce-averaged wave structure and their kinetic pressure response cancels with their fluid pressure response so that the symmetric mode is stable.

For antisymmetric modes the energetic trapped-particle pressure response vanishes in a bounce period, and the instability threshold of the antisymmetric mode is determined by the energetic-particle fluid-free energy. Pressure anisotropy with larger perpendicular pressure reduces the beta threshold. The antisymmetric mode changes from a ballooning mode with dominant transverse magnetic-field components at isotropic pressure to a hybrid ballooning-mirror-type mode with comparable transverse and compressional magnetic-field components near the equator as pressure anisotropy increases. The antisymmetric field-aligned wave structure resembles the multi-satellite observation of compressional Pc 5 wave structure.[63]

Plasma Properties during Compressional and Transverse Pc 4-5 Wave Events in the Ring Current Region

From the AMPTE/CCE particle and magnetic-field data observed during Pc 4-5 wave events, the ballooning-mirror instability parameters have been computed and a correlation study with the theoretical instability threshold performed.[64]

The Pc 4-5 wave events observed near the dipole equator by AMPTE/CCE are selected to analyze CHEM particle data. The pitch-angle and energy-distribution of H^+ is relatively well determined and is used to compute the plasma beta and ballooning-mirror stability parameters: the pressure anisotropy and the pressure-gradient magnetic-field curvature parameters.

The contribution of O^+ to plasma beta can be as large as 30% during storm time. But, due to low counting statistics, the O^+ pitch-angle distribution is not well determined and is not used. The transverse waves are radially polarized Pc 4 waves observed on the dayside. When the transverse waves are observed (typically around $4 < L < 6$), the proton beta is enhanced, but remains relatively smaller than unity. Ballooning-mirror instability parameters are well below the theoretical instability threshold, and they are probably related to other resonant-type ballooning instabilities. The compressional waves have longer period than the transverse waves. When the compressional waves are observed (typically around $6 < L < 10$), the proton beta is greatly enhanced and becomes larger than one with large pressure anisotropy. The ballooning-mirror stability parameters are either near or above the theoretical stability threshold for antisymmetric ballooning-mirror modes, and they can be identified as ballooning-mirror modes. For the transverse wave events, the contribution of O^+ to plasma beta can be important and needs to be included to understand the excitation mechanism of transverse waves.

Wave Propagation in Dielectrics

A new computational model has been developed[65,66] in order to study linear and nonlinear wave propagation in a dielectric materials such as optical fibers using a particle simulation model. The model may be applied to test new ideas on nonlinear optical fiber devices such as switches.

Collaborations

The Theory Division is involved in a wide variety of projects with non-PPPL scientists from the U.S. and abroad. A sampling of the collaborative efforts during FY94 includes:

- Transference of the NOVA-K code to the Doublet III-D (DIII-D) at General Atomics to analyze energetic particle behavior in the DIII-D plasmas.
- Using the PEST code, MHD analysis of edge localized modes in JT-60U plasmas, in collaboration with Drs. Azumi, Kamada, Ozeki, and Tokuda, and development of an interface between their equilibrium code and PEST, which will be useful for future collaborations with PEST and other Princeton codes.
- Use by General Atomics of the Laboratory's FULL comprehensive stability code, interfaced with DIII-D equilibria, especially for the analysis of H-mode and VH-mode plasma discharges.
- Development with K.H. Burrell of a theoretical model for L-mode to H-mode and H-mode to VH-mode transitions on DIII-D at General Atomics.
- Collaboration with X. Garbet, V. Basiuk, and M. Zabiego at Cadarache, France, completing a joint International Atomic Energy Agency paper on sawtooth stabilization, and transference of the ORBIT guiding center code to the Tore Supra group there to study ICRF-induced stabilization, as well as ripple-induced beam ion loss.
- Further development of the PIES code and applications, in collaboration with Peter Merkel (Garching) and Angel Salas (CIEMAT, Madrid, Spain).
- A Stellarator Power Plant study in collaboration with the ARIES team.
- Collaborative research with the Fermi National Accelerator Laboratory on the numerical simulation of space charge effects in high-energy synchrotron accelerators has recently been initiated. The initial focus has been on the negative-mass instability at transition crossing. The work is presently funded internally and is a part of the lab-wide non-fusion research initiative.
- Cooperative Research and Development Agreement (CRADA) funding has been obtained to initiate numerical modeling of the electron beam injected in air in collaboration with Charged Injection Corporation (CIC). The goal of the modeling is to understand the charging of paint particulates and their properties to be applied to the SPRAYTRON device invented by CIC.

Graduate Education

The Theory Division staff plays a key role in the training of graduate students through teaching courses and supervising Ph.D. theses and the second-year theory projects. During FY94, six of the eleven graduate plasma physics courses offered by the Department of Astrophysical Sciences were taught by members of the Theory Division, three theoretical theses were completed, and eight second-year projects were pursued on a range of topics, including high-beta equilibria, gyrokinetic simulations, alpha-channeling, and the question of Onsager symmetries in turbulent transport.

References

[1] N. Pomphrey, S.C. Jardin, J. Bialek, *et al.*, "MHD Regimes and Feedback Stabilization in Advanced Tokamaks," in *Plasma Physics and Controlled Nuclear Fusion Research 1994* (Proc. 15th Int. Conf., Seville, Spain, 1994), Paper IAEA-CN-60/D-1-I-4, to be published by the International Atomic Energy Agency in 1995.

[2] A. Bondeson and D.J. Ward, "Stabilization of External Modes in Tokamaks by Resistive Walls and Plasma Rotation," Phys. Rev. Lett. **72** (1994) 2709.

[3] J. Myra, "Two- and Three-Dimensional Tokamak Equilibrium Modifications Driven by the Localized Ponderomotive Force of Applied Radio Frequency Waves," Phys. Fluids **31** (1988) 1190.

[4] W. Park, S. Parker, H. Biglari, *et al.*, "Three-Dimensional Hybrid Gyrokinetic-Magnetohydrodynamics Simulation," Phys. Fluids B **4** (1992) 2033-2037.

[5] G.Y. Fu and W. Park, "Nonlinear Hybrid Simulation of Toroidicity-Induced Alfvén Eigenmode," Princeton University Plasma Physics Laboratory Report PPPL-3017 (1994) 14 pp.

[6] F.M. Levinton, L. Zakharov, S.H. Batha, *et al.*, "Stabilization and Onset of Sawteeth in TFTR," Phys. Rev. Lett. **72** (1994) 2895.

[7] M.S. Chance, S.C. Jardin, J. Bialek, *et al.*, "Coupling the PEST and SPARK Codes for δW Stability Analyses with Three Dimensional Wall Configurations," Proc. 15th Int. Conf. on the Numerical Simulation of Plasmas (Valley Forge, Pennsylvania, USA, 1994), Paper 3A2.

[8] A.H. Reiman and H.S. Greenside, "Computation of Zero β Three-Dimensional Equilibria with Magnetic Islands," J. Comput. Phys. **87** (1990) 349-365.

[9] P. Merkel, "Solution of Stellarator Boundary Value Problems with External Currents," Nucl. Fusion **27** (1987) 867-871.

[10] P. Merkel, J.L. Johnson, D.A. Monticello, *et al.*, in *Plasma Physics and Controlled Nuclear Fusion Research 1994* (Proc. 15th Int. Conf., Seville, Spain, 1994), Paper IAEA-CN-60/D-P-II-10, to be published by the International Atomic Energy Agency in 1995.

[11] A. Reiman, "Singular Surfaces in the Open Field Line Region of a Nonaxisymmetric Poloidal Divertor [Abstract]," Bull. Am. Phys. Soc. **39** (1994) 1714.

[12] L.E. Zakharov and A.H. Glasser, "Sweeping Technique to Solve Elliptic Equations as a Cauchy Problem," Proc. 15th Int. Conf. on the Numerical Simulation of Plasmas (Valley Forge, Pennsylvania, USA, 1994), Paper 1A2.

[13] M.S. Chance, J.L. Johnson, and R.M. Kulsrud, "The Validity of the Extended Energy Principle," Plasma Phys. and Cont. Fusion **36** (1994) 1233-1239.

[14] B. Lehnert, "Comments on the Extended Energy Principle," Plasma Phys. and Cont. Fusion **35** (1993) 873-884.

[15] I.B. Bernstein, E.A. Frieman, M.D. Kruskal, and R.M. Kulsrud, "An Energy Principle for Hydromagnetic Stability Problems," Proc. Roy. Soc. (London) **A244** (1958) 17.

[16] G. Rewoldt, W.M. Tang, and R.J. Hastie, "Collisional Effects on Kinetic Electromagnetic Modes and Associated Quasilinear Transport," Phys. Fluids **30** (1987) 807.

[17] G. Rewoldt, W.M. Tang, and M.S. Chance, "Electromagnetic Kinetic Toroidal Eigenmodes for General Magnetohydrodynamic Equilibria," Phys. Fluids **25** (1982) 480-490.

[18] C. Kessel, J. Manickam, G. Rewoldt, and W.M. Tang, "Improved Plasma Performance in Tokamaks with Negative Magnetic Shear," Phys. Rev. Lett. **72** (1994) 1212.

[19] S. Kaye, private communication (1994).

[20] M. Artun and W.M. Tang, "Nonlinear Electromagnetic Gyrokinetic Equations for Rotating Axisymmetric Plasmas," Phys. of Plasmas **1** (1994) 2682.

[21] S.E. Parker, W.W. Lee, and R.A. Santoro, "Gyrokinetic Simulation of Ion Temperature Gradient Driven Turbulence in 3D Toroidal Geometry," Phys. Rev. Lett. **71** (1993) 2042.

[22] J.C. Cummings, W.W. Lee, and S.E. Parker, "Generation and Damping of Sheared Perpendicular Flows in Electrostatic Toroidal Gyrokinetic Simulations of η_i Mode Turbulence [Abstract]," Bull. Am. Phys. Soc. **39** (1994) 1665.

[23] H.E. Mynick and S.E. Parker, "Transport in Gyrokinetic Tokamaks," Phys. Plasmas **2** (1995) 1217.

[24] H.E. Mynick and S.E. Parker, "Analysis of Transport in Gyrokinetic Tokamaks," Phys. Plasmas **2** (1995) 2231.

[25] Z. Lin, W.W. Lee, and W.M. Tang, "Simulation of Sheared Flow Effects on Neoclassical Transport in Toroidal Plasmas [Abstract]," Bull. Am. Phys. Soc. **39** (1994) 1616.

[26] M.A. Beer, "Gyrofluid Models of Turbulent Transport in Tokamaks," Ph.D. Dissertation, Princeton University, 1994.

[27] R.E. Waltz, R.R. Dominguez, and G.W. Hammett, "Gyro-Landau Fluid Models for Toroidal Geometry," Phys. Fluids B **4** (1992) 3138.

[28] W. Dorland, "Gyrofluid Models of Plasma Turbulence," Ph.D. Dissertation, Princeton University, 1993.

[29] M.A. Beer, S.C. Cowley, and G.W. Hammett, "Field-Aligned Coordinates for Nonlinear Simulations of Tokamak Turbulence," Princeton University Plasma Physics Laboratory Report PPPL-3040 (1994) 45 pp.

[30] W. Dorland, M. Kotschenreuther, M.A. Beer, *et al.*, "Comparisons of Nonlinear Toroidal Turbulence Simulations with Experiment," in *Plasma Physics and Controlled Nuclear Fusion Research 1994* (Proc. 15th Int. Conf., Seville, Spain, 1994), Paper IAEA-CN-60/D-P-I-6, to be published by the International Atomic Energy Agency in 1995.

[31] M. Kotschenreuther, W. Dorland, M.A. Beer, and G.W. Hammett, "Quantitative Predictions of Tokamak Energy Confinement from First-Principles Simulations with Kinetic Effects," Phys. Plasmas **2** (1995) 2381.

[32] G.W. Hammett, M.A. Beer, J.C. Cummings, *et al.*, "Advances in Simulating Tokamak Turbulent Transport," in *Plasma Physics and Controlled Nuclear Fusion Research 1994* (Proc. 15th Int. Conf., Seville, Spain, 1994), Paper IAEA-CN-60/D-2-II-1, to be published by the International Atomic Energy Agency in 1995.

[33] T.C. Luce, C.C. Petty, K.H. Burrell, *et al.*, "Experimental Constraints on Transport," in *Plasma Physics and Controlled Nuclear Fusion Research 1994* (Proc. 15th Int. Conf., Seville, Spain, 1994), Paper IAEA-CN-60/A-2-III-2, to be published by the International Atomic Energy Agency in 1995.

[34] T.S. Hahm, "Rotation Shear Induced Fluctution Decorrelation in a Toroidal Plasma," Phys. Plasmas **1** (1994) 2940.

[35] T. H. Dupree, "Nonlinear Theory of Drift-Wave Turbulence and Enhanced Diffusion," Phys. Fluids **10** (1967) 1049-1055.

[36] J. Bowman, "Realizable Markovian Statistical Closures: General Theory and Application to Drift-Wave Turbulence," Ph.D. Dissertation, Princeton University, 1992.

[37] J. Bowman, J.A. Krommes, and M. Ottaviani, "The Realizable Markovian Closure. I. General Theory, with Application to Three-Wave Dynamics," Phys. Fluids B **5** (1993) 3558-3589.

[38] J.A. Krommes, "Statistical Descriptions and Plasma Physics," in *Handbook of Plasma Physics*, edited by A.A. Galeev and R.N. Sudan (North-Holland, Amsterdam, 1984), Vol. **2**, Ch. 5.5, p. 183.

[39] A. Hasegawa and M. Wakatani, "Plasma Edge Turbulence," Phys. Rev. Lett. **50** (1983) 682-686.

[40] A. Hasegawa and K. Mima, "Pseudo-Three-Dimensional Turbulence in Magnetized Nonuniform Plasma," Phys. Fluids **21** (1978) 87-92.

[41] M. Ottaviani and J.A. Krommes, "Weak- and Strong-Turbulence Regimes of the Forced Hasegawa-Mima Equation," Phys. Rev. Lett. **69** (1992) 2923-2926.

[42] G. Hu, J.A. Krommes, and J.C. Bowman, "Resistive Drift-Wave Plasma Turbulence and the Realizable Markovian Closure," Phys. Lett. A **202** (1995) 117-125.

[43] A.E. Koniges, J.A. Crotinger, and P.H. Diamond, "Structure Formation and Transport in Dissipative Drift-Wave Turbulence," Phys. Fluids B **4** (1992) 2785-2793.

[44] N.J. Fisch and M.C. Herrmann, "Utility of Extracting Alpha Particle Energy by Waves," Nucl. Fusion **34** (1994) 1541-1556.

[45] N.J. Fisch and J.M. Rax, "Interaction of α-Particles with Intense Lower Hybrid Waves," Phys. Rev. Lett. **69** (1992) 612.

[46] N.J. Fisch, E.J. Valeo, C.F.F. Karney, and R. Majeski, "Possibility of using Ion Bernstein Waves for Alpha Power Extraction in Tokamaks," in *Controlled Fusion and Plasma Physics* (Proc. 21st EPS Conf., Montpellier, France, 1994), edited by E. Joffrin, P. Platz, and P.E. Stott, Contributed Papers Vol. **18B** (Part II), (European Physical Society, 1994) 640.

[47] E.J. Valeo and N.J. Fisch, "Excitation of Large-k_θ Ion Bernstein Waves in Tokamaks," Phys. Rev. Lett. **73** (1994) 3536-3539.

[48] H.E. Mynick and N. Pomphrey, "Frequency-Sweeping: A New Technique for Energy-Selective Transport," Nucl. Fusion **34** (1994) 1277.

[49] C.T. Hsu, C.Z. Cheng, P. Helander, *et al.*, "Particle Dynamics in Chirped-Frequency Fluctuations," Phys. Rev. Lett. **72** (1994) 2503-2507.

[50] R.B. White and Y. Wu, "Numerical Evaluation of High Energy Particle Effects in Magnetohydrodynamics," Princeton University Plasma Physics Laboratory Report PPPL-2973 (1994) 40 pp.

[51] Y. Wu and R.B. White, "Self-Consistent Study of the Alpha-Particle-Driven Toroidicity-Induced Alfvén Eigenmode," Phys. Plasmas **1** (1994) 2733.

[52] C.Z. Cheng and M.S. Chance, "Low-*n* Shear Alfvén Spectra in Axisymmetric Toroidal Plasmas," Phys. Fluids **29** (1986) 3695-3701.

[53] C.Z. Cheng, "Kinetic Extensions of Magnetohydrodynamics for Axisymmetric Toroidal Plasmas," Phys. Reports **211** (1992) 1-51.

[54] C.Z. Cheng, R. Budny, L. Chen, *et al.*, "Energetic/Alpha Particle Effects on (MHD) Modes and Transports," in *Plasma Physics and Controlled Nuclear Fusion Research 1994* (Proc. 15th Int. Conf., Seville, Spain, 1994), Paper IAEA-CN-60/3-3-III-2, to be published by the International Atomic Energy Agency in 1995.

[55] G.Y. Fu, "Existence of Core Localized Toroidicity-Induced Alfvén Eigenmode," Phys. Plasmas **2** (1995) 1029.

[56] Y.Wu, C.Z. Cheng, and R.B. White, "Alpha Particle Effects on the Internal Kink and Fishbone Modes," Phys. Plasmas **1** (1994) 3369-3377.

[57] B. Coppi, S. Migliuolo, F. Pegoraro, and F. Porcelli, "Global Modes and High-Energy Particles in Ignited Plasmas," Phys. Fluids B **5** (1990) 927-943.

[58] N.N. Gorelenkov and C.Z. Cheng, "Excitation of Alfvén Cyclotron Instability by Charged Fusion Products in Tokamaks," Princeton University Plasma Physics Laboratory Report PPPL-2998 (1994) 31 pp.

[59] H. Okuda, "Numerical Simulation of Neutral Gas Release Experiments in the Ionosphere," Phys. Fluids **1** (1994) 1669.

[60] C.Z. Cheng, "Magnetospheric Equilibrium with Anisotropic Pressure," J. Geophys. Res. **97** (1992) 1497-1510.

Divertor Modeling

The divertor is a critical component of a tokamak fusion reactor such as the International Thermonuclear Experimental Reactor (ITER). It is responsible for removing the alpha-particle energy, for pumping the helium ash, and for controlling impurities. The tokamak divertor is particularly challenging to understand because of the complex geometry and because of the interaction of the plasma with material surfaces and with neutral atoms and molecules. For this reason, computer codes are needed to model the physics of the divertor in existing experiments to provide the necessary input for the design of future experiments.

The work undertaken in 1994 utilizes a neutral transport code, DEGAS, a plasma transport code, PLANET, and a simplified one-dimensional plasma code. These have been applied to experiments on Alcator C-Mod, at the Massachusetts Institute of Technology (described also in the section on Collaborations), on the Tokamak Fusion Test Reactor (TFTR), and for studies of ITER. In addition, work is under way on a new neutral transport code, DEGAS-2, which will provide substantial improvements over DEGAS in terms of execution speed and the ease with which new physics can be included.

DEGAS Applications

The most important components of the DEGAS atomic physics package are the reaction rates used to describe the interaction of neutral and ionized hydrogen with plasma electrons. Under conditions typical of most fusion devices, one needs to consider both the radiative and collisional processes undergone by neutral hydrogen atoms (excited as well as ground state). The "collisional radiative" model used heretofore in DEGAS to describe the electron-hydrogen interactions is in the process of being revised. Following some changes in the physics basis for the model, replacement of the atomic physics cross sections with ones from a new database published by the International Atomic Energy Agency has begun.

Comparisons of the spectrum of hydrogen Balmer-alpha emissions as calculated by DEGAS with those seen in TFTR are continuing. The width of these spectral lines provides information about the velocity distribution of neutral hydrogen. Hence, it should be possible to benchmark the atomic and surface physics which give rise to that distribution in DEGAS against the experiment. Initial simulations matched the experimental spectra very well. However, it is felt that part of this agreement is the result of some dissociation products of hydrogen molecular ions having unexpectedly large energies (more than 30 eV).

For this case, the experimental plasma data have been obtained from the time-independent SNAP analysis code. Because of the greater reliability of the results from the time-dependent TRANSP code, the input for DEGAS is now based on its output. However, it has been noted that the plasma temperatures directly in front of the limiter provided by TRANSP are consistently higher than those gotten from SNAP; the errors on these measurements are too large to warrant dismissal of either set of values. The DEGAS-simulated spectra obtained with these higher temperatures are much narrower in wavelength space than they had been previously. Consequently, the agreement with the experimental spectra is now much poorer.

The search for other explanations led to the examination of work by David Ruzic (University of Illinois) who has suggested that the sputtering of hydrogen isotopes from the limiter surface could be a significant source of neutral atoms in DEGAS. Ruzic's group employed the VFTRIM code to generate several sets of sputtering data specific for TFTR conditions. The energy distribution of the sputtered atoms is roughly what is needed to fill in the gap between the simulated and measured spectra. However, it has not yet been demonstrated that this sputtering pro-

cess is responsible for the discrepancy between the simulated and measured spectra.

PLANET Simulations

The PLANET fluid plasma code has been used to model both high-recycling and detached-divertor operation in Alcator C-Mod. This code assumes a Braginskii description of the hydrogen plasma and a diffusive model for the neutral gas. A constant concentration, coronal equilibrium carbon impurity is included; charge-exchange impurity recombination is accounted for in this model.

Two modes of high-density divertor operation have been simulated: high recycling and detached. The former occurs at low powers and low neutral gas injection rates; it is characterized by relatively high (10 eV) plate electron temperatures and particle fluxes. The detached plasmas have lower plate electron temperatures (less than 5 eV) and a substantial amount of impurity radiation.

Good agreement is found between the PLANET simulations and the measured upstream profiles. However, the resulting profiles at the plate are too broad. In particular, the densities in the private flux region are too high. This strongly suggests that the radial transport is, in reality, much less below the X-point than above it. Good agreement with measurements at the plate, near the separatrix, can be achieved if the transport coefficients are reduced by an order of magnitude from the ones required upstream.

Qualitatively, the simulations show the same general characteristics as the experiments. In the high-recycling mode, the electron temperature is lowest and density highest over the portion of the plate where the power is the highest; that is, this is where the particle flux from the main plasma and, therefore, the flux amplification also peak. In this way, the preconditions for radiation and, subsequently, detachment are established.

In general, due to the geometry of the plate, the simulations are very sensitive to a number of parameters. For example, the results depend on the ion temperature (not measured) through the equations used to model the neutral transport in the simulation. Taking into account reactions involving molecular hydrogen could also affect the profiles, since there are definite indications that the simulated neutral transport in the vicinity of the plate is larger than it should be.

Carbon radiation, which peaks at about 10 eV, reduces the heat flux and the temperature near the plate sufficiently to greatly reduce hydrogen ionization and, consequently, particle flux amplification. This, together with the lowering of the plasma density, are the defining characteristics of plasma detachment. Within the radiation region, which can be anywhere between the plate and the X-point, the plasma density remains high. However, this region is always close to the separatrix because only here is the density high enough. The combination of high upstream and low plate densities and temperatures (between 1 and 2 eV) are possible because of the radial loss of momentum, which results in a plasma pressure drop.

Due to the simplicity of the impurity model (density proportional to the electron density), only qualitative agreement can be expected. However, the onset temperature at the plate (electron temperature between 5 and 10 eV), the radial extent of detachment, and the location of the radiation front are correctly predicted.

One-Dimensional Gas Target Divertor Modeling

In order to handle the high plasma energy flux flowing in the scrape-off layer, ITER designers envision effectively replacing the physical divertor plate "target" with a "gas target," a region of high neutral gas density which intercepts the plasma power flux and dissipates the energy through various atomic processes. Also of interest is the process of divertor plasma detachment which has been observed in several tokamaks (notably the Joint European Torus, the Doublet-III-D, and Alcator C-Mod), and may be a mechanism by which the immense heat flux expected in ITER could be dissipated in steady-state.

One gas target divertor concept, proposed by Watkins and Rebut, is based on transferring essentially all of the plasma power directly to neutral particles via charge-exchange. A "flame front" is envisioned in which the plasma heat flux is "extinguished" as the plasma energy and momentum are transferred primarily to charge-exchange neutrals. A one-dimensional time-dependent computational model has been constructed, based on a coordinate transformation to incorporate two-dimensional effects following the Watkins and Rebut formulation. This model includes the transport of ions and four neutral species, momen-

tum, and ion and electron energy both along and across the magnetic-field lines. A full radiative-collisional model is used for the ionization, recombination, and radiation of hydrogen neutrals. The four species of neutral particles are "cold" atoms and molecules formed by recycling processes at the wall and "hot" atoms and molecules formed via collisions with plasma ions.

The one-dimensional model described above has been applied to DIII-D (Doublet-III-D) and Alcator C-Mod divertor conditions. In applying the model to the Alcator C-Mod divertor plasma, certain parameters were fixed (e.g., input power, geometry, carbon impurity concentration) while the plasma density at the machine midplane was varied. One consequence of detachment in this model is the formation of a high-density, highly radiating region, and the movement of this region away from the divertor plate to a position closer to the core plasma. Simultaneously, the electron temperature undergoes a sharp drop through the radiative region, and after full detachment, the model predicts that the electron temperature at the plate remains constant at 1 eV and comparable fractions of the input power escape the system in impurity radiation and neutral particles. One-dimensional modeling is able to reproduce the decrease in plasma heat flux, plasma pressure, and charged-particle flux to the plate observed in detached divertor experiments. However, in this one-dimensional model, the decrease in plasma pressure is compensated by an increase in the neutral pressure (many times greater than the neutral pressures measured in experiments), and the charged-particle flux is reduced due to volume recombination (while detached divertor electron temperature values are typically reported in the 2 to 5 eV range, for which recombination is not a dominant process). It is clear that two-dimensional processes (such as neutral transport and plasma fluid drifts) must be properly modeled in order to understand divertor plasma detachment as observed in existing experiments, and to predict with reasonable confidence the performance of the ITER divertor.

High-Field Magnet Project

The goal of the High-Field Magnet Project is the construction of a pulsed solenoid (see Fig. 1) that produces central magnetic fields of the order of 60 Tesla using the available power supplies at the Princeton Plasma Physics Laboratory's (PPPL) C-Site. For the period October 1, 1993 through February, 1994, the effort concentrated on two main objectives: completion of the magnetic design and an analysis of magnet safety.

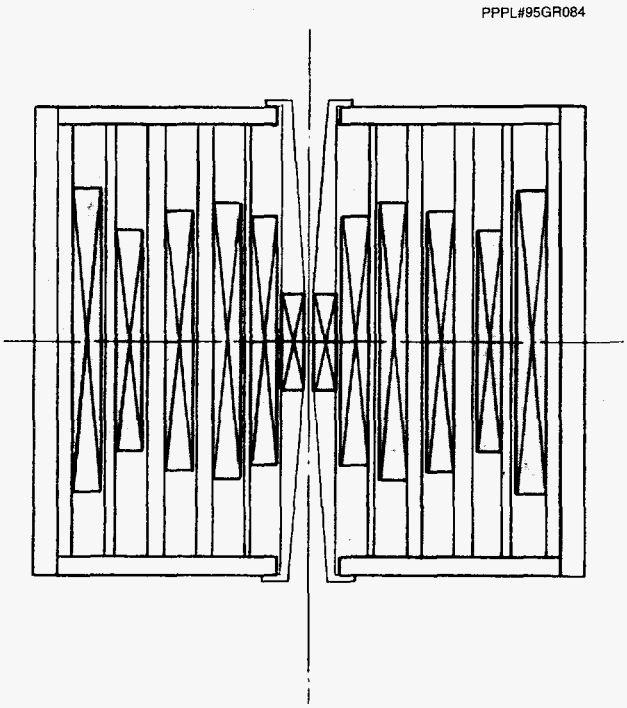

Figure 1. *Cross section of the six-coil magnet with internal support cylinders. The magnetic coils are represented by the shaded rectangles.*

Magnet Design

Magnet design work included selection of current densities and materials for the small coil at the magnet bore (Coil #1) and thermomechanical analysis of all the coils (Coils #1 through #6), with particular emphasis on the coil crossovers and terminal connections. These latter items are sometimes the limiting factors in coil performance.

The four nested cylindrical helical layers of Coil #1 produce nearly 20 Tesla in a 20-mm bore. The inner two layers use the high-conductivity BeNiCu (Beryllium-Nickel-Copper) conductor (Alloy 17510) and the outer two layers use the more conventional BeCu (Beryllium-Copper) conductor (Alloy 17200). The material selection permits maximization of current density, hence field production, within each layer without exceeding a limiting temperature or stress level. The power supply provides a coil current of 20 kA. The necessarily large cross section per turn for this small diameter coil precludes fabrication by winding; wire electric discharge machining of tubes to form coil turns is the chosen alternative manufacturing technique.

The larger diameter wound coils (Coils #2 through #6) use an 8 by 12 millimeter rectangular conductor and are six layers deep. Each coil is inserted into its' supporting structural tube and impregnated with an epoxy resin. This concentric nest has small annular gaps for liquid nitrogen coolant flow between coils. For Coils #2 through #5 the Lorentz forces are too high to be supported by any known, sufficiently conductive, material acting alone. Structural reinforcement is essential and the support cylinders make use of the stronger alloys available for cryogenic applications, i.e., the manganese-nitrogen stainless steels and the maraging steels. Each coil is sufficiently thin and has few enough insulation layers to allow a cool-down time between pulses of an hour or so.

Safety Analyses

Magnets of this class, which operate near the performance limits of the construction materials, must include analyses of possible electrical and structural failures. Two related major safety concerns have been addressed. First, whether any toxic aerosols are produced by an arc resulting from an internal coil short

and, second, the mechanical control or containment of an explosive failure.

A literature search found no test data on the first question. One analysis does indicate very low-vapor pressures over molten pools of BeCu. The second point has been analyzed using models to determine the energy deposition in the arc and the pressure produced if the magnet is contained by a vessel. Further work is needed to estimate the heating of the vaporized conductor and the degree of condensation within the containing vessel. An enclosure of heavy concrete is considered in addition to the thick-walled dewar.

Project Status

Approximately one year of a three-year budget has been expended to produce a design considerably different from that initially proposed. A new proposal has been submitted to the National Science Foundation for continuation of the project.

Engineering and Technology Development Department

The Engineering and Technology Development Department (ETDD), formerly the Engineering Department, is primarily responsible for managing the Princeton Plasma Physics Laboratory's (PPPL) engineering resources. The Department underwent a substantial reorganization during the past year resulting in a new name which underscores the additional responsibility to develop applicable technologies for fusion and/or spin-off to the commercial and industrial sector. The organization changed to a function-oriented (design, fabrication, operations, etc.) structure from a discipline-oriented (mechanical, electrical, etc.) structure. Divisions of the Department are: Design and Analysis, Computer Systems, Technical Systems, Facilities and Environmental Management, Fabrication and Assembly, and the Office of Technology Transfer. Although reporting separately to the PPPL Director, the Tokamak Fusion Test Reactor (TFTR) Shutdown and Removal Project also falls under the direction of the Engineering and Technology Development Department Head.

Major research activities supported by the ETDD during the past fiscal year include TFTR deuterium-tritium (D-T) operations and the Tokamak Physics Experiment (TPX) design activity. While some engineering staff are assigned to project organizations (primarily TFTR), the majority of staff are assigned to the Engineering and Technology Development Department Divisions where their work is managed. It is anticipated that most of the Laboratory's engineering activities will be performed by the ETDD following the end of TFTR experimental operations. More detailed progress is reported, by Division, below.

Design and Analysis

The Design and Analysis Division was formed during the July 1994 reorganization of the Engineering Department by expanding the analysis-oriented Engineering Analysis Division (EAD) to include enhanced electrical design, mechanical design, and systems engineering capabilities. The Division now has about 35 engineers grouped into the following branches: Plasma Engineering, Thermomechanical Engineering, Mechanical Design, Electrical Design, and Systems Engineering.

Since the reorganization of the Engineering Department took place near the end of the fiscal year, the Design and Analysis Division section of the Engineering and Technical Development Department report will cover only the branches that were formerly part of the Engineering Analysis Division: The Plasma Engineering and Thermomechanical Engineering Branches. Services provided by the former EAD included conceptual and preliminary engineering design, evaluation and planning of new and upgraded experiments, and systems engineering.

Plasma Engineering Branch

The Plasma Engineering Branch performs design analysis in systems engineering, electromagnetics, power supply and energy storage, and neutronics. Most of the effort in this fiscal year was focused on the Tokamak Physics Experiment, with the balance of time spent on the TFTR, the International Thermonuclear Experimental Reactor (ITER), and several smaller projects.

Tokamak Physics Experiment

Support for the TPX Project was provided in neutronics, power system design, electromagnetics, and plasma control. Survey calculations for in-vessel material radioactivity inventory and activation dose rates were completed. Preliminary three-dimensional shielding analyses of ion cyclotron heating and lower-hybrid designs were performed. The effect of a borated water shielding design on delayed gamma dose rates was examined. No significant perturbations of the dose rates were found. These calculations were verified by Oak Ridge National Laboratory and Los Alamos National Laboratory. Three-dimensional calculations of nuclear heating rates in the toroidal-field coils were performed to provide source terms for the thermo-mechanical analysis of the coils. Estimates were made of total nuclear heating rates in the poloidal-field coils and radiation damage levels of coil insulation.

Work in support of TPX power systems included poloidal-field (PF) power system revisions, plasma position control system development, and research and development of superconducting coil protection. An analysis of the power system requirements for the PF coils, based on PF current scenarios, was performed in support of the effort to optimize the use of TFTR facilities. A PF dump simulation included a quantitative analysis of PF current decay and a time integral of the square of the current for a desired protection scheme, in order to estimate better the hot spot temperatures of a superconducting coil during a quench and dump event. Thermal simulations of heat run tests on Transrex power supplies and associated equipment were performed for evaluation of proposed power supply control schemes. An analysis of results from the Princeton Beta Experiment-Modification (PBX-M) pulsing measurements was performed to predict voltage and load transients on the network grid during TPX experimental pulses. An initial study of an even current sharing strategy for TPX PF needs was performed.

Electromagnetics work centered on the analysis of the TPX vacuum vessel and passive stabilizers. Finite element models of the complete vacuum vessel, and inner and outer passive stabilizers, were generated. From these models, axisymmetric equivalent models of the vessel and stabilizers were created. A combined model of cryostat, vacuum vessel, and passive stabilizers was created.

An algorithm based on concepts of dynamic programming for determining PF coil locations was developed. A large number of PF coils are placed on a contour of allowed positions. The algorithm sequentially removes each coil, calculates the equilibrium at the critical points in the plasma discharge, and eliminates the coil that minimizes coil stored energy. The procedure is continued until the number of coils remaining is sufficiently low.

A plasma shape control method was developed. This approach attempts to keep the poloidal magnetic flux at specified points in space equal to the plasma x-point flux. A small number of critical points are controlled using all of the PF coils, resulting in a multiple input and output control problem. The algorithm has been successfully tested in the TSC code.

Tokamak Fusion Test Reactor

As part of the effort to upgrade TFTR for six tesla operation, various power system studies were performed. An analysis of the TFTR power system at elevated current was conducted, addressing the adequacy of all components of the power chain at elevated currents and at elevated voltages. In support of this analysis, an electrical model of the motor generators was developed and calibrated against measurements. A model of the total power chain was developed to evaluate the impact of circuit changes. General Electric of Canada was consulted for an evaluation of the impact of these changes on the life expectancy of components such as the motor generators.

International Thermonuclear Experimental Reactor

A simulation of the ITER long-pulse plasma discharge is being performed to determine PF coil current and voltage requirements, control requirements, plasma evolution and flux consumption, and stable plasma operating scenarios. This work is scheduled for completion in March 1995.

Reactor Studies

The PULSAR long-pulse inductive reactor study was completed. A follow-on to the ARIES (Advanced Reactor Innovation Evaluation Study) reactor studies, this work was performed in conjunction with Dr. Robert Conn of the University of California at San Diego. The MHD (magnetohydrodynamic) equilibrium and stability analysis showed that the constraint of steady-state Ohm's Law, with neoclassical corrections, on the plasma profile severely limited the class of

stable plasma configurations to beta values of 3.0 or less. These equilibria were found to be prescribed by the density, temperature, and total plasma current.

Other Work

In collaboration with AT&T Bell Labs, PPPL has been involved in the development of submicron lithography using the photocathode electron projection technique. Focusing and image distortion problems associated with the generation, transport, and registration of photoelectrons were studied. Necessary conditions and parameters for achieving a 3:1 image reduction for features in the 100 nm range have been identified.

Thermomechanical Engineering Branch

The Thermomechanical Engineering Branch performs mechanical and thermal design and analysis in support of projects at PPPL and at other laboratories. Stress analysis, fracture mechanics, fluid flow, heat transfer and temperature calculations, and design criteria development are the primary functions of the Branch. This year, work performed by the Branch was divided between TPX, TFTR, and several smaller projects.

Tokamak Physics Experiment

An in-depth study of the U.S. Department of Energy (DOE) seismic requirements at the Laboratory site was completed. The resulting report will be used to justify the seismic design criteria and peak seismic accelerations to be used for TPX structures, systems, and components. An analysis of the superconducting strand to be used in the TPX toroidal-field coils was initiated. The intrinsic strain caused by reacting the strand and then cooling it to 4 degrees Kelvin was examined.

The System Description Documents and System Requirements Documents for the vacuum vessel and the plasma facing components were reviewed prior to award of those contracts. After contract awards, the Branch provided oversight of the Ebasco Division of Raytheon Engineers and Constructors, Inc. vacuum vessel contract.

Tokamak Fusion Test Reactor

A detailed analysis was performed in support of the proposed six tesla upgrade. This included the development of a new lookup table for the coil protection calculator and detailed structural analyses of the toroidal-field coil and case, lead stems, and water fittings.

The Test Cell structure was analyzed to see if it would be adequate for the increased crane capacity needed by the TFTR Shutdown and Removal (S&R) Project. Also in support of the TFTR Shutdown and Removal Project, planning work for vacuum system removal was performed.

Princeton Spherical Tokamak Experiment

The structural analysis and design for the Princeton Spherical Tokamak Experiment (PSTX) was completed. Using MSC/NASTRAN finite element models (Fig. 1), the responses to dead loads, vacuum loads, eddy current forces due to normal operation and plasma disruptions, and seismic loads were evaluated. A comprehensive model representing one quarter of the machine was used for the symmetric loads. A 360-degree model was used for seismic loads.

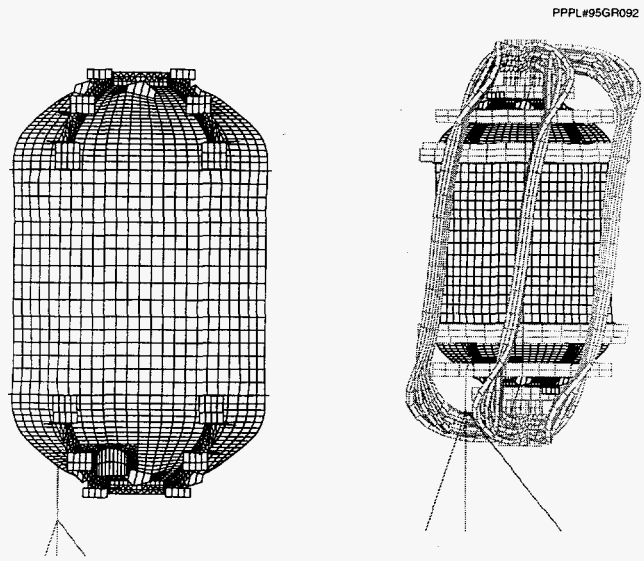

Figure 1. *Finite element model of the Princeton Spherical Tokamak Experiment (PSTX).*

Magnetic Reconnection Experiment

The flux core design for the Magnetic Reconnection Experiment (MRX) was completed and fabrication was begun. This assembly contains 36 conductors of the toroidal-field windings and four conductors for the poloidal-field coil system. A stress analysis of the MRX vacuum vessel was completed (Fig. 2) and used to verify that the design was adequate.

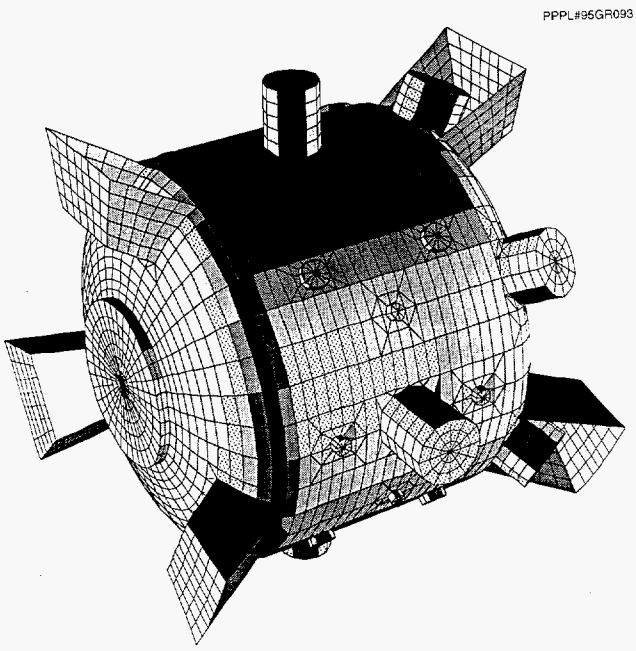

Figure 2. Finite element model of the Magnetic Reconnection Experiment (MRX) vacuum vessel.

Computer Systems

The Computer Systems Division (CSD) is responsible for all scientific and engineering computing at PPPL. The Division accomplishes this mission through the planning, procurement, design, implementation, and operation of computing and networking hardware and software systems associated with general purpose and special purpose computing in both central and distributed computing environments.

In FY94, support focused on providing a high degree of operational reliability for the PPPL experimental projects. In addition, the general user community was provided with both the tools and the expertise necessary to migrate to and develop applications for newer technologies. Support was provided to an evolving UNIX workstation environment. A Video Conferencing Center was procured. A World Wide Web server was installed at PPPL. Through the Internet, users all over the world can easily gain insight and knowledge about the Laboratory and its science.

Project Support

Tokamak Fusion Test Reactor

The TFTR produces more than 114 MBytes of data per full load shot. For each shot, approximately 220 result waveforms are computed automatically and made available for graphical display. Providing reliable computing facilities for acquiring, analyzing, storing, and archiving these large amounts of data was a continuing challenge. The computer systems' availability for FY94 reached a record high of 97.1%.

Two major additions to the Tritium Remote Control and Monitoring System (TRECAMS) were completed during the year. The first was the integration of instrumentation to track tritium transfers between the Tritium Storage and Delivery System (TSDS) and TFTR. To take full advantage of this new instrumentation, a tritium inventory accounting capability was added to track tritium as it is transferred between the TSDS Holding Volumes, the Tritium Gas Delivery Manifold (TGDM), 14 "Use Point" holding volumes, and the TFTR torus. Daily summaries for delivery and injection activities were provided.

The second major addition was the network integration of TRECAMS to a Digital Equipment Corporation VAX workstation and the development of new software on the VAX to transfer, display, and print the TRECAMS trend data files.

In preparation for the D-T experiments, the TFTR neutral-beam computer system was expanded to pro-

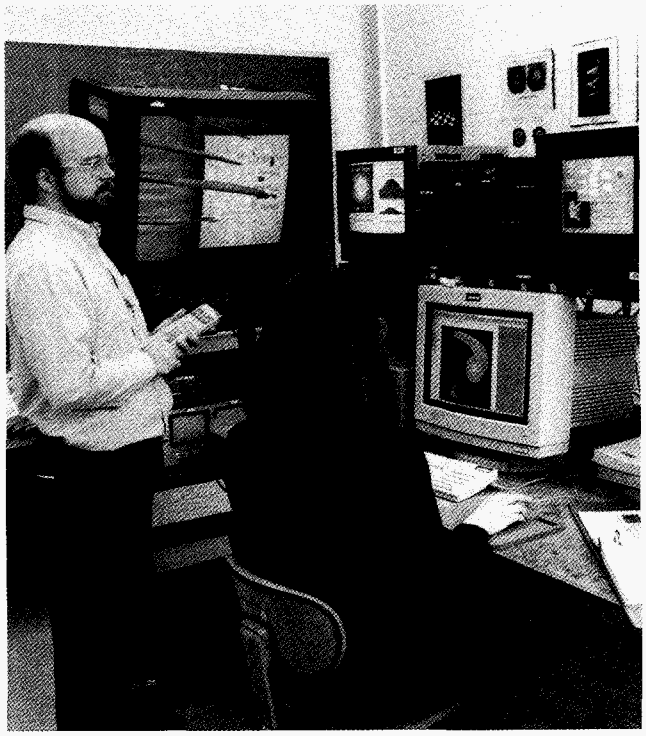

Figure 3. Movie making in progress in PPPL's Visualization Laboratory. (94A0215)

vide an easy-to-use windows and graphics environment for the TFTR neutral-beam injection system. Expanded software capabilities included development of a complete set of diagnostic software (thermocouple, optical multichannel analyzer, and waterflow), a real-time database interface, and support for operational software.

Extensive work was performed on the alpha scattering diagnostic, including control and acquisition software. Analysis software was provided for the alpha charge-exchange recombination spectroscopy (CHERS) diagnostic, which enabled determination of ion temperatures. Enhancements to analysis software were provided for alpha charge-exchange, microwave reflectometer, Mirnov loops, and several of the neutron diagnostics. New neutron power waveforms were provided to support the tritium experiments.

Princeton Beta Experiment-Modification

The Princeton Beta Experiment-Modification's (PBX-M) most recent experimental run period ended in early fiscal year 1994. During that period, the principal PBX-M data analysis computer was upgraded from a VAX 4300 to a 4500 and both its disk storage and memory were expanded. Two DECstation, 3100 AXP workstations, were procured for data analysis, particularly transport analysis.

A computer code designed to give a quick approximation to the CRAY-based equilibrium analysis code was modified to run automatically after every shot. Pseudo-color animations were produced automatically between shots for hard X-ray pinhole camera data.

Plans were developed for the design and implementation of a sophisticated plasma position control system, to advance the goal of current profile control during future runs. The data acquisition hardware had been fully tested and maintained for PBX-M start-up.

Tokamak Physics Experiment

Work in the central instrumentation and control (I&C) area during fiscal year 1994 was consistent with the decision to schedule the I&C design as late as practical to enable the integration of rapidly improving cost and performance trends.

A Small Business Technology Transfer (STTR) application was submitted by Datachron, Inc., of Anaheim, California, naming PPPL as a partner. Their proposal offered to design and build a synchronization system, one that reflects the future requirements of the fusion community. The new system will need greater stability for steady-state operation and will need to support VME and VME/VXI systems.

A background effort was initiated to explore the requirements and design issues involved with supporting a steady-state waveform system. The CSD personnel also produced papers entitled the "TPX Grounding for Equipment and Personnel Safety Specification" and the "TPX Implementation Plan for DOE Orders."

International Thermonuclear Experimental Reactor

The CSD continued to support efforts to improve electronic communications within the ITER community. Support for the U.S. Home Team ITER file sharing system was provided with an upgrade to the server and the addition of more disk space. A World Wide Web (WWW) Server was enhanced to provide information about the ITER Project.

General Support

Networking

The CSD is responsible for the planning, design, implementation, and operation of high-speed networks for the Laboratory's local area network and for providing engineering support for the wide area interface of the Energy Sciences Network (ESnet). High-speed computer communications and peer-to-peer networking are seen as the essential fabrics required for the distributed computing environment at PPPL. This network infrastructure allows PPPL researchers and engineers the ability to collaborate and interact with colleagues and associates around the world. The high bandwidth capability allows researchers the ability to study and interact with scientific data in fundamentally new ways.

PPLnet

In fiscal year 1994, high priority was given to the establishment of the basic 10 megabytes per second Ethernet throughout the 26 buildings comprising PPPL's B-, C-, and D-sites. An additional 450 data service outlets were installed, bringing the total to much more than 1,000. Several miles of fiber optic cable was installed, linking all areas of PPPL with the network infrastructure base. A Sun Microsystems workstation was put in place running Cabletron Spectrum Network Management software. This package will provide Asynchronous Transfer Mode (ATM) net-

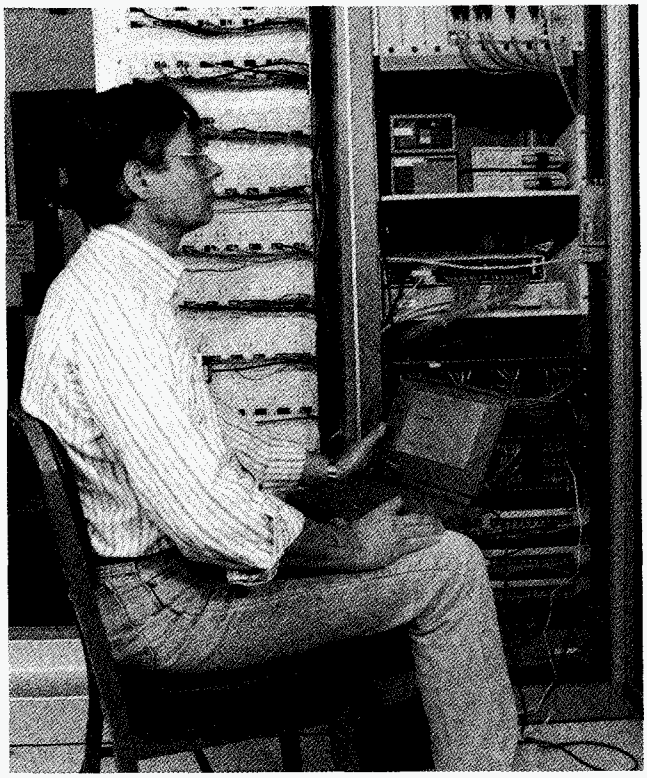

Figure 4. Communications Specialist monitors the Laboratories High-Speed Local Area Network. (94A0213)

work configuration capabilities needed for fiscal year 1996 and beyond. Nearly eight tons of old communication cable installations were removed from drop ceilings at the PPPL C-Site facilities.

The planning and design of the next phase of networking, which will provide 100 megabytes to 1 gigabyte bandwidth service, was begun. The new network technology was chosen to be the ATM-connection-based networking system. The ATM has matured substantially during the year, and is the network technology on which the DOE ESnet will be based. Within five years, this service will be required for advanced scientific visualization, desktop video, and audio distribution.

ESnet

The Laboratory continues to be a major contributor to the growth of the Energy Sciences Network (ESnet). This is due to PPPL's proximity to international and high-density communication centers and to the large amount of circuits and network traffic handled by the PPPL node. Multiple international and domestic communication circuits were established this year, bringing ESnet costs for circuits at PPPL to nearly one million dollars annually. Planning, site preparation, and staging equipment for ESnet high bandwidth connections was a major activity for the CSD. In fiscal year 1994, ESnet installed a 45 MByte per second T3 circuit between PPPL and the Lawrence Livermore National Laboratory. An additional 45 MByte per second ATM circuit provided by Sprint was installed as part of initial tests of the future ESnet ATM backbone. A Silicon Graphics Inc. Indigo workstation was installed on the local ESnet fiber distribution data interface ring to support ESnet high-speed network management. A Digital Equipment Corporation Alpha AXP workstation was installed to support the ESnet Multicast Backbone. An uninterruptible power supply installation was completed in fiscal year 1994. This facility will provide sensitive ESnet and PPPL network equipment continuous power during scheduled and unscheduled power outages.

Computer-Aided Design and Drafting

Laboratory engineers and designers employed Computer-Aided Design (CAD) and Drafting tools to create models and drawings in support of the Laboratory's projects and facilities. The CAD capabilities presently range from traditional two-dimensional representation to three-dimensional modeling. Visualization software presents picture-like renderings of three-dimensional design models, which are used for design integration, checking, and display. The CAD configuration consists of six SUN workstations, one server, and 25 PC workstations running Computervision CAD application software. Four plotters are employed to generate prints for construction and documentation.

A file server was added to accommodate TPX computer-aided design data storage needs. The Sun SPARC workstation, with 14 GBytes of disk capacity, acts as the central storage system for approved and "in work" drawings. Collaborative partners for TPX can access the CAD binary and Initial Graphics Exchange Specification files for TPX project drawings.

A Tektronix Phaser IISDX dye sublimation A-size color printer was added to produce high-quality renderings of engineering designs, primarily for presentation purposes. The printer can accommodate large double-precision solid models.

A CALCOMP 800 dpi E-size scanner was added to capture drawing data associated with existing paper prints of the TFTR facilities.

Central Computing Services

VMScluster Computing Facility

The VMScluster Computing Facility at PPPL, manufactured by Digital Equipment Corporation (DEC), continued to evolve in very significant ways during fiscal year 1994. The VMS central computing facility is routinely used by more than 100 scientists and engineers for data analysis in support of both TFTR and PBX-M. There are currently 29 computers on the PPPL VMScluster. In fiscal year 1994, seven powerful DEC Alpha workstations were integrated into the cluster. Several other cluster nodes, whose bus architecture is required by much of PPPL's data acquisition hardware, were upgraded.

Extensive performance tuning and reconfiguration of roles of VMScluster members resulted in a dramatic improvement of the VMScluster's ability to provide TFTR with the required throughput and response needed to process the significant increase in the TFTR data load. The data load rose from about 90 MBytes at the start of FY94 to approximately 114 MBytes per shot at the end of FY94.

Five older RA82s disks were replaced with RA92s disks bringing the total storage to 45 GBytes. By the end of the fiscal year, all the remaining drives (thirty 1.5 gigabyte RA92s) were interchangeable. Additionally, small computer system interconnect and digital storage system interconnect-based drives were addition to various workstations in the VMScluster. Platters in the PPPL Optical Disk Jukebox were rewritten on double-density disks, enabling it to hold more than 300 GBytes. This added storage space has greatly facilitated off-line analysis for research purposes.

System administration changes were made to simplify the computer configurations and to reduce the load on support staff. Software licensing agreements for IMSL, NAG, and Ingres were negotiated that will greatly reduce long-term costs and greatly increase the flexibility of deployment of this software. All of these enhancements have significantly increased TFTR's and PBX-M's between-shot data analysis capabilities, providing more timely and complete guidance for experimental operations.

A study was completed outlining the planned evolution for VMS computing over the next 3-5 years at PPPL. The procurement of an Alpha AXP server is planned which will reduce maintenance costs and increase computing capabilities to more than 300 million instructions per second (MIPS).

Central UNIX Services

Central UNIX Services provide support for general purpose computing, particle transport analysis, theory and modeling, electronic mail hub, World Wide Web, and various other applications.

The general purpose laboratory computer is a multiprocessor Silicon graphics UNIX machine that provides computing services for all general engineering and scientific computing requirements at the Laboratory. The particle transport analysis code systems consist of eight DEC 3000/300 OSF UNIX systems used for the TFTR and PBX-M experiments. The performance of these systems was greatly enhanced this year by conversion to DEC Alpha machines. This conversion increased the computational power by more than a factor of four.

The theory and modeling systems are Sun UNIX systems which run as part of a UNIX cluster; they are scheduled to be merged with the Silicon Graphics system and other UNIX systems. A distributed file system, AFS, was added to the theory Sun machines, giving users simpler and faster access to files while providing much better security. Significant new computational capabilities exist on theory Sun workstations with the addition of new high-powered software including Mathematica, Macsyma, Maple, and NCAR graphics.

The Laboratory's electronic mail hub system runs on a Sun UNIX system. A ListServe capability was added to the e-mail system, greatly enhancing the Laboratory's e-mail capability. In fiscal year 1994, the theory mail system was merged into the Laboratory mail system.

There are some UNIX machines which provide information about the Laboratory and its experiments through the World Wide Web. A user can find the PPPL home page (describes the Laboratory and its roles) through the Mosaic program by referencing http://www.pppl.gov/ . The server (which is known as www.pppl.gov) is now available on the Internet and has been servicing 1,000-2,000 requests per week. Exploration into using these capabilities for a much wider range of services at the Laboratory is now underway.

Video Conferencing

Video conferencing technology provides a functionality which will change and enhance the way workers and organizations function. The new collaborative efforts associated with the TPX and ITER experimen-

tal programs have caused PPPL to plan for the installation and integration of a new VTEL video conferencing subsystem. The subsystem is due for delivery in early FY95.

Desktop Computing

The Distributed Computing Services (DCS) User Support Group provides customer service and support to PPPL staff members. During fiscal year 1994, this included support for more than 1,000 Macintosh personal computers, more than 500 IBM personal computers, and peripherals. Users in need of assistance with hardware or software or answers to general computer-related questions call a centralized facility referred to as the Help Desk. User requests are handled immediately over the phone or by a scheduled service call. Service calls completed during fiscal year 1994 exceeded 6,000.

The DCS User Support Group manages the Help Desk located in the Computer Resource Center which is open Monday through Friday from 8:30 AM to 4:30 PM. This center provides access to IBM PCs, Macintosh computers, scanners, a color printer, and laser printers. A wide variety of equipment and services are available at the Center. Short-term loan of desktop equipment for office use or portable equipment for individuals traveling on Laboratory business was available.

During fiscal year 1994, a significant amount of time was spent installing network software on IBM-PCs. With this software, IBM-PC users are able to have desktop mail and to share files over the network. In addition, this has also opened the entire Internet to IBM-PC users by using programs such as Mosaic.

Introductory and specialized classes for the Macintosh and IBM were offered upon request. A variety of instruction options were used: in-house classroom instruction taught by User Support Group staff or PPPL employees, one-on-one training, and self-paced training. Approximately 160 employees attended 20 classes in fiscal year 1994. Also during this period, an Introduction to the Internet course was given and attended by about 20 people. Additional classes were scheduled upon request.

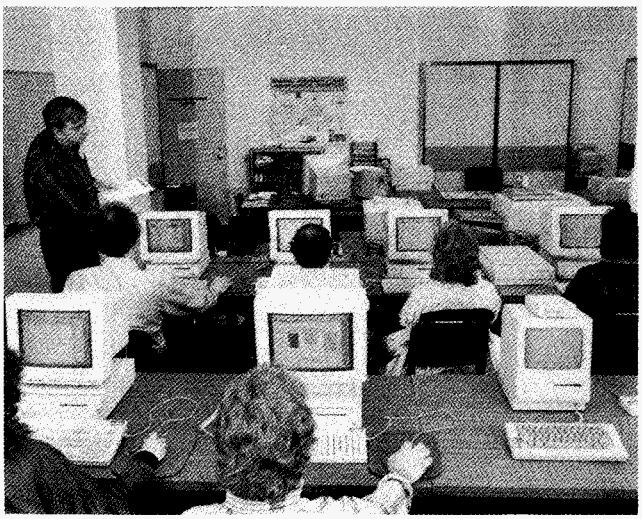

Figure 5. *Microcomputer training in progress at PPPL's Computer Resource Center. (94A0218)*

Strategic Planning

In the middle of fiscal year 1994, "Focus Groups" were formed to examine several specific functions supported by the Computer Systems Division. The individual functions addressed included:

- Networking.
- Microcomputer support.
- Experimental computing support.
- UNIX support.
- General Laboratory support (including e-mail, Internet access, etc.).

The charter of these groups was to:

- Discuss a 3-5 year vision for the particular area of focus.
- Develop the mission (WHY), vision (WHAT), and midterm direction (HOW) for each function.
- Examine current short-term to midterm budgets for how they support the mission, vision, and direction.
- Provide recommendations for modifications to the current direction and budget proposals, if necessary.

Members of the "Focus Groups" consisted of both customers (users) and CSD staff members. Group reports have been completed and were used in the short-term planning process for the Division. The reports will also be used as input for the fiscal year 1995 revision of the CSD Site Statement of Strategy of Computing at PPPL.

Technical Systems

The Technical Systems Division is organized into six skill and activity units. For the report period, the majority of the staff was deployed in a matrix structure supporting the operation of TFTR. For the most part, work performed by the Technical Systems staff is reported in the individual sections of the host projects. Work activities directly managed by the home organization are described in the following sections.

During FY94, this Division provided the engineering support for operations activities associated with the highly successful TFTR tritium experimental campaign. Operation and routine maintenance of TFTR in a safe and environmentally acceptable manner has been demonstrated.

Neutral Beams

The bulk of plasma core heating and tritium fueling for TFTR is supplied by the neutral-beam injection system. All twelve neutral-beam systems injected tritium during FY94 and completed the year operable at full power. Experimental time for TFTR experiments was maximized by performing the cryopanel regenerations, which move the beamline and torus effluent to the tritium systems for processing, during third shifts. This effluent was successfully reduced without impacting beam reliability by increasing the neutral-beam recycle time 20%.

Maintenance of the neutral-beam ion sources, vacuum systems, and cryogenic equipment was required during this year to assure the continuation of full system capability. Special considerations for decontamination and handling procedures for tritium systems are needed when maintenance requires a breach of primary tritium containment. These "line breaks" have been, and are, routinely and safely performed on the diagnostic systems, the tritium gas handling systems, and the neutral-beam systems. In June, 1994, all twelve neutral-beam ion sources were decontaminated, removed, repaired, and reinstalled successfully and without incident.

Radio-Frequency Systems

During FY94, the ICRF (ion cyclotron range of frequencies) Source Operation Group continued to support ICRF experiments in TFTR. The group operates and maintains six multimegawatt radio-frequency (rf) sources at 43 MHz and 64 MHz. One of the largest undertakings for FY94 was the conversion of two of the sources so that they could use Thomson as well as Varian high-power vacuum tubes. Major changes had to be made to the sources' large cavities and input circuits to accommodate the new tubes. These modifications were completed and the sources commissioned in time to support TFTR operations in the summer.

In order to increase overall system reliability, the protection systems for the sources' high-power vacuum tubes were reengineered to dynamically limit tube current and power dissipation. These systems permit the high-power output tubes to operate reliably under unpredictable load conditions while still maintaining the highest possible power output.

TFTR Power Systems

The field coil power conversion systems for TFTR maintained a 97% availability for FY94. Major modifications to the toroidal-field system to allow 5.6 tesla operation included moving four equilibrium-field power supplies to the toroidal-field power system and 1,200 MVA operation of the Motor Generator Sets. Installation and testing of these modifications was primarily done on TFTR nonoperating shifts in order to maximize TFTR experimental time.

AC Power Section

Activities of the AC Power Section for FY94 include the following:

- An extensive TFTR ac power system short circuit and coordination study review was completed, problem areas identified, and system correction initiated. Completion of this large-scale effort is expected by the end of CY94.
- Portable load survey instrumentation was installed at selected D-Site load areas, and the information obtained was used to improve system protection and performance. A broadening of this effort is planned as a result of the initial successful surveys.
- The reliability of the Laboratory's ac power system continues to be high, the result of a well planned and skillfully implemented preventative maintenance program.
- Transient recording expertise was provided to support a TPX investigation of future pulse-power impact on the existing 138-kV system

voltage. Support included coordinating the investigation among the power company, project, and sponsor.

- In support of 1,200 MVA, 5.6-tesla operation, strategic protection control system changes were implemented that permitted continued use of existing medium-voltage, variable-frequency circuit breakers.
- A spare uninterruptible power supply was upgraded and performance tested for use with the Energy Science Network system. Installation will be completed during the early part of FY95.
- Other activities included the replacement of inert gas systems for the switchyard 138-kV transformers, the technical oversight for the replacement of underground fuel tanks with above ground tanks for the C- and D-Site standby diesel generators, and technical review of a water deluge system.

A broad range of support activities were also provided by the AC Power Section in FY94. These included evaluation of load-addition requests; the design, development, cost, and schedule estimates for the almost seven hundred Laboratory panelboards; and continuation of the panelboard local circuit verification program.

Motor Generator Section

The Motor Generator (MG) Section is responsible for the maintenance, repair, upgrade, and operation of two equipment constellations. One, consisting of three shafts and twelve generators, is located at C-Site and supplies energy for PBX-M and other small experimental devices. The second MG set, which consists of two vertical shaft machines, is located at D-Site and supplies energy to TFTR.

The motor generator system for the TFTR Project operated in FY94 with an availability of 99.5%. Table I gives the total starts and stops, operating hours, and pulses for each MG set since fiscal year 1989. Figure 6 shows the trends for pulses, operating hours, and start/stop for each MG set by fiscal year. Since initial start-up in December 1981, MG #1 has a total of 18,223 operating hours with 1,876 start and stop cycles. Motor Generator #2 has operated for a total of 15,626 hours with 1,415 start and stop cycles since July 1984. The used life expectancy for the MG sets for pulses is 6.0 % and for start and stop cycles 18.8%.

In support of 5.6-tesla operation and after extensive evaluative testing, both MGs were successfully operated at 600 MVA, which is 25% over rating. An additional 140 MJ of energy is provided at this operating level. In order to accomplish this, control settings were made to the both cycloconvertors and the exciters and control circuit modifications were made. Motor Generator Set #1 was rebalanced to reduce shaft runout to acceptable operating limits.

Discussion is underway, with an equipment manufacturer, to develop a new process to improve the operation of the direct current high-speed circuit breakers used for the C-Site motor generators.

Facilities and Environmental Management

The Facilities and Environmental Management (FEM) Division provides engineering and technical support to PPPL. While many FEM personnel are well-

Table I. Total Starts and Stops, Operating Hours, and Pulses for D-Site Motor Generator Sets #1 and #2. (Fiscal Year 1989 through 1994)

	FY89		FY90		FY91		FY92		FY93		FY94	
	MG #1	MG #2	MG #1	MG #2	MG #1	MG #2	MG #1	MG #2	MG #1	MG #2	MG #1	MG #2
Start and Stops	44	39	265	262	47	35	116	110	84	88	152	152
Operating Hours	576	570	3,726	3,784	519	392	1,567	1,493	991	1,036	2,029	2,007
Number of Pulses	1,474	1,684	13,269	13,229	3,324	1,702	7,074	6,691	3,918	3,918	6,440	6,436

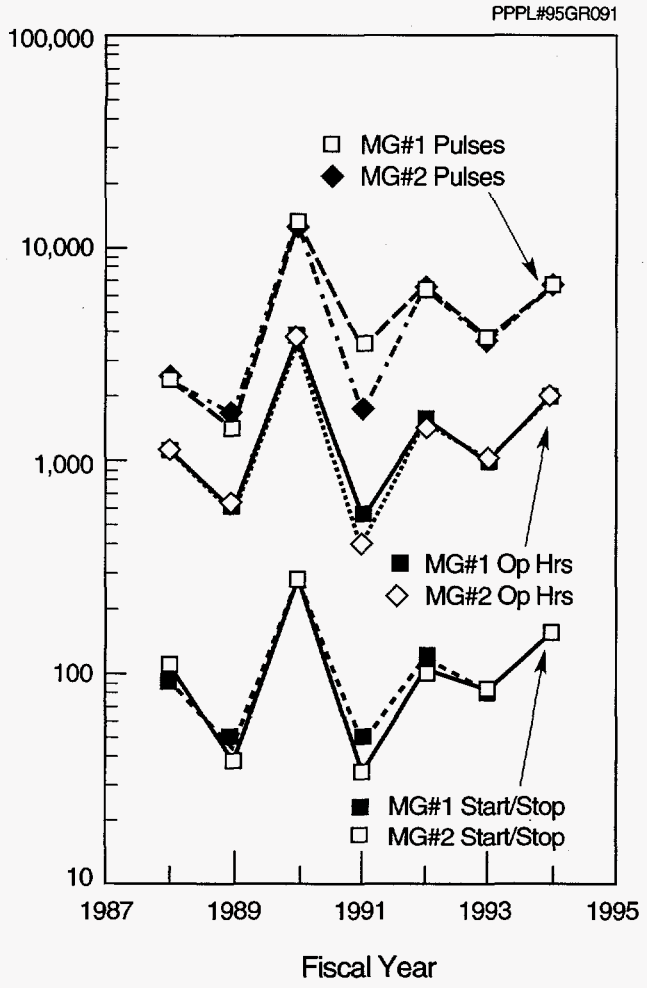

Figure 6. *Motor generator operation trends for pulses, operating hours, and starts and stops.*

recognized throughout the facility, many of the tasks they perform take place "behind the scenes." Their work serves to ensure that facilities are operated effectively and efficiently. The Division is composed of six branches: Maintenance Operations, Maintenance Engineering, Project Engineering, Environmental Restoration and Waste Management Administration, Fire Protection Engineering, and Utility Management.

Fiscal year 1994 was a challenging and successful year for the FEM Division. The mission of the Division has evolved over the past one to two years with the addition of new responsibilities. For example, the FEM Division has an increasing role in the support of TFTR with the addition of responsibility for the maintenance and operation of the TFTR heating, ventilating, and air-conditioning (HVAC) and liquid effluent collection systems. In addition, a Laboratory reorganization added the functions of Environmental Restoration and Waste Management Administration and Radioactive Waste Management to the FEM organization. The reorganization also increased the accountabilities of the Division and provided additional technical talent and expertise to the staff.

Maintenance Operations

Fiscal year 1994 was a productive year for the Maintenance Operations Branch. It was a year when the challenge of "do more with less" was the goal for the staff. Staffing was reduced by 16% to 60 people and nonlabor expenses were reduced an average of 11% from the previous year. In order to prioritize the work load, the decision was made to limit work to maintenance, repair, and operation of existing systems and equipment. Requests for new installations, facility improvements, and material handling were given a low priority. Highest priority was given to safety concerns and the TFTR Project. At the close of FY94, a total of 5,115 work orders had been completed by the staff.

Extensive efforts went into preparing for the final D-T Operational Readiness Review and the record setting experiments by TFTR. Assisted by a System Engineer, the Maintenance Operations Branch had direct responsibility for the HVAC and liquid effluent collection systems. Both systems are performing reliably and without incident.

A major safety problem that developed as the year progressed was the extreme winter weather which gripped the Princeton area. There were seventeen recordable snow and ice storms which required constant shoveling, plowing, sanding and salting. The severe weather also caused a shutdown of natural gas delivery and complicated fuel oil deliveries. The Maintenance Operations staff overcome these complications and worked to ensure that the facilities remained operational.

The backlog of work requests and preventative maintenance actions continue to run at a high rate. At the close of FY94, the maintenance backlog stood at approximately 9,500 hours. The backlog is managed such that work requests are evaluated for merit and only important requests are kept "active." Other work requests are either rejected (and the requestor informed of such) or placed in a "deferred" file. In this manner, the backlog is kept at a manageable level with the goal of accomplishing important tasks in a timely manner.

Maintenance Engineering

Operating Expense Projects

An important component of facility improvements is accomplished through the OPEX (**OP**erating **EX**pense) Program. The mid-sized OPEX Projects bridge the gap between routine maintenance work and the larger General Plant Projects accomplished by Project Engineering. OPEX projects focus on correcting safety concerns and improving the operation of infrastructure systems. Although the OPEX budget was reduced from FY93, more than a dozen OPEX projects were initiated during the year. Project requests are evaluated and prioritized by the Maintenance Engineering Branch and reviewed by the Technical Resources Committee. Some of the FY94 projects included:

- Completion of the five-year maintenance program for the three central plant centrifugal chillers.
- Replacement of TFTR Air Compressor AC-102.
- Multiple fire protection system improvements.
- Upgrade of electrical service in the Radiological Environmental Monitoring Laboratory (REML).
- Installation of new lighting in the Cafeteria serving area, the Theory wing hallways, and the D-Site parking lot.

Energy Studies and Retrofit Projects

During 1994, Engineering Department management reemphasized the importance of effective energy management. Although budgets continued to shrink, an organization modification was enacted which redistributed internal staffing to the In-House Energy Management Program. Responsibility for Energy Management functions was moved to the Maintenance Engineering Branch. As a result, the efforts of two Maintenance Engineers and the Branch head are focused on improving energy conservation performance. Progress in FY94 includes:

- A new energy project to convert Boiler #3 to dual fuel capability was requested and approved.
- An energy study of the C-Site Energy Monitoring and Control System and the Power Line Carrier System has been completed and submitted to DOE.
- An energy study of C-Site lighting room sensors was completed.
- An energy study was requested and funded by DOE to reevaluate the feasibility of replacing the existing transite walls for the RF and CS Buildings. The study was completed within one month and submitted to DOE with energy conservation opportunities identified.
- An energy study of HVAC controls calibration has been completed and submitted to DOE.
- An energy study of chilled water, steam, condensate and steam traps has resumed.
- An energy study of group relamping and fixture retrofits has resumed.
- An energy study was requested and funded by DOE to reevaluate the feasibility of a standby generator for electrical peak demand limiting.

Project Engineering

The Project Engineering Branch is responsible for the design and construction of site improvements, new facilities, and the modification to existing facilities throughout the Laboratory. In this capacity, the Project Engineering Branch acts as the interface between the DOE/Princeton Area Office and Laboratory management in developing construction project priorities; formulation of design concepts; and the development of engineering design, drawings, and specifications for the solicitation of bids. The FEM Project Engineering provides technical support to the Procurement Department in contractor selection for both architect and engineering design and small business construction contractor services.

The Branch provides project management and oversight during the construction phase of all projects, serving as the focal point for the coordination of a variety of activities including compliance with Davis Bacon requirements through the DOE/Princeton Area Office, quality management through the proper integration of Quality Assurance personnel, adherence of Occupational Safety and Health Administration (OSHA) and specialized Laboratory training requirements, and field supervision of construction operations performed by contractor personnel. The activity level in this arena was particularly elevated in FY94 due

to the large number of construction projects initiated through a variety of funding sources and the launching of complex General Plant Projects (GPPs) which have extended design and construction schedules suitable for multiyear funding. By the close of the fiscal year, FEM Project Engineering provided construction and design management services on 25 General Plant Projects, 10 fire and life safety projects, and a major Environmental Restoration and Waste Management (ER/WM) remediation project for underground fuel storage tank removals at both C- and D-Sites of the Laboratory. The eleven projects closed-out (or with construction completed) include:

- Two projects which added 17,102 square feet of new space to the Laboratory.
- Seven projects focused on safety-oriented modifications to existing facilities.
- Two projects dedicated to upgrade facilities to satisfy current operational needs.

Project Engineering is also responsible for compliance with DOE Orders for Site Development Planning, (DOE Order 4320.1B and the related Order 4320.2). In June 1994, Project Engineering completed and submitted to DOE the Laboratory's Integrated Facility Plan detailing PPPL's site development growth projections and identifying facility requirements necessary to satisfy and support future programmatic goals and objectives. Project Engineering has been conducting a comprehensive site mapping program over the last three years to collect site profile data information for use in site planning and project design development. The Geographic Information System (GIS) Program was launched in February of 1992 when baseline information was obtained with aerial photography. The GIS, when completed, will provide site topographic data; delineate wetlands and flood plains which limit site development; accurately locate all structures, utilities, and paved areas; and identify existing land use for site development planning. In FY94, site wetlands and flood plains delineated under the ongoing GIS site planning program were verified and accepted by the New Jersey Department of Environmental Protection.

During FY94, FEM Project Engineering Site Utilization and Building Space Utilization planning activities were audited by DOE as part of a Real Property Management Appraisal. Both activities received ratings of "Excellent" by DOE, with the evaluation conclusion stating "Building and site information have been entered into a computer system making building and site information readily available. This has been found to be a useful management tool."

Environmental Restoration and Waste Management

The Environmental Restoration and Waste Management (ER/WM) Branch has three main roles within its mission: budget and financial planning for environmental restoration and waste management projects; remediation of areas of hazardous contamination on site; and management of the hazardous, radioactive, and mixed waste generated from research, maintenance, and remedial activities at the Laboratory.

In fiscal year 1994, the administrative function of ER/WM expanded significantly because of expanded Department of Energy Office of Environmental Management financial and project planning requirements. One of the major activities completed in 1994 was the preparation and submission of the FY96-00 Environmental Management Activity Data Sheets and related budget documents. These Data Sheets are the funding mechanism for all environmental restoration and waste management activities at PPPL. As a corollary to these budget documents, ER/WM completed a detailed Environmental Restoration project baseline that describes the scope of activities, milestones, deliverables, and funding requirements for all on-site remedial activities. This project baseline has been approved by the Princeton Area Office, the Chicago Field Office, and Department of Energy Headquarters.

The ER/WM Branch also prepared Current Year Work Plans for both remedial and waste management activities. These work plans have been used as models for other laboratories within the Chicago complex. Through all of these financial planning and budgeting efforts, ER/WM has been able to attract $9.2 M in target level funding for Laboratory activities for fiscal year 1996.

During fiscal year 1994, ER/WM staff identified funding resources within existing waste management projects and reassigned these funds to the construction of 52 Type-B Disposable Molecular Sieve Beds (DMSB). The DMSBs are specialized containers for transportation of tritium off-site for recycling at Savannah River or disposal at Hanford. The DMSBs are

a critical component for tritium operations in TFTR. The ER/WM Branch also participated in the TFTR Shutdown & Removal (S&R) Conceptual Design Review and S&R Project planning. Environmental Management funding of waste packages, transportation, and disposal are a critical element to the success of the S&R Project.

The ER/WM Branch made progress on the site-wide remedial investigation to identify the extent of potential on-site contamination. This remedial investigation is being conducted under a Memorandum of Understanding between the New Jersey Department of Environmental Protection (NJDEP) and Princeton University. Activities for this project included preparation and submittal of the Activity Data Sheets and Project Baseline documents to allow funding of the project. An ER/WM subcontractor prepared draft work plan documents (Remedial Investigation Work Plan, Field Sampling Plan, Quality Assurance Project Plan, and Health and Safety Plan), and ER/WM submitted them to NJDEP. The NJDEP's comments were incorporated into the final documents and these documents are awaiting final NJDEP approval. The ER/WM staff conducted expedited soil and ground water sampling in order to facilitate construction of improvements to the Hazardous Material Storage Facility and to meet Program Execution Guidance milestones.

In addition to the site-wide remedial restoration, ER/WM staff worked closely with the Project Engineering Branch to achieve the removal of numerous underground storage tanks at the site. The ER/WM provided field oversight, environmental sampling and analysis, and waste management services to support this activity. Approximately 570 tons of contaminated soil was excavated and transported to an asphalt paving plant for recycling. The ER/WM staff also assisted the Project Engineering Branch with the Detention Basin Upgrade Project by conducting post-excavation soil sampling to address past PCB contamination prior to installation of an impermeable liner in the basin.

Representatives of the ER/WM Branch continued their involvement in the Environmental Management Office of Technology Development Technical Program Manager's Network. This network serves as the focal point for facilities throughout the DOE complex to share information on environmental technology development activities. In this effort, ER/WM works closely with PPPL's Office of Technology Transfer and the Plasma Science and Technology Department to identify possible applications of plasma technology to environmental cleanup and other areas for PPPL involvement in environmental technology development.

The ER/WM Branch also supported the Tritium Systems Division's packaging and shipment of Type-B Disposable Molecular Sieve Beds to Savannah River and the Hanford Burial Site. Waste management staff also provided asbestos remediation services in support of maintenance operations.

During fiscal year 1994, the ER/WM Branch received an "Excellent" rating from the Chicago Field Office Hazardous Materials Transportation Appraisal. In addition, ER/WM staff prepared the Annual Hazardous Waste Generator Report for submission to the NJDEP. This report is a summary of all hazardous waste generated and shipped for disposal on an annual basis. Waste management staff also joined members of the Quality Assurance and Reliability Division staff in conducting audits of four hazardous waste treatment and disposal facilities. Also, waste management staff completed the development and implementation of a Hazardous Waste Generator Program for the Laboratory. Finally, the ER/WM Branch lead the development and approval of the Final Design Requirements document for the proposed Radioactive Waste Handling Facility.

Fire Protection Engineering

The primary focus of the Fire Protection Branch is centered around the Safety and Fire Protection Improvement (SFPI) Line Item Project. This $4.8 million, multiyear project provides for improvements in fire protection system design and correction of Life Safety Code Discrepancies. The following work was completed as part of the SFPI Project:

- Building alarm system improvements were completed in the FEM Building, Emergency Services Building, QA Facility, and REML and are nearly completed in the C-Site MG Building, Rectifier Building, and ESAT Building.
- Design was completed on a site fire alarm reporting and recording system and construction is under way.
- Construction was completed on a variety of Life Safety Code compliance projects and sprinkler projects were completed in the C-Site MG Building, Rectifier Building, ESAT Building, QA Facility, REML, and C-Site Cooling Tower Pump House.

- New carbon dioxide suppression systems were installed in four areas of the CS Building.

In addition to the SFPI Project, a project was completed which provides smoke detection in the HVAC ducts at D-Site and another project is in progress which provides an automatic second source of fire protection water. Through the provision of alternate detection and suppression systems, the Laboratory has decommissioned 12 of 30 (40%) Halon systems during FY94. That brings the total number of systems decommissioned to date to 16 (53%) and the pounds of Halon taken out of service to 9,506 (67%). Approximately 6,000 pounds of Halon was excessed to the Strategic Petroleum Reserve (SPR) to assist the SPR with a Halon shortfall.

PPPL has been required to meet increased testing and inspection requirements due to changes in our systems configuration and upgraded requirements by the National Fire Protection Association code, which underwent major revision in 1993. Nearly 3,400 manhours were expended performing preventive maintenance and testing of fire protection systems. A DOE Appraisal assessing the Fire Protection program was performed during May, 1994, which resulted in an evaluation of "Good."

Utility Management

Utility Management includes the planning and administration of all the Laboratory's utility contracts, and providing direct liaison with all utility companies. There are nineteen utility contracts which include for example, electric, natural gas, fuel oil, propane gas, and potable water. The total cost for these services was more than $5,330,000 (after savings adjustments). All utility invoices were technically and financially evaluated for correctness before approval for payment. Verifications of utility billing(s) included, but were not limited to, utility costs versus rate schedules, utility usage, profiles, engineering and statistical analysis, and database maintenance. The Laboratory realized savings of nearly $3,000,000 in fiscal year 1994 through:

- The PSE&G Electric Interrupt Service and the Electric Curtailment Service Programs.
- The Demand Monitor Program.
- The Electric Bill Apportionment Program.

Fabrication and Assembly

The Fabrication and Assembly Division (FAD) was created when the Engineering Department was reorganized and renamed the Engineering and Technology Development Department. It is comprised of the Project Management Staff, the Engineering Support Branch, and the Central Drafting and Technical Shops.

A large percentage of the FAD staff is assigned to projects via the matrix structure implemented by the Laboratory in 1988. The FAD provides engineering and technician services to the projects, as well as the home division through this matrix structure. These services include project engineering management, engineering calculation checking and sign-off, seismic analysis, weld engineering, design review, writing of technical policies and procedures, setup and maintenance of hoisting and rigging procedures and management of critical lifts, modification and maintenance of the non-TFTR experimental utility hardware and equipment, and shop services. A summary of the shops and their services is given below.

Engineering Support and Technical Shops

Six shops provide mechanical, welding, electrical, vacuum brazing, machining, and material test technology to the Laboratory's experimental projects and facility maintenance and operations. The shops provide qualified and certified technicians using up-to-date tools and equipment to perform a wide variety of tasks. The tasks range from vacuum oven brazing of dissimilar materials to ultrahigh vacuum welding and leak checking, as well as precision machining, shop fabrication, and on-site installation of hardware. Major tasks the FAD shops provided in support of projects in FY94 are listed below.

Princeton Beta Experiment-Modification

Technician and machine shop support for PBX-M shutdown was provided. Activities included the rebuilding of the Biasing Bus, Fenwall instrumentation calibration, and in-vessel work and modifications.

Tokamak Fusion Test Reactor

On the TFTR the following tasks were accomplished:

- Fabrication of more than 60 Type-A and Type-B tritium waste containers.
- Preliminary modifications to the TFTR Maintenance Manipulator in support of TFTR S&R.
- Upgrade of the TFTR decontamination facility, including installation of an oven and new laundry equipment.
- Engineering support and installation support for the TFTR tritium purification system in the decontamination facility at D-Site.
- Fabrication and Assembly of vacuum pump oil change carts for tritiated oil.
- Preparation of test sample from the TFTR toroidal-field coils in preparation of the TF coil cutting studies to be performed in FY95.

Drafting

Primarily, fiscal year 1994 efforts were in support of preparations for the shutdown and removal tasks for TFTR. Support was also provided for the tritium purification system interfaces design and to the TPX Project.

A program to assist the Drafting Section in the release and control of drawings and a drawing database file was completed. This system allows users to search to files via user-friendly on-line software.

In FY94, the Drafting Section acquired a large document scanner. It has the capability to scan large, manually created engineering drawings for importing into computer-aided design and drafting applications. In addition, it reduces paper storage requirements and provides archiving capabilities.

TFTR Shutdown and Removal

The Tokamak Fusion Test Reactor (TFTR) is scheduled to complete its deuterium-tritium (D-T) experiments in September, 1995. The D-T operations will result in the TFTR machine structure becoming activated and the plasma facing and vacuum components becoming contaminated with tritium. The resulting machine activation levels after a two-year cooldown period will allow hands-on dismantling for external structures, but may require remote or semi-remote dismantling for the vacuum vessel. The primary objective of the TFTR Shutdown and Removal (S&R) Project is to provide a facility available by August, 1999, for the construction of a new Department of Energy (DOE) experimental fusion device.

The TFTR S&R Project schedule calls for a two-year shutdown period when tritium decontamination of the vacuum vessel, neutral-beam injectors, and other components will occur. Shutdown will be followed by an 18-month period of removal operations for the device itself. The technical objectives of the TFTR S&R Project are to: (1) Safely dismantle and remove components from the Test Cell complex. (2) Package disassembled components in accordance with applicable regulations. (3) Ship packages to a DOE-approved disposal or material recycling site. (4) Develop expertise using semi-remote disassembly techniques on a large-scale fusion facility.

Project Objectives

The primary objective of the TFTR S&R Project is to render the facility suitable for construction of the next DOE fusion device, the Tokamak Physics Experiment (TPX), by mid-1999. To reach this objective, it will be necessary to remove activated and tritium-contaminated machine components so the facility can be downgraded from a "Category 3 Nonreactor Nuclear Facility" to a "General Use Radiological Facility." This will be achieved while keeping the dose to workers as low as reasonably achievable (ALARA).

Technical Objectives

The technical objectives for the TFTR S&R Project are similar to the objectives for dismantling a nuclear power facility. Technology from the nuclear fission industry will be utilized wherever possible to safely dismantle activated and contaminated systems. Due to the activation and contamination levels, it will be necessary to use semi-remotely operable equipment to dismantle some components. Disassembled components will be packaged in compliance with DOE, Department of Transportation (DOT), and waste receiver requirements. The certified packages will then be transported to a DOE-approved waste repository for low-level radioactive waste disposal. The TFTR S&R Project differs from a typical decontamination and decommissioning project in that the facility will not be returned to "greenfield" conditions nor will it be released for unrestricted use. The Laboratory will retain ownership and reuse of the facility for the next-generation fusion device.

Schedule Objectives

The major milestones for the TFTR S&R Project are as follows:

Major Milestones for TFTR Shutdown and Removal

Conceptual Project Review	July 1994 (complete)
End Operations and Commence Shutdown	September 1995
Preliminary Design Review for Tokamak Removal	June 1996
Final Design Review for Tokamak Removal	June 1997
Begin Tokamak Removal	October 1997
Test Cell Available for TPX Occupancy	August 1999

PPPL#95GR090

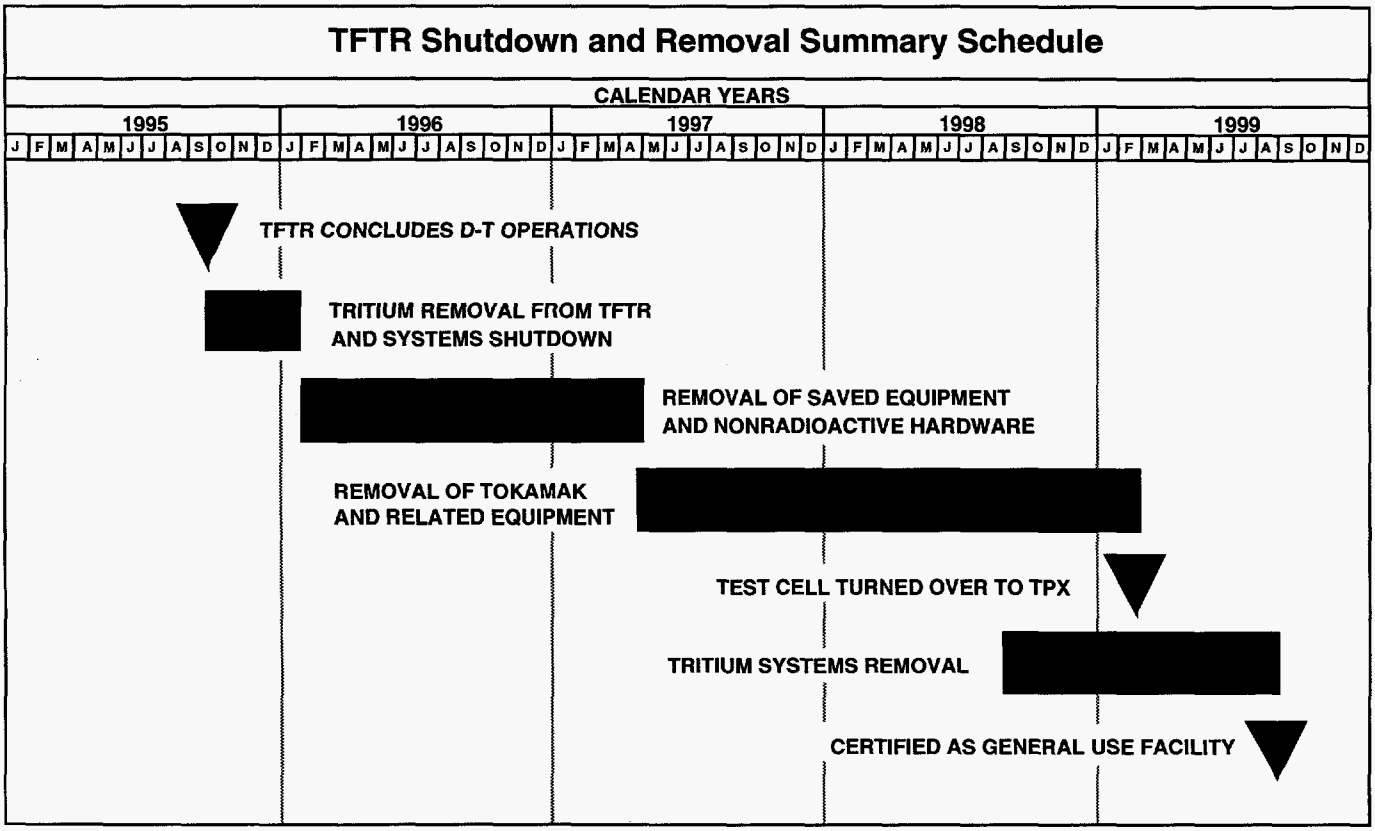

Figure 1. *Summary Schedule for the Tokamak Fusion Test Reactor Shutdown and Removal.*

S&R Plan

The first phase of the TFTR S&R Project will be the bulk removal of tritium from the vacuum vessel and the neutral beams. This will begin with a two-to-four week period of neutral-beam conditioning followed by up to five months of glow-discharge cleaning and bakeout. The first step will preclude other activities in the machine areas, while the second step will only preclude activities directly on or under the tokamak.

The second phase of the TFTR S&R Project will start with the safing and removal of most items being saved for reuse. This will be followed by the removal of almost all items in the Test Cell Basement, Hot Cell, and Data Acquisition Rooms (DARMs). This phase is expected to last up to 18 months.

The third phase of the TFTR S&R Project will be the removal of items from the Test Cell. The plan is based on the assumptions that a total of 2×10^{21} neutrons will be produced, and all plasma facing components, neutral-beam injectors and machine vacuum components will be tritium contaminated. This results in Test Cell activation and contamination levels requiring precautionary measures for workers.

The final phase of the TFTR S&R Project will be the removal of the tritium systems from the tritium area of the Test Cell Basement. Each equipment skid will be isolated and then packed into customized type A containers for shipment and burial. Only the gas holding tank will be left behind, but it will be thoroughly decontaminated and sealed.

Site preparation includes shutdown of the TFTR at the conclusion of D-T operations. This includes the removal from the site of all tritium storage inventories; decontamination of systems and components; de-energize, lockout, and tagout of electrical and mechanical systems that are not required to support tokamak shutdown and removal activities or are to be dismantled; radiological characterization of the experimental areas; and visual inspections and surveillance. Dismantling and removal of nonradioactive and salvageable components will be completed during the

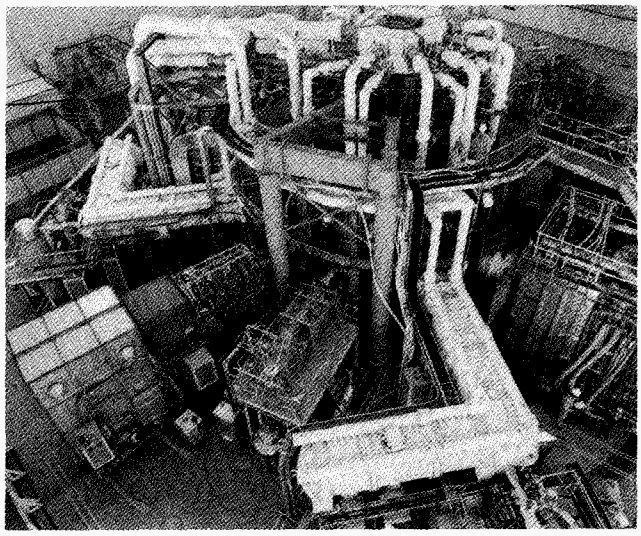

Figure 2. *The Tokamak Fusion Test Reactor. (PPPL#89E0306)*

shutdown phase. Tritium decontamination of internal systems will be difficult because of their complex configuration, materials of construction, and large surface areas. The majority of the retained tritium will be adsorbed into the vacuum vessel graphite tiles or in the co-deposited layer of graphite on the vacuum vessel walls. The neutral-beam injectors will also be contaminated because they operate with tritium and collect tritium from the plasma with their cryogenic pumping panels.

The effectiveness of various tritium removal techniques such as plasma etching, moist air soaking, and gas purging is presently being investigated. A decontamination plan will be developed and implemented based on these results and the experience of other tritium facilities. The majority of the decontamination operations will occur during the early stages of the TFTR S&R Project. Localized decontamination will continue as required throughout the Project to reduce subsequent personnel exposures, waste generated, and to minimize overall shutdown and removal costs.

Radionuclide characterization will occur immediately after the conclusion of D-T operations and will provide the information required to finalize the planning of the shutdown and removal activities. It will affect the work schedule and manpower requirements, particularly those related to personnel exposure. Projected personnel exposures have been calculated from a Laboratory computer model. The model is continually checked against actual dose rates attained during D-T plasma operations. Based on the projected contact dose figures, all dismantling work from the toroidal-field coils to the center of the machine will be performed with remotely or semi-remotely operable tooling and equipment.

Plasma arc cutters, hydraulic shears, and other mechanical cutters will be used to perform the dismantling tasks. Due to geometric constraints, disassembly of the vacuum vessel may involve cutting operations inside the torus. Containment structures will be used to limit the spread of contamination during dismantling operations.

Calculations of radioactive material inventories for TFTR components indicate that the shutdown and removal waste will be Class A low-level radioactive waste. This will consist of stainless steel and aluminum structures, piping and components, copper coils and bus bars, stabilized radioactive liquids, and personnel protective equipment. All radwaste will be packaged and transported to a DOE approved waste repository. The total neutron-induced radioactivity inventory to be disposed of has been estimated at 50 TBq (1400 Ci). The amount of radwaste generated during shutdown and removal, including stabilizer and void space filler, is estimated to be 2300 tons. At present, the repository is assumed to be the Westinghouse Hanford Company (WHC) site. Packaging of the waste will be in compliance with DOE and DOT regulations, PPPL procedures, and WHC waste acceptance requirements.

Figure 3. *The Tokamak Fusion Test Reactor Test Cell in 1981 prior to machine installation. (PPPL#81E1297)*

FY94 Accomplishments

During FY94, a number of activities led up to a successful Conceptual Project Review in July. A Work Breakdown Structure (WBS) and the associated WBS dictionary were developed, draft Statements of Work for each WBS element were prepared, schedules and preliminary cost estimates were refined, a Project Management Plan was written and submitted to the Princeton Area Office of the Department of Energy, and an Advance Acquisition Plan was developed.

In addition, a preliminary study of the cables and raceways to be removed was prepared and a Master Equipment List outlining the disposition (save, scrap, trash, or submit to radwaste) of all items at D-Site was drafted and approved by both the TFTR S&R Project and the Tokamak Physics Experiment Project. The need for a Radwaste Storage Building and a temporary storage building to support the TFTR S&R Project was defined and associated Statements of Work were prepared so procurements could begin.

Summary

The TFTR will be the first tritium-fueled fusion facility to undergo shutdown and removal. The experience gained from tritium decontamination, implementation of remote-handling techniques, and lessons learned from TFTR's shutdown and removal will provide valuable information for the design of future large-scale fusion devices, such as the International Thermonuclear Experimental Reactor. Since shutdown and removal costs have become a major expenditure for nuclear facilities, it is important to develop detailed estimates at the inception of a new project. Shutdown and removal cost and schedule estimates for future fusion projects can be based on actual data taken from the TFTR S&R Project.

References

1 U.S. Department of Energy Order 5820.2A, "Radioactive Waste Management," U.S. DOE, 1988.

2 G.R. Walton and J.C. Commander, "The Preliminary Decontamination and Decommissioning Plan for the Tokamak Fusion Test Reactor," D&D-0012-DDOC, Princeton Plasma Physics Laboratory, February, 1993.

3 L.P. Ku and S.L. Liew, "Global Dose Rate in TFTR Due to Neutron Induced Residual Radioactivities During DT Operation," in *Fusion Engineering* (Proc. 15th IEEE/NPSS Symp., Hyannis, Massachusetts, 1993) Vol. **1** (Institute of Electrical and Electronics Engineers, New Jersey, 1994) 313-316.

4 "Hanford Site Solid Waste Acceptance Criteria," Westinghouse Hanford Company Report WHC-EP-0063-4 (November, 1993).

5 "Environmental Assessment for the Tokamak Fusion Test Reactor Decontamination and Decommissioning Project and the Tokamak Physics Experiment at the Princeton Plasma Physics Laboratory," U.S. Department of Energy Report DOE/EA-0813 (draft) February, 1994.

Technology Transfer

The Office of Technology Transfer (OTT) is responsible for the transfer of Princeton University Plasma Physics Laboratory (PPPL) technologies to the private sector as defined by the National Competitiveness Technology Transfer Act of 1990. The OTT is staffed by a full-time senior professional staff member with full-time secretarial support. The Head of the OTT is the Laboratory representative to the Federal Laboratory Consortium (FLC), a federally mandated organization of Technology Transfer Officers of all laboratories funded by the Federal Government.

The Office of Technology Transfer is engaged in a variety of programs to promote transfer technology to industry, including:

- Cooperative Research and Development Agreements (CRADAs), whereby industry and Laboratory researchers work together on problems of mutual interest.
- Sponsored research (Work For Others), whereby industry pays the Department of Energy (DOE) for work performed at PPPL.
- Personnel Exchange Programs, where researchers from industry assume a Laboratory work assignment or Laboratory staff work in an industrial setting.
- Technology Maturation Projects, where technologies in the first stages of development at the Laboratory are developed further to bring them closer to commercialization.
- Licensing of inventions or technologies.

In addition to the routine activities of initiating CRADAs, in FY94 a major effort was concentrated on the development of new avenues for the Technology Transfer programs at PPPL.

- The Laboratory applied for and was granted membership in the American Textile (AMTEX) Partnership CRADA.
- More emphasis was placed on developing Nonfederal Work For Others as a source of Technology Transfer opportunities and outside funding.
- The Laboratory was a strong advocate for the elimination of the DOE added factor and depreciation costs on Nonfederal Work for Others for small business and Not for Profit organizations. This policy was placed into effect by DOE on August 25, 1994.

As a technology resource, PPPL seeks to provide its unique expertise to solutions of industrial problems. PPPL has also endeavored to enhance its contact with area small business and to provide technological help and guidance where possible.

Cooperative Research and Development Agreements

Cooperative Research and Development Agreements are one of the primary means for transferring technology from the federal laboratories to the private sector. A CRADA is a contractual agreement between a federal laboratory and one or more industrial or university partners, in which collaboration, cost sharing, and the results of a particular R&D program are equitably shared. One of the limitations on the ability of PPPL to enter into a CRADA is the requirement that the CRADA research must be either in a programmatic area related to PPPL funding or must be funded by a DOE agency willing to sponsor the particular CRADA. The CRADAs below are in various stages of development.

CRADAs in Development

Sapphire-to-Metal Bonding

PPPL's first CRADA is with Saphikon, Inc., a small business located in New Hampshire that develops high-performance products based on sapphire. This CRADA is to develop a sapphire-to-metal bond-

ing technique that can produce a firm seal for the end caps on high-intensity lamps to be manufactured by Saphikon. Over the years, PPPL has developed a method of bonding ceramics to metals using a titanium hydride technique which is suitable for applications that must withstand extreme thermomechanical loads. The CRADA combines the contributions of Saphikon, which include the sapphire material, expertise in the design and testing of high-intensity lamps, and commercial manufacturing, with PPPL's existing knowledge and experience in bonding ceramic to metal. The goal is to develop a seal between the metal and the sapphire that can withstand intense conditions of high temperature, thermal shock, and operation under a vacuum. Two of the advantages of the new high-intensity lamps are that the source of light will be less yellow than present sources and that the source of illumination will approach a point source of light. Applications for the high-intensity lamps, which can operate as high as 35,000 watts, include rapid thermal drying, lithography, and robotic recognition of circuit boards by TV cameras. This CRADA will be concluded in FY95.

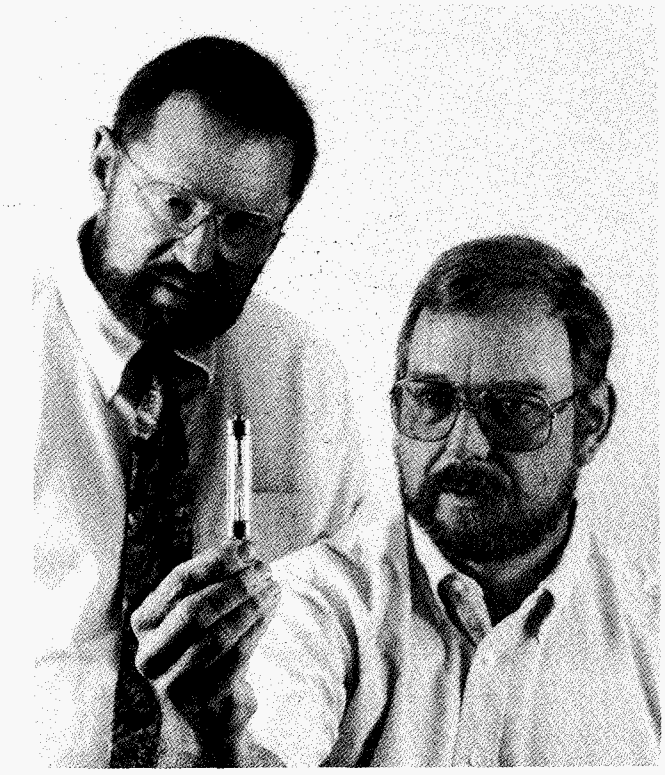

Figure 1. *A sapphire-to-metal bonding technique to produce a firm seal for the end caps of high-intensity lamps is being developed through a PPPL CRADA with a small business in New Hampshire. (PPPL #94A0457)*

Plasma Chemical Synthesis

PPPL's second CRADA, with a major chemical company, is to explore the potential for synthesizing a chemical of proprietary interest and with commercially viable purity and yields. The CRADA supports a proof-of-principle study in which a small-scale reactor will be constructed and a plasma composed of the feed stock chemicals created. In the microwave-heated moderate pressure 1-10 Torr plasma, energetic electrons dissociate the feed stock chemicals. The study will determine the optimum conditions for the dissociated products to recombine into the chemical of interest. The dissociated species will be monitored using plasma spectroscopy. The chemical produced will be analyzed to determine which chemical reaction paths are in play, the process efficiency, and the optimization of quality and yield. Much of the reactor was constructed during FY94. Initial tests are expected in early FY95.

Chemical Tracking and Report Generating System

This CRADA is for the enhancement of the Chemical Tracking and Report Generating System developed at PPPL and its upgrading for commercial applications. This computer application can provide industrial users of chemicals the means to generate all of the necessary Environmental Protection Agency state and federal forms, and the capability to track all information regarding the purchasing, storing, and use of chemicals. The industrial participant is Vertére Inc., a small woman-owned business located in Rhode Island.

Advanced Computer Modeling Environment Project

This CRADA is for the development of a high-level computational environment that allows diverse computational modules to be rapidly and easily integrated into a computer model by the end user. Applications exist both in the fusion energy program and the commercial sector. The industrial participant is Dynamic Research Corporation. This CRADA is expected to be completed in early FY95.

Advanced Computer Modeling AMBER and SAGE

This CRADA is for the development of an advanced computation modeling environment which will

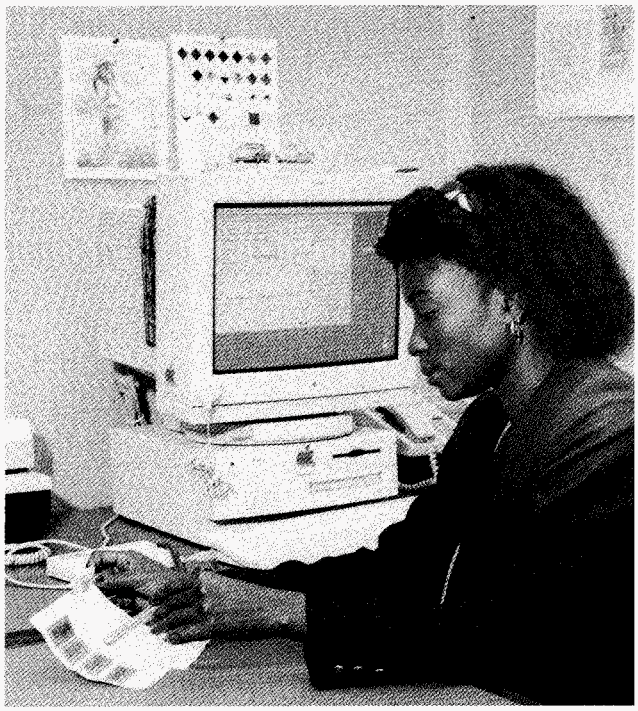

Figure 2. *Bar coding allows the tracking of chemicals "from cradle to grave" via a software package being developed through a CRADA between PPPL and a small woman-owned business. (PPPL #94A0371)*

allow users of existing modeling programs written in various languages to integrate those programs into a single modeling environment using two of the industrial partner's programs AMBER and SAGE. Applications exist both in the fusion energy program and the commercial sector. The industrial participant is Dynamic Research Corporation. This CRADA is a three-year effort which was started in FY94.

Investigation of Electron Beams in Air

This CRADA is with a small business, "Charged Injection Corporation." It is for the development of theoretical models for use in designing equipment for spray coatings and other applications in which electrostatically charged particles are directed in an electromagnetic field. Applications exist in the automotive industry and other industrial processes. A new experimental facility has developed from this CRADA.

Investigation of Tokamaks as a Source of Radiation for Lithography

Negotiations for the terms of this CRADA with the small business Applied Physics Technology and the Massachusetts Institute of Technology were held during FY94. This is PPPL's first three-way CRADA. The Project is for developing and evaluating techniques and optics to obtain radiation from fusion research plasma devices known as tokamaks and for determining the optimum wavelengths usable for lithography applicable to the manufacture of integrated circuits.

Personnel Exchanges

Two Personnel Exchanges, funded by Energy Research-Laboratory Technology Transfer (ER-LTT) were initiated in FY94.

- Two electronic engineers from PPPL worked at the David Sarnoff Research Laboratory on designs related to single integrated circuit power supplies for industrial florescent lighting and other remote power distribution techniques. The engineers applied their knowledge and experience of digital feedback techniques to the project.
- PPPL Engineering Analysis Division staff participated on a project at AT&T Bell Telephone Laboratories, Murray Hill, New Jersey, to develop computer codes for the design of magnetic-field trajectories for electron beam etching of integrated circuits.

Technology Maturation Project

The PPPL has initiated funding through the ER-LTT program for a Technology Maturation Project in conjunction with Caltech to investigate magnetic-field techniques to stabilize the electric arcs in electric arc furnaces. The techniques are similar to those used to control the plasma position in fusion machines. A small-scale experiment, to simulate an electric arc furnace, has been constructed at PPPL for initial studies. Asea Brown Boveri is the industrial partner.

Licensing

The Office of Technology Transfer actively promotes the licensing of inventions and software through the Princeton University Office of Research and Technology Assessment. Two technologies were licensed in FY94.

- A license was negotiated with the American Institute of Physics for the use of the software XMACRO. XMACRO was developed at PPPL to transmit documents in which many equations are embedded.
- A license was negotiated with the Laboratory's CRADA partner Vertére for the Chemical Waste Tracking and Report Generating System software. The software was developed at PPPL to track and report chemicals on-site at the Laboratory.

Princeton University has retained the rights for future licensing for a PPPL-invented high level nuclear waste containment system and an associated weld technique. United States and foreign patents have been filed on both technologies, and a licensing and marketing company has been retained to commercialize the technology. British Technologies Group (BTG) has elected to manage the technologies under their Technology Transfer Enabling Agreement of August 1991 with Princeton University. The BTG has filed the foreign patents (at its expense) and is active in the marketing, licensing, and commercialization of the technologies. Presently, talks are being held with two major industrial companies. Now that this technology has been waived to Princeton University, the Laboratory is no longer able to support its development under the Technology Transfer program.

Small Business Contacts

Another method of enhancing U.S. competitiveness through technology transfer is work with small businesses in the local area. The PPPL Office of Technology Transfer has maintained contact with the Small Business Development Center in New Jersey, the Corporation for the Application of Rutgers Research, and the Technology Executives Roundtable (a forum for the owners of small high-tech businesses in central New Jersey). Typical areas in which the PPPL Office of Technology Transfer has played a role with small high-tech business is to make them aware of the technologies available from PPPL, as well as the access they have through the PPPL Office of Technology Transfer to the Federal Laboratory Consortium for specific help solving technical problems.

Another mechanism for PPPL to enhance the technology transfer activities of small business is through Small Business Innovative Research (SBIR) Partnerships. PPPL provided technical support for four SBIR submissions in FY94. Lodestar Research Corporation of Boulder, Colorado, who was granted an award for ponderomotive feedback stabilization for control of external kink modes and disruptions in tokamaks, conducted research at PPPL on its project in fiscal year 1994.

A new mechanism for PPPL to interact with small business is the DOE Small Business Technology Transfer Program (STTR) program. This year, PPPL had three submissions with small businesses for the fusion-related portion of the STTR solicitation.

NASA Center for Technology Commercialization

The National Aeronautics and Space Administration's (NASA) New Jersey Center for Technology Commercialization (CTC) grew in size and activity in FY94. The CTC, which is funded by NASA and for which PPPL provides the facilities, visits companies around the state of New Jersey, as well as attending state and federal meetings and programs, to augment technology transfer efforts using resources and databases developed by NASA. The NJ CTC sponsored a successful Advanced Materials Technology Fair at the David Sarnoff Research Center in Princeton in April, 1994, and held a well-attended symposium on Defense Conversion in June, 1994. One of the major efforts of the CTC office in FY95 will be to promote the Technology Reinvestment Program, in which military technology is converted to peaceful uses.

Major Marketing Meetings

In FY94, three marketing conferences were attended:

- NASA Technology 2003, Technology Transfer Exhibit, Anaheim, CA.
- Technology Transfer Conference, New York, NY.

Patent Awareness Program

The primary vehicle for protection of the intellectual property associated with technological developments at PPPL is the Patent Awareness Program. The Committee on Inventions has as its charter the fostering of disclosure of inventions and the copywriting of software. This is done by raising the consciousness

of the staff to the value of intellectual property by providing appropriate recognition and modest monetary rewards to the inventors. Twenty-two invention disclosures were filed (see PPPL Invention Disclosures for Fiscal Year 1994, page 189) in fiscal year 1994 and forty-six staff members shared in the distribution of $4,700 in incentives.

Three patent applications were submitted in FY94.

- Direct Current Sputtering of Boron from Boron/Carbon Mixtures.
- Method of High Level Radioactive Waste Management.
- Lower Hybrid Current Drive in Tokamak Reactors Using Alpha Particles.

Also, in FY94, three patents were issued:

- Method and Apparatus for Welding Precipitation Hardenable Materials.
- Means for Positively Seating a Piezoceramic Element in a Piezoelectric Valve During Inlet Gas Injection.
- Apparatus and Method for Uniform Microwave Plasma Processing Using TE_{11} and TM_{01}.

Figure 3. *PPPL staff who have filed invention disclosures through the Patent Awareness Program in FY94. (PPPL #94PR040-2A)*

Environment, Safety, and Health and Quality Assurance

Environment, Safety, and Health

In fiscal year 1994 the Environment, Safety, and Health (ES&H) Division responded to self-assessments, unresolved Tiger Team audit findings, Department of Energy (DOE) audits, and ES&H issues dealing with an active Deuterium-Tritium (D-T) Program on the Tokamak Fusion Test Reactor (TFTR). Also, ES&H support was provided for planning and design efforts for the TFTR Shutdown and Removal (S&R) and Tokamak Physics Experiment (TPX) projects. The ES&H documents were updated, and the ES&H internal document control system was expanded to meet new requirements. Environmental issues continued to be a high priority. Environmental status and monitoring were reported to the DOE and to the general public through the 12th Annual Site Environmental Report.[1]

The ES&H staff stabilized in 1993 but was decreased in 1994 due to funding shortages. The decrease came in industrial and occupation safety staff (1), electrical safety staff (1.5), clerical (1), and health physics (2). The remaining staff worked extra hours required by a very busy D-T program.

The ES&H staff participated in and attended many DOE workshops and conferences on topics such as the National Environmental Policy Act (NEPA), Occupational Safety and Health Administration (OSHA), and DOE Energy Research Environment, Safety, and Health, so that the DOE philosophy and changing policy and programs can be quickly implemented into the Princeton Plasma Physics Laboratory (PPPL) culture. The ES&H Division staff also participated in the PPPL Educational Outreach Programs. This included providing safety input for Trenton schools as part of a partnership on science in education with the Trenton school system.

Commitment to the technical community was demonstrated by the ES&H staff's active participation in professional and governmental committees such as the New Jersey State Commission for Regulating Utility Transmission Lines, and as a member of the National Fire Protection Association Technical Committee for Electrical Equipment, the Health Physics Society Standards Committee, the DOE Training and Resources Data Exchange, the New Jersey Low-Level Radioactive Waste Disposal Facility Siting Board, Joint Working Groups between the U.S.-Japan and U.S.-Russian Federation on safety in the transfer of collaborators and equipment in fusion-related projects, and the DOE-sponsored Fusion Safety Standard Steering Committee. In addition, a tutorial article on fusion was written for the radiation protection community,[2] research into future tritium accountability methods using calorimetry were studied,[3] and standards development processes were participated in and reported on.[4,5]

Safety

The Industrial Safety Branch is staffed by an Industrial Safety and OSHA Engineer, Construction Safety Engineer, and an Area Safety Coordinator/Cognizant Area Supervisor (ASC/CAS) Program Coordinator and Trainer. The tasks assigned to this group remained active due to a busy D-T schedule. As the key OSHA compliance arm of ES&H, the staff must be cognizant of industrial hygiene, electrical, environmental, hazardous materials, health physics, and fire protection issues.

The ASC/CAS program continued to provide the main focus for line-safety responsibilities. A total of four new training courses were developed and presented to the line-safety organization. Areas covered included back safety, office ergonomics, bloodborne pathogens, and emergency evacuation and response

training. Other training was wholly developed or partially developed for the Laboratory in machine guarding, back safety for material handlers, laser safety, general employee training, ladder safety, forklift safety, lockout and tagout, and lead safety. This year ASCs also participated in one-on-one consultations with the ASC/CAS Program Coordinator, as needed, to provide support and technical assistance.

The ASC/CAS incentive program continued with the third annual recognition luncheon for all ASCs and CASs (Fig. 1). In addition, two ASCs attended the National Safety Council Convention and Exposition and DOE's Occupational Safety program, held in conjunction with the National Safety Council meeting. The incentives are provided to line-organization personnel who make a special effort to ensure the safety of fellow employees, Laboratory property, and the environment.

Industrial Safety Branch staff are also active members of the Princeton University program for assisting local schools. Assistance was provided to local high schools in the areas of hazardous material control and bloodborne pathogen safety.

Figure 1. *Eight PPPL Department Award Area Safety Coordinator winners received plaques recognizing six PPPL departments. Winners, from left, are Gerald Satkofsky (TFTR Project), William Persely (Engineering Department), George Peak, Jr. (Miscellaneous Groups), Susan Pontani (Engineering Department), Michael Karl (Office of Resource Management), and Gloria Pollitt (Office of Human Resources and Administration). Department winners not pictured are Joseph Carson (Physics Department) and Joseph Frangipani (TFTR Project). At the podium is Joe Smith from ES&H. Joseph Frangipani and Susan Pontani were named ASCs of the Year and attended DOE's Third Annual Occupational Safety and Health Conference and the National Safety Council Congress and Exposition. (94PRO45-33)*

The Occupational Safety section of the ES&H Manual for PPPL had been finalized, with 13 chapters rewritten and two new chapters added. Due to changes in OSHA regulations and DOE policy, the Personnel Protective Equipment and Machine Guarding chapters will be reissued in early FY95.

The annual DOE Occupational Safety and Health inspection found ten deficiencies (six findings and four recommendations). This is a stark contrast from the FY92 and FY93 inspections—126 findings in FY92, 30 findings in FY93. These improvements may be largely credited to the efforts of the Departmental Safety Officers (DSOs), CASs, and ASCs. At the conclusion of FY94, there were approximately 160 open items in the Laboratory ES&H deficiency reporting system. This was an improvement from the approximately 280 open items earlier in the year (and 600 the year before).

The ES&H Division's Industrial Safety Branch provided oversight and offered cost-effective alternatives for Lab-wide issues. Examples include reducing paperwork for accident investigations, obtaining Federal Aviation Administration concurrence for the discontinuance of costly maintenance of the water tower warning lights, and receiving DOE-Chicago concurrence concerning guarding of belt sanding equipment, metal sawing machines, abrasive wheel equipment, and woodworking machines. This latter item was a significant milestone to establish a mutually agreeable criteria between PPPL and DOE concerning machine guarding policy. It is anticipated that all Tiger Team findings concerning machine guarding will be closed in FY95.

The Construction Safety Engineer oversaw such projects as lining of the detention basin, installation of above-ground fuel storage tanks and spill containment facilities, Ethernet cabling projects, site fire alarm system upgrades, Phase II parking improvements, upgrades to the decon facility, and initiation of the tritium purification system installation. In addition, Construction Safety personnel had a busy schedule with work-site inspections, bid reviews, and compliance assistance. The Construction Safety Engineer follow-up reporting system rates the subcontractors' adherence to safety on the job and reports violations found and corrected. This information has been used for overall bid evaluations made by the subcontractors on future projects. The Construction Safety Engineer continues to provide support to the Industrial Safety and Occupational Safety and Health Ad-

ministration Engineer in the Machine Guarding Assessment Project.

The Electrical Safety staff participated in design reviews and inspections of electrical installations. The staff produced requirements documents for safety and accident prevention tags and signs. Electrical Safety and RF (radio-frequency), Microwave, and Magnetic Field sections of the ES&H Manual were upgraded. The staff took part in RF leakage and magnetic-field-strength surveys. Biannual in-service reinspections of stored-energy systems and recertification of their accessors continued, as did reinspections of the facility's active personnel safety-interlock systems.

The Electrical Safety Engineer participated on the technical committee of the National Fire Protection Association (NFPA), which completed a pilot program to harmonize the 1994 version of NFPA79, "Electrical Equipment of Industrial Machinery," with its corresponding international Electrotechnical Commission Standard (IEC 240). Audits were conducted of the line organization to assure compliance with electrical safety requirements. The Electrical Safety Program was audited by DOE-Headquarters and was found to be adequate.

The Electrical Safety staff submitted to the Principal Deputy Assistant Secretary for ES&H, DOE, a number of recommendations for areas of research to be conducted on the effects of electromagnetic-field exposure to humans. An electrical staff member participated as a member of the state of New Jersey Non-Ionizing Radiation Commission for the regulation of distribution and transmission electric power lines.

The 4.8 million dollar Fire and Life Safety Improvement Project continued in FY94. As of October, 1994, the sprinkler, fire barriers, and life-safety portion of the Project have been completed. The site-wide, fire-alarm reporting system work continues with a mid-1995 projected completion date. The Fire and Life Safety Improvement Project has resulted in all major buildings of the Laboratory being protected with at least sprinklers and has permitted the Laboratory to reduce the number of Halon fire suppression systems from 30 to 11, with a final reduction to six Halon systems planned in 1995.

Environment and Health

The Nuclear and Environmental Engineer continued to coordinate ES&H reviews of all proposed changes to the TFTR configuration through membership on the TFTR Configuration Review Board, as well as changes to the TPX baseline design through reviews of TPX engineering change proposals. The National Environmental Policy Act (NEPA) reviews ensure that all existing PPPL activities and proposed new activities are reviewed for environmental considerations in accordance with NEPA and the implementing guidelines of the Council on Environmental Quality and DOE. Approximately 115 such actions received NEPA review during FY94.

Coordination of efforts continued for completion of the combined Environmental Assessment (EA) for the proposed Shutdown and Removal of TFTR and for the proposed Tokamak Physics Experiment (TPX) at PPPL.[6] This EA also addresses construction of a Radioactive Waste Storage Building for temporary storage of low-level radioactive waste prior to shipment off site and construction of a second detention basin for storm water management. Comments from DOE-EH on the EA were received and resolved. Review of the Environmental Assessment by the New Jersey Department of Environmental Protection (NJDEP) was completed and its comments were resolved. A Proposed Finding of No Significant Impact (PFONSI) was published in the *Federal Register* by DOE for a 30-day public review on October 5, 1994.

Support was provided for preparation of Amendment #3 to the TFTR Final Safety Analysis Report (FSAR).[7] The DOE's comments on FSAR Amendment #3 were received and resolved, and DOE approved this Amendment on October 4, 1994. Since Amendment #3 was prepared and issued to DOE for comment in January, 1994, about 160 Unreviewed Safety Question Determinations have been prepared by the Nuclear and Environmental Engineer in accordance with the requirements of DOE Order 5480.21.[8] Approved by the TFTR Project, these Unreviewed Safety Question Determinations document the review against the TFTR Authorization Basis of facility changes and changes to information and analyses affecting the TFTR Nuclear Boundary.

The Nuclear and Environmental Engineer coordinated with the Idaho National Engineering Laboratory Fusion Safety Group to produce a draft Preliminary Safety Analysis Report (PSAR) for the TPX. The draft PSAR for TPX was prepared in accordance with the "graded approach" outlined in newly issued DOE Standard 3009-94 on Safety Analysis Report preparation, and will be issued for DOE review in December, 1994.

Support was given in the revision and review of TFTR Procedure OP-AD-77, which prescribes the Operating Parameter Requirements for TFTR. These Operating Parameter Requirements help ensure that features (e.g., tritium monitors, HVAC, fire protection) designed to enhance the safety of TFTR during D-T operations will be operating or fully operational when needed.

Support was provided to the TFTR S&R Project in determining the applicability of requirements for preparation of applications to the Environmental Protection Agency (EPA) under the radionuclide National Emissions Standards for Hazardous Air Pollutants regulations. Support was also provided in the preparation of a draft TFTR FSAR Amendment #4 to cover S&R activities and in the determination of regulatory requirements for operation of an evaporator for the liquid effluent collection tanks.

The Environmental Section applied for modifications to the existing air permits for three boilers based on an inspection by the NJDEP in July, 1994. The boilers were modified to burn natural gas and fuel oil; however, the permit applications were not submitted to NJDEP at the time the modifications occurred. In FY95, modifications will be performed on the remaining boiler so that this boiler can burn natural gas and fuel oil, as appropriate.

Five underground storage tanks were removed under the guidelines of the NJDEP-approved Facility UST [Underground Storage Tank] Closure Plan. These tanks ranged in size from 1,000 to 30,000 gallons and contained diesel fuel, #4 fuel oil, and unleaded gasoline.

Halon inventories were submitted to the DOE/Princeton Area Office (PAO) through the PPPL Halon Phaseout Plan documentation and the Halon Repository Questionnaire. Nineteen of the 30 Halon systems have been decommissioned and total remaining inventories of Halon 1211 and 1301 are 1,140 and 9,191 pounds, respectively.

The New Jersey Pollutant Discharge Elimination System (NJPDES) surface water permit was approved and became effective on March 1, 1994. One surface and one storm water sampling locations were added to the permit (discharge serial number or DSN002 and DSN003, respectively); a requirement to conduct chronic toxicity monitoring studies for DSN001 was also added to the permit conditions.

Modifications to the detention basin began in August, 1994. These modifications included the installation of an impermeable liner, reconstruction of the outfall structure, and the placement of rip-rap in the receiving ditch (DSN001). These activities are expected to be completed in FY95.

The NJPDES quarterly ground water permit monitoring continued. Volatile organic compounds continued to be detected in three of the wells. The NJPDES ground water permit expires in December, 1994. In July 1994, PPPL and DOE submitted to the NJDEP the renewal application, which included a summary report on ground water quality from 1989 to 1993.

Freshwater Wetlands Applications for fire main installations, the Hazardous Materials Storage Building Upgrade Project, and maintenance around the 26-kV tower were submitted to NJDEP in accordance with its Letter of Interpretation on the PPPL wetlands boundaries.

In accordance with DOE Order 5400.1 (Programs and Plans), an Environmental Protection Implementation Plan (EPIP) was updated and issued; the 1993 Annual Site Environmental Report[1] was prepared; and the Environmental Monitoring Plan is undergoing revision.

The Industrial Hygiene Section revised the confined-space training program to reflect the changes in the permit-required confined-space program and upgraded the handling and procedures surrounding the issuance of permits to improve efficiency and emphasize compliance with record-keeping issues.

The baseline sampling program was continued into FY94 and was included as an integral part of the overall Industrial Hygiene Program. The Lab-wide Job Hazard Analysis Program was pushed into the forefront of industrial hygiene activities and is expected to be completed in mid-1995. An industrial hygienist was assigned the Job Hazard Analysis Program as a primary duty to ensure the priority is maintained and the project remains on schedule. New requirements for OSHA, including the survey for use of personal protective equipment and training requirements, have been incorporated into the Job Hazard Analysis Program.

Industrial Hygiene staff participated in numerous design reviews and oversight of projects. The chemical and waste management tracking and report-generating system is in the process of being implemented Lab-wide and will be designed to co-exist with existing procurement and materiel control systems to ensure ease of use and comprehensive inclusion of all

chemicals brought on-site. Designed by PPPL, the system is comprised of software packages for personal computers and will be available on-line across the PPPL network.

The Hazard Communication Program was streamlined to include improvements in record keeping and training. The Material Safety Data Sheet (MSDS) tracking system was upgraded in FY94 and includes the placement of more than 50 Right-to-Know Information Stations throughout the Laboratory. Stations are controlled to provide constant updates for the MSDSs and indexes.

The Industrial Hygiene section began a proactive look into indoor air quality at PPPL. The program includes survey and inspection forms, as well as questionnaires for the personnel in areas of concern. Site-wide surveys of indoor air quality concerns have begun. The local Exhaust Ventilation Certification Program was strengthened to include requirements for monitoring of TFTR elephant trunk systems. The Respiratory Protection Program was expanded to include the potential use, as well as maintenance and inventory, of fully encapsulated (bubble-suit) airline respiratory protection.

The chemical procurement process was improved to enhance traceability and to decrease turnaround time. The Superfund Amendment Reauthorization Act (SARA) Title III and Toxic Release Inventory reports were filed (Toxic Release Inventory for the first time, as per DOE requirement). Industrial Hygiene personnel participated in HAZWOPER (Hazardous Waste Operations Training) and additional confined-space entry training. Industrial Hygiene training has been further strengthened with improvements to all courses, including the General Employee Training Program.

Health Physics

During FY94, The Health Physics Branch provided oversight and support to PPPL projects in the areas of training, material control and accountability (MC&A) of nuclear materials, radiation measurements, field operations, radiological environmental monitoring, and radioactive waste operations.

Support of TFTR tritium operations was a major function of the Health Physics Branch. Operational methods for monitoring tritium airborne and surface contamination were proven to be effective in assessing operations and maintaining excellent radiological performance indicators. Laboratory personnel have gained valuable experience in the safe handling of tritium and operations and maintenance of tritium systems.

The first full-power series of D-T plasmas in December, 1993, resulted in world-record fusion power levels, which led to even greater accomplishments during FY94. The Health Physics Branch staff performed extensive radiation measurements in support of D-T experiments, which characterized the radiation profiles at the TFTR site and verified the adequacy of shielding of the TFTR machine, the safety of PPPL personnel and the public, and compliance with regulatory requirements. Additional areas of new health physics operating experience included occupational differential tritium analysis, tritium internal dosimetry, activated air measurements, and radiological profiles of D-T neutron-induced activation products. All of these "lessons learned" provided information relevant to future D-T fusion devices and to tritium technology.

The Radiological Environmental Monitoring Laboratory (REML) monitored air, water, soil, sod, and biota with tritium and gamma spectroscopy analyses during FY94. Additionally, a sample oxidizer was commissioned that measures tritium concentrations in materials such as oils and solids, which are combustible. This capability greatly enhanced the analytical capability of the REML for quantifying tritium concentrations in media. The REML continued to verify the environmental attractiveness and safety of fusion technology.

The Calibration and Service Laboratory personnel calibrated, maintained, and serviced tritium process, area, and stack monitors, which were an essential element in support of safe D-T operations. Experience with activated air monitoring in the presence of tritium provided valuable experience relevant to future D-T fusion devices.

The PPPL material control and accountability program tracked and accounted for approximately 350 kiloCuries (kCi) of tritium, which was used to fuel the TFTR during D-T operations. The PPPL program was the first implemented for a D-T fusion facility and has been optimized for fusion technology. This program determines how much tritium is in the TFTR vacuum vessel and ensures compliance with regulatory requirements.

Training was a continued process at PPPL to ensure that personnel working in radiologically con-

trolled areas had the greatest level of knowledge about conduct of operations and radiation safety. As evidenced by the excellent radiological performance indicators, the training programs have been highly effective.

The Radioactive Waste Program completed a successful audit by the disposal site during FY94 and retained authorization from the disposal site to ship waste. This program was instrumental in maintaining a site inventory of tritium that met regulatory requirements.

Quality Assurance and Reliability

The Quality Assurance and Reliability (QA/R) Division is organized into two branches: Quality Assurance and Quality Control.

Quality Assurance

Quality Assurance, with more than 150 years of technical experience including more than 110 years of quality experience, is available to assist senior management in the establishment of Laboratory-wide quality programs; assist projects to establish project-specific quality programs; assist cognizant personnel to assure that the required quality of their procurements are met; assist PPPL to assure that the Laboratory's systems meet requirements specified in federal and state laws and regulations, DOE requirements, and PPPL policies and procedures; and to assist PPPL to assure that the implementations of these systems are effective, from risk, quality, and cost-benefit perspectives.

Institutional QA Plan

Work began on the revision of the PPPL Institutional QA Plan to reflect the requirements of 10CFR830.120, Nuclear Safety. This rule is part of the Price Anderson Act Amendments applicable to TFTR as a nuclear facility. The revised Institutional QA Plan and its associated Implementation Plan describing PPPL's status with respect to these requirements and any future actions necessary to meet the requirements are due at DOE in November, 1994.

Tracking and Trend Analysis System

The tracking and trending system established in 1992 continued throughout FY94. This system including the mailing of open item status to assigned individuals and their managers and the monthly tracking and trending report.

TFTR Availability Analysis

Fiscal year 1994 was an excellent year for the operation of TFTR with the introduction of tritium. Other sections of the Annual Report describe the results. For FY94, the availability was 80.5%. The system availabilities are given in Table I.

Figure 2 is a plot of TFTR availability versus time from October 1984 until September 1994.

Table I.
TFTR Systems Availability for Fiscal Year 1994

AC/MG	97.1%
Computing	97.4%
Diagnostics	98.9%
Energy Conversion System	97.1%
Neutral Beams	96.5%
Radio-Frequency	99.6%
Tokamak	92.7%

Procurement Quality Assurance

Work continued on enhancements to the QA database in order to assist cognizant engineers and others in applying standardized quality assurance and inspection requirements to major and critical procurements.

Auditing of vendors providing critical environmental, safety, or health services continued in FY94.

- Two hazardous waste transporters, storage, and disposal facilities were audited under a program established in FY92 to make sure that PPPL's responsibility for hazardous waste is properly assured.
- One analytical laboratory was audited under a program, established in FY92, to assure compliance with established federal and state regulatory protocols.
- Two ground water sampling operations were surveilled under a program instituted in FY93 to assure the identification and traceability of

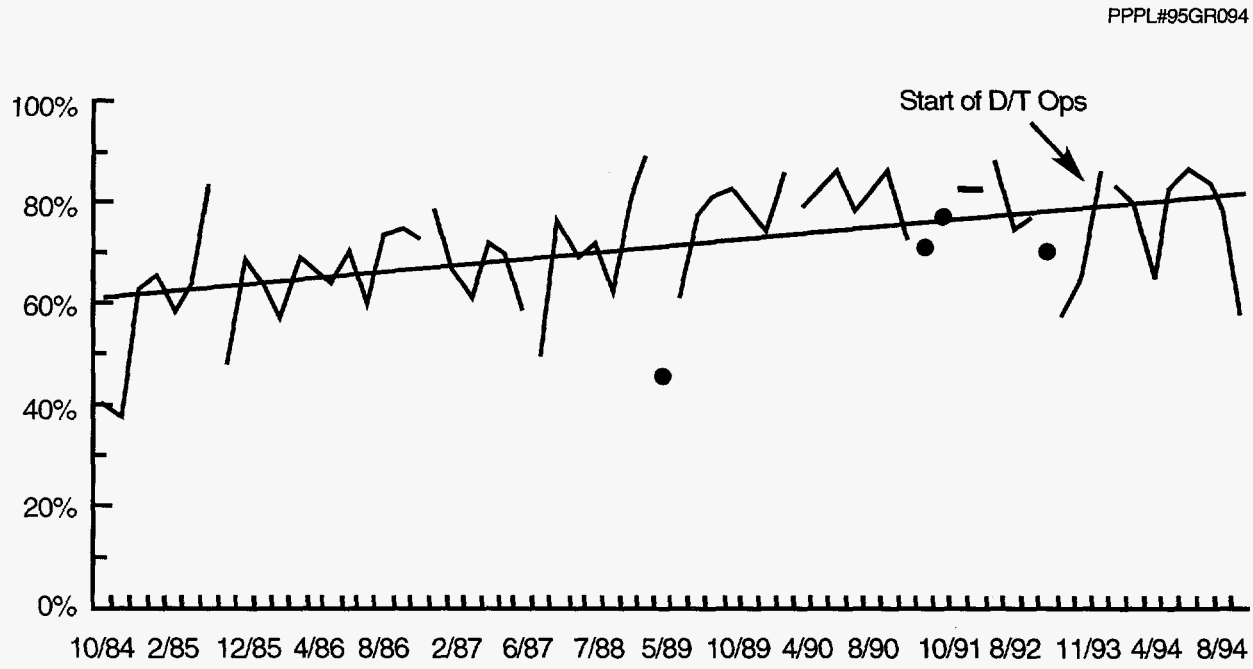

Figure 2. *Long-term TFTR availability chart from 1 October 1984 through 30 September 1994. The straight line represents the long-term trend of TFTR availability for this period. Machine openings are indicated by the breaks in the actual TFTR availability. Experimental run periods contained within one calendar month and preceded and followed by openings are represented by a dot. The beginning of deuterium-tritium operations is indicated.*

samples from the time a sample is obtained by subcontractor site personnel to the final analysis report issued by the analytical laboratory.

- A post-award survey was performed on a provider of computer software for characterization of radioactive waste material generated at PPPL, as well as tracking of radioactive material, auditing of radwaste shipments, and providing required documentation for shipments.

Quality Assurance staff reviewed Statements of Work and evaluated bid packages by hazardous waste shipping container fabricators for QA provisions and performed QA activities including pre-award and post-award surveys and several follow-up visits of high integrity container fabricators. A pre-award survey of a Type-A container fabricator was performed for application during TFTR Shutdown and Removal activities. Quality Assurance staff reviewed statements of work and evaluated bid packages by low-level radwaste volume reduction vendors.

The PPPL QA has become actively involved with the Supplier Quality Information Group (SQIG) that promotes sharing and standardization of supplier evaluation information throughout the DOE Complex. Currently, there are seventeen DOE contractors participating in the SQIG who have performed hundreds of supplier evaluations. The ability to share information and capitalize on cost savings is promoted by SQIG. Recently, PPPL QA saved about $3,000 using SQIG vendor data. The PPPL also benefits by participation in quarterly SQIG meetings held at various DOE contractor sites by providing a forum for networking, discussing lessons learned, and developing best industry practices for the future. Recently, QA staff attended the Standardization of Analytical Laboratories Evaluations (SALE) Workshop. The SALE is a working group of SQIG that has been developed to standardize analytical laboratory evaluations for DOE contractors.

Quality Assurance staff performed reviews of Statements of Work and specifications for TPX, performed pre-award evaluations of the proposed subcontractors, and were actively involved in Special Procurement Evaluation Boards. Reviews of subcontractor's QA programs and procedures were also performed on behalf of TPX. Subsequently, QA arranged and conducted a meeting at the TPX Project with the major subcontractors Ebasco Division of Raytheon Engineers and Constructors, Inc., and

General Atomics, and subtier vendors McDonnell Douglas and Rocketdyne, on the QA approach for the vacuum vessel and plasma facing components.

TPX Quality Assurance

Progress, although at a slower rate than planned due to funding changes, continued on the Tokamak Physics Experiment. The QA engineer assigned to the project as TPX Quality Assurance Manager has moved into the project office building. The percentage of time spent on TPX Project activities has gradually increased to roughly 90% of his time.

A TPX Project QA Plan was approved by the DOE Princeton Area Office and issued in December 1993. This is the highest level in the project's QA documentation hierarchy. Work is progressing on the next tier, the TPX Participant (Lawrence Livermore National Laboratory, Oak Ridge National Laboratory and PPPL) QA Plans. These plans describe the systems used at each laboratory to meet the requirements of the TPX Project QA Plan. All of the TPX Participant Plans are progressing toward issuance by the end of CY94.

Quality Assurance personnel have been working as advisors to the Subcontract Proposal Evaluation Boards established for the major subcontracts and as reviewers of the Statements of Work. Two of the major PPPL contracts, one for design of the vacuum vessel and the other for design of the plasma facing components, were awarded to industry teams in FY94. Both the TPX Quality Assurance Manager and QA personnel have been working with the prime and secondary contractors to ensure that acceptable quality programs are implemented for these contracts.

A third major PPPL contract, to be issued in FY95, is for Systems Integration Support. This contractor will establish and manage most of the centralized control systems such as document control, drawing control, configuration management, and design integration. The TPX Quality Assurance Manager has been working with TPX Systems Engineering and Project Control to define and establish interim systems and to develop the procedures for these systems. He has been active in the effort to define TPX Project standards that are intended to obtain acceptably consistent output from the diverse project collaborators.

There were two quality assessments of the TPX Project in FY94. Tokamak Physics Experiment Project Engineering and Design was audited by PPPL Quality Assurance toward the end of April. This audit resulted in one finding concerned with the lack of documented TPX procedures. The DOE-Chicago Office included TPX design and program development in their annual assessment in May. This did not result in any actions for TPX.

Quality Audits and Surveillances

Five internal audits on PPPL systems and five vendor audits were performed in FY94. The internal audits included Health Physics, Environmental Program Compliance, TPX Engineering Systems, Welding Program, and the Emergency Preparedness Program. Two surveillances (mini-audits) were performed — the log keeping for the Material Test Equipment calibrations and surface water sampling performed by PPPL staff.

Quality Control

Quality Control (QC) is responsible for on-site inspections of installations on research devices, fabrication inspection of critical components in shops, inspections of facility-related work, receiving inspections of components fabricated by vendors, mechanical calibration of tools for eleven shops within the Laboratory, and nondestructive examinations of material and lift equipment at PPPL. The QC Staff, with more than 130 years of technical inspection experience and more than 50 years of construction and electrical design experience, is available to assist cognizant personnel to assure compliance to required codes and safety requirements.

Work Permits

The TFTR Work Permit System requests Quality Control to verify that: (1) all work performed in the Test Cell and Tritium Area follows procedures and is approved by TFTR Operations prior to implementation, (2) the system and location where the work will take place is identified, (3) the lead person and individuals performing the work have been identified, and (4) the work is inspected upon completion to assure that it has been performed correctly and that all tools have been removed from the work area. Quality Control was involved with approximately 1,590 work permits during FY94.

Inspection Activities

Inspection activities are based on the importance of the task being performed. Due to limited resources, unless special requests for inspection services are re-

ceived, only those items considered to be critical are inspected. In order to evaluate the importance of the task, a Risk Assessment Plan (RAP) is generated for each job. Within the RAP a determination is made whether to perform an inspection and if so, what type of inspection. In some cases, only a final inspection is performed, while in other cases the task is inspected as the operation proceeds. In FY94, one hundred ninety-two Risk Assessment Plans were generated by Quality Control.

One-hundred and twenty-one RAPs were generated for the TFTR Project in FY94. Quality Control responsibility for these tasks required daily monitoring during ongoing activities, weld inspections, termination inspections, torque verification, testing verification, assuring compliance to procedures and drawings, and final walk-down inspections. Major activities included inspection activities for Tritium Gas Injection System for D-T operations and inspection and traceability documentation for the Type A and B Disposable Molecular Sieve Bed Drums.

Fabrication shops throughout the Laboratory are monitored on a daily basis. Inspection plans were developed for critical components being fabricated as part of the work request system and special processes performed during the fabrication. Included in this was the verification by Quality Control that all code welding throughout the Laboratory is performed by qualified welders using qualified procedures. Approximately 200 weld inspection reports were documented consisting of approximately 1,900 welds that were inspected. Most of the welds were for tritium-related work and the Disposable Molecular Sieve Bed Drum Project.

Quality Control inspections are also conducted on Facility Construction Branch projects. During FY94, fifteen RAPs were developed requiring the following types of activities: concrete inspection and testing, weld inspection, electrical and mechanical system testing, and final inspections.

Inspection of critical vendor components is performed either at PPPL Receiving Inspection or at the vendor's site. In FY94, fifty-five RAPs for vendor inspections were generated. One hundred and fifteen material inspection reports were made for the parts that passed through Receiving Inspection. Quality Control performed "in-process" inspections at the vendors site when requested.

Finally, the PPPL Lift Program requires Quality Control involvement for visual inspection of lifting equipment (hooks and lifting fixtures), witnessing of critical lifts, and load testing lifting equipment.

Nonconformances

Whenever inspections identify a process or work performed differently than specified in drawings, procedures or specifications, a nonconformance report is generated. A total of 84 nonconformance reports were generated in FY94, including 16 for material and items supplied by vendors. A total of 204 lots with 9,913 pieces were inspected at PPPL Receiving. Table II shows the number and types of nonconformances for FY94.

Table II.
Type and Number of Nonconformance Reports in Fiscal Year 1994.

Type of Nonconformance Report	Number in FY94
Deviation from Documents or Procedures	16
Workmanship Problems	13
Out of Tolerance	39
Identification or Control of Items	3
All Others	11
Total	82

Mechanical Calibration

Quality Control is responsible for the calibration and maintenance of all mechanical inspection devices throughout the Laboratory site. The calibration is typically performed on a quarterly basis during the operational period of TFTR when inspection activity is reduced. During FY94, a total of 398 items were cleaned, calibrated, and adjusted as necessary.

Certification and Training

In addition to the PPPL regularly sponsored courses such as Radiation Protection or Confined Space, the following courses were taken:

- One mechanical inspector was trained and certified as an American Welding Society Weld Inspector.

- Two inspectors went to a DOE sponsored National Electric Code inspectors certification course in Dallas, Texas.
- One quality engineer received training on the DOE Performance Indicator Database System from EG&G Idaho.
- Two quality engineers received International Standards Organization audit training.
- One quality engineer attended the DOE Environmental Audit and Assessment seminar.
- One quality engineer took a one-day course in requirements for underground storage tanks in preparation for the environmental audit.

In addition, some staff members completed college-level courses on their own time in order to increase their skills and knowledge base.

References

[1] V.L. Finley and M.A. Wieczorek, "Princeton Plasma Physics Laboratory (PPPL) Annual Site Environmental Report for Calendar Year 1993," Princeton University Plasma Physics Laboratory Report PPPL-3043 (January 1995) 146 pp.

[2] J.R. Stencel, J.D. Gilbert, J.D. Levine, and G. Ascione, "Radiation Protection Aspects of Fusion Reactors," Radiation Protection Management, Vol. 11 (July/August 1994) 27-52.

[3] J.A. Mason, N. Bainbridge, and J. Stencel, "Isothermal Calorimetry and Tritium Accountability," in *18th Symposium on Fusion Technology*, Karlsruhe, Germany, August 1994, to be published in proceedings.

[4] J.R. Stencel and S.Y. Chen, The HPSSC Standards Process, Presentation made at DOE Technical Standards Program Workshop, October 1994.

[5] J.R. Stencel, and S.Y. Chen, Activities of HPS Standards Committees in Environmental Remediation, Presentation made at American Nuclear Society Winter Meeting, Washington, D.C., November, 1994, to be published in ANS proceeding.

[6] Environmental Assessment, "The Tokamak Fusion Test Reactor Decontamination and Decommissioning Project and the Tokamak Physics Experiment at the Princeton Plasma Physics Laboratory," DOE/EA-0813, May 1994.

[7] Final Safety Analysis Report, Amendment No. 3, "Tokamak Fusion Test Reactor," DTSD-FSAR-17, October 1994.

[8] U.S. DOE Order 5480.21, "Unreviewed Safety Questions," 1991.

[9] J.A. Malsbury, presentation at the Fifth Annual Workshop on Management in Basic and Applied Research Environments, Tucson, Arizona, September 1994.

Office of Human Resources and Administration

In FY94, the Office of Human Resources and Administration continued to devote considerable effort in support of the Tokamak Fusion Test Reactor (TFTR) Project, with particular emphasis upon a proactive Public Relations Program to heighten the public's awareness and attention to the outstanding deuterium-tritium experimental program that resulted in the attainment of nine megawatts of fusion power in May of 1994.

The Laboratory produced and distributed a video news release (VNR) reporting the first successful high-power results in December, 1993. The VNR reached approximately fifty-seven million viewers; it was the second most heavily viewed VNR in the United States for 1993.

As a result of the planned extension of TFTR operations, an extensive effort has continued in the training, qualification, and certification of TFTR Operations personnel.

Human Resources implemented a Voluntary Separation Program and a voluntary and involuntary Reduction-In-Force during the course of the fiscal year.

Emergency Services worked closely with the Princeton Area Office (PAO) of the Department of Energy (DOE) in creating fire protection response criteria comparable to recommendations of the National Fire Protection Association, while continuing to downsize and reduce the cost of operations.

The Laboratory Directorate instituted a series of Council retreats geared toward Management Skills Development, and management operations issues within the Princeton University Plasma Physics Laboratory (PPPL). The retreats were highlighted by a two and one-half-day program in Stephen Covey's "'7' *Habits of Highly Effective People.*"

Finally, as a commitment toward promoting and maintaining the highest quality-of-life standards at PPPL facilities, the Laboratory announced that, effective November, 1994, all Laboratory buildings and vehicles would become smoke-free.

Occupational Medicine Office

The Occupational Medicine Office (OMO) staff performs standardized physical examinations, specific medical evaluations, and acute medical care in addition to providing a number of other wellness-related functions.

In FY94, OMO's participation in the monitoring and management of the Temporary Total Disability and Worker's Compensation Program increased. A DOE Audit of the OMO was conducted in March and no significant functional findings [deficiencies] were identified. Other OMO activities are highlighted below:

- A highly successful Blood Donor Drive was conducted in April, 1994, in support of the Regional Red Cross Program; there were fifty-one participants.
- A seminar on Stress Recognition and Stress Management was presented to PPPL employees through the Employee Assistance Program.
- A new vendor was contracted to provide better quality safety eye wear and improved service.
- A Diabetes Detection Program was offered. No new cases of diabetes were discovered among the thirty-seven participants.
- A Smoking Cessation Program was offered and conducted at the Laboratory in anticipation of the implementation of PPPL's No Smoking Policy on November 14, 1994. Twenty-five employees attended.
- Changing conditions and functions at the Laboratory resulted in the consideration to use the "Bubble Suit" as personal protective equipment. Other Laboratories where the "suit" is used

were surveyed, and selection criteria for personnel qualification were drafted.

Security and Emergency Preparedness

The Security and Emergency Preparedness Division continued its comprehensive "around-the-clock" support in the areas of security, fire protection, medical emergency response, and emergency management and planning. Emphasis was placed on providing a cost-effective and efficient organization in support of the Laboratory's major goals. Several projects were undertaken by the Division during FY94.

The Division worked closely with the Department of Energy (DOE) to develop fire protection response criteria consistent with the recommendations of the National Fire Protection Association. This work resulted in more comprehensive and efficient fire protection response criteria and reduced the cost of "day-to-day" Division operations.

The Division's upgraded "performance based" training program was fully implemented in FY94, further enhancing the skills of Division personnel. The Division also worked closely with Rutgers University to provide Hazardous Materials and Confined-Space Training Programs through a DOE Grant.

Security Unit management conducted an extensive assessment of the physical security system and completed an upgrade to the security reporting system. The assessment was reviewed by key Security personnel in the DOE Chicago Operations Office; it received excellent marks.

The Laboratory's aggressive emergency response drill and exercise program continued during FY94. This year's exercise and response program was directed at communication and response planning with the external agencies who support the Laboratory through Memorandums of Understanding. A complex "off-hours" exercise was conducted in conjunction with federal, state, and local agencies. The results of the exercise were deemed by all to be a success. The Emergency Preparedness Unit also developed an extensive Emergency Readiness Assurance Plan, which was evaluated and accepted by the DOE without major comments.

The Division continued to play a key role in support of the Laboratory's TFTR program by implementing, evaluating, and revising its policies and procedures for the protection of critical systems and experimental source materials.

Certification and Training

"Our commitment is to provide the best possible training services to the PPPL community in support of the Laboratory's mission." These words articulate the mission of the Office of Certification and Training at PPPL. Accordingly, the Office is responsible for training, qualification, and certification of Laboratory personnel so they can perform their jobs competently and safely and can develop professionally in their occupations.

Major efforts in FY94 focused on: qualification and certification programs, "lessons learned," and training programs for TFTR personnel in support of Deuterium-Tritium Operations; the development of training and examinations to implement the DOE Radiological Control Manual and DOE Environmental Restoration and Waste Management programs; support of the Princeton Beta Experiment-Modification Conduct of Operations program; the development of training and qualification requirements for a proposed Fusion Standard; and the initiation of senior management workshops and retreats.

Several training initiatives were launched during FY94 that will continue into the next fiscal year. Computer-based instruction and multimedia presentations were designed and are now used for General Employee Training. Instruction in Quality Learning from the U.S. Chamber of Commerce and the Professional Development Series from American Management Association were conducted via satellite downlink. Office of Certification Training Specialists assumed responsibility for the technical and environmental, safety, and health (ES&H) training courses. A comprehensive PPPL Information Handbook was published; it will be maintained on an ongoing basis. Cross-training of PPPL personnel to assume new operations positions with TFTR was initiated and will continue through the life of the TFTR Project.

The effort to develop comprehensive and innovative training programs at PPPL continues. Self-paced instruction modules for TFTR Access Training, Hoisting, Rigging, and Crane Training, Hazardous Waste Generator Training, and Forklift Operator Training were written and are in use. An extensive technical training text for Tritium Systems was also written and published.

This year, the Office of Certification and Training revised and approved many ES&H courses. A major program providing Hazardous Waste Operations training, under a grant from the National Institute for Environmental Health Sciences to DOE, was also implemented. Advanced Electrical Safety was completed and presented in FY94. General Employee Training was expanded to include General Employee Radiological Training for all Laboratory personnel, as required by the Rad Con Manual.

In support of TFTR Deuterium-Tritium Operations, system engineers and technicians were trained in the design and function of tritium systems. Operators and support personnel were trained in safe tritium handling at Ontario (Canada) Hydro's Chalk River facility. Technicians were instructed in tritium leak detection methods. A program to prepare and conduct prejob briefings for TFTR installation, operations, maintenance, and repair activities was instituted in fiscal year 1994 and is an integral part of the work-planning process. In accordance with Department of Energy good practices, the development of qualification materials to support qualified and certified positions continued as a major undertaking of this Office.

Since Deuterium-Tritium Operation has been extended, the training, qualification, and certification of operations personnel (including training on the operating, emergency, and alarm response procedures) and support positions initiated in FY93 continued in FY94 and will continue throughout FY95.

Along with scheduling ES&H and technical training, this Office also coordinates other training. A comprehensive training plan for Managers and Supervisors was initiated in FY94. Specialized technical training in the National Electric Code and the American Society of Mechanical Engineers Piping Code was conducted for Engineers and Engineering support personnel. A Requisitioner's Training course was presented jointly by procurement specialists from PPPL and the DOE Princeton Area Office. A series of computer skills training courses was implemented for administrative and support staff.

Fiscal year 1994 saw a number of other accomplishments by this Office: alternate test forms and test bank items were created, employee development courses were introduced in cooperation with Princeton University Main Campus organizations, the video library was updated to include quality improvement and TQM (Total Quality Management) videos, and the resource system for training videos and catalogs was expanded.

In order to support TFTR, this Office develops and maintains all of the TFTR operations qualification and certification program documents and procedures, and has developed qualification procedures for support groups such as Health Physics and Facilities Engineering.

The Office also coordinates the registration and scheduling of training sessions; sends out training scheduling memoranda; publishes a monthly training calendar; assists instructors in planning their training sessions; arranges and sets up the training facilities and audiovisual equipment; and prepares the attendance sheets, course materials, and tests for use. There is also a system that notifies managers, on a monthly basis, of retraining needed by personnel under their supervision. This written notification is provided for the upcoming three-month period.

The centralized record keeping system continues to be revised to accurately capture all training completed by employees (regular and temporary). Employee training is recorded in a database that provides training information for all employees. The database is also a source of information for all courses given internally and externally. This computerized training system is complemented by a hard-copy record system which was devised to handle course attendance sheets, training materials, and training correspondence. For record protection and security, special fire retardant files are used.

Information Services

The Information Services Division provides services supporting the preparation and dissemination of information pertaining to PPPL. Included are public and employee information, technical information, graphic arts, photography, printing, duplication, records management, and telecommunications.

Public and Employee Information

The Information Services Division is responsible for providing up-to-date information on PPPL's program for the public, news media, representatives of government and industry, and PPPL employees. Brochures, information bulletins, and other publications are designed and written for the layperson. In addition, two employee newsletters, *PPPL Hotline* and

PPPL News Alert are issued. The Division staff coordinates a speakers bureau, a Laboratory tour program, as well as news media and community relations activities. Responsibilities also include the development and fabrication of stationary and traveling exhibits about PPPL's magnetic fusion program and technology transfer activities.

Activities defined in PPPL's public relations plan, developed during FY93, were continued. Early in FY94, a strategy was planned and implemented relating to TFTR's unprecedented deuterium-tritium high-power experiments scheduled for December 1993. The objective was to maximize and sustain the interest of national, state, and local print and broadcast journalists in the magnetic fusion energy program.

PPPL's media distribution list was greatly expanded. In November, 1993, background materials on magnetic fusion, the upcoming TFTR experiments, and plans for the Tokamak Physics Experiment and the International Thermonuclear Experimental Reactor were mailed to journalists worldwide. This resulted in the publication of several advance stories, including the *New York Times'* weekly science supplement. Several leading science writers and local journalists were briefed personally and invited to be present for the high-power experiments on December 9. They gathered in the M.B. Gottlieb auditorium where a remote control television system enabled them to witness activities in the TFTR control room on the large-screen projection system. Television monitors were set up for viewing the plasma and a fusion power light diagnostic provided a graphic representation of the neutrons produced during the world-record three-million-watt burst of fusion power produced that evening.

As a result, on December 10, front-page stories appeared in the *New York Times*, the *Washington Post*, the *Star Ledger*, and a major *Associated Press* wire story was distributed throughout the country. Hundreds of newspaper stories appeared throughout the world. The high level of public interest continued well into 1994, with a multitude of follow-up articles in newspapers, science magazines, and educational publications. The subsequent production of nine million watts of fusion power by TFTR in May, 1994, resulted in renewed media interest in the Laboratory and magnetic fusion energy.

For the benefit of broadcast journalists, plans were developed late in FY93 for the production and distribution of a Video News Release (VNR) reporting the high-power results. Interviews with PPPL's senior scientists and activities in the TFTR control room, including the jubilation on the attainment of three million watts, were captured on video during the evening of December 9. Editing of the VNR was completed overnight and the production was ready for distribution via satellite early the next day.

On the morning of December 10, as a result of the barrage of inquiries from the nation's major television networks and local area stations, a news conference was held, followed by one-on-one TV news interviews with representatives of PPPL and the USDOE. Many of the broadcasts reported the achievement of six-million watts by TFTR in the late afternoon on December 10. The VNR was uplinked for satellite distribution around the world and copies were provided to broadcast journalists attending the news briefing. Use of the VNR was monitored electronically. The final report noted 197 uses in 95 markets nationally, reaching approximately 56.9 million viewers. PPPL's VNR was the second most heavily viewed VNR in the United States for 1993.

Other significant public information projects during FY94 included the development of a twenty-four-foot portable exhibit describing PPPL's mission and accomplishments. The exhibit was displayed at the Fusion Energy Forum in Washington, D.C. in March, 1994, and at the American Nuclear Society's Meeting on the Technology of Fusion Energy in New Orleans in June, 1994. When not on the road, the exhibit stands in PPPL's main lobby.

During the later half of FY94 a plan was developed for the public review of the preliminary Finding of No Significant Impact (FONSI) relating to the shutdown and removal of TFTR and the construction and operation of Tokamak Physics Experiment. The plan, which was approved by PPPL senior management and the USDOE, called for the distribution of the preliminary FONSI for review by federal, state, and local officials during a thirty-day comment period which was to be held early in FY95.

During FY94, fifteen individual news releases were issued on a variety of topics including staff awards, appointments, technology transfer activities, and the award of two major industrial subcontracts for the design of Tokamak Physics Experiment components. Work began on the writing and production of an updated, upgraded PPPL Overview booklet and a brochure summarizing the lifetime accomplishments of TFTR. All totaled, sixteen issues of the *PPPL*

Hotline were produced, along with fifty issues of the *PPPL News Alert.*

Technical Information

The technical Information Section of the Information Services Division is responsible for administering the Reports and Patents function. During FY94, sixty-six PPPL Report Preprints were distributed, thirty articles published in professional journals, and two-hundred eighty-two scientific and technical reports presented at conferences. Twenty-two invention disclosures and one patent application were filed during the year. Three patents were issued. The PPPL Patent Awareness program recognized forty-three inventors for invention disclosures, patent applications, and patents issued in FY94.

Graphic Arts and Photography

The Information Services Graphic Arts Section has built a comprehensive capability in the utilization of Macintosh computers for the generation of two- and three-dimensional graphics and the design of publications, presentations, and illustrations utilizing Adobe Illustrator, Adobe Photoshop, and Aldus PageMaker software. A total of eleven hundred pieces of line art were produced during the year. To meet the demand for color graphics, a color scanner was added to the Graphic Services Section during fiscal year 1994.

Photographic Services are provided by PPPL's photographer, including studio and location photography and all related processing with the exception of color printing, which is performed by a subcontractor. During FY94, twelve-thousand one-hundred seventy-five pieces were processed, including black and white prints, color negatives, 35-mm slides, and vugraphs. This, together with location and studio photography, comprised eight-hundred-fifteen individual jobs.

Duplicating and Printing

Production in the Duplication Center during FY94 totaled 5.9 million impressions. In late FY93, the modernization of the Duplicating Center was completed with the installation of the Xerox 5090 high-speed duplicator. The number of individual printing procurements through the US Government Printing Office in FY94 was thirty-seven, with an associated cost of thirty-three thousand dollars.

Records Management

The U.S. DOE's Site Specific Record Inventorying and Scheduling Project requires that all PPPL's records, including paper, electronic, and photographic, be inventoried and appropriately scheduled for retention by the close of FY95. A substantial Lab-wide effort will be required to meet this deadline.

During FY94, a Records Management Plan was developed defining the schedule and resources required. By the end of the fiscal year, responsibilities were delineated, a consultant was on board, and staff training programs were ready for implementation. A software package is being developed to collect comprehensive data on Laboratory records, with the ability to generate all required DOE and National Archives and Records Administration forms. PPPL will conduct a two-phase effort, deferring TFTR-related records to the second half of FY95.

Telecommunication Services

The Telecommunications Office is responsible for the provision of cost-effective voice communication services throughout the Laboratory. The Telecommunications Office recommends the selection of carriers and specifies systems and hardware for both wireline and wireless services. The Office also supervises and coordinates the installation, repair, and billing for these services and equipment. In FY94, the Telecommunications Office processed three-hundred-six requests for telephone installations, moves and changes, and one-hundred-thirty requests for radio and paging changes and repairs.

Of significance also were the Office's efforts to provide Telecommunications services to the remotely sited Environmental Waste Management Facility and the installation of Integrated Services Digital Network facilities for off-site computing.

Human Resources

The Human Resources Division was reorganized to accommodate new responsibilities for maintenance of the data for the new Princeton University payroll and personnel system and to consolidate work due to attrition. A thorough review of all functions of the Division by the entire staff with an outside facilitator resulted in shifting of Division responsibilities to provide better customer service.

Policy Development and Implementation

In order to support the establishment of twelve-hour shift workdays for Emergency Services Units and some TFTR Operations personnel, all aspects of the Practices and Procedures Manual and University Policy were reviewed to determine the specific interpretation required for these unique work schedules. Guidelines were developed to address issues such as overtime, sick time, and holidays.

The Extended Relocation Policy was reviewed for PPPL employees working on the International Thermonuclear Experimental Reactor Project in San Diego and in Naka, Japan. Extra effort was made to insure equity between PPPL employees and Lawrence Livermore National Laboratory employees also working in Naka. These efforts included a review of Goods and Services differentials, housing, and annual trips home. In spite of early efforts to develop similar policies, each laboratory has variations in policy development. This has required countless hours of communication between the PPPL Human Resources and Accounting Divisions and other laboratories. Modifications to the Policy are under review for FY95.

The Drug Testing Policy was implemented in December of 1993 and random testing of fifty percent of those in positions designated for Drug Testing are under way. Employees newly hired or transferred into testing positions were also tested as a condition of employment.

The Smoking Policy was revised, with final approval from the Provost to allow the Laboratory to be a nonsmoking facility beginning in November, 1994. Employees were surveyed, resulting in overwhelming support for the new policy. Special classes on smoking cessation were provided prior to the November effective date for those who wish to stop smoking.

Affirmative Action

The Director's Advisory Committee on Women and the Director's Minority Advisory Committee, formed in FY92 to assist the Director in meeting the Laboratory's Affirmative Action commitments, continued to develop new areas for study and support.

The Director's Minority Advisory Committee, which recommended a Skills Development Program for minority employees in FY93, successfully completed the first phase of a pilot program in FY94. In FY95, the Program has been expanded to include development of a variety of skills for minority employees through on-the-job mentoring, as well as formal education outside the Laboratory.

The Director's Advisory Committee on Women reviewed concerns with the Director, resulting in a Laboratory-wide meeting with the Director and the Head of Human Resources to discuss issues of respect and career advancement for women at PPPL. In addition, the Committee sponsored a very successful "Take-Your-Daughter-To-Work Day" in cooperation with the Princeton University Women's Organization. The program attracted more than fifty young women, with thirty PPPL employees providing tours, demonstrations, and one-on-one shadowing of a typical workday, from administrators to engineers.

For the third consecutive year, a pay study was conducted that resulted in the review and adjustment of salaries for some minorities and women, based on an analysis of salaries by rank within each staff.

Employee Relations

The Human Resources Division staff developed and implemented two Voluntary Separation Programs in FY94—one in November of 1993 and one in September of 1994. Both were successful, attracting thirty-seven employees in November, 1993, and forty-four employees in September, 1994. A special incentive package for those employees with Continuing Appointment was developed to encourage participation in the Voluntary Separation Program.

An Involuntary Separation Program was also developed and implemented. All policies related to involuntary termination were reviewed. An outplacement request for proposal was developed and bids were reviewed with five different vendors. The selected vendor—Manchester Associates—provided services for the affected employees, including termination counseling and a workshop on preparing for the job search. Ten indirect positions were eliminated.

Modifications were made this year to the Performance Appraisal form for all General Council Members. All other Performance Appraisal forms were reviewed to provide a consistent format and rating system for all staffs. For ease of access, all forms were available on a file server and disks.

As a continuation of the Supervisors' Training Program in Sexual Harassment Awareness, the Divi-

sion developed a follow-up program for all employees. The Director has required all employees to participate in small group meetings. Approximately half the employees attended training programs in FY94. Workshops are held and will continue to be held on a weekly basis until the entire Laboratory staff has attended this training.

Human Resources Information System

Princeton University completed the initial design and development of a new human resources and payroll system (TESSERACT). The PPPL Human Resources Division filled a position vacated by a retired Benefits Assistant with a transferred employee. The employee in the new position—Information Systems Specialist—learned the new system, as well as the internal PPPL financial systems, and will be the focal point of all salary actions and record keeping. The Specialist is required to input data for all personnel actions, including salaries and benefits. Division staff have been trained to use the system by the Information Systems Specialist. During FY95, the staff will be further trained to input data and will be helped to develop new skills in data management and reporting.

As a result of the new TESSERACT software, the Division has taken on the responsibility previously managed by the Accounting Division of entering and maintaining all personnel-related information on both the University system and the Laboratory's financial system, as well as managing the position requisition process and developing the official monthly headcount report.

Administrative Services

The Office of Administrative Services provides a variety of Laboratory-wide administrative functions. The staff oversees the Cafeteria operations and manages PPPL-leased apartments for intermediate and long-term foreign and domestic visitors. It maintains the responsibility for processing and controlling Department of Energy security clearances; prepares and monitors budgets; and maintains official Laboratory organization charts and supervisors and managers lists.

The Office has responsibility for planning, organizing, and managing the Laboratory's social and recreational activities. There was a bus excursion to a retail outlet mall, a cruise on the Delaware River aboard the "Spirit of Philadelphia," and a memorable day-long trip to Ellis and Liberty Islands.

During our Service Awards Program, one hundred twenty-eight employees were recognized with a gift of their choice for achieving a new five-year milestone in their years of service with the Laboratory. Additionally, two Retirement Awards Ceremonies were held to honor a total of forty-six employees who retired during the year.

In December, the Annual Laboratory Dinner-Dance was held in the spirit of the holiday season and in June, the Laboratory sponsored a free picnic-style lunch for all employees. Both events were well received.

PPPL Invention Disclosures for Fiscal Year 1994

Type "B" Disposable Molecular Sieve Bed
F. Tulipano, R. Rossmassler, L. Ciebiera, and S. Vinson

Segmented Chuck for RF Biasing Large Substrates
J. Stevens and J. Cecchi

Improved Low Energy Neutral Beam Source for Plasma Materials Processing
J. Stevens

Automatic Video Monitoring System
T.E. O'Connor

Arc Detection Using 2nd Harmonic Signal
J. Rogers, P. LaRue, and Unknown

Use of Magnetic Field Pitch Angle Measurements for Real-Time Tokamak Plasma Control
R. Kaita and F. Levinton

Toxic Chemical System (TCS)
P. Del Gandio

Electro-brazing
D.K. Owens

Control of Stochastic Ripple Loss of Alpha Particles and Fast Ion in Fusion Plasmas
M. Redi, R. White, and M. Zarnstorff

Using the Ion Bernstein Wave to Extract Power from Alpha-particles
N. Fisch, C.F.F. Karney, R. Majeski, and E. Valeo

Large Scale Chemical Synthesis System Using Plasmas
S. Yoshikawa

Method to Detect Arsenic Precipitates Buried Inside Silicon Surfaces
C. Skinner

Reconditioning Magnet Assembly of DC Switchgear
M. Awad, R. Pressberger, F. Wasylenko, and W. Persely

Active Induction of Transort Barrier in Plasma by Ion Bernstein Wave Power
B. LeBlanc, M. Ono, and S. Sesnic

A Compact m = ±1 Helicon Mode Plasma Source Utilizing a Planar Antenna Structure
J. Stevens and J. Cecchi

Method to Detect Calcium in Biological Tissues in a Natural State
C. Skinner

A Simple Experimental Kit for Middle School Students
S. Yoshikawa

Sling Tension Unit
R. Snead, J. Desandro, and J. Wioncek

Method for Controlling Instabilities at the Edge of a Diverted Tokamak
A. Reiman

Compensation Loop Technique to Measure Radiation Effects on Fibers
A. Ramsey

Chemical Elements Mapping Soft X-Ray Reflection Microscope
S. Suckewer

Optimized Use of the Ion-Bernstein Wave in Channelling Alpha-Particle Power
E. Valeo and N. Fisch

Office of Resource Management

The Office of Resource Management (ORM) provides the Princeton Plasma Physics Laboratory (PPPL) with financial, procurement, property, and other administrative services. The Office of Resource Management consists of the following six activities: Budget Office, Accounting and Financial Controls, Information Resource Management, Procurement, Materiel Control, and Cost and Schedule Control. During FY94, the Environmental Restoration and Waste Management Division was transferred to the Engineering and Technology Development Department.

Fiscal year 1994 was another challenging year for the Office of Resource Management. The Department's budget for FY94 was established approximately 3% below FY93 costs. When coupled with inflation, ORM's FY94 budget represented a real decrease in spending power of approximately 7%. Since the Department's cost structure is labor intensive, meeting the FY94 budget target required the reduction of staff. Accordingly, ORM's staff level decreased from seventy nine on 30 September 1993 to seventy one on 30 September 1994.

The Department was generally able to meet its mission requirements notwithstanding the reductions in resources described above. The various audits and appraisals conducted during FY94 by the various organizations who have responsibility for these reviews, with the exception of the Contractor Purchasing System Review (CPSR), generally resulted in "excellent" adjectival ratings and usually resulted in no findings or only minor findings. The CPSR surfaced some significant issues, which the Procurement Division responded to in a very aggressive manner; much progress was made during the fiscal year toward resolving these issues. Lastly, the Department pursued numerous initiatives to improve the service provided to its Laboratory customers by restructuring processes, reassigning staff, and eliminating no-value and low-value activities.

The succeeding paragraphs will focus on each of the six activities comprising the Office of Resource Management and provide highlights and overviews for each. Tables I and II give the financial activities and staffing levels of the Laboratory for the last five years, respectively.

Budget Office

During FY94, the Budget Office provided analytical support to Laboratory management for budget and human resource planning. A program to reduce staff was implemented during the latter part of the fiscal year based on the initial Department of Energy (DOE) funding profile for FY95, which indicated a decrease in the Laboratory's net budget. As a result, the Budget Office staff reviewed and restructured its operations to compensate for the reduction of one employee.

The Budget Manual was updated to include changes to Budget Office policies and procedures and to incorporate information included in the DOE Budget Formulation Handbook. The revised manual was issued September 30, 1994.

One of the key issues facing the Budget Office in FY94 was the development of a new methodology for the liquidation of General and Administrative (G&A) on a causal and beneficial basis as required by the Department of Energy and Cost Accounting Standards. The methodology developed was utilized for the Field Work Proposals commencing with budgets prepared for fiscal year 1995. A review was conducted by DOE which resulted in two minor revisions to the proposed methodology. This methodology will be in effect for FY95.

The 39th Annual DOE Laboratory Budget Officers' Meeting was chaired by PPPL. Budget personnel from fifteen DOE laboratories attended the meeting, which provides the opportunity to exchange practices and experiences on various budget subjects in an effort to improve budget management and processes throughout the DOE system.

Accounting and Financial Controls

The Accounting and Financial Controls Division is responsible for recording and reporting the finan-

Table I. Princeton Plasma Physics Laboratory Financial Summary by Fiscal Year.
(Thousands of Dollars)

	FY90	FY91	FY92	FY93	FY94
OPERATING (Actual Costs)					
Department of Energy					
TFTR Diagnostics	$11,384	$10,084	$ 9,822	$ 7,400	$ 9,426
TFTR Physics Program	4,406	4,329	4,316	6,470	7,905
TFTR Computer Facility	4,214	3,863	4,063	3,902	4,568
TFTR Heating	20,873	19,728	15,534	15,040	16,991
TFTR Tokamak Operations	19,673	15,075	20,217	24,916	29,087
TFTR DT Systems	1,027	5,904	22,216	21,246	1,041
TFTR Decontamination & Decommissioning	—	—	—	716	4,503
TFTR Other	—	—	—	—	—
Subtotal TFTR	$61,577	$58,983	$76,168	$79,690	$73,521
CIT/BPX/TPX	17,073	17,750	14,830	14,691	15,550
PBX-M	3,913	5,201	9,940	8,535	3,913
CDX/CDX-U	440	585	479	585	677
Theory	2,597	2,769	2,882	2,560	2,503
ITER	513	565	937	1,691	2,146
Applied Physics	1,195	1,142	810	1,253	1,248
Other Operating - Fusion	364	579	740	539	615
Change in Inventories	1,230	(123)*	4	(96)*	(1,915)
X-ray Laser Development	1,004	8	—	—	—
Energy Management Studies	66	—	41	115	65
Environmental Restoration/Waste Mgt	451	677	1,376	3,434	4,811
Science Education	—	71	19	334	406
Technology Transfer	—	—	3	50	66
Work for Others	1,309	1,372	839	1,370	490
Total Operating	$91,732	$89,579	$109,240	$114,751	$104,096
EQUIPMENT (Budget Authorization)					
Capital Equipment not Related to Construction	$1,746	$1,108	$3,140	$1,395	$ 371
CONSTRUCTION (Budget Authorization)					
Compact Ignition Tokamak	—	—	—	—	(63)**
General Plant Projects	$1,479	$1,608	$1,858	$2,400	$1,848
Energy Management Projects	783	431	(350)**	(972)**	(17)**
Safety and Fire Line Item	—	—	2,600	2,200	—
Total Construction	$2,262	$2,039	$4,108	$3,628	$1,768

* Change of the inventory levels on hand at the end of the fiscal year compared to the previous fiscal year.
** Deobligation of funds for completed or canceled projects.

Table II. Princeton Plasma Physics Laboratory Staffing Summary by Fiscal Year.

	FY90	FY91	FY92	FY93	FY94
Faculty	4	6	7	7	7
Physicists	104	99	102	100	97
Engineers	173	172	171	171	156
Technicians	330	360*	358	351	306
Administrative	102	108	126	131	121
Office and Clerical Support	73	73	72	69	57
Total	786	818	836	829	744

* Includes the transfer of 29 security staff from Princeton University to PPPL.

cial transactions of the Laboratory. The transactions include payments, accruals, commitments and requisitions for labor, materials, other operating expenses, equipment, and construction costs. The Division is also responsible for all financial reporting and for maintaining the financial records of the Laboratory in accordance with the requirements of the Department of Energy, Princeton University, the accounting industry, and other funding sources.

During FY94, the Accounting and Financial Controls Division continued to place emphasis on system enhancements, review of internal controls, updating policies and procedures, and providing service to the Laboratory at minimum cost.

Some of the more significant accomplishments during the year were as follows:

- The Accounting Division reinstated the procedure for monitoring the amount of time worked by hourly employees. This will ensure that hourly employees do not exceed the 1,000 hours limit that would entitle them to benefits provided to regular employees.
- The Laboratory Accounting Manual was revised and issued in FY94. In addition, all Accounting Policies and Procedures that generally impact Laboratory personnel in their day-to-day operations were submitted to be incorporated in the Laboratory Procedure Manual in the early part of FY95.
- The Travel Voucher reimbursement form was revised to simplify the form, to include some of the key travel policies, and to provide space for employees to give justification and/or clarification for unusual transactions.
- The Petty Cash Reimbursement Guidelines were modified to streamline the documentation requirements, while maintaining assurance that all transactions are valid. Also, the limit for each reimbursement was raised from $200 to $300.
- The Labor Accrual Policy and Procedures were modified to ensure that all wages and benefits earned by employees (but not paid) are recorded in the financial records at the close of each accounting period.
- There were 7 audits and reviews conducted by the Princeton University Internal Auditors, the DOE Chicago Operations Office and the DOE Office of the Inspector General in FY94. There were no findings identified in these audits.

Information Resource Management

During FY94, Information Resource Management (IRM) continued the support and maintenance of the PPPL administrative systems, continued working toward completion of the RAMIS-to-FOCUS conversion, and initiated a number of new projects. The majority of IRM's efforts during FY94 were to install and configure ORM's Ethernet software and to develop systems and system enhancements to reduce manual effort in the PPPL administrative systems. Some of the Division's key initiatives are summarized below.

RAMIS-to-FOCUS Conversion. The Phone Cost Distribution System was the only new system to be converted to FOCUS during FY94; however, the Personnel and Payroll systems were activated and a number of enhancements were added to them. Significant effort was required to change the Personnel and Payroll systems to work with Princeton University's new personnel system which was installed in FY94.

ORM Ethernet Systems. During FY94, IRM configured a suit of Windows applications to be used by the administrative departments as their standard configuration. The software is being installed on all ORM PCs and training courses are being scheduled. This configuration brings e-mail, word processing, spreadsheets, and terminal emulation to all users.

Labor Reduction Initiatives. IRM developed the software and applications necessary to put local printers in all major areas of the Laboratory. Low-cost HP Laserjets have been used to provide user printing from the mainframe, as well as from PCs. By moving the printing from a central location to remote locations, users get faster turn around on printing, as well as less wasted time picking up output. Coupled with the local printing, IRM developed software to allow users to "post" their own data instead of submitting a post to be entered by a central operator. With the new system, IRM also developed a complete security and logging system which controls user access to posting and provides data to managers and users on posts submitted to the system, sorted by user's name.

TESSERACT Support. IRM organized and managed the interface and training required for PPPL to participate in the activation of Princeton University's new on-line personnel system called TESSERACT. This new system required training of personnel in PPPL's Human Resources Division and significant redesign of PPPL's systems.

FIS to MARS Conversion. The PPPL interface to DOE's Financial Information System (FIS) was modified to support the new Management Analysis Reporting System (MARS) format. During the redesign, the system mappings were documented for inclusion in the accounting manual.

Budget/Accounting System Modification. The RAMIS Budget System was modified to support pricing past 1999, the G&A programs were modified to support a two-level G&A rate (see Budget Office Section), new Tech Centers were added to the systems to support reorganizations in the Lab and bi-weekly staff labor accruals were added to Accounting.

Excess Property System Developed. A system to track and report on excess property was developed and installed.

Procurement DOE Reports Automated. A number of manually prepared DOE reports were automated, which resulted in labor savings and an increase in reliability of the data.

Procurement System Redesign. The method of operation in the Procurement Division was analyzed and system changes were designed to reduce paper and manual effort. Initial changes are reflected in some of the above progress statements. Future initiatives include an on-line requisition, electronic purchase order preparation, and automated subcontract preparation.

Procurement

The Procurement Division is responsible for obtaining all goods and services necessary for the Laboratory's continued operation and mission accomplishment. The Division's goal is to accomplish its work in a timely manner, under the most favorable terms possible, in accordance with applicable laws and government regulations, and consistent with good business practice.

FY94 ushered in substantive changes for the Division. The Director of Procurement retired in December 1993. Also in December, a triennial Contractor Purchasing System Review (CPSR) conducted by the DOE Office of Contract Management and Administration identified a number of opportunities for improvements in the Procurement Division's policies, procedures, and operations. Beginning in January and continuing throughout the spring and summer, the Procurement Division staff collectively developed and implemented a systematic corrective action plan addressing all issues identified by the CPSR team.

This year the Division also underwent a follow-up surveillance conducted by the Department of Energy's Princeton Area Office, a review by Princeton University's internal auditors, and an examination by Princeton University's Office of Internal Audit. None of these reviews generated significant new findings.

FY94 saw decreases both in the number of procurement actions and dollars awarded, reflecting the anticipated wind-down of the Tokamak Fusion Test Reactor (TFTR) operations and the

more national nature of the Tokamak Physics Experiment Project activities. The total number of actions decreased by 28.6%, while dollars decreased by 11.3%. The Division awarded 12,150 actions with an aggregate value of more than $38.3 million. This included the initial funding of two large hardware design subcontracts for the Tokamak Physics Experiment Project — one for plasma facing components (approximately $26 million over a three and one-half year period) and another for the vacuum vessel (approximately $8 million over a three-year period). Both of these actions were competitive, cost-plus-award fee type subcontracts with fixed price options for component manufacture. The Division began activities in support of TFTR Shutdown and Removal (S&R), including development of a procurement plan for selection of the primary S&R subcontractor.

In fiscal year 1994, the Division was composed of two branches — Purchasing and Subcontracts — both reporting to the Director of Procurement. Division staffing decreased throughout the year. The position of Procurement Director was vacant from December, 1993, through September, 1994, with the Head, Office of Resource Management serving in an acting capacity. The Manager of Purchasing was absent on medical disability from December, 1993, through June, 1994. By the end of FY94, the Subcontracts Branch staff had been reduced from six to five Subcontract Administrators by elimination of a temporary position. The Purchasing Branch staff was reduced from five to four Buyers by attrition. Management continued to review the Division's staffing levels and organizational structure with the goal to improve both the effectiveness and the efficiency of the Division's operations.

The Division continued to actively pursue and expand its outreach efforts to small and small disadvantaged businesses. Procurement representatives attended four minority business fairs in various regions of the U.S. In September, 1994, the Division cosponsored a Small Disadvantaged and Women-Owned Business Procurement Breakfast with the International Minority Business Corporation (IMBC). Representatives from sixty-five firms attended. As a result of these and other initiatives, the Division exceeded its Small Business Subcontracting Plan goals for the first time in six years, awarding 40% of procurement dollars to Small Businesses and 5.7% of procurement dollars to Small Disadvantaged Businesses. Our goals were 34.5% and 4.0%, respectively.

Materiel Control

The Materiel Control Division is responsible for providing effective stores, warehousing, property, and transportation services in support of Laboratory projects and administrative activities. Division staffing was reduced from 24 to 21 in FY94, in order to achieve required cost reductions in Laboratory indirect activities. The operational impact of the staff reduction was minimized, to some extent, by eliminating or reducing certain Division services, consolidating some functions, tasks, and personnel, and identifying opportunities to streamline operations through automation of labor intensive activities.

Another major event occurring during FY94 was a Contractor Personal Property Management Review (CPPSR) performed in March by DOE Headquarters and the DOE Chicago Operations Office. The review lasted nearly two weeks and found that the PPPL property management system effectively protects the interests of the Government and that Laboratory property management activities are conducted in accordance with applicable requirements. The CPPSR report noted that the Laboratory property system is responsive to the protection, accountability, and control of Government personal property. The report also highlighted two noteworthy practices: the idle and excess property walk-through program and the management of equipment and materials being held for future projects. In addition to the CPPSR, three other DOE reviews were also performed in FY94: (1) a DOE/Chicago Headquarters Environmental, Safety, and Health appraisal which rated the Division's Packaging and Transportation program as "excellent"; (2) an Inspector General audit on the use of Government Supply Sources, which found no material weaknesses in the Laboratory's property or acquisition systems; and (3) a DOE and Princeton Area Office annual appraisal which rated the Property Management System as "excellent."

In other areas, two improvement projects were undertaken and completed by the Division this year: the stock level and inventory control process for common use stores inventory was improved, resulting in a $40 K reduction in on-hand inventory and the average time for delivery of incoming material was reduced from 3.5 days to 2.5 days by streamlining the material staging and delivery process.

The Warehouse Operations Branch performed an annual review of equipment and material held for fu-

ture projects. As a result, there was a reduction of 3,500 square feet of storage area. The Branch processed 3,500 purchase orders for more than 6,500 line item receipts. Delivery of receivables to user groups totaled more than 10,300 pieces. The Branch maintained an outstanding transportation safety record while making twenty-five hundred shipments to international and domestic locations and handling a 56% increase in hazardous materials shipments.

The Property Administration Branch completed the FY94 statistical sampling of capital equipment inventory and processed more than 20,500 property transactions. The Branch sold 200 tons of scrap metal and held two public sales of government property where 327 line items were sold. These activities resulted in a combined return to the Laboratory of $40 K. Reutilization of 41 equipment items, valued at nearly $203 K, was also accomplished.

In the Transportation Services Section, more than 600 preventive maintenance inspections and repair actions were performed on Laboratory vehicles and equipment. Additionally, more than 1,800 vehicle dispatches were made. The automated maintenance and management program continued to provide up-to-date management information on preventive maintenance requirements and costs. In September, a new gasoline and fuel dispensing station was made available. The station is a microprocessor-based fuel control and data acquisition system enabling fuel availability around the clock.

In Stores Operations this year, 23,000 withdrawals were processed with sales totaling $732 K. An Inventory Investment Quality Improvement Team was formed with the goal of reducing the common use stores inventory by $35 K, while maintaining a high fill rate. The goal was surpassed by $5 K with a fill rate of 98%. Spares Parts had sales of $1.96 M, with $131 K in receipts which resulted in a $1.85 M reduction of on-hand inventory.

Cost and Schedule Control

The Cost and Schedule Control Division coordinates implementation of the Laboratory's Project Controls System. The Project Controls System provides the basic management functions necessary for the successful completion of PPPL projects, namely: organization, planning, authorization, budgeting, accounting, analysis, and change management. Benefits derived from the system include:

- A formal process for organizing PPPL work efforts.
- Assignment of responsibilities and accountability for work scope via the Work Breakdown Structure system.
- A formal process for planning and estimating work in support of DOE funding and milestone guidance.
- A formal process for the authorization of work through the Lab Work Authorization Process.
- A formal process for monitoring work progress via monthly progress statusing.
- A formal process for identifying, reporting, and analyzing schedule and cost problems via the PPPL variance analysis process.
- Electronic data access to accounting, budget, performance measurement, and procurement data and reporting systems.

Specific accomplishments in FY94 include:

- Developed and maintained an integrated cost and schedule database for the TFTR Project. Specific areas receiving focus included: Tritium systems maintenance and operations. Field maintenance and installation "rollover" scheduling. Tritium Purification System installation. Shutdown and Removal conceptual design cost and schedule baselines.
- Developed and implemented PPPL's major acquisition schedules providing monthly visibility to PAO and PPPL management on the Laboratory's critical procurements, and ensuring that both the cognizant procurement and project staffs are working toward identical goals.
- Developed and maintained PPPL Institutional Plan and PPPL manpower studies.

Graduate Education: Plasma Physics

Among the major facilities in the world for research in plasma physics and controlled fusion, the Princeton Plasma Physics Laboratory (PPPL) is unique in its direct ties and close proximity to a leading university. For more than 30 years, PPPL has maintained an even and sensitive balance between education, fundamental research, and leadership in the fusion program. That thirty-five to forty top-notch graduate students work side-by-side with PPPL staff members is a circumstance that provides invaluable training and experience for these students and youthful stimulation and expert assistance for the research staff.

The Plasma Physics Program was first offered at Princeton University in 1959 and two years later was incorporated into the Department of Astrophysical Sciences. In an environment that, over the past three decades, has seen enormous changes in the fields of plasma physics and controlled fusion, the Program has consistently focused on fundamentals in physics and applied mathematics and on intense exposure to contemporary experimental and theoretical research in plasma physics.

Graduate students entering the Plasma Physics Program at Princeton spend the first two years in classroom study, acquiring a foundation in the many disciplines that make up plasma physics: classical and quantum mechanics, electricity and magnetism, fluid dynamics, hydrodynamics, atomic physics, applied mathematics, statistical mechanics, and kinetic theory. Table I lists the departmental courses offered this past academic year. These courses are taught by the members of the Princeton Plasma Physics Laboratory's research staff who also comprise the sixteen-member plasma physics faculty (see Table II). The curriculum is supplemented by courses offered in other departments of the University and by a student-run seminar series in which PPPL physicists share their expertise with the graduate students.

Most students hold Assistantships in Research at PPPL through which they participate in the Laboratory's experimental and theoretical research programs. In addition to formal class work, first- and second-year graduate students work directly with the research staff, have full access to Laboratory and computer facilities, and learn firsthand the job of a re-

Table I. Plasma Physics Courses Offered in FY94 and Instructors.

Fall 1993

Course Title	Instructor
General Plasma Physics I	N.J. Fisch
Plasma Waves and Instabilities	M. Ono and T.H.Stix
Experimental Plasma Physics	R.J. Goldston
Analytical Techniques in Differential Equations	A.H. Reiman
Seminar in Plasma Physics	S. Yoshikawa
Turbulence in Plasma	J.A. Krommes

Spring 1994

Course Title	Instructor
General Plasma Physics II	R.M. Kulsrud and W.M. Tang
Irreversible Processes in Plasmas	C.F.F. Karney
Advanced Plasma Dynamics	R.B. White
Seminar in Plasma Physics	H.P. Furth
Laboratory in Plasma Physics	S.A. Cohen

Table II. Astrophysical Sciences and Plasma Physics Faculty.

Faculty Members	Title
Nathaniel J. Fisch	Professor of Astrophysical Sciences; Director, Program in Plasma Physics; and Associate Director for Academic Affairs, PPPL
Samuel A. Cohen	Principal Research Physicist and Lecturer with rank of Professor
Ronald C. Davidson	Professor of Astrophysical Sciences; Director, PPPL
Harold P. Furth	Professor of Astrophysical Sciences; Director Emeritus, PPPL
Robert J. Goldston	Professor of Astrophysical Sciences; Head, Research Council, PPPL
Stephen C. Jardin	Principal Research Physicist and Lecturer with rank of Professor
Charles F.F. Karney	Principal Research Physicist and Lecturer with rank of Professor
John A. Krommes	Principal Research Physicist and Lecturer with rank of Professor
Russell A. Kulsrud	Professor of Astrophysical Sciences
Masayuki Ono	Principal Research Physicist and Lecturer with rank of Professor
Allan H. Reiman	Principal Research Physicist and Lecturer with rank of Professor
Paul H. Rutherford	Lecturer with rank of Professor; Associate Director for Research, PPPL
Thomas H. Stix	Professor of Astrophysical Sciences; Director Emeritus, Program in Plasma Physics, PPPL
William M. Tang	Principal Research Physicist and Lecturer with rank of Professor
Roscoe B. White	Principal Research Physicist and Lecturer with rank of Professor
Shoichi Yoshikawa	Principal Research Physicist and Lecturer with rank of Professor

search physicist. First-year students assist in experimental research areas including Tokamak Fusion Test Reactor diagnostics development, the Princeton Beta Experiment-Modification, the Current Drive Experiment-Upgrade, materials fabrication process plasmas, and X-ray and free-electron laser development and applications. In a similar fashion, second-year students assist in theoretical research. After passing the Department's General Examination, students concentrate on the research and writing of a doctoral thesis under the guidance of a member of the PPPL staff. Of the forty-two graduate students in residence this past year, twenty-four were engaged in thesis projects—ten on experimental topics and fourteen on theoretical topics. Table III lists the doctoral thesis projects completed this fiscal year.

During FY94, two students held a Natural Science and Engineering Research Council of Canada Fellowship, three held DOE Magnetic Fusion Science Fellowships, three had National Science Foundation Fellowships, and one held a DOE Computational Science Fellowship. Other students held awards from the Fannie and John Hertz Foundation and Office of Naval Research. Some of these fellowships are supplemented by partial research assistantships. Table IV lists the students admitted in FY94 and their undergraduate institutions.

Overall, the plasma physics graduate studies program in Princeton University's Department of Astrophysical Sciences has had a significant impact on the field of plasma physics. One hundred and sixty-five have received doctoral degrees from Princeton. The roster includes many of today's leaders in plasma research and technology in academic, industrial, and government institutions. The process continues as the Laboratory trains the next generation of scientists, preparing them for the challenging and diversified problems of the 2000s.

Table III. Recipients of Doctoral Degrees in FY94.

Mehmet Artun
Thesis: Low-frequencies Microinstabilities in Rotating Tokamak Plasmas
Advisor: William M. Tang
Employment: University California at Los Angeles

David P. Coster
Thesis: Tokamak Divertor Modelling with Fluid and Kinetic Codes
Advisor: Charles F.F. Karney
Employment: Max-Planck Institute for Plasma Physics, Garching, Germany

Karl M. Krushelnick
Thesis: Coherent Soft X-ray Generation Using a Powerful Subpicosecond Laser
Advisor: Szymon Suckewer
Employment: Laboratory for Plasma Studies, Cornell University

Robert A. Santoro
Thesis: Gyrokinetic Particle Simulation of a Multi-ion Species Plasma
Advisor: Wei-li Lee
Employment: University of California at Irvine

Giorgos Vetoulis
Thesis: Global Structures of Alfvén-ballooning Modes in Magnetospheric Plasmas
Advisor: Liu Chen
Employment: Universtiy of California at San Diego

Christopher D. Zuiker
Thesis: Laser-induced Fluorescence Measurements in an Electron-cyclotron Resonance Plasma Etch Reactor
Advisor: Joseph Cecchi
Employment: Argonne National Laboratory

Table IV. Students Admitted to the Plasma Physics Program in FY94.

Student	Undergraduate Institution	Major Field
Stanislav Boldyrev	Moscow Institute of Physics and Technology	Physics
Chan Feng	Tsinghua University	Physics
Xiaohu Li	University of Science and Technology of China	Physics
Mikhail Malyshev	Moscow Institute of Physics and Technology	Physics
Tobin Munsat	University of North Carolina	Physics

Graduate Education: Program in Plasma Science and Technology

One of the most significant benefits of the Princeton Plasma Physics Laboratory's (PPPL) association with Princeton University is the existence of faculty and graduate students engaged in science and technology research areas which are related to areas of interest to the Laboratory and which complement its strengths. The Laboratory's expertise in plasma physics is highly relevant and complementary to Princeton University research groups which utilize plasmas for applications in the plasma processing of materials, lasers, ion thrusters, and plasma sources for analytical beams. The Program in Plasma Science and Technology, a graduate program within the University's School of Engineering and Applied Science, provides a focus for graduate studies involving the application of plasmas in high-technology fields and provides a vehicle for enhancing the collaboration between PPPL and the science and engineering departments of the University. These collaborations provide important extensions of the Laboratory's technology needs within the fusion program and also a significant coupling for the transfer of Laboratory technology to other plasma areas of near-term application within industry. The most important products of the Program are highly qualified Ph.D.'s who have broad interdisciplinary training in the important field of plasma science and technology. These scientists and engineers will fill prominent research and development positions in fusion research, other areas of plasma technology, and government.

The Program is administered by an Interdepartmental Committee. The Committee comprises faculty members representing the departments of astrophysical sciences, chemical engineering, chemistry, electrical engineering, mechanical and aerospace engineering, and physics. Each of the members is engaged in research in areas pertinent to the Program and each also serves as a departmental representative to communicate the broader Program interests of their respective departments. The current areas of interest for each department are listed in Table I. Additionally, the Committee is responsible for ensuring that graduate courses are available within the participating departments to cover the curriculum needs of the students.

Table I. Research Areas of the Program in Plasma Science and Technology

Department	Research Area
Astrophysical Sciences	Divertor Operation and Materials Plasma-Surface Interactions Hyperthermal Neutral Phenomena Magnetic Reconnection Fusion Reactor Design
Chemical Engineering	Plasma Etching Plasma Polymerization Nanostructures
Chemistry	Plasma-Generated Radical Sources Surface Chemistry Molecular Dynamics
Electrical Engineering	Plasma Etching Plasma Deposition of Amorphous Silicon Electronic Materials and Devices
Mechanical and Aerospace Engineering	Advanced Lasers X-ray Laser Microscopy Composite Materials Plasma Ignitors Ion Propulsion Microengineering Processes and Devices
Physics	Plasma Processing of Thin Films Polarized Nuclei

Extensive facilities exist at the PPPL and in the Engineering Quadrangle for plasma science and technology research. A laboratory at PPPL is devoted to the plasma production of low-energy neutral particles to study low-earth orbit spacecraft phenomena and the interaction of plasmas with dense gases. Research on plasma disposal of toxic waste, plasma-assisted aerosol formation, free-electron lasers, and plasma chemical synthesis are growing in importance at PPPL. Projects on these are available to Princeton students.

In the area of plasmas for thin-film processing, the PPPL Plasma Deposition and Etching Laboratory facilities include a lower-hybrid-wave-heated etch tool for plasma-processing diagnostic development and an electron-cyclotron-wave-heated magnetron for neutral particle etching of submicron devices. The Department of Chemical Engineering has a reactive ion etch (RIE) tool that is being used for the development of real-time etching process monitors based on reflection infrared spectroscopy. The Department of Electrical Engineering operates four reactors for plasma-enhanced chemical vapor deposition. Its main interests are the fabrication of amorphous silicon films for photovoltaics and large-area transistor electronics and the processing of devices for integrated circuits.

Facilities of the Department of Mechanical and Aerospace Engineering include the X-ray Laser Laboratory, Powerful Subpicosecond Laser Laboratory, X-ray Imaging Laboratory, and Electric Propulsion Laboratory. The latter comprises four vacuum test chambers, one for electrostatic spraying and the others for magnetoplasmadynamic (MPD) thrusters in the megawatt range or hybrid MPD and thermal thrusters in the kilowatt range. The X-ray Laser Laboratory provides research opportunities in utilizing plasmas for the generation of short-wavelength radiation and its applications to X-ray microscopy and lithography

A number of departments participate in the Advanced Technology Center for Surface Engineered Materials. The activities of this center include the application of plasmas for thin-film processing, such as advanced techniques for process and surface characterization and microengineered structures.

Many activities within this Program, especially those involving plasma processing of materials and the X-ray laser, are closely associated with Princeton's Photonic and Optoelectronic Materials (POEM) Center and the Princeton Materials Institute (PMI).

During 1994, ten students were enrolled in the Program and represented four departments: Astrophysical Sciences, Chemistry, Electrical Engineering, and Mechanical and Aerospace Engineering. Sources of support for students in the program were Laboratory funds, departmental funds, National Aeronautics and Space Administration support, as well as grants.

Three students supported by the Program were awarded advanced degrees in 1994 and are listed in Table II.

Table II. Recipients of Graduate Degrees in Fiscal Year1994.

John N. Bullock
Department: Electrical Engineering
Advisor: Sigurd Wagner
Degree: Ph.D.
Thesis: Experimental and Theoretical Attacks on Meta-Stable Defect Creation in Hydrogenated Amorphous Silicon

Gordon Chiu
Department: Astrophysical Sciences
Advisor: Samuel A. Cohen
Degree: Ph.D.
Thesis: Studies of Magnetized Plasmas Interacting with Neutral Gas

Zeljka Matutinovic-Krstelj
Department: Electrical Engineering
Advisor: James Sturm
Degree: Ph.D.
Thesis: Base Doping Effects and Design of Si/SiGe/Si Heterojunction Bipolar Transitors

Science Education Program

The mission of the Science Education Program is to use the facilities and resources of the Princeton University Plasma Physics Laboratory (PPPL) to improve the science, math, and technology education of students in elementary and secondary schools.

During 1994, the Science Education Program outreach activities continued to increase in size and scope. The staff interacted with students, teachers, administrators, and the community at-large. In addition, staff members of the Science Education Program participated in a number of workshops and seminars to ensure the incorporation of "best practice" in all of the Laboratory's education programs.

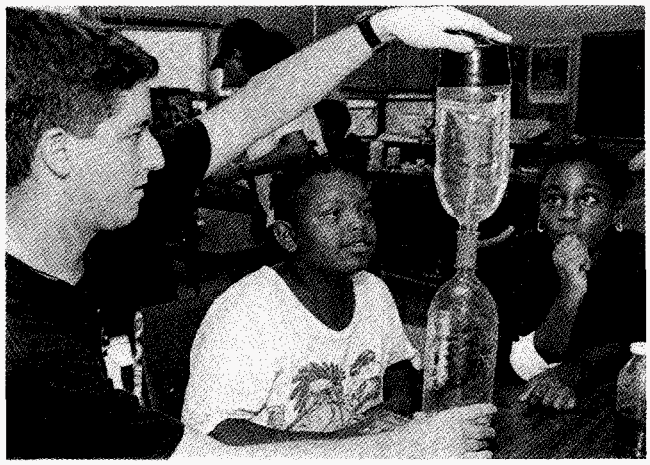

Princeton University students serving as mentors and tutors helped young people from inner-city Trenton to improve their science and math skills. (95PR070-18)

Research Opportunities

The Princeton Plasma Physics Laboratory conducted the Summer Science Awards Program (SSA) for high-school students. SSA '94 provided an eight-week research experience for 17 high-school students from various school districts in central New Jersey, including four students from Trenton Central High School in Trenton, NJ. Students worked on a variety of projects including computer simulation, plasma etching, and transport simulation codes. Students were placed in several divisions of the Laboratory including, TFTR Diagnostics and Data Analysis, PBX-M, Engineering and Technology Development, and the Computer Division.

The Teacher Research Associates Program (TRAC) was open to secondary science, mathematics, and technology education teachers. Funded by the U.S. Department of Energy, participants were selected by draft from a national pool of applicants, as well as from teachers living and working in New Jersey. In 1994, PPPL hosted two national and eight regionally selected teachers. The teachers participated in various research projects throughout the Lab, and workshops were conducted to facilitate the transfer of their research experience to the classroom, including one aimed at developing strategies to integrate interaction and communication in the classroom with the process of academic inquiry. As a result of the program, one teacher has conducted a week-long, district-wide training workshop for physics teachers; another developed a unit based on analysis of data collected during his research project, and another collaborated on a paper presented the 1994 Division of Plasma Physics' meeting of the American Physical Society.

The Science Education Program's Undergraduate Research Opportunities Program provided summer research experiences to students who previously participated in our program for high-school students, as well as those undergraduates attending local universities, including Princeton and Rutgers. Research opportunities were offered to two Princeton University

students and to two students who previously participated in our program for high-school students: one from Rutgers University and one from Massachusetts Institute of Technology. Summer research experiences were also offered under a program for students who attend Historically Black Colleges and Universities (HBCU). In addition, PPPL hosted a physics professor and two of his students under the HBCU-Visiting Faculty and Student Program sponsored by the Oak Ridge Institute for Science and Education (ORISE). Projects for this summer's undergraduates included the study of ion cyclotron range of frequencies heating, simulation software programming, coil circuits design and their analysis for the Magnetic Reconnection Experiment, computer simulation of plasma etching; the study of U.S. science policy related to fusion energy research, and modifications to a three-dimensional magnetohydrodynamic equilibrium code.

National Undergraduate Fellowship Program

In FY94, PPPL's Science Education Program administered the National Undergraduate Fellowship Program. The program, proposed by the University Fusion Association in conjunction with PPPL, provided an opportunity for 28 students from 25 different colleges and universities to participate in research opportunities relevant to fusion research, while providing capable assistants for fusion research projects. The ten-week program was composed of a one-week introductory course on plasma physics and fusion engineering, held at PPPL, followed by nine weeks of research at a variety of facilities around the country engaged in fusion research—five participants remained at PPPL for their research assignment. Following the program, several participants have enrolled in plasma physics classes, and others have decided to base their senior theses on their summer research. One student, who was awarded a Rhodes Scholarship, attributed his scholarship to his summer experience in the National Undergraduate Fellowship Program.

Programs

Fractals, Chaos, and Dynamics

In 1994, the PPPL Science Education Program conducted a symposium entitled Fractals, Chaos, and Dynamics. The presenters at this five-day workshop included some of the leaders in the field of basic research in fractals, chaos, and dynamics, as well as those who are leading the effort to bring discussions of fractals, chaos, and dynamics into the classroom including, Heintz-Otto Peitgen, Deitmar Saupe, Lee Yunker, Evan Malestsky, Terry Perciante, Richard Voss, and Harlheinz Haas. A special workshop was conducted by Jhane Barnes, a New York fashion designer who discussed fractals and fabrics. Classroom activities developed by the participants in the 1993 workshops were presented as well. All of the 120 attendees stated that they gained valuable new ideas for implementing and enhancing the teaching of fractals. The symposium provided an opportunity for mathematics and science educators to gain additional knowledge in the emerging fields of fractal geometry and chaos theory.

Summer Teachers' Leadership Institutes

During the summer of 1994, PPPL ran four institutes. Each of the workshops was designed with a specific target audience in mind: teachers of science and mathematics of grades K-2, teachers of science and mathematics in grades 3-5, teachers of science and mathematics of grades 5-8, and teachers of mathematics of grades 6-12. Applicants were recruited from central New Jersey. A total of 114 teachers were selected

Gaining hand-ons on experience in science was one of the focuses of the Summer Teachers' Leadership Institutes conducted by PPPL's Science Education Program and attended by more than one hundred Central New Jersey Teachers. (94PR064-8A)

from more than two-hundred applicants. The three objectives of the workshops were: to increase teachers' content knowledge in science and mathematics, to promote thinking and problem solving skills in the classroom, and to increase teachers' knowledge of pedagogy. The workshops were conducted by PPPL staff and local teachers. Lectures were inquiry-based and followed by hands-on activities. All activities were integrated across the curriculum focusing on connections among science, mathematics, literature, art, and music.

Kids-Network

A workshop in conjunction with the National Geographic Society, Oak Ridge Institute for Science and Education, Ames Laboratory and sponsored by the U.S. Department of Energy entitled, "What's in Our Water," was held for teachers of grades 3-7, including 15 teachers from Trenton. The workshop focused on building computer skills, while addressing environmental issues surrounding water quality.

Science on Saturday

From January 9 to March 20, PPPL sponsored a Science on Saturday program. The program was a nine-week series of talks on a variety of topics geared toward high-school students, but open to teachers, parents, and the community. Russell Hulse, a 1993 Nobel Prize winner for Physics, gave the final lecture in the series. A complete list of the speakers, their affiliations, and the topics they spoke about are given in Table I.

Science Bowl 1994

In February, PPPL Science Education Program, with the help of approximately 40 PPPL volunteers, hosted the New Jersey Regional Competition of the National Science Bowl®. Sponsored by the U.S. Department of Energy and modeled after academic competitions such as "The G.E. College Bowl," sixteen teams from high schools in area school districts participated in this exciting event. The winning team went on to represent New Jersey at the National Science Bowl® held in Washington D.C.

PPPL-Trenton Partnership

Fiscal year 1994 marked the fourth year of the PPPL-Trenton School District Partnership. Building on the success of the previous years, the Partnership made remarkable strides in the following areas.

Table I. Science on Saturday 1994 Lecture Series.

Speaker	Affiliation	Topic
Dr. Richard Voss	IBM Research Laboratories	The Practical Fractal
Dr. Dale Meade	Princeton Plasma Physics Laboratory	Deuterium-Tritium Results on the Tokamak Fusion Test Reactor
Professor Patrick Hanrahan	Princeton University	Computer Graphics in Terminator II and Other Films
Professor Edward Cox	Princeton University	How Animals Develop their Shape and Form
Professor Edward Witten	Institute for Advanced Study	The Magic of Four Dimensions
Professor Richard Lutz	Rutgers University	Amazing Creatures at Hot Water Springs in the Deep Sea
Professor Edwin Turner	Princeton University	Looking at the Universe through Gravity's Lenses
Dr. Leslie Johnson	Princeton University	Sex Differences in Animals—What For?
Dr. Russell Hulse	Princeton Plasma Physics Laboratory	The Discovery of the Binary Pulsar

Curriculum Revision

Discussions to revise the Trenton Public Schools science curriculum were begun during the 1992-1993 school year. During the summer of 1994, the elementary school curriculum committee met at PPPL during July and August. Working with PPPL staff, activities manuals were constructed for grades K-5. The teaching of activity-based science for forty minutes per day during the second and fourth marking periods is now mandatory in Trenton. The new science curriculum is modeled after the proposed New Jersey Science Content Standards.

Professional Development of Teachers and Administrators

Another main focus of the Partnership is the continued professional development of teachers and administrators. In 1994, PPPL staff conducted six weeks of summer workshops, providing more than 3,560 teacher-hours of staff development. In addition, thirty-five workshops were held during the school year in the afternoons and on Saturdays, providing more than 4,200 teacher-hours of staff development.

Visiting Scientists and School Support

An important part of the PPPL-Trenton Partnership is the PPPL staff volunteers, who are available to visit classrooms to meet with teachers and talk to students on a variety of topics in science, technology, and mathematics. These professional scientists, engineers, technicians, and administrators serve both as technical resources and role models.

Scientists in Residence

In cooperation with the Princeton Chapter of Sigma Xi, scientists in residence have been placed in all of Trenton's 23 schools. Science Advisors, SciAds, as they are called, visit their schools every two weeks for two or three hours. PPPL's science education staff meet with SciAds on a regular basis to help address their needs.

Princeton Student Volunteer Council

During the summer of 1994, fifteen Princeton University students participated in five community-based programs in Trenton and served as tutors and mentors to nearly 350 young people who reside in the inner city. The primary focus of the programs was on the improvement of inner-city students' science and mathematics skills.

A Princton University tutor helps inner-city children from Trenton during the summer of 1994. (95PR070-24)

Section Coordinators

Awards and Honors
Patti Wieser

Tokamak Fusion Test Reactor
David W. Johnson

Princeton Beta Experiment-Modification
Robert Kaita

Current Drive Experiment-Upgrade
Masayuki Ono
Yong-Seok Hwang

Tokamak Physics Experiment
John A. Schmidt

International Thermonuclear Experimental Reactor
Ned R. Sauthoff

Collaborations
Kenneth M. Young

Low-Temperature Plasma Research
Samuel A. Cohen

Electron Diffusion Gauge Experiments
Stephen Paul

Theoretical Studies
Harry E. Mynick

Divertor Modeling
Charles F.F. Karney

High-Field Magnet Project
Peter Bonanos

Engineering and Technology Development Department
Michael D. Williams

Design and Analysis Division
Robert A. Ellis, III

Computer Systems Division
Dori J. Barnes

Engineering and Technology Development Department (Continued)
Technical Systems
Alfred von Halle

Facilities and Environmental Management
J.W. Anderson

Fabrication and Assembly
Lawrence E. Dudek

TFTR Shutdown and Removal
Erik D. Perry

Technology Transfer
Michael D. Williams
Lewis D. Meixler

Environment, Safety, and Health and Quality Assurance
John W. DeLooper

Environment, Safety, and Health
Joseph Stencel

Quality Assurance
Judith A. Malsbury

Office of Human Resources and Administration
Steven M. Iverson

PPPL Invention Disclosures for Fiscal Year 1994
Marilyn J. Hondorp

Office of Resource Management
Edward H. Winkler

Graduate Education: Plasma Physics
Nathaniel J. Fisch

Graduate Education: Program in Plasma Science and Technology
Samuel A. Cohen

Science Education Program
Diane L. Carroll

Princeton Plasma Physics Laboratory Reports Fiscal Year 1994

PPPL-2941, October 1993, 67 pp

Transport Effects of Low (m,n) MHD Modes on TFTR Supershots

Z. Chang, E.D. Fredrickson, J.D. Callen, K.M. McGuire, M.G. Bell, R.V. Budny, C.E. Bush, D.S. Darrow, A.C. Janos, L.C. Johnson, H. Park, S.D. Scott, J.D. Strachan, E.J. Synakowski, G. Taylor, R.M. Wieland, M.C. Zarnstorff, S.J. Zweben, and TFTR Group

PPPL-2943, October, 1993, 25 pp

Modeling of MeV Alpha Particle Energy Transfer to Lower Hybrid Waves

J. Schivell, D. Monticello, N. Fisch, and J. Rax

PPPL-2944, October 1993, 22 pp

Role of Neutral-Beam Fueling Profile in Energy Confinement and Neutron Emission on TFTR

H.K. Park, M.G. Bell, W.M. Tang, G. Taylor, M. Yamanda, R.V. Budny, D.C. McCune, and R. Wieland

PPPL-2945, November 1993, 36 pp

Wall Conditioning Experiments on TFTR Using Impurity Pellet Injection.

J.D. Strachan, D.K. Mansfield, M.G. Bell, J. Collins, D. Ernst, K. Hill, J. Hosea, J. Timberlake, M. Ulrickson, M.J. Terry, E. Marmar, and J. Snipes

PPPL-2946, November 1993, 17 pp

Spectroscopic Observation of 0-300 keV ^{3}He Ions Produced by ICRF Heating in the TFTR Tokamak

B.C. Stratton, R.J. Fonck, G. McKee, T. Thorson, G. Hammett, C.K. Phillips, and E.J. Synakowski

PPPL-2947, March 1994, 45 pp

The Generalized Accessibility and Spectral Gap of Lower Hybrid Waves in Tokamaks

H. Takahashi

PPPL-2948, January 1994, 37 pp

ICRF Heating of TFTR Deuterium Supershot Plasmas in the ^{3}He Minority Regime

G. Taylor, J.R. Wilson, R.C. Goldfinger, J.C. Hosea, D.J. Hoffman, R. Majeski, C.K. Phillips, D.A. Rasmussen, J.H. Rogers, G. Schilling, J.E. Stevens, M.G. Bell, R.V. Budny, C.E. Bush, Z. Chang, D. Darrow, D.R. Ernst, E. Fredrickson, G. Hammett, K. Hill, A. Janos, D. Jassby, D.W. Johnson, L.C. Johnson, S.S. Medley, H.K. Park, J. Schivell, J.D. Strachan, E. Synakowski, and S. Zweben

PPPL-2949, November 1993, 13 pp

Summary of the IEA Workshop on Alpha Physics and Tritium Issues in Large Tokamaks.

C.Z. Cheng, C.S. Pitcher, B. Stratton, and S.J. Zweben

PPPL-2951, January 1994, 73 pp

Cyclotron Subharmonics Resonant (CSR) Heating

H. Abe

PPPL-2952, January 1994, 17 pp

Experimental Study of Magnetic Reconnection during a Sawtooth Crash in a High Temperature Tokamak Plasma

M. Yamada, F.M. Levinton, J. Manickam, Y. Nagayama, and N. Pomphrey

PPPL-2953, November 1993, 16 pp

The Theory of Stabilization of Sawtooth Oscillations in TFTR Supershots

L. Zakharov, F. Levinton, S. Migliuolo, and B. Rogers

PPPL-2954, January 1994, 34 pp

Guiding-Center Equations for Electrons in Ultraintense Laser Fields

J.E. Moore and N.J. Fisch

PPPL-2955, March 1994, 13 pp

Global Structures of Alfvén-Ballooning Modes in Magnetospheric Plasmas

G. Vetoulis and L. Chen

PPPL-2956, January 1994, 37 pp

Poloidal Flux Linkage Requirements for the International Thermonuclear Experimental Reactor

S.C. Jardin, C. Kessel, and N. Pomphrey

PPPL-2957, February 1994, 15 pp

Are the Invariance Principles Really Truly Lorentz Covariant?

V. Arunasalam

PPPL-2959, March 1994, 38 pp

Nonlinear Coupling of Low-n Modes in PBX-M

S. Sesnic, R. Kaita, S. Kaye, M. Okabayashi, R.E. Bell,G.M. Gammel, A. Holland, H.W. Kugel, B. LeBlanc, F.M. Levinton, H. Takahashi, E.J. Powers, and S. Im

PPPL-2960, February 1994, 17 pp

Lower Hybrid Current Drive and Ion Bernstein Wave Heating Experiments on PBX-M

S. Bernabei and the PBX-M Group

PPPL-2961, February 1994, 16 pp

Periods of Enhanced Transport During H-Mode in PBX-M

S. Sesnic, J. Dunlap, R. Kaita, S.M. Kaye, and M. Okabayashi

PPPL-2962, February 1994, 7 pp

Performance of the PBX-M Passive Plate Stabilization System

H. W. Kugel, R. Bell, S. Bernabei, T.K. Chu, A. England, G. Gettelfinger, R. Hatcher, P. Heitzenroeder, R. Isler, S. Jones, R. Kaita, S. Kaye, B. LeBlanc, M. Ono, M. Okabayashi, N. Sauthoff, L. Schmitz, S. Sesnic, H. Takahashi, W. Tighe, J. Timberlake, S. von Goeler, A. Post-Zwicker, and the PBX-M Group

PPPL-2963, February 1994, 22 pp

MHD Stability Regimes for Steady State and Pulsed Reactors

S.C. Jardin, C.E. Kessel, and N. Pomphrey

PPPL-2964, March 1994, 10 pp

Influence of Radial Electric Field on Alfvén-Type Instabilities

T.S. Hahm W.M. and Tang

PPPL-2965, March 1994, 34 pp

Comparisons of Gyrofluid and Gyrokinetic Simulations

S.E. Parker, W. Dorland, R.A. Santoro, M.A. Beer, Q.P. Liu, W.W. Lee, and G.W. Hammett

PPPL-2966, April 1994, 13 pp

An Overview of PBX-M H-Mode Results

S.M. Kaye, H. Kugel, B. LeBlanc, S. Sesnic, and the PBX-M Group; J.L. Dunlap and the ORNL Group; and L. Schmitz, G. Tynan, and the UCLA Group

PPPL-2867, April 1994, 9 pp

ELM-Related Fluctuations in PBX-M H Modes

S.M. Kaye, T.S. Hahm, S. Sesnic, W. Tang, P. Roney, W. Davis, J.L. Dunlap, and H. Harris

PPPL-2968, March 1994, 16 pp

Stabilization and Onset of Sawteeth in TFTR

F.M. Levinton, L. Zakharov, S.H. Batha, J. Manickam, and M.C. Zarnstorff

PPPL-2970, February 1994, 16 pp

Frequency-Sweeping: A New Technique for Energy-Selective Transport

H.E. Mynick and N. Pomphrey

PPPL-2971, March 1994, 31 pp

Study of High Energy Ion Loss during Hydrogen Minority Heating in TFTR

J. Park and S.J. Zweben

PPPL-2972, March 1994, 34 pp

Bootstrap Current in a Tokamak

C.E. Kessel

PPPL-2973, March 1994, 40 pp

Numerical Evaluation of High Energy Particle Effects in Magnetohydrodynamics

R.B. White and Y. Wu

PPPL-2974, March 1994, 26 pp

Ballooning-Mirror Instability and Internally Driven Pc 4-5 Wave Events

C.Z. Cheng, Q. Qian, K. Takahashi, and A.T.Y. Lui

PPPL-2976, March 1994, 35 pp

Nonlinear Electromagnetic Gyrokinetic Equations for Rotating Axisymmetric Plasmas

M. Artun and W.M. Tang

PPPL-2977, March 1994, 14 pp

Confinement and Heating of a Deuterium-Tritium Plasma

R.J. Hawryluk, H. Adler, P. Alling, C. Ancher, H. Anderson, J.L. Anderson, D. Ashcroft, C.W. Barnes, G. Barnes, S. Batha, M.G. Bell, R. Bell, M., Bitter, W. Blanchard, N.L. Bretz, R. Budny, C.E. Bush, R. Camp, M. Caorlin, S. Cauffman, Z. Chang, C.Z. Cheng, J. Collins, G. Coward, D.S. Darrow, J. DeLooper, H. Duong, L. Dudek, R. Durst, P.C. Efthimion, D. Ernst, R. Fisher, R.J. Fonck, E. Fredrickson, N. Fromm, G.Y. Fu, H.P. Furth, C. Gentile, N. Gorelenkov, B. Grek, L.R. Grisham, G. Hammett, G.R. Hanson, W. Heidbrink, H.W. Herrmann, K.W. Hill, J. Hosea, H. Hsuan, A. Janos, D.L. Jassby, F.C. Jobes, D.W. Johnson, L.C. Johnson, J. Kamperschroer, H. Kugel, N.T. Lam, P.H. LaMarche, M.H. Loughlin, B. LeBlanc, M. Leonard, F.M. Levinton, J. Machuzak, D.K. Mansfield, A. Martin, E. Mazzucato, R. Majeski, E. Marmar, J. McChesney, B. McCormack, D.C. McCune, K.M. McGuire, G. McKee, D.M. Meade, S.S. Medley, D.R. Mikkelsen, D. Mueller, M. Murakami, A. Nagy, R. Nazikian, R. Newman, T. Nishitani, M. Norris, T. O'Connor, M. Oldaker, M. Osakabe, D.K. Owens, H. Park, W. Park, S.F. Paul, G. Pearson, E. Perry, M. Petrov, C.K. Phillips, S. Pitcher, A. Ramsey, D.A. Rasmussen, M.H. Redi, D. Roberts, J. Rogers, R. Rossmassler, A.L. Roquemore, E. Ruskov, S.A. Sabbagh, M. Sasao, G. Schilling, J. Schivell, G.L. Schmidt, S.D. Scott, R. Sissingh, C.H. Skinner, J. Snipes, J. Stevens, T. Stevenson, B.C. Stratton, J.D. Strachan, E. Synakowski, W. Tang, G. Taylor, J.L. Terry, M.E. Thompson, M. Tuszewski, C. Vannoy, A. von Halle, S. von Goeler, D. Voorhees, R.T. Walters, R. Wieland, J.B. Wilgen, M. Williams, J.R. Wilson, K.L. Wong, G.A. Wurden, M. Yamada, K.M. Young, M.C. Zarnstorff, and S.J. Zweben

PPPL-2978, March 1994, 16 pp

Fusion Power Production from TFTR Plasmas Fueled with Deuterium and Tritium

J.D. Strachan, H. Adler, P. Alling, C. Ancher, H. Anderson, J.L. Anderson, D. Ashcroft, C.W. Barnes, G. Barnes, S. Batha, M.G. Bell, R. Bell, M. Bitter, W. Blanchard, N. Bretz, R. Budny, C.E. Bush, R. Camp, M. Caorlin, S. Cauffman, Z. Chang, C.Z. Cheng, J. Collins, G. Coward, D.S. Darrow, J. DeLooper, H. Duong, L. Dudek, R. Durst, P.C. Efthimion, D. Ernst, R. Fisher, R.J. Fonck, E. Fredrickson, N. Fromm, G.Y. Fu, H.P. Furth, C. Gentile, N. Gorelenkov, B. Grek, L.R. Grisham, G. Hammett, G.R. Hanson, R.J. Hawryluk, W. Heidbrink, H.W. Herrmann, K.W. Hill, J. Hosea, H. Hsuan, A. Janos, D.L. Jassby, F.C. Jobes, D.W. Johnson, L.C. Johnson, J. Kamperschroer, H. Kugel, N.T. Lam, P.H. LaMarche, M.J. Loughlin, B. LeBlanc, M. Leonard, F.M. Levinton, J. Machuzak, D.K. Mansfield, A. Martin, E. Mazzucato, R. Majeski, E. Marmar, J. McChesney, B. McCormack, D.C. McCune, K.M. McGuire, G. McKee, D.M. Meade, S.S. Medley, D.R. Mikkelsen, D. Mueller, M. Murakami, A. Nagy, R. Nazikian, R. Newman, T. Nishitani, M. Norris, T. O'Connor, M. Oldaker, M. Osakabe, D.K. Owens, H. Park, W. Park, S.F. Paul, G. Pearson, E. Perry, M. Petrov, C.K. Phillips, S. Pitcher, A.T. Ramsey, D.A. Rasmussen, M.H. Redi, D. Roberts, J. Rogers, R. Rossmassler, A.L. Roquemore, E. Ruskov, S.A. Sabbagh, M. Sasao, G. Schilling, J. Schivell, G.L. Schmidt, S.D. Scott, R. Sissingh, C.H. Skinner, J.A. Snipes, J. Stevens, T. Stevenson, B.C. Stratton, E. Synakowski, W. Tang, G. Taylor, J.L. Terry, M.E. Thompson, M. Tuszewski, C. Vannoy, A. von Halle, S. von Goeler, D. Voorhees, R.T. Walters, R. Wieland, J.B. Wilgen, M. Williams, J.R. Wilson, K.L. Wong, G.A. Wurden, M. Yamada, K.M. Young, M.C. Zarnstorff, and S.J. Zweben

PPPL-2979, August 1994, 11 pp

Alpha Particle Effects on the Internal Kink Modes

Y. Wu and C.Z. Cheng

PPPL-2980, April 1994, 12 pp

Evolution of the Alpha Particle Driven Toroidicity Induced Alfvén Mode

Y. Wu, R.B. White, and C.Z. Cheng

PPPL-2981, April 1994, 36 pp

Doppler-Shifted Neutral Beam Line Shape and Beam Transmission

J.H. Kamperschroer, L.R. Grisham, N. Kokatnur, L.J. Lagin, R.A. Newman, T.E. O'Connor, T.N. Stevenson, and A. von Halle

PPPL-2982, April 1994, 14 pp

The Validity of the Extended Energy Principle

M.S. Chance, J.L. Johnson, and R.M. Kulsrud

PPPL-2983, May 1994, 39 pp

Fracture Testing and Performance of Beryllium Copper Alloy C17510

H.A. Murray and I.J. Zatz

PPPL-2984, April 1994, 29 pp

Self-Consistent Study of the Alpha Particle Driven TAE Mode

Y. Wu and R.B. White

PPPL-2985, June 1994, 20 pp

Rotation Shear Induced Fluctuation Decorrelation in a Toroidal Plasma

T.S. Hahm

PPPL-2986, April 1994, 25 pp

Comparison of Initial Value and Eigenvalue Codes for Kinetic Toroidal Plasma Instabilities

M. Kotschenreuther, G. Rewoldt, and W.M. Tang

PPPL-2987, April 1994, 29 pp

Preparations for Deuterium-Tritium Experiments on the Tokamak Fusion Test Reactor

R.J. Hawryluk, H. Adler, P. Alling, C. Ancher, H. Anderson, J.L. Anderson, J.W. Anderson, V. Arunasalam, G. Ascione, D. Ashcroft, C.W. Barnes, G. Barnes, D.B. Batchelor, G. Bateman, S. Batha, L.A. Baylor, M. Beer, M.G. Bell, T.S. Biglow, M. Bitter, W. Blanchard, P. Bonoli, N. Bretz, C. Brunkhorst, R. Budny, T. Burgess, H. Bush, C.E. Bush, R. Camp, M. Caorlin, H. Carnevale, Z. Chang, L. Chen, C.Z. Cheng, J. Chrzanowski, I. Collazo, J. Collins, G. Coward, S. Cowley, M. Cropper, D.S. Darrow, R. Daugert, J. DeLooper, H. Duong, L. Dudek, R. Durst, P.C. Efthimion, D. Ernst, J. Faunce, R.J. Fonck, E. Fredd, E. Fredrickson, N. Fromm, G.Y. Fu, H.P. Furth, V. Garzotto, C. Gentile, G. Gettelfinger, J. Gilbert, J. Gioia, R.C. Goldfinger, T. Golian, N. Gorelenkov, M.J. Gouge, B. Grek, L.R. Grisham, G. Hammett, G.R. Hanson, W. Heidbrink, H.W. Herrmann, K.W. Hill, S. Hirshman, D.J. Hoffman, J. Hosea, R.A. Hulse, H. Hsuan, E.F. Jaeger, A. Janos, D.L. Jassby, F.C. Jobes, D.W. Johnson, L.C. Johnson, J. Kamperschroer, J. Kesner, H, Kugel, S. Kwon, G. Labik, N.T. Lam, P.H. LaMarche, M.J. Loughlin, E. Lawson, B. LeBlanc, M. Leonard, J. Levine, F.M. Levinton, D. Loesser, D. Long, J. Machuzak, D.K. Mansfield, M. Marchlik, E.S. Marmar, R. Marsala, A. Martin, G. Martin, V. Mastrocola, E. Mazzucato, M.P. McCarthy, R. Majeski, M. Mauel, B. McCormack, D.C. McCune, K.M. McGuire, D.M. Meade, S.S. Medley, D.R. Mikkelsen, S.L. Milora, D. Monticello, D. Mueller, M. Murakami, J.A. Murphy, A. Nagy, G.A. Navratil, R. Nazikian, R. Newman, T. Nishitani, M. Norris, T. O'Connor, M. Oldaker, J. Ongena, M. Osakabe, D.K. Owens, H. Park, W. Park, S.F. Paul, Yu.I. Pavlov, G. Pearson, F. Perkins, E. Perry, R. Persing, M. Petrov, C.K. Phillips, S. Pitcher, S. Popovichev, A.L. Qualls, S. Raftopoulos, R. Ramakrishnan, A. Ramsey, D.A. Rasmussen, M.H. Redi, G. Renda, G. Rewoldt, D. Roberts, J. Rogers, R. Rossmassler, A.L. Roquemore, S.A. Sabbagh, M. Sasao, J. Scharer, G. Schilling, J. Schivell, G.L. Schmidt, R. Scillia, S.D. Scott, T. Senko, R. Sissingh, C. Skinner, J. Snipes, P. Snook, J. Stencel, J. Stevens, T. Stevenson, B.C. Stratton, J.D. Strachan, W. Stodiek, J. Swanson, E. Synakowski, W. Tang, G. Taylor, J. Terry, M.E. Thompson, J.R. Timberlake, H.H. Towner, M. Ulrickson, A. von Halle, C. Vannoy, R. Wieland, J.B. Wilgen, M. Williams, J.R. Wilson, K. Wright, D. Wong, K.L. Wong, P. Woskov, G.A. Wurden, M. Yamada, A. Yeun, S. Yoshikawa, K.M. Young, L. Zakharov, M.C. Zarnstorff, and S.J. Zweben

PPPL-2988, September 1994, 13 pp

Observation of Nonlinear Neoclassical ∇_p-Driven Tearing Modes in TFTR

Z. Chang, J.D. Callen, C.C. Hegna, E.D. Fredrickson, R.V. Budny, K.M. McGuire, M.C. Zarnstorff, and the TFTR Group

PPPL-2989, May 1994, 60 pp

Utility of Extracting α-Particle Energy by Waves

N.J. Fisch and M.C. Herrmann

PPPL-2990, June 1994, 32 pp

Numerical Studies on the Electromagnetic Properties of the Nonlinear Lorentz Computational Model for the Dielectric Media

H. Abe and H. Okuda

PPPL-2992, June 1994, 33 pp

Numerical Studies on the Soliton Propagation in the Dielectric Media by the Nonlinear Lorentz Computational Model

H. Abe and H. Okuda

PPPL 2993, June 1994, 21 pp

First Measurements of Tritium Recycling in TFTR

C.H. Skinner, H. Adler, R.V. Budny, J. Kamperschroer, L.C. Johnson, A.T. Ramsey, and D.P. Stotler

PPPL-2994, June 1994, 27 pp

Alpha Particle Effects on the Internal Kink and Fishbone Modes

Y. Wu, C.Z. Cheng, and R.B. White

PPPL-2995, June 1994, 14 pp

Comments on Finite Larmor Radius Models for Ion Cyclotron Range of Frequencies Heating in Tokamaks

C.K. Phillips, J.R. Wilson, J.C. Hosea, R. Majeski, and D.N. Smithe

PPPL-2996, June 1994, 14 pp

Observation of Doppler-Shifted Tα Emission from TFTR Tritium Neutral Beams

J.H. Kamperschroer, L.R. Grisham, L.J. Lagin, T.E. O'Connor, R.A. Newman, T.N. Stevenson, A. von Halle, and K.E. Wright

PPPL-2997, June 1994, 29 pp

Core Fueling to Produce Peaked Density Profiles in Large Tokamaks

D.R. Mikkelsen, K.M. McGuire, G.L. Schmidt, S.J. Zweben, S.E. Attenberger, W.A. Houlberg, and S.L. Milora

PPPL-2998, August 1994, 31 pp

Excitation of Alfvén Cyclotron Instability by Charged Fusion Products in Tokamaks

N.N. Gorelenkov and C.Z. Cheng

PPPL-3000, September 1994, 13 pp

Excitation of Large-Θ Ion-Bernstein Waves in Tokamaks

E.J. Valeo and N.J. Fisch

PPPL-3002, August 1994, 27 pp

Reflectometer Measurements of Density Fluctuations in Tokamak Plasmas

R. Nazikian and E. Mazzucato

PPPL-3003, August 1994, 15 pp

Effects of Turbulent Fluctuations on Density Measurements with Microwave Reflectometry in Tokamaks

E. Mazzucato and R. Nazikian

PPPL-3004, September 1994, 23 pp

Investigation of Magnetic Reconnection during a Sawtooth Crash in a High Temperature Tokamak

M. Yamada, F. Levinton, N. Pomphrey, R. Budny, J. Manickam, and Y. Nagayama

PPPL-3005, August 1994, 49 pp

Model for Collisional Fast Ion Diffusion into Tokamak Fusion Test Reactor Loss Cone

C.S. Chang, J. Schivell, R. Budny, S. Scott, and S.J. Zweben

PPPL-3006, August 1994, 21 pp

Electron Heating and Current Drive by Mode Converted Slow Waves

R. Majeski, C.K. Phillips, and J.R. Wilson

PPPL-3011, September 1994, 63 pp

Collisional Stochastic Ripple Diffusion of Alpha Particles and Beam Ions on TFTR

M.H. Redi, M.C. Zarnstorff, R.B. White, R.V. Budny, J.F. Schivell, S.D. Scott, and S.J. Zweben

PPPL-3013, September 1994, 23 pp

Deuterium-Tritium Experiments on the Tokamak Fusion Test Reactor

J. Hosea, H. Adler, P. Alling, C. Ancher, H. Anderson, J.L. Anderson, J.W. Anderson, V. Arunasalam, G. Ascione, D. Ashcroft, C.W. Barnes, G. Barnes, S. Batha, M.G. Bell, R. Bell, M. Bitter, W. Blanchard, N. Bretz, C. Brunkhorst, R. Budny, T. Burgess, H. Bush, C.E. Bush,

R. Camp, M. Caorlin, H. Carnevale, S. Cauffman, Z. Chang, C.Z. Cheng, J. Chrzanowski, J. Collins, G. Coward, M. Cropper, D.S. Darrow, R. Daugert, J. DeLooper, H. Duong, L. Dudek, R. Durst, P.C. Efthimion, D. Ernst, J. Faunce, R. Fischer, R.J. Fonck, E. Fredd, E. Fredrickson, N. Fromm, G.Y. Fu, H.P. Furth, V. Garzotto, C. Gentile, G. Gettelfinger, J. Gilbert, J. Gioia, T. Golian, N. Gorelenkov, B. Grek, L.R. Grisham, G. Hammett, G.R. Hanson, R. Hawryluk, W. Heidbrink, H.W. Herrmann, K.W. Hill, H. Hsuan, A. Janos, D.L. Jassby, F.C. Jobes, D.W. Johnson, L.C. Johnson, J. Kamperschroer, J. Kesner, H, Kugel, S. Kwon, G. Labik, N.T. Lam, P.H. LaMarche, E. Lawson, B. LeBlanc, M. Leonard, J. Levine, F.M. Levinton, D. Loesser, D. Long, M.J. Loughlin, J. Machuzak, D.K. Mansfield, M. Marchlik, E.S. Marmar, R. Marsala, A. Martin, G. Martin, V. Mastrocola, E. Mazzucato, R. Majeski, M. Mauel, M.P. McCarthy, B. McCormack, D.C. McCune, K.M. McGuire, D.M. Meade, S.S. Medley, D.R. Mikkelsen, S.L. Milora, D. Mueller, M. Murakami, J.A. Murphy, A. Nagy, G.A. Navratil, R. Nazikian, R. Newman, T. Nishitani, M. Norris, T. O'Connor, M. Oldaker, J. Ongena, M. Osakabe, D.K. Owens, H. Park, W. Park, S.F. Paul, Yu.I. Pavlov, G. Pearson, F. Perkins, E. Perry, R. Persing, M. Petrov, C.K. Phillips, S. Pitcher, S. Popovichev, S. Pysher, A.L. Qualls, S. Raftopoulos, R. Ramakrishnan, A. Ramsey, D.A. Rasmussen, M.H. Redi, G. Renda, G. Rewoldt, D. Roberts, J. Rogers, R. Rossmassler, A.L. Roquemore, E. Ruchov, S.A. Sabbagh, M. Sasao, G. Schilling, J. Schivell, G.L. Schmidt, R. Scillia, S.D. Scott, T. Senko, R. Sissingh, C. Skinner, J. Snipes, P. Snook, J. Stencel, J. Stevens, T. Stevenson, B.C. Stratton, J.D. Strachan, W. Stodiek, E. Synakowski, W. Tang, G. Taylor, J. Terry, M.E. Thompson, J.R. Timberlake, H.H. Towner, A. von Halle, C. Vannoy, R. Wester, R. Wieland, J.B. Wilgen, M. Williams, J.R. Wilson, K. Winston, K. Wright, D. Wong, K.L. Wong, P. Woskov, G.A. Wurden, M. Yamada, A. Yeun, S. Yoshikawa, K.M. Young, M.C. Zarnstorff, and S.J. Zweben

PPPL-3015, September 1994, 7 pp

Isotopic Mass and Alpha Heating Effects in TFTR DT Plasmas

R.V. Budny, M.G. Bell, D.K. Mansfield, J.D. Strachan, S. Zweben, H. Adler, C.E. Bush, Z. Chang, D. Ernst, E. Fredrickson, B. Grek, M. Murakami, H. Park, A.T. Ramsey, J. Schivell, S.D. Scott, C.H. Skinner, E. Synakowski, G. Taylor, and M.C. Zarnstorff

Glossary of Abbreviations, Acronyms, Symbols

A	Ampere
Å	Angstrom unit; 10^{-8} cm
ac	Alternating Current
ACT-I	Advanced Concepts Torus-I (now the CDX-U at PPPL)
ACX	Alpha Charge-Exchange
A/D	Analog-to-Digital
ADP	Automated Data Processing
ADPE	Automated Data Processing Equipment
ADS	Activity Data Sheets
AFSOR	Air Force Office of Scientific Research
AIHA	American Industrial Hygiene Association
ALADDIN	A Labeled Atomic Data Interface—an atomic physics data base for fusion applications.
ALARA	As Low As Reasonably Achievable
Alcator	A family of tokamak devices being developed and built at the Massachusetts Institute of Technology (from the Italian for high-field torus)
ALT-I	Advanced Limiter Test on TEXTOR (Jülich, Germany); Version I
ALT-II	Version II of ALT
AM	Amplitude Modulation
amu	Atomic Mass Unit
ANL	Argonne National Laboratory, Argonne, Illinois
ANSI	American National Standards Institute
APS	American Physical Society
ARIES	Advanced Reactor Innovation Evaluation Study
ARPS	Automated Receipts Processing System at PPPL
ASC	Area Safety Coordinator at PPPL
ASDEX	Axially Symmetric Divertor Experiment (Max-Planck-Institut für Plasmaphysik, Garching, Germany)

ASDEX-U	ASDEX Upgrade (also AUG)
Asher	A plasma magnetron. A device to create plasma using a longitudinal magnetic field and a radial electric field.
ASME	American Society of Mechanical Engineers
ASQC	American Society of Quality Control
ATC	Adiabatic Toroidal Compressor (at PPPL in the 1970's)
ATF	Advanced Toroidal Facility (a stellarator at the Oak Ridge National Laboratory, Oak Ridge, Tennessee)
ATF-1	Advanced Toroidal Facility-1
ATM	Asychronous Transfer Mode
AUG	ASDEX Upgrade (also ASDEX-U)
AWAFT	Automatic Work Approval Form Transfer (system) at PPPL
AWS	American Welding Society
B2	A PPPL edge plasma modeling code
BALDUR	A PPPL one-dimensional tokamak transport code
BBGKY	Bogoliubov-Born-Green-Kirkwood-Yvon
BES	Beam Emission Spectrometer
BETAS	A three-dimensional equilibrium code
BOFT	Beginning of Flattop
BPX	Burning Plasma Experiment (now the Tokamak Physics Experiment)
BS	Beta Scintallator Detector
Bytes	
CAD	Computer-Aided Design
CADD	Computer-Aided Design and Drafting (Facility)
CAMAC	Computer-Automated Measurement and Control (System)
CAMEO	Computer-Aided Management of Emergency Operations (Program)
CAR	Cost Analysis Report
CAS	Cognizant Area Supervisor at PPPL
CASL	Calibration and Service Laboratory at PPPL
CCD	Capacitor Charge/Discharge
CCD	Charge-Coupled Device
CCF	Central Computer Facility
CCT	Continuous Current Tokamak (at the University of California, Los Angeles)

CD	Conceptual Design
CDA	Conceptual Design Activity
CDR	Conceptual Design Review
CDX	Current-Drive Experiment at PPPL
CDX-U	Current Drive Experiment-Upgrade at PPPL
CEA	Commisariat A L'Energie Atomique
CEBAF	The US Department of Energy's Continuous Electron Beam Accelerator Facility located in Newport News, Virginia
CENA	Charge-Exchange Neutral Analyzer
CERT	Constant Elongation Rate Tensile
CESEP	Combined Electrical and Sample Exposure Probe
CFC	Carbon Fiber Composite
CFC	Chlorofluorocarbon
CFFTP	Canadian Fusion Fuels Technology Project
CH	Chicago Headquarters
CH-mode	Core H-mode
CHERS	Charge-Exchange Recombination Spectrometer
CHIRPS	Chicago Headquarter's Incident Reporting Programs
Ci	Curies
CICADA	Central Instrumentation, Control, and Data Acquisition (System) at PPPL
CICC	Cable in Conduit Conductor
CIEMAT	Centro de Investigaciones Energetics Medioambientales y Technologicas in Madrid, Spain
CIT	Compact Ignition Tokamak (now the Tokamak Physics Experiment)
cm	Centimeter
CMA	Cylindrical Mirror Analyzer
CMP	Configuration Management Plan
COE	Chief Operating Engineer
COO	Chicago Operations Office
COS	Console Operating Station
COXRALM	Composite Optical Soft X-Ray Laser Microscope at PPPL
CPC	Coil Protection Calculator
CPS	Coil Protection System
CPSR	Contractor Procurement System Review

CPU	Central Processing Unit
CRADAs	Cooperative Research and Development Agreement(s)
CRAY	A brand of computer made by Cray Research, founded by S. Cray
CRB	Configuration Review Board
CSD	Computer System Division at PPPL
CSR	Cost and Schedule Review
CTC	Center for Technology Commercialization (a NASA-based organization)
CTEM	Collisionless Trapped-Electron Mode
CTR	Controlled Thermonuclear Research
CX	Charge-Exchange
CXRS	Change-Exchange Recombination Spectroscopy
CY	Calendar Year (January 1 to December 31)
°	Degrees
°C	Degrees Centigrade
D/A	Digital-to-Analog
DARM	Data Acquisition Room
DAS	Data Acquisition System
DATS	Differential Atmospheric Tritium Sampler at PPPL
DAX	DAS supplemental system (uses a VAX computer)
dc	Direct Current
DCS	Distributed Computer Services
D&D	Decontamination and Decommissioning (now Shutdown and Removal)
D-D	Deuterium-Deuterium
DDC	Disruptive Discharge Cleaning
DEAR(s)	Department of Energy Acquisition Regulation(s)
DEC	Digital Equipment Corporation
DEGAS	A PPPL computer code for studying the behavior of neutrals in plasma
DEGAS-2	Revised DEGAS code
DEMO	Demonstration Power Reactor
DIALOG	An interactive online information retrieval system used by the PPPL Library
DIFFUSE	A computer code used to calculate the one-dimensional diffusion and trapping of atoms in a wall
DIII	Doublet-III—A tokamak located at General Atomics in San Diego, California

DIII-D	Doublet-III-D (upgrade of DIII with D-shaped plasma)
DITE	Divertor and Injection Tokamak Experiment (Culham Laboratory, United Kingdom)
DMSB	Disposable Molecular Sieve Bed
DN	Double Null
DNB	Diagnostic Neutral Beam
DOE	Department of Energy
DOE/RECON	An interactive online information retrieval system used by the PPPL Library
DOT	Department of Transportation
DPI	Deuterium Pellet Injector
dpm	Disintegrations per Minute
D-T	Deuterium-Tritium
DVC	Diagnostic Vacuum Controller
DVS	Diagnostic Vacuum System
EA	Environmental Assessment
ECE	Electron Cyclotron Emission
ECH	Electron Cyclotron Heating
ECR	Electron Cyclotron Resonance
ECRF	Electron Cyclotron Range of Frequencies
ECRH	Electron Cyclotron Resonance Heating
ECS	Energy Conversion System
EDA	Engineering Design Activity
EDG	Electron Diffusion Gauge
EF	Equilibrium Field
EH	Environmental and Health Office (at USDOE)
EIRENE	Monte Carlo neutral transport code (developed at Kernforschungsanlage, Jülich, Germany)
EIS	Environmental Impact Statement
ELMs	Edge Localized Modes
E-Mail	Electronic Mail
EMCS	Energy Monitoring and Control System at PPPL
EMEQ	Electrodynamic Moment Equilibrium
EMI	Electromagnetic Interface

EML	(DOE's) Environmental Measurements Laboratory
ENS	Emergency Notification System at PPPL
EPA	Environmental Protection Agency
EPFL	Ècole Polytechnique Fédérale de Lausanne
EPIP	Environmental Protection Implementation Plan
EPRI	Electric Power Research Institute
ER	Energy Research
ERAP	Emergency Readiness Assurance Plan
ERB	Engineering Review Board
ERI	Electron-Ripple Injection
ERP	Edge Relaxation Phenomena
ER/WM	Environmental Restoration and Waste Management
ESAAB	Energy Systems Acquisition Advisory Board
ESB	Executive Safety Board
ES&H	Environment, Safety, and Health
ESnet	Energy Sciences Network
ESO	Emergency Services Officer(s)
ESU	Emergency Services Unit at PPPL
ETACS	Equipment Tracking and Control System at PPPL
ETDD	Engineering and Technology Development Department
ETR	Engineering Test Reactor
ETS	Engineering Test Station
Eudora	A program developed at the National SuperComputer Center (University of Illinois) to handle electronic mail
eV	Electron Volt
EZB	Exclusion Zone Boundary
FAR	Federal Acquisition Regulation(s)
FAST	Fast Automatic Transfer System
FCPC	Field Coil Power Conversion
FDDI	Fiber Distribution Data Interface
FDR	Final Design Review
FEA	Finite Element Analysis
FEAC	Fusion Energy Advisory Committee
FEC	Field Error Correction

FED	Facilities Engineering Division at PPPL
FED	Fusion Engineering Device
FEDC	Fusion Engineering Design Center (at the Oak Ridge National Laboratory Oak Ridge, Tennessee)
FELIX	Fusion Electromagnetic Induction Experiment at the Argonne National Laboratory, Argonne, Illinois
FEM	Finite Element Modeling or Finite Element Method
FER	Fusion Engineering Reactor
FIDE	Fast Ion Diagnostic Experiment
FIR	Far-Infrared
FIS	(Department of Energy) Financial Information System
FLC	Federal Laboratory Consortium
FLOPSY	Flexible Optical Path System
FMECA(s)	Failure Mode Effects and Criticality Analyses
FMIT	Fusion Materials Irradiation Test
FONSI	Finding of No Significant Impact
FPAC	Fusion Power Advisory Committee
FPAT	Fusion Physics and Technology
FPSTEL	Computer code used to solve the ripple-bounce-averaged Fokker-Planck equation numerically
FSAR	Final Safety Analysis Report
FTE	Full-Time Equivalent
FTP	Field Task Proposal(s)
FTP	File Transfer Protocol
FTS	Federal Telecommunications System
FVPC	Fast Vertical Position Control
FWCD	Fast-Wave Current Drive
FWHM	Full Width at Half Maximum
FY	Fiscal Year (October 1 to September 30)
G	Gauss
G&A	General and Administrative (cost or expense)
GA	General Atomics, San Diego, California
GAE	Global Alfvén Eigenmode
GAO	General Accounting Office

gBL	Generalized Balescu-Lenard
GDC	Glow Discharge Cleaning
GHT	Gas Holding Tank
GHz	Gigahertz; 10^9 cycles per second
GIS	Geographic Information System
gk	gyrokinetic
GJ	Gigajoule, a unit of energy; 10^9 joules
GLOBUS-M	A low-aspect-ratio tokamak at the Ioffe Institute
GPC	Grating Polychromator
gpm	Gallons Per Minute
GPP	General Plant Projects
GRD	General Requirements Document
GSA	General Services Administration
GSF	Gross Square Feet
GTD	Gas-Target Device
GUI	Graphical User Interface
HAIFA	Hydrogen Alpha Interference Filter Array
HARD	High-Aspect Ratio Design (for ITER)
HAX	High-Level Data Analysis (system); uses a VAX computer
HEDL	Hanford Engineering Development Laboratory
HELIAC	A computer code used to calculate vacuum magnetic surfaces in nonaxisymmetric three-dimensional toroidal geometries
HF	Horizontal Field
HFIX	High-Field Ignition Experiment
HLDAS	High-Level Data Analysis System; equivalent to HAX
H-mode	High-Confinement Mode
HP	Health Physics (Branch) at PPPL
HPA	High Power Amplifier
HPP	High Power Pulsing (Operations)
HPPCI	High Performance Computing and Communication Initiative
HSD	Health and Safety Directive
HTA	Hard Tube Amplifier
HV	High Voltage
HVAC	Heating, Ventilating, and Air Conditioning

HVE	High-Voltage Enclosure(s)
HVPS	High-Voltage Power Supplies
HVST	High-Voltage Switch Tube
HXIS	Horizontal X-Ray Imaging System
HXR	Hard X-Ray
IAEA	International Atomic Energy Agency, Vienna, Austria
IBW	Ion-Bernstein Wave
IBWH	Ion-Bernstein-Wave Heating
I&C	Instrumentation and Control
IC	Internal Control
IC	Ion Cyclotron
ICCD	Intensified Charge-Coupled Device
ICE	Independent Cost Estimate
ICH	Ion Cyclotron Heating
ICRF	Ion Cyclotron Range of Frequencies
ICRH	Ion Cyclotron Resonance Heating
ID	Inner Diameter
IDEAL	ITER Divertor Experiment and Laboratory
IDL	Interactive Data Language
IEC	International Electrotechnical Commission Standard
IG	Inspector General
IGNITOR	Ignited Torus
IHEM	In-House Energy Management Program
IMAPS	Interstellar Medium Absorption Profile Spectrograph
IMF	Interplanetary Magnetic Field
INEL	Idaho National Engineering Laboratory, Idaho Falls, Idaho
INTOR	International Tokamak Reactor
I/O	Input/Output
I_p	Plasma Current
IPA	Intermediate Power Amplifier
IPP	Initial Protective Plates
IPP	Institut für Plasmaphysik at Garching, Germany
IPSG	Ignition Physics Study Group

IR	Infrared
IRM	Information Resource Management
ISCUS	ITER Steering Committee United States
ISDN	Integrated Services Digital Network
ISP	Ignition Studies Project
ISS	Internal Support Structure
ISTP	Integrated Systems Test Procedure
ISX	Impurity Study Experiment (at the Oak Ridge National Laboratory, Oak Ridge, Tennessee)
ISX-B	B version of ISX
ITER	International Thermonuclear Experimental Reactor
ITG	Ion Temperature Gradient
ITGDT	Ion-Temperature Gradient-Driven Turbulence
ITOC	Ignition Technical Oversight Committee
ITR	Ignition Test Reactor
IVV	In-Vessel Vehicle
IXRALM	Imaging Soft X-Ray Laser Microscope
JAERI	Japan Atomic Energy Research Institute, Japan
JCT	Joint Central Team (for the International Thermonuclear Experimental Reactor)
JET	Joint European Torus (at the Culham Laboratory, United Kingdom)
JIPPT-U-U	Fusion Device at the National Institute of Fusion Studies, Nagoya, Japan
JT-60	JT stands for JAERI Tokamak and 60 means plasma volume in m^3. A tokamak device in Japan.
JT-60SU	JT-60 Super Upgrade
JT-60U	JT-60 Upgrade
K	Kelvin–Thermodynamic Temperature
kA	Kiloamperes
KBM	Kinetic Ballooning Mode
kbytes	1000 bytes
KERMA	A factor which, when multiplied by newton flux, gives volume-averaged nuclear heating
keV	Kilo-Electron-Volts
KFA	Kernforschungsanlage Jülich, Germany

KfK	Kernforschungszentrum Karlsruhe, Germany
kG	Kilogauss
kHz	Kilohertz
kJ	Kilojoule
kMHDBM	Kinetically Calculated Magnetohydrodynamic Ballooning Mode
ksi	Kilopounds Per Square Inch (Pressure, Stress)
kV	Kilovolt
kV A	Kilovolt Ampere
kW	Kilowatt
kW h	Kilowatt Hour
LaB_6	Lanthanum Hexaboride
LANL	Los Alamos National Laboratory, Los Alamos, New Mexico
LAN(s)	Local Area Network(s)
LAR	Low-Aspect-Ratio
LART	Low-Aspect-Ratio Tokamak
LBL	Lawrence Berkeley Laboratory, Berkeley, California
LBM	Lithium Blanket Module
LCC	Lithium Comparison Code
LCCs	Local Control Centers
LCFS	Last Closed Flux Surface
LCP	Large Coil Program
LEC	Liquid Effluent Collection
LED	Light Emitting Diode
LENS	Low Energy Neutral System
LEO	Low Earth Orbit
LH	Lower Hybrid
LHCD	Lower Hybrid Current Drive
LHCP	Left-Hand Circularly Polarized
LHe	Liquid Helium
LHRF	Lower Hybrid Range of Frequencies
LHRH	Lower Hybrid Resonance Heating
LIF	Laser-Induced Fluorescence
LITE	Laser-Injected Trace Element (System)

LITE	Long-Pulse Ignited Test Experiment (at the Massachusetts Institute of Technology, Cambridge, Massachusetts)
LLBL	Low-Latitude Boundary Layer
LLNL	Lawrence Livermore National Laboratory, Livermore, California
LLRW	Low-Level Radioactive Waste
L-mode	Low-Confinement Mode
LMS	Leak Mitigation Systems
LO	Local Oscillator
LOB	Laboratory Office Building at PPPL
LOTUS	Nuclear testing facility at École Polytechnique Fédérale de Lausanne in Switzerland
LPG	Liquid Propane Gas
LPI	Lithium Pellet Injector
LPIS	Long-Pulse Ion Source
LSC	Lower Hybrid Simulation Code
LSM	Layered Synthetic Microstructures
μm	Micrometer; equivalent to micron
μsec	Microsecond
m	Meter
MA	Megamperes
MARFE(s)	Region(s) of enhanced edge radiation localized poloidally on the inner major-radius side of a plasma
MARS	Mirror Advanced Reactor Study (Lawrence Livermore National Laboratory, Livermore, California)
Mb	Megabyte; 1,000,000 bytes
MByte	Megabyte or Mb
MC&A	Material Control & Accountability
MCCB	Management Configuration Control Board
MCNC	Multichannel Neutron Collimator
MCNP	Monte-Carlo Neutron and Proton Code
MeV	Mega-Electron-Volt
MFAC	Magnetic Fusion Advisory Committee
MFE	Magnetic Fusion Energy
MFENET	Magnetic Fusion Energy Network
MFETF	Magnetic Fusion Energy Technology Fellowship (Program)

MFTF	Mirror Fusion Test Facility at the Lawrence Livermore National Laboratory, Livermore, California
MG	Motor Generator
MH3D	Magnetohydrodynamic Three-Dimensional Code
MHD	Magnetohydrodynamics
MHz	Megahertz
mil	A unit of length equal to 0.001 inch
MIPS	Million Instructions Per Second
MIRI	Multichannel Infrared Interferometer
MIST	Multiple Ionization State Transport code. A computer code which follows impurity species through various stages of ionization, charge-exchange, radiation, and transport within the plasma.
MIT	Massachusetts Institute of Technology, Cambridge, Massachusetts
MJ	Megajoules
mm	Millimeter
MMA	Maintenance Manipulator Arm (for TFTR)
M&O	Management and Operating (contractors)
MOSFET	Metal Oxide Semiconductor Field Effect Transistor
MPa	Mega-Pascal (Pressure, Stress)
MPD	Magnetoplasmadynamic
MRX	Magnetic Reconnection Experiment (at PPPL)
MSDS	Material Safety Data Sheet
MSE	Motional Stark Effect
msec	Millisecond
MTBF	Mean Time Between Failure
MTL	Material Test Laboratory
MTX	Microwave Tokamak Experiment at the Lawrence Livermore National Laboratory, Livermore, California
MVA	Megavolt Ampere
mW	Milliwatt
MW	Megawatt
NASA	National Aeronautics and Space Administration
NASA/RECON	An interactive online information retrieval system used by the PPPL Library
NASTRAN	A structural analysis code

NB	Neutral Beam
NBCD	Neutral-Beam Current Drive
NBETF	Neutral-Beam Engineering Test Facility
NBI	Neutral-Beam Injection
NBIS	Neutral-Beam Injection System
NBLs	Neutral Beamlines
NBPC	Neutral-Beam Power Conversion (Building)
NBPS	Neutral-Beam Power Supply
NBTC	Neutral-Beam Test Cell
NBTGI	Neutral-Beam Tritium Gas Injector(s)
NBVS	Neutral-Beam Vacuum System
NCR	Nonconformance Report
NCTTA	National Competitiveness Technology Transfer Act of 1990
NEPA	National Environmental Policy Act
NERSC	National Energy Research Supercomputer Center [formerly the National Magnetic Fusion Energy Computer Center (NMFECC)]
NESHAPS	National Emission Standards for Hazardous Air Pollutants
NET	Next European Torus
NFPA	National Fire Protection Association
NFS	Network File System
NIST	National Institute of Standards and Technology
NJDEPE	New Jersey Department of Environmental Protection and Energy
NJIT	New Jersey Institute of Technology
nm	Nanometer
NMFECC	National Magnetic Fusion Energy Computer Center (now the National Energy Research Supercomputer Center)
NOAA	National Oceanic and Atmospheric Administration
NOVA-K	A nonvariational stability code with kinetic effects
NPB	Neutral Probe Beam
NRC	Nuclear Regulatory Commission
nsec	Nanosecond
NSF	National Science Foundation
NSTX	National Spherical Tokamak
NTIS	National Technical Information Service

NTP	National Tokamak Project (a national consortium sponsored by the U.S. Department of Energy for the High Performance Computing and Communication Initiative)
1-D	One Dimensional
OD	Outer Diameter
OER	Office of Energy Research
OFE	Office of Fusion Energy
OH	Ohmic Heating
OMA	Optical Multichannel Analyzer
OMO	Occupational Medicine Office at PPPL
ONS	Office of Nuclear Safety
OPEX	Operating Expenses
ORM	Office of Resource Management at PPPL
ORB	Operations Review Board
ORC	Operations Review Committee
ORNL	Oak Ridge National Laboratory, Oak Ridge, Tennessee
ORR	Operational Readiness Review
OSB	Occupational Safety Branch
OSES	Operations System Engineering Support
OSHA	Occupational Safety and Health Administration
OTT	Office of Technology Transfer at PPPL
PAC	Program Advisory Committee (for Tokamak Physics Experiment)
PACE	Plant and Capital Equipment
PADS	Procurement Automated Data Processing System
PAO	Princeton Area Office
PBX	Princeton Beta Experiment (now the PBX-M)
PBX-M	Princeton Beta Experiment-Modification at PPPL
PC	Personal Computer
pC	Pico Coulomb
PCB	Polychlorinated Biphenyl
PCS	Projects Control System at PPPL
PCX	Pellet Charge-Exchange

PDC	Pulse-Discharge Cleaning
PDI	Proportional-Derivative-Integral
PDR	Preliminary Design Review
PDS	Princeton Divertor Simulator (a linear plasma device)
PDX	Poloidal Divertor Experiment (now the PBX-M) at PPPL
PEMs	Photoelastic Modulators
PEP-Hmodes	Pellet-Enhanced Profile H-Mode
PEST	Princeton Equilibrium, Stability, and Transport Code
PF	Poloidal Field
PFC	Plasma Facing Component
PFC	Plasma Fusion Center (at the Massachusetts Institute of Technology, Cambridge, Massachusetts)
PHA	Pulse-Height Analyzer
PID	Proportional, Integral, Differential
PIES	Princeton Iterative Equilibrium Solver Code
PIV	Plenum Interface Valve
PLANET	A two-dimensional transport code used to study the scrape-off region created by divertors and limiters
PLC	Programmable Logic Controller
PLCS	Power Line Carrier System
PLT	Princeton Large Torus (at PPPL in the 1970s and 1980s)
PM	Preventive Maintenance
PMP	Project Management Plan
PMS	Performance Management System
PMS	Performance Measurement System
POP	Post Office Protocol
PP-Lasers	Powerful, Picosecond Lasers
PPLCATS	A PPPL Library data base of fusion-related articles
PPLCC	Plasma Physics Laboratory Computer Center
PPM	Parts per Million
PPPL	Princeton University Plasma Physics Laboratory, Princeton, New Jersey
PQA	Procurement Quality Assurance
PSC	Pittsburgh Supercomputer Center
psec	Picosecond
PSE&G Co.	Public Service Electric and Gas Company (New Jersey)

psi	Pounds Per Square Inch
psig	Pounds Per Square Inch Gauge
PSPL	Powerful Subpicosecond Laser
PSTX	Princeton Spherical Tokamak Experiment
PUBSYS	Public System [PPL Public Information System (installed on the Princeton University IBM 3081 computer)]
PUCC	Princeton University Computer Center
PVT	Pressure, Volume, Temperature
PWB	Princeton Weekly Bulletin
QA	Quality Assurance
QA/R	Quality Assurance and Reliability
QC	Quality Control
QE	Quantum Efficiency
QMS	Quadpole Mass Spectrometer
RAM	Random Access Memory
RAM	Reliability, Availability, and Maintainability
RAP	Risk Assessment Plan
RAX	TFTR off-line data reduction system (uses a VAX computer)
R&D	Research and Development
REML	Radialogical Environmental Monitoring Laboratory
RESA	Research Equipment Storage and Assembly
rf	Radio-Frequency
RFBA	Request for Baseline Adjustment
RFI	rf-Inductively Coupled Plasma Reactor
RFP	Request for Proposal
RFP	Reversed-Field Pinch (device) at Los Alamos National Laboratory, Los Alamos, New Mexico
RFTF	Radio-Frequency Test Facility
RGA	Residual Gas Analyzer
RHCP	Right-Hand Circularly Polarized
RIE	Reactive Ion Etch (tool)
RIF	Reduction-in-Force
RIPLOS	Ripple Loss Code

RIV	Rapid Intervention Vehicle
RLIN	Research Libraries Information Network
RLW	Rebut-Lallia-Watkins
RMC	Realizable Markovian Closure
rms	Root-Mean-Square
RPI	Repeating Pellet Injector also Repeating Pneumatic Injector
rpm	Revolutions Per Minute
RTD	Resistive Thermal Detector
S-1 Spheromak	A compact toroid device (formerly at PPPL)
S-1 Upgrade	S-1 Spheromak Upgrade
SAD	Safety Assessment Document
SBD	Surface Barrier Diode
SBIR	Small Business Innovative Research
sccm	Standard Cubic Centimeter Per Minute
SCR	Silicon Controlled Rectifier
S/DB	Small and Disadvantaged Businesses
SDS	Safety Disconnect Switch(es)
SEAB	Secretary of Energy Advisory Board
SEAS	School of Engineering and Applied Science at Princeton University
sec	Second
SEM	Scanning Electron Microscope
SF	Shaping Field, equivalent to EF
SF_6	Sulfur Hexafluoride
SFPI	Safety and Fire Protection Improvement (Project)
SHEILA	Australian Heliac
SIMS	Secondary-Ion Mass Spectroscopy
SIR	Statutory Invention Registration
SM	Slave Manipulator
SMTP	Simple Mail Transfer Protocol
SN	Single Null
SNAP	Time-independent power equilibrium code
SNL	Sandia National Laboratories, Albuquerque, New Mexico and Livermore, California
SOL	Scrape-Off Layer

SOP	Safe Operating Procedure(s)
SOXMOS	Soft X-Ray Monochromator Spectrometer
SPARK	A general geometry computer code that calculates transient eddy currents and the resulting fields
SPEB	Subcontract Proposal Evaluation Panel
SPICE	A general purpose circuit simulation code
SPRED	Survey, Power Resolution, Extended Domain Code
SPRED	Ultraviolet survey spectrometer
SPS	Surface Pumping System
S&R	Shutdown and Removal
Sr	Steradian
SR	Safety Requirements
SRD	System Requirements Document
SSA	Summer Science Awards
SSAT	Steady-State Advanced Tokamak
SSC	Superconducting Supercollider
SST	Site Specific Plan
SSTR	Steady-State Tokamak Reactor
START-UP	A computer code which evaluates free boundary axisymmetric equilibria and transport
STEP	Stellarator expansion equilibrium and stability code
STTR	Small Business Technology Transfer Program
Supershots	Low-current, high-density plasma discharges combined with intensive neutral-beam heating that are fired in a machine where the walls have been scrupulously conditioned via high-power discharges to remove adsorbed deuterium
SUR	Surveillance Requirement
SURF	Synchrotron Ultraviolet User Facility (at the National Bureau of Standards)
SURFAS	A fast between-shot moments code
SXL	Soft X-Ray Laser
SXR	Soft X-Ray
2-D	Two-Dimensional
3-D	Three-Dimensional
T3	A toroidal W' solver

TAB	Technical Advisory Board
TAC	Technical Advisory Committee
TAE	Toroidicity-Induced Alfvén Eigenmode or Toroidal Alfvén Eigenmode
TCS	Torus Cleanup System
TCV	Tokamak Condition Variable—a tokamak under construction at École Polytechnique Fédérale de Lausanne in Switzerland.
TDMX	TFTR Data Management System
T_e	Electron Temperature
TEM	Transmission Electron Microscope
TEXT	Texas Experimental Tokamak at the University of Texas, Austin, Texas
TEXTOR	Tokamak Experiment for Technologically Oriented Research (Jülich, Germany)
TF	Toroidal Field
TFCD	Tokamak Fusion Core Device
TFCPC	Toroidal Field Coil Power Conversion (Building)
TFCX	Tokamak Fusion Core Experiment
TFD	Telemetry Fault Detector
TFM	TFTR Flexibility Modification
TFTR	Tokamak Fusion Test Reactor at PPPL
TGDM	Tritium Gas Delivery Manifold
TGI	Tritium Gas Injection
TGIA	Tritium Gas Injection Assembly
THICS	Tritium Hardware Interlock Control System
T_i	Ion Temperature
TIBER	Tokamak Ignition/Burn Experiment
TIV	Torus Interface Valve
TLD	Thermoluminescent Dosimeters
TMPs	Turbomolecular Pumps
TMX	Tandem Mirror Experiment at the Lawrence Livermore National Laboratory, Livermore, California
TMX-U	Tandem Mirror Experiment Upgrade at the Lawrence Livermore National Laboratory, Livermore, California
TNB	Tritium Neutral Beam (System)
Tore-Supra	Tokamak at Cadarache, France
Torr	A unit of pressure equal to 1/760 of an atmosphere

TOS	Terminal Operating Station
TPI	Tritium Pellet Injector
TPS	Tritium Purification System
TPX	Tokamak Physics Experiment, a National Project, to be located at PPPL
TQM	Total Quality Management
TRAC	Teacher Research Associates Program at PPPL
TRADE	Training Resource and Data Exchange (an annual DOE meeting of training professionals)
TRAGB	Tritium Receiving and Analytical Glove Box
TRANSP	Time-dependent transport analysis code
TRECAMS	Tritium Remote Control and Monitoring System
TRS	Tritium Regeneration System
TSC	Tokamak Simulation Code
TSCALE	A computer code that scales plasma equilibrium parameters over a wide range of major radius and aspect ratio
TSDCS	Tritium Storage and Delivery Cleanup System
TSDS	Tritium Storage and Delivery System
TSS	Tokamak Simulation System (Project)
TSTA	Tritium Systems Test Assembly
TVCS	Tritium Vault Cleanup System
TVPS	Torus Vacuum Pumping System
TVTS	TV Thomson Scattering
U-Bed	Uranium Getter Beds
UCLA	University of California at Los Angeles
UHF	Ultrahigh Frequency
ULF	Ultralow Frequency
UPS	Uninterruptible power supply
US	United States
USC	User Service Center at PPPL; implemented on a Digital Equipment Corporation (DEC) PDP-10 computer
USGS	United States Geological Survey
USNRC	United States Nuclear Regulatory Commission
UV	Ultraviolet

V	Volt
VAX	Digital Equipment Corporation computer; "Virtual Address Extension"
VC	Variable Curvature
VCD	Viscous Current Drive
VDE	Vertical Display Event
VEAPC	Vacuum Exhaust Active Pressure Control
VF	Vertical Field
VH-Mode	Very High Confinement Mode
VHF	Very High Frequency
VIPS	Visible Impurity Photometric Spectrometer
VMEC	Variational Method for Equilibrium Calculations (Code)
VSWR	Voltage Standing Wave Ratio
VUV	Vacuum Ultraviolet
VV	Vacuum Vessel
VXCS	Vertical X-Ray Crystal Spectrometer
W	Watt
WAF	Work Approval Form (system)
WFO	Work for Others
WBS	Work Breakdown Structure
WHIST	A one-dimensional transport code developed by the Oak Ridge National Laboratory, Oak Ridge, Tennessee
WKB	Wentzel-Kramers-Brillouin (A method for analyzing wave behavior if propagation characteristics depend on position.)
W-VIIAS	Wendelstein VII Stellarator Modified (at Garching, Germany)
WWW	World Wide Web
XCS	X-Ray Crystal Spectrometer
XIS	(Horizontal) X-Ray Imaging System
XP	Experimental Plan
XUV	Extreme Ultraviolet
0-D	Zero-Dimensional
ZT-H	A 4-MA reversed-field pinch experiment at the Los Alamos National Laboratory, Los Alamos, New Mexico

Notice

Available from:

National Technical Information Service
U.S. Department of Commerce
5285 Port Royal Road
Springfield, Virginia 22161

(703) 487-4650

Editor: Carol A. Phillips

Graphic Arts: G. Terry Birch
Gregory Czechowicz

Photography: Dietmar Krause

Manuscript Preparation: Kelly Forkel
Lillian Saquing
Patti Wieser

Layout: Carol A. Phillips
Lillian Saquing
Patti Wieser

The Princeton Plasma Physics Laboratory is operated by Princeton University under contract to the U.S. Department of Energy. For additional information, please contact:

Information Services
Princeton University
Plasma Physics Laboratory
P.O. Box 451
Princeton, N.J. 08543

Telephone: 609-243-2750
Fax: 609-243-2751
e-mail: pppl_info@pppl.gov
Internet: http://www.pppl.gov